Alkali Activation of Iranian Natural Pozzolans for Producing Geopolymer Cement and Concrete

Dali Bondar BSc, MSc

Thesis submitted in fulfilment of the requirements for the degree of Doctor of Philosophy

Department of Civil and Structural Engineering
University of Sheffield

June 2009

ABSTRACT

The challenge for the civil engineering community in the near future will be to realize the building of structures in harmony with the concept of sustainable development, through the use of high performance materials which have low environmental impact and can be produced at reasonable cost. Geopolymers are novel binder materials that could provide a route towards this objective. Although research on geopolymer has advanced, most of the previous research conducted on geopolymers has dealt with pastes and concentrated on the material's chemistry and microstructure. There is little information available concerning the engineering and durability properties of geopolymer concrete and none considering the use of natural pozzolans for production of geopolymer concrete.

This investigation has studied the potential of using five natural pozzolans from Iran as geopolymer precursors. Most of the raw materials contain zeolites and clay minerals and have a high loss on ignition. Therefore, trials were made where samples were calcined at 700, 800 and 900°C. The solubility of both the raw and calcined materials in an alkaline solution was used as an indicator for pozzolanic activity. Improvements in pozzolanic properties due to heat treatment and elevated curing temperatures (20, 40, 60, and 80°C) were studied by using alkali solubility, XRD and compressive strength tests. It has been found that geopolymer binders can be synthesized by activating natural pozzolans and condensing them with sodium silicate in a highly alkaline environment. A new model is presented which allows the prediction of the alkali activated pozzolan strength from information on their crystallinity, chemical compositions and alkali solubility.

Two types of Iranian natural pozzolans, namely Taftan which can be activated without calcination and Shahindej which was calcined were selected for further activation to study the effect of the alkaline medium on the strength of the alkali-activated natural pozzolan. The effect of the type, form, and concentration (molarities =2.5, 5.0, 7.5, 10.0 M) of the alkaline hydroxide, the modulus of sodium silicate (SiO_2/Na_2O ratio =2.1, 2.4, 3.1) and different curing conditions on the geopolymerisation of the above two natural pozzolans were studied. The optimum range and contributions for each factor is suggested based on their effect on compressive strength.

An optimum paste formulation has been developed for concrete mixing together with the procedure of addition of the raw materials to the reaction mixture and suitable curing methods for producing the geopolymer concrete derived from them. The properties of this geopolymer concrete in both the fresh and hardened states have been investigated in terms of setting time, workability, air content, compressive strength, splitting tensile strength, static modulus of elasticity, ultrasonic pulse velocity, and drying shrinkage. Studies related to durability such as gas permeability, chloride ion penetration, and sulphate resistance have been undertaken and compared to these for typical OPC concretes. Some problems were encountered in applying the standard concrete durability tests. In this study attempts have been made to determine the relationships between the different properties of geopolymer concrete with its compressive strength and compared to results for OPC concrete, to help to explain the differences between alkali-activated natural pozzolan concrete and OPC concrete. In the countries which have large resources of natural pozzolan, geopolymer concrete based on alkali activation of these resources can help decrease the energy consumption and environmental impacts involved in using traditional cement pastes.

ACKNOWLEDGMENTS

The author would like to extend her deepest gratitude to Dr. Cyril Lynsdale for his invaluable supervision and guidance throughout the progress of this manuscript. I am also indebted to my co-supervisor, Professor Neil Milestone for many insightful discussions and helpful criticism and advice. Their help and support have allowed me to complete my thesis successfully.

The author wishes to express her gratitude to Dr. N. Hassani the manager of the Natural Disasters Research Centre, Iran, for his encouragement and support rendered throughout this experimental research programme, which was carried out at the concrete technology laboratory of Power and Water University of Technology Tehran, Iran.

A special thank you is also extending to Professor A.A.Ramezanianpour for his valuable suggestions.

Thanks are also due to the technical staff of the concrete technology and chemistry laboratory of P.W.U.T. for their helpful assistance during the various stages of the project.

I would like to express my thanks to Dr. Nik Reeves in the Department of Materials, Sheffield University in Sheffield, U.K. and the technical staff of the Kansaran Binaloud X-ray, Kavoshyar, I.P.P.I., Material and Energy Research Centre laboratories in Tehran, Iran for their essential assistance on XRD, XRF, ICP-AES, FTIR, SEM/EDX.

Thanks to all of the friends of the author that have made her stay in England once more a memorable and valuable experience.

Heartfelt gratitude goes to the author's parents for their encouragement and prayers back home and her husband and children for their understanding and patience.

TABLE OF CONTENTS

ABSTRACT i
ACKNOWLEDGMENTS ii
TABLE OF CONTENTS iii
LIST OF TABLES vi
LIST OF FIGURES viii
GLOSSARY xv
NOTATION xvii
LIST OF ABBREVIATIONS xvii
1. INTRODUCTION 1
1.1 Introduction 1
1.2 Objectives and Scope of Work 2
1.3 Thesis Outline 4
2. LITERATURE REVIEW 6
2.1 Introduction 6
2.2 Geopolymers 6
2.2.1 Chemical properties of geopolymers 7
2.2.1.1 Set of reactions for geopolymerization 7
2.2.1.2 Chemical factors affecting geopolymerization structure 12
2.2.2 Physical properties of geopolymers 12
2.2.3 Mineralogical properties of geopolymers 13
2.3 Natural pozzolan and an overview of the activation of its reactivity 16
2.3.1 Pozzolanic activities of natural pozzolan 17
2.3.2 Main Factors affecting pozzolanic activity 17
2.3.3 Methods of activating natural pozzolan 18
2.3.3.1 Thermal activation methods 18
2.3.3.2 Mechanical activation method 19
2.3.3.3 Chemical activation method 20
2.4. Activators 22
2.4.1 Type of activators 22
2.4.2 Dosage of activators 23
2.4.3 Modulus of water glass solution 23
2.5. Geopolymer concrete 24
2.5.1 Properties of fresh geopolymer concrete 24
2.5.2 Properties of hardened geopolymer concrete 26
2.5.2.1 Alkali activated slag 27
2.5.2.2 Alkali activated fly ash 28
2.5.3 Durability properties of geopolymer concrete 29
2.6 Summary 30
3. CHARACTERISTICS OF NATURAL AND CALCINED POZZOLANS USED IN THE INVESTIGATION 35
3.1 Introduction 35
3.2 Shahindej Dacite 36
3.2.1 Mineralogical Composition 36
3.2.2 Chemical Composition 37
3.2.3 Physical Composition 38
3.3 Sahand Dacite 39
3.3.1 Mineralogical Composition 39

3.3.2 Chemical Composition 40
3.3.3 Physical Composition 40
3.4 Sirjan Dacite 40
3.4.1 Mineralogical Composition 41
3.4.2 Chemical Composition 41
3.4.3 Physical Composition 42
3.5 Rafsanjan Dacite 42
3.5.1 Mineralogical Composition 43
3.5.2 Chemical Composition 43
3.5.3 Physical Composition 44
3.6 Taftan Andesite 44
3.6.1 Mineralogical Composition 44
3.6.2 Chemical Composition 45
3.6.3 Physical Composition 45
3.7 Summary 46
4. THE SELECTION OF POZZOLAN FOR PRODUCING GEOPOLYMER BASED ON SIMPLE TESTS 59
4.1 Introduction 59
4.2 Measurement of Pozzolanic Activity of Natural Pozzolans 59
4.3 Experimental investigations 60
4.4 Pozzolanic activity of five pozzolans in their natural state and after heat treatment 61
4.4.1 Shahindej Dacite 61
4.4.2 Sahand Dacite 62
4.4.3 Sirjan Dacite 63
4.4.4 Rafsanjan Dacite 63
4.4.5 Taftan Andesite 64
4.5 A Simplified Model for the Prediction of Pozzolanic Behaviour 65
4.5.1 Activity Index 66
4.5.2 Alkali percentage 67
4.5.3 Alkali Solubility Index 68
4.5.4 Loss on Ignition (L.O.I.) 68
4.5.5 The activity ratio [(SiO_2+Al_2O_3+CaO) in solution/ (SiO_2+Al_2O_3+CaO) mineral] obtained from ICP tests 69
4.5.6 The quartz percentage 69
4.6 Correlation for Compressive Strength 70
4.7 Results and Suggestion 72
5. THE EFFECT OF ALKALI ACTIVATOR TYPE AND MINERAL ADDITIVES ON ALKALI ACTIVATION 87
5.1 Introduction 87
5.2 Chemical Activators and Materials 87
5.3 Experimental investigations 88
5.4 Experimental results 91
5.4.1 Type of Alkaline Activator 91
5.4.2 Dosage of Alkali Component 91
5.4.3 Form of Sodium Silicate Activator 94
5.4.4 Modulus of Water-glass Solution 94
5.4.5 Various Ratios of Alkaline Hydroxide to Water-glass 95
5.5 XRD Results for Geopolymerised Alkali Activated Natural Pozzolans 96
5.6 The Effect of Mineral Additives 97

5.7 Optimum Paste Proportions for Geopolymer Concrete Production 101
5.8 Summary 101
6. MIX DESIGN AND PROPERTIES OF FRESH GEOPOLYMER CONCRETE 124
6.1 Introduction 124
6.2 Mix Design Procedure 124
6.2.1 Alkali-Activated Natural Pozzolan Mixes 124
6.2.2 Determination of Water to Binder Ratios 124
6.2.3 Aggregates and Sieve Analysis Results 126
6.2.3.1 Fine Aggregate 126
6.2.3.2 Coarse Aggregate 126
6.2.4 Aggregate to Binder Content 126
6.2.5 Designing of Control Mixes 127
6.2.6 Mix Proportions and Mix Notation 127
6.3 Mortar and Concrete Mixing Procedure 128
6.4 Casting and Curing 129
6.5 Workability 131
6.5.1 Workability tests 131
6.5.2 Slump Test 131
6.5.3 Vebe time Test 132
6.5.4 Results and Discussions 132
6.6 Setting Time 133
6.6.1 Test Procedure 133
6.6.2 Results and Discussion 133
6.7 Air Content 135
6.7.1 Test Procedure 135
6.7.2 Results and Discussion 136
6.8 Summary 136
7. ENGINEERING PROPERITIES OF GEOPOLYMER CONCRETE 146
7.1 Introduction 146
7.2 Compressive Strength 146
7.2.1 Test Procedure 147
7.2.2 Results and Discussion 148
7.3 Splitting Tensile Strength 149
7.3.1 Test Procedure 149
7.3.2 Results and Discussion 150
7.4 Static Modulus of Elasticity 151
7.4.1 Test Procedure 151
7.4.2 Results and Discussion 152
7.5 Ultrasonic Pulse Velocity 153
7.5.1 Test Procedure 153
7.5.2 Results and Discussion 154
7.6 Drying Shrinkage properties 154
7.6.1 Test Procedure 154
7.6.2 Results and Discussion 155
7.7 Relationship between Engineering Properties 156
7.7.1 Relationship between Compressive and Tensile Strength 156
7.7.2 Relationship between Compressive Strength and Modules of Elasticity 158
7.7.3 Relationship between Compressive Strength and Ultrasonic Pulse Velocity 161

7.8 Summary 162
8. DURABILITY PROPERTIES OF GEOPOLYMER CONCRETE 188
8.1 Introduction 188
8.2 Oxygen permeability 189
8.2.1 Samples Preparation 189
8.2.2 Test Procedure 190
8.2.3 Results and Discussion 191
8.3 Chloride permeability 192
8.3.1 Samples Preparation 193
8.3.2 Test Procedure 193
8.3.3 Results and Discussions 195
8.4 Sulphate Resistance 197
8.4.1 Sample Preparation and Test Method for Sulphate Resistance 199
8.4.2 Test Procedure 199
8.4.2.1 Compressive Strength 199
8.4.2.2 Expansion Test 200
8.4.2.3 X-ray Diffraction Test 200
8.4.3 Results and Discussions 200
8.5 Relationship between Oxygen Permeability and Compressive Strength 202
8.6 Relationship between Chloride Permeability and Compressive Strength 204
8.7 Relationship between Chloride Permeability and Oxygen Permeability 205
8.8 Concluding summary 205
9. CONCLUSIONS AND RECOMMENDATIONS FOR FUTURE RESEARCH 221
9.1 Introduction 221
9.2 Activation of Natural Pozzolans for Production of Geopolymer Binder 221
9.3 Mix Design, Procedure and Curing Temperature 222
9.4 Fresh Properties of AANP Concrete 223
9.5 Engineering Properties of AANP Concrete 223
9.6 Durability Properties of AANP Concrete 224
9.7 Evaluation of Carbon footprint and Cost for AANP Concrete 224
9.7. 1 Environmental Benefits 225
9.7.2 Supply and Cost of activators 225
9.8 Application Aspects of AANP Concrete 226
9.8 Future Research on AANP Concrete 226
REFERENCES 230
APPENDIX 252

LIST OF TABLES

Table 3.1-a- Mineral compositions of the pozzolanas conducted by Kansaran Binaloud X-ray laboratory in Tehran, Iran 47
Table 3.1-b - Mineral compositions of the calcined pozzolanas conducted by Kansaran Binaloud X-ray laboratory in Tehran, Iran 48
Table 3.2 – The properties of Zeolite and Clay Minerals of the materials used in this investigation as described by F.Ezatian (1998) 49
Table 3.3-a Chemical composition (oxide percent) of the materials used in this investigation conducted by Kansaran Binaloud X-ray laboratory in Tehran, Iran (2005-2006) 50

Table 3.3-b Chemical composition (oxide percent) of the calcined materials used in this investigation conducted by Kansaran Binaloud X-ray laboratory in Tehran, Iran (2005-2006) 50
Table 3.4 Variability in the Chemical composition (oxide percent) of the materials used in this investigation 51
Table 4.1 ICP results of the filtrates from rapid alkali solubility test measured by the Kavoshyar laboratory in Tehran, Iran 74
Table 4.2 The measured parameters used for model input in present study 75
Table 4.3 The replacement of missing parameters used for model input in present study 76
Table 4.4 Linear and nonlinear regression coefficients and correlation coefficient (R^2) for pozzolans in natural and calcined form cured at 3 different temperatures ... 77
Table 5.1 Alkali Activation Solutions (grams per 100ml solution) 104
Table 5.2 ICP-AES results for Taftan pozzolan leaching tests (conducted by I.P.P.I. laboratory, Tehran, Iran) 104
Table 5.3 Weight percentage concentration observed in EDX (conducted by Material and Energy Research Centre laboratory, Tehran, Iran) 105
Table 5.4 Chemical composition of mineral additives used in this investigation conducted by Kansaran Binaloud X-ray laboratory in Tehran, Iran 105
Table 5.5 Mix proportion, strength, specific strength (SS), specific strength of mineral additive effect (SSME) of geopolymer cement 106
Table 5.6 Weight percentage concentration observed in EDX (conducted by Material and Energy Research Centre laboratory, Tehran, Iran) (TN=Taftan, TNK=Taftan added Kaolinite, TNSH=Taftan added Calcined Shahindej, TNL=Taftan added Burnt Lime) 107
Table 5.7 – Optimum Paste Proportion for Geopolymer Concrete 107
Table 6.1 Grading for the fine and coarse aggregates 138
Table 6.2 Concrete Mix Proportion 139
Table 6.3 Fresh concrete properties of the mixes investigated 140
Table 6.4 Initial and Final setting time of different mixes (with different activator concentration and mix temperature) 140
Table 7.1 The pulse velocity and the corresponding compressive strength of different mixes 164
Table 7.2 Quality Criteria Suggested by Central Water and Power Research Station Khadakwasla (India) 164
Table 8.1 The measured parameters used as input for finding nonlinear model to predict permeability of alkali activated Taftan pozzolan 207
Table 8.2 Nonlinear regression coefficients and correlation coefficient (R^2) for predicting permeability of alkali activated Taftan pozzolan 207
Table 8.3 Chloride diffusion coefficient and total integral chloride% to 45mm depth after 90 days ponding 207
Table 8.4 Summary of X-ray diffraction results show the existence of sulphate phases and achieved from the powder prepared from the surface and the middle of the samples immersed in sulphate solution 208
Table 8.4 Summary of X-ray diffraction results show the existence of sulphate phases and achieved from the powder prepared from the surface and the middle of the samples immersed in sulphate solution (continued) 209
Table 9.1 Mineralogy of investigated pozzolans 228
Table A7.1 Relation between splitting tensile strength and compressive strength .. 253

Table A7.2 Relation between static modulus of elasticity and cube compressive strength 254
Table A7.3 Relation between static modulus of elasticity and cylinder compressive strength 255
Table A7.4 Relation between static modulus of elasticity and splitting tensile strength 256
Table A8.1 Relation between oxygen permeability and compressive strength 257
Table A8.2 Relation between chloride permeability and compressive strength 258

LIST OF FIGURES

Figure 2.1a Computer molecular graphics of polymeric Mn-(-Si-O-Al-O-)n poly(sialate) and Mn-(-Si-O-Al-O-Si-O-)n poly(sialate-siloxo) and related frameworks (Devidovits, 1991, 1994) 33
Figure 2.1b Proposed structural model for K-poly(sialate-siloxo) geopolymer (Devidovits, 1991, 1994 and Barbosa, 2000) 33
Figure 2.2 Room temperature setting for concrete for concrete made of geopolymeric cement and Portland cements (Devidovits, 1991, 1994) 34
Figure 2.3 Cumulative intrusion volume vs. pore diameter plotted from MIP results. The characteristic pore size decreased as the molar % of KOH was increased (Bell and Kriven, 2004) 34
Figure 3.1 Location of pozzolans on geology map of Iran (Geology Survey of Iran/WWW.GSI.IR) 52
Figure 3.2-a Mineralogical composition of Shahindej dacite (testing was carried out in the Department of Engineering Materials, University of Sheffield) 53
Figure 3.2-b Mineralogical composition of calcined Shahindej dacite (testing was carried out in the Department of Engineering Materials, University of Sheffield) ... 53
Figure 3.2-c Mineralogical composition of Sahand dacite (testing was carried out in the Department of Engineering Materials, University of Sheffield) 54
Figure 3.2-d Mineralogical composition of Sirjan dacite (testing was carried out in the Department of Engineering Materials, University of Sheffield) 54
Figure 3.2-e Mineralogical composition of Rafsanjan dacite (testing was carried out in the Department of Engineering Materials, University of Sheffield) 55
Figure 3.2-f Mineralogical composition of Taftan andesite (testing was carried out in the Department of Engineering Materials, University of Sheffield) 55
Figure 3.2-g Comparison of X-ray diffraction of five untreated pozzolans conducted by Kansaran Binaloud X-ray laboratory in Tehran, Iran 56
Figure 3.3-a The XRD pattern of Shahindej and Sahand pozzolans at various calcination temperatures conducted by Kansaran Binaloud X-ray laboratory in Tehran, Iran A=Albite; Ca= Calcite; Cl=Clinoptilolite; MH=Magnesiohornblende; Q=Quartz 57
Figure 3.3-b The XRD patterns of Sirjan and Rafsanjan pozzolans at various calcination temperatures conducted by Kansaran Binaloud X-ray laboratory in Tehran, Iran A=Albite; B=Biotite; MH=Magnesiohornblende; M=Montmorillionite; Mu=Muscovite 58
Figure 4.1 Effect of boiling time on alkali solubility of various pozzolans studied in this research 78
Figure 4.2 Effect of boiling time and calcination on alkali solubility for different pozzolans studied in this research 79

Figure 4.3 Effect of calcinations temperature on alkali solubility for different pozzolans studied in this research 80
Figure 4.4 Comparing the compressive strength of different pozzolans in natural form or after calcination in various temperatures 81
Figure 4.5 Comparison of the effect of calcination on compressive strength of different alkali activated pozzolans at different curing temperature 82
Figure 4.6 Comparing the results of compressive strength of different untreated and calcined pozzolans at different curing temperature 83
Figure 4.7 Correlation between observed and predicted compressive strength at 28 days for untreated and calcined pozzolans resulted from linear model 84
Figure 4.8(a) and (b) Correlation between observed and predicted compressive strength at 28 days for untreated and calcined pozzolans resulted from nonlinear model 85
Figure 4.8(c) and (d) Correlation between observed and predicted compressive strength at 28 days for untreated and calcined pozzolans resulted from nonlinear model 86
Figure 5.1 Effect of type and concentration of activators on Taftan geopolymer compressive strength for different curing conditions 108
Figure 5.2 FTIR results for leached Taftan pozzolan with different concentration of activator conducted by I.P.P.I. FTIR laboratory, Tehran, Iran 109
Figure 5.3 Effect of concentration of activators on Shahindej geopolymer compressive strength for different curing conditions 109
Figure 5.4 FTIR results for untreated Shahindej pozzolan and alkali activated form of it conducted by I.P.P.I. FTIR laboratory, Tehran, Iran 110
Figure 5.5 Effect of sodium silicate form on activation of natural pozzolan 110
Figure 5.6 Effect of sodium silicate ratio on activation of Taftan pozzolan with different content of CaO 111
Figure 5.7 Effect of sodium silicate ratio on activation of untreated and calcined Shahindej pozzolan 111
Figure 5.8 X-ray diffraction traces of untreated (ARSH) and calcined (ACSH) Shahindej dacite activated with different ratio of sodium silicate (testing was carried out in the Department of Engineering Materials, University of Sheffield) 112
Figure 5.9 Influence of amount of sodium silicate on compressive strength of activated pozzolans (samples dimensions were 20x20x20 mm in these experiments) 113
Figure 5.10 Strength contour for different concentration of KOH and various ratio of KOH/Na_2SiO_3 for Taftan Pozzolan (24 samples were tested) 114
Figure 5.11 Strength contour for different concentration of KOH and various ratio of KOH/Na_2SiO_3 for Shahindej Pozzolan (16 samples were tested) 115
Figure 5.12(a) Mineralogical composition of Taftan andesite (testing was carried out in the Department of Engineering Materials, University of Sheffield) 116
Figure 5.12(b) Mineralogical composition of activated Taftan andesite at 90 days (testing was carried out in the Department of Engineering Materials, University of Sheffield) 116
Figure 5.13(a) Mineralogical composition of Shahindej dacite (testing was carried out in the Department of Engineering Materials, University of Sheffield) 117
Figure 5.13(b) X-ray diffraction traces of activated utreated Shahindej dacite (ARSH) at different ages (28 and 90 days) (testing was carried out in the Department of Engineering Materials, University of Sheffield) 117

Figure 5.14(a) Mineralogical composition of calcined Shahindej dacite (testing was carried out in the Department of Engineering Materials, University of Sheffield) . 118
Figure 5.14(b) X-ray diffraction traces of activated calcined Shahindej dacite (ACSH) at different ages (28 and 90 days) (testing was carried out in the Department of Engineering Materials, University of Sheffield)..... 118
Figure 5.15 Specific compressive strength of mixes containing kaolinite..... 119
Figure 5.16 Specific compressive strength of mixes containing calcined Shahindej 119
Figure 5.17 Specific compressive strength of mixes containing burnt lime 119
Figure 5.18-a SEM of activated Taftan pozzolan cured at 25 °C carried out in Material and Energy Research Centre laboratory, Tehran, Iran-(G) Geopolymer Matrix (T) Non reacted Taftan Pozzolan 120
Figure 5.18-b SEM of activated Taftan pozzolan cured at autoclave condition carried out in Material and Energy Research Centre laboratory, Tehran, Iran-(G) Geopolymer Matrix (T) Non reacted Taftan Pozzolan 120
Figure 5.19-a SEM of activated Taftan pozzolan mixed with Kaolinite Cured at 25°C carried out in Material and Energy Research Centre laboratory, Tehran, Iran-(G) Geopolymer Matrix (K) Non reacted Kaolinite 121
Figure 5.19-b SEM of activated Taftan pozzolan mixed with Kaolinite Cured at autoclave condition carried out in Material and Energy Research Centre laboratory, Tehran, Iran (G) Geopolymer Matrix (K) Non reacted Kaolinite..... 121
Figure 5.20-a SEM of activated Taftan pozzolan mixed with calcined Shahindej and cured at 25°C carried out in Material and Energy Research Centre laboratory, Tehran, Iran (G) Geopolymer Matrix (Z) zeolite (SH) Non reacted Shahindej Pozzolan 122
Figure 5.20-b SEM of activated Taftan pozzolan mixed with calcined Shahindej and cured at autoclave condition carried out in Material and Energy Research Centre laboratory, Tehran Iran(Z) Zeolite 122
Figure 5.21-a SEM of activated Taftan pozzolan mixed with burnt lime at 25°C carried out in Material and Energy Research Centre laboratory, Tehran, Iran(G) Geopolymer Matrix (CSH) Calcium Silicate Hydrate (T) Non reacted Taftan Pozzolan 123
Figure 5.21-b SEM of activated Taftan pozzolan mixed with burnt lime at autoclave condition carried out in Material and Energy Research Centre laboratory, Tehran, Iran(G) Geopolymer Matrix (CSH) Calcium Silicate Hydrate (Ca-C) Calcium Carbonate 123
Figure 6.1 Grading limits and size distribution curves for the fine and coarse aggregates..... 141
Figure 6.2 Compressive strength contour of activated untreated Shahindej pozzolan versus different amount of water to binder and binder to aggregate ratio (16 samples were tested) 142
Figure 6.3 Slump values for mixes investigated..... 143
Figure 6.4 Vebe results for the mixes investigated..... 143
Figure 6.5 Influence of activator concentration and mix temperature on final setting time..... 144
Figure 6.6 Initial and final setting time for different mixes..... 144
Figure 6.7 Air content values for different mixes investigated..... 145
Figure 7.1 Early-age and long-term compressive strength development for different mixes under sealed curing condition (CM1, CM2, and ACSH were cured at 20°C, ATAF1 and ATAF2 were cured at 40°C and ARSH was cured at 60°C which were the best curing temperature in each case) 165

Figure 7.2 Effect of curing conditions on compressive strength development of CM1 mix 166
Figure 7.3 Effect of curing conditions on compressive strength development of CM2 mix 167
Figure 7.4 Effect of different curing condition and curing temperature on compressive strength development for activated Taftan pozzolan with water to binder ratio equal to 0.4 168
Figure 7.5 Effect of different curing condition and curing temperature on compressive strength development for ATAF1 mix and comparing with CM1 mix 169
Figure 7.6 Effect of different curing condition and curing temperature on compressive strength development for activated Taftan pozzolan with water to binder ratio equal to 0.5 170
Figure 7.7 Effect of different curing condition and curing temperature on compressive strength development for ATAF2 mix and comparing with CM2 mix 171
Figure 7.8 Effect of water to binder ratio on compressive strength development for activated Taftan pozzolan cured at 20°C 172
Figure 7.9 Effect of water to binder ratio on compressive strength development for activated Taftan pozzolan cured at 40°C 173
Figure 7.10 Effect of water to binder ratio on compressive strength development for activated Taftan pozzolan cured at 60°C 174
Figure 7.11 Compressive strength at 28 days versus water to binder ratio(W/B)for alkali activated Taftan pozzolan 175
Figure 7.12 Long-term indirect tensile strength development for different mixes under sealed curing condition (CM1, CM2, and ACSH were cured at 20°C, ATAF1 and ATAF2 were cured at 40°C and ARSH was cured at 60°C which were the best curing temperature in each case) 175
Figure 7.13 Effect of different curing condition and curing temperature on indirect tensile strength development for ATAF1 and ATAF2 mixes 176
Figure 7.14 Effect of water to binder ratio on indirect tensile strength development for activated Taftan pozzolan cured at different curing condition (sealed and fog) and temperatures 177
Figure 7.15 Long-term static modulus of elasticity development for different mixes under sealed curing condition (CM1, CM2, and ACSH were cured at 20°C, ATAF1 and ATAF2 were cured at 40°C and ARSH was cured at 60°C which were the best curing temperature in each case) 178
Figure 7.16 Effect of different curing condition and curing temperature on static modulus of elasticity development for ATAF1 and ATAF2 mixes 179
Figure 7.17 Ultrasonic pulse velocity for different mixes under sealed curing condition (CM1, CM2, and ACSH were cured at 20°C, ATAF1 and ATAF2 were cured at 40°C and ARSH was cured at 60°C which were the best curing temperature for each one) 180
Figure 7.18 The comparator and concrete prism 181
Figure 7.19 Effect of length, temperature and condition of curing on drying shrinkage development with age for ATAF1 mix with comparison with OPC 182
Figure 7.20 Effect of length, temperature and condition of curing on drying shrinkage development with age for ATAF2 mix with comparison with OPC 183
Figure 7.21 Effect of Calcination and length of curing on drying shrinkage development with age for Shahindej mixes 184

Figure 7.22 Relation between the splitting tensile strength and the compressive strength of alkali activated natural pozzolans 185
Figure 7.23 Correlation between cube and cylinder compressive strength 185
Figure 7.24 Relation between the static modulus of elasticity and the cube compressive strength of Alkali activated natural pozzolans 186
Figure 7.25 Relation between the static modulus of elasticity and the cylinder compressive strength of Alkali activated natural pozzolans 186
Figure 7.26 Relationship between compressive strength and UPV 187
Figure 8.1 Oxygen permeability apparatus 210
Figure 8.2 Oxygen permeability development of different mixes under Sealed Curing Condition (CM1, CM2, and ACSH were cured at 20°C, ATAF1 and ATAF2 were cured at 40°C and ARSH was cured at 60°C which were the best curing temperature for each one)..... 211
Figure 8.3 Effect of curing conditions on oxygen permeability of alkali activated Taftan pozzolan..... 212
Figure 8.4 Top: Vacuum saturation and Bottom: Rapid chloride permeability test apparatus 213
Figure 8.5 Chloride permeability of various mixes at different ages under Sealed Curing Condition (CM1, CM2, and ACSH were cured at 20°C, ATAF1 and ATAF2 were cured at 40°C and ARSH was cured at 60°C which were the best curing temperature for each one)..... 214
Figure 8.6 Effect of curing on chloride permeability for ATAF1 and ATAF2 Mixes 215
Figure 8.7 Chloride [% wt. of concrete] versus depth of samples for different material and curing conditions 216
Figure 8.8 Compressive strength for ATAF1 and ATAF2 Mixes cured at different condition and temperature, ARSH, and ACSH in and out of the sulphate solution 217
Figure 8.9 Expansion at various ages for geopolymer mortar mixes based on alkali activated natural pozzolan in sulphate solution 218
Figure 8.10 Correlation between the percentage of expansion and reduction of strength at various ages for geopolymer mortar mixes based on alkali activated natural pozzolan in sulphate solution (W/B for mixes is same)..... 218
Figure 8.11 Relation between the oxygen permeability and the compressive strength of geopolymer concrete based on alkali activated natural pozzolans 219
Figure 8.12 The relationship between the predicted and observed permeability..... 219
Figure 8.13 Relation between the chloride permeability and the compressive strength of geopolymer concrete based on alkali activated natural pozzolans 220
Figure 8.14 Relation between the chloride permeability and the oxygen permeability of geopolymer concrete based on alkali activated natural pozzolans 220
Figure 9.1 Different calcination and curing temperatures with related compressive strengths of investigated pozzolans..... 228
Figure 9.2 Comparison of compressive strength of different investigated AANP concrete mixes and OPC concrete control mixes..... 229
Figure 9.3 Comparison of the oxygen permeability of different AANP concrete mixes and OPC concrete control mixes 229
Figure A7.1 Relation between the splitting strength and the compressive strength of CM1 and CM2 under different curing conditions..... 259
Figure A7.2 Relation between the splitting strength and the compressive strength of ATAF1 and ATAF2 under different curing conditions 260

Figure A7.3 Relation between the splitting tensile strength and the compressive strength of activated Taftan Pozzolan 261
Figure A7.4 Relation between the splitting tensile strength and the compressive strength of ARSH and ACSH mixes 262
Figure A7.5 Relation between the splitting tensile strength and the compressive strength of alkali activated Shahindej mixes 262
Figure A7.6 Relation between the static modulus of elasticity and the cube compressive strength of CM1 and CM2 under different curing conditions 263
Figure A7.7 Relation between the static modulus of elasticity and the cube compressive strength of ATAF1 and ATAF2 under different curing conditions 264
Figure A7.8 Relation between the static modulus of elasticity and the cube compressive strength of Alkali activated Taftan pozzolan 265
Figure A7.9 Relation between the static modulus of elasticity and the cube compressive strength of ARSH and ACSH Mixes 266
Figure A7.10 Relation between the static modulus of elasticity and the cube compressive strength of alkali activated Shahindej mixes 266
Figure A7.11 Relation between the static modulus of elasticity and the cylinder compressive strength of ATAF1 and ATAF2 under different curing conditions 267
Figure A7.12 Relation between the static modulus of elasticity and the cylinder compressive strength of Alkali activated Taftan Mixes 268
Figure A7.13 Relation between the static modulus of elasticity and the cylinder compressive strength of ARSH and ACSH Mixes 269
Figure A7.14 Relation between the static modulus of elasticity and the cylinder compressive strength of Alkali activated Shahindej Mixes 269
Figure A7.15 Relation between the static modulus of elasticity and the splitting tensile strength of CM1 and CM2 under different curing conditions 270
Figure A7.16 Relation between the static modulus of elasticity and the splitting tensile strength of ATAF1 and ATAF2 under different curing conditions 271
Figure A7.17 Relation between the static modulus of elasticity and the splitting tensile strength of Alkali activated Taftan Mixes 272
Figure A7.18 Relation between the static modulus of elasticity and the splitting tensile strength of ARSH and ACSH mixes 273
Figure A7.19 Relation between the static modulus of elasticity and the splitting tensile strength of Alkali activated Shahindej Mixes 273
Figure A7.20 Relation between the static modulus of elasticity and the splitting tensile strength of Alkali activated natural pozzolans 274
Figure A8.1 (a) X-ray diffraction traces for ATAF1 Mix cured at 20°C sealed condition after 3 month exposure in sulphate solution 275
Figure A8.1 (b) X-ray diffraction traces for ATAF1 Mix cured at 40°C fog condition after 3 month exposure in sulphate solution 276
Figure A8.1 (c) X-ray diffraction traces for ATAF2 Mix cured at 40°C fog condition after 3 month exposure in sulphate solution 276
Figure A8.1 (d) X-ray diffraction traces for ATAF1 Mix cured at 40°C sealed condition after 3 month exposure in sulphate solution 277
Figure A8.1 (e) X-ray diffraction traces for ATAF2 Mix cured at 40°C sealed condition after 3 month exposure in sulphate solution 277
Figure A8.1 (f) X-ray diffraction traces for ATAF1 Mix cured at 60°C sealed condition after 3 month exposure in sulphate solution 278
Figure A8.1 (g) X-ray diffraction traces for ATAF2 Mix cured at 60°C sealed condition after 3 month exposure in sulphate solution 278

Figure A8.1 (h) X-ray diffraction traces for ACSH Mix cured at 20°C sealed condition after 3 month exposure in sulphate solution 279
Figure A8.1 (i) X-ray diffraction traces for ARSH Mix cured at 60°C sealed condition after 3 month exposure in sulphate solution 279
Figure A8.2 Relation between the oxygen permeability and the compressive strength of CM1, CM2 and OPC concrete generally under different curing conditions 280
Figure A8.3 Relation between the oxygen permeability and the compressive strength of ATAF1, and ATAF2 mixes under different curing conditions 281
Figure A8.4 Relation between the oxygen permeability and the compressive strength of geopolymer concrete based on alkali activated Taftan pozzolan 282
Figure A8.5 Relation between the oxygen permeability and the compressive strength of ARSH and ACSH mixes separately and totally 283
Figure A8.6 Relation between the chloride permeability and the compressive strength of CM1, CM2 and OPC concrete generally under different curing conditions 284
Figure A8.7 Relation between the chloride permeability and the compressive strength of ATAF1, and ATAF2 mixes under different curing conditions 285
Figure A8.8 Relation between the chloride permeability and the compressive strength of geopolymeric concrete based on alkali activated Taftan pozzolan..... 286
Figure A8.9 Relation between the chloride permeability and the compressive strength of ARSH and ACSH mixes separately and totally 287

GLOSSARY

The following definitions were modified from Wikipedia encyclopedia:

Monomer: A **monomer** is a small molecule that may become chemically bonded to other monomers to form a polymer (from Greek mono "one" and meros "part").

Dimer: A **dimer** is a chemical entity consisting of two structurally similar subunits called monomers, which are held together by either intramolecular forces (covalent bonds) or weaker intermolecular forces.

Trimer: In chemistry a **trimer** is a reaction product of three identical molecules. Trimers are typically encountered as cyclic trimers. Chemical compounds that very easily form trimers are cyanic acids as an early intermediate in a polymerisation process.

Oligomer: In chemistry, an **oligomer** consists of a limited number of monomer units (*oligos,* is Greek for "a few"), in contrast to a polymer which, at least in principle, consists of an unlimited number of monomers

Polymer: A **polymer** (from Greek po´li-s for much, many and meros meaning part) is a large molecule (macromolecule) composed of repeating structural units typically connected by covalent chemical bonds. While *polymer* in popular usage suggests plastic, the term actually refers to a large class of natural and synthetic materials with a variety of properties.

Dacite: A type of igneous, volcanic rock. It is intermediate in composition between andesite and rhyolite. Typically it will contain about 65% SiO_2. Being volcanic the rock has a glassy or very fine grained texture.

Andesite: A type of igneous, volcanic rock, of intermediate composition, with grains varying in size or of uniform very fine or glassy texture. The mineral assemblage is typically dominated by plagioclase plus pyroxene and/or hornblende. Magnetite, zircon, apatite, ilmenite, biotite, and garnet are common accessory minerals. Alkali feldspar may be present in minor amounts. Being of intermediate composition the rock contains 52-65% SiO_2.

Classification of andesites may be refined according to the most abundant phenocryst, for example: hornblende-phyric andesite, if hornblende is the principal accessory mineral.

Rhyolite is an igneous, volcanic (extrusive) rock, of felsic (silicon-rich) composition (typically >69% SiO2). It may have any texture with grains varying from uniformly very fine grained or glassy from aphanitic to porphyritic. The mineral assemblage is usually quartz, alkali feldspar and plagioclase (in a ratio > 1:2 — see the QAPF diagram). Biotite and hornblende are common accessory minerals.

Rhyolite can be considered as the extrusive equivalent to the plutonic granite rock but due to its high content of silica and low iron and magnesium contents, rhyolite lava is highly polymerized and thus viscous. Rhyolite may also occur as breccias or in volcanic plugs and dykes. Very rapid cooling of rhyolite lavas produces a glass called obsidian.

Slower cooling forms microscopic crystals in those results in textures such as flow foliations, spherulitic, nodular, and lithophysal structures. Some rhyolite is highly vesicular pumice. Rhyolite eruptions may be highly explosive; resulting in deposits of fallout tephra and/or ignimbrites.

NOTATION

AANP = Alkali activated Natural Pozzolan

A=Alkali percentage in mineral

BO = Bridging Oxygen

CO_2 = Carbon dioxide

DC = Direct Current

Ec = Static Modulus of Elasticity (GPa)

f_c = Compressive Strength (MPa)

f_{cu} = Cubic Compressive Strength (MPa)

fcyl= Cylinder Compressive Strength (MPa)

f_t = Splitting Tensile Strength (MPa)

Kax=The activity index or the ratio of $[(Al_2O_3+CaO+Fe_2O_3+MgO)/SiO_2]$ in the mineral

Kalr = The activity ratio $[(SiO_2+Al_2O_3+CaO)$ in solution/ $(SiO_2+Al_2O_3+CaO)$ mineral]

LL = Liquid Limit

L.O.I = Loss on Ignition

Ms = Modulus of water-glass solution which is the ratio of SiO_2/Na_2O

NBO = Non Bridging Oxygen

PL = Plastic Limit

SL = Shrinkage Limit

Sol=Alkali solubility index

SSD = Saturated Surface Dry

LIST OF ABBREVIATIONS

AASHTO = American Association of State Highway and Transportation Officials

ASTM = American Society for Testing and Materials

BRE = Building Research Establishment

BS = British Standard

FTIR = Furrier Transverse Infrared Spectroscopy

ICP-AES = Inductively Coupled Plasma with Atomic Emission Spectroscopy

IR = Infrared Spectroscopy

OPC = Ordinary Portland cement

RCPT = Rapid Chloride Permeability Test

SEM/EDX = Scanning electron microscopy / Energy Dispersive X-ray

XRD = X-ray Diffraction

XRF = X-ray Fluorescence

1. INTRODUCTION

1.1 Introduction

It is expected that in the near future, the civil engineering community will have to produce structures in harmony with the concept of sustainable development, through the use of high performance materials with low environmental impact that are produced at reasonable cost. Geopolymer cement provides one route towards this objective.

Unfortunately, the production of Portland cement, a major component of concrete used in construction, releases large amounts of CO_2 into the atmosphere. It is estimated that the production of 1 tonne of OPC results in the release of 1 tonne of CO_2, a major contributor to the greenhouse effect and the global warming of the planet (Bilodeau and Malhotra, 2003). Given the huge amounts of concrete used worldwide (one cubic metre of concrete per person per year), cement production is estimated to contribute around 7% of global CO_2 emissions. Geopolymer cement, on the other hand, uses lesser amounts of calcium-based raw materials, lower manufacturing temperature and lower amounts of fuel, resulting in reduced carbon dioxide emissions during manufacture (Davidovits, 1994). Geopolymer materials are inorganic polymers based on alumina and silica units and are synthesized from a wide range of de-hydroxylated alumina-silicate powders including natural pozzolan, condensed with sodium silicate in a highly alkaline environment (Xu and Deventer 2000, 2003). Although the sodium silicate and alkaline hydroxide must be manufactured from refined products, geopolymer cement manufacture remains of lower environmental impact compared to OPC manufacture (Shi et al., 2006). In addition, materials based on alumina-silicates are naturally abundant worldwide and are present in many wastes and by-products, and geopolymer cement may be manufactured using existing concrete works; therefore no new expenditure is necessary (Davidovits, 1994). The mechanical properties of these novel materials produce the competitive properties for geopolymer cement in comparison with Portland cement (Davidovits, 1994, Barbosa et al., 2000, and Hardjito et al., 2004). It is claimed that geopolymer cement will account for about 47% of the world cement market in 2015 (Davidovits, 1994).

Geopolymer concrete is concrete produced with a geopolymer cement matrix binding fine and coarse aggregates. It has also been referred to in the literature as rock-concrete (Davidovits, 2003) since the finished product is almost identical to natural rock in appearance. With geopolymer cement it is possible to produce a mixture that can be poured, moulded, worked, and which sets faster and harder than normal Portland cement concrete (Taylor, 1997). Despite claims that this technology is based on a very old principle of construction materials such as that which was used in the Great Pyramids, it is only in the last 35 years that it has been rediscovered and attention has been drawn to its useful chemical and physical properties. It is evident from the literature that factors governing the formation of geopolymers and their setting and hardening are not fully understood. In addition there is little knowledge about the behaviour of activated natural pozzolans as geopolymer cement. Therefore it is worthwhile to study these alkali activated pozzolans as well as the properties of concrete constructed with this type of binder.

1.2 Objectives and Scope of Work

The use of alkali-activated natural pozzolan as a construction material is not well known. Therefore the principal aim of this research is to investigate the intrinsic nature of reacted Iranian natural pozzolans with the aim of establishing the optimum concentration of alkali solution for producing geopolymer cement from natural pozzolan and discover a suitable molar composition, and curing method for producing geopolymer cement derived from them. These all lead to the formulation of viable paste and concrete mixtures and the characterisation of their properties and performance in terms of compressive and tensile strengths, static modulus of elasticity, drying shrinkage, gas permeability, chloride ion penetration and sulphate resistance with the overall aim of assessing the potential of this type of geopolymer cement for the production of structural grade concrete and comparing this AANP concrete with typical OPC concrete control mixes.

The research programme has the following main objectives:

1) To investigate natural pozzolans as raw materials for producing geopolymer cement with emphasis on their chemical, physical and mineral characteristics. The aims of determining these characteristics are conducive for finding a

model to assess the reactivity of the pozzolans before using these materials for the production of geopolymer cement and concrete.

2) To select a method suitable for activating natural pozzolan as a geopolymer cement.
3) To determine AANP paste and concrete mix design in order to achieve acceptable setting time and compressive strength.
4) To study the properties of AANP concrete in both fresh and hardened states and evaluating its durability performance.

In order to achieve the above aims, the following additional objectives have been identified:

1) Study the effect of alkali type and concentration on compressive strength of paste.

2) Investigate the effect of the silica modulus of sodium silicate on the compressive strength of paste.

3) Determine the influence of selected kaolinite, calcined pozzolan, and lime as mineral additives on the compressive strength of geopolymer paste.

4) Examine the microstructure of reacted geopolymer derived from activated natural pozzolan with selected molar compositions cured at different temperatures or autoclave.

5) Suggest an optimum mix design for AANP concrete using the optimum paste obtained in previous steps considering the properties of fresh concrete such as slump, workability and setting time.

6) Study the effect of water to binder ratio and concrete age on the compressive and tensile strength and static modulus of elasticity of AANP concrete.

7) Measure drying shrinkage of AANP concrete.

8) Investigate the oxygen permeability of AANP concrete.

9) Determine the chloride ion penetration for AANP concrete.

10) Evaluate the resistance of the AANP concrete to sulphate attack.

1.3 Thesis Outline

The research project is reported in this thesis in 9 chapters. Following this introductory chapter, the other chapters are organised as follows:

Chapter 2 presents a review of the literature available on the subject of geopolymers and their properties, natural pozzolan and the methods of activation, the influence of different properties of various activators on producing geopolymers, and the properties of geopolymer concrete.

Chapter 3 deals with the characterization including chemical, physical and mineralogical properties of five types of natural pozzolans in raw and calcined forms.

Chapter 4 is dedicated to study the pozzolanic reactivity of five pozzolans in their natural state and after heat treatment at different calcination and curing temperatures. This was done based on simple tests including solubility and compressive strength and their efficiency in producing geopolymer cement was compared to select two natural pozzolans among them to continue the research. Furthermore a model is developed to allow prediction of the alkali activated pozzolan strength versus their crystallinity, chemical compositions and alkali solubility.

Chapter 5 deals with chemical activation of these materials to find out the most suitable activators in terms of type, dosage, form and ratio. It also assesses the usefulness of mineral additives in compensating for the deficiencies of the main oxides, such as SiO_2, Al_2O_3 and CaO in natural pozzolans with the aim of improving the strength of geopolymer cement.

Chapter 6 covers mix design and the properties of fresh concrete made with alkali activated natural pozzolan such as workability, setting time and air content.

Chapter 7 is dedicated to the evaluation of the engineering properties of the AANP concrete including compressive strength, splitting tensile strength, static modulus of elasticity, ultrasonic pulse velocity and the drying shrinkage behaviour of the

different mixes and factors affecting them. It also includes the relationships between different properties of this type of concrete and its compressive strength.

Chapter 8 deals with the properties related to the AANP concrete durability including oxygen permeability, rapid chloride permeability, and sulphate resistance.

Chapter 9 presents the main conclusions and recommendations for future research.

The list of references is presented at the end of the thesis.

2. LITERATURE REVIEW

2.1 Introduction

The purpose of this chapter is to review and discuss the available literature on geopolymers including the nature of starting materials and properties of alkaline solutions for producing geopolymer cements as an environmental concrete binder. The published research on the properties of various types of natural pozzolans as raw material and the different ways of activating these materials are reviewed here to enhance our knowledge in the use of natural pozzolans in production of this new construction material.

2.2 Geopolymers

The term "geopolymer" describes a family of mineral binders that have a polymeric silicon-oxygen-aluminium framework structure, similar to that found in zeolites. Geopolymers are often viewed as the amorphous equivalents of zeolites because they have approximately the same Al:Si ratio as a comparable zeolite but without the crystal structure (Davidovits, 1999). Highly alkaline solutions are used to induce the silicon and aluminium ions in the source materials to dissolve and form the geopolymer cement.

The three main steps in the process are similar to those for synthesis of zeolites:

1) Dissolution of any pozzolanic compound or source of silica and alumina that is readily dissolved in alkaline solution, with the formation of mobile precursors of alumino-silicate oxides through the complex action of hydroxide ions.
2) Partial orientation of mobile precursors as well as the partial internal restructuring of the alkali poly-sialates.
3) Re-precipitation of the particles from the initial solid phase where the whole system hardens to form an inorganic polymeric structure.

A geopolymerisation process can transform a wide range of alumina-silica wastes or natural materials such as fly-ash (coal and lignite), oil fuel ash, rice husk ash, blast furnace and steel slag, silica fume, metakaolin, and natural pozzolans into building

products (Davidovits, 1994). These materials can provide poly-condense alumina silica behaviour just like organic polymers, at temperatures lower than 100°C. Geopolymerization involves the chemical reaction of alumina-silicate oxides with alkali poly-silicates yielding polymeric Si-O-Al bonds; the amorphous or semi-crystalline three dimensional silico-aluminate structures (Davidovits, 1991). Davidovits defined three basic forms to describe building blocks (Figure 2.1):

a) Poly (sialite) (-Si-O-AL-O-)
b) Poly (sialate-siloxo) (-Si-O-Al-O-Si-O-)
c) Poly (sialate-disiloxo) (-Si-O-Al-O-Si-O-Si-O-)

The distribution and relative amounts of each of the different Al and Si building blocks affect the chemical and physical properties of the final product.

2.2.1 Chemical properties of geopolymers

It is worthwhile discussing briefly, the chemistry and molecular structure of geopolymers. For the chemical designation of geopolymers based on silico-aluminates, poly (sialate) was suggested. The sialate network consists of approximately equal number of SiO_2 and AlO_4 tetrahedral linked alternately by sharing all the oxygen. Positive ions (Na^+, K^+, Li^+, Ca^{++}, Ba^{++}, NH_4^+, H_3O^+) must be present in the framework cavities to balance the negative charge of Al_3^+ in IV-fold coordination (Davidovits, 1999).

2.2.1.1 Set of reactions for geopolymerization

The set of reactions for geopolymerization can be divided into three stages as below (Hanzlicek and Steinerov, 2002, Palomo and Lopez de la Fuente, 2003):
In the first stage, M-O, Al-O-Si, Al-O-Al, and Si-O-Si bonds in raw material should be ruptured. This needs a stimulus, for example the variation of the ion force of the medium when adding ions with electro-donor properties (alkaline-metals). The result is a redistribution of the electronic density over the silicon atoms that favour the Si-O-Si bond breaks. The hydroxylation degree of silicon may increase above 2 or 3 units forming unstable intermediate complexes that decompose to give place to silicic acid $Si(OH)_4$ and $Si\text{-}O^-$ anions. The presence of cations of alkaline metals balances the negative electrical load of these anions, producing $Si\text{-}O\text{-}Na^+$ bonds.

These alkaline silicates are due to ion-exchange reaction with co-valance ions and result in Si-O-Ca-OH complexes. Hydroxyl groups affect Al-O-Si bonds in a similar way and $Al(OH)_4^-$, $Al(OH)_5^{-2}$, $Al(OH)_6^{-3}$ complexes are due to the pH value of the alkaline aqueous solution and existence of aluminates in it.

In the second stage, condensation of un-separated elements causes favourable contacts and creates a coagulation structure. Therefore when pH>7 rupture of Si-O-Si bonds are substituted with hydroxyl complexes of $Si(OH)_4$ which stabilize it as a dimmer molecule. Here OH^- behaves as a catalyst. All of the phenomena, combinations and stability of the products in this stage are affected by the amount of alkaline in the system. At a specific moment, due to the reduction of the pH in the liquid phase, mechanical strength will develop. This is due to the absorption and reaction of alkaline, hydro-silicates and hydro-aluminates. If the alkaline acts as a catalyst phenomenon in the destructive stage, it will act as a structural conforming element in the next stage. Basic factors that influence the chemical reactions in the low temperature syntheses are the interlinking of $AlO_2(OH)_4$ octahedrons and SiO_4 tetrahedrons and changes in alumina-silicate structure in the course of the de-hydroxylation. In the complete de-hydroxylation and disintegration of mineral material on heating, the Al atom coordination number changes from 6 to 4 or to 5 (Xu and Deventer, 2000). The possible change in Al coordination could be described as:

$$AlO_2(OH)_4 = AlO_4 + 2\ H_2O \qquad (2\text{-}1)$$

Finally, these two stages conduct the polymerization of raw material. This requires that condensation of the structure and of the particles from the initial solid phase is produced (strongly exothermal step), which involves the appearance of a cementitious material with a poorly ordered structure but having a high mechanical strength (Van Jaarsveld and Van Deventer et al. 2002; Palomo and Lopez de la Fuente 2003). The chemical reaction schemes for the dissolution of Al-Si minerals and silicates under strong alkaline conditions, condensation and polymerization of elements are discussed as follows:

Based on the above preliminary general description, the details of chemical reaction of geopolymerization are as follows. Normally, the possible chemical process for the dissolution of Al–Si minerals and silicates under strong alkaline conditions can be

expressed as the following reaction schemes (Babushkin et al., 1985; McCormick et al., 1989b) (M represents the Na or K).

$$\text{Al–Si solid particle} + OH^-(aq) \leftrightarrow \underset{\text{monomer}}{Al(OH)_4^-} + \underset{\text{monomer}}{^-OSi(OH)_3} \quad (2\text{-}2)$$

$$^-OSi(OH)_3 + OH^- \leftrightarrow {}^-OSi(OH)_2O^- + H_2O \quad (2\text{-}3)$$

$$\begin{array}{c} O^- \\ | \\ {}^-OSi(OH)_2O^- + OH^- \leftrightarrow {}^-OSi(OH)O^- + H_2O \end{array} \quad (2\text{-}4)$$

$$\underset{\text{monomer}}{M^+} + \underset{\text{monomer}}{^-OSi(OH)_3} \leftrightarrow M^+{}^-OSi(OH)_3 \quad (2\text{-}5)$$

$$\underset{\text{monomer}}{2M^+ + {}^-OSi(OH)_2O^-} \leftrightarrow \underset{\text{monomer}}{M^+{}^-OSi(OH)_2O^-{}^+M} \quad (2\text{-}6)$$

$$\begin{array}{c} O^- \qquad\qquad O^-{}^+M \\ | \qquad\qquad | \\ 3M^+ + {}^-OSi(OH)O^- \leftrightarrow M^+{}^-OSi(OH)O^-{}^+M \end{array} \quad (2\text{-}7)$$

$$\underset{\text{monomer}}{M^+ + Al(OH)_4^-} + OH^- \leftrightarrow \underset{\text{monomer}}{M^+{}^-Al(OH)_3^-} + H_2O \quad (2\text{-}8)$$

$$\underset{\text{monomer}}{^-OSi(OH)_3} + \underset{\text{monomer}}{M^+{}^-OSi(OH)_3} + M^+ \leftrightarrow \underset{\text{dimmer}}{M^+{}^-OSi(OH)_2\text{-}O\text{-}Si(OH)_3} + MOH \quad (2\text{-}9)$$

$$\underset{\text{monomer}}{^-OSi(OH)_2O^-} + \underset{\text{monomer}}{M^+{}^-OSi(OH)_3} + M^+ \leftrightarrow M^+{}^-OSi(OH)_2\text{-}O\text{-}Si(OH)_2O^- + MOH \quad (2\text{-}10)$$

$$\begin{array}{cc} O^- & O^- \\ | & | \\ {}^-OSi(OH)O^- & + M^+{}^-OSi(OH)_3 + M^+ \end{array} \underset{\substack{\text{monomer} \\ \text{monomer} \\ \text{dimmer}}}{\leftrightarrow} M^+{}^-OSi(OH)\text{-}O\text{-}Si(OH)_2O^- + MOH \quad (2\text{-}11)$$

$$2\text{Silicate monomer}^- + 2\ \text{Silicate dimmer}^- + 2M^+ \leftrightarrow M^+{}^-\text{cyclic trimmer} + M^+{}^-\text{linear trimer} + 2OH^- \quad (2\text{-}12)$$

With concentrated silicate anion addition, the tetramer, pentamer, hexamer, octamer, nonamer, and their compounds will appear (Hendricks et al., 1991). The dissolution reaction (2-2), for a fixed particle size, is a function of MOH concentration, the structure and the surface properties of the minerals. From the 11 reactions given above, it can be seen that increasing the concentration of alkaline solution favours all reactions (2-2) to (2-8) shifting to the right hand side. Eqs (2-2) - (2-4) are chemical hydration reactions, where the OH^- anions react with the Al-Si solid surface to form $Al(OH)_4^-$, $^-OSi(OH)_3$, divalent orthosilicic acid and trivalent orthosilicic acid ions. Reactions (2-5) to (2-8) are physical electrostatic reactions, where the alkali metal cation M^+ reacts with $Al(OH)_4^-$, $^-OSi(OH)_3$, divalent orthosilicic acid and trivalent orthosilicic acid ions to balance coulombic electrostatic repellence. Reactions (2-9) to (2-12) are cation-anion pair condensation interactions based on Coulombic electrostatic attraction. In reactions (2-8) to (2-12), the M^+ cations reacts with $Al(OH)_4^-$ and species of orthosilicic acid ions to form ion pairs of $M^{+-}Al(OH)_4$ monomer and silicate monomer, dimmer and trimmer ions, which reduce the amount of free $Al(OH)_4^-$ and the species of ortosilicic acid ions, therefore shifting reactions (2-2)-(2-4) to the right hand side. According to Dent Glasser and Hervey (1984a) there is no cation-anion pair reaction directly on $Al(OH)_4$ tetrahedral, which limits the dissolution of Al, so that the concentration of Al is always lower than the corresponding concentration of Si. Reactions (2-5) to (2-12) suggest that the alkali-metal cation affects extend of the dissolution of an alumina-silicate. As Na^+ and K^+ have the same electric charge, their different effects are as result of their different ionic sizes. It has been shown that cation-anion pair interaction becomes less significant as the cation size increases. The cation with the smaller size favours the ion-pair reaction with smaller silicate oligmers, such as silicate monomers, dimmers, and trimers. Thus we can expect that Na^+ with the smaller size will be more active in reactions (2-5) to (2-12) than K^+, which should result in a higher extent of dissolution of minerals in the NaOH solution. The fact that sodalite structure is stabilized by sodium but not by potassium may be the reason why sodalite, in contrast with the other minerals, shows a higher extent of dissolution in KOH than in NaOH solution (Xu and Deventer, 2000). Experimental data shows that dissolution of Al and Si depends strongly on ionic strength and aqueous pH. Si dissolution increases with a decrease of ionic strength and an increase of aqueous pH and Al dissolution does just the opposite. On the other hand, fundamental factors that mostly influence the

formation and stability of the gel as a precursor of new materials as well as the preparation of such materials are:

- The de-hydroxylation of raw material
- Size of particles
- Value of pH of the alkaline aqueous solution
- Mixing (the intensity and time of mass transportation) (Babushkin, 1985; McCormick, 1989)

Therefore, promoted hydrolytic reaction, or alkali-activation of the alumina-silicate raw materials, is followed by the polymerization of the dissolved species (including the added soluble silicates) to form an alumina-silicate gel (the binding phase) and the subsequent solid state transformation of the gel. With the assumption that Al is always in the fourth coordination, a simplified hydrolytic reaction on an alumina-silicate can be shown in the scheme below:

$$M^{+}\text{-}(Al\text{-}O\text{-}Si)\ \text{raw} + 2M^{+}OH^{-} \rightarrow M^{+}\text{-}(Al^{-}\text{-}O^{-}\text{-}M^{+}) + (M^{+}\text{-}O^{-}\text{-}Si)^{-} + H_2O \quad M=Na \text{ or } K \qquad (2\text{-}13)$$

From the scheme, it is clear that during alkali activation; every bridging oxygen atom (BO) of the original alumina-silicate is replaced by two negative charged non bridging oxygen atoms (NBO) which are charged compensated by alkalis. Addition of alkalis as network modifiers to an (alumina) silicate is known to generate greater concentration of NBOs within the structure. The TO_4 (T=Al or Si) units within the silicate network become more isolated within increasing alkali inclusion and thus lower the molecular vibration force constant of the T-O bond. As a result, an infrared (IR) band attributable to the T-O-Si asymmetric stretching vibration of the TO_4 tetrahedral of an (alumina) silicate glass has been found to shift to the lower energy end with increasing alkali content. The extent of the shift is approximately linear to the alkali content. With the view that a greater extent of alkali activation of alumina silicates should give rise to a product of greater NBO concentrations, it is possible that similar trends can also be observed in the geopolymerization of alumina-silicates especially at the early stage (Lee and Deventer, 2003). IR spectroscopy provides a useful method for the following changes occurring during reaction: the bands at 1080 and 460 cm^{-1} are Si-O vibrations, while the Al-O vibration band has shifted to

800cm^{-1}. This band is characteristic of tetrahedral coordinated Al. The geopolymer IR spectrum is quite different. The Si-O vibration bands have moved to lower frequencies (1000 and 440 Cm^{-1}) and in this spectrum the bands due to Al-O vibrations are located at 850 and 700 Cm^{-1} (Palomo et al, 1997).

2.2.1.2 Chemical factors affecting geopolymerization structure

Davidovits et al. indicate that certain composition criteria have to be met for geopolymerization to occur (in Jaarsveld et al, 1997, Rahier et al. 1996, 1997, Hos et al., 2002). These include: (1) The molar ratio SiO_2:M_2O must be between 3.0:1 and 6.6:1 in the aqueous soluble silicate solution where M is an alkali metal cation, (2) The alumino-silicate oxide must contain Al which is readily soluble and (3) The overall molar ratio Al_2O_3:SiO_2 must be between 1: 3.3 and 1:6.5.

Therefore the nature of the starting materials (Al-Si minerals) and actual concentrations of alkali in solution affect the formation and setting of this gel phase. The concentrations of Si are higher than the corresponding Al, which could be caused partly not only by the higher content of Si than Al in the minerals, but also by the higher intrinsic extent of dissolution of Si than Al. Minerals have a higher extent of dissolution with increasing concentrations of alkaline as well(Xu and Deventer, 2000).

Previous works show that factors such as the %CaO, the molar Si-Al in the original mineral, the extent of dissolution of Si, the molar Si/Al ratio in solution, the hardness of the mineral and the use of KOH as an activator have positive effects on the final compressive strength of geopolymer cement while %K_2O in the original mineral and use of NaOH show a negative correlation. Of all the factors mentioned above, the type of alkali, %K_2O in the mineral and ppm Si in solution are identified as having a significant effect on strength (Xu and Deventer, 2000).

2.2.2 Physical properties of geopolymers

Inorganic polymers harden in a few hours at 30°C, a few minutes at 85°C and a few seconds if subjected to micro waves (Davidovits, 1999). Compressive strengths of geopolymer cement rise with time for up to about 28days; for example, while

compressive strengths may be 20MPa after four hours at 20°C (Figure 2.2), 28day compressive strengths are in the range 70-100MPa (Davidovits, 1988).

Physical strength is not only an advantage for the utilization of these products in certain building applications but also provides means for physical encapsulation of toxic material. Physical properties, such as compressive strength and porosity, can be utilized in distinguishing between different matrices (Van Jaarsveld et al., 1997).

It is found that variation of alkali choice may be used as a means to tailor pore size. This could allow geopolymers to be applied to areas such as catalysts and filtration. The majority of the intrusion volume occurs from 0.1 to 0.01μm pore diameter for different geopolymers and consistently decreases as the molarity of KOH increases; however, this is contrary for NaOH solution. The plot of differential intrusion volume versus pore diameter indicates that the pore size distribution may be bimodal. Mercury Intrusion Porosimetry (MIP) data show that the inherent pore size of an autoclaved geopolymer is between 10-100 nm (Figure 2.3). Using the autoclave processing technique effectively rids the sample of large pores (Bell and Kriven, 2004).

It is noteworthy that the curing of geopolymers is achieved by one of three routes, at ambient temperatures up to (40-80°C), warm pressing (between two sheets at 80°C and ~18MPa load for 2 hour) or curing in a high pressure autoclave (iso-statically pressed at 20MPa while being heated at 80°C for 24h) (Kriven and Bell, 2004).

In addition, the evolution of geopolymers with temperature will involve three stages comprising the loss of constitutional water at about 150°C, transformation in nepheline ($Na_3KAl_4Si_4O_{16}$) or silica-under saturated aluminosilicate at about 900°C and melting at about 1300°C (Palomo et al., 1997).

With respect to density, inorganic polymer density is typically from 1300 to 2100 kg/m^3.

2.2.3 Mineralogical properties of geopolymers

Single phase geopolymers such as anorthite ($CaAl_2Si_2O_8$) or albite ($NaAlSi_3O_8$) may be thought of as porous, alumina-silicate glass or as metastable, amorphous zeolite

which due to the insufficiency of water and hence diffusion paths, do not have an opportunity to crystallize. The microstructure of fully reacted geopolymers consists of amorphous nano-particles separated by nanopores whose features are the order of ≤10nm (Kriven et al., 2003). The subsequent geopolymeric products are therefore, amorphous to semi-crystalline materials, which distinguishes geopolymers from the well crystallized zeolite products, and contributes to the superior mechanical strength of geopolymers (Xu and Deventer, 2002). The amorphous nature of geopolymers makes structural investigations by X-ray powder diffraction inconclusive. Other techniques such as Infrared Spectroscopy and Magic Angle Spinning Nuclear Magnetic Resonance (MAS-NMR) developed for studies of zeolitic structures, have been employed with varying degrees of success (Van Jaarsveld et al., 1997).

When crystalline alumina-silicates partially dissolve in a concentrated alkaline medium, an amorphous geopolymeric gel is formed interspersed with un-dissolved crystalline particles. Geopolymers invented by Davidovits in the late 1970s (1991, 1994), are amorphous to semi-crystalline three-dimensional alumina-silicate polymers. Geopolymeric reactants could range from kaolinite or metakaolinite to a group of materials rich in SiO_2 and/or Al_2O_3 oxides, e.g., fly ash, slag, construction waste, and natural minerals. It should be noted that the geopolymer binders (polysialate, polysialate-siloxo, and polysialate-disoloxo) characterised by Davidovits were evenly dispersed (Davidovits, 1991) amorphous to semi-crystalline products synthesised at a temperature higher than 100°C and pressure higher than 1 At. using kaolinite or calcined kaolinite as the sole alumina-silicate source. In contrast, most geopolymers synthesised from different starting materials are mixtures of crystalline alumina-silicate particles and semi-crystalline and amorphous alumina-silicate gel. Due to the complex composition of such geopolymers and the difficulties of separating the crystalline alumina-silicates particles from the semi-crystalline and amorphous gel phases, characterization of the structural composition of geopolymers has not been conducted. As a mixture of amorphous to semi-crystalline and crystalline phases, the mechanical strength of a geopolymer should be the result of both the amorphous gel phase as binder and the crystalline alumina-silicate particles as filler. Hence, an understanding of the structural composition as well as the gel phase of a geopolymer will aid the development of improved geopolymers (Xu and

Deventer, 2002). The mechanism of conforming crystalline and amorphous geopolymers could be as below:

1) Crystalline Poly (sialate) (-Si-O-Al-O-)n: With the geopolymeric precursor kaolinite Si_2O_5, $Al_2(OH)_4$, hydrothermal poly-condensation at 150°C and 5-10Mpa with NaOH, yields well crystallized sodalite based Na-Poly(sialate) Na-PS(Si_2O_4, Al_2O_4, 2Na), $3H_2O$, within 20 seconds, according to the scheme as follow:

$$\text{Kaolinite} + \text{NaOH} \xrightarrow[\text{10-20sec}]{\text{150°C, 20 MPa}} \text{Sodium-poly-sialate (Na-Ps)}$$

The 3-dimentional framework evolves from the poly-condensation of the dimmer: cyclo-di-sialate (CDS). For zeolite A, the primary condensation unit is tetramer cyclo-tetra-sialate which is formed in the solution prior to crystallization. With longer reaction time, 45-60min, only the denser Na-PS is formed (Davidovits, 1991).

2) Amorphous Poly (sialate-siloxo) (Si-O-Al-O-Si-O)n, (Na, K)-PSS, (Ca, K)-PSS and K-PSS: It is known that the mechanism of the formation of crystalline zeolitic species with the ratio Si/Al>2 requires the silico-aluminate gels to be crystallized in a closed hydrothermal system at temperature to about 175°C. In some cases, higher temperatures to 300°C are used. The pressure is generally the auto-genus pressure approximately equivalent to the saturated vapour pressure (spa) of water at the temperature designated.

The time required for crystallization varies from a few hours to several days. Aging time at room temperature is 24 hours; crystallization time at 100°C from 50 to 100 hours (Breck, 1974). For the K_2O-Al_2O_3-SiO_2 system, crystallization temperatures have a range from 150°C to 230°C. Yet geopolymer binders generally do not implement these hydro-thermal conditions. One hardening mechanism among others, involves the chemical reaction of geopolymeric precursors such as alumina-silicate oxides (Al^{3+} in IV-fold coordination) with alkali poly-silicates yielding polymeric Si-O-Al bonds. This will occur at temperatures below 100°C and when the ratio of

SiO_2/Al_2O_3 is from 1.5 to 6.5 (Davidovits, 1991). Poly (sialates) has the empirical formula:

$$Mn \{-(SiO_2)\ z\text{-}AlO_2\}\ n,\ wH_2O \qquad (2\text{-}14)$$

Wherein M is a cation such as potassium, sodium or calcium, and «n» is a degree of poly-condensation; «z» is 1, 2, and 3. Poly (sialates) is chain and ring polymers with Si^{4+} and Al^{3+} in IV-fold coordination with oxygen (Davidovits, 1991).

2.3 Natural pozzolan and an overview of the activation of its reactivity

The term "pozzolan" comes from the US simplification of "pozzolana" which is derived from the location "Pozzuoli, Italy" and is used in UK and EU standards. Here the Romans found a reactive silica-based material of volcanic origin which they called "Pulvis puteolanus". Today, both the terms "pozzolan" and "pozzolana" are used (Shi et al., 2006).

Natural pozzolan is one of the oldest construction materials. According to ASTM C 618 (2003), a pozzolan is defined as a "siliceous or siliceous and aluminous material which in itself possesses little or no cementitious value but will, in finely divided form and in the presence of moisture, chemically reacts with calcium hydroxide at ordinary temperature to form compounds possessing cementitious properties". Lorenz (1985) estimated that about 5% of the solid surface of the earth is covered by volcanic rocks or effusive deposits (Shi et al., 2006).

These rocks can be classified according to their origin and essential active constituents as below (Massazza, 2003):

- Volcanic, incoherent, rich in unaltered or partially altered glass is produced from fusion. (A characteristic feature of these pozzolanas is the high alkali content which can exceed 10 percent. Loss on ignition (L.O.I) generally ranges between three percent and six percent but it can be higher in some altered materials).

- Volcanic glass which has been transformed, entirely or partially, into zeolite compounds including tuffs by the action of ground waters on volcanic glass under high temperature. Many factors such as the characteristics of the

volcanic glass ground water properties, temperature and pressure, affect the zeolitization process. (In these pozzolanas, the L.O.I. value is considered to be an index of the intensity of the transformation that the original volcanic material underwent owing).

- Sedimentary: rich in opaline diatoms usually formed from the precipitation of silica from solution or from the remains of organisms. (A high alumina percentage means that the main component of pozzolana, opal, is associated with clay minerals. The presence of clay creates some problems since it can reduce the workability, increase the water demand and lower the strength of mortar and concrete).

- Diagenetic: rich in amorphous silica, resulting from the weathering siliceous rocks. (In some countries, pozzolanic materials with very high silica content occur. This can be due to the transformation of the original minerals into silica gel by the action of hot springs. Silica prevails with proportions reaching 90 percent).

2.3.1 Pozzolanic activities of natural pozzolan

The pozzolanic activity includes two parameters, the maximal amount of lime that a pozzolana can combine with and the rate at which this occurs. These depend on the content of dissolved SiO_2 or Al_2O_3+SiO_2. Lime absorption, solubility of a pozzolan in saturated $Ca(OH)_2$, alkali, acid, or alkali and then acid solution or electrical conductivity change of a solution due to the dissolution of a pozzolan may be used for evaluation of pozzolanic reactivity of natural pozzolans (Shi et al., 2006). The performance of a hardened paste depends not only on the reaction rate and degree, but also on the nature of reaction products (Shi et al., 2006). Takemoto and Uchikawa (1980) also suggested that the quality of natural or artificial pozzolanic cement should be evaluated by strength tests. Many standards now use compressive or tensile strength of mortars to show the quality of pozzolans (Shi et al., 2006).

2.3.2 Main Factors affecting pozzolanic activity

The main factors affecting the pozzolanic reaction are (Massazza, 2003):

- Nature and composition of the active phases and their content in pozzolana.

- Specific surface
- The lime/pozzolana ratio of the mix
- The water/mix ratio
- The curing time and temperature

2.3.3 Methods of activating natural pozzolan

Lime-pozzolan cements have been used for several thousand of years and have an excellent reputation for their durability. Pozzolans are widely used as a cement replacement in Portland cement concrete because of their advantageous properties which include cost reduction, reduction in heat evolution, decreased permeability, alkali aggregate expansion control, increased chemical resistance, reduced concrete drying shrinkage, and the improvement of the properties of fresh concrete. Therefore using pozzolans for producing concrete has the advantages of lower costs and better durability; however, they also have a longer setting time and lower early strengths compared with pure Portland cement. Different techniques have been tried to increase the reactivity of natural pozzolans to overcome these disadvantages. The activation methods for increasing the reactivity of natural pozzolan can be classified into three categories: thermal, mechanical, and chemical activation. These are discussed below and a comparison based on the strength-cost relationship indicates that the chemical activation method is the most effective and the cheapest (Shi and Day, 1993, 2001).

2.3.3.1 Thermal activation methods

Thermal activation methods refer to those processes related to heat treatment, and can be classified into two categories: calcination of pozzolans and elevated temperature curing of pastes containing pozzolans. The thermal activation decreases the ultimate strength but is a useful method for high alumina percentage pozzolan associated with clay minerals (Shi, 2001, Massazza, 2003). The calcination of clay minerals changes their crystalline structures into amorphous structures and increases pozzolanic reactivity significantly. The most common example is metakaolin which results from the calcination of kaolinite. The optimum calcination temperature is in the range of 650-870°C, and higher temperatures than this result in decreased reactivity. Therefore the effect of calcination is a combination of two opposite effects

depending on the reactivity of the vitreous, zeolitic, and clay phases together with de-activation depending on the specific surface area and soluble fraction decrease and the crystalline increase (Shi, 2001). Generally calcination of a zeolite between 600 and 900°C can improve its pozzolanic reactivity since heating destroys the alumina and silica tetrahedral and makes the material more vulnerable to OH^- attack (Shi et al., 2006). Raising the temperature is more helpful to the reaction processes with higher reaction activation energies than to those with lower reaction activation energies. It has been found (Shi and Day 1993a) that the pozzolanic reaction between lime and natural pozzolan has much higher apparent reaction activation energy than that for the hydration of Portland cement. Thus, the hydration of lime-pozzolan mixtures is more susceptible to temperature than that of Portland cement. It is therefore essential for lime-pozzolan cement to be cured at elevated temperatures to obtain useful strengths within a reasonable period. Different pozzolans show different responses to temperature rise. Recently, the thermal activation of lime–pozzolan cements consisting of 80% natural pozzolan and 20% hydrated lime were studied in detail (Shi and Day 1993*a*, 2000*a*). It was found that the early strength of lime–pozzolan pastes is significantly increased as the curing temperature is elevated. Statistical analysis indicated that the strength development rate constant increased exponentially with curing temperature from 23 to 65°C, but the ultimate strength of these pastes decrease linearly with curing temperature (Shi and Day 1993a). Shi and Day (1993) have shown that when the curing temperature is 35°C the strength of lime-natural pozzolan pastes has the best development (in Shi, 2001).

2.3.3.2 Mechanical activation method

Prolonged grinding not only increases the surface area of a material, but also the number of active centres which exist at the edges, corners, projections, and places where the interatomic distances are abnormal or are embedded with foreign atoms. These centres are in a higher energy state than in the normal structure. The more active centres there are, the more reactive the pozzolan is (Gregg1961; Dave 1981). It has been found that impaction and friction milling of high alumina cement alters its crystallinity and notably modifies its hydraulic behaviour (Scian et al. 1991). In a study (Day and Shi 1994), it was found that the strength of lime–pozzolan pastes consisting of 80% natural pozzolan and 20% hydrated lime correlates linearly well

with the Blaine fineness of the natural pozzolan. Controversial results are also obtained from the prolonged grinding of different pozzolans (Heath and Brandenburg 1953). Some lime-pozzolan mixtures and Portland pozzolan cements give higher strength by the use of prolonged ground pozzolan, but some show an opposite trend. Different pozzolans have different quantities and nature of reactive components. It cannot be expected that a unique relationship exists between reactivity and surface area for all pozzolans. Some pozzolans are very porous and the N_2 (Nitrogen) adsorption method is usually used to measure the surface area of these pozzolans, although the reactants may not be able to enter the small pores inside the pozzolan that can be filled by N_2. Thus, the products formed in the open pores or channels that are inside pozzolans do not contribute to the strength of hardened pastes and it is not surprising that no significant correlation exists between the N_2 absorption surface area of a pozzolan and its lime absorption and the strength of its lime–pozzolan mixture. However the prolonged grinding of the natural pozzolan accelerates the pozzolanic reaction during the first 3 days. Costa and Massazza (1974) observed that the correlation between combined lime (pozzolanic activity) and surface area was valid only before seven days, and the activity of pozzolans depended on the reactive content (SiO_2+Al_2O_3). But Mortureux et al. (1980) found no correlation between the fixed $Ca(OH)_2$ and the surface areas for different pozzolans in another research (Shi et al., 2006).

2.3.3.3 Chemical activation method

Chemical activation is the most efficient and feasible method for the activation of natural pozzolan. The reactivity of an effective pozzolan can be greatly increased, particularly at early stages, by acid-treatment (Alexander 1955*b*). The degree of activation depends on the concentration of acid, and reaches a maximum in the region of 10N in the case of hydrochloric acid. No further activation was produced by raising the temperature of the concentrated acid or by increasing the duration of the treatment beyond the 10 min period used (Shi, 2001). The experimental results indicated that acid treatment processes were more effective than prolonged grinding or the addition of NaOH to mixing water. Acid treatment can only increase the pozzolanic reactivity of low-Ca pozzolan particularly at early ages while in high-Ca pozzolan, Ca is dissolved and its pozzolanic reactivity is reduced (Berry et al. 1988;

Hemmings et al. 1989). Note that the acid treatment is not practical because it is too expensive and the operation is too dangerous.

In all cases, pozzolans are activated with alkaline solutions containing alkaline hydroxides and alkali silicates. Alexander (1955*a*) found that the addition of NaOH increased the early strength of both lime-pozzolan and Portland-pozzolan cements, and the magnitude of the increase was greater for larger additions up to 2% based on the mass of lime-pozzolan blends. The long-term results confirmed that the addition of small quantities of NaOH to lime-pozzolan cements greatly increased the later-age strength. The beneficial effect was less with greater addition and became negligible at the 2% level. On the other hand, the addition of alkali to Portland cement results in a reduction of strength after 3 or 7 days, because the hydration chemistry and the morphology of the hydration products are changed due to the presence of alkali (Johansen 1976; Jawed and Skalny 1978, 1983).

Shi and Day (Shi and Day 1992*a*, 1992*b*; Day and Shi 1994) conducted extensive work on the chemical activation of pozzolans. The results indicated that the addition of Na_2SO_4 or $CaCl_2$ can increase the strength of lime-pozzolan pastes significantly. The addition of 4% Na_2SO_4 or1% $CaCl_2 \cdot 2H_2O$ based on the mass of lime-pozzolan blends significantly increases the early strength and the ultimate strength of lime-pozzolan mixtures by 50 to 90%. The presence of 4% $CaCl_2 \cdot 2H_2O$ is not helpful to the early strength of lime-pozzolan pastes, especially at low temperatures, but greatly improves the ultimate strength, by two or more times compared to the control pastes. $CaSO_4 \cdot 0.5H_2O$ improves the strength of lime-pozzolan cement at 28 days and thereafter. NaCl does not have an effect on the strength development of the hardened lime–pozzolan cement pastes up to 5% dosage levels and at age of 180 days. The further results confirmed that the above findings are not only applicable for natural pozzolans, but also for fly ash and blast furnace slag. The addition of 4% Na_2SO_4 significantly amplifies the early strength of the lime-natural pozzolan pastes. $CaCl_2$ pastes display lower strength than the control pastes during early ages, and surpass the control and Na_2SO_4 pastes at later ages. The later age strength of the hardened cement pastes with $CaCl_2$ is about 2.2 to 2.6 times higher than that of control pastes, while the strength of pastes with Na_2SO_4 is only about 1.5 to 1.7 times higher. The use of chemical activators changes hydration products and accelerates pozzolanic

reactions, which results in faster strength development rates and higher ultimate strength (Shi and Day 2000*b*; 2001).

2.4. Activators

The formation of zeolites and geopolymers require reactive precursor materials besides the concentrations of the reagents (especially of OH^-) (Palomo et al, 1992). High alkaline solutions are used to induce the silicon and aluminium ions in the source materials to dissolve and form the geopolymer paste (Davidovits, 1999). Several activators have been reported as suitable for activation of alumino-silicates. Theoretically, any alkali or alkali earth cation such as alkali hydroxide (MOH), non-silicate salts of weak acids (M_2CO_3, M_2SO_3, M_2S, M_3PO_4 and MF), non-silicate strong acid salts (M_2SO_4) and silicate salts ($M_2O.nSiO_2$) can be used as the alkali element (M). Of all these activators, NaOH, Na_2CO_3, $Na_2O.nSiO_2$ and Na_2SO_4 are the most widely available and economical chemicals. Some potassium compounds have also been used in laboratory studies. However, their potential applications will be very limited due to their lack of availability and high costs. It has been reported that soluble alkali silicates are the most effective activators for most alkali-activated cementing materials (Shi et al., 2006).

2.4.1 Type of activators

The type of activator may also play an important role. Although, the limited research regarding the activation of the natural alumina silicates has focused on the effect of sodium and/or potassium hydroxide combined (or not) with sodium silicate, it seems that KOH usually shows better reaction products than NaOH (Xu and Deventer, 2000, 2003). Minerals have a higher extent of dissolution with increasing concentrations of alkaline particularly in the NaOH than KOH solution; despite all the minerals demonstrating higher compressive strengths after geopolymerisation in the latter. The longer K^+ favours the formation of large silicate oligomers (polymer consisting of only a few monomer units) with which $Al(OH)^-_4$ prefers to bind. Therefore in KOH solutions, more geopolymer exist which results in better setting and stronger compressive strength of the geopolymer than in the case of NaOH activation (Xu and Deventer, 2000).

When compared to the use of alkali hydroxide only, the addition of soluble silicates makes the reaction occur at higher rates and also improves the final binder (Palomo, Grutzeck et al, 1999: Lee and Deventer, 2004; Fernandez-Jimenez and Palomo 2005).

2.4.2 Dosage of activators

The alkali activation dosage may be expressed in many different ways, such as activator molarities, oxides or activator weight percentage and oxides molar ratios. The optimum dosage differs according to the type of alumina-silicate used and the type of activation solution. Palomo et al (1999) suggested that an excess of OH^- concentration in the system can lead to a strength decrease of the alkali cement. It is possible to say that the molarities of KOH used ranges from 5M to 10M for the activation of natural minerals (Xu and Deventer, 2000). Increasing the activator concentration beyond a certain alkali content (depending on mineral, activator and curing conditions), may not result in further increase in strength, and detrimental effects such as efflorescence and brittleness resulting from the effects of high free alkali in the product have been reported (Xu and Deventer 2000).

2.4.3 Modulus of water glass solution

Addition of extra Na_2SiO_3 is essential because the more long-chain silicate oligomers there are; the more geopolymer precursor is formed (Xu and Deventer, 2000). The composition of alkali silicate solution can be expressed by two parameters: one is the modulus of solution which is the ratio of SiO_2/Na_2O, and the other is SiO_2 or M_2O content, or the sum of SiO_2+M_2O (Shi et al., 2006). Increasing the SiO_2/Na_2O ratio affects the degree to which, polymerization significant occurs (Xu and Deventer, 2000). Commercial liquid sodium silicates have a modulus of 1.6 to 3.85. Sodium silicate liquids outside of the range have limited stability and are not practical. The pH value is the most important characteristic determining stability of high-modulus silicate solution, that is, their inclination to the formation of gel or coagulation (Shi et al., 2006). As the formation of silica gel makes a significant contribution to strength in geopolymerisation, there is an obvious interaction between modulus and Na_2O. That is, if the Na_2O content is kept constant, the alkaline activation effect can be considered the same, the higher the modulus the more the contribution from silica gel

and the higher the strength within a certain range. However, if the sodium silicate solid content is kept constant, the higher the modulus the lower the Na_2O content and smaller the alkaline activation effect but the greater the amount of silica gel. These competing effects result in a variable optimum modulus depending on the raw material and curing condition. When alkaline activation is insufficient and thus becomes the main factor slowing down the activation of aluminosilicate, a lower modulus is preferred; otherwise a higher modulus is preferred (Wang et al, 1994). NaOH is added to a sodium silicate solution with a high modulus to produce a sodium silicate solution with a lower modulus. However, it can be expected that, for a given modulus and concentration, the attenuated silicate solution may have different species as compared with the one manufactured directly. Korneev and Brykov (2000) proposed a method to produce amorphous hydrated alkali silicate with modulus over 1. In this method organic solvents mixed with water are used to extract hydrated silicate after the ground silicate is dissolved in a dissolver. This method allows direct production of water-glasses of the optimal modulus and concentration (Shi et al., 2006). The dissolution of solid sodium silicate is an endothermic reaction and the dissolution rate and solubility of vitreous silicates decreases as the modulus increases. The dissolution of alkali silicate glass with a modulus greater than 2 is a very complicated incongruent process and is still not well understood (Shi et al., 2006).

2.5. Geopolymer concrete

In geopolymer concrete, the geopolymer paste serves to bind not only the coarse and fine aggregates but any un-reacted material. Geopolymer concrete can be utilized to manufacture pre-cast concrete, structural and non-structural elements, to make concrete pavements, immobilize toxic waste, and produce concrete products that are resistant to heat and aggressive environments (Hardjito et al, 2004).

2.5.1 Properties of fresh geopolymer concrete

The nature of the fresh geopolymer concrete is that of a stiff paste with high viscosity and low workability (Hardjito et al, 2004*a*, 2004*c*). Much literature reports on the workability of alkali activated slag binders which states that many factors such as the nature of slag and activators, dosage of activator(s), fineness of slag, chemical

admixtures, addition of lime, mineral admixtures and timing for the addition of activators have an effect on the rheological properties of alkali activated slag cement pastes (Al-Otaibi et al., 2001, Shi et al., 2006). During the activation of slag, Collins and Sanjayan (1999) and Qing-Hua and Sarkar (1994) found that the workability decreased as the content of alkali activator (Na_2O) was increased. Rapid loss of workability was also reported by Douglas et al. (1991) when the reaction happened in the presence of sodium silicate. In addition, the state and modulus of the silicate can also play an important role in workability. When the modulus is lower than 0.5, the workability is low and when the modulus is between 0.5 and 1.0 the workability is very high. Where the modulus of sodium silicate is greater than 1, the workability of the paste decreases markedly with the increase of the modulus of the silicate (Costa et al., 2007, Shi et al., 2006). The little information about the workability of activated alumina silicate explain that the water content in the mixture plays an important role with regard to workability of fresh geopolymer concrete. By keeping the molar H_2O-to-M_2O ratio of the mixture constant, the water content may be adjusted to produce the desired workability for a specified compressive strength of hardened concrete (Hardjito et al, 2004*a*, 2004*c*).

Although there are plenty of literature reports regarding the setting of activated slag binders, there is very little information about the setting of activated alumina silicate minerals. A geopolymer mix can be timed to set either fast or slow, by adjusting the mixture components. Depending on the synthesis conditions, structural integrity and reasonable strength were attained in a short time, sometimes in as little as sixty minutes (Van Jaarsveld et al., 1997). Using granulated blast furnace slag as the source material with the addition of metakaolinite, Cheng and Chiu (2003) found that the setting time of the geopolymer paste was affected by curing temperature, type of alkaline activator and the composition of source material. They stated that the setting time of above geopolymer paste was between 15 to 45 minutes at 60°C. The time available between the end of mixing and the start of casting of fresh geopolymer concrete may be more relevant in practical applications and measuring the setting time at elevated temperatures may not be appropriate. The laboratory experience by Hardjito et al. (2003*a*) showed that the fresh geopolymer concrete could be handled for at least 120 minutes after mixing, without any sign of setting and degradation in compressive strength. These results depended on the composition of the source

material, higher CaO contents giving faster setting. The presence of components other than Al_2O_3 and SiO_2 in the source material may also delay the setting. In materials of pure geological origin (say calcined kaolin), the dominant chemical contents are only Al_2O_3 and SiO_2, whereas by-product materials such as fly ash may contain other compounds e.g. Fe_2O_3. Therefore, it appears that pure geological materials may be more reactive with alkaline activators and induce a reduction in initial setting time (in Hardjito et al, 2004). Fly ash based geopolymers showed faster initial setting time at higher temperatures with the final setting of these mortars occurring 15 to 25 minutes after the initial setting (Costa et al., 2007).

2.5.2 Properties of hardened geopolymer concrete

There are many different views as to which are the main parameters that affect the compressive strength and other mechanical properties of geopolymer concrete. Palomo et al. (1999) stated that the significant factors affecting the compressive strength are the type of alkaline activator, the curing temperature and the curing time (in Hardjito et al, 2004*a*, 2004*c*). However, other researchers have reported that the important parameters for satisfactory polymerization are the relative amounts of Si, Al, K, Na, molar ratio of Si to Al present in solution, the ratio of alumina silicate mineral to kaolinite (when kaolinite is added), the type of alkaline activator, the water content, and the curing temperature (Xu and Deventer, 2000, Barbosa et al., 2000, Rowles et al., 2003). The presence of silicate ions in the alkaline solution substantially improves the mechanical strength and modulus of elasticity values but has a slightly adverse effect on the otherwise very strong matrix/aggregate and matrix/steel bond (Fernandez-Jimenez et al, 2006). Experimental results show that the H_2O/M_2O molar ratio in the mixture composition significantly affects the compressive strength of fly ash based geopolymer concrete, whereas the influence of the Na_2O/SiO_2 molar ratio is less significant (Hardjito et al, 2004*a*, 2004*c*). An increase of the H_2O/M_2O molar ratio and water to geopolymer solids ratio decreases the compressive strength of geopolymer (Hardjito et al, 2004*a*, 2004*c*). In addition, Van Jaarsveld et al. (2002) found that curing at elevated temperatures for long periods of time may weaken the structure of hardened material. The research on fly ash-based geopolymer binder, Palomo et al. (1999*b*) has confirmed that curing temperature and curing time significantly influence the compressive strength but this

does not seem to be same for different aluminosilicates. Longer curing time and higher curing temperature increased the compressive strength in fly ash based geopolymer concrete, although the increase in strength may not be as significant for curing at more than 60°C and for periods longer than 48 hours (in Hardjito et al, 2004*a*, 2004*c*). In most cases, 70% of the final compressive strength is developed in the first 4 hours of setting. Because the chemical reaction of the geopolymer paste is a fast polymerization process, the compressive strength does not vary greatly with the age of concrete, after it has been cured for 24h. This observation is in contrast to the well-known behaviour of OPC concrete, where the hydration process extends over a long time period and hence strength increases over time (in Hardjito et al, 2004*a*, 2004*c*). Another kinetic difference between Portland cement and alkaline activated systems is the existence of a relatively low threshold temperature in the former, above which thermal curing can have an adverse effect on the mechanical development and even on material durability. For an activated ash, on the contrary, a suitable choice of reaction time and curing temperature can yield a different reaction products without detracting from material durability, because according to Fernandez et al. (2006) increases in the curing temperature go hand-in-hand with decreases in the amount of Al incorporated into the final product and a concomitant improvement in mechanical properties. Such improvements parallel the formation of a homogeneous aluminaosilicate matrix (Fernandez-Jimenez et al., 2006).

Different pathways for preparation of a synthetic geopolymer, including the order of addition of the raw materials, show different evolutions of compressive strength of the materials. The best method is to prepare an alkaline solution (mixing MOH and water and stirring for 2 minutes), adding pozzolan to alkaline solution for 15 minutes in a mixer, followed by sodium silicate, and mixing for 15 minutes (Palomo et al, 1997).

2.5.2.1 Alkali activated slag

When alkali-activated slag cement concrete is cured in water, compressive strength of the concrete keeps increasing until 365 days. However, if the concrete is cured in a sealed condition, the strength stopped increasing at about 90 days. This may be attributed to the lack of moisture available for the hydration of slag inside the concrete. The concrete exposed to air exhibits the lowest strength all the time and

strength retrogression occurs at ages greater than 28 days. The strength reaches a maximum after 14 to 28 days of hydration, and then starts to decrease (Shi et al., 2006). For Portland cement concrete, the effect of inadequate water on strength is greater at higher water to cement ratio, lower strength development and in the presence of fly ash or slag (Neville, 1995).

2.5.2.2 Alkali activated fly ash

Although there are only a few reports regarding the flexural strength and elastic modulus of alkali activated fly ash (AAFA), it seems that both show inferior values to those of Portland cement. Puertas et al. (2003) reported that the flexural strength of alkali activated PFA mortars are 5.79 MPa while OPC based mortars are 7.76 MPa. They also showed that the elastic modulus of OPC mortars was 5679 MPa, also higher than the values for PFA mortars activated with 8M NaOH(4441 MPa).

Fernandez-Jimenez et al. (2006) found that the addition of soluble silicates in the alkaline solution improved the modulus of elasticity in PFA-based geopolymer concrete. However, this improvement was not sufficient and the alkali activated PFA concrete showed a much lower static modulus of elasticity than expected. The values presented for OPC concrete ranged from 30.3 to 32.3GPa while for geopolymer concrete they ranged from 10.7 (without silicate) to 18.4 GPa (with silicate). Hardjito et al. (2004) observed better elastic modulus results for a concrete samples made in similar conditions: 22.95 to 30.84 GPa.

Apart from their short setting times compared to conventional concrete, geopolymers also attain higher unconfined compressive strengths and shrink much less on setting than OPC (for 7 days only 0.2% that of OPC while for 28 days it is 0.5% of OPC). (Van Jaarsveld et al., 1997). One explanation for this behaviour may be found in the microstructural characteristic of the new binder which in alkali activation of fly ash can form a zeolite-type phase. Zeolite properties and microstructure are widely known to be unaffected by the loss of the water incorporated during their synthesis because not only water loss is reversible in most zeolites but also they are able to absorb water from the humidity in atmosphere (Fernandez-Jimenez et al, 2006). The drying shrinkage strains are extremely small indeed and the ratio of creep strain-to-elastic strain (that is, creep factor) reached a value of 0.30 in approximately 6 weeks

after loading on the 7th day with a sustained stress of 40% of the compressive strength. Beyond this time the creep factor increased only marginally (Hardjito et al, 2004). For normal condition the value of 1.6 is suggested in BS 5400-4:1990 for creep factor of OPC concrete, although it depends on environmental conditions, maturity of the concrete at the age of loading and composition of it. Kaewmanee and Okamura (2001) reached to a value of 1.35 in their works on OPC self compacted concrete loading on the 7th day with a sustained stress of 40% of the compressive strength while Tarek and Sanjayan (2008) have shown that the rate of creep factor evolution with time for slag mixes is lower than of OPC mix which is 1.49 at the time of cracking.

2.5.3 Durability properties of geopolymer concrete

Glukhovsky (1957) hypothesized that the superior durability of ancient plain (un-reinforced) concretes resulted from the coexistence of cements containing calcium silicate hydrate (C-S-H) with some form of alkaline alumina-silicate hydrates. The latter are essentially impure forms of current day geopolymers. It can be seen that the alkali-activated slag cement paste exhibits not only a lower porosity but also a finer pore structure than Portland cement paste (Shi et al., 2006). Therefore, low permeability (10^{-9} cm/s) is another property that favours the use of these materials for the immobilization for toxic metals (Devidovits, 2002). Acidic corrosion of hydrated cement based materials has attained more importance in the recent decade due to fears over the deteriorating effects of acidic media (e.g. acidic rains, acidic ground-waters, etc) on Portland cement-based materials. At the same time, development of geopolymer cements (a new class of alkali activated material) with better chemical resistance necessitates more detailed investigation. Chemically activated alumina-silicate tested for durability properties and resistance of concrete to chemical attack by mineral acids such as sulphuric, nitric, hydrochloric, and organic acids was claimed to be far better than that of Portland cement concrete (Allahverdi and Skvara, 2001). To evaluate the resistance of geopolymer concrete to sulphate attack, it was shown by that after 12 weeks of exposure for specimens soaked in a 5% sodium sulphate (Na_2SO_4) solution, there were no significant changes in the compressive strength, mass, and the length of test specimens. Davidovits (1999) reported that geopolymer materials do not generate any dangerous alkali-aggregate

reaction, even in the presence of high alkali content. In addition, Paolomo et al. (1999) reported that metakaolin-based geopolymer mortars remained stable and showed negligible deterioration in microstructure and strength after being soaked in ASTM sea water, sodium sulphate solution (4.4% by mass), and sulphuric acid solution (0.001 M) for 9 months (Hardjito et al, 2004). These materials also have good resistance to freeze-thaw cycles as well as a tendency to drastically decrease the mobility of most heavy metal ions contained within the geopolymeric structure (Van Jaarsveld et al., 1997).

2.6 Summary

The following conclusions can be summarised from the literature:

1. It is clear from the literatures that certain composition criteria have to be met for geopolymerization to occur. These include: (a) The molar ratio SiO_2:M_2O in the aqueous soluble silicate solution must be between 3.0:1 and 6.6:1 where M is an alkali metal cation, (b) The alumino-silicate oxide must contain Al which is readily soluble and (c) The overall molar ratio Al_2O_3:SiO_2 of the finished product must be between 1: 3.3 and 1:6.5.

2. Previous work show that in the nature of the starting materials (Al-Si minerals) factors such as increasing the %CaO, increasing the molar Si-Al ratio, or the extent of dissolution of Si and the molar Si/Al ratio in solution and the hardness of the mineral have positive effects on the final compressive strength of geopolymer cement while $\%K_2O$ in the original mineral shows a negative correlation. Of all the factors mentioned above, $\%K_2O$ in the mineral and ppm Si in solution are identified as having a significant effect on strength.

3. The subsequent geopolymeric products are found to be amorphous to semi-crystalline materials. Thus the amorphous nature of geopolymers makes structural investigations by X-ray powder diffraction inconclusive.

4. Solubility of a pozzolan in an alkali may be used for evaluation of pozzolanic reactivity of natural pozzolans. Many standards now use compressive

strength of mortars made with specified cement pozzolan to show the quality of pozzolans.

5. Calcination is a useful method for preparing an active pozzolan in samples with a high alumina percentage associated with clay minerals. Generally calcination of a zeolite between 600 and 900°C can improve its pozzolanic reactivity. Thus it seems the pozzolanic reactivity can be improved by calcination before reacting them with alkali to produce geopolymer cement.

6. It was shown in the literature that for lime-natural pozzolan pastes, the strength development rate increased exponentially with curing temperature from 23 to 65°C but the ultimate strength of these pastes decrease linearly with curing temperature and when the curing temperature is 35°C the strength has the best development. These curing temperatures were taken in consideration with the present investigation and improvement in pozzolanic properties due to elevated curing temperature was studied.

7. The best alkali activator is potassium hydroxide (KOH) used with sodium silicate (Na_2SiO_3). The potassium hydroxide favours the formation of large silicate oligomers (polymer consisting of only a few monomer units) with which $Al(OH)^-_4$ prefers to bind and adding the sodium silicate is essential because the more long-chain silicate oligomers there are; the more geopolymer precursor forms.

8. The literature shows that if the sodium silicate solid content is kept constant, the higher the modulus, the lower the Na_2O content and smaller the alkaline activation effect but the greater the amount of silica gel. These competing effects result in a variable optimum modulus depending on the raw material.

9. The reviewed literature introduces geopolymer concrete as a stiff one with high viscosity and low workability generally. The workability of geopolymer concrete is said to depend on the modulus of sodium silicate and decreases markedly with an increase in the modulus of the sodium silicate.

10. Alkali-activated cement concrete needs sufficient moisture available for reaction and it is really important to affect positively on strength. Other

significant factors affecting the compressive strength are the relative amounts of Si, Al, K, and Na, the molar ratio of Si to Al in solution, the type of alkaline activator, the curing temperature and the curing time.

11. The reviewed literature indicates that in general, good strength and durability can be achieved with concrete produced from alkali activated cements and geopolymers based on alkali activated fly ash in comparison with OPC concretes. In the present work an attempt to achieve these properties for geopolymer based on alkali activated natural pozzolan was followed.

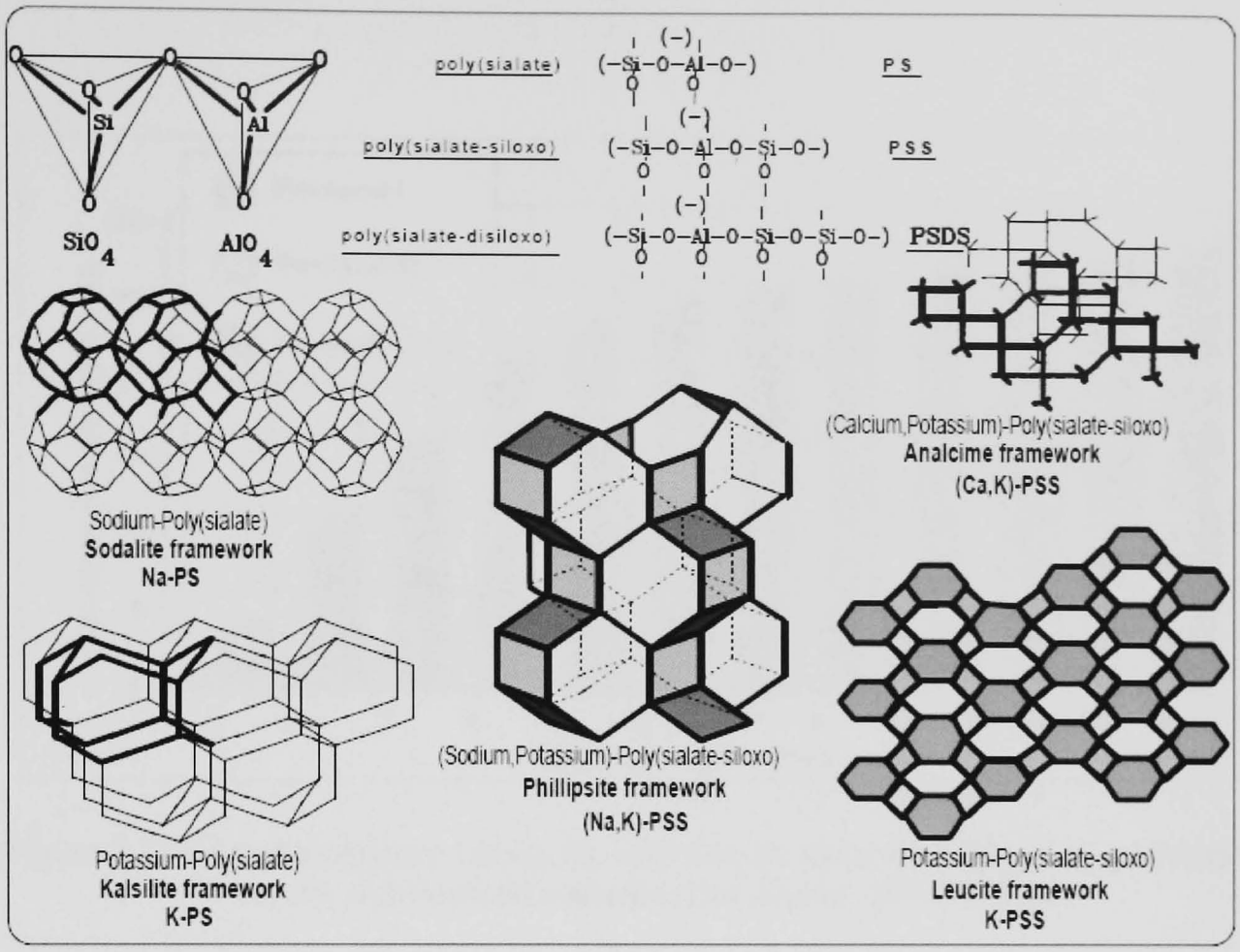

Figure 2.1a Computer molecular graphics of polymeric Mn-(-Si-O-Al-O-)n poly(sialate) and Mn-(-Si-O-Al-O-Si-O-)n poly(sialate-siloxo) and related frameworks (Devidovits, 1991, 1994)

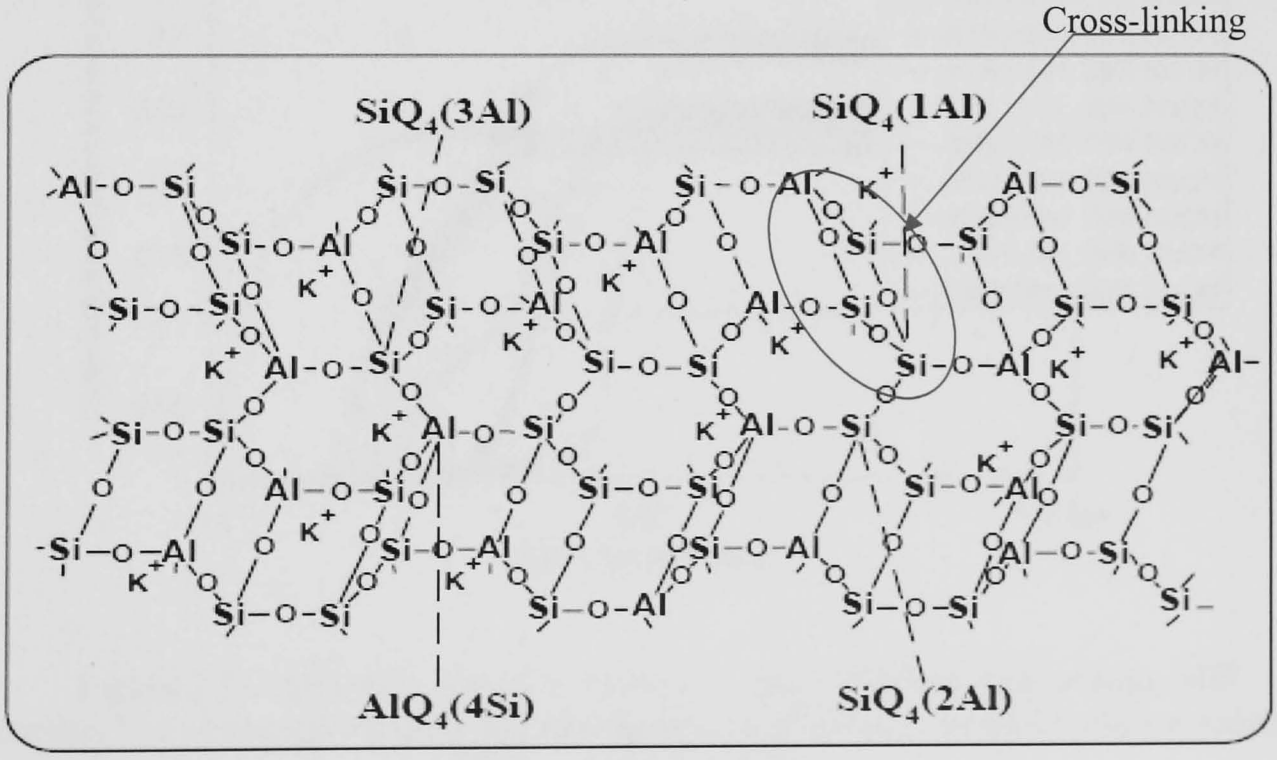

Figure 2.1b Proposed structural model for K-poly(sialate-siloxo) geopolymer (Devidovits, 1991, 1994 and Barbosa, 2000)

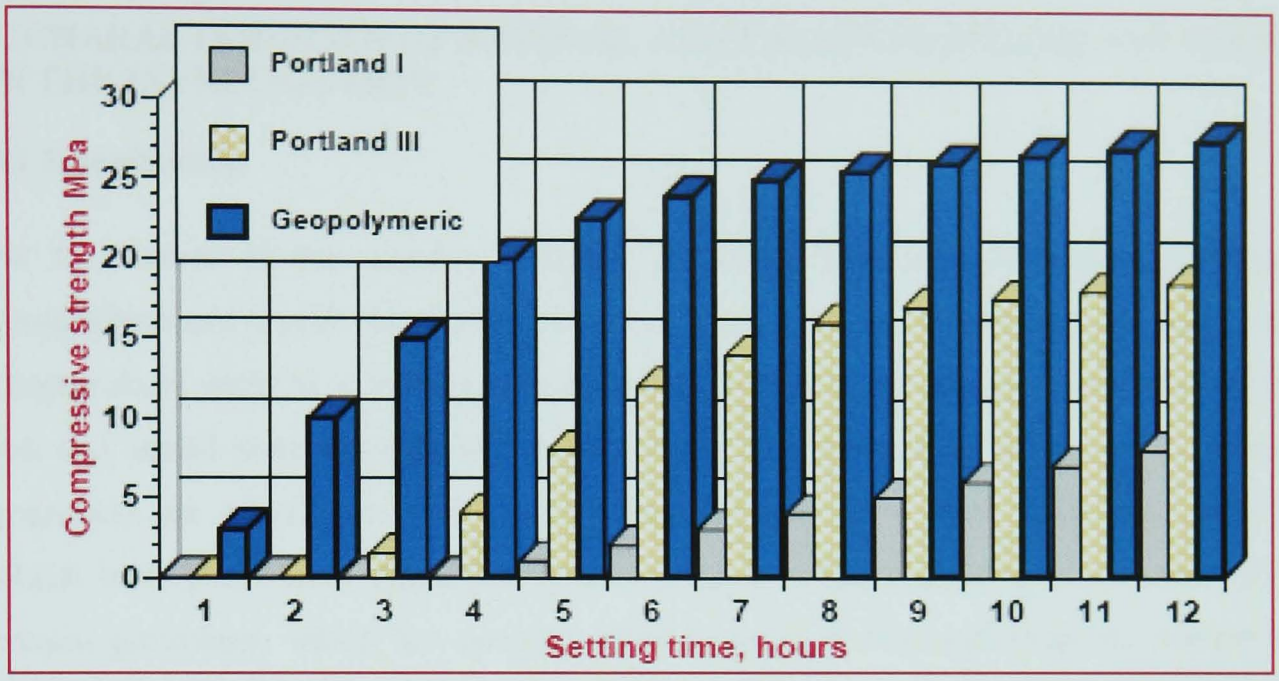

Figure 2.2 Room temperature setting for concrete for concrete made of geopolymeric cement and Portland cements (Devidovits, 1991, 1994)

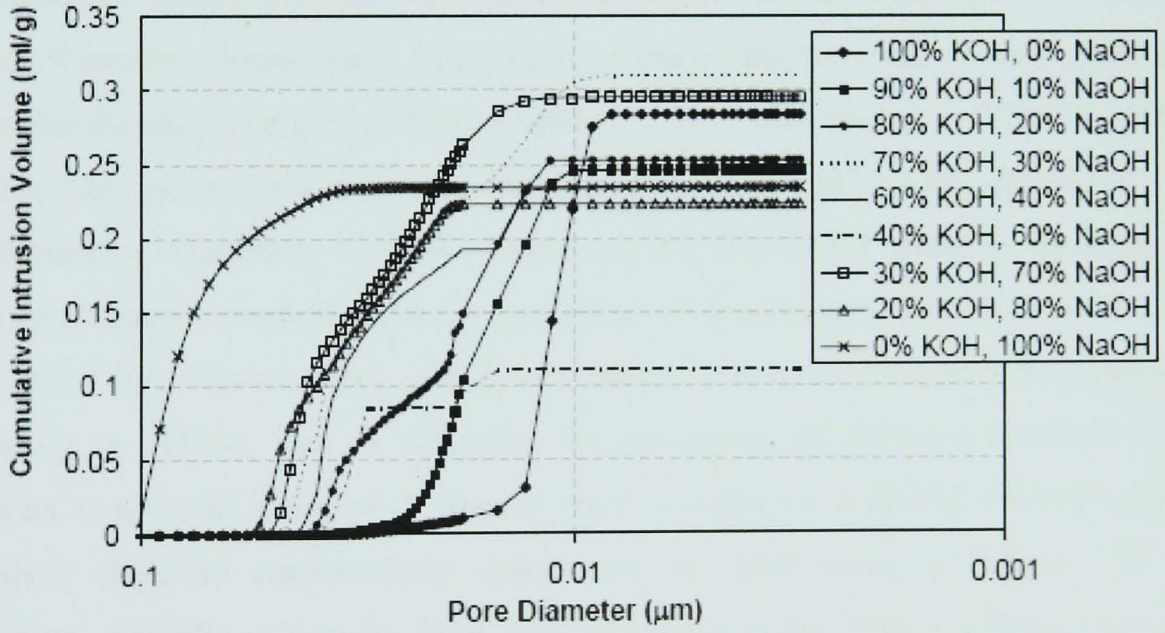

Figure 2.3 Cumulative intrusion volume vs. pore diameter plotted from MIP results. The characteristic pore size decreased as the molar % of KOH was increased (Bell and Kriven, 2004).

3. CHARACTERISTICS OF NATURAL AND CALCINED POZZOLANS USED IN THE INVESTIGATION

3.1 Introduction

As the nature of the starting materials including mineral composition, chemical composition and crystal structure affects the formation of the geopolymer gel phase; this chapter deals with the mineralogy, chemical composition and physical properties of the raw and heated materials used in the present research. Several different types of natural pozzolans are quarried in Iran. The volcanic ashes studied were dacite and andesite, which have pozzolanic properties in their natural state or after heat treatment. Five natural pozzolans, which are currently used to produce Portland pozzolan cement by Iranian Cement Factories, have been considered in this work. These are Shahindej and Sahand dacite from the North West, Sirjan and Rafsanjan dacites, and Taftan andesite from the South East of Iran. All were prepared with a particle size of 100% less than 75μm, and used to produce Portland pozzolan cement by Ourmia, Ardebil, Kerman (use two sources of pozzolanic materials including Sirjan and Rafsanjan dacites) and Khash Cement Factories, respectively. Since most of these raw materials contain zeolites and clay minerals and have a high loss on ignition, they were heated at 700 and 800°C to improve their pozzolanic properties. X-ray differaction (XRD) was carried out in the Department of Materials, Sheffield University by the author using a Siemens D500 machine to study the mineralogical composition of these natural pozzolans. Quantitative XRD and X-Ray Fluorescence (XRF) were carried out in the Kansaran Binaloud X-ray laboratory in Tehran, Iran to determine the percentage of different minerals in each pozzolan as detected from XRD. Spectra were recorded on a Philips PW1800 machine and their chemical compositions determined by XRF using a Philips PW 1480 instrument. Samples in powder form were examined in the Philips diffractometer with nickel-filtrated CuKα radiation generated at 40 KV and 30 mA. The mineralogy, chemical composition and physical properties of these five pozzolans in their natural state and after calcining were compared in this chapter to determine their pozzolanic reactivity.

3.2 Shahindej Dacite

The Urumiyeh-Bazman volcanic belt runs parallel to the Sanandaj-Sirjan zone on the NE side of Iran, and owes its existence to widespread and intensive volcanic activity which developed on the Iranian plate from the upper Cretaceous to Recent times. The Urumiyeh-Bazman volcanic belt is believed to have resulted from the collision of the Arabian and central Iranian continental plate margins. Urumiyeh Dokhtar Magmatic Arc is a part of this belt composed mainly of tholeitic, calc-alkaline and K-rich alkaline intrusive and extrusive rocks and associated volcanics. It is represented by sub-alkaline volcanics that vary in composition from basaltic through andesitic to dacite and rhyolitic. The material from this site used by the Ourmia Cement Factory in kiln is composed mainly of vitric tuff of acidic composition about rhyodacite, which has pozzolanic application due to its high amount of acidic vitroclastic glass shards and low fraction of fine crystalline particles. These properties were studied by the Iranian Cement Guild (Ezatian, 2004) through light microscopic investigation on solid samples.

3.2.1 Mineralogical Composition

The quantitative XRD patterns of the Shahindej pozzolan in Table 3.1-a show it to be a mixture of minerals with different percentages, while the mineralogical composition is presented on Figure 3.2-a. It has high percentages of zeolites minerals (clinoptilolite), and its pozzolanic properties can be changed by heat treatment and also elevated temperature curing (Figure 3.3-a). In order to study the effect of thermal treatment on the properties of Shahindej pozzolan, it was heated at 700°C and 800°C where the results of the variation of mineralogical composition are presented on Table 3.1-b and Figure 3.3-a. Comparing the quantitative XRD results indicates that when this material is calcined at 700°C and 800°C clinoptilolite percentage had decreased and that this mineral had converted to mordenite and opal with properties shown briefly in Table 3.2. respectively. The comparison of XRD patterns of natural Shahindej dacite heated at various temperatures on Figure 3.3-a, shows quartz increasing for Shahindej when treated at 700°C and this mostly composed of quartz which does not react in normal condition with activators. Continued increase the calcination temperature shows that the crystalline phase related to clinoptilolite and the peaks related to calcite have decreased

in Shahindej treated at 800°C thus these minerals appeared as a minor phase only. This fact and changing of clinoptilolite to opal which reacts intensively with alkaline solution (Table 3.2) makes Shahindej treated at 800°C more reactive. Therefore the untreated Shahindej and the one treated at 800°C seem to be the states of Shahindej pozzolan which have the potential of activation while the latter might have better reactivity (Figure 3.3-a, Table 3.1-a, Table 3.1-b).

3.2.2 Chemical Composition

The chemical composition of untreated Shahindej pozzolan was analysed by XRF and presented on Table 3.3-a. In X-Ray Fluoresence analysis, the quantitative data is only collected on the atoms of elements present. Most ceramic and rock materials can be approximated to oxygen lattices with cations added for charge balance. Within a fused bead environment all cations present will indeed be present as fully oxidised species. As a result when calibrations are prepared, the major components in these systems as oxide weight percent are calculated. As a rule of thumb in these systems the sum of the major component oxides should come to a value close to 100%. The proportion of a particular element be required can easily be calculated considering the atomic weights of the element and oxygen plus the molecular weight of the oxide.

Considering the diagram of total alkalis versus SiO_2 (TAS; Le Bas et al., 1986), Shahindej dacite is an acidic tuff with respect to its chemical composition. Untreated Shahindej pozzolan contains SiO_2 and Al_2O_3 with the SiO_2 content equal to 70.13 wt. % and Al_2O_3 content equal to 11.11 wt. %. It has a high amount of L.O.I. equal to 10.28 wt. % and higher content of K_2O relative to Na_2O. These features were found to give a negative affect on geopolymeric paste strength (Xu and Deventer, 2000). However, the high percentage of silica and alumina (SiO_2+Al_2O_3), which is equal to 81.24 wt. %, were found to overcome the above negative effect. CaO content in this pozzolan resulted equal to 2.52 wt. %. Whereas in the previous section comparing the XRD results shows that the intensity peaks for Shahindej untreated and treated at 800°C seem to prepare the potential of activation for Shahindej pozzolan, the chemical composition of Shahindej pozzolan treated at 800°C was analysed by XRF as well and presented on Table 3.3-b.

For calcined Shahindej pozzolan at 800°C, the loss on ignition decreases to 5.78 wt. % and the amount of SiO_2 increases to 73.44 wt. % which causes the amount of silica and alumina (SiO_2+Al_2O_3) to increase to 85.32 wt. %. Other component has not changed significantly.

3.2.3 Physical Composition

In order to measuring the specific gravity of pozzolan it is weighed first in air, then while immersed in kerosene; the difference in the two weights divided by the specific weight of kerosene, according to Archimedes' principle , is the weight of the kerosene displaced by the volume of it. The specific gravity of the pozzolan is the ratio of its weight in air to the difference between its weight in air and its weight immersed in kerosene (ASTM D-854, ASTM D5550). The Shahidej pozzolan was passed through a 4.75mm (No.4) sieve before testing and the specific gravity of it, as supplied by the manufacturer, was measured using a pycnometer according to the mentioned method. The measurement was reported to be equal to 2.2.

Specific surface of Shahindej pozzolan was measured, by the manufacturer, using the Blaine air permeability method. This method tends to measure only the external surfaces of particles (Ramezanianpour and Cabrera, 1987). The principle of this test is based on the relation between the flow of air through the pozzolan bed and the surface area of the particles comprising that. The pozzolan bed in the permeability cell is 1cm thick and 2.5cm in diameter. Knowing the density of pozzolan the weight required to make a pozzolan bed of porosity of 0.475 can be calculated and placed in the permeability cell in a standard manner. Air was passed slowly through the pozzolan bed at a constant pressure difference and the rate of air flow until the flow meter shows a difference in the range of 30-50cm in the outlet tube is measured. The specific surface (S_w) is then determined from relationship between the differential pressure and flow rate in steady flow conditions.

The pozzolan was ground for 4 hours and passed through a 75μm sieve before testing. The specific surface of Shahindej pozzolan was found equal to 10621cm^2/g (resulted the

same as whatever was measured and reported in Evaluation of Pozzolans of Iran by Ramezanianpour and Ghazi Moradi, 1992).

Sodic plagioclase and oligoclase crystalline particles with 25 to 75 micron sizes and crushed quartz particles from 10 to 25 micron sizes are observed and reported in the sample of Shahindej pozzolan by Iranian Cement Guild (Ezatian, 2004).

3.3 Sahand Dacite

Mount Sahand which is located in the south eastern part of Tabriz is 3600m high. Its vast cone is made of tuff and ash. Existence of high volume of ash and pumice pieces far away from Sahand indicates a vigorous explosion of this mountain occurred (Darvishzadeh, 1983).The composition of Sahand lava are rhyolite, dacite, and andesite. The activity of this volcano started from early Quaternary, and today it is in a relatively calm period. The materials from this volcano are used by Ardebil Cement Factory in kiln which is near Mameghaneh Azarshahr. These materials were studied by Iranian Cement Guild (Ezatian, 2004) using light microscopy on solid samples and reported to be composed mainly of trachydacite including mostly albite.

3.3.1 Mineralogical Composition

The mineral compositions of the Sahand pozzolan were identified by XRD and are presented in Figure 3.2-c, while the quantitative XRD patterns of the Sahand dacite used in this work are shown in Table 3.1-a. The Sahand dacite has the lowest pozzolanic activity due to a lack of amorphous material in its make-up. In fact it is mainly composed albite which composes 75% of its mass. However, its reactivity can be improved by heat treatment up to 800°C. The results of the variation of mineralogical composition percentage for calcined samples are presented in Table 3.1-b, while the XRD diffractograms of the untreated and calcined samples at different temperatures are presented in Figure 3.3-a. It appears that it is hornblende that becomes disordered at 800°C as its peaks disappear and Sahand pozzolan calcined at 800°C might have the potential for activation.

3.3.2 Chemical Composition

The chemical composition of Sahand dacite was analysed by XRF and the results are presented on Table 3.3-a. The main constituents in untreated Sahand pozzolan are SiO_2 and Al_2O_3 with SiO_2 content equal to 64.67 wt. % and Al_2O_3 content equal to 11.85 wt. % and the sum of silica and alumina at 76.52 wt. %, which satisfies the requirements of ASTM C-311/ASTM C-618 for natural pozzolans. Other constituents are Fe_2O_3, CaO, MgO, K_2O and Na_2O. In Sahand dacite the amount of K_2O is equal to 4.26 wt. % and more than 2.3 wt. % was detected for Na_2O. The CaO content, which according to Xu and Deventer (2000) is positively correlated to the compressive strength, is equal to 6.79 wt. %. The loss on ignition is 5.15 wt. %. Whereas in the previous section comparing the XRD results shows that the reactivity of Sahand can be improved by heating it up to 800°C, the chemical composition determined by XRF analysis of Sahand pozzolan heated to 800°C is presented in Table 3.3-b. For calcined Sahand pozzolan at 800°C, the loss on ignition decreases to 2.90 wt. % and the amount of SiO_2 and Al_2O_3 increases to 67.4 and 11.87 wt. % respectively, which causes the amount of silica and alumina (SiO_2+Al_2O_3) to increase to 79.27 wt. %. The amount of K_2O decreases to 3.41 wt. % and Na2O is detected at 1.9 wt. %. Other components did not change significantly.

3.3.3 Physical Composition

The specific gravity of Sahand pozzolan used in this work was measured using a pycnometer according to ASTM D-854/ASTM D5550 method and reported by Ardebil Cement Factory to be equal to 2.7.

Specific surface of Sahand pozzolan was measured, by the manufacturer, using the Blaine air permeability method. The specific surface of Sahand pozzolan was found to be equal to 6331 cm^2/g (resulted the same as whatever was measured and reported in Evaluation of Pozzolans of Iran by Ramezanianpour and Ghazi Moradi, 1992).

3.4 Sirjan Dacite

The Sanandaj-Sirjan zone was first recognized as a separated linear structural element by Sticklin (1968). The zone lies between the main Zagros thrust in the SW and the

Urumiyeh-Bazman volcanic belt in the NE. It joins to the Taurus Orogenic belt in Turkey. Part of the zone is characterized by Palaeozoic volcanism and Hercynian metamorphism. This source is used by Kerman Cement Factory in kiln and is composed mainly of glassy pumicite brecciate tuff, with the composition of dacite igneous rock.

3.4.1 Mineralogical Composition

XRD shows the mineralogical composition of Sirjan Dacite (Figure 3.2-d); while the mineralogical percentages are presented in Table 3.1-a. Sirjan pozzolan has a vitroclastic texture with comminute crystalline plagioclase including more than 40% albite. Therewith more than 5% of this pozzolan is composed of brown biotite and the rest is composed of glassy pumicite particles which sit on a brown glassy texture including hematite. The percentage of glass shards is about 30%, which is determined by subtracting the sum of the crystalline phase percentages from the sum of the major phases should come to a value close to 100%.

It can be seen that the reactivity of Sirjan dacite cannot be improved by heat treatment as the intensity of peaks for the material calcined at 700°C has changed only a little, which is due to the conversion to muscovite of 5% biotite and 10% montmorillonite in the main phases of Sirjan dacite (Table 3.1-b and Figure 3.3-b).

3.4.2 Chemical Composition

The chemical composition of Sirjan pozzolan determined by analysis XRF is presented in Table 3.3. The main constituents are SiO_2 and Al_2O_3 with SiO_2 content equal to 68.51 wt. %, Al_2O_3 content equal to 11.84 wt. % and the sum of silica and alumina equal to 80.35%. This satisfies the requirements of ASTM C 311/ASTM C 618 for natural pozzolan. Other constituents are Fe_2O_3, CaO, MgO, K_2O and Na_2O. In Sirjan dacite the amount of K_2O is equal to 3.19% and more than 1.62% is detected for Na_2O. The loss on ignition was resulted equal to 6.14%. In the previous section comparing the XRD results shows that the intensity peaks for Sirjan were improved slightly by heating it up to 700°C, thus the chemical composition of Sirjan pozzolan treated at 700°C was analysed by XRF as well and presented in Table 3.3-b. For calcined Sirjan pozzolan at 700°C, the

loss on ignition decreased to 2.2 wt. % and the amount of SiO_2 detected was equal to 68.36 wt. %. The percentage of Al_2O_3 increased to 13.40 wt. %, which caused the amount of silica and alumina (SiO_2+Al_2O_3) to increase to 81.76 wt. %. The amount of K_2O decreases to 2.66 wt. % and Na_2O increased to 2.78 wt. %. Other components including Fe_2O_3, CaO, MgO were 4.41, 3.90, and 1.2%, respectively.

3.4.3 Physical Composition

The specific gravity of Sirjan pozzolan was measured, by the manufacturer, using a pycnometer according to ASTM D-854/ASTM D5550 method and reported to be 2.28.

Specific surface of Sirjan pozzolan was measured using the Blaine air permeability method in the Kerman cement factory. The specific surface of Sirjan pozzolan was resulted equal to 6348 cm^2/gr (the same as whatever was measured by BHRC, Tehran, Iran and reported by Maghsoudi, 2001).

3.5 Rafsanjan Dacite

Godarkhoon Sorkh is located 40 to 50 km to the south part of Kerman and east of the Kaleh Gavi Mountains. This is a vast part of Urumiyeh volcanic belt which stretches more than 1000 km from northwest to southeast of Iran. In the upper part of the Pliocene deposits in this zone, there is a thick layer of light grey brecciate tuffs which adjacent to the river, include 0.5-3 cm of white pumice and red and grey glassy magma particles. These brecciate tuffs show are the result of acidic exploding volcanic activity in a dry environment. They lie in a NW alignment and form a hill 40 to 50 m high adjacent to the contiguous plain. A 2 to 3 m thick layer of grey dacite which includes biotite and feldspar in a glassy texture extends over this layer, which has resulted from the explosive eruption of lava. Towards the east, pumiced brecciate tuffs and an overlying dacite lava are in turn succeeded by loose Quaternary conglomerate. The lower part include the outcrop of a 400m long, 150m wide by 40-50m thick forms a strip of brecciate tuffs which dips a 10 to 15 degree slope towards the east (Maghsoudi, 2001). The brecciate tuff which is composed mainly of glassy brecciate vitric material with composition near to about that of dacite, presently used to produce Portland pozzolan

cement by the Kerman Cement Factory in kiln. Rafsanjan pozzolan has a vitroclastic texture including euhedral crystalline of sodic plagioclase.

3.5.1 Mineralogical Composition

The mineral composition of the Rafsanjan pozzolan was identified by qualitative XRD (Figure 3.2-e), where the composition is given in Table 3.1-a. Rafsanjan dacite is an acidic tuff and its pattern indicates albite, montmorillonite, hornblend, biotite, calcite, quartz and amorphous minerals. It contains 25% of the clay mineral montmorillonite and as shown in Figure 3.3b heat treatment increases its pozzolanic reactivity as the clay present is dehydroxylated. It has been pointed out that the optimal calcination temperature for destruction of Na-montmorillonite is 800°C (Murat and Driouche, 1988). The effect of calcination on the reactivity of the pozzolan depends on the combination of the two reverse effects including activation depending on the reactivity of clay phase and deactivation depending on the decrease of soluble fraction and increase of crystalline fraction. Therefore, calcinations of Rafsanjan sample at 700°C activated montmorillonite, which makes up 25% of mineralogical components, but also decreased the amorphous phases from 25% to 10%. Continued to increases in the calcination temperature shows that at 800°C Rafsanjan dacite has a slight potential of activation (Figure 3.3-b, Table 3.1-a, Table 3.1-b).

3.5.2 Chemical Composition

The chemical composition of Rafsanjan pozzolan was analysed by XRF and the results are shown in Table 3.3-a. The major inorganic oxides which are SiO_2 and Al_2O_3 are equal to 68.31 wt. % and 12.59 wt. %, respectively. The sum of these major inorganic oxides is equal to 80.9% and satisfies the ASTM C 311/ASTM C 618 requirements for natural pozzolan to have a good pozzolanic activity. In Rafsanjan dacite the amount of K_2O is equal to 3.26% and more than 2.4% is detected for Na_2O. The Rafsanjan dacite has loss on ignition equal to 4.41 percent as presented in Table 3.3-a. Since according to the previous section the optimal calcination temperature for calcining Rafsanjan pozzolan seems to be 800°C, thus the chemical composition of Rafsanjan pozzolan treated at 800°C was analysed by XRF as well and presented in Table 3.3-b. For

calcined Rafsanjan pozzolan at 800°C, the loss on ignition decreased to 2.48 wt. % and the amount of SiO_2 increase to 71.53 wt. %. The percentage of Al_2O_3 is detected equals 12.46 wt. %, which causes the amount of silica and alumina (SiO_2+Al_2O_3) to increase to 83.99 wt. %. The amount of K_2O and Na_2O is detected equal to 2.53 wt. % and 1.87 wt. % respectively. Other components have not changed significantly.

3.5.3 Physical Composition

The specific gravity of Rafsanjan pozzolan used in this work determined by the pycnometer according to the ASTM D-854/ASTM D5550 method, was measured and reported by Kerman Cement Factory to be equal to 2.08.

Specific surface of Rafsanjan pozzolan was measured, by the manufacturer, using the Blaine air permeability method. The specific surface of Rafsanjan pozzolan resulted was equal to 4870 cm^2/gr (the same as whatever was measured by BHRC, Tehran, Iran and reported by Maghsoudi, 2001).

3.6 Taftan Andesite

Mount Taftan is a semi-active 4050m high starto-type volcano. It is the highest peak in Baluchestan and is located near Khash City. Taftan lavas are andesitic. Various sulphuric springs surround this mountain and gas emissions from its highest peak provide evidence of an active volcano. It has been reported that molten material came out from Taftan in 1970 and 1971 (Darvishzadeh, 1983). The materials used from this area by Khash Cement Factory in kiln and mill are composed mainly of vitric tuff of acidic composition about andesitic, which has pozzolanic application due to its high amount of acidic vitroclastic glass shard and low dissection and fine crystalline particles. These properties were obtained by Iranian Cement Guild (Ezatian, 2004) through light microscopic investigation on solid samples.

3.6.1 Mineralogical Composition

The qualitative XRD is shown in Table 3.1-a, while the mineralogical composition is presented in Figure 3.2-f. Optical microscopy by Iranian Cement Guild (Ezatian, 2004),

revealed feldspar (sodic plagioclase), amphibole, quartz, and biotite. The background was glassy which due to oxidation was converted in to clayey minerals although this section is prepared from powder samples and not quite clear. In fact pumice and glassy particles are sometimes seen in samples.

3.6.2 Chemical Composition

The chemical composition of Taftan pozzolan was analysed by XRF and is presented on Table 3.3-a. It has the lowest amount of L.O.I. equal to 1.85% amongst the five natural pozzolans selected in this study and higher content of Na_2O relative to K_2O which has a positive affect on geopolymeric paste strength (Xu and Deventer, 2000). In Taftan andesite the amount of K_2O is equal to 2.12 wt. % and less than 3.21 wt. % was detected for Na_2O. Untreated Taftan pozzolan contains SiO_2 and Al_2O_3 as the major constituents (the same as other pozzolans) with the SiO_2 content equal to 61.67 wt. % and Al_2O_3 content equal to 15.9 wt. %. The percentage of silica and alumina (SiO_2+Al_2O_3) is equal to 77.57%. The study shows that calcining the Taftan pozzolan does not change its behaviour.

3.6.3 Physical Composition

The specific gravity of Taftan pozzolan, as supplied by the manufacturer, is 2.22. This property was measured using a pycnometer and according to ASTM D-854/ ASTM D5550 standards.

The Kash Cement Factory measured the specific surface of Taftan pozzolan using the Blaine air permeability method, which gave a value of 3836 cm^2/g. This is the same as the value reported in Evaluation of Pozzolans of Iran by Ramezanianpour and Ghazi Moradi (1992).

Crystalline particles of sodic plagioclase, quartz, amphibole and biotite of 20 to 75 microns size were observed and reported in samples of Taftan pozzolan by Iranian Cement Guild (Ezatian, 2004).

3.7 Summary

1. The properties of five natural pozzolan were discussed in this chapter and the variability in composition of these materials, based on published data or from cement works themselves, are shown in Table 3.4.

2. Pozzolans contain sodic zeolites, especially clinoptilolite, such as Shahindej dacite, after calcination at 800°C, convert to opal which reacts rapidly with an aqueous alkaline solution and seems to be suitable for producing geopolymers.

3. The hornblende peaks in the XRD of Sahand pozzolan disappeared due to calcination and it seems by calcination to temperatures of 800-1000°C would result even more than 800°C provides a more reactive material, although it might not be economic.

4. The effect of calcination on the reactivity of the pozzolans such as Sirjan and Rafsanjan which contain more altered minerals such as montmorillonite, depends on the combination of two reverse effects including activation depending on the reactivity of clay phase and deactivation depending on the decrease of soluble fraction and increase of crystalline fraction. It was observed that the reactivity of Sirjan dacite cannot be improved by heat treatment and the Rafsanjan treated at 800°C seems to have a slight potential for activation.

5. Taftan has the lowest L.O.I., highest soluble calcium content and higher content of Na_2O relative to K_2O which all have positive affects on the geopolymeric paste strength according to the literatures, might be the best case to be activated in alkaline solution to provide geopolymer cement.

6. All of these Pozzolans were studied for their alkali solubility and compressive strength for selection for geopolymer cement production in the next chapter.

Table 3.1-a- Mineral compositions of the pozzolanas conducted by Kansaran Binaloud X-ray laboratory in Tehran, Iran

Material	Main and Minor Minerals									
	Feldspars		Clays		Mafics					
	Albite $NaAlSi_3O_8$	Clinoptilolite $KNa_2Ca_2(Si_{29}A_{17})O_{72}.24H_2O$	Montmorillonite $Na0.3(AlMg)_2Si_4O_{10}(OH)_2$	Muscovite-Illite $KAl_2Si_3AlO_{10}(OH)_2$	Hornblende $Ca_2(Fe.Mg)_4Al(Si_7Al)O_{22},(OH)_2$	Biotite $K(Mg,Fe)_3(Al,Fe)Si_3O_{10}(OH)_2$	Calcite $CaCO_3$	Quartz SiO_2	Amorphous	Total
Shahindej dacite	14%	40%	-	-	-	-	11%	32%	-	97
Sahand dacite	75%	-	-	2%	12%	-	-	9%	-	98
Sirjan dacite	43%	-	10%	-	-	5%	-	7%	33%	98
Rafsanjan dacite	20%	-	25%	-	12%	7%	5%	4%	25%	98
Taftan andesite	41%	-	-	-	20%	6%	-	6%	25%	98

Note: ***Qualitative*** Analysis usually involves the identification of a phase or phases in a specimen by comparison with "standard" patterns (i.e., data collected or calculated by someone else), and relative estimation of proportions of different phases in multiphase specimens by comparing peak intensities attributed to the identified phases. ***Quantitative*** analysis of diffraction data usually refers to the determination of amounts of different phases in multi-phase samples. Quantitative analysis may also be thought of in terms of the determination of particular characteristics of single phases including precise determination of crystal structure or crystallite size and shape. In quantitative analysis, an attempt is made to determine structural characteristics and phase proportions with quantifiable numerical precision *from the experimental data itself.*

Table 3.1-b - Mineral compositions of the calcined pozzolanas conducted by Kansaran Binaloud X-ray laboratory in Tehran, Iran

Material		Main and Amorphous Minor Minerals									
		Feldspars				Clays	Mafics				
		Albite $NaAlSi_3O_8$	Clinoptilolite $KNa_2Ca_2(Si_{29}Al_7)O_{72}.24H2O$	Mordenite $Na_2K_2Ca(Al_2Si_{10})O_{24}.7H_2O$	Opal(amorphous) $SiOnH_2O$	Muscovite-Illite $KAl_2Si_3AlO_{10}(OH)_2$	Hornblende $Ca_2(Fe.Mg)_4Al(Si_7Al)O_{22}(OH)_2$	Hematite	Quartz SiO_2	Amorphous	Total
Shahindej dacite	700C		12%	26%					60%		98
	800C	15%			38%	4%	5%		37%		99
Sahand dacite	700C	64%					10%		25%		99
	800C	63%				3%	15%		18%		99
Sirjan dacite	700C	54%				10%			4%	30%	98
	800C	57%				6%		1%	3%	30%	97
Rafsanjan dacite	700C	65%				4%	14%		5%	10%	98
	800C	47%				5%	12%	2%	8%	25%	99

Note: ***Qualitative*** Analysis usually involves the identification of a phase or phases in a specimen by comparison with "standard" patterns (i.e., data collected or calculated by someone else), and relative estimation of proportions of different phases in multiphase specimens by comparing peak intensities attributed to the identified phases.
Quantitative analysis of diffraction data usually refers to the determination of amounts of different phases in multi-phase samples. Quantitative analysis may also be thought of in terms of the determination of particular characteristics of single phases including precise determination of crystal structure or crystallite size and shape. In quantitative analysis, an attempt is made to determine structural characteristics and phase proportions with quantifiable numerical precision *from the experimental data itself.*

Table 3.2 – The properties of Zeolite and Clay Minerals of the materials used in this investigation as described by F.Ezatian (1998)

Minerals		Description
Tectosilicates (Zeolite group)	Clinoptilolite $KNa_2Ca_2(Si_{29}Al_7)O_{72}.24H2O$	Clinoptilolite forms as a devitrification product (the conversion of glass to crystalline material) of volcanic glass in tuffs. Tuffs are consolidated pyroclastic rocks. The devitrification occurs when the glass is in contact with saline waters. Clinoptilolite is one of the more useful natural zeolites and has high resistance to extreme temperatures and chemically neutral basic structure while its pozzolanic properties can be changed by heat treatment.
Tectosilicates (Zeolite group)	Mordenite $Na_2K_2Ca(Al_2Si_{10})o_{24}.7H_2O$	Mordenite is an abundant naturally occurring zeolite with relatively low cation exchange properties. The degree of exchange of Na + of mordenite for other cations decreases with increasing polarizing ability of the cation and the acid resistance of cationic forms of it increases with increasing polarizing ability of the exchange cation.
Tectosilicates (Albite group)	Albite $NaAlSi_3O_8$	Kaolinite, illite and serisite are the most important minerals resulting from albite breaking up. These are economic minerals and used to produce glass and ceramics. Melting them at 1100 to 1300°C and adding kaolin and quartz to it, makes a dense white material called porcelain.
Tectosilicates (Silica group)	Opal(amorphous) $Sio.nH_2O$	Opal tends to convert to calcedonic crystals, that reacts intensively with alkaline aqueous and is soluble in strong and hot alkaline solutions.
Phyllosilicates (Muscovite-Illite group)	Muscovite-Illite $KAl_2Si_3AlO_{10}(OH)_2$	Reaction relationships between muscovite and potassium feldspars can be observed at more than 700 °C. Muscovite is resistant to weathering and due to absorbing water; breaks down to illite, montmorillonite and kaolinite clays respectively.
Phyllosilicates (Montmorillonite group)	Montmorillonite $Na0.3(AlMg)_2Si_4O_{10}(OH)_2$	Montmorillonite clays are mainly result of the erosion of basic igneous rocks containing Mg and Ca. It may form kaolinite due to the presence of water and generate chlorite or illite.

Table 3.3-a Chemical composition (oxide percent) of the materials used in this investigation conducted by Kansaran Binaloud X-ray laboratory in Tehran, Iran (2005-2006)

Material	LOI	SiO_2	Al_2O_3	Fe_2O_3	CaO	MgO	TiO_2	K_2O	Na_2O	Total
Shahindej dacite	10.28	70.13	11.11	1.27	2.52	0.92	0.14	2.25	1.01	99.63
Sahand dacite	5.15	64.67	11.85	3.03	6.79	1.11	0.537	4.26	2.3	99.70
Sirjan dacite	6.14	68.51	11.84	3.73	2.90	1.43	0.366	3.19	1.62	99.73
Rafsanjan dacite	4.41	68.31	12.59	2.70	3.88	1.37	0.263	3.26	2.40	99.18
Taftan andesite	1.85	61.67	15.90	4.32	7.99	2.04	0.438	2.12	3.21	99.54

Table 3.3-b Chemical composition (oxide percent) of the calcined materials used in this investigation conducted by Kansaran Binaloud X-ray laboratory in Tehran, Iran (2005-2006)

Material	LOI	SiO_2	Al_2O_3	Fe_2O_3	CaO	MgO	TiO_2	K_2O	Na_2O	Total
Shahindej dacite-800°C	5.78	73.44	11.88	1.30	2.55	0.98	0.147	2.30	1.10	99.48
Sahand dacite-800°C	2.90	67.40	11.87	3.10	6.87	1.18	0.564	3.41	1.90	99.19
Sirjan dacite-700°C	2.20	68.36	13.40	4.41	3.90	1.20	0.508	2.66	2.78	99.42
Rafsanjan dacite-800°C	2.48	71.53	12.46	2.76	3.93	1.46	0.276	2.53	1.87	99.3

Table 3.4 Variability in the Chemical composition (oxide percent) of the materials used in this investigation

Material	LOI	SiO_2	Al_2O_3	Fe_2O_3	CaO	MgO	TiO_2	K_2O	Na_2O	Consideration & References
Shahindej dacite	12.1	62.2	12.82	4.24	5.01	-	-	1.52	-	Ourmia Cement Company, 2004
	10.62	71.43	8.29	1.49	3.72	1.04	0.23	1.88	1.03	Conducted by Kansaran Binaloud X-ray laboratory, 2004
	10.28	70.13	11.11	1.27	2.52	0.92	0.14	2.25	1.01	Conducted by Kansaran Binaloud X-ray laboratory, 2005
Sahand dacite	-	62.7	18.25	3.57	2.65	1.05	-	0.41	0.19	Ardebil Cement Company, 2004
	5.15	64.67	11.85	3.03	6.79	1.11	0.537	4.26	2.3	Conducted by Kansaran Binaloud X-ray laboratory, 2005
Sirjan dacite	9.8	60.9	14.0	3.77	5.3	0.39	-	1.88	2.4	Ghadrooni Dam Project report, 2005
	5.2	63.6	17.72	3.68	5.6	0.8	-	2.4	0.22	Maghsoudi, 2001
	3.24	62.92	19.55	4.16	3.52	0.2	-	3.1	3.5	Kerman Cement Company, 2004
	6.14	68.51	11.84	3.73	2.9	1.43	0.366	3.191	1.62	Conducted by Kansaran Binaloud X-ray laboratory, 2005
Rafsanjan dacite	1.9	74.4	13.6	1.6	0.84	1.2	-	6.2	0.14	Maghsoudi, 2001
	4.41	68.31	12.59	2.7	3.88	1.37	0.263	3.26	2.4	Conducted by Kansaran Binaloud X-ray laboratory, 2005
Taftan andesite	2.2	60.1	18	6.8	7.2	1.6	-	-	-	A.Ghazi Moradi, 1992
	2.66	61.17	18.77	4.68	6.98	-	-	-	-	Khash Cement Company, 2004
	1.64	58.35	12.98	4.86	15.01	1.69	0.58	1.61	2.7	Conducted by Kansaran Binaloud X-ray laboratory, 2004
	1.85	61.67	15.9	4.32	7.99	2.04	0.438	2.12	3.21	Conducted by Kansaran Binaloud X-ray laboratory, 2005

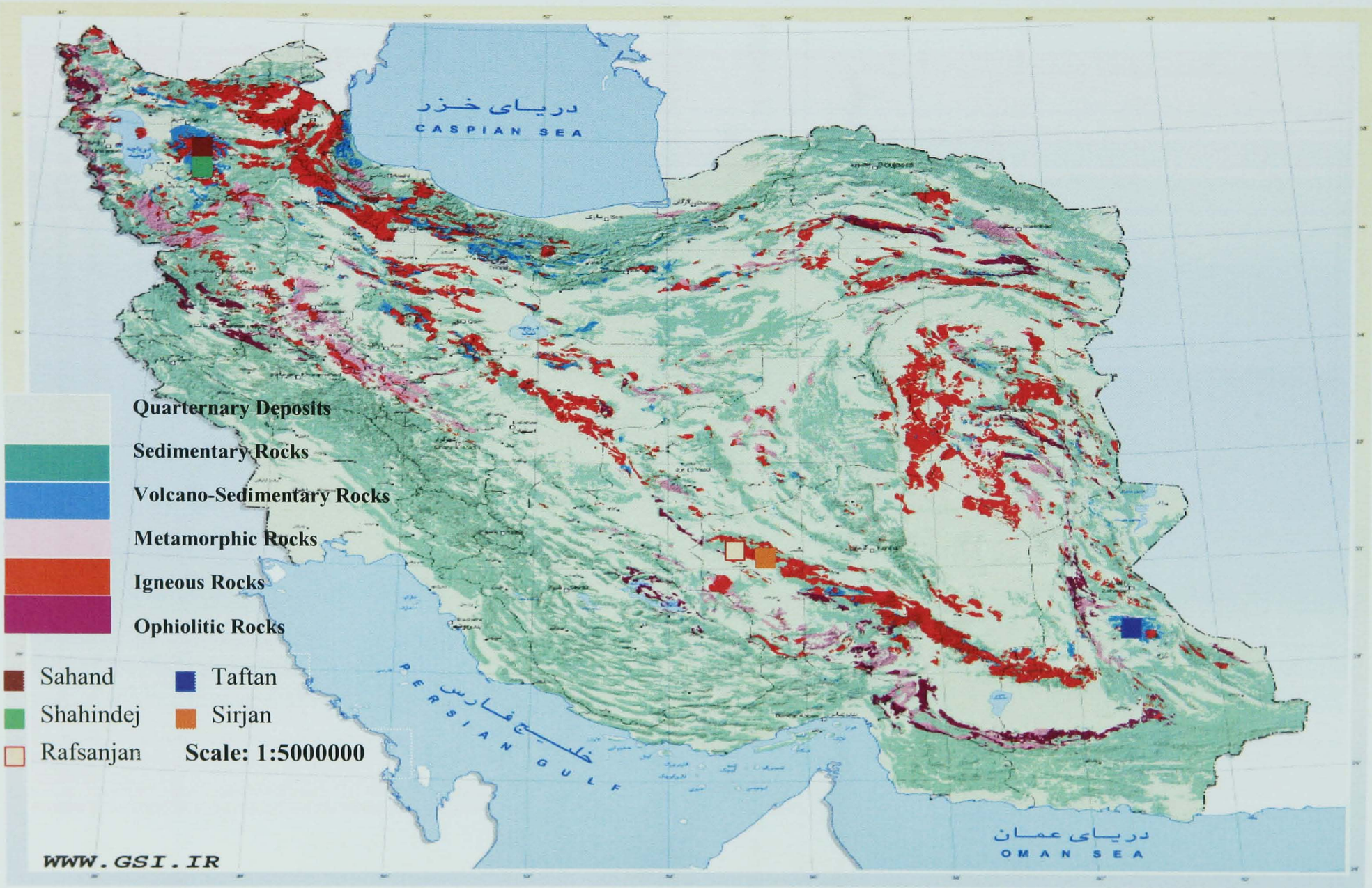

Figure 3.1 Location of pozzolans on geology map of Iran (Geology Survey of Iran/WWW.GSI.IR)

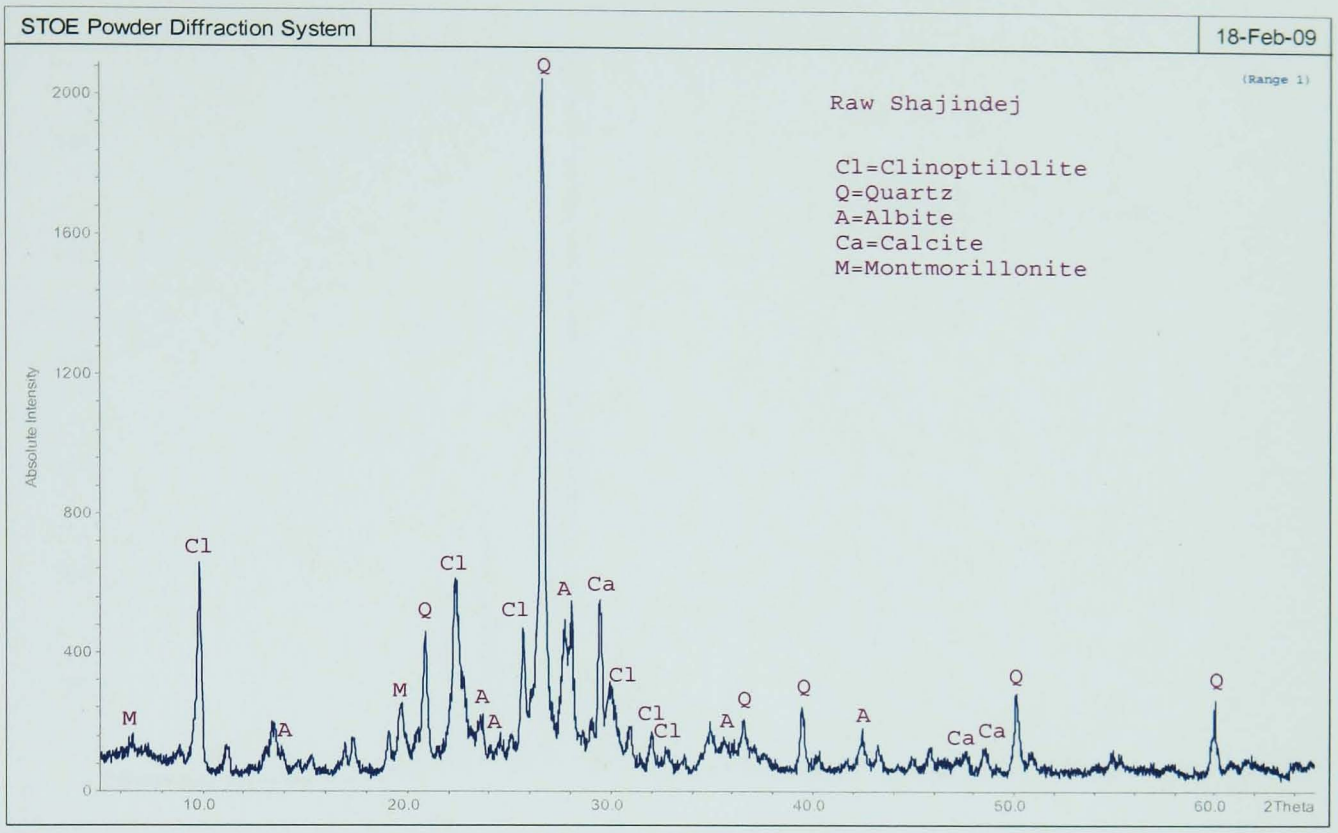

Figure 3.2-a Mineralogical composition of Shahindej dacite (testing was carried out in the Department of Engineering Materials, University of Sheffield)

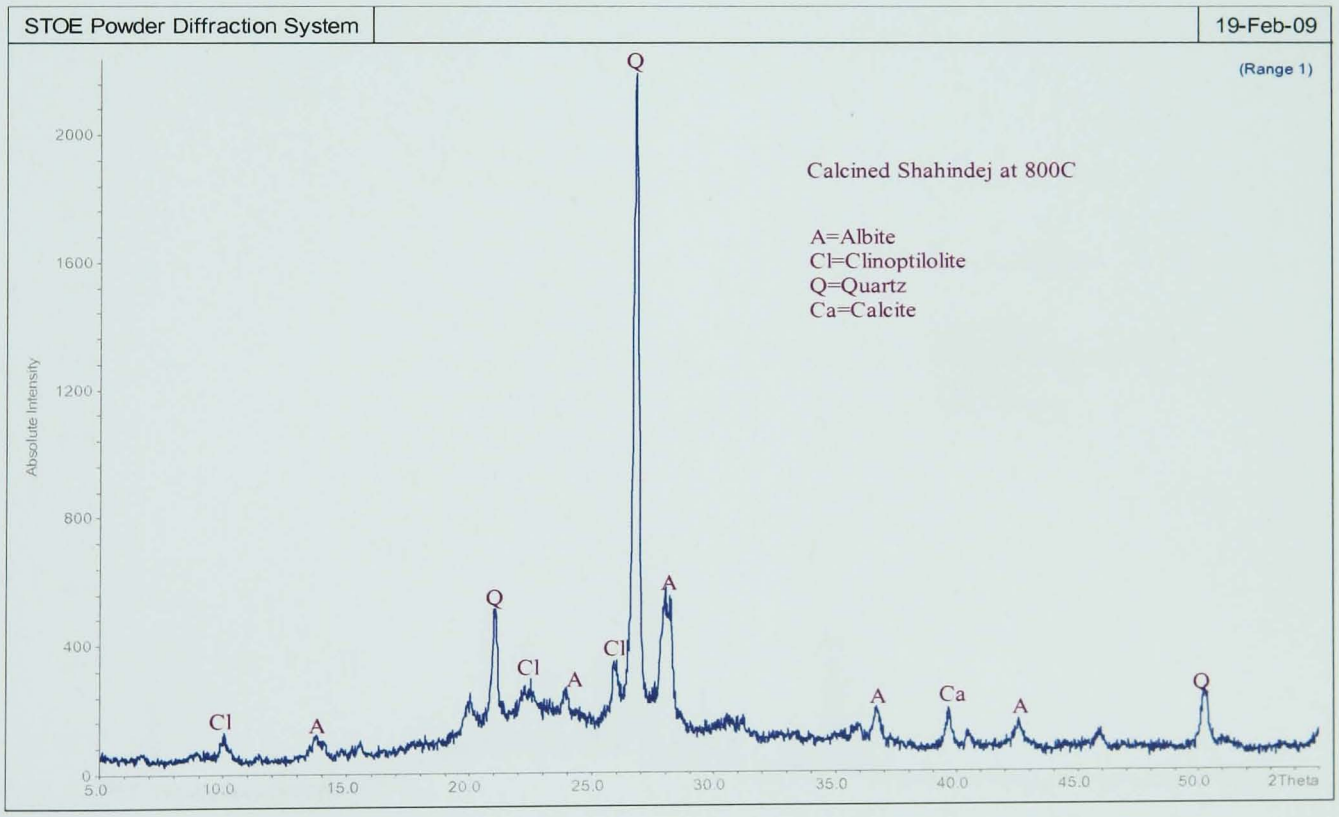

Figure 3.2-b Mineralogical composition of calcined Shahindej dacite (testing was carried out in the Department of Engineering Materials, University of Sheffield)

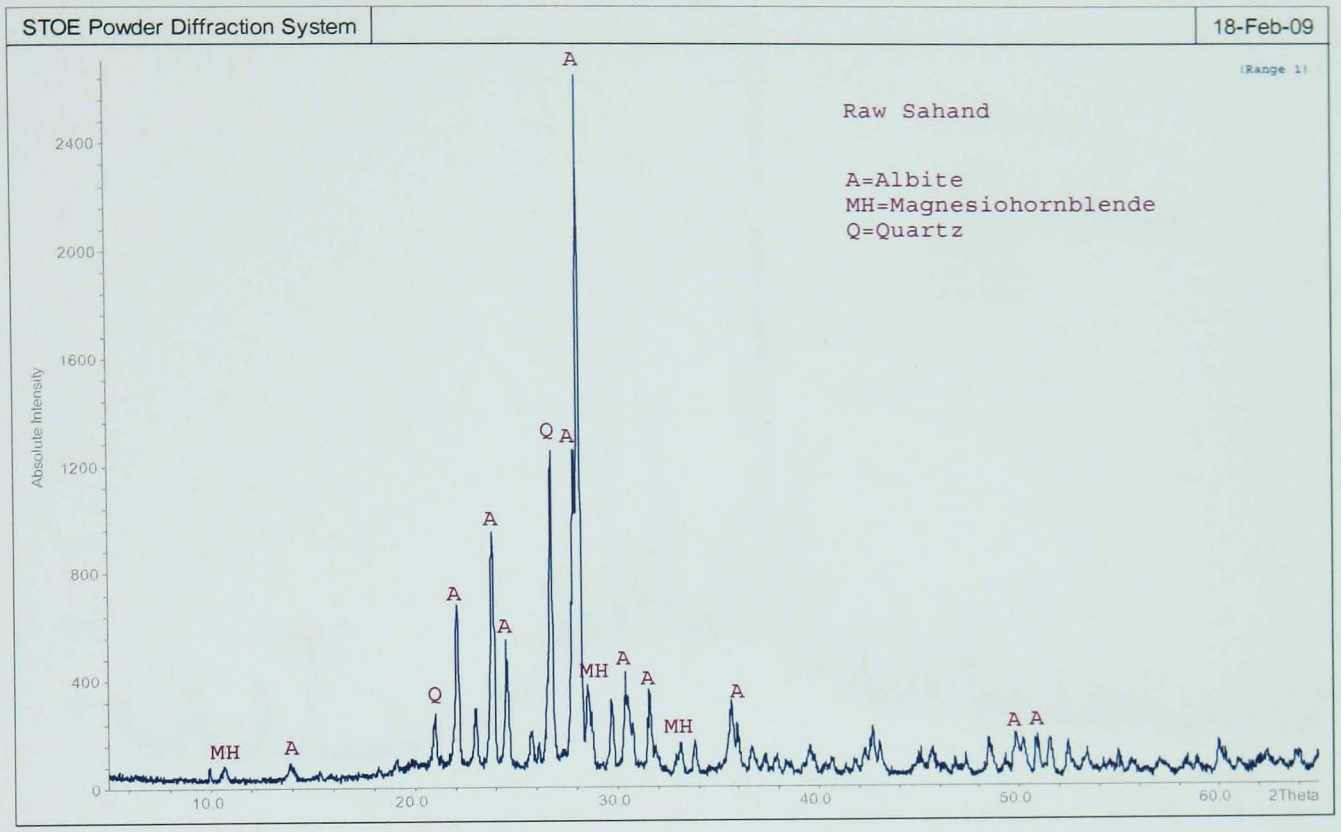

Figure 3.2-c Mineralogical composition of Sahand dacite (testing was carried out in the Department of Engineering Materials, University of Sheffield)

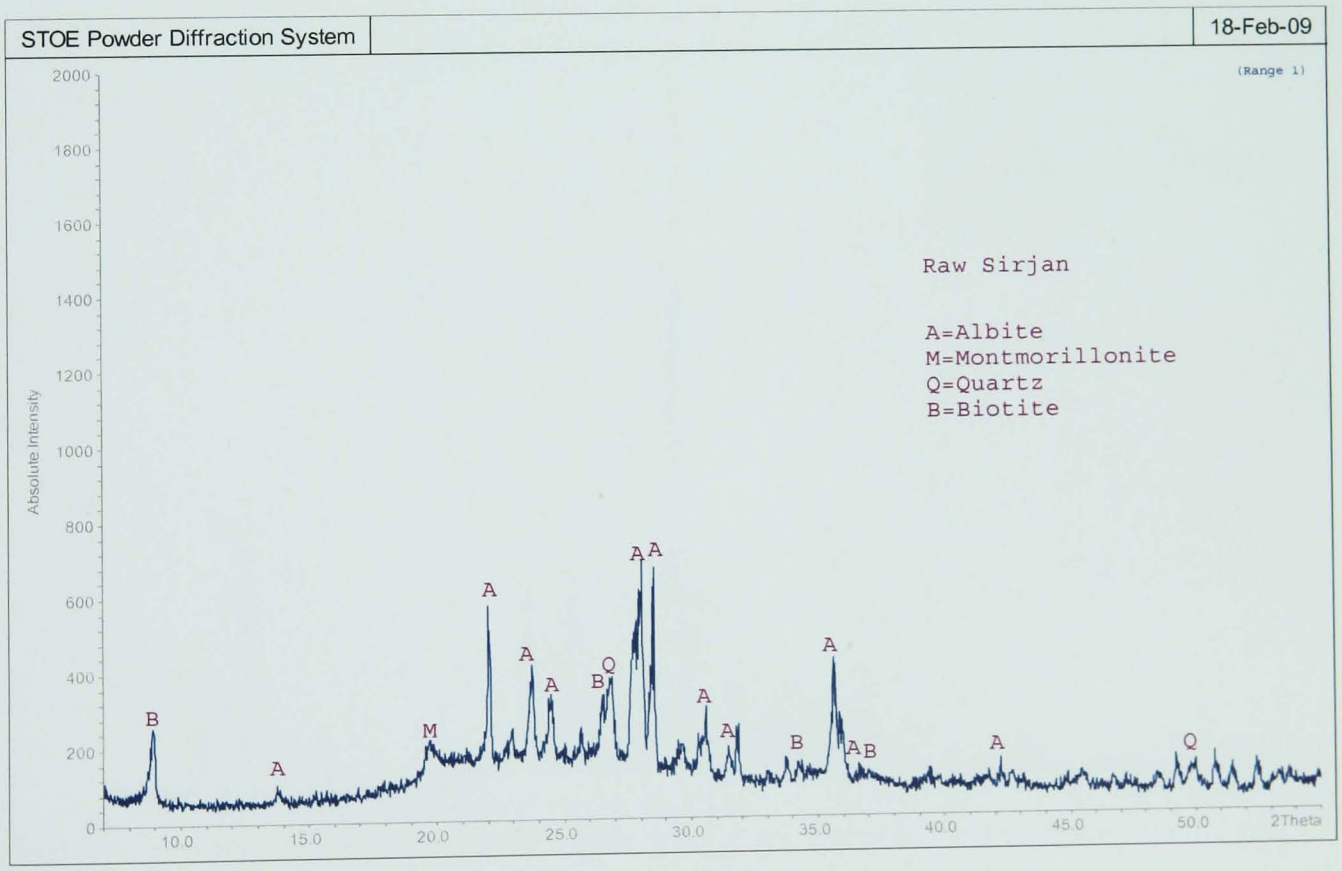

Figure 3.2-d Mineralogical composition of Sirjan dacite (testing was carried out in the Department of Engineering Materials, University of Sheffield)

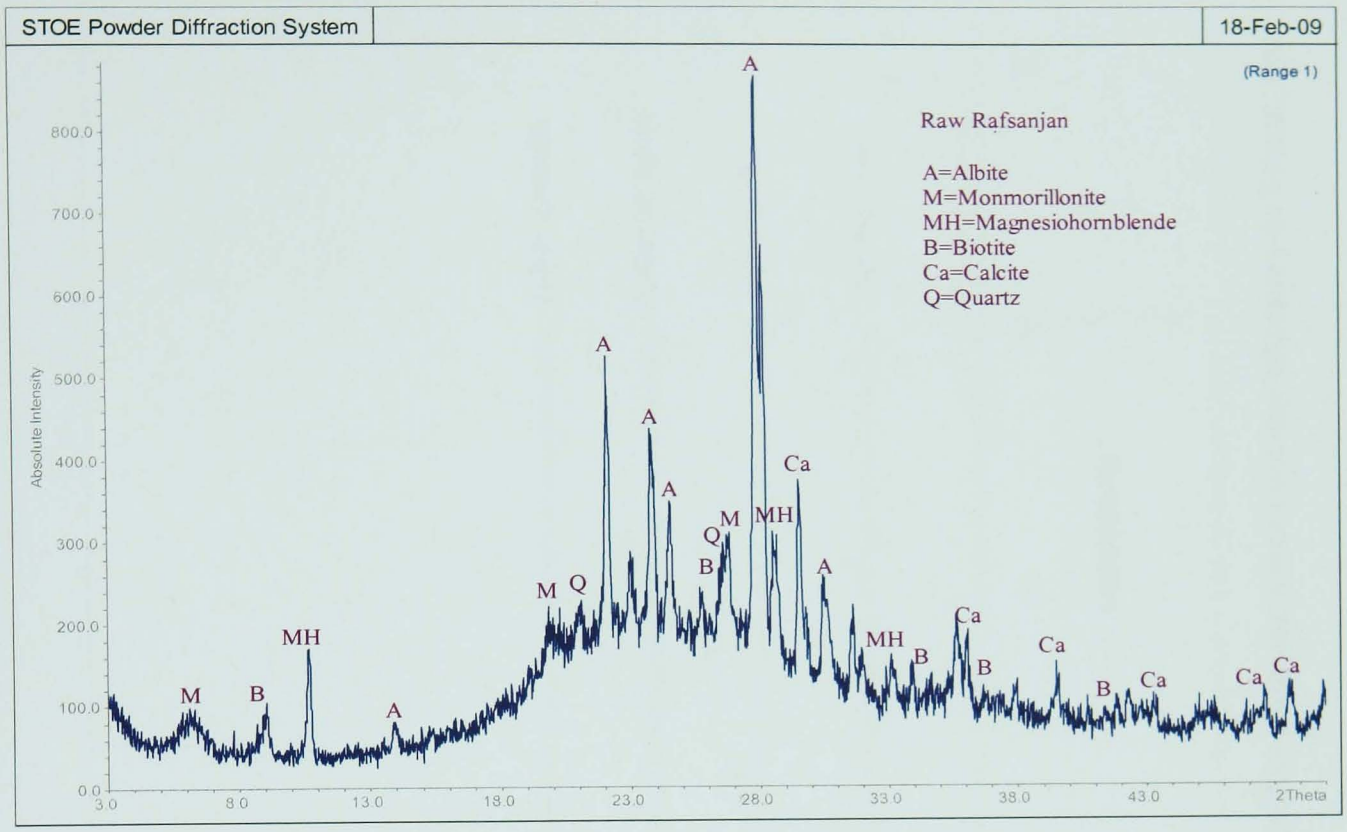

Figure 3.2-e Mineralogical composition of Rafsanjan dacite (testing was carried out in the Department of Engineering Materials, University of Sheffield)

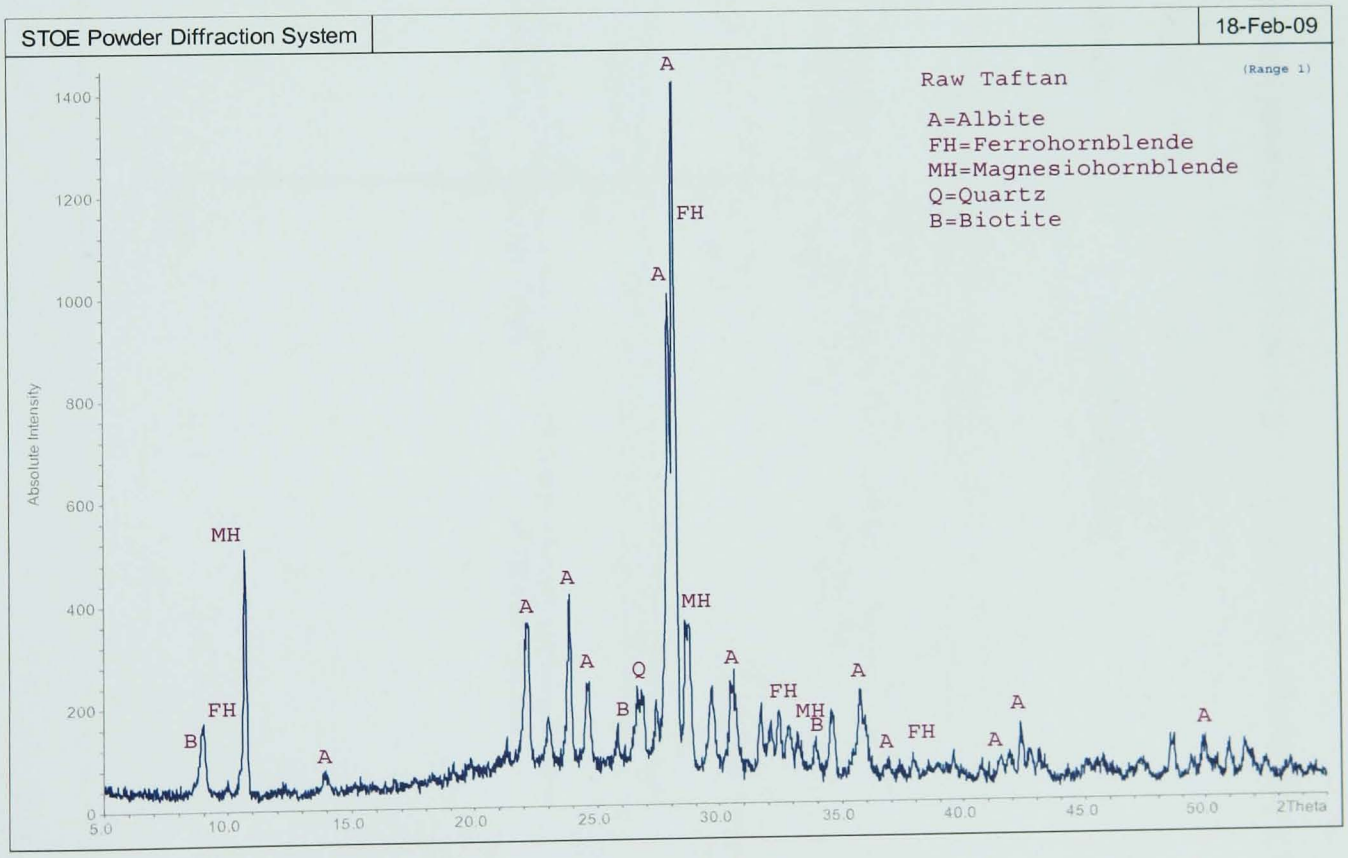

Figure 3.2-f Mineralogical composition of Taftan andesite (testing was carried out in the Department of Engineering Materials, University of Sheffield)

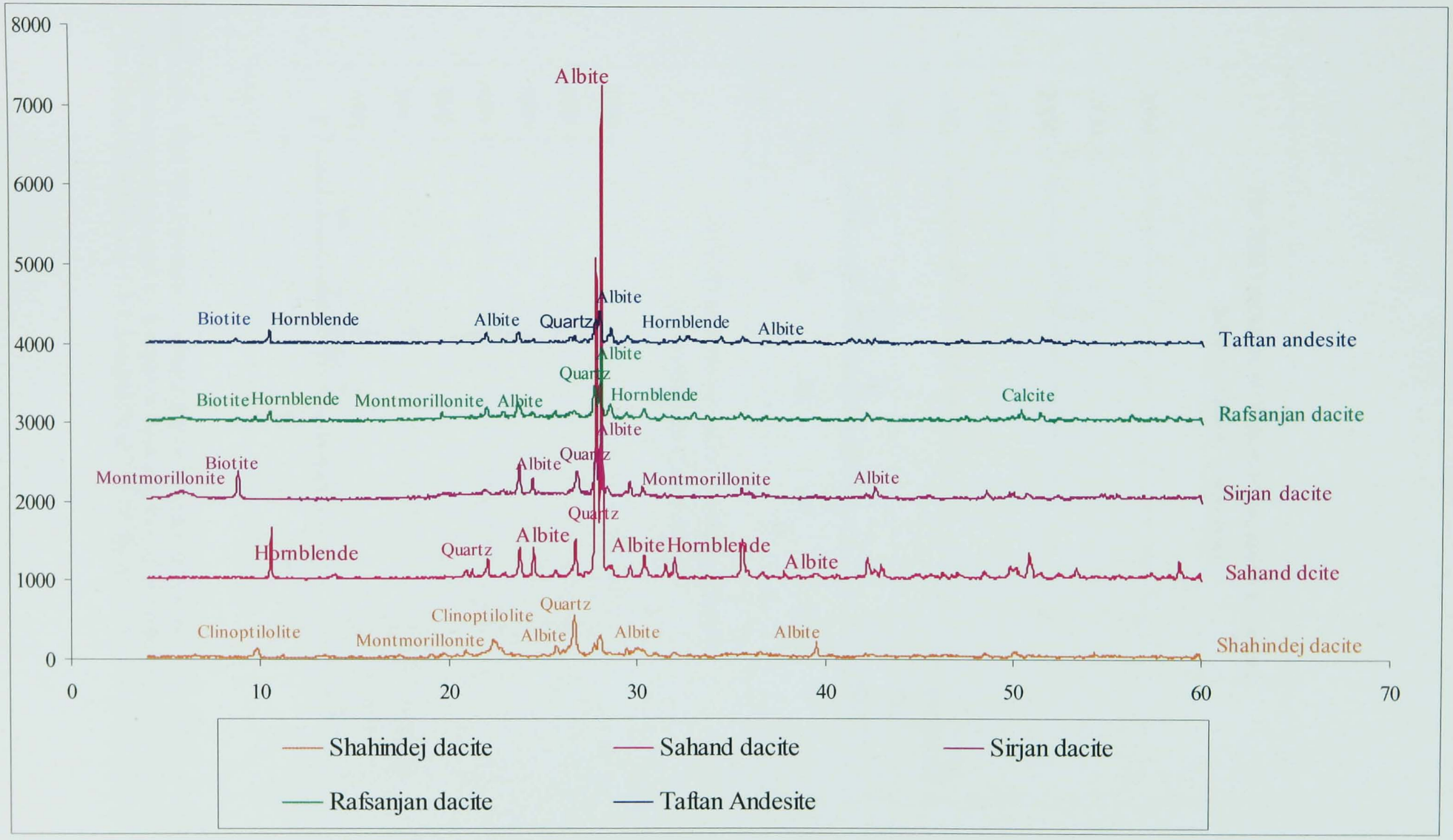

Figure 3.2-g Comparison of X-ray diffraction of five untreated pozzolans conducted by Kansaran Binaloud X-ray laboratory in Tehran, Iran

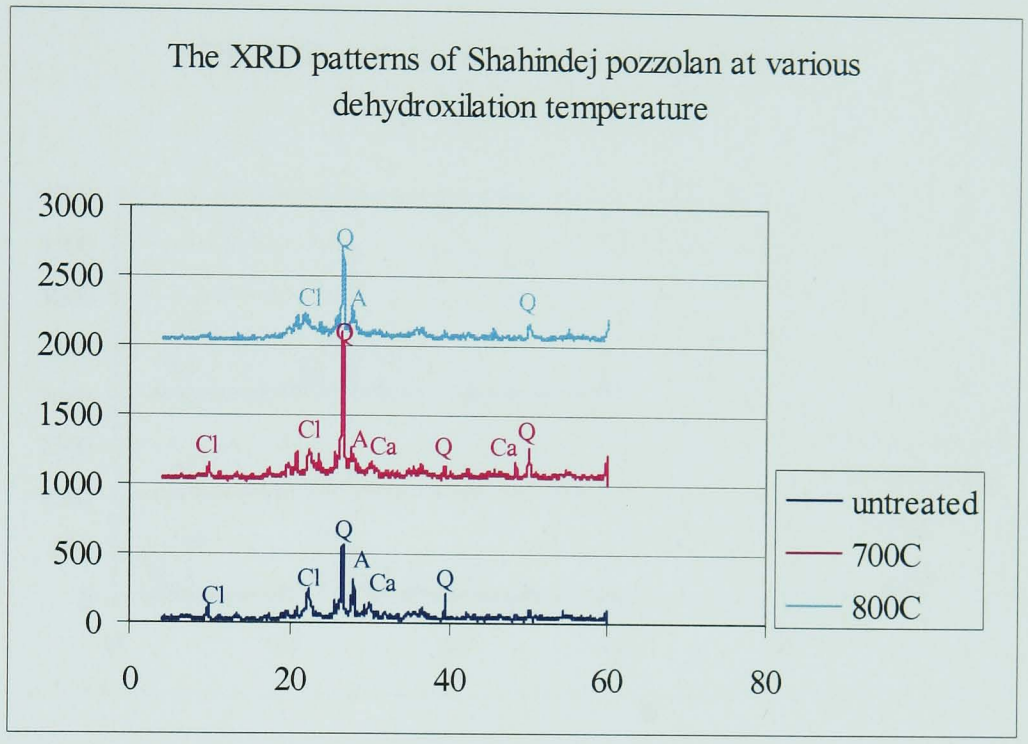

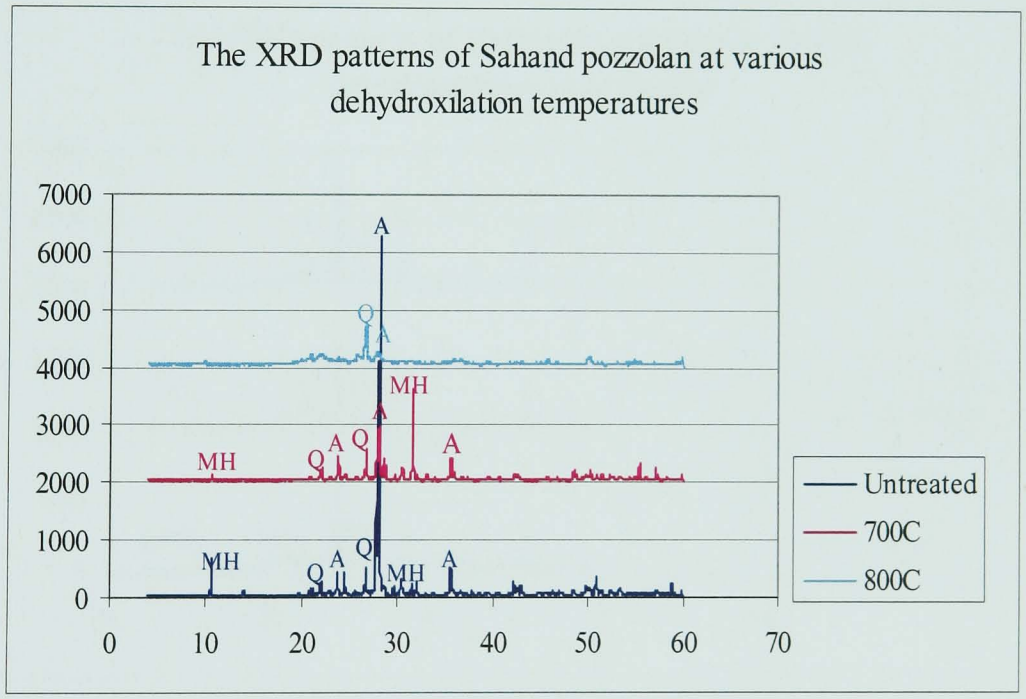

Figure 3.3-a The XRD pattern of Shahindej and Sahand pozzolans at various calcination temperatures conducted by Kansaran Binaloud X-ray laboratory in Tehran, Iran
A=Albite; Ca= Calcite; Cl=Clinoptilolite; MH=Magnesiohornblende; Q=Quartz

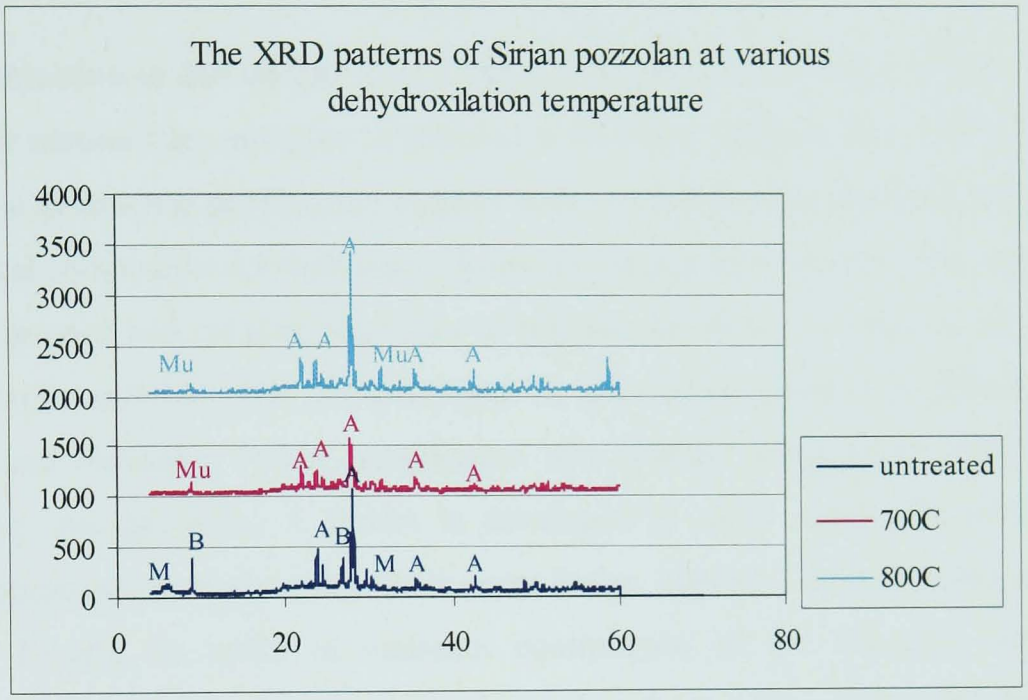

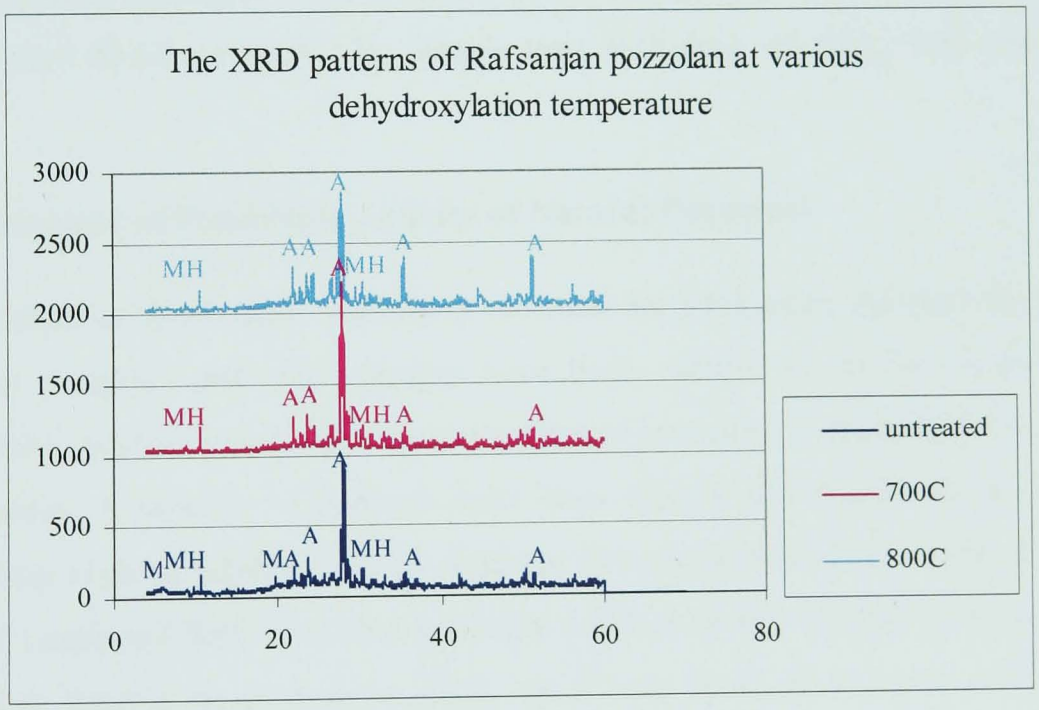

Figure 3.3-b The XRD patterns of Sirjan and Rafsanjan pozzolans at various calcination temperatures conducted by Kansaran Binaloud X-ray laboratory in Tehran, Iran
A=Albite; B=Biotite; MH=Magnesiohornblende; M=Montmorillionite; Mu=Muscovite

4. THE SELECTION OF POZZOLAN FOR PRODUCING GEOPOLYMER BASED ON SIMPLE TESTS

4.1 Introduction

The main objective of this chapter is to study the pozzolanic reactivity of five pozzolans both in their natural state and after calcination at different temperatures, comparing their efficiency in producing geopolymer cement with respect to their minerals, crystallinity and chemical compositions which were studied in the previous chapter. The solubility of both the untreated and calcined materials in alkaline solution was taken as an indicator for pozzolanic activity. The improvement in pozzolanic properties following heat treatment and elevating curing temperature was studied using alkali solubility and compressive strength tests. A model is developed to allow prediction of the alkali activated pozzolan strength versus their crystallinity, chemical compositions and alkali solubility. Finally, in order to maintain continuance of the research, Taftan and Shahindej natural pozzolans were selected based on engineering judgement from x-ray diffraction and fluorescence results, simple tests including solubility and compressive strength.

4.2 Measurement of Pozzolanic Activity of Natural Pozzolans

The assessment of pozzolanic activity is essential for estimating the performance of a material as pozzolan and many studies have been carried out to find a general test method which, besides being valid for every type of pozzolan, is acceptable for accuracy and quickness. A number of methods have been suggested for estimating pozzolanic activity. These can be subdivided into chemical and physical tests. In chemical tests, the amount of combined lime in a lime-pozzolan solution or the amount of silica or silica and alumina soluble in an acid or alkali, have been used as an index of pozzolanic activity. In physical tests, unconfined compressive strength has been used for assessing pozzolanic activity (Shi, 2001). Both the American Standards (ASTM) and British Standards (BS) define indices based on the ratio between the compressive strength of a specified cement pozzolan mortar and a control mortar with plain cement.

In the present research, the solubility of a natural pozzolan in boiling 0.5M NaOH which Milestone (1978) reported as a rapid chemical test for evaluating pozzolanic reactivity, was used for assessing pozzolanic activity. Compressive strengths have also been used to determine pozzolanic activity. The general procedure is to make samples of a certain size from different alkali activated pozzolans pastes with same alkali concentration, and then test the samples in compression after 28 days. Variations in the type and concentration of alkali influence the strength significantly, and therefore must be specified to enable comparison of results.

4.3 Experimental investigations

In the rapid chemical test, for measuring solubility of different natural pozzolans described in Report No. C.D. 2273 of Department of Scientific and Industrial Research of New Zealand (Milestone, 1978), 0.15g of the material, which has been dried at 105°C, is accurately weighed into a 300ml nickel beaker. 200 ml of boiling 0.5M NaOH is poured in to the beaker and the resulting suspension brought back to boiling as quickly as possible. After boiling for different times, the suspension is cooled quickly with cold water and filtered. The residue is well washed with cold water and the residue dried at 105°C overnight. The weight of undissolved material is determined by reweighing. The alkali solubility is the percentage of material dissolved. Then Silica, aluminium, and calcium were determined by ICP tests in the filtrate of samples and the results are presented in Table 4.1.

In order to determine the compressive strength of pozzolanic materials, 4ml of 7.5M KOH solution was added to 15g pozzolan powders and blended for 5 min before the addition of 0.5 ml of sodium silicate solution with a solid content equal to 2.1%. Each of the subsequent slurries was mixed for 5 min and transferred to PVC moulds measuring 20x20x20 mm. Samples were removed from the mould after 24 hrs and cured at 20, 40, 60, and 80°C for 27 days after which the compressive strength of these samples was measured. Three samples of each condition were tested with average compressive strength values reported as the results.

4.4 Pozzolanic activity of five pozzolans in their natural state and after heat treatment

All 5 pozzolans contain SiO_2 and Al_2O_3 with the SiO_2 content varying from 61.67 wt.% in Taftan andesite to 70.13 wt.% in the Shahindej dacite. The Al_2O_3 content varies from 11.11 wt.% in Shahindej dacite to 15.90 wt.% in Taftan andesite while the CaO content varies from 2.52 wt. % in Shahindej to 7.99 wt.% in Taftan andesite (Table 3.3a).

The XRD patterns for the pozzolans in Table 3.1 shows that all of them to be mixture of minerals with various degrees of crystallisation. All of these pozzolans contain albite as main mineral phase varying from 14 wt.% in Shahindej dacite to 75 wt.% in Sahand dacite. Four of them, Shahindej, Sahand, Sirjan, and Rafsanjan, contain both zeolites and clay minerals and three, Sirjan, Rafsanjan and Taftan, contain about 30% amorphous material.

The nature of the starting materials including chemical composition, mineral composition and crystal structure affects their pozzolanic activity and the formation of the geopolymer gel phase. Two types of heat treatment can be used; those which involve calcination of the pozzolans and those where elevated temperature curing of pozzolan pastes is used. Often the two processes must be combined. The pozzolanic activity of pozzolans in their natural state and after heat treatment has been assessed by measurement of rapid alkali solubility and 28 days compressive strength and, as can be observed in Table 4.1, calcination significantly increases the solubility of all pozzolans, except Taftan.

4.4.1 Shahindej Dacite

Shahindej dacite, in spite of having high L.O.I. and higher content of K_2O relative to Na_2O which can have a negative affect on geopolymeric paste strength, the extent of dissolution of Si and the molar Si/Al ratio of the dissolved material in solution has a significant effect on compressive strength (Table 4.1).

The solubility of Shahindej dacite in untreated and calcined forms was measured after 3, 5, and 7 minutes boiling in 0.5M NaOH in order to determine the ideal time for boiling.

The results of alkali solubility versus boiling time for the Shahindej dacite are shown in Figures 4.1 and 4.2 for both the untreated and calcined forms. Three minutes was selected for this pozzolan when untreated and calcined at 800°C and five minutes for calcination at 700°C and 900°C as the optimum boiling time, since for longer boiling times, the dissolution of this pozzolan is reduced. The alkali solubility results of the untreated and calcined forms of Shahindej pozzolan show solubility increases due to calcining up to 700°C (Figures 4.2, 4.3 and Table 4.1).

When compared with the parameters which indicate the pozzolanic activity, the compressive strength of the geopolymeric paste prepared with dacite tuff calcined at 700°C attains the highest value equal to 42.5MPa at the usual curing temperature of 40°C (Figure 4.4). This is thought to be due to activation of the zeolite which converts from clinoptilolite to mordenite at 700°C. Continued calcination up to 800°C; converts mordenite to opal which reacts strongly with alkaline solutions giving a compressive strength of 68.5MPa when cured at 20°C, 37.6MPa at 40°C and 60.4MPa at 80°C curing. Untreated Shahindej dacite gives a strength of the geopolymeric paste that varies from 22MPa at 40°C to 81.5MPa at 80°C (Figure 4.4). Thus Shahindej pozzolan in an untreated form and cured at 60°C or calcined at 800°C and cured at 20°C might be useful for producing structural concrete (Figures 4.4, 4.5).

4.4.2 Sahand Dacite

Sahand dacite has the lowest pozzolanic activity due to the lack of amorphous material in its mineralogy components. The solubility of Sahand dacite in untreated and calcined forms was measured after 3, 5, and 7 minutes boiling in 0.5M NaOH as well to determine the ideal time for boiling. The results of alkali solubility versus boiling time for the untreated and calcined Sahand dacite are shown in Figures 4.1 and 4.2. respectively. Five minutes was selected as the optimum boiling time for this pozzolan since for longer times of boiling the dissolution of this pozzolan is reduced. However, as it is obvious from the measurements of the alkali solubility and the results of the compressive strengths, its reactivity can be improved by heat treatment up to 900°C. By calcining this pozzolan, the solubility was increased from 45% to 67% for calcined

sample at 900°C (Figure 4.3). Therefore, the solubility of the Sahand dacite can be improved significantly by calcining which increases its compressive strength from 5MPa to 19.3MPa for the sample calcined at 800°C which curing at 40°C (Figure 4.4). Calcined samples at 900°C show higher compressive strengths of up to 32.9MPa when cured at 80°C and might be used to produce precast concretes (Figures 4.4, 4.5).

4.4.3 Sirjan Dacite

The solubility of Sirjan dacite in untreated and calcined forms was measured in 0.5M NaOH solution at three different boiling times (3, 5, and 7 minutes) to determine the ideal time of boiling. The results of alkali solubility versus boiling time for the untreated and calcined Sirjan dacite are shown in Figures 4.1 and 4.2, respectively. Three minutes was selected as the optimum boiling time for this pozzolan, since for longer times of boiling the dissolution of this pozzolan is reduced. Sirjan dacite reactivity is not improved by calcining. Calcination decreases alkali solubility, the maximum solubility corresponding to the untreated sample at 63.75%. Increasing the calcination temperature from 700°C to 900°C increases the alkali solubility from 39.18% to 52.36% which is still less than the solubility of untreated form (Figures 4.2, 4.3).

Although the geopolymeric paste prepared with the untreated form of Sirjan pozzolan shows moderate compressive strength when cured at 60°C, XRD results (Table 3.1), confirm that calcination has not had any significant effect on Sirjan dacite reactivity. This is mirrored in the compressive strength results which are maximum for the untreated form and equal to 13MPa at 40°C curing and 29MPa at 60°C curing (Figures 4.4, 4.5).

4.4.4 Rafsanjan Dacite

The solubility of Rafsanjan dacite in untreated and calcined forms was measured after 3, 5, and 7 minutes boiling in 0.5M NaOH in order to determine the ideal time of boiling. The results of alkali solubility versus boiling time for the untreated and calcined states are shown in Figures 4.1 and 4.2, respectively. Three minutes was selected as the optimum boiling time for this pozzolan to avoid dissolution of non-pozzolanic material.

As it is apparent from these curves the solubility reduces after 3 minutes boiling, but it increases further due to the dissolution of secondary conformed minerals. Increasing the temperature of calcination from 700°C to 800°C increases the percentage of amorphous phase from 10% to 25% the same as in the raw sample and shows the same solubility. Thereafter, solubility decreases with increasing the temperature up to 900°C (Figures 4.2, 4.3).

The calcined form of Rafsanjan dacite at 700°C is less reactive than the raw samples with a drop of compressive strength from 22.3MPa to 2.5Mpa at 60°C curing temperature (Figures 4.4, 4.5). It can be observed in Figure 4.4 that increasing the temperature of calcination up to 800°C increases the compressive strength which increased from 26.5Mpa at 40°C curing temperature to 42.4MPa at 80°C curing temperature, while calcination has no significant effect on improving reactivity at 60°C curing temperature (Figures 4.4, 4.5).

4.4.5 Taftan Andesite

Results of alkali solubility versus boiling time for the Taftan andesite are shown in Figure 4.2 for the untreated and for the calcinated forms. The optimum boiling time for Taftan pozzolan is 3 minutes and as it is apparent from these curves, the solubility reduces after 3 minutes boiling but it increases further due to the dissolution of secondary conformed minerals. Calcination has no significant effect on the properties of Taftan andesite and its solubility remains approximately constant, varying from 56.7% for the untreated sample to 57.1% for sample calcined at 700°C (Figures 4.2, 4.3). Taftan andesite has a higher pozzolanic activity than the others in its untreated form which makes it more economical to use and it has lower environmental impact. The untreated Taftan andesite produces a paste with moderate to high compressive strength ranging from 25.8MPa with 40°C curing to 53.1MPa at 60°C. Increasing the curing temperature above 60°C does not change its compressive strength significantly (Figures 4.4, 4.5). It can be seen from Figure 4.6 that the most suitable pozzolan for continuing this research is the Taftan andesite which gives high compressive strength without any requirement for calcining.

4.5 A Simplified Model for the Prediction of Pozzolanic Behaviour

The correlation between type, main and soluble chemical composition, and quantity of glassy and quartzite phases of pozzolans with compressive strength is reviewed in this section. A simplified linear model based on above properties has been proposed for assessment of pozzolanic reactivity of pozzolans in natural and calcined forms in terms of compressive strength of pozzolanic based geopolymeric cement paste and developed as a nonlinear model. The model using a least squares technique is fitted for alkali activated natural pozzolan for 28 days of curing period. The pozzolanic behaviour of calcined and untreated natural pozzolans can be evaluated directly using the compressive strength development with time of the alkali activated paste. By being able to assess the pozzolanic behaviour indirectly by means of rapid alkali solubility, the test period can be reduced so development of a predictive model can save both resources and time. The pozzolanic behaviour depends upon the type, chemical compositions such as alkali percentage, solubility, L.O.I, and quantity of glassy and quartzite phases, both for the calcined and untreated natural pozzolans.

In the mathematical model developed for predicting the strength of alkali activated natural pozzolan using chemical, physical and mineralogical factors, the following parameters are considered: the activity index [$(Al_2O_3+CaO+Fe_2O_3+MgO)/SiO_2$], used for the first time by Smith (1967) sited in Bao-min (2004), as the gelatinization coefficient of pozzolans; alkali (Na_2O+K_2O) percentage derived from X-Ray Fluoresence analysis of the untreated and calcined pozzolans; L.O.I.; alkali solubility index; the ratio of [$(SiO_2+Al_2O_3+CaO)$ in solution/$(SiO_2+Al_2O_3+CaO)$ mineral] obtained from ICP measurements, which Lian Huizehen (2001) sited in Bao-min (2004), defined as the activity ratio of pozzolans (this parameter not only reflects the chemical reactivity properties of pozzolans, but also relates to many physical properties such as degree of fineness and content of crystal); and the percentage of quartz in the calcined or untreated pozzolan powder. All of these parameters are presented in Table 4.2 where missing points were obtained by mean of nearby points and replaced in Table 4.3. As a first step the best curve fit to relate the strength for each parameter was found.

Analysis of the experimental results shows that the gel strength decreases linearly with the alkali percentage of each material and increases linearly with the alkali solubility index. The relation of the strength to activity index [$(Al_2O_3+CaO+Fe_2O_3+MgO)/SiO_2$], L.O.I., the ratio of [$(SiO_2+Al_2O_3+CaO)$ in solution/ $(SiO_2+Al_2O_3+CaO)$ mineral] resulting from the ICP tests and the quartz percentage was not found to be linearly related.

The linear model has been proposed for assessment of pozzolanic reactivity of pozzolans in natural and calcined form in terms of compressive strength of pozzolanic based geopolymeric cement paste. Alkali percentages of each material and alkali solubility index are two parameters that related linearly with the gel strength. In addition to these, eliminating one of the result points, activity index [$(Al_2O_3+CaO+Fe_2O_3+MgO)/SiO_2$] might be related linearly to strength as well. Therefore considering these three parameters a linear model is proposed which shows that the predicted and observed values are correlated 75%. In the linear model different temperatures of curing are considered as a variable which has interactive effect on linear equations between each parameter and the compressive strength of pozzolanic based geopolymeric cement paste.

This model was developed in to a non-linear model considering the other three parameters including L.O.I., the ratio of [$(SiO_2+Al_2O_3+CaO)$ in solution/ $(SiO_2+Al_2O_3+CaO)$ mineral] from ICP tests and the quartz percentage to obtain better correlation between the predicted and observed values of compressive strength of pozzolanic based geopolymeric cement paste.

The correlation between compressive strength and each parameter is presented in section 4.5.1 to section 4.5.6.

4.5.1 Activity Index

According to the activity index [$(Al_2O_3+CaO+Fe_2O_3+MgO)/SiO_2$] the compressive strength can be assessed with respect to the following relations at different curing temperatures.

I) Considering linear regression, ignoring the Taftan result

At 40°C: $Y_{40} = 82.7\text{-}222.58K_{ax}$ ($R=0.777$, $R^2=0.604$, Sig $=0.005$) (4-1a)

At 60°C: $Y_{60} = 99.43\text{-}264.32K_{ax}$ ($R=0.838$, $R^2=0.702$, Sig $=0.001$) (4-1b)

At 80°C: $Y_{80} = 145.51\text{-}405.64K_{ax}$ ($R=0.759$, $R^2=0.576$, Sig $=0.007$) (4-1c)

II) Considering nonlinear regression

At 40°C: $Y_{40} = 192.73\text{-}1005.99K_{ax}+1358.41K_{ax}^2$ ($R=0.816$, $R^2=0.665$, Sig $=0.007$) (4-1e)

At 60°C: $Y_{60} = 263.3\text{-}1443.22K_{ax}+2064.93K_{ax}^2$ ($R=0.885$, $R^2=0.783$, Sig $=0.001$) (4-1f)

At 80°C: $Y_{80} = 357.49\text{-}1921.36K_{ax}+2639.98K_{ax}^2$ ($R=0.800$, $R^2=0.640$, Sig $=0.01$) (4-1g)

Where Y=Compressive Strength (MPa) and K_{ax}=Activity Index

In this case the number of measurements is at least (N=11). Therefore the degree of freedom would be (N-2=9) and (N-3=8) for linear and nonlinear regression and R should more than 0.602 and 0.632, respectively which has occurred for all of the above equations. On the other hand, R^2 shows that this parameter justifies the variation more than 57.6% alone. The amount of statistical significance indicates that the curve fit is correct with more than 99% confidence as well.

4.5.2 Alkali percentage

The second parameter is the alkali percentage (Na_2O+K_2O)% found by X-Ray Fluoresence analysis of pozzolans which decreases the compressive strength linearly. The relation is given by the following at the different curing temperatures:

At 40°C: $Y_{40} = 65.66\text{-}9.79A$ ($R=0.791$, $R^2=0.625$, Sig $= 0.002$) (4-2a)

At 60°C: $Y_{60} = 72.9\text{-}9.98A$ ($R=0.63$, $R^2=0.397$, Sig $= 0.028$) (4-2b)

At 80°C: $Y_{80} = 109.6\text{-}16.71A$ ($R=0.708$, $R^2=0.501$, Sig $= 0.01$) (4-2c)

Where Y=Compressive Strength (MPa) and A=alkali percentage in pozzolanic materials.

The number of measurements is (N=12), therefore the degree of freedom would be (N-2 = 10) and R should be more than 0.576 which is quite satisfied. R^2 shows that this parameter justifies the variation more than 40% alone. The amount of statistical

significance indicates that the regression assumption is correct with more than 97.2% alone.

4.5.3 Alkali Solubility Index

The influence of solubility on strength shows that these two can be related linearly. Considering different curing temperature:

At 40°C : $Y_{40}= 0.82Sol-29.73$ (R=0.539, R^2 =0.291, Sig = 0.017) (4-3a)

At 60°C : $Y_{60}=1.07Sol-37.94$ (R=0.544, R^2 =0.296, Sig = 0.016) (4-3b)

At 80°C : $Y_{80}=1.57Sol-60.99$ (R=0.644, R^2 =0.415, Sig = 0.003) (4-3c)

Where Y=Compressive strength (MPa) and Sol=Alkali solubility index

With respect to the number of test results which is (N=19) degree of freedom would be (N-2=17) and therefore R should be more than 0.456 which is satisfied for all of the above equations. Square of R for all the equations shows that this parameter justifies the variation more than 29% alone. The amount of statistical significance indicates that the regression assumption is correct with more than 98.3% confidence as well.

4.5.4 Loss on Ignition (L.O.I.)

The influence of L.O.I. on strength shows that these two are related as follows. Considering different curing temperature:

At 40°C : $Y_{40}= 40.33(2.72)^{L.O.I.} (L.O.I.)^{-3.81}$ (untreated Shahindej result was eliminated.)
(R=0.704, R^2 =0.495, Sig =0.055) (4-4a)

At 60°C : $Y_{60}=55.84(1.72)^{L.O.I.} (L.O.I.)^{-2.42}$ (R=0.626, R^2 =0.392, Sig =0.063) (4-4b)

At 80°C : $Y_{80}=65.49(2.02)^{L.O.I.} (L.O.I.)^{-3.0}$ (R=0.712, R^2 =0.507, Sig =0.054) (4-4c)

Where Y=Compressive strength (MPa) and L.O.I. =loss on ignition

In this case the number of measurements is at least (N=11). Therefore the degree of freedom would be (N-3=8) and R should more than 0.632 which has occurred for all of the above equations. On the other hand R^2 shows that this parameter justifies the

variation more than 39.0% alone. The amount of statistical significance indicates that the curve fit is correct with more than 93.7% confidence.

4.5.5 The activity ratio [(SiO_2+Al_2O_3+CaO) in solution/ (SiO_2+Al_2O_3+CaO) mineral] obtained from ICP tests

The relation between the activity ratio [(SiO_2+Al_2O_3+CaO) in solution/ (SiO_2+Al_2O_3+CaO) mineral] resulting from ICP test data and the compressive strength are found as follows at different curing temperatures:

At 40°C: $Y_{40} = (0.03+1866.1K_{alr}-8.77x10^6 K_{alr}^2)^{-1}$ ($R=0.768$, $R^2=0.590$, Sig $=0.003$) (4-5a)

At 60°C: $Y_{60}=(-0.04+3505.97K_{alr}-17.65x10^6 K_{alr}^2)^{-1}$ ($R=0.807$, $R^2=0.651$, Sig $=0.0$) (4-5b)

At 80°C: $Y_{80}=(-1.15+60050.58K_{alr}-6.25x10^8 K_{alr}^2)^{-1}$ ($R=0.774$, $R^2=0.599$, Sig $=0.003$)(4-5c)

Where Y = Compressive Strength (MPa) and K_{alr} =the activity ratio [(SiO_2+Al_2O_3+CaO) in solution/ (SiO_2+Al_2O_3+CaO) mineral] resulted from leaching tests

The number of results is (N=10) therefore the degree of freedom is (N-3=7) and R should be more than 0.666 which has occurred for all of the above equations. R^2 shows that this parameter justifies the variation more than 59.0% alone and the amount of statistical significance shows that the curve fit is correct with more than 99.7% confidence as well.

4.5.6 The quartz percentage

The last parameter that seems to affect the strength is the percentage of quartz that exists in calcined or untreated pozzolan powder since the rupture of its bonding occurs at more than 2000°C (Ezatian, 1998) and presence of it can reinforce the synthesized gel.

Considering different curing temperature:

At 40°C: $Y_{40}= 10.51e^{0.02Q}$ ($R=0.721$, $R^2=0.519$, Sig $=0.085$) (4-6a)

At 60°C: $Y_{60}=14.24\ e^{0.02Q}$ (untreated Taftan result was eliminated.)
($R=0.590$, $R^2=0.348$, Sig $=0.11$) (4-6b)

At 80°C: $Y_{80}=12.86\ e^{0.04Q}$ (700°C treated Shahindej result was eliminated.)
($R=0.656$, $R^2=0.430$, Sig $=0.091$) (4-6c)

Where Y=Compressive strength (Mpa) and Q=the percentage of quartz

The number of results is at least (N=12) therefore the degree of freedom would be (N-2=10) and R should be more than 0.576 which has occurred for all of the equations. R^2 shows that this parameter at least justifies the variation more than 34.8% separately and the amount of statistical significance shows that the regression assumption is correct with more than 89% confidence.

4.6 Correlation for Compressive Strength

At first a simplified linear model is proposed to predict compressive strength which incorporates activity index, alkali percentage derived from X-Ray Fluoresence analysis of the untreated and calcined pozzolans and alkali solubility index. Different linear models were tried combining these three parameters with curing temperatures as a variable, as inputs using the least squares technique. It is found that Eq. (4-7) fits the above model. The coefficients of Eq. (4-7) are given in Table 4.4.

$$Y=b_0+b_1Sol+b_2\,(1.77-0.01T^{1.05})^{-1}+b_3\,(1.77-0.01T^{1.05})^{-1}\,Sol+b_4A+b_5\,(0.166-0.001T^{1.06})^{-1}A$$
$$+b_6\,K_{ax}+b_7(-437.84+10.36T-0.12T^2)+b_8(-437.84+10.36T-0.12T^2)K_{ax} \qquad (4\text{-}7)$$

Where Y=Compressive strength (MPa), Sol=Alkali solubility index, A=Alkali percentage, K_{ax}=Activity index, T=Curing temperature (°C) and b_0-b_8 are the coefficients determined by the least square technique.

Figure 4.7 shows typical results of the variation between predicted and observed compressive strength of pozzolans as determined by the above linear analysis. The predicted and observed values are compared in terms of correlation coefficient (R^2). Dropping the variables including Sol, A, and K_{ax} one by one and separately reduces the correlation coefficient from 0.745 to 0.660, 0.706, and 0.614, respectively.

The above simplified linear model has been further developed to a nonlinear form for predicting compressive strength and incorporating three further parameters including loss on ignition, the ratio of dissolution of the main elements, and quartz percentages. The model is developed for 28 days compressive strength of alkali activated pozzolans pastes with the same type and concentrations of alkali at three different curing

temperatures. Different models were tried with combinations of input parameters for the above six models using a least squares technique. It is found that following equations fit well for the above model. The coefficients of Eq. (4.8) are given in Table 4.4.

Non-linear analysis was completed using each relationship data after replacing missing ones and considering curve fits to each parameter with compressive strength to define the primer coefficients. Then considering nonlinear regression the following models was found out and confirmed with back substituting:

At 40°C: $Y_{40}=b_0+b_1Sol+b_2A+b_3.(192.73-1005.99K_{ax}+1358.41K_{ax}^2)+b_42.72^{LOI}(LOI)^{-3.81}$
$+b_5e^{0.02Q}+b_6/(0.03+1866.18K_{alr}-8.77x10^6K_{alr}^2)$ (4-8a)

At 60°C: $Y_{60}=b_0+b_1Sol+b_2A+b_3.(263.3-1443.22K_{ax}+2064.93K_{ax}^2)+b_41.72^{LOI}(LOI)^{-2.42}$
$+b_5e^{0.02Q}+b6/(-0.04+3505.97K_{alr}-17.65x10^6K_{alr}^2)$ (4-8b)

At 80°C: $Y_{80}=b_0+b_1Sol+b_2A+b_3.(357.49-1921.36K_{ax}+2639.98K_{ax}^2)+b_42.02^{LOI}(LOI)^{-3.0}$
$+b_5e^{0.04Q}+b6/(-1.15+60050.58K_{alr}-6.25x10^8K_{alr}^2)$ (4-8c)

Where Y=Compressive strength (MPa), K_{ax}=Activity index, A=Alkali percentage, and Sol=Alkali Solubility Index, LOI=loss on ignition, Q=Quartz percentage and K_{alr}= the ratio of solving main elements measured from leaching test results and b_0-b_6 are the coefficients determined by the least square technique. While dropping the variables including Sol, A, and K_{ax}, LOI, Q, and K_{alr} one by one and separately reduces the correlation coefficient 15%, 1%, 15%, 2%, 2%, and 10%, respectively.

F-ratios based upon the ratio of the model mean squares divided by the mean squared error, which estimates the variance of the deviations around the model, are equal to 9.816, 252.899 and 172.657 for Eq. 4-2a to 4-2c, respectively. Theses amounts for the first and third equations are between standard F-ratio which is more than 9.35 for P=0.1 and less than 199.4 for P=0.005 corresponding to model while the other seems to significant more for P less than 0.005 and error degree of freedom (D.F. for model and error are equal to 7 and 2, respectively). Thus the model is significant.

Figure 4.8 shows typical results of the variation between predicted and observed compressive strength of pozzolans as determined from the above analysis. The predicted and observed values are compared in terms of correlation coefficient (R^2).
Models show that the most important factors are activity index, the percentage of alkali and the alkali solubility index.

4.7 Results and Suggestion

Pozzolans in their natural state and after calcination can be activated and condensed with sodium silicate in an alkaline environment to synthesize a high performance cementitious construction material with a low environmental impact.

The effects that the chemical and phase compositions of natural pozzolans have on the compressive strength of geopolymers made from them have been investigated in this study. It is the properties of the main mineral phases which govern the behaviour of the pozzolans.

By correlating the parameters which give rise to the relationship of pozzolanic activity with compressive strength, a pozzolan containing the sodium zeolite clinoptilolite, such as Shahindej dacite which has high soluble silicates (Table 3.1-a, 3.3-a, 4.1) can be used to prepare a moderate to high compressive strength binder by both elevated temperature curing and calcination.

Calcination seems to impart disorder in hornblende in Sahand pozzolan as its XRD peaks disappear (Figure 3.2-a). The compressive strength of the geopolymer obtained when Sahand pozzolan which contained no amorphous phase and only a small amount of soluble silicate was used.

For the pozzolans which contain more altered minerals such as montmorillonite resulting from the alteration of basic igneous rocks (Ezatian, 1998), as in Sirjan and Rafsanjan, calcination is effective in improving the reactivity of altered minerals, but it also deactivates the amorphous phase and increases the crystalline fraction. Calcination improves the properties of this type of pozzolan. The Sirjan pozzolan which contains

less altered minerals, shows better reactivity at 60°C curing temperature but is not suitable after calcination, while calcination has no significant effect on improving reactivity of the Rafsanjan pozzolan at 60°C curing temperature.

The highest reactivity obtained was shown for Taftan which has the minimum L.O.I. and highest soluble calcium content which was shown to be an important factor in the original mineral according to Xu and Deventer (2000) (Tables 3.3, 4.1). The overall molar ratio of soluble SiO_2:Al_2O_3 is equal to 4.65 and as found out by Rahier and Hos et al. (1996, 2002) is in the range where it is highly unlikely that all of the silica and alumina actually takes part in the synthesis reaction.

With respect to the above results, Taftan and Shahindej Pozzolan were selected for geopolymer cement production and a pilot study was carried on sets of trial mixes of paste, mortar and concrete.

For assessing the pozzolanic reactivity of pozzolans in both natural and calcined forms in terms of compressive strength of the pozzolanic based geopolymer binder, the relationship between compressive strength of alkali activated pozzolans and relevant parameters to its reactivity which include the alkali solubility, alkali content and activity index (Sol, A, K_{ax}) were modelled by a linear power equation and included the effect of curing temperatures. This model was improved by using a non-linear model and considering three further parameters including loss on ignition, the ratio of (SiO_2+Al_2O_3+CaO) in solution to (SiO_2+Al_2O_3+CaO) mineral (obtained from ICP measurements) and quartz percentage (L.O.I., K_{alr} and Q). A good correlation ($R^2 > 0.9$) between predicted and observed values was achieved for this non-linear model.

Table 4.1 ICP results of the filtrates from rapid alkali solubility test measured by the Kavoshyar laboratory in Tehran, Iran

Sample	Si (ppm)	Al (ppm)	Ca (ppm)	Si/Al
Shahindej	49	4	5	12.2
Shahindej dacite-700°C	158	20	3	7.9
Sahand	13	2	4	6.5
Sahand dacite-700°C	33	2	3	16.5
Sirjan	13	1	5	13
Sirjan dacite-700°C	109	8	3	13.6
Rafsanjan	25	2	4	12.5
Rafsanjan dacite-700°C	138	2	2	69
Taftan	14	3	7	4.67
Taftan andesite-700°C	18	2	3	9.0

Note: In the above ICP results of the filtrates from rapid alkali solubility test, the quantity detected for Taftan samples seems to be low which may be due to quick repercipitation of the sample. The ratios of element which seems to be more accurate are more important in diagnosis of suitability of the pozzolan for producting geopolymer.

Table 4.2 The measured parameters used for model input in present study

Material	Kax	A(%)	Sol(%)	LOI(%)	Kalr	Q(%)	S-40 (MPa)	S-60 (MPa)	S-80 (MPa)
Shahindej dacite-raw	0.23	3.26	67.5	10.28	6.92E-05	32	21.92	47.48	81.55
Shahindej dacite-700°C			71.74		2.16E-04	60	42.47	35.32	26.74
Shahindej dacite-800°C	0.227533	3.4	67.49	5.78		37	37.56	37.56	60.43
Shahindej dacite-900°C			61.88				0	6.82	28.88
Sahand dacite-raw	0.35225	6.56	44.86	5.15	2.28E-05	9	5	7.5	7.88
Sahand dacite-700°C			53.51		4.56E-05	25	2.63	8.22	7.13
Sahand dacite-800°C	0.341543	5.31	54.95	2.9		18	19.34	19.34	21.63
Sahand dacite-900°C			67.02				18.98	13.56	32.88
Sirjan dacite-raw	0.290469	4.81	63.75	6.14	2.28E-05	7	12.74	28.88	16.94
Sirjan dacite-700°C	0.335138	5.44	39.13	2.2	1.40E-04	4	8.83	2.79	0
Sirjan dacite-800°C			48.65			3	8.47	8.47	13.14
Sirjan dacite-900°C			52.36				0	2	8.94
Rafsanjan dacite-raw	0.300688	5.66	62.5	4.41	3.66E-05	4	10.09	22.27	20.8
Rafsanjan dacite-700°C			39.8		1.67E-04	5	2.4	2.55	2.57
Rafsanjan dacite-800°C	0.288131	4.4	61.43	2.48		8	26.52	26.52	42.36
Rafsanjan dacite-900°C			52.18				10.73	10.19	14.28
Taftan andesite-raw	0.490514	5.33	56.7	1.85	2.81E-05	6	25.74	53.03	50.08
Taftan andesite-700°C			57.12		2.69E-05		17.84	55.25	63.54
Taftan andesite-900°C			55.43				47.48	48	28.55

The terms are defined in the table of notation and in section 4.5 of the text.

Table 4.3 The replacement of missing parameters used for model input in present study

Material	Kax	A(%)	Sol(%)	LOI(%)	Kalr	Q(%)	S40 (MPa)	S60 (MPa)	S80 (MPa)
Shahindej dacite-raw	0.23	3.26	67.5	10.28	6.92E-05	32	21.92	47.48	81.55
Shahindej dacite-700°C	0.228766	3.33	71.74	8.03	2.16E-04	60	42.47	35.32	26.74
Shahindej dacite-800°C	0.227533	3.4	67.49	5.78		37	37.56	37.56	60.43
Shahindej dacite-900°C			61.88				1	6.82	28.88
Sahand dacite-raw	0.35225	6.56	44.86	5.15	2.28E-05	9	5	7.5	7.88
Sahand dacite-700°C	0.346897	5.94	53.51	4.02	4.56E-05	25	2.63	8.22	7.13
Sahand dacite-800°C	0.341543	5.31	54.95	2.9		18	19.34	19.34	21.63
Sahand dacite-900°C			67.02				18.98	13.56	32.88
Sirjan dacite-raw	0.290469	4.81	63.75	6.14	2.28E-05	7	12.74	28.88	16.94
Sirjan dacite-700°C	0.335138	5.44	39.13	2.2	1.40E-04	4	8.83	2.79	1
Sirjan dacite-800°C			48.65			3	8.47	8.47	13.14
Sirjan dacite-900°C			52.36				1	2	8.94
Rafsanjan dacite-raw	0.300688	5.66	62.5	4.41	3.66E-05	4	10.09	22.27	20.8
Rafsanjan dacite-700°C	0.294409	5.03	39.8	3.45	1.67E-04	5	2.4	2.55	2.57
Rafsanjan dacite-800°C	0.288131	4.4	61.43	2.48		8	26.52	26.52	42.36
Rafsanjan dacite-900°C			52.18				10.73	10.19	14.28
Taftan andesite-raw	0.490514	5.33	56.7	1.85	2.81E-05	6	25.74	53.03	50.08
Taftan andesite-700°C			57.12		2.69E-05		17.84	55.25	63.54
Taftan andesite-900°C			55.43				47.48	48	28.55

Table 4.4 Linear and nonlinear regression coefficients and correlation coefficient (R^2) for pozzolans in natural and calcined form cured at 3 different temperatures

Coefficients	Linear mode	Nonlinear		
		Cured at 40°C	cured at 60°C	Cured at 80°C
b_0	-55.47	-23.117	-57.629	-86.491
b_1	0.334	0.063	0.872	0.711
b_2	28.188	2.000	1.934	7.667
b_3	0.362	1.006	0.795	0.652
b_4	-6.244	-0.279	17.687	33.885
b_5	0.309	-1.310	-4.991	-1.659
b_6	222.53	0.591	0.165	0.269
b_7	-0.154	-	-	-
b_8	0.628	-	-	-
Correlation coefficient (R^2)	0.745	0.933	0.997	0.997

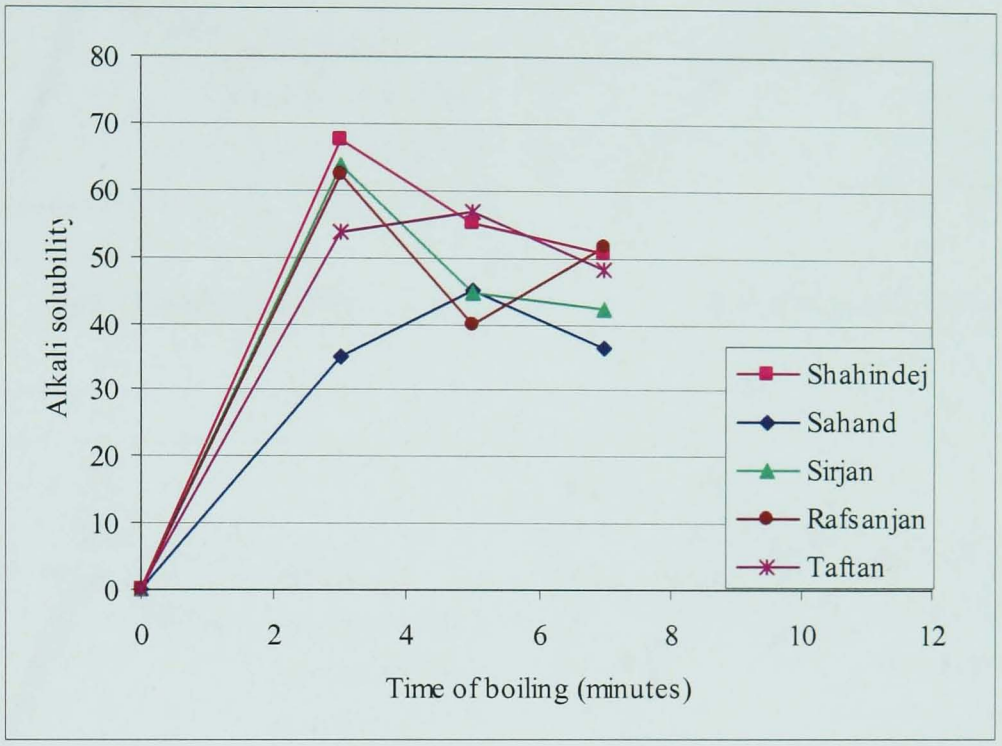

Figure 4.1 Effect of boiling time on alkali solubility of various pozzolans studied in this research

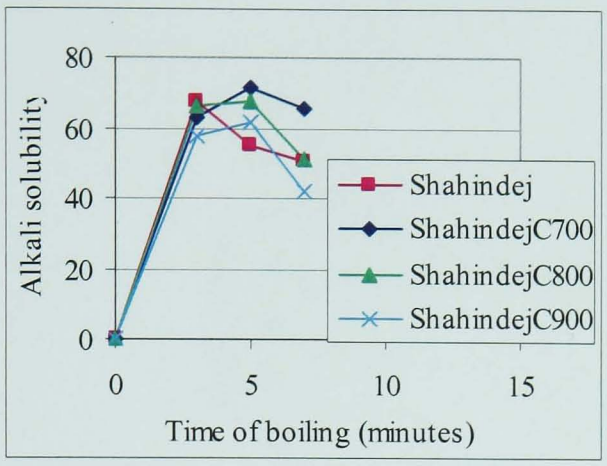

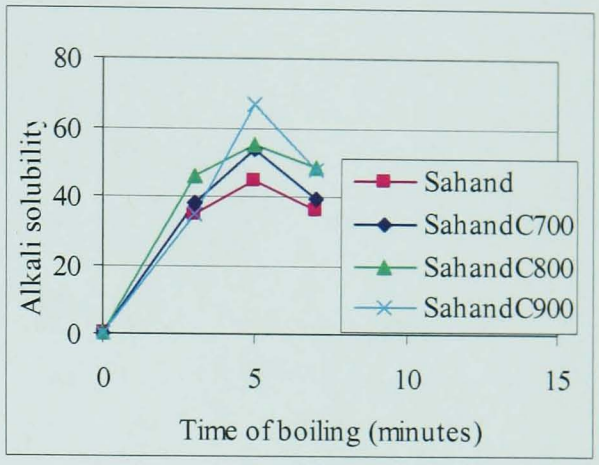

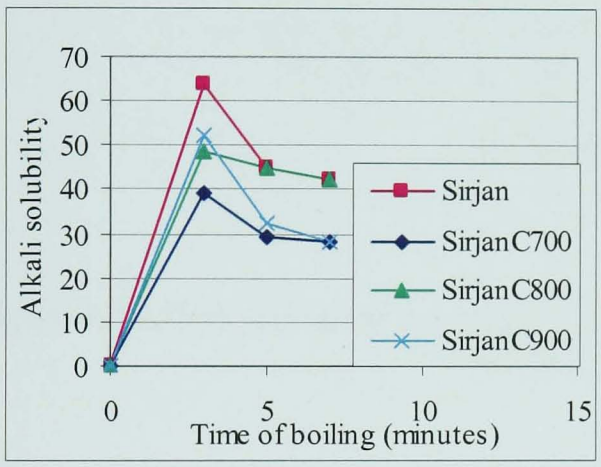

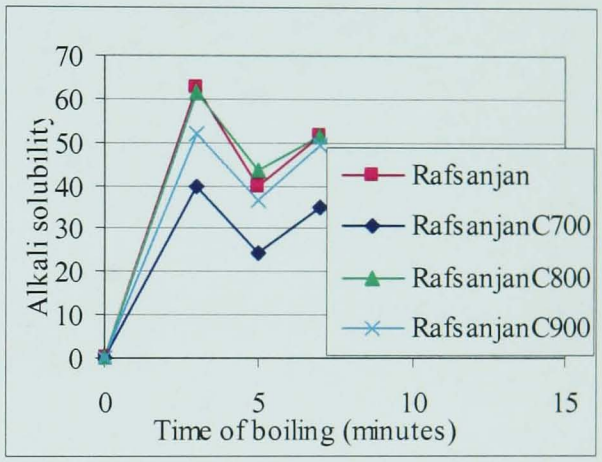

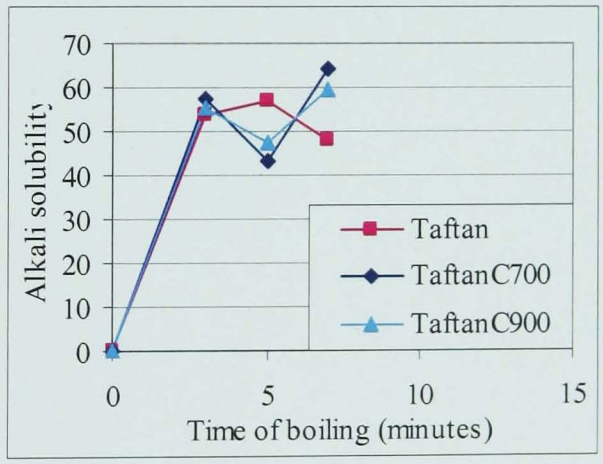

Figure 4.2 Effect of boiling time and calcination on alkali solubility for different pozzolans studied in this research

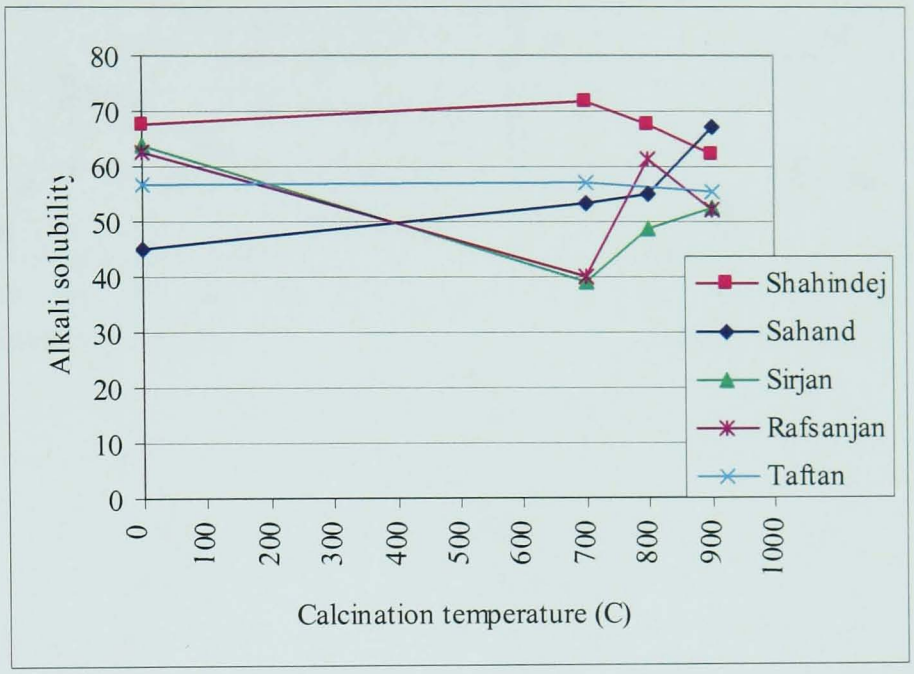

Figure 4.3 Effect of calcination temperature on alkali solubility for different pozzolans studied in this research

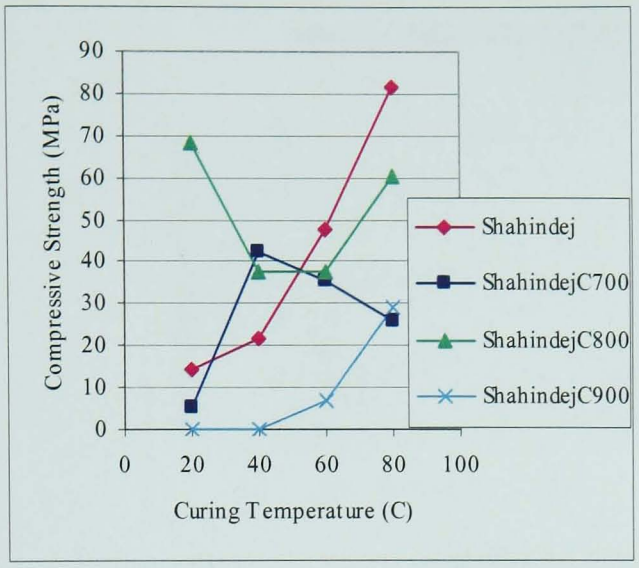

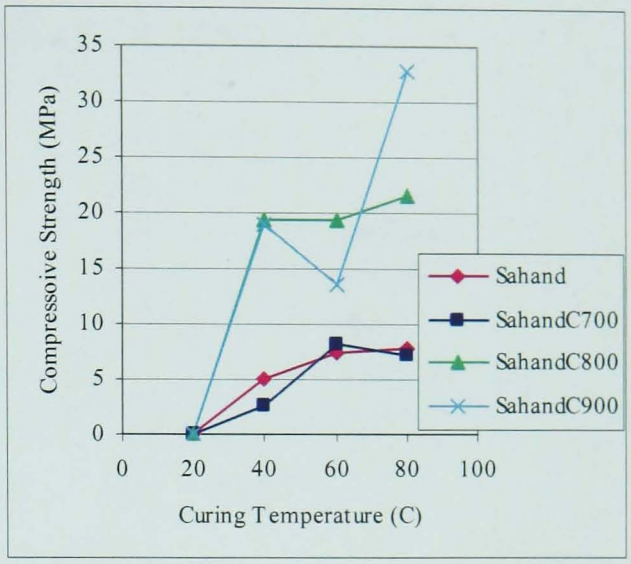

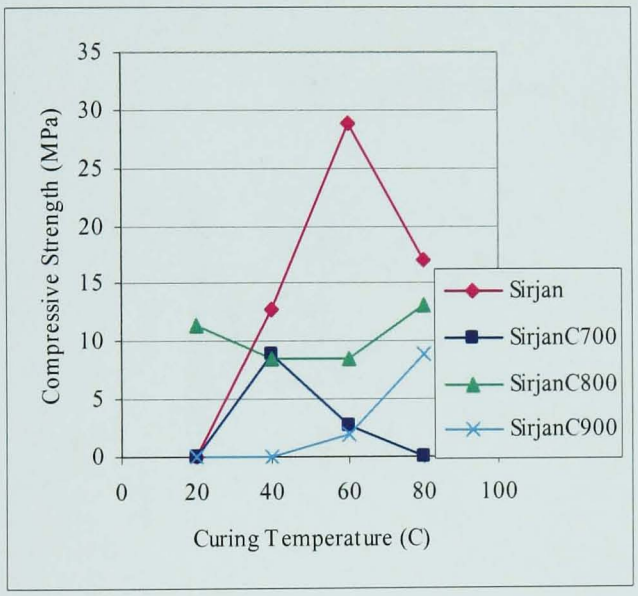

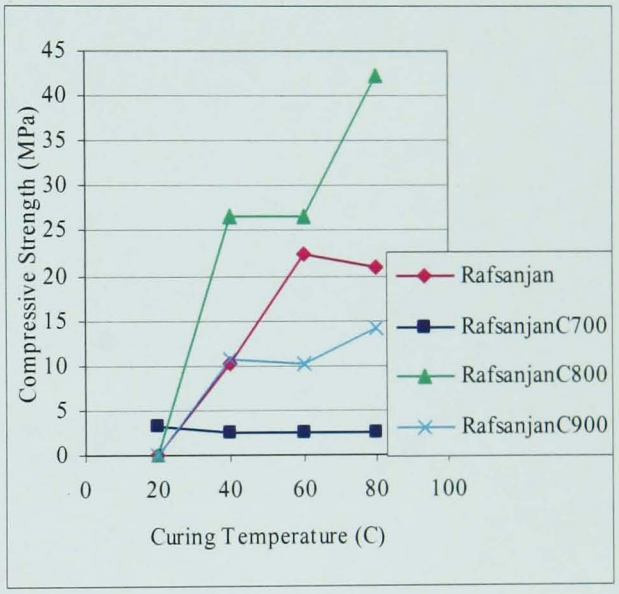

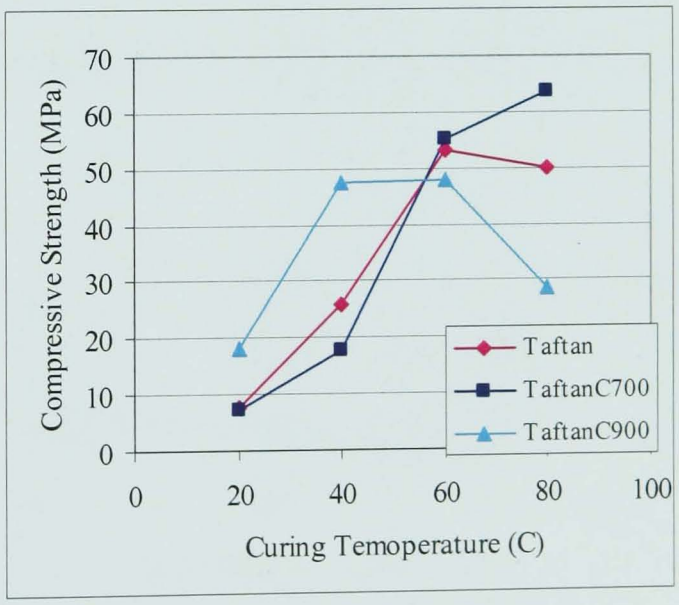

Figure 4.4 Comparing the compressive strength of different pozzolans in natural form or after calcination in various temperatures

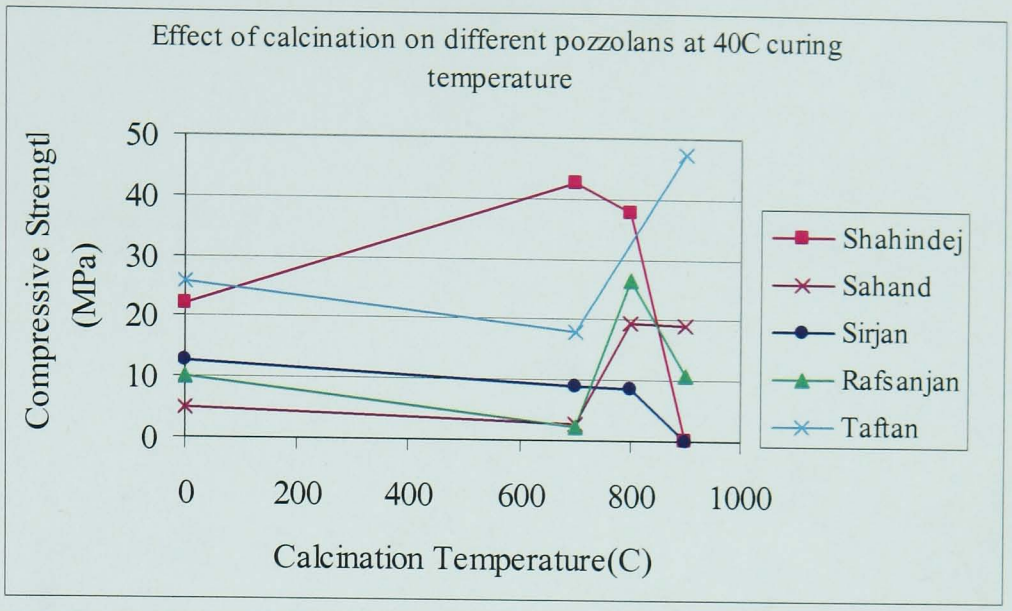

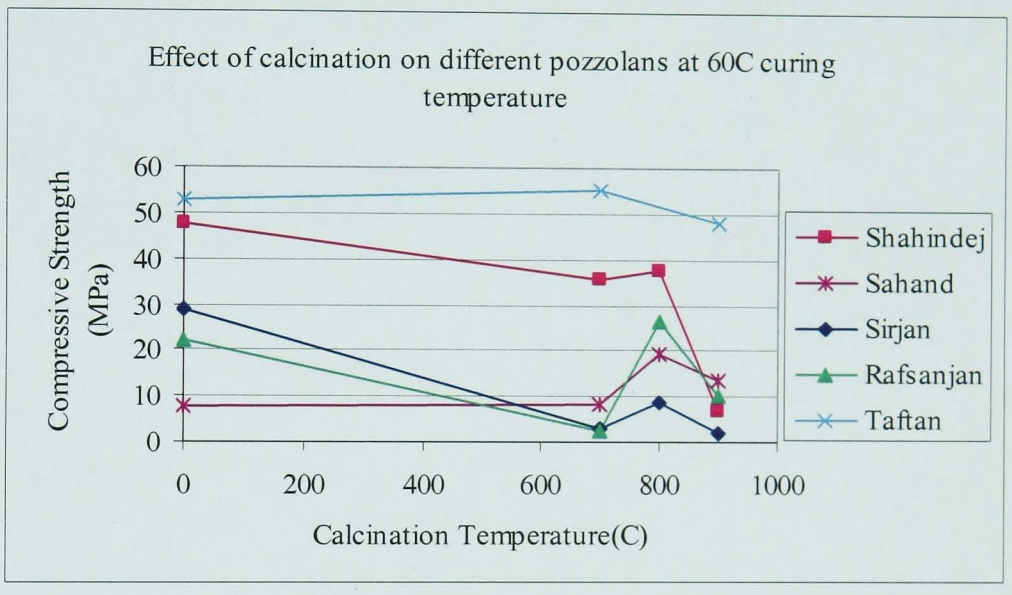

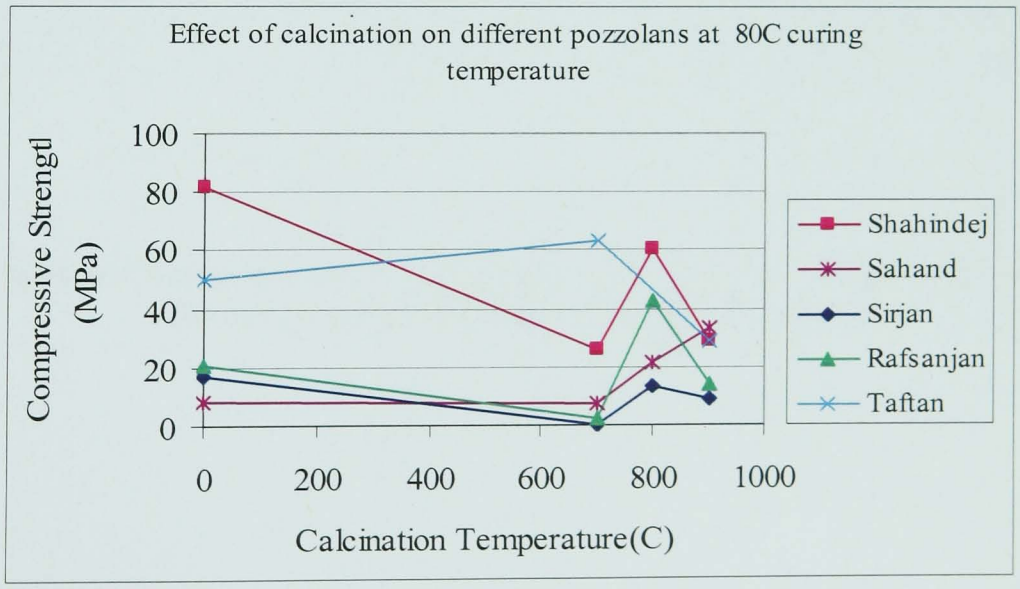

Figure 4.5 Comparison of the effect of calcination on compressive strength of different alkali activated pozzolans at different curing temperature

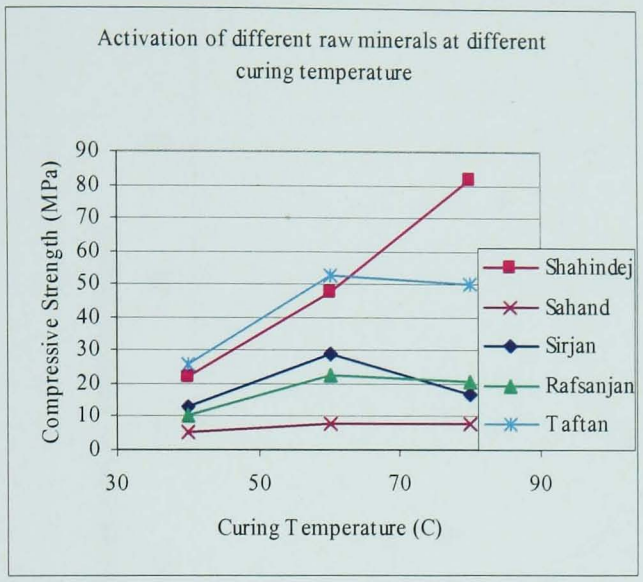

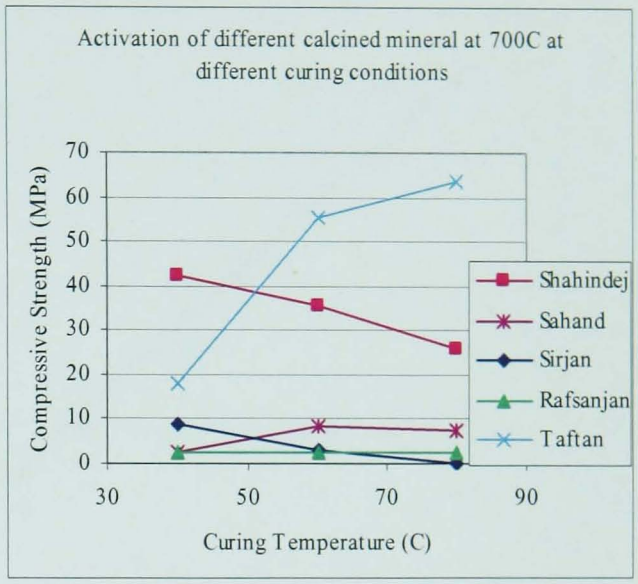

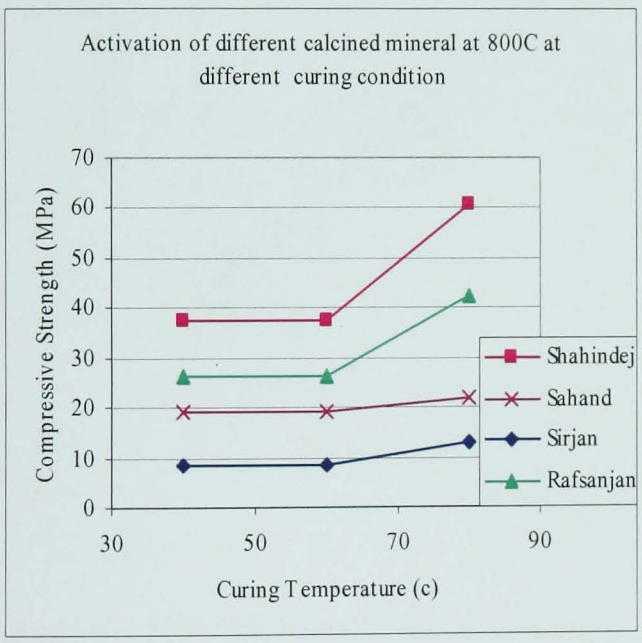

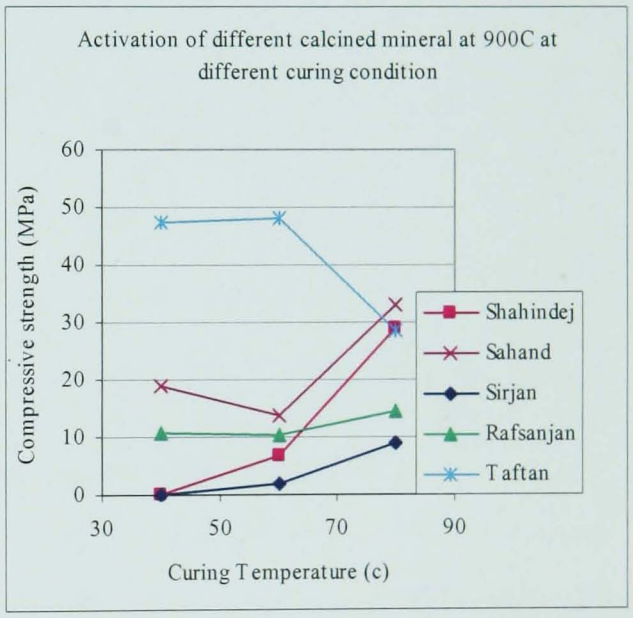

Figure 4.6 Comparing the results of compressive strength of different untreated and calcined pozzolans at different curing temperature

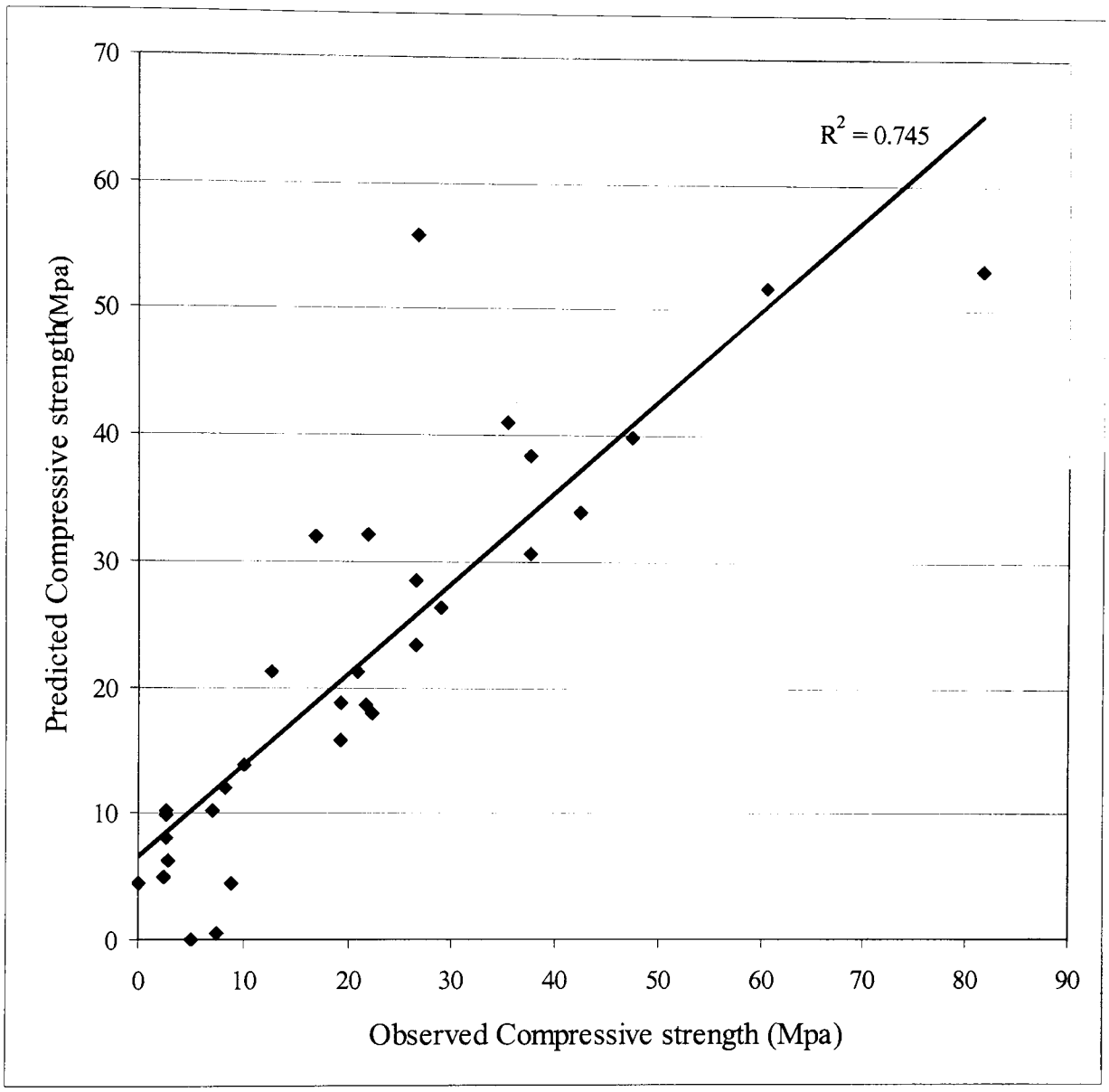

Figure 4.7 Correlation between observed and predicted compressive strength at 28 days for untreated and calcined pozzolans resulted from linear model

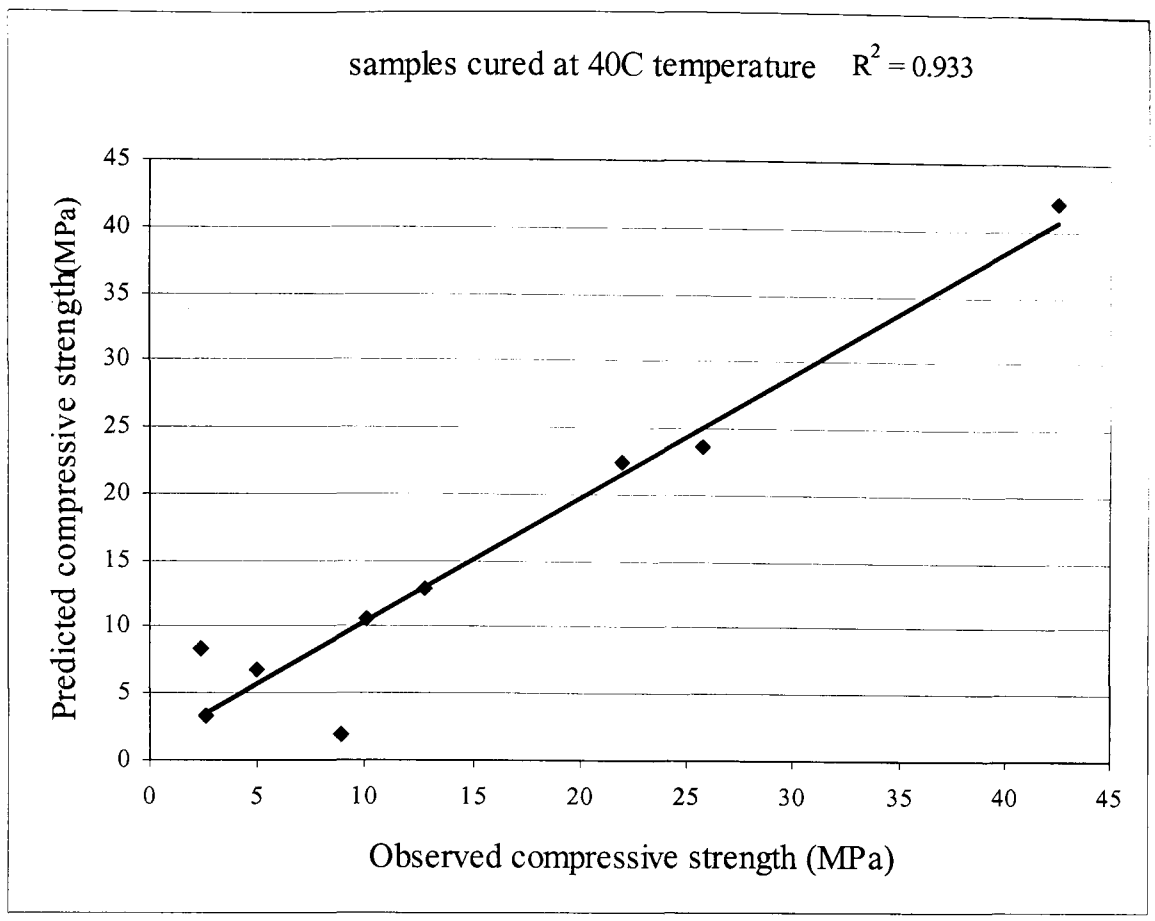

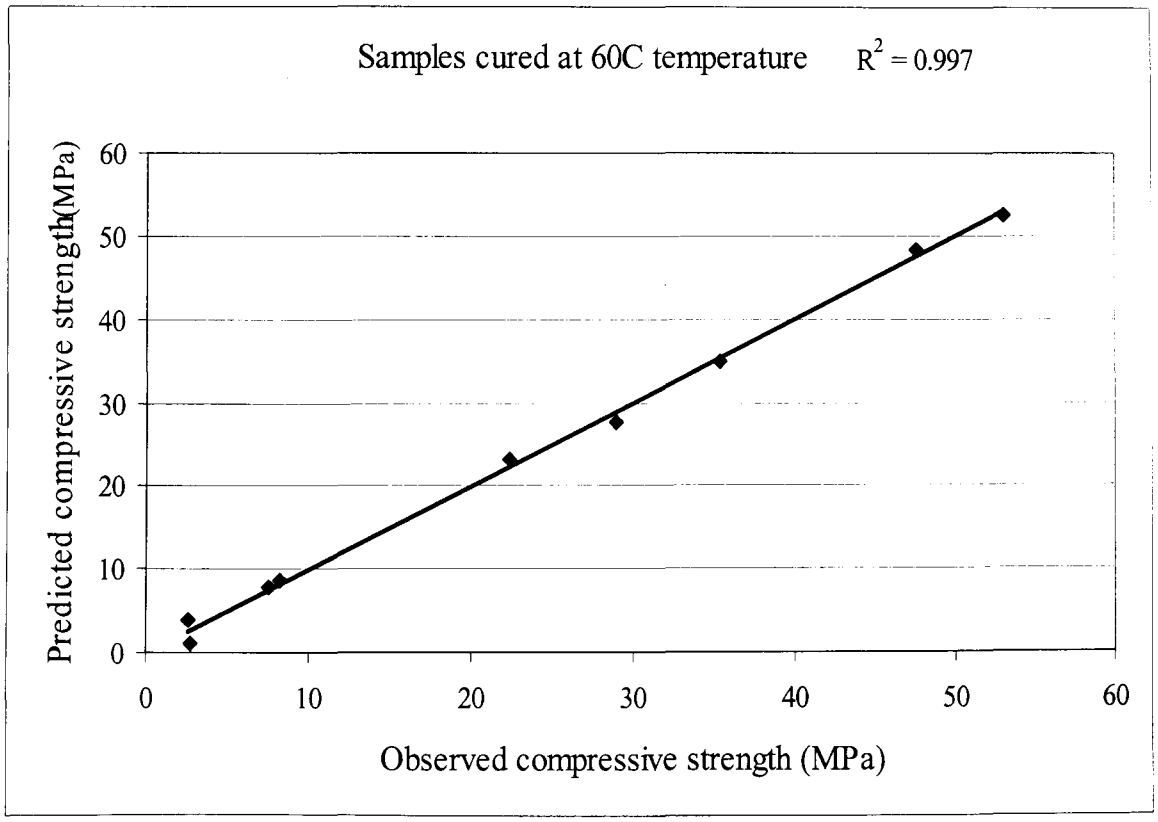

Figure 4.8(a) and (b) Correlation between observed and predicted compressive strength at 28 days for untreated and calcined pozzolans resulted from nonlinear model

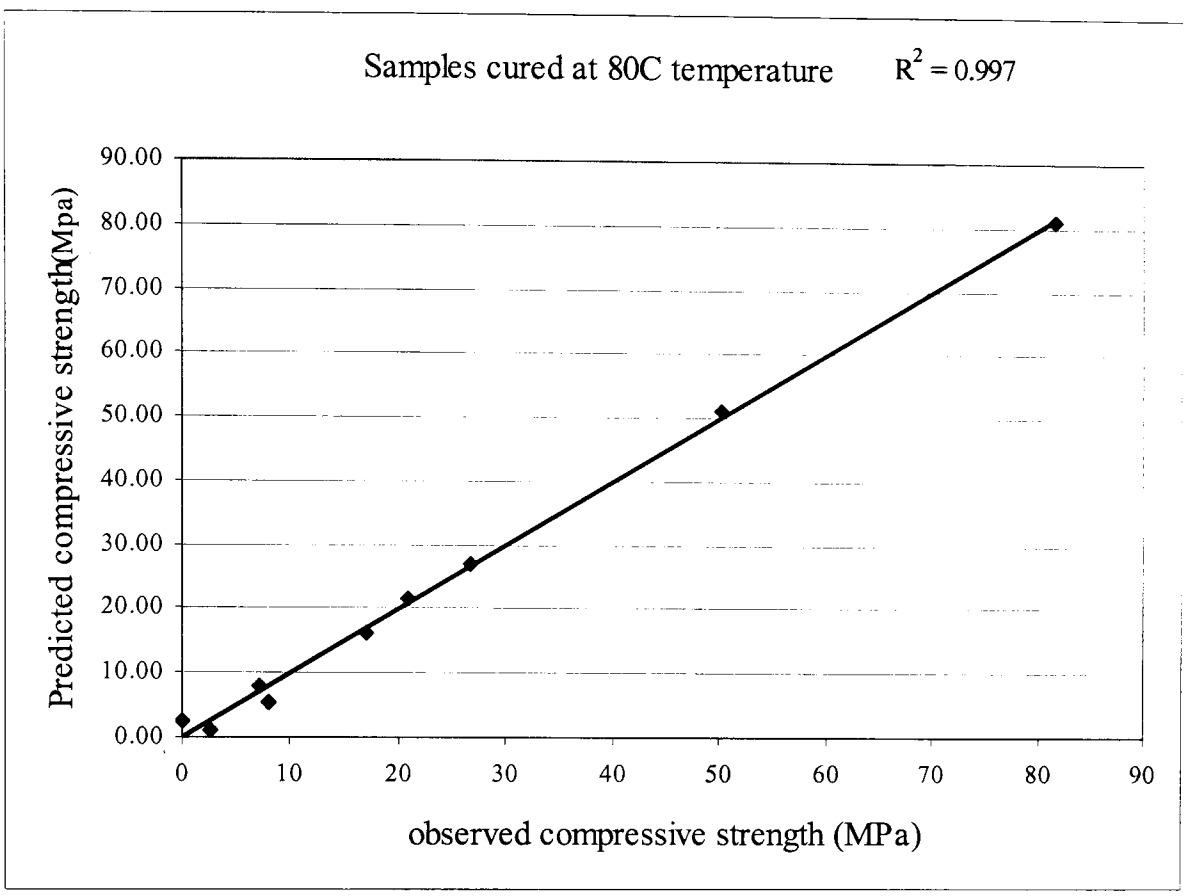

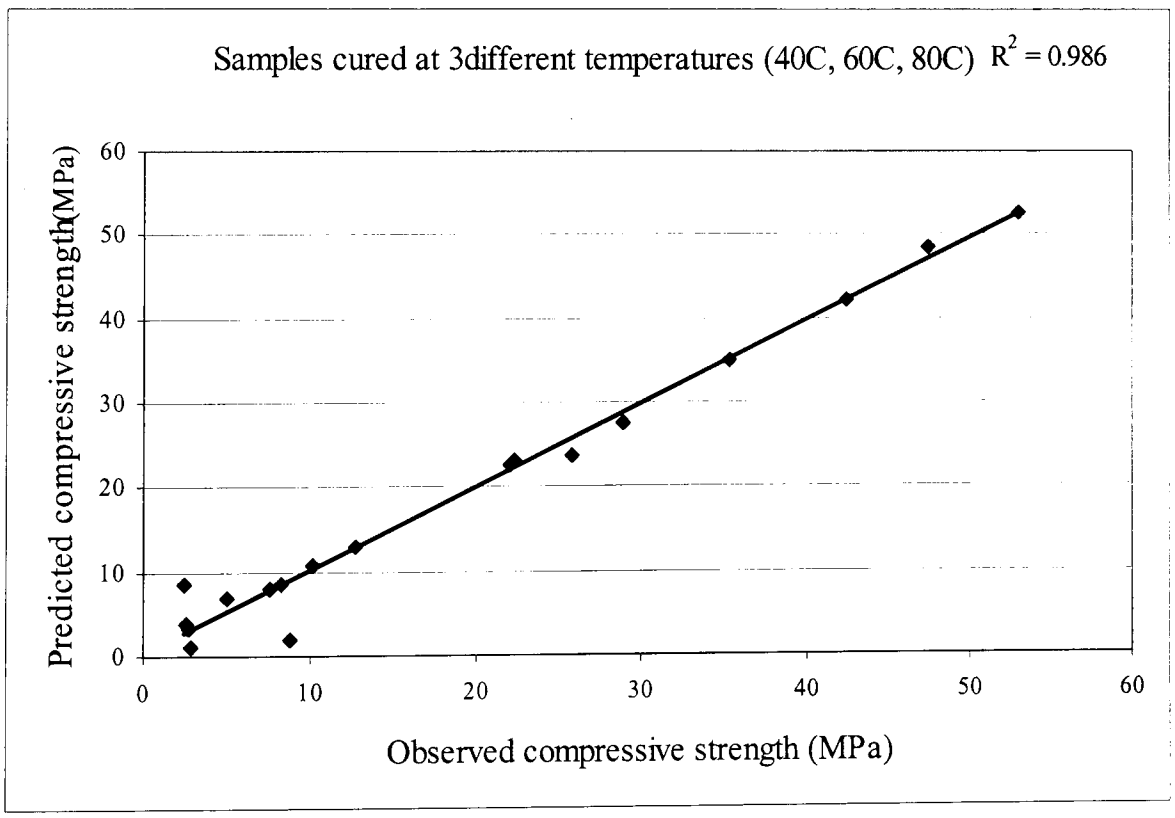

Figure 4.8(c) and (d) Correlation between observed and predicted compressive strength at 28 days for untreated and calcined pozzolans resulted from nonlinear model

5. THE EFFECT OF ALKALI ACTIVATOR TYPE AND MINERAL ADDITIVES ON ALKALI ACTIVATION

5.1 Introduction

The aim of this chapter is to study the effect of alkaline activator type, the form on which it is added, the dosage of alkali, and the SiO_2/Na_2O ratio (silica modulus, Ms) when using water-glass solution at different curing conditions on the geopolymerisation of natural pozzolans. Taftan andesite was selected as the most reactive natural pozzolan in Iran and activation of natural and calcined pozzolan for production of geopolymer binder was verified by the use of Taftan andesite and Shahindej dacite as a solid precursors. The optimum range and features for each factor are suggested based on their effect on compressive strength. The concentration of dissolving silicon, aluminium and calcium in alkaline solution, the formation of gel phase and the factors affecting these have been studied using leaching tests, ICP-AES, FTIR, and SEM/EDX.

In addition, the concept that mineral additives can affect the properties of geopolymer cement is introduced. Taftan andesite was selected as the solid precursor and the effect of adding mineral additives including kaolinite, other calcined pozzolans such as Shahindej pozzolan, and lime on the strength of geopolymer cement was investigated. Scanning electron microscopy (SEM) / energy dispersive X-ray (EDX) was used to determine the composition of gel phase and to compare it to the gel that was produced from alkali-activated Taftan pozzolan without addition of mineral additives.

At the end of this chapter, the optimum proportions of activator, precursor and additive, based on the above investigations aspects, are proposed.

5.2 Chemical Activators and Materials

According to Massazza (2003) activated natural pozzolans have the advantages of lower costs and better concrete durability than OPC in aggressive environments. However, their use leads to a longer setting times and lower early strengths compared to pure Portland cement. Different techniques have been tried to increase the reactivity of natural pozzolans to overcome these disadvantages, including chemical activation,

which is suggested in the literature to be the most effective and cheapest method. Thus, alkali activation of selected materials to produce a geopolymer is considered to continue the research in the direction of chemical activation.

In this investigation the following materials were used as chemical activators to activate the natural pozzolans selected in previous chapter with or without mineral additives:

Potassium or sodium hydroxide (KOH/NaOH) pellets, supplied by MERK International Ltd. These were dissolved to produce the alkaline solutions for geopolymeric paste production.

Sodium silicate, which was provided by Iran Silicate Industrial Company in the form of granules, powder (with SiO_2/Na_2O=2.1) and solution (water glass). The chemical composition of the solution provided by the manufacture was:

a) 12.6% of sodium oxide (Na_2O), 26.5% of silicon oxide (SiO_2) and 60.9% of water; pH=13

b) 11% of sodium oxide (Na_2O), 26.5% of silicon oxide (SiO_2) and 62.5% of water; pH=12.2

c) 8.5% of sodium oxide (Na_2O), 26.5% of silicon oxide (SiO_2) and 65% of water; pH=11.4

The paste was prepared by adding the hydroxide solutions (No. 1 to 8 in Table 5.1) to the natural pozzolans and mixing for 15 min. The mixing was continued with the addition of sodium silicate solutions (No. 9 to 11).

5.3 Experimental investigations

In order to determine the compressive strengths and follow the effect of different activators on alkali activation of natural pozzolans, KOH or NaOH were added with stirring to deionised water to provide the alkaline hydroxide solution and cooled. The samples for alkali activation were prepared by adding alkaline hydroxide solution to pozzolan followed by adding sodium silicate solution. The ratio of alkaline hydroxides (ml)/ alkali silicates Na_2SiO_3 (ml) and total dry mix (g)/total solution (ml) were 7.7 and 3.2, respectively. At first to study the effect of alkaline activator type and dosage, different molarities of alkaline hydroxide equal to 2.5, 5, 7.5, 10 are considered while the properties of sodium silicate solution used corresponded to type (c) in previous

section. In the next stage to find the effect of silica modulus of sodium silicate solution. different types of this solution were used while the molarity of alkaline hydroxide was constant and equal to 7.5molar, found the optimum concentration of alkaline hydroxide for activating natural pozzolans. The mixture was then blended using a Hobart Canada N-50-1425rpm blender. The resulting paste was transferred to polyvinyl chloride (PVC) 50mm cubic moulds and left at room temperature for 24 hr covered by a plastic sheet. After being removed from the mould, three samples for each formulation were cured in an autoclave at 2MPa pressure and 150°C for 3hr. The rest were wrapped and insulated in a special plastic bag (which had been tested and proved adequate to prevent evaporation) and left in the oven to further setting and hardening for 27 days at 40°C and 60°C temperatures. At 28 days, the compressive strength according to ASTM C39 of three samples for each formulation was measured.

The optimum concentration of KOH solution which generated geopolymers with highest compressive strength has been determined and was presented in section 5.4.2. The composition of components dissolved by each concentration of activator in a leach test, were determined by inductively coupled plasma with atomic emission spectroscopy (ICP-AES) carried out at the I.P.P.I. laboratory, Tehran, Iran. For the leaching tests, a specified mass of natural pozzolan (2.5g) was mixed with 25cc of the appropriate KOH (hydroxide pellets 5012 MERK added to deionised water and stirred) solution with molarities equal to 2.5, 5, 7.5, 10 in a polypropylene beaker at room temperature for 5 hours using a magnetic stirrer. The solution and residue were separated by centrifuging for 25 minutes at 6000 rpm. After centrifuging, the clear liquid solution was diluted and neutralized to pH<1 with HCl and analyzed using JY-124 Sequential Jobin-Yvon ICP-AES to determine the concentration of Si, Al, and Ca that had been transferred into the solution so as to generate a gel phase.

In order to investigate the extent of development of alkali-activation of the pozzolans as precipitation reactions, the resultant filter cake from leaching was washed with 200 ml distilled water in two stages broken up, scattered on a watch glass and dried for 48 hrs at 60°C. Pellets were prepared by the common method (0.5mg of dried solid residue

ground to fine powder and 150mg of KBr) dried in an oven at 60°C over night and pressed in to a disc before scanning. The powder was analyzed by a Bruker Equinox55FTIR spectrometer with an aperture selected at $8cm^{-1}$ and a total of 64 scans in each spectrometer in the I.P.P.I. laboratory in Tehran, Iran.

In order to study the effect of mineral additives as compensation for the lack of mineral elements (Si, Al and Ca), three additives, kaolin, calcined Shahindej pozzolan, and lime were chosen as the mineral additives and added to Taftan pozzolan before activating, to observe how they affected the compressive strength and the composition of the gel phase and its structure; kaolin SL-KAD has a particle size of 66% less than 2μm and 0.1% greater than 45μm,; Shahindej pozzolan from NW of Iran, (particle size of 100% less than 75μm) used to produce Portland pozzolan cement by Ourmia Cement Factory was calcined at 800°C for 12hr; and burnt lime with the same particle size were used. Chemical compositions of the mineral additives were analysed by X-ray Fluorescence (XRF) analysis at the Kansaran Binaloud X-ray laboratory in Tehran, Iran using a Philips PW 1480 instrument and are shown in Table 5.4.

In order to determine the compressive strength and follow the effect of adding different minerals to natural pozzolans, The samples for alkali activation were prepared by mixing Taftan natural pozzolan with or without the mineral additives above at different ratios (the mineral additives were dry mixed with Taftan pozzolan at specified mass ratios for 5 minutes) before the addition of the potassium hydroxide solution to the pozzolan followed by the sodium silicate solution and pursued the same as the first paragraph of this section unless the samples were cured at room temperature (25°C).

To investigate the microstructure of pastes, samples were cut by a diamond wheel saw from the epoxy-impregnated cubes, polished and carbon-coated for examination by scanning electron microscopy and microanalysis (SEM and EDX) using a Cambridge 2000EX scanning electron microscope equipped with EDX analysis system at the Material and Energy Research Centre laboratory, Tehran, Iran.

5.4 Experimental results

5.4.1 Type of Alkaline Activator

From Figure 5.1 it can be seen that activation with KOH always achieved higher compressive strength at ambient temperature curing conditions, especially at 60°C, compared to NaOH activation. According to Xu and Deventer (2000) as Na^+ and K^+ have the same electrical charge; their different effects must be the result of their different ionic sizes. The smaller size cation, Na^+ favours an ion-pair reaction with smaller silicate oligomers. The use of K^+ is expected to result in the formation of large silicate oligomers which is favourable from the strength point of view due to the greater condensation of the resulting gel phase. Consequently, aluminosilicates demonstrate higher compressive strength after geopolymerisation in KOH than NaOH. However, from the cost view point, the use of NaOH rather than KOH may be more desirable, especially under conditions of accelerated curing. Figure 5.1 shows that the same compressive strength (44.0Mpa) has been achieved using 5Molar NaOH compared to 7.5Molar KOH in autoclave curing.

5.4.2 Dosage of Alkali Component

The compressive strength of geopolymer cements made from Taftan pozzolan activated with either KOH or NaOH at concentrations of 2.5, 5, 7.5, 10M are shown in Figure 5.1. KOH concentrations in the range of 5-7.5M were found to generate geopolymers with the highest compressive strengths. The results of the ICP-AES tests are shown in Table 5.2. At 7.5M KOH, the optimum concentration for strength development, 274.4 and 68.22 ppm Si and Al, are dissolved respectively. Increasing the alkali concentration to 10M did not have a significant effect on the levels of Si and Al leached.

With lower activator concentrations (i.e. less than 5M KOH) there is significantly lower dissolution of natural pozzolan (see Table 5.2) resulting in the formation of a gel phase with lower binding strength. However, the higher viscosity of the alkaline hydroxide solution at concentration greater than 7.5M means that the resultant geopolymer pastes need a longer time and/or a higher temperature for the excess water to evaporate from

the system before forming a monolithic geopolymer, in which full strength is gained due to the development of the 3-D network of aluminosilicate. Thus, the alkali content reaches a certain value (which depends on mineral type, activator type and curing condition), beyond which there is no further significant increase in strength, and according to Xu and Deventer (2000) detrimental features such as efflorescence and brittleness may arise due to the increased free alkali content in the product. Therefore, trying to increase the strength by increasing the alkali dosage is not recommended, from both economic and properties points of view.

Some additional tests and elemental analyse were carried out on alkali activated Taftan pozzolan to understand the gel conformation and its composition. Figure 5.2 depicts the FTIR spectra recorded for Taftan powders before and after leaching in 2.5, 5.0, 7.5M KOH. Before leaching there were two main peaks at 1032 and 1089 cm^{-1} with several smaller peaks. After leaching, the band centred at $1032cm^{-1}$ is shifted towards a lower wave number with increasing alkali concentration showing that as the silicate and/or aluminosilicate structures in the natural pozzolan are significantly depolymerised based on electrostatic reactions.

According to Lee and Deventer (2003), during alkali activation every bridging oxygen atom (BO) on the surface of the original aluminosilicate is replaced by two negatively charged non-bridging oxygen atoms (NBO), which are charge compensated by alkalis. As a result, the infrared (IR) band attributable to the T-O-Si asymmetric stretching vibration of the TO_4 tetrahedral of an alumino silicate in glass has been found to shift to lower energy with increasing alkali content. The shift observed for Taftan pozzolan in Figure 5.2 would suggest that on leaching, all the polymerised alumina-silicate has dissolved leaving layered silicates with a number of siloxyl groups since this corresponds to stretching vibration which is corroborated by the wave number equal to $995cm^{-1}$ and its structure is exclusively formed by Si-O-Al bridges.

Generally, the mid IR of these pozzolans contains a number of peaks from 800 to 1200 and the surfaces display a substantially higher degree of Al-Si disorder with bands

becoming broader. This phenomenon suggests that the disordering of the primary structure of aluminosilicate and conforming de-polymers during the treatment could result in some type of Al-Si precipitates forming on the surfaces of un-reactive Taftan pozzolan particles.

All samples display a new absorbance in the region of 1404-1471cm^{-1} which increases after leaching (Figure 5.2). This absorbance could be due to a vibration of carbonate salts formed on the surface of the residues (Lee and Deventer, 2003) and with the band around 870cm^{-1} it might imply that some type of hydrated carbonates and K^+ related aluminates are precipitated on the surfaces of the residues produced during leaching.

The standard molar oxide ratio of SiO_2/Al_2O_3 in geopolymer composition were suggested by Davidovits et al. (1994) to be between 3.3 and 6.5 for finished product (in Jaarsveld et al, 1997, Rahier et al. 1996, 1997, Hos et al., 2002). This seems to be optimized for simplicity and potential to approach full reactivity while a variety of composition may be chosen for the fully reacted mixture (Kriven et al., 2003). In this work, the "standard" geopolymer composition given by Rahier et al. (1996), Barbosa et al. (2000) and Hos et al. (2002) was followed and scanning electron microscopy (SEM)/energy dispersive X-ray (EDX) was used to determine the chemical composition of the gels made from Taftan pozzolan activated with KOH at concentrations of 5 and 7.5, which were found to generate the geopolymers with a higher compressive strength and optimum leaching in the previous tests, in order to compare to the standard to confirm that certain composition criteria have been met for geopolymerization to occur. Table 5.3 lists the SEM/EDX results for the mean compositions of the gel phases of three samples of Taftan pozzolan. It is found from Table 5.3 that for Taftan activated with 5M and 7.5M KOH Sealed at 40°C, and Taftan activated with 7.5M KOH and cured in an autoclave at 2MPa, respectively, the mean ratios of weight percentage concentration for SiO_2 to Al_2O_3 are 5.3, 4.7, and 5.3. Thus in all of the three samples, the standard composition criteria have been met for geopolymerization to occur.

Activation of Shahindej pozzolan with 5, 7.5, 10 and 15M KOH gives the compressive strengths shown in Figure 5.3 at two different curing temperatures with the highest strength of 32.2MPa at 40°C and 56.2MPa at 60°.

Figure 5.4 depicts the PAS-FT-IR spectra recorded for Shahindej powders before and after leaching in 7.5M KOH. The spectrum before treatment contained one main peak at 1055 cm^{-1} which display Al-O-Si and Si-O-Si stretching bands. After leaching, the vibration band for untreated Shahindej pozzolan with its maximum at 1060cm^{-1} is shifted to a lower wave number. Therefore, the original silicate and/or alumina-silicate structures in the natural pozzolan have been significantly depolymerised based on electrostatic reactions.

5.4.3 Form of Sodium Silicate Activator

There are three forms of sodium silicate, granular, powder and solution. The present work confirms that higher strengths are obtained when sodium silicate is added as a solution (strengths of 20.7 and 43.0MPa corresponding to 40 and 60°C curing temperatures respectively) than when it is added in solid state by powder forms (strengths of 15.3 and 41.7MPa corresponding to 40 and 60°C curing temperatures, Fig. 5.5). The addition of solid alkali silicate not only results in lower strength but also produces much greater strength fluctuation, which can be attributed to lower solubility in the mix and availability of alkali for reaction. The solid alkali silicate might absorb moisture during storage which will inhibit its activating action. Another interesting point is that using hydrous water-glass / sodium meta-silicate containing chemically bound water in the solid form produces low strength 11MPa (Fig. 5.5) under normal curing conditions equal.

5.4.4 Modulus of Water-glass Solution

The most important property of sodium silicates is the molar ratio of SiO_2 to Na_2O. Silicates are commercially produced in the SiO_2:Na_2O ratio range of 1.5 to 3.2. In general, high ratio silicates (i.e. 3.2) are most suitable for chemical bonding since it is the siliceous portion of the silicate that reacts with cations. Due to the importance of

maintaining a high alkali concentration, it has been recommended that lower ratio silicates, e.g. (2.0), are used for activation of pozzolans (McDonald and Thompson, 2004).

In the present work, three industrial sodium silicate solutions with SiO_2/Na_2O ratios of 2.1, 2.4 and 3.1 were used to form geopolymers with two samples of Taftan pozzolans which contained 8% and 15% CaO (Table 3.4). It was found that the pozzolan with higher CaO content gives rise to higher strengths (maximum 28days compressive strength of 43.0MPa) with a SiO_2/Na_2O ratio of 3.1. However, for the natural pozzolan with the lower content of CaO it is the amount of alkali that is more important for activation (Figure 5.6).

Figure 5.7 shows that for pozzolans containing sodic zeolites such as Shahindej dacite that are not thermally treated and which exhibit high soluble silicate, lower SiO_2 to Na_2O ratios give higher strengths (at 28days the compressive strength is 39.0MPa with SiO_2/Na_2O equal to 2.1) but when calcined the reverse is true (at 28days, the compressive strength of 33.4MPa was obtained with the SiO_2/Na_2O ratio of 3.1). However, beyond 40 days the best compressive strengths were obtained with higher amounts of silicate in the system so at 90days the compressive strengths were 49.7MPa and 39.8Mpa respectively, both with a SiO_2/Na_2O ratio equal to 3.1.

The study of geopolymers produced based on untreated and calcined Shahindej pozzolan with different amounts of water-glass ratio using X-ray diffraction and comparing the results, confirms the above results as is presented in Figure 5.8. It can be observed that for calcined Shahindej when the water-glass with the SiO_2 to Na_2O ratio of 3.1 is used, the intensity of peaks is less and more activation is occurred while this happens for untreated Shahindej when the water-glass with the SiO_2 to Na_2O ratio of 2.1 is used.

5.4.5 Various Ratios of Alkaline Hydroxide to Water-glass

To study the effect of different contents of sodium silicate on improving the compressive strength, mixes were prepared with different volume range of sodium silicate solution from 0.15 to 1.0cc while the concentration of potassium hydroxide and water content

were keeping constant and the compressive strength was measured. This was repeated for different concentration of alkaline hydroxide (KOH). The effect of Na_2SiO_3 on the development of compressive strength (Figure 5.9) shows that the optimum amount of Na_2SiO_3 for achieving strength in a range suited for structural concrete is 0.25cc to 0.5cc. The ratios of the alkaline hydroxide (KOH) to sodium silicate in the above mixes were calculated and the strength contours versus different molarities of KOH and various ratio of KOH/Na_2SiO_3 are shown in Figure 5.10 and 5.11. The islands of ideal compositions show that the minimum ratio of KOH to Na_2SiO_3 volume corresponding to the optimum concentration of KOH for achieving high compressive strengths are 7.1 and 7.7 for Taftan and Shahindej pozzolan, respectively. The reason for conforming three islands of ideal compositions in Figure 5.11 might be that different molarities of KOH against various ratio of KOH/Na_2SiO_3 provide various circumstances for different relative amounts of SiO_2 and Al_2O_3 of the Shahindej pozzolan to be solved. This phenomena affects on the chemical reaction of alumina-silicate oxides with alkali yielding polymeric Si-O-Al bonds with different dimensional silico-aluminate structures such as Poly(sialite) (-Si-O-AL-O-), Poly(sialate-siloxo) (-Si-O-Al-O-Si-O-), or Poly(sialate-disiloxo) (-Si-O-Al-O-Si-O-Si-O-) with different Al and Si building blocks, which affect the chemical and physical properties of the final product. Considering the price of KOH and Na_2SiO_3, the minimum ratio was found to be the most adequate from the economical point of view.

5.5 XRD Results for Geopolymerised Alkali Activated Natural Pozzolans

The study of geopolymers using X-ray diffraction as mentioned by Jaarsveld and Deventer (1997) is made difficult by the fact that a large part of the structure is amorphous to X-rays. Nuclear Magnetic Resonance (MAS-NMR) spectroscopy provides some insight into the molecular framework (Lee and Deventer, 2003) but as this was expensive and inaccessible, so X-ray diffraction analysis was carried out to monitor the progress of activation of natural pozzolan. X-ray diffraction chart traces for geopolymerisation of alkali activated natural pozzolan pastes at age of 28 and 90 days are shown in Figures 5.12 to 5.14.

X-ray diffraction of alkali-activated Taftan pozzolan during the aging process indicates that the intensity of peaks related to albite, a major feldspar phase at $20 \leq 2\Theta \leq 30$ have decreased up to 50% with respect to those for untreated Taftan pozzolan after 90 days and the peaks related to quartz and the crystalline phase related to hornblende have decreased so these minerals appeared as a minor phase only (Figures 5.12(a) and (b)).

Figure 5.13 shows that for alkali activated untreated Shahindej cured at 60°C, the reduction of the intensity of peaks related to clinoptilolite shows that the maximum reaction depends on this mineral. While the intensity of peaks related to quartz and albite decline slightly after 90 days. It seems this type of pozzolan takes time to react, although comparing Figures 5.13(a) and 5.13(b), shows that the rate of the reaction is quicker at early ages.

X-ray diffraction of calcined Shahindej cured at 20°C shows that the intensity of peaks related to quartz have decreased by 10% while the peaks related to albite declines by about 30% after 90 days and the reduction of the peaks related to clinoptilolite and calcite bring these minerals to appear as a minor phase (Figures 5.14(a) and (b)).

Thus the above results indicate that as the material ages, the reactions of silica, alumina and alkali produce the geopolymerisation reaction resulting in reduction in the crystalline phases and increase in the amorphous.

5.6 The Effect of Mineral Additives

The aluminosilicate used for the production of a geopolymer cement must contain Al which is readily soluble with an overall molar ratio of Al_2O_3:SiO_2 lying between 1:3.3 and 1:6.5 (Jaarsveld et al, 1997, Rahier et al. 1996, 1997, Hos et al., 2002). However, these ratios are not critical and are for the most part only an indicator of approximate composition. The reason for this is that while these compositional ratios are based on chemical analysis, but it is highly unlikely that all of the silica or alumina actually take part in the synthesis reaction (Jaarsveld and Deventer 1996). Often the rate of dissolution of Al from natural aluminosilicates is insufficient to produce a gel of desired composition (Xu and Deventer, 2000). Kaolinite is a relatively inexpensive

aluminosilicate which might be used as a secondary source of soluble Si and Al when added to natural pozzolans to synthesize geopolymers. Consequently, when an optimum amount of kaolinite is added to natural aluminosilicates activated by alkaline solutions, a desired gel composition can be produced with a longer setting time. However, if kaolinite on its own is used without the presence of other natural minerals, a weak structure is formed.

Additionally, the calcium content is also an important factor affecting the setting time and final strength in concrete, and there are indications that it may also affect the properties of geopolymers (Xu and Deventer, 2000). Therefore by adding an optimum amount of CaO content to a natural aluminosilicate may also increase the strength of an alkali-activated natural pozzolan.

Natural pozzolans are geological deposits with a wide range of chemical compositions which vary from batch to batch but they are usually high in available SiO_2. Deficiencies in the SiO_2, Al_2O_3 and CaO content in a natural pozzolan might be compensated for by adding mineral additives, such as kaolinite or lime enabling them to be used as a geopolymer cement.

In the present section, to determine the effect of active mineral additives on compressive strength in geopolymer cements and to describe the behaviour of their reaction, the method of specific strength determination (SS) devised by Pu (1999) was carried out. Specific compressive strength can be defined as the contribution 1 wt% of a natural pozzolan makes to the strength of a geopolymer cement at 28 days. It equals the real 28 days compressive strength divided by the percentage of the natural pozzolan, namely Taftan, in this research. The results are given in Table 5.5 and Figures 5.15 to 5.17 for the different mineral additives. At 28 days of age, the specific strength increased when mineral additives were used compared to activation of pure natural pozzolan as a geopolymer cement at room temperature. It can be seen that for each mineral additive there is an optimum addition although it does depend on temperature. Specific strength is also increased with an increase of aluminium or calcium containing additives up to

that optimum amount after which increasing the amount of mineral additive has no significant effect on the increase of the specific strength.

The strength of a geopolymer cement containing active mineral additives can be considered to consist of two parts. The main contributor to strength for this type of cement is the polymerised Al and Si network obtained from the reaction between active silica and alumina oxides in the main pozzolan. Addition of the active mineral additives provides additional aluminium or silicon to enhance the three dimensional amorphous and/or semi-crystalline polymer structures with alkali metal cations compensating the negative charges caused by Al substitution. The secondary part of strength is contributed by formation of semi-crystalline tobermorites (C-S-H) or calcium aluminosilicate hydrates (Pu, 1999). In this research, kaolinite and calcined Shahindej pozzolan have been used as mineral additives to provide additional aluminium and silicon sources. The maximum strength which resulted when 20% kaolinite was used giving 45.6 and 19.3MPa for autoclave and sealed curing at 25°C, respectively. Similar results were obtained by adding 16.7% calcined Shahindej pozzolan as an additive where 45.6 and 25.3MPa were obtained for autoclave and sealed curing at 25°C, respectively. Using burnt lime the maximum strength resulted when 3.4% lime was used giving 27.8 and 19.6MPa for autoclave and sealed curing at 25°C, respectively (Table 5.5).

Figures 5.18, 5.19, 5.20, and 5.21 show some of the microstructural characteristics as seen by SEM of the binder obtained resulting from the alkaline activation of a natural pozzolan with and without addition of different minerals, and cured at both 25°C and autoclave conditions. The samples studied have quite different microstructures. Autoclaving samples has made the structure micro-crystalline, dense and this resulted in higher strength. EDX results were measured for three points within the gel and the average is shown in Table 5.6. It can be observed that in all of the samples, the standard composition criteria have been met for geopolymerization to occur. In Table 5.6, the increase of the SiO_2 content in the autoclaved samples can be explained by an increased dissolution of the pozzolan upon autoclaving. The percentage of reacted pozzolans can be found by dividing the weight percentage of silicon concentration observed in the

binders (Table 5.6) by the total amount of the silicon content in the Taftan pozzolan and the mineral additives, considering the optimum percent of mixture, in each case (Table 5.4 and 5.5). It should be mentioned that the reacted pozzolan in different formulation gives rise to the geopolymer gel, zeolites and calcium silicate hydrate in the different cases.

When Taftan pozzolan was activated after mixing with kaolinite as an aluminum source, this produced an impermeable sticky gel. Autoclave curing at 2MPa pressure and 150°C for 3hrs resulted in a more uniform microstructure for the gel produced (Figure 5.19-b). The average molar ratios for the reaction product when the sample was cured at 25°C, were SiO_2/Al_2O_3=3.1 and K_2O/Al_2O_3=1.1 while for autoclave curing, the K_2O/Al_2O_3 ratio decreased to 0.59. The aluminium oxide content was increased in the finished product compared to that of Taftan pozzolan activated without adding kaolinite (Table 5.6).

The binder obtained from the activation of Taftan pozzolan and calcined Shahindej is more porous than when mixed with kaolinite but it still has a uniform texture (Figures 5.19-a and 5.20-a). Using the Taftan and calcined Shahindej mix to produce geopolymers seems to show the best gel. When autoclave cured this shows a uniform micro crystalline texture. Thus autoclave curing seems to produce a zeolitic form that consists of a potassium aluminosilicate (Figure 5.20-b and Table 5.6). The average molar ratios found in this reaction product when cured at 25°C, were SiO_2/Al_2O_3=4.58 and K_2O/Al_2O_3=1.31 while for autoclave curing, the SiO_2/Al_2O_3 ratio increased to 4.96. The silica content was increased in the finished product compared to when Taftan pozzolan was activated without adding calcined Shahindej (Table 5.6).

The type of additive mineral used affects the development of reactions. When $Ca(OH)_2$ was used as an additive, the materials obtained following activation showed the co-existence of a geopolymer formed from natural pozzolan particles which had reacted with the alkali forming a potassium aluminosilicate gel together with a calcium silicate hydrate and particles of calcium carbonate likely to form from the carbonation process when calcium hydroxide reacts with carbon dioxide, CO_2, from atmosphere. This has

increased the compressive strength of the product immediately (Figure 5.21). The average molar ratios for this product cured at 25°C were SiO_2/Al_2O_3=3.77 and K_2O/Al_2O_3=0.82 while for autoclave curing, the SiO_2/Al_2O_3 ratio increased to 4.33. Taftan pozzolan has variation in chemical composition from batch to batch. Batches with low content of CaO were used in this work when lime was added as mineral additives and compared to the same batch was activated without adding lime. The calcium oxide content in the finished product had increased compared to when Taftan pozzolan was activated without adding burnt lime (Table 5.6).

Compared to the above materials, the gel obtained from the activation of natural pozzolan without a mineral additive has higher gel porosity (Figures 5.18 to 5.21). This formation at lower curing temperature produces more uniform gel although when the product was cured at a higher curing temperature the compressive strength was increased (Figure 5.18).

5.7 Optimum Paste Proportions for Geopolymer Concrete Production

Considering the above discussion on the optimum concentration of KOH, ratios of alkaline hydroxide to water glass and suitable modulus of water glass solution for activation for each type of pozzolan the details of the different paste proportions for production of geopolymer concrete are presented in Table 5.7.

5.8 Summary

From the results obtained in this chapter, several factors for achieving optimum strength of alkali-activated natural pozzolan concrete have been determined which are summarized as follows

1) A combination of potassium hydroxide with a sodium silicate solution provides the best activator. KOH solutions between 5 – 7.5 M dissolve the greatest amount of material from the precursor and also give the highest values for compressive strength. The alkaline hydroxide first breaks up the Al-Si bonds and dissolves Al ions which catalyses the polymerisation and formation of the gel from hydrated alkaline alumina-

silicates created by adding soluble sodium silicate. These follow the pattern reported by Xu and Van Deventer, (2000, 2003).

2) For natural pozzolans with low CaO content and for pozzolans containing sodic zeolites that are not thermally treated, such as Shahindej dacite with its high soluble silicate, the optimum water glass modulus (SiO_2 /Na_2O ratio) is 2.1 but increases to 3.1 for natural pozzolans with high CaO or which have been calcined.

3) The optimum dosage of activator and the optimum ratios of alkaline hydroxide to sodium silicate were determined by examining the islands of ideal compositions determined from a new method which draws the strength contours versus different molarities of alkaline hydroxide and various ratio of alkaline hydroxide to alkaline silicate. It would be worthwhile to extend the model found in chapter 4 to include the properties of activators in future works.

4) The optimum curing temperature to achieve the highest strength for alkali-activated Taftan pozzolan was 60°C. However, 40°C was found to be adequate for achieving strength in a range suited for structural concrete (Figure 5.1).

5) Comparable strengths to those obtained at 60°C curing can be obtained by autoclaving alkali-activated Taftan pozzolan at 2.5MPa and 150°C for three hrs (Figure 5.1).

6) As described in section 4.4.1, Natural Shahindej pozzolan must be cured at 60°C to produce structural concrete (Figure 5.3) but when calcined at 800°C can be cured at 20°C.

7) Mineral additives including kaolinite and other calcined pozzolans such as Shahindej and slaked lime when added to Taftan pozzolan as a solid precursor gives approximately the same strength as when the pozzolan is activated without mineral additives, although it seems that the gel obtained is more impermeable (Figures 5.18-b and 5.19-b).

8) In the present research, since the pozzolans selected seem to satisfy the compositional ratios based on chemical analysis, the use of additive mineral is not necessary. It seems the deficiency of main oxides such as SiO_2, Al_2O_3 and CaO in natural pozzolans can be compensated for by adding mineral additives to increase the level of oxides in the final product before activation (Table 5.6).

Table 5.1 Alkali Activation Solutions (grams per 100ml solution)

No.	Notation	K_2O	Na_2O	SiO_2	Total Solid
1	2.5M NaOH	/	7.75	/	10
2	5M NaOH	/	15.5	/	20
3	7.5M NaOH	/	23.25	/	30
4	10M NaOH	/	31.0	/	40
5	2.5M KOH	11.75	/	/	14
6	5M KOH	23.5	/	/	28
7	7.5M KOH	32.25	/	/	42
8	10M KOH	47	/	/	56
9	WG(SiO_2/Na_2O ratio of 2.1)	/	12.33	26.626	38.959
10	WG(SiO_2/Na_2O ratio of 2.4)	/	10.83	25.992	36.822
11	WG(SiO_2/Na_2O ratio of 3.1)	/	8.54	26.474	35.014

Table 5.2 ICP-AES results for Taftan pozzolan leaching tests (conducted by I.P.P.I. laboratory, Tehran, Iran)

(KOH)	(Si)ppm	(Al) ppm	(Ca) ppm
2.5M	29.75	Not detectable	28
5.0M	147.99	Not detectable	98.25
7.5M	274.4	68.22	74.98
10M	235.2	69.36	51.43

Table 5.3 Weight percentage concentration observed in EDX (conducted by Material and Energy Research Centre laboratory, Tehran, Iran)

Compositions	Taftan 5M KOH Sealed at 40°C	Taftan7.5M KOH Sealed at 40°C	Taftan7.5M KOH Autoclaved at 2MPa
SiO_2	52.090	50.071	51.87
Al_2O_3	9.921	10.770	9.85
K_2O	13.507	16.810	12.856
CaO	19.984	18.038	20.926
Fe_2O_3	4.497	4.309	5.281
MgO			
TiO_2			

Table 5.4 Chemical composition of mineral additives used in this investigation conducted by Kansaran Binaloud X-ray laboratory in Tehran, Iran

Material	LOI	SiO_2	Al_2O_3	Fe_2O_3	CaO	MgO	TiO_2	K_2O	Na_2O
Kaolin	13.84	52.2	30.90	0.45	0.26	0.24	0.125	0.90	0.45
Calcined Shahindej pozzolan	5.78	73.44	11.88	1.3	2.55	0.98	0.147	2.3	1.1
Burnt Lime	10	-	-	-	90	-	-	-	-

Table 5.5 Mix proportion, strength, specific strength (SS), specific strength of mineral additive effect (SSME) of geopolymer cement

Mix Proportion (%)		**Mix 1**	**Mix 2**	**Mix 3**	**Mix 4**	**Mix 5**	**Mix 6**	
Taftan Pozzolan		100	85.7	83.3	80	73.33	60	
Kaolinite		0	14.3	16.7	20	26.67	40	
W/B		0.31	0.31	0.31	0.31	0.31	0.31	
compressive strength(MPa)		44.03	23.85	24.21	45.61	22.9	22.36	Autoclave Curing
	28 days	19.48	18.61	19.04	19.26	16.81	10.49	25°C Curing
SS of pozzolan in the cement (MPa)		0.44	0.27	0.29	0.57	0.31	0.37	Autoclave Curing
		0.195	0.22	0.23	0.24	0.23	0.17	25°C Curing
SS of mineral effect (MPa) (SSME)		0	-0.17	-0.15	0.13	-0.13	0	Autoclave Curing
		0	0.025	0.035	0.045	0.035	0	25°C Curing
Mix Proportion (%)		**Mix 7**	**Mix 8**	**Mix 9**	**Mix 10**			
Taftan Pozzolan		100	85.7	83.3	0			
Calcined Shahindej Pozzolan		0	14.3	16.7	100			
W/B		0.31	0.31	0.31	0.31			
compressive strength(MPa)		44.03	37.22	45.56	0			Autoclave Curing
	28 days	19.48	15.53	25.28	16.07			25°C Curing
SS of pozzolan in the cement (MPa)		0.44	0.43	0.55	0			Autoclave Curing
		0.195	0.18	0.3				25°C Curing
SS of mineral effect (MPa) (SSME)		0	-0.01	0.11				Autoclave Curing
		0	-0.015	0.105				25°C Curing
Mix Proportion (%)		**Mix 11**	**Mix 12**	**Mix 13**	**Mix 14**			
Taftan Pozzolan		100	98.3	96.66	93			
Burnt lime		0	1.7	3.4	7			
W/B		0.31	0.31	0.31	0.31			
compressive strength(MPa)		44.03	16.33	27.8	14.98			Autoclave Curing
	28 days	19.48	10.84	19.6	17.19			25°C Curing
SS of pozzolan in the cement (MPa)		0.44	0.17	0.29	0.16			Autoclave Curing
		0.195	0.11	0.2	0.18			25°C Curing
SS of mineral effect (MPa) (SSME)		0	-0.27	-0.15	-0.28			Autoclave Curing
		0	-0.085	0.005	-0.015			25°C Curing

Table 5.6 Weight percentage concentration observed in EDX (conducted by Material and Energy Research Centre laboratory, Tehran, Iran)
(TN=Taftan, TNK=Taftan added Kaolinite, TNSH=Taftan added Calcined Shahindej, TNL=Taftan added Burnt Lime)

Compositions	TN	TN-Au	TNK	TNK-Au	TNSH	TNSH-Au	TNL	TNL-Au
SiO_2	48.803	55.814	44.807	52.275	52.09	56.829	55.88	58.197
Al_2O_3	12.41	15.304	14.264	16.876	11.362	11.447	14.81	13.441
CaO	7.233	8.743	19.327	14.231	15.042	12.254	10.055	10.646
Fe_2O_3	4.108	3.881	2.981	3.466	3.109	3.215	3.38	3.591
MgO	1.062	0.795	0.821	0.838	0.916	0.968	0.899	0.777
Na_2O .	2.523	2.682	2.083	1.829	2.274	2.060	2.452	1.897
K_2O	13.36	12.211	15.463	10.006	14.885	12.751	12.105	10.967
TiO_2	0.5	0.57	0.254	0.479	0.322	0.475	0.42	0.484
Densities(gr/cm^3)	1.88	1.91	1.92	1.76	1.96	1.66	2.18	1.75
Pozzolan reacted (%)	79.1	90.5	75	87.5	82.5	90	93.7	97.6

Table 5.7 – Optimum Paste Proportion for Geopolymer Concrete

Raw Materials (Pozzolan)	**KOH/Na_2SiO_3**	**S/W**	**KOH Concentration**	**Composition of the Sodium Silicate Solution (%)**			
				Ratio	**Na_2O%**	**SiO_2%**	**Water%**
Taftan	7.1	3.33	7.5M	2.1	12.6	26.5	65
Shahindej	7.7	2.63	7.5M	2.1	12.6	26.5	65
Calcined Shahindej	7.7	2.63	7.5M	3.1	8.5	26.5	65

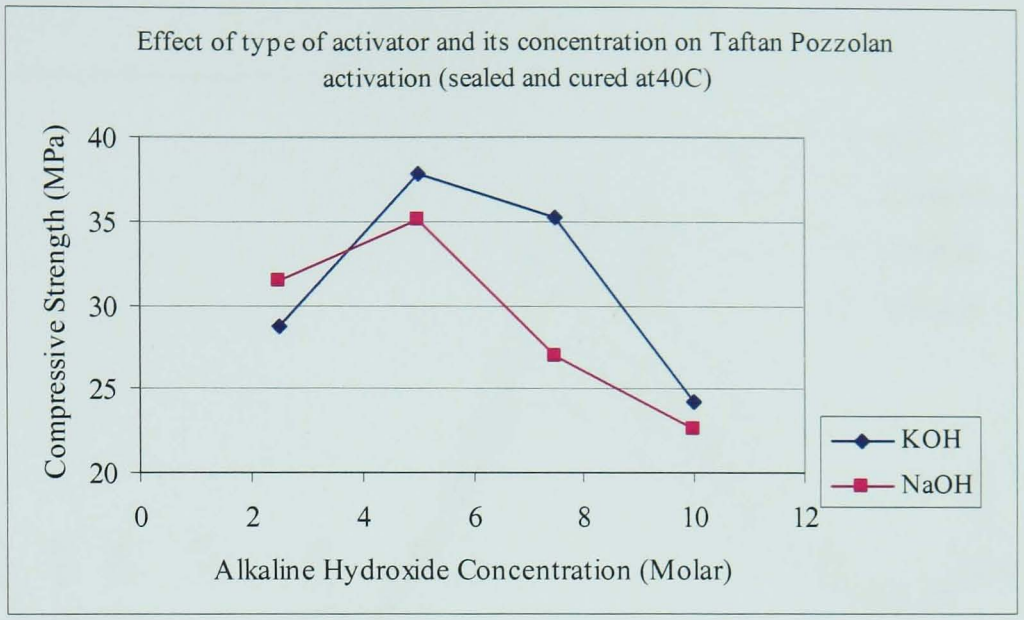

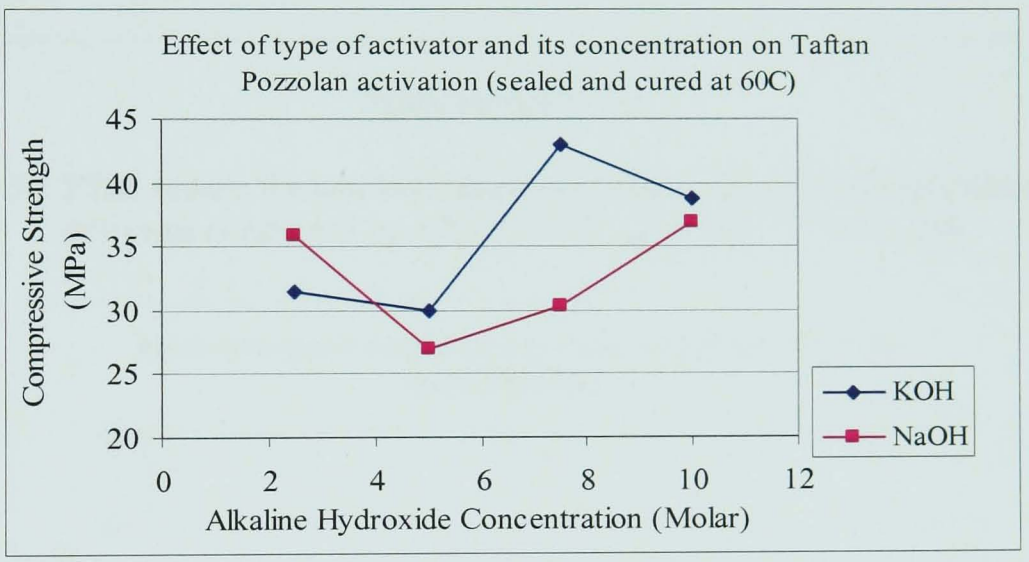

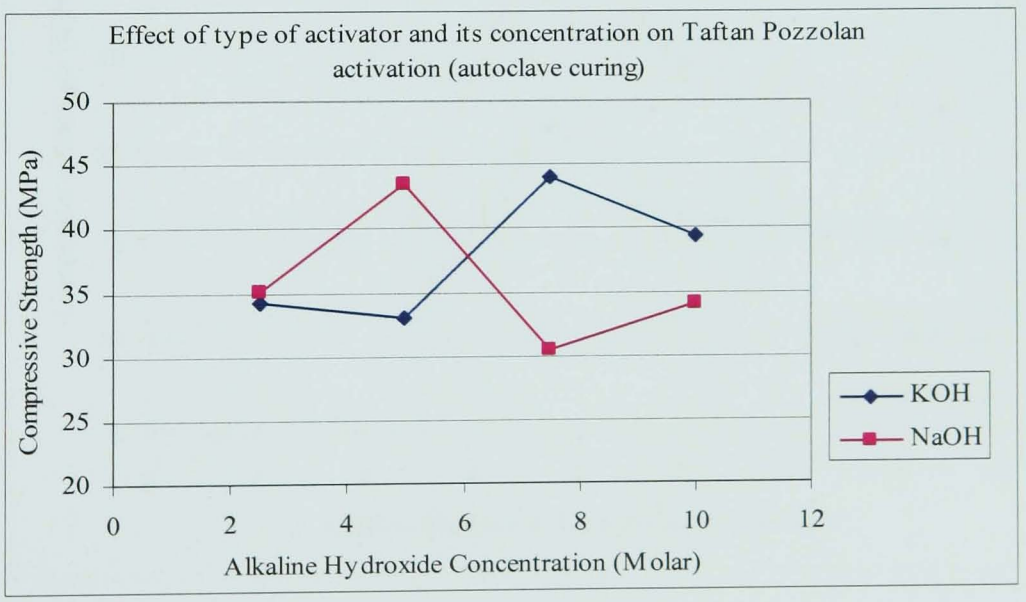

Figure 5.1 Effect of type and concentration of activators on Taftan geopolymer compressive strength for different curing conditions

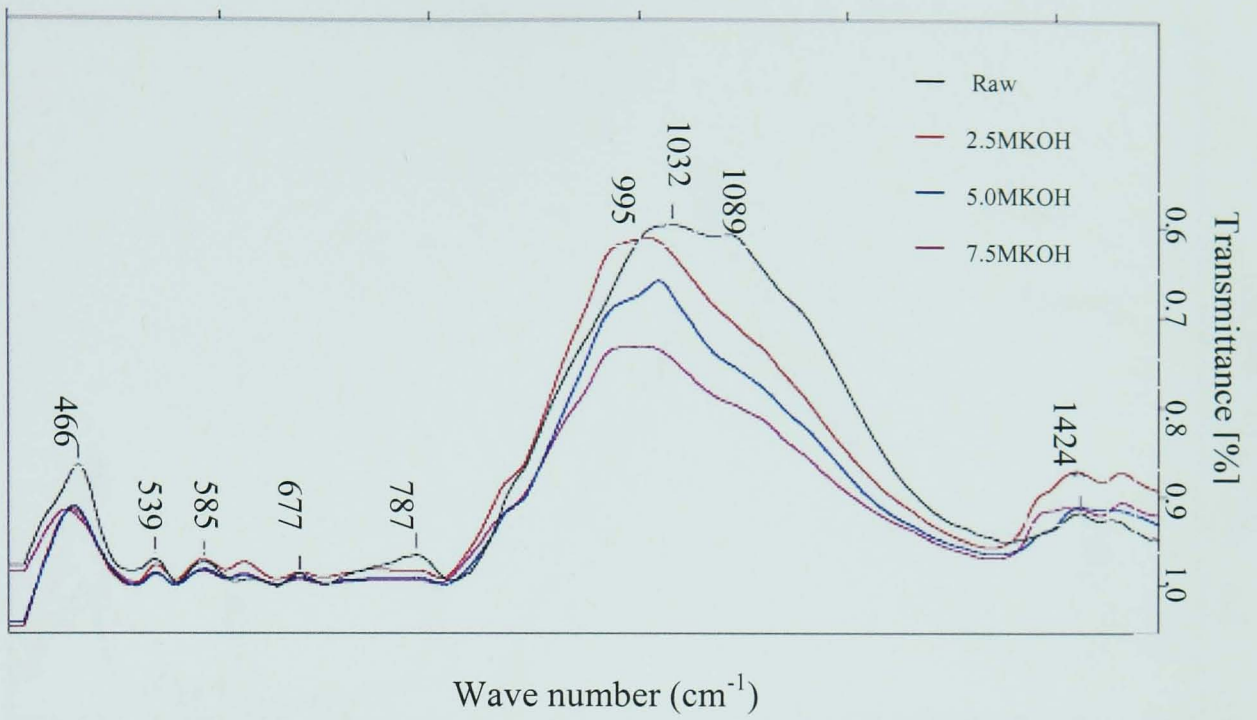

Figure 5.2 FTIR results for leached Taftan pozzolan with different concentration of activator conducted by I.P.P.I. FTIR laboratory, Tehran, Iran

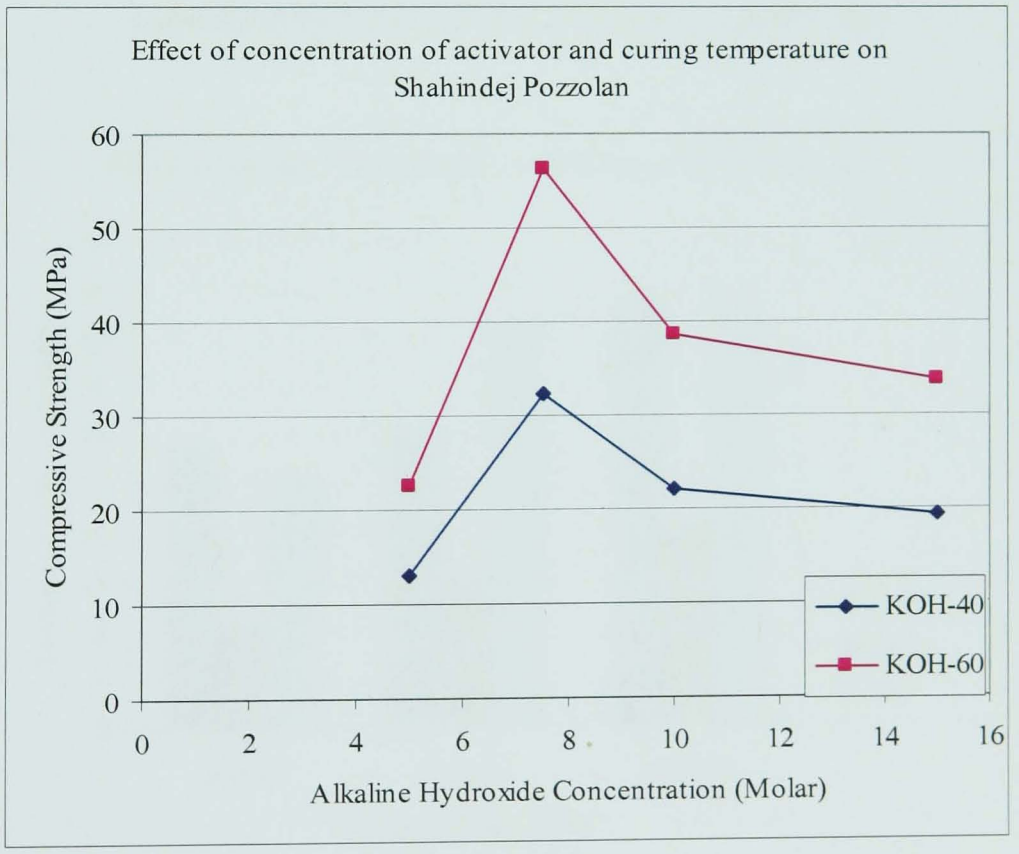

Figure 5.3 Effect of concentration of activators on Shahindej geopolymer compressive strength for different curing conditions

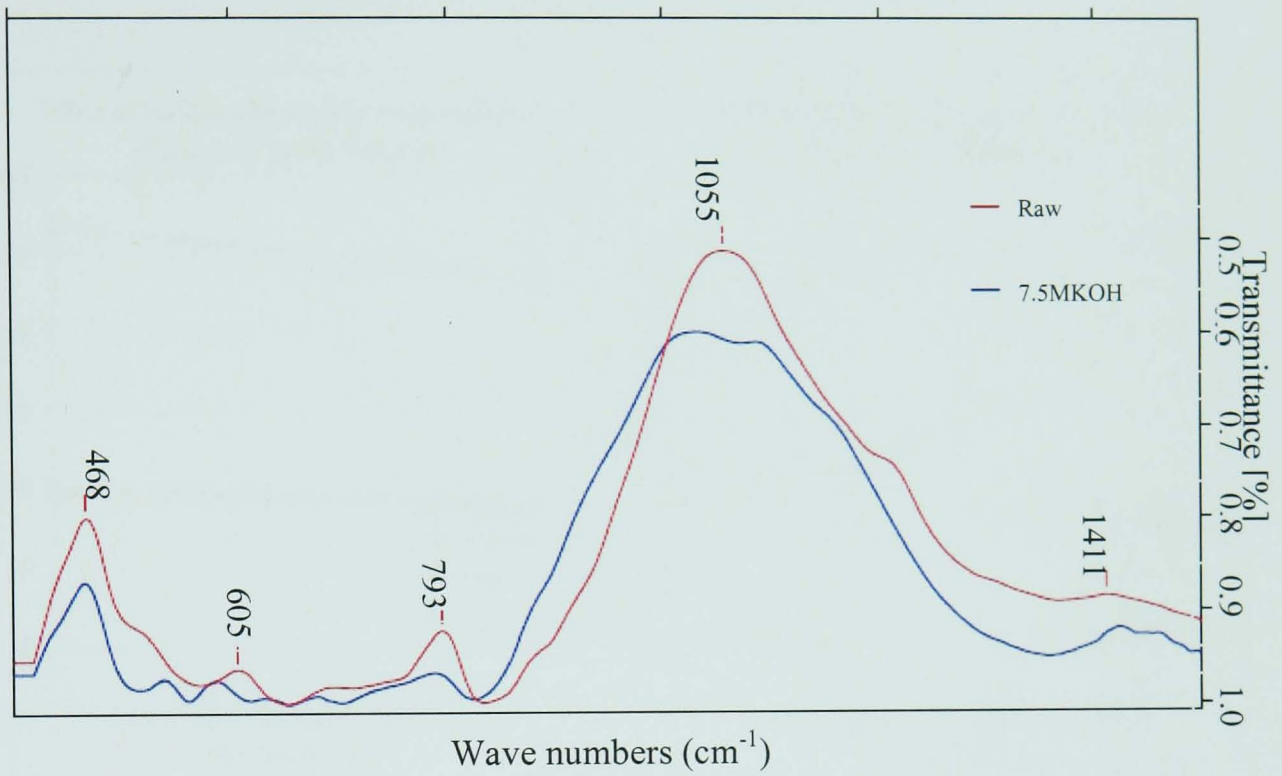

Figure 5.4 FTIR results for untreated Shahindej pozzolan and alkali activated form of it conducted by I.P.P.I. FTIR laboratory, Tehran, Iran

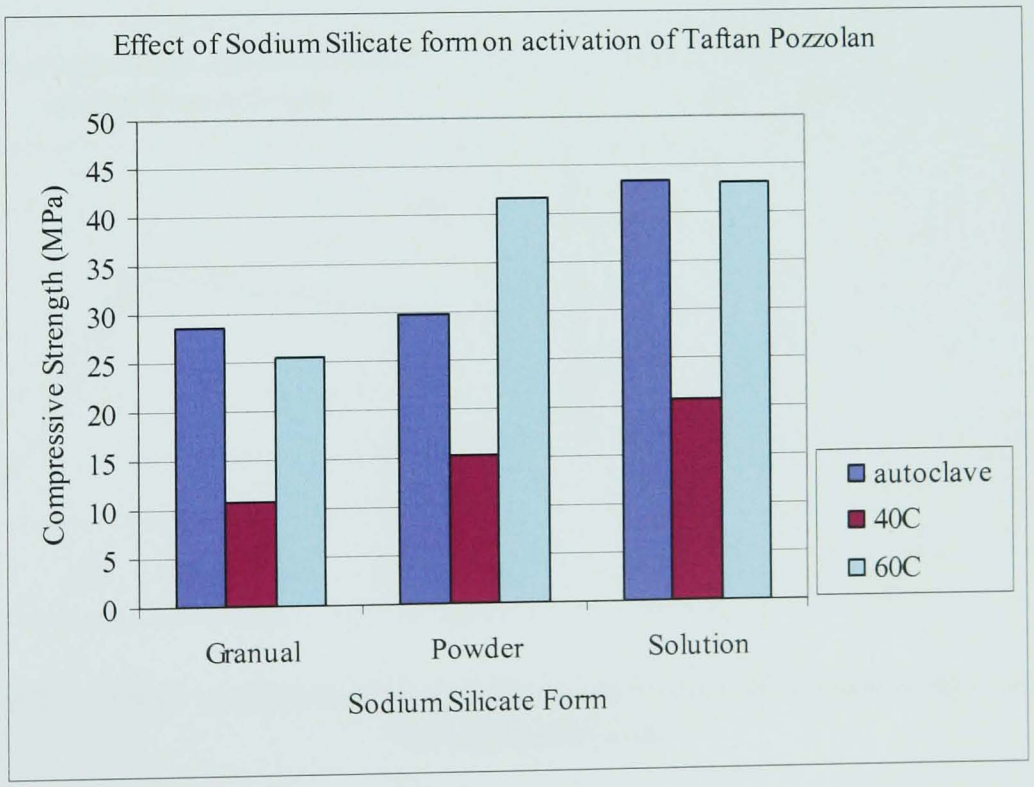

Figure 5.5 Effect of sodium silicate form on activation of natural pozzolan

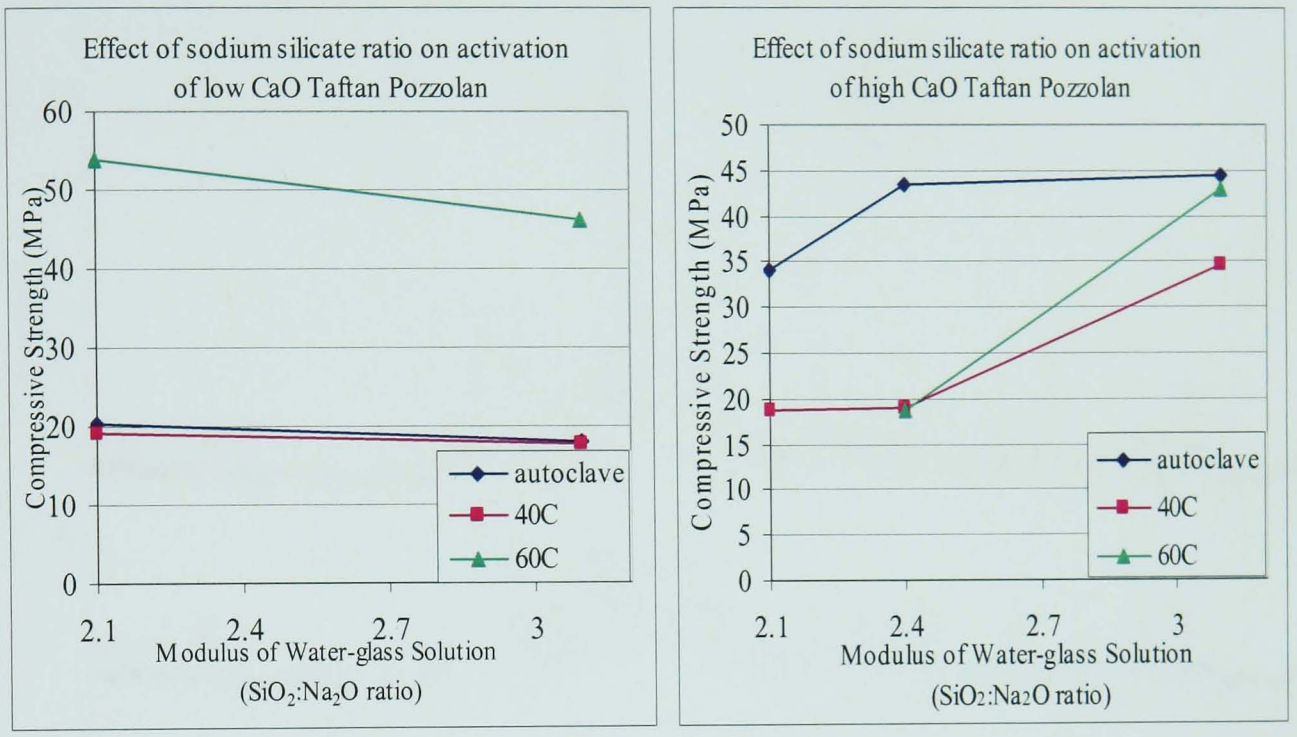

Figure 5.6 Effect of sodium silicate ratio on activation of Taftan pozzolan with different content of CaO

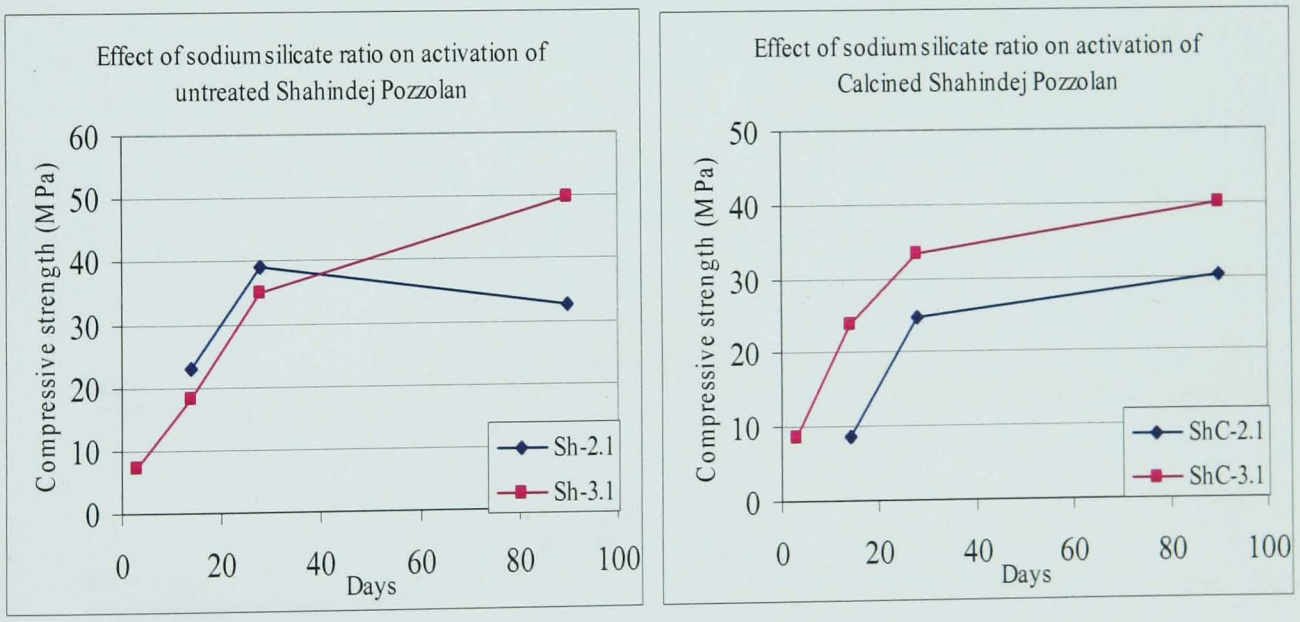

Figure 5.7 Effect of sodium silicate ratio on activation of untreated and calcined Shahindej pozzolan

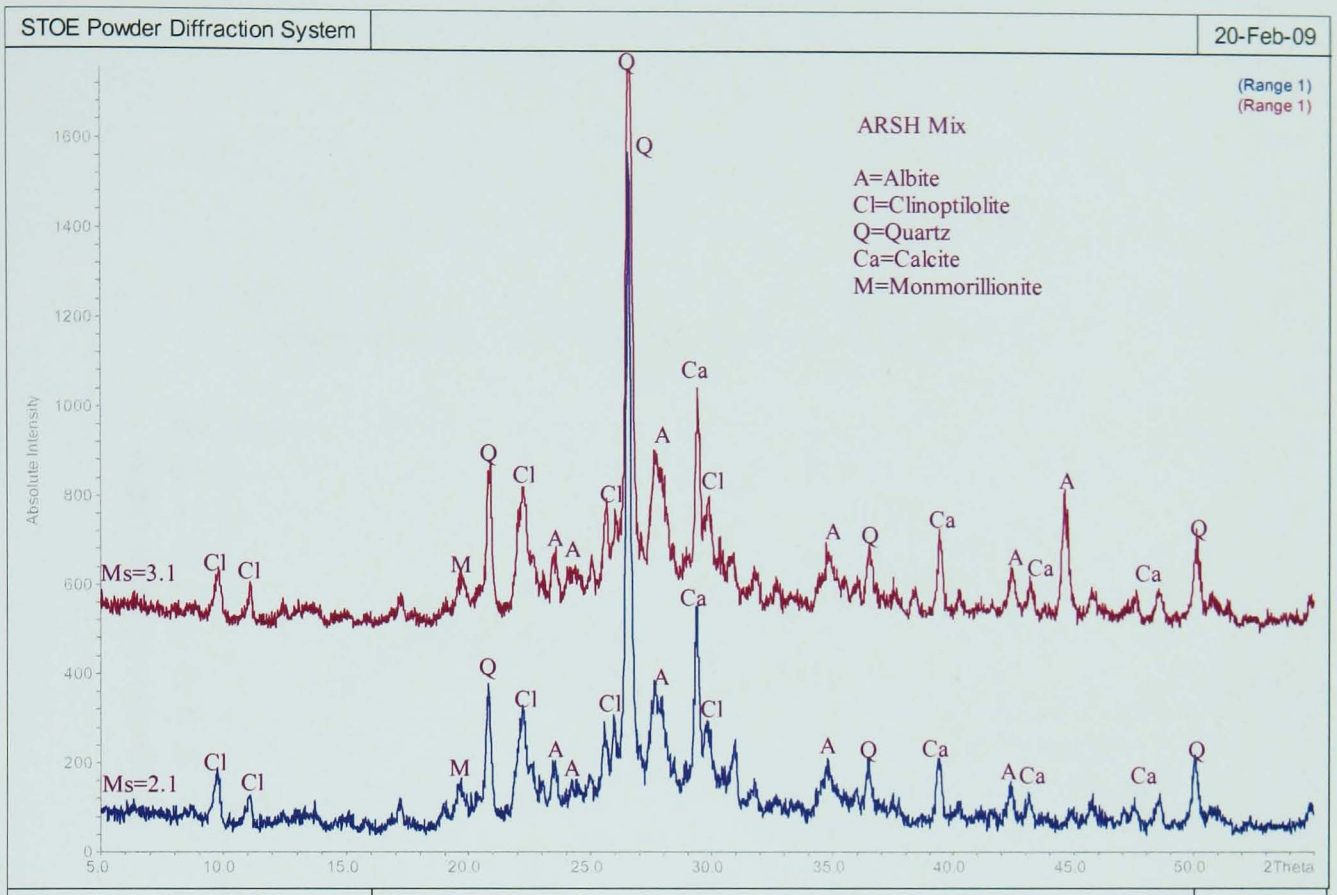

Figure 5.8 X-ray diffraction traces of untreated (ARSH) and calcined (ACSH) Shahindej dacite activated with different ratio of sodium silicate (testing was carried out in the Department of Engineering Materials, University of Sheffield)

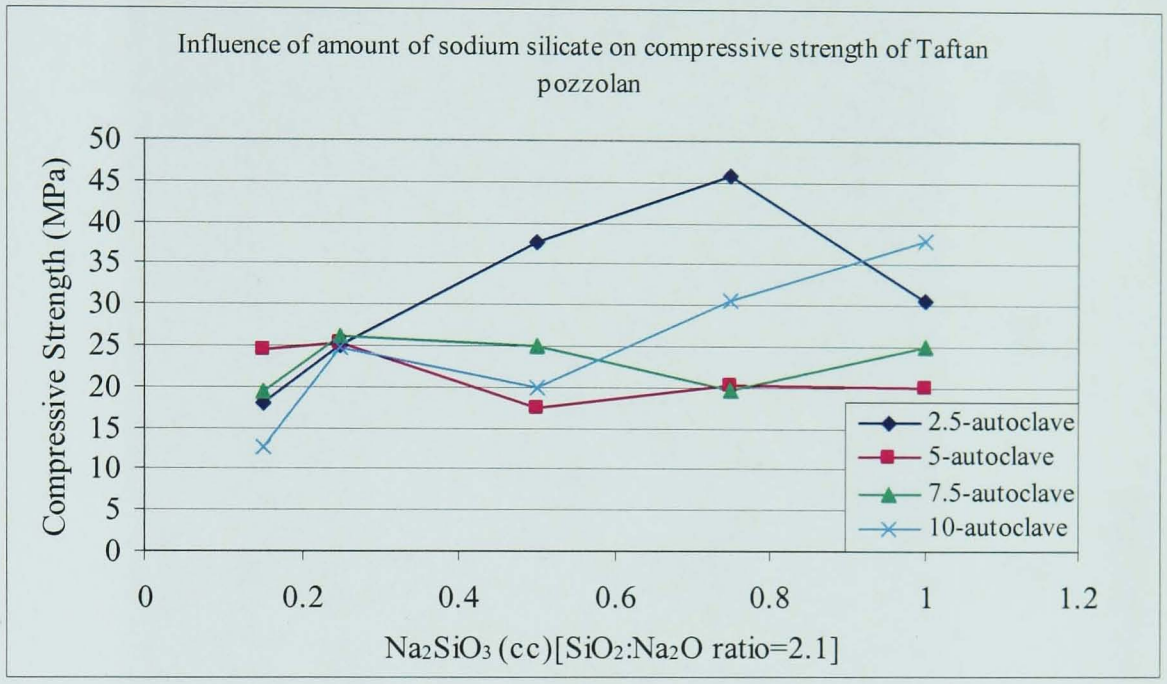

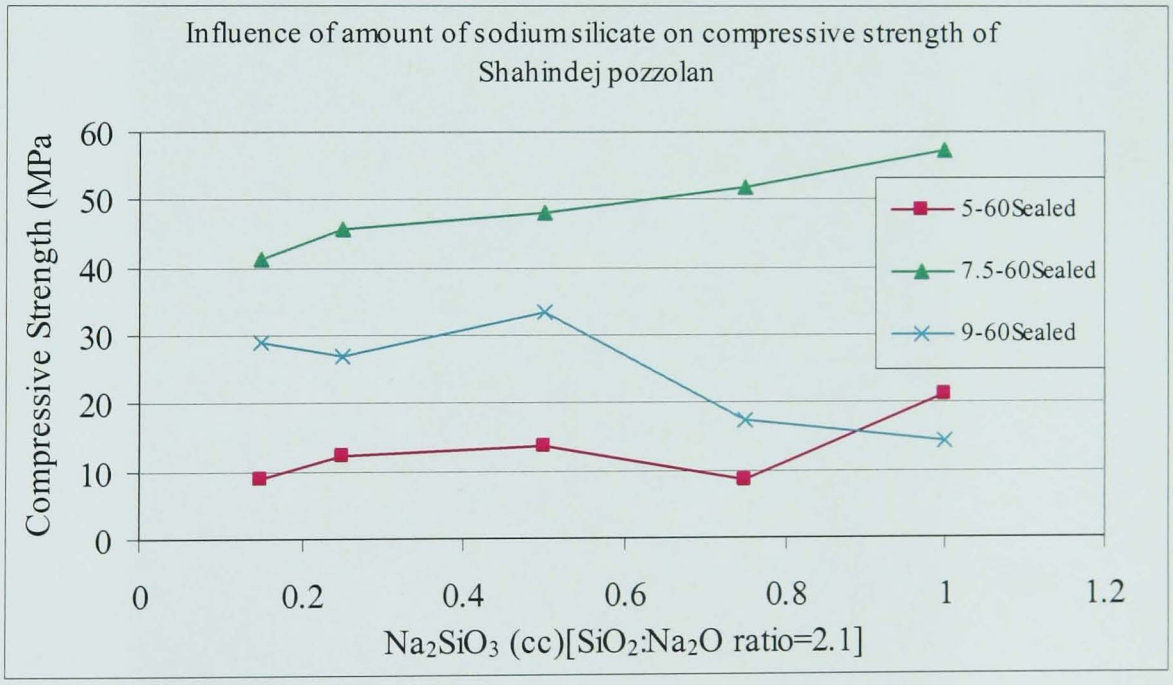

Figure 5.9 Influence of amount of sodium silicate on compressive strength of activated pozzolans (samples dimensions were 20x20x20 mm in these experiments)

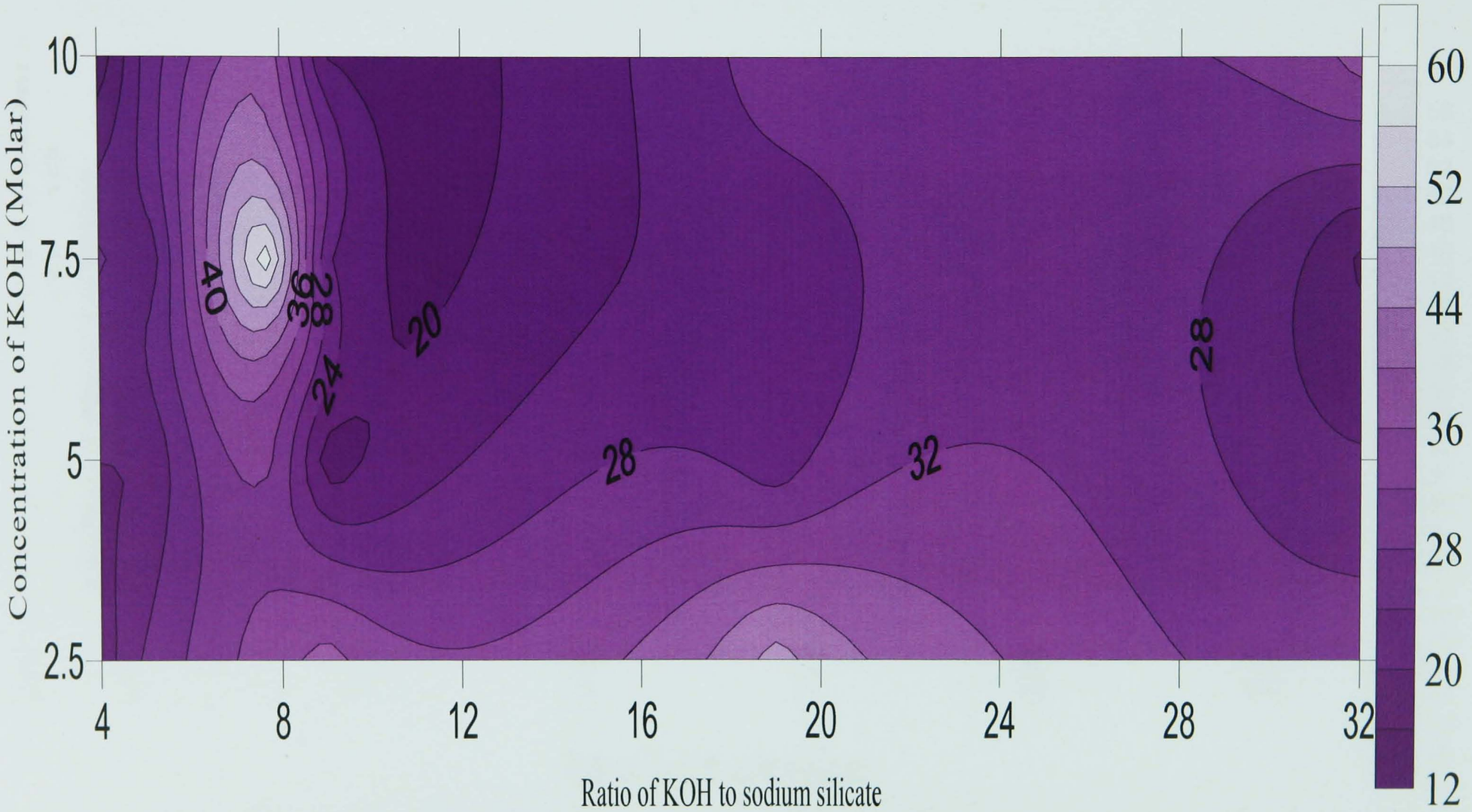

Figure 5.10 Strength contour for different concentration of KOH and various ratio of KOH/Na_2SiO_3 for Taftan Pozzolan (24 samples were tested)

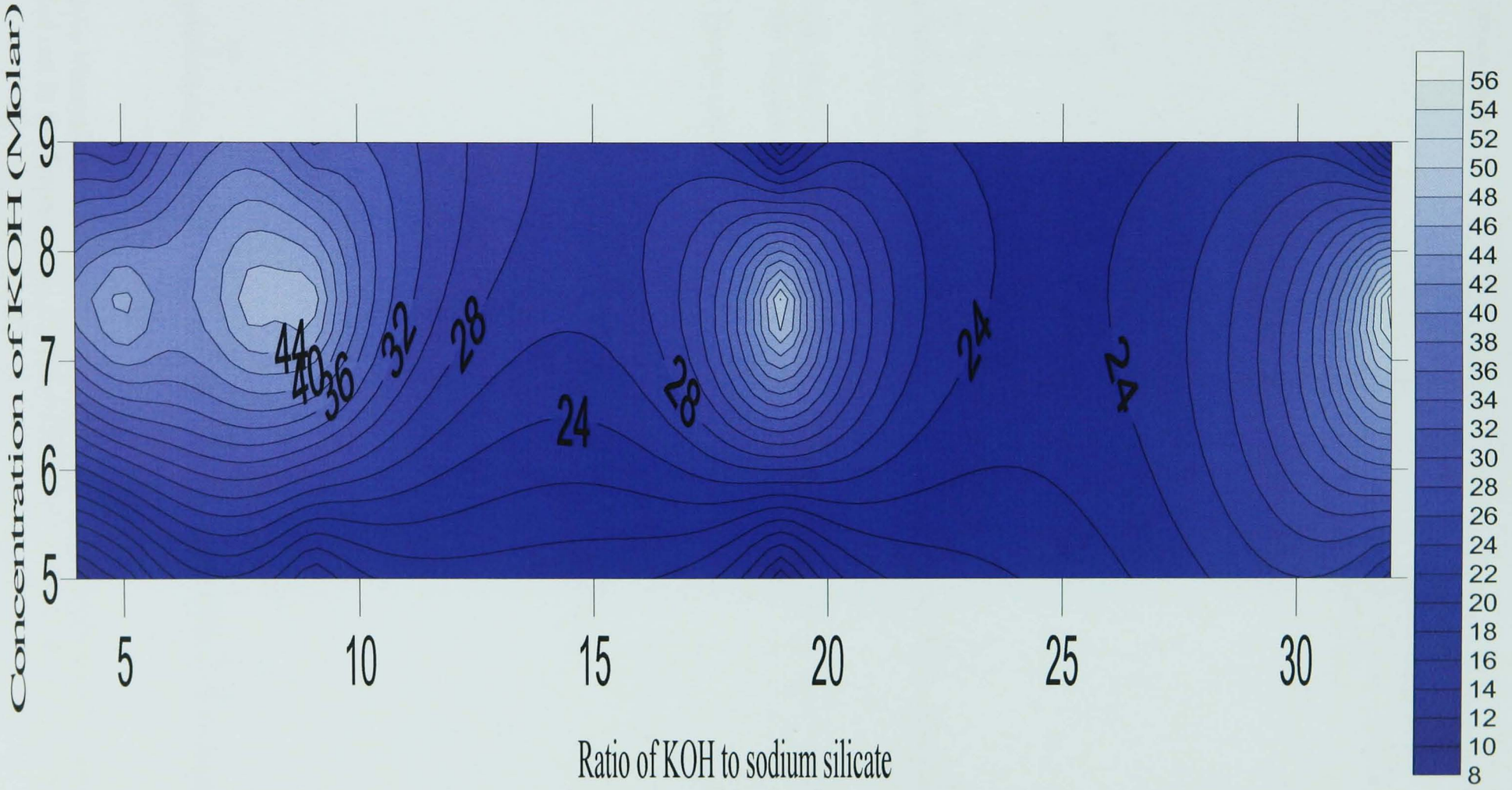

Figure 5.11 Strength contour for different concentration of KOH and various ratio of KOH/Na_2SiO_3 for Shahindej Pozzolan (16 samples were tested)

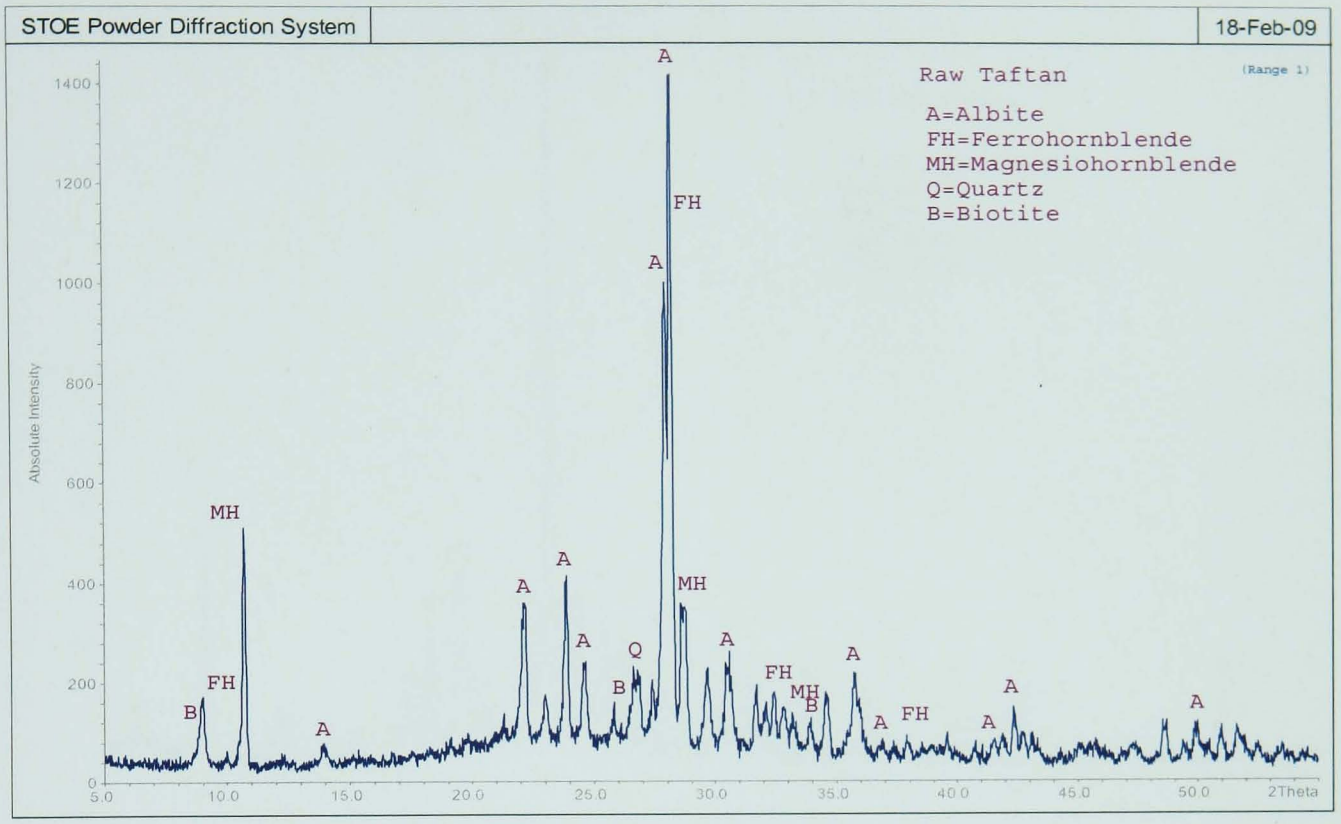

Figure 5.12(a) Mineralogical composition of Taftan andesite (testing was carried out in the Department of Engineering Materials, University of Sheffield)

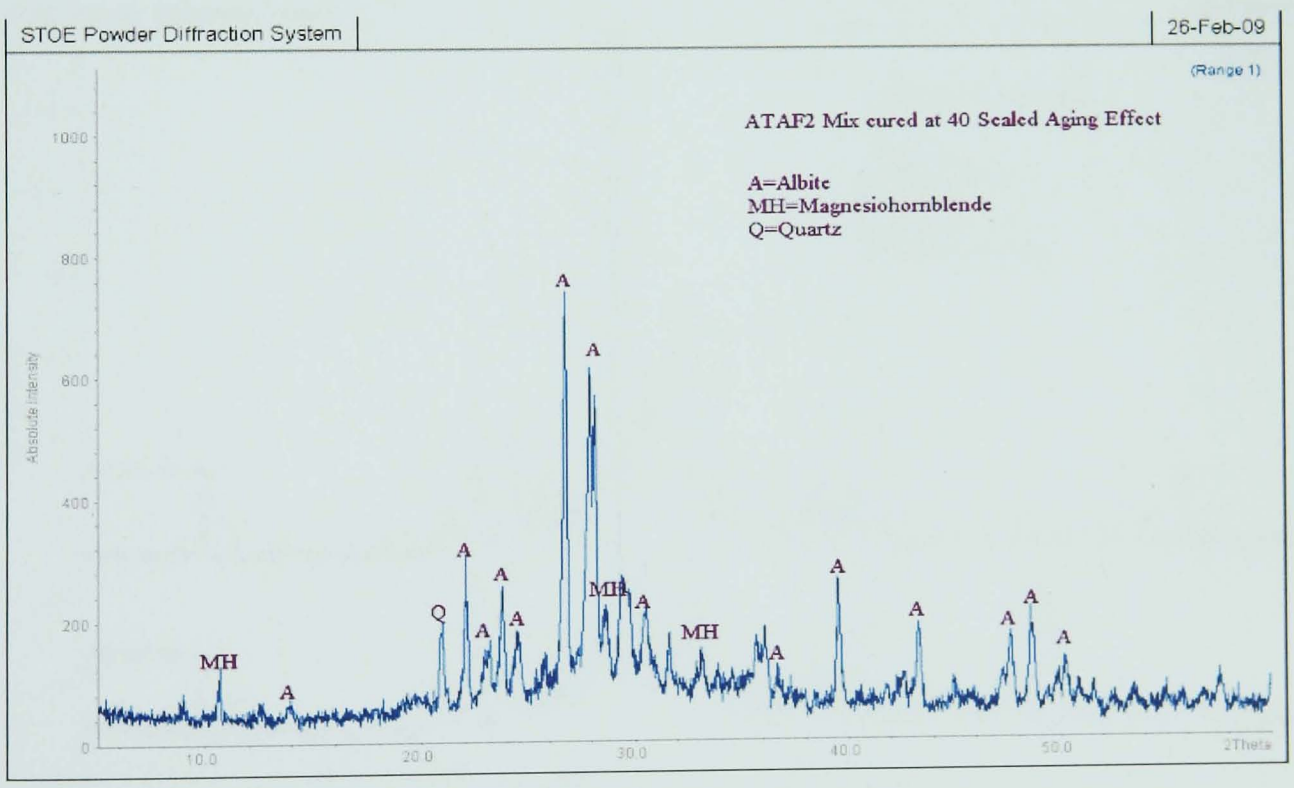

Figure 5.12(b) Mineralogical composition of activated Taftan andesite at 90 days(testing was carried out in the Department of Engineering Materials,University of Sheffield)

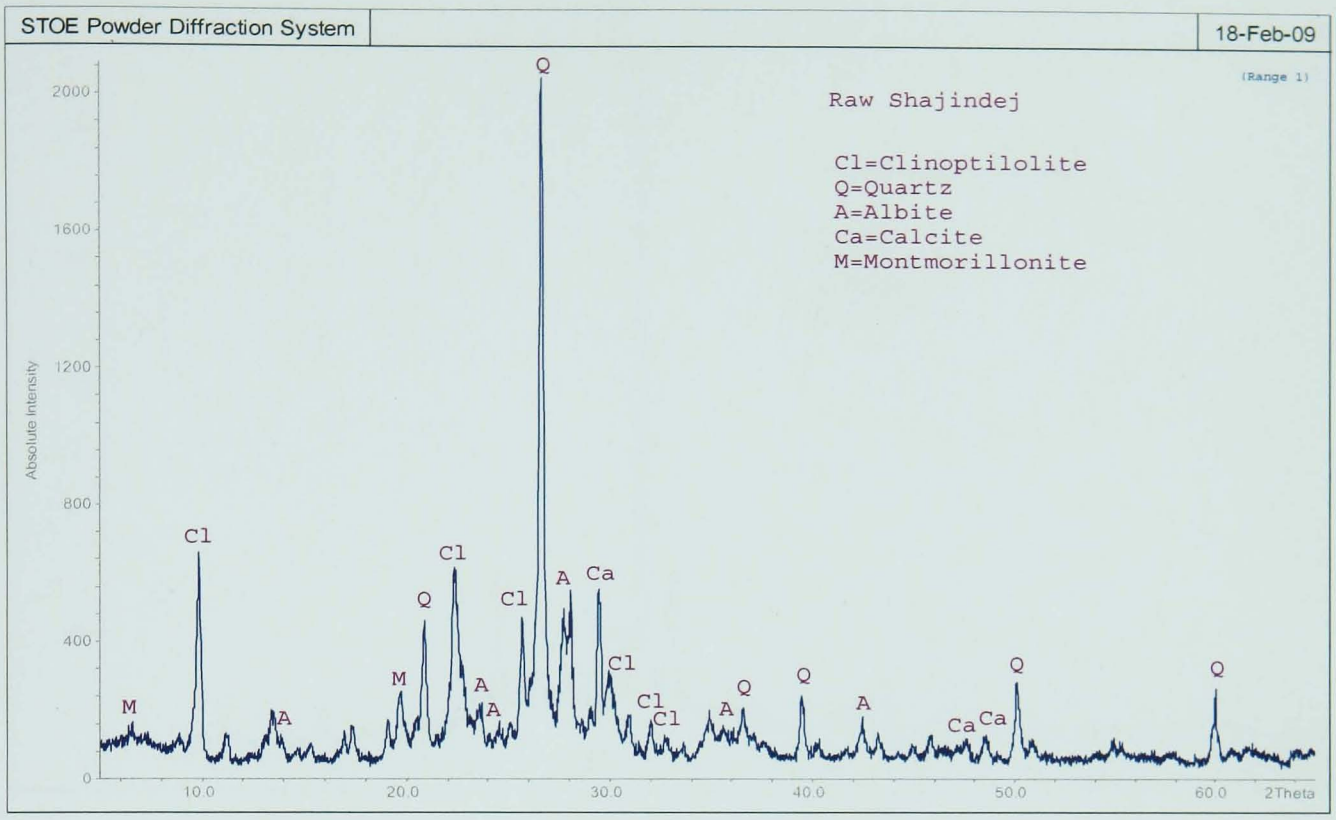

Figure 5.13(a) Mineralogical composition of Shahindej dacite (testing was carried out in the Department of Engineering Materials, University of Sheffield)

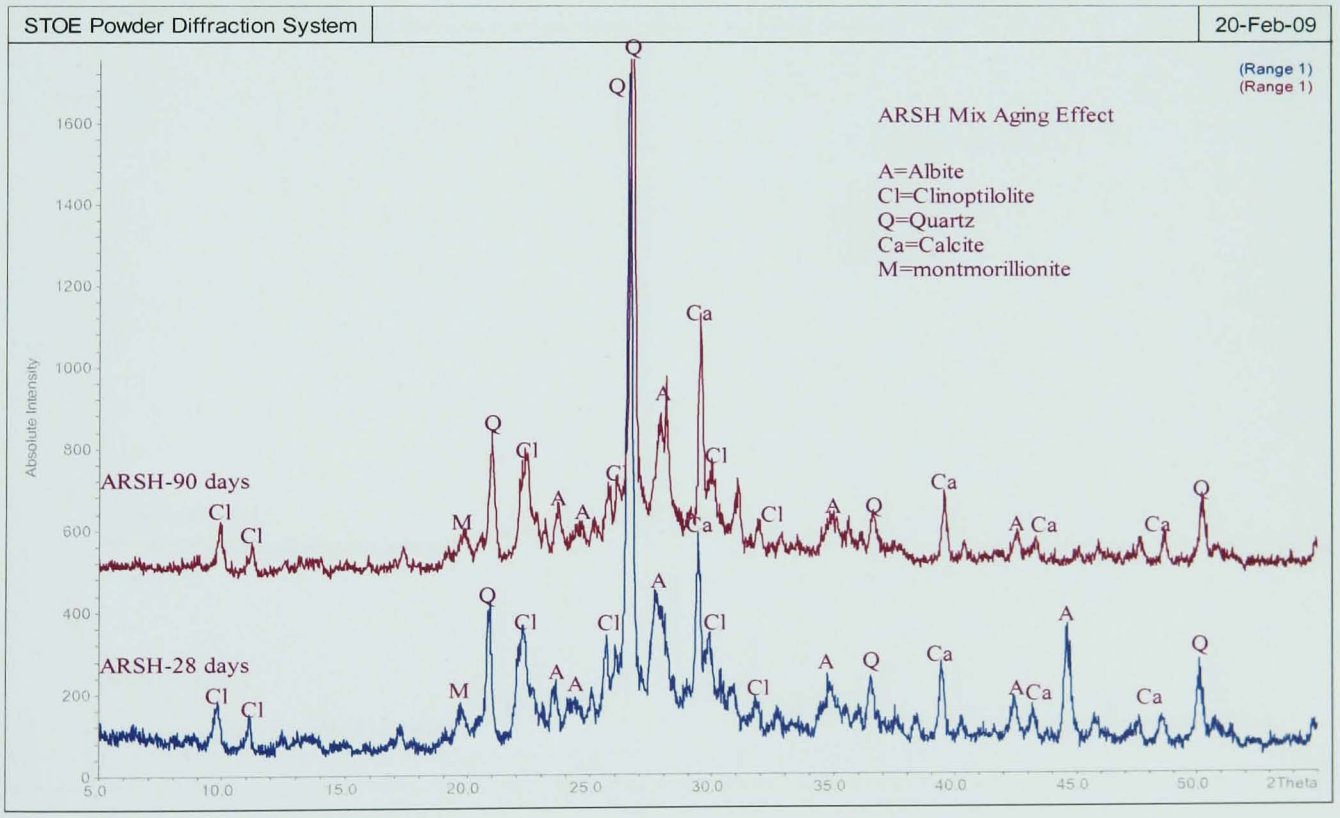

Figure 5.13(b) X-ray diffraction traces of activated utreated Shahindej dacite (ARSH) at different ages (28 and 90 days) (testing was carried out in the Department of Engineering Materials, University of Sheffield)

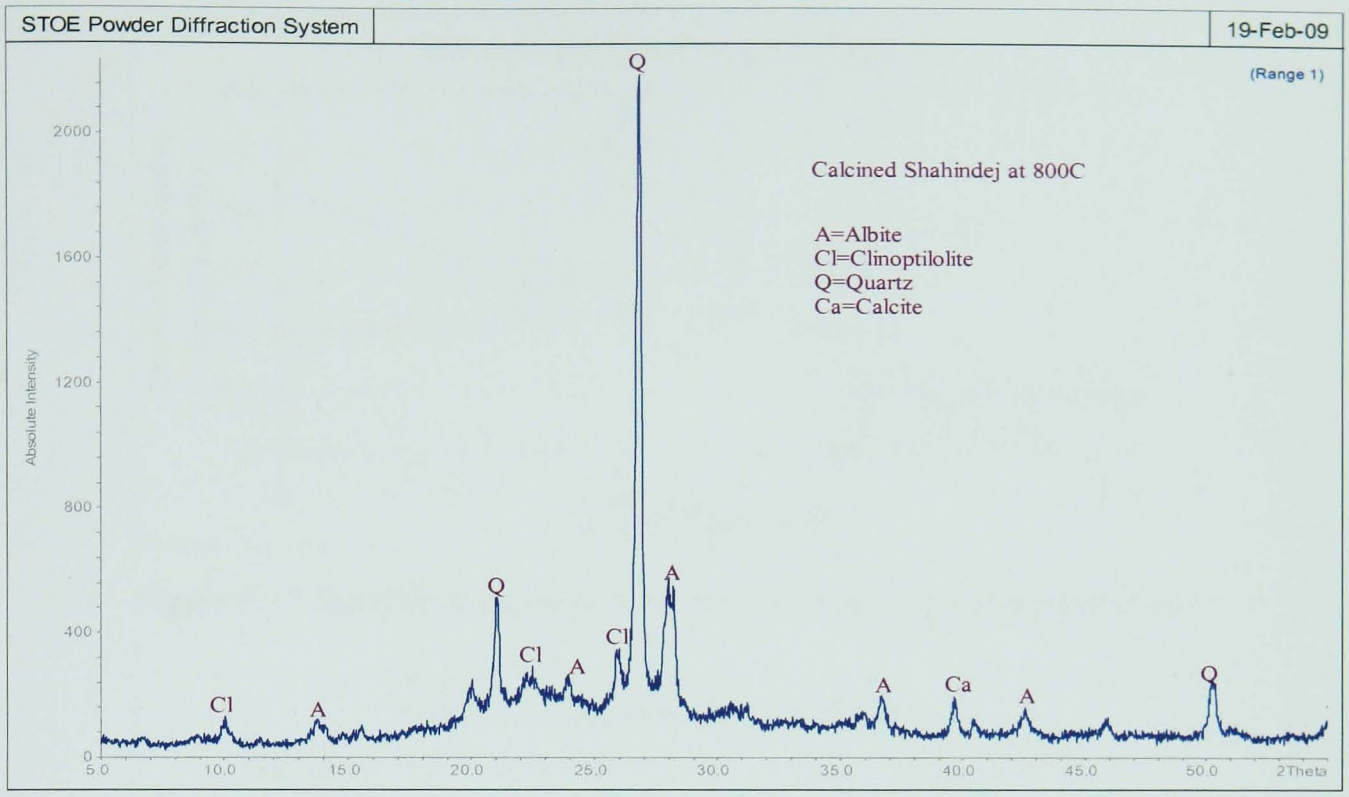

Figure 5.14(a) Mineralogical composition of calcined Shahindej dacite (testing was carried out in the Department of Engineering Materials, University of Sheffield)

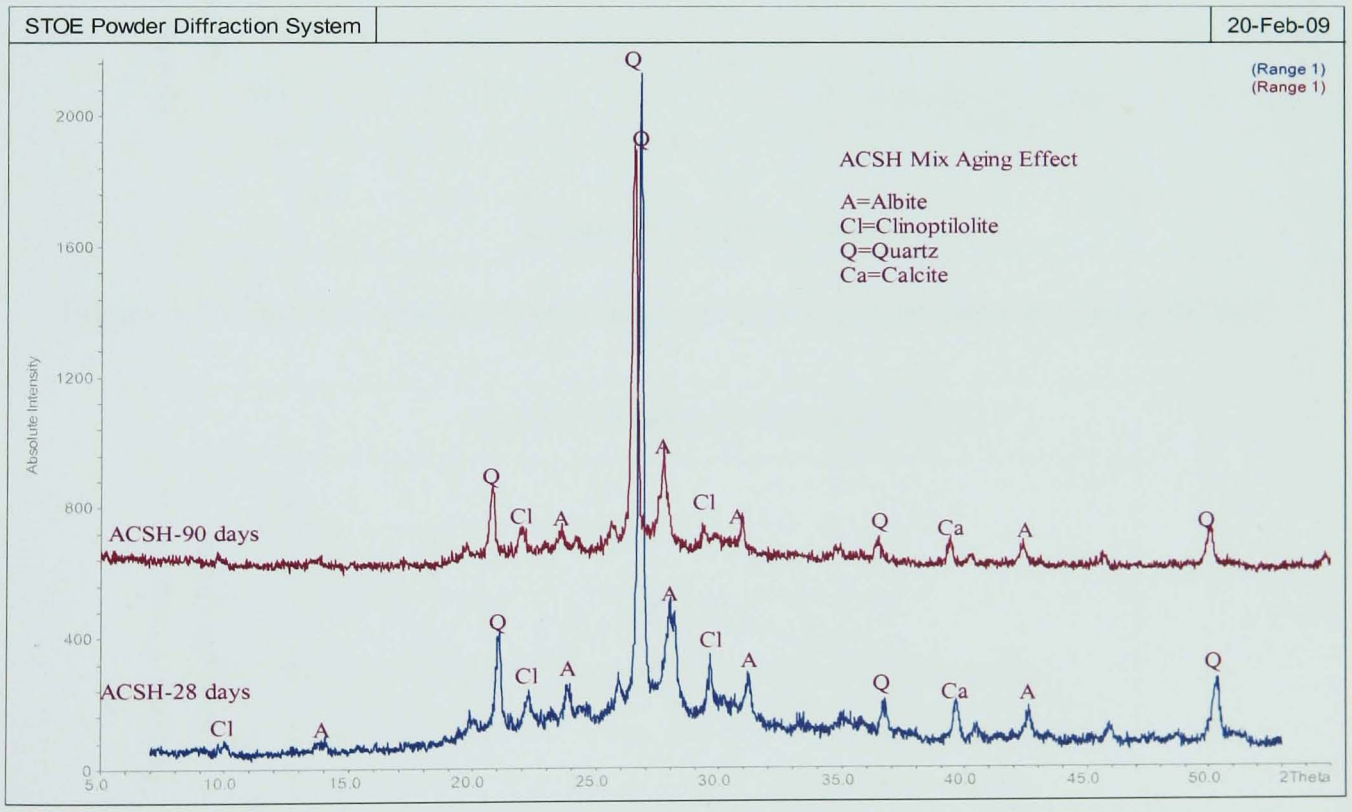

Figure 5.14(b) X-ray diffraction traces of activated calcined Shahindej dacite (ACSH) at different ages (28 and 90 days) (testing was carried out in the Department of Engineering Materials, University of Sheffield)

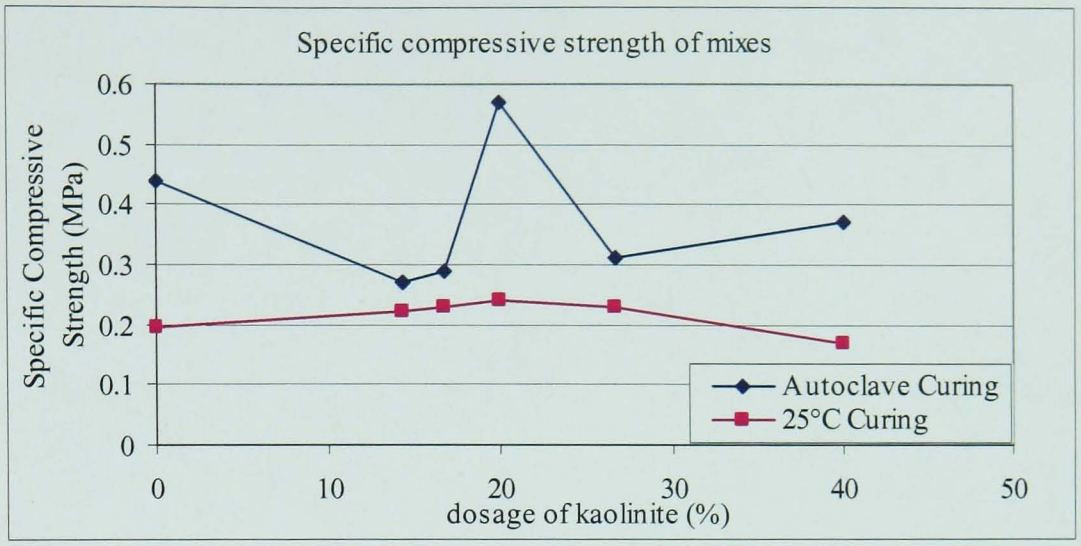

Figure 5.15 Specific compressive strength of mixes containing kaolinite

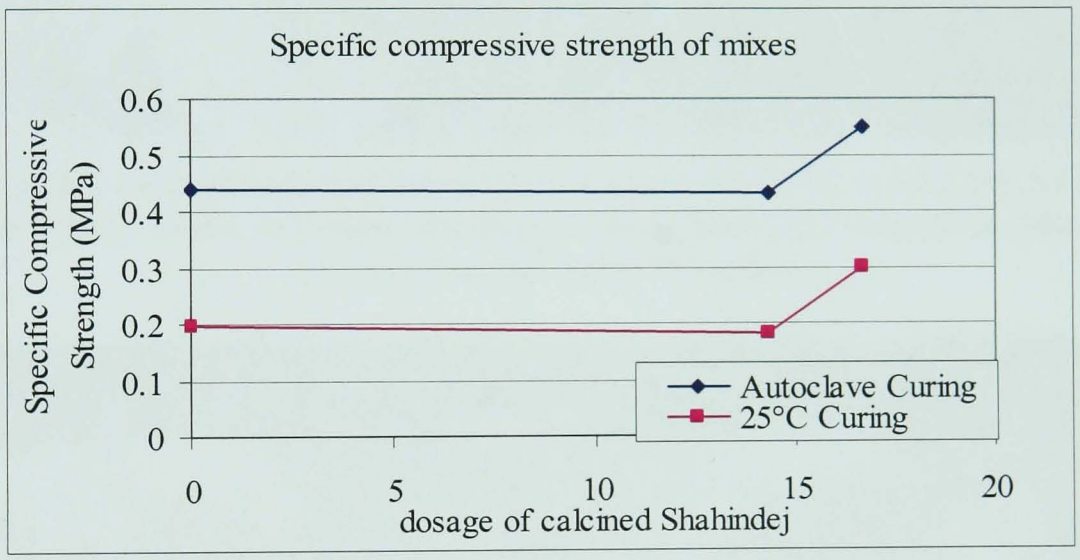

Figure 5.16 Specific compressive strength of mixes containing calcined Shahindej

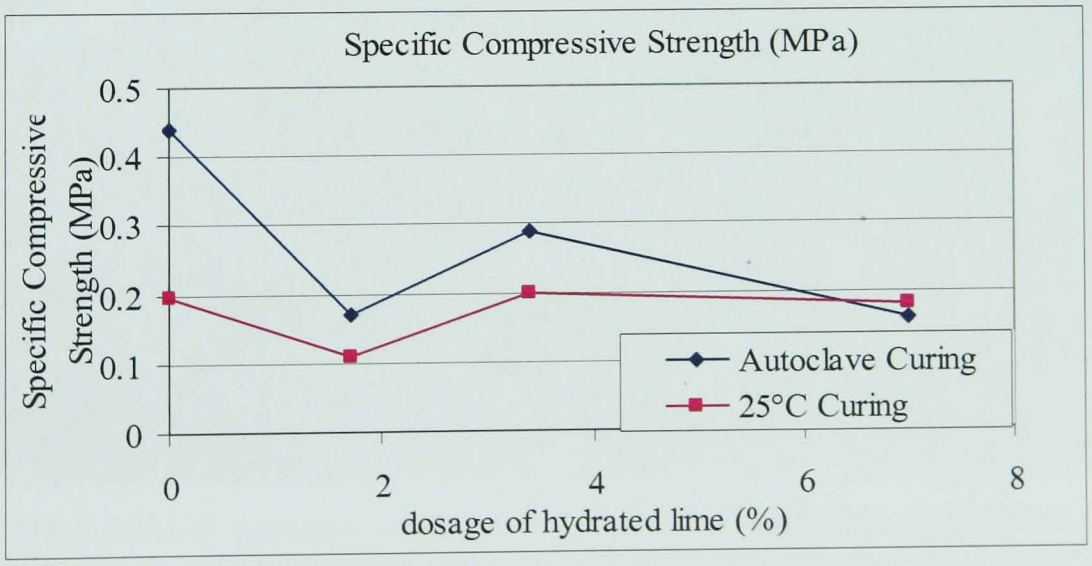

Figure 5.17 Specific compressive strength of mixes containing burnt lime

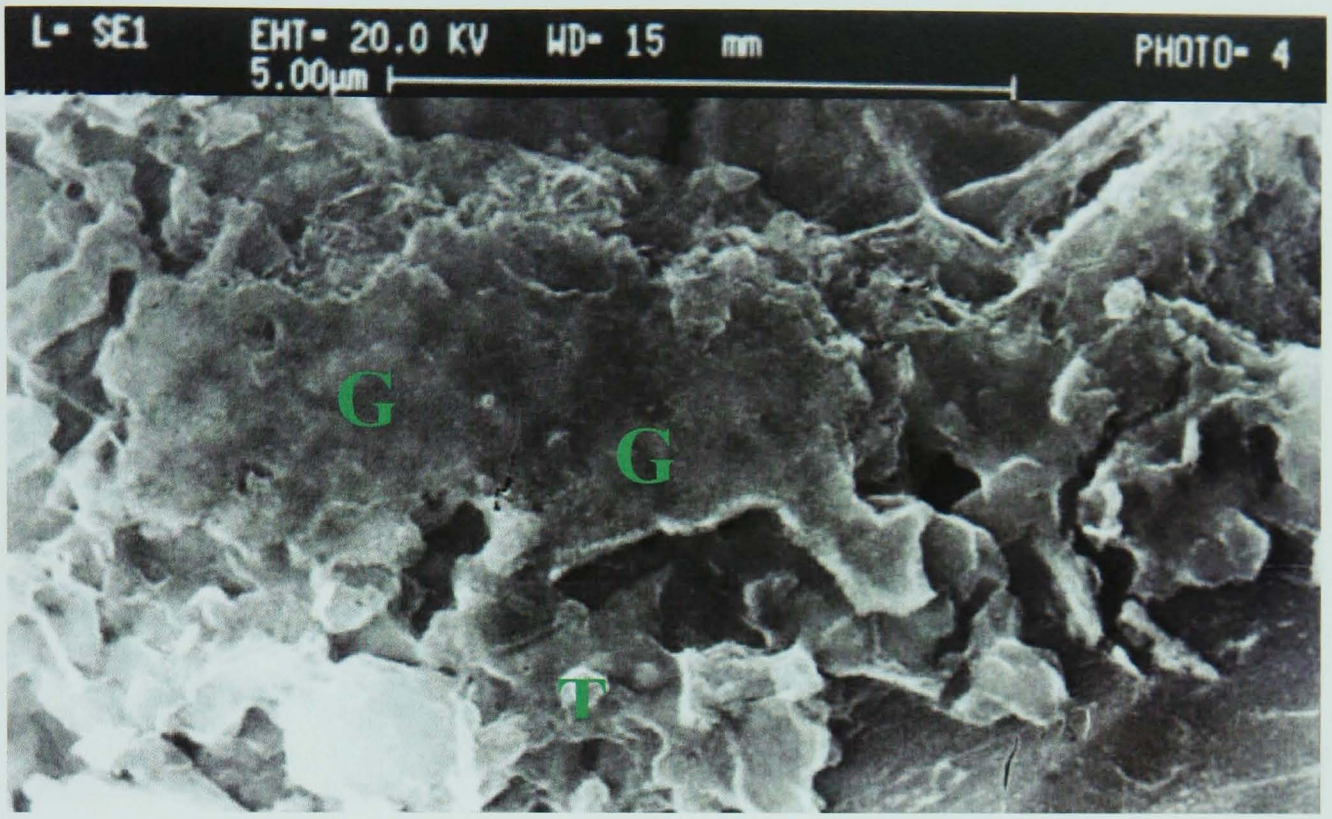

Figure 5.18-a SEM of activated Taftan pozzolan cured at 25 ºC carried out in Material and Energy Research Centre laboratory, Tehran, Iran-(G) Geopolymer Matrix (T) Non reacted Taftan Pozzolan

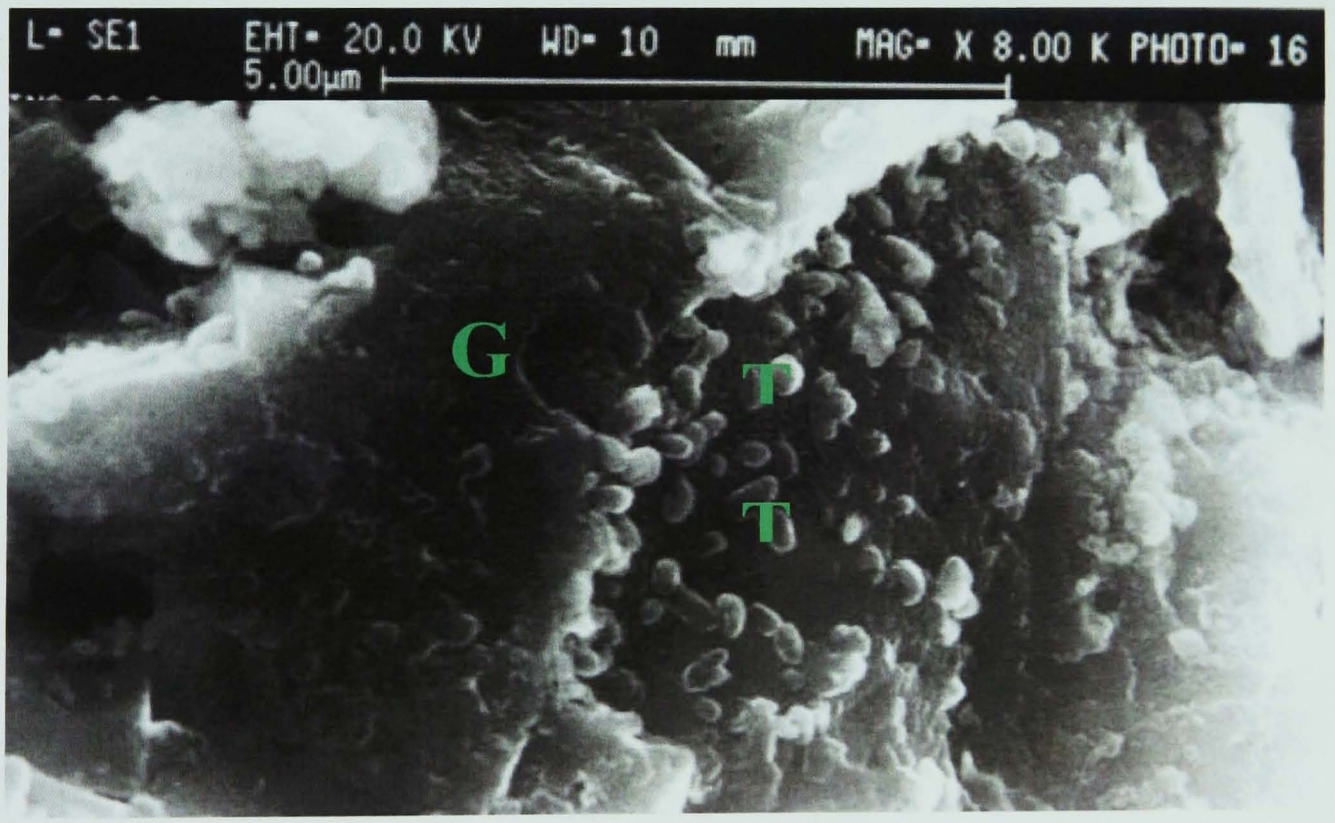

Figure 5.18-b SEM of activated Taftan pozzolan cured at autoclave condition carried out in Material and Energy Research Centre laboratory, Tehran, Iran-(G) Geopolymer Matrix (T) Non reacted Taftan Pozzolan

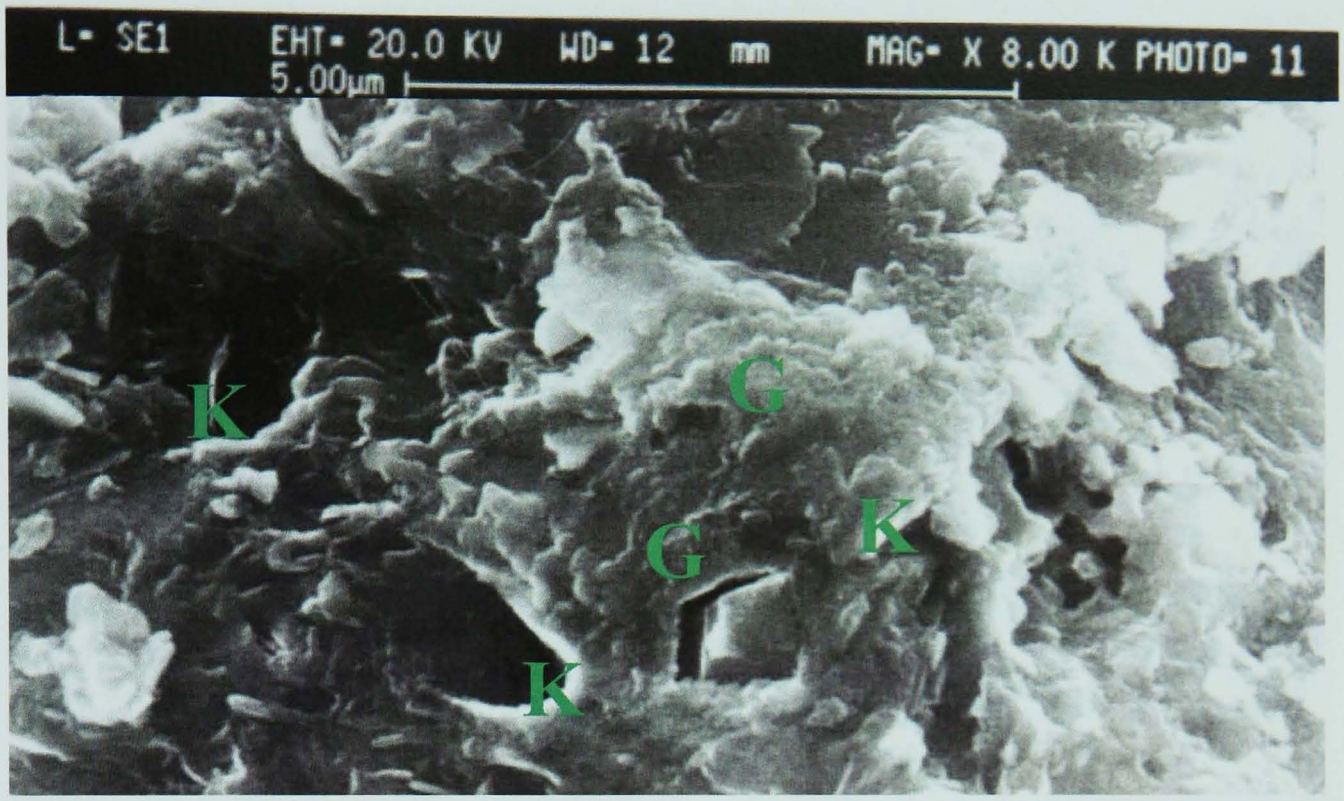

Figure 5.19-a SEM of activated Taftan pozzolan mixed with Kaolinite Cured at 25°C carried out in Material and Energy Research Centre laboratory, Tehran, Iran-(G) Geopolymer Matrix (K) Non reacted Kaolinite

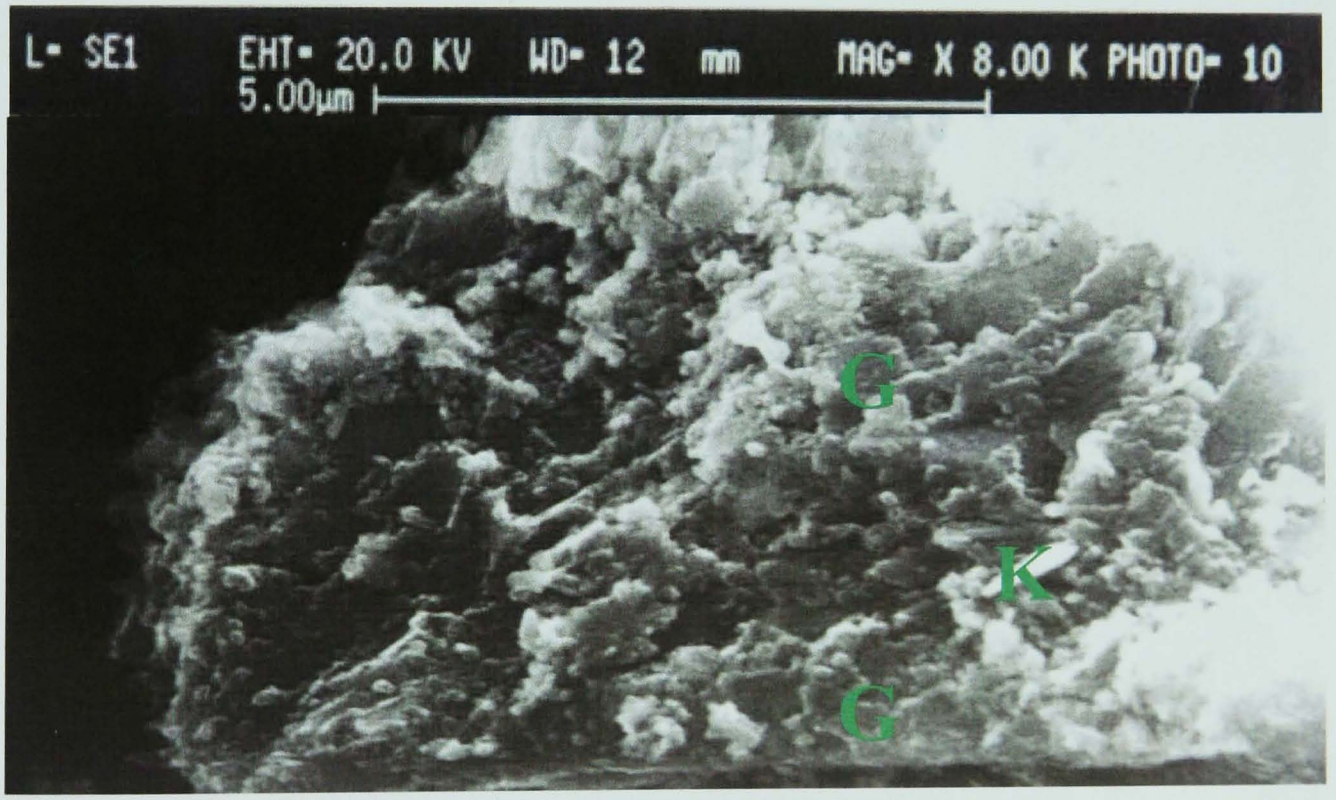

Figure 5.19-b SEM of activated Taftan pozzolan mixed with Kaolinite Cured at autoclave condition carried out in Material and Energy Research Centre laboratory, Tehran, Iran (G) Geopolymer Matrix (K) Non reacted Kaolinite

Figure 5.20-a SEM of activated Taftan pozzolan mixed with calcined Shahindej and cured at 25°C carried out in Material and Energy Research Centre laboratory, Tehran, Iran (G) Geopolymer Matrix (Z) zeolite (SH) Non reacted Shahindej Pozzolan

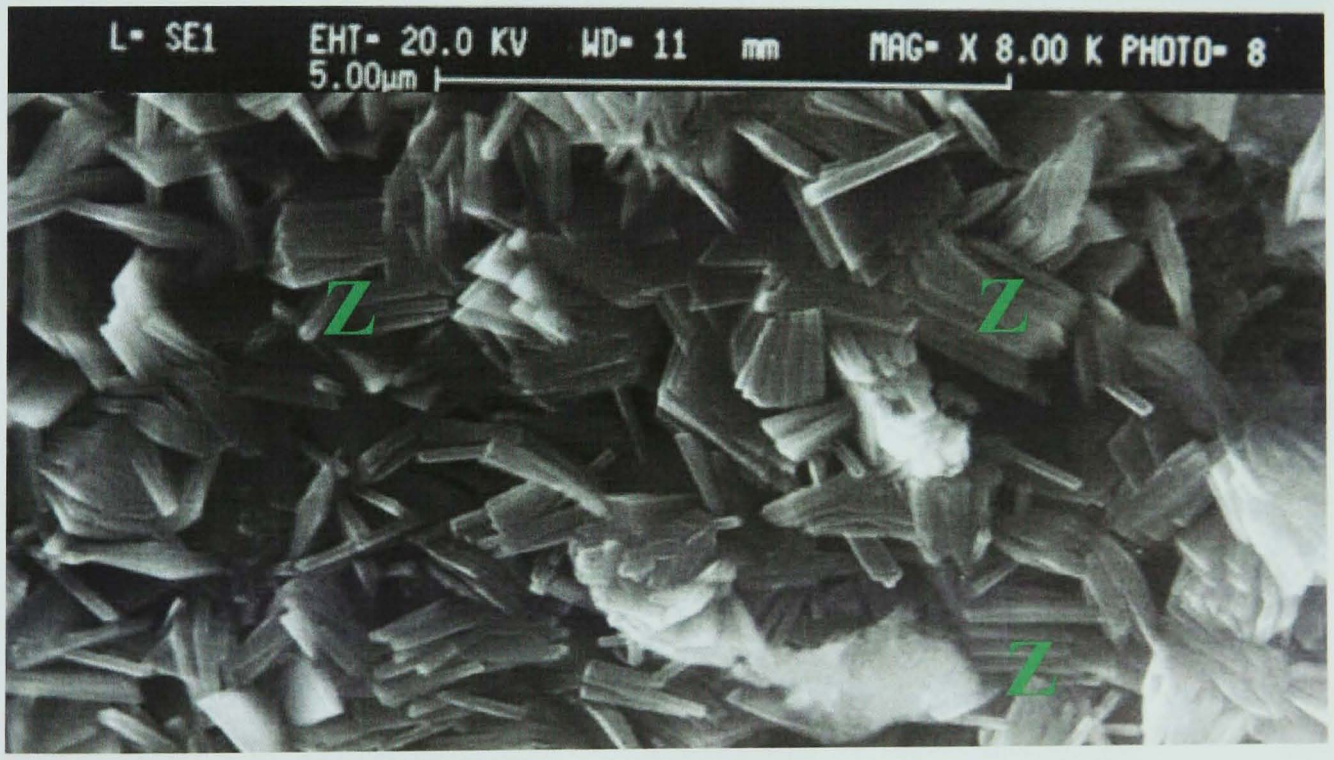

Figure 5.20-b SEM of activated Taftan pozzolan mixed with calcined Shahindej and cured at autoclave condition carried out in Material and Energy Research Centre laboratory, Tehran, Iran(Z) Zeolite

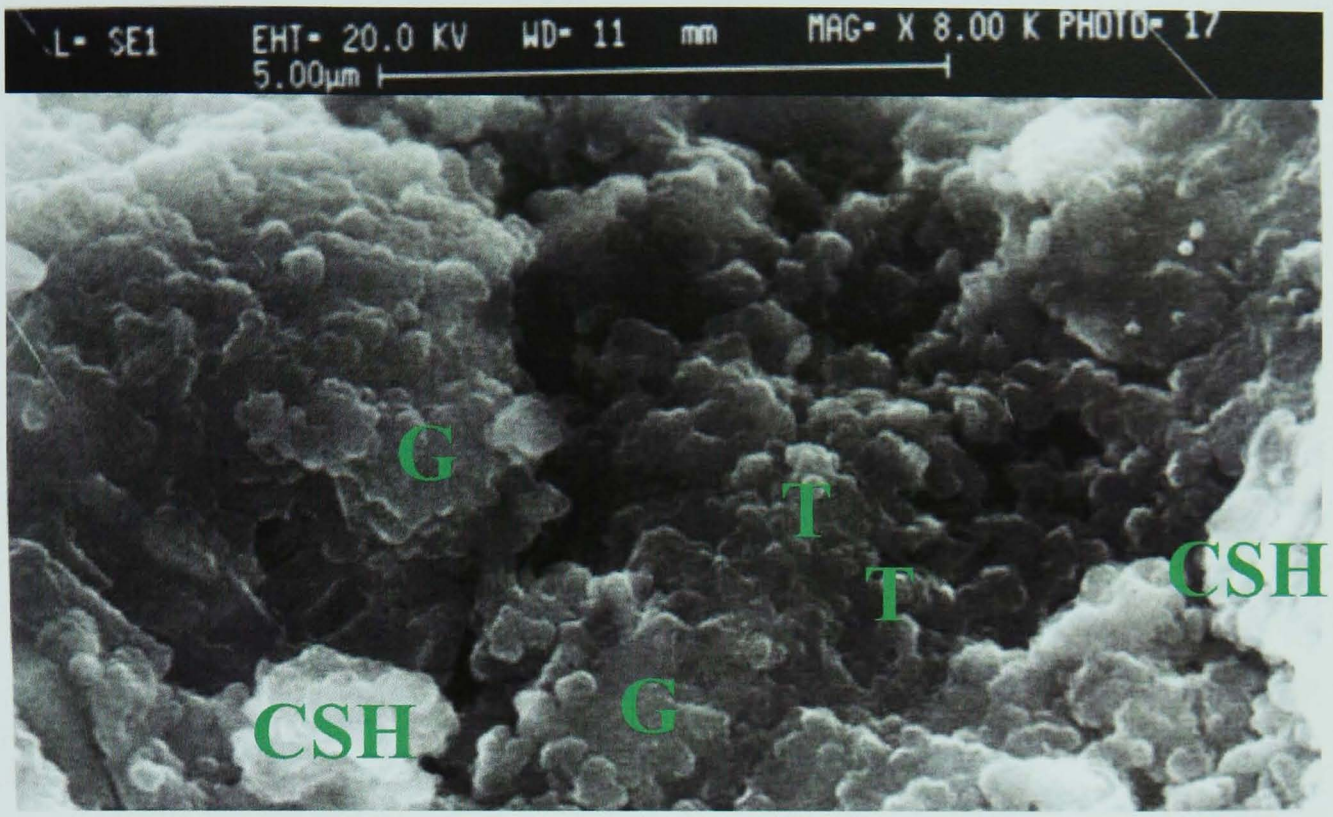

Figure 5.21-a SEM of activated Taftan pozzolan mixed with burnt lime at 25°C carried out in Material and Energy Research Centre laboratory, Tehran, Iran(G) Geopolymer Matrix (CSH) Calcium Silicate Hydrate (T) Non reacted Taftan Pozzolan

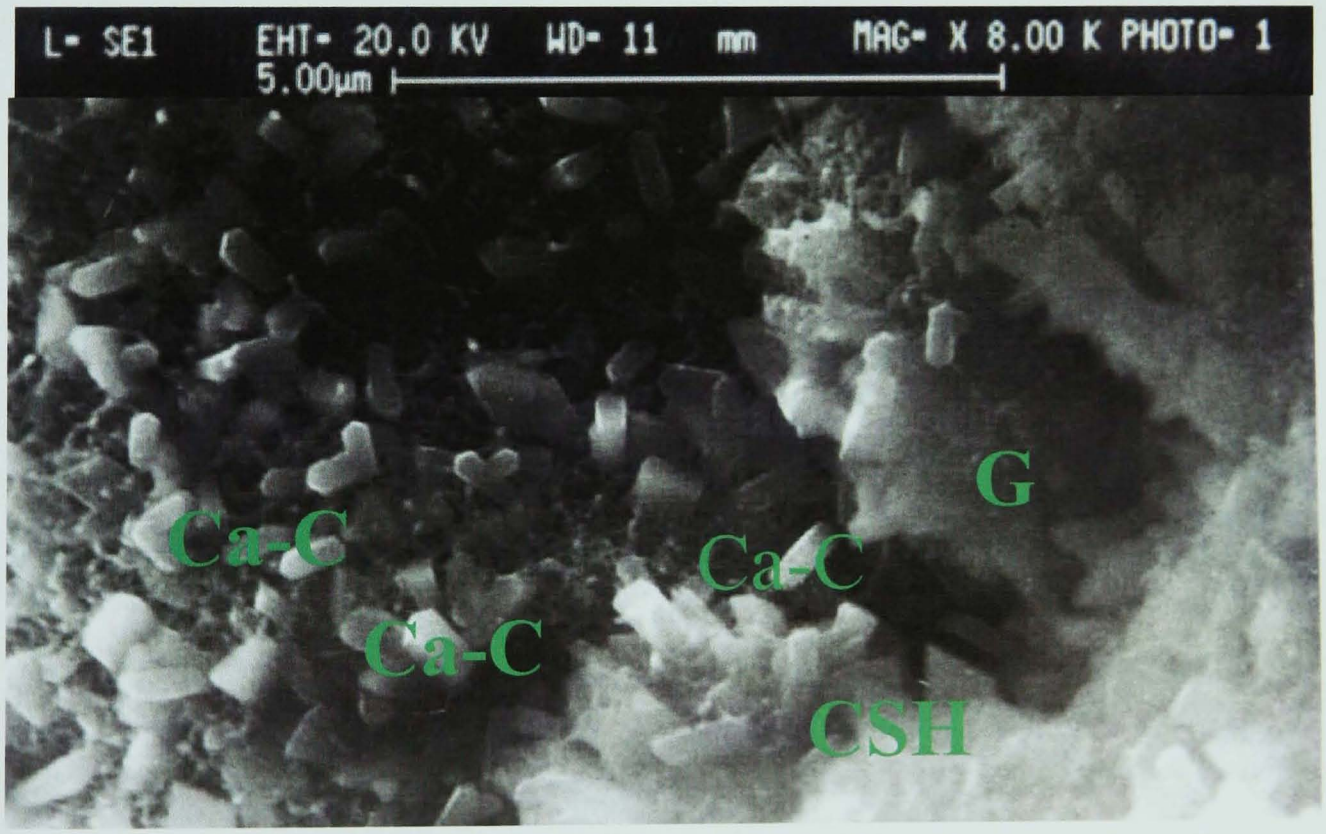

Figure 5.21-b SEM of activated Taftan pozzolan mixed with burnt lime at autoclave condition carried out in Material and Energy Research Centre laboratory, Tehran, Iran(G) Geopolymer Matrix (CSH) Calcium Silicate Hydrate (Ca-C) Calcium Carbonate

6. MIX DESIGN AND PROPERTIES OF FRESH GEOPOLYMER CONCRETE

6.1 Introduction

In this chapter, the different mix designs including the selection of ingredients, blending proportions, mixing procedures and curing regimes used, are presented.

Another aim of this chapter is to study the fresh geopolymer concrete properties influenced by the incorporation of natural pozzolan and the addition of alkali activators. Fresh geopolymer concrete based on activated natural pozzolan is a freshly mixed material that can be moulded into any shape. The inherent properties and relative quantities of activators of natural pozzolan, in addition to the amount of water mixed in, control the properties of the wet state as well as the hardened state of the concrete. This chapter reports on the workability of the geopolymer concrete mixes based on their slump and vebe time (rod normally VB) results. The setting time results for the mixes are presented, followed by the air content of the concrete.

6.2 Mix Design Procedure

The widespread use and complex structural application of concrete require design of mixes possessing high strength and durability. Mix proportioning is based on determining the quantities of the ingredients, when mixed together and cured properly will produce workable concrete that achieves the desired strength and durability when hardened. Therefore different variables including desired workability measured by slump, water to binder ratio, binder content and aggregate proportions should be considered in the mix design procedure.

6.2.1 Alkali-Activated Natural Pozzolan Mixes

The mixture calculations were made based on the optimum amount of activator needed to activate the pozzolan which resulted from sections 5.4, 5.6, and 5.7. The water in the activator is also taken as part of the total mix water.

6.2.2 Determination of Water to Binder Ratios

Soil concept approaches are used to determine the amount of water required in no slump concrete mix design such as roller compacted concrete by determining the

optimum moisture amount to achieve maximum density (Hansen and Rinehart, 1992). In this investigation in view of the low workability of geopolymer concrete, the Atterberg consistency limits for cohesive soils were utilized to determine the minimum water to binder ratios for making mixtures with these natural materials. In soil mechanics these limits are used to define the behaviours of a cohesive soil as its moisture content is changed. The values are influenced by grain size and the amount and character of the clay minerals present. When dry, a cohesive soil behaves as a solid (no workability) but as water is added it first turns to a semi-solid, then to a plastic, and finally to a liquid (workable) state. The moisture contents at the boundaries between these states are referred to as the shrinkage limit (SL), the plastic limit (PL) and the liquid limit (LL), respectively (Bell, 2000).

The consistency of cohesive soils depends on the interaction between the particles. Any decrease in moisture content results in a decrease in cation layer thickness and an increase in the net attractive forces between particles. For a soil to exist in the plastic state, the magnitude of the net inter particle forces must be such that the particles are free to slide relative to each other but with cohesion between them being maintained (Bell, 2000).

The plasticity index defines the range of water content for which the soil behaves like a plastic material and the amount of water content, which causes the soil to change from a plastic to semi-solid, is called the plastic limit. A falling cone test was used to determine the liquid and plastic limits of both pozzolans and the beginning point for water to binder ratio for concrete mixtures should be considered at least equal to the summation of the plastic limit and aggregate water absorption which are as below for different pozzolans:

Taftan Pozzolan: 21.0% + 0.9% = 21.9%
Shahindej Pozzolan: 38.9% + 0.9% = 39.8%

Using the values obtained from the above method, and considering the workability of mixtures, several trial batches were made to achieve the target strength with a cohesive, workable mix. It was found that for pozzolans containing zeolites and clayey minerals such as Shahindej the above water to binder ratio is the optimum amount to give high compressive strength.

6.2.3 Aggregates and Sieve Analysis Results

6.2.3.1 Fine Aggregate

The fine aggregate used was obtained from deposits from the Karaj River in northwest of Iran. A sieve analysis was carried out on representative samples in accordance with BS EN 12620:2002. The analysis showed that the sand needed some modification to fall in zone F. Therefore it was sieved through the specified sieves and particles between each two sieves were stored separately. Then suitable proportions of sand were selected and remixed to give a curve which fell within zone F as specified by BS EN 12620:2002. The final sieve analysis is given in table 6.1. The sand has a water absorption coefficient of 0.6 percent and a bulk specific gravity, saturated surface dry (SSD) of 2.62, both determined in accordance with BS 812: Part 2.

6.2.3.2 Coarse Aggregate

The coarse aggregate used for this study was clean and well graded gravel with a maximum size of 14 mm. Gravel was obtained from the same location as the fine aggregate. A sieve analysis test showed that the coarse aggregate conformed to the limits set out in BS EN 12620:2002 and the results are given in Table 6.1. The bulk specific gravity (SSD) of this gravel was 2.6 and its water absorption was 0.9 percent.

6.2.4 Aggregate to Binder Content

In the RRL method (Road Note 4 Method, Neville, 1995), the aggregate to cement ratios for OPC concrete are worked out on the basis of type of aggregate, maximum size of aggregate and different levels of workability. This method leads to very high cement contents and thus is becoming obsolete, but it can be used as a starting point. The values of aggregate to cement ratio are suggested for angular rounded or irregular coarse aggregate and for different levels of workability ranging from low to high. Therefore for irregular coarse aggregate and very low workability, this ratio suggested values of aggregate to cement ratio are 4.7, 5.7, and 7.3 while for low workability it is 3.8, 4.6, and 6 for the water to binder ratios equal to 0.4, 0.45, and 0.55, respectively. Thus, using the BRE method and specific gravity to arrive at

correct mix design calculations, the resulted aggregate to binder content compared to the above ratio to be verified.

The untreated Shahindej pozzolan was found to be sensitive to the ratio of binder to aggregate. Hence, this parameter and water to binder ratio were considered together to find the optimum for these two in a model that may be suitable to use for this type of pozzolan and is shown in Figure 6.2. To do this, different samples were made with different aggregate to binder ratios while the other factors were kept constant and the compressive strength was measured at 28 days. This was repeated for samples with different water to binder ratios and the whole results were plotted to find the ideal islands of these two ratios. As can be observed in Figure 6.2 at higher binder to aggregate ratio in spite of normal cases the compressive strength reduces which seems to be related to main mineral phases in untreated Shahindej pozzolan.

6.2.5 Designing of Control Mixes

The control mixes were designed using the BRE method (Neville, 1995) targeting a 40 MPa 28 days compressive strength and a slump 60 mm. With respect to the values obtained from this method several batches were carried out to achieve the target strength with a workable mix. To compare the mixes on equal W/B ratio, OPC control mixes were used with the cement content and the W/C ratio the same as the binder content and the W/B ratio in Taftan geopolymer concrete. For untreated and calcined Shahindej pozzolan the binder content was 25kg/m^3 more and the W/B ratio was 3% less than the corresponding amounts in OPC control mix. These are the least to achieve strength in a range suited for structural concrete with Shahindej pozzolan.

6.2.6 Mix Proportions and Mix Notation

The proportioning of the concrete mixture was based on the BRE method targeting a 40 MPa (28 days) compressive strength and a slump of 60 mm considering the earlier approaches for determining the minimum water to binder ratio (i.e. the optimum amount for Shahindej pozzolan with zeolite minerals) and the optimum aggregate to binder ratio was found for activated Shahindej pozzolan mix. Hence, the water to binder ratio selected according to the workability and the above method might not be less than the pozzolan plastic limit plus aggregate water absorption

which was discussed in section 6.2.2, and would be expected to result the highest compressive strength especially in cohesive pozzolans. The amount of cement was substituted with the same quantity of natural pozzolan plus the solids in water glass and the amount of water was ignored since there was already water in the alkali solutions. In other words, the calculated amount of water was considered to make alkali solutions. Then the mixture calculations were made to calculate the required amount of activator by weight, which would provide the chosen dosage in Table 5.7. The BRE method was used only to decide what is a common ratio of binder, sand and coarse aggregates, it was not expected that the actual 28 days compressive strength or the slump would be in accordance with the values designed. The details of the different mixes are presented in Table 6.2 and the notations for the mixes are as follows:

CM1: PC control mix with w/c=0.45

CM2: PC control mix with w/c=0.55

ATAF1: Activated Taftan pozzolan mix with w/b=0.45

ATAF2: Activated Taftan pozzolan mix with w/b=0.55

ARSH: Activated Raw Shahindej pozzolan mix with w/b=0.42

ACSH: Activated Calcined Shahindej pozzolan mix with w/b=0.42

6.3 Mortar and Concrete Mixing Procedure

In the initial investigation, the study also concentrated on the mixing procedure, in terms of the order of the addition of the raw materials to the reaction mixture, in a small pilot study on whatever was reported by Palomo et al. (1992). Two different pathways for obtaining the geopolymers were considered while compressive strength of the products so obtained was studied. This was found that the compressive strengths are higher in geopolymers made by adding alkaline hydroxide solution to natural pozzolan first followed by a sodium silicate solution, instead of adding alkaline and sodium silicate as a mixed solution to natural pozzolan. Compressive strength increased about 33% in Taftan pozzolan due to the former mix procedure with rises from 44.4 to 59.08MPa considering other parameters similarly. It seems

that by adding alkaline hydroxide solution first, the Al-Si bonds are broken up, thus causing a higher degree of the Al-Si disorder. Then gel formation in hydrated alkaline alumina-silicates is generated by sodium silicate. However, adding alkaline and sodium silicate as a mixed solution creates two opposite reactions. Therefore the mixing of the geopolymer mortar was carried out in a Hobart Canada N-50-1425rpm mixer (2 litre capacity) using the procedure below:

.

i. The alkaline hydroxide solution was made by dissolving KOH pellets in the mixing water, using a magnetic stirrer and left to cool down. Then it was added to natural pozzolan in the Hobart mixer.
ii. Mixing proceeded for the next 10 minutes at low speed.
iii. The mixer was stopped to scrape the mixture off the sides of the bowl and turned on again for another 5 minutes at medium speed.
iv. Then the sodium silicate solution was added to the above mixture and the mixing continued for another 10 minutes.
v. Sand was added to the slurry and the mixing continued for the next 5 minutes at low speed before the mixtures were cast into the moulds in three layers.

The mixing of the geopolymeric concrete was carried out in two phases of mixing. The paste was prepared in a Hobart mixer (2 litre capacity) as above (i to iv steps) and added to a horizontal pan mixer (20 litre capacity) which contained the aggregates. The reason for choosing two sequences of mixing was preventing the direct contact of alkaline solutions with aggregates. It seems adding alkaline solutions directly to the aggregates causes a surface layer of alkaline around them which makes they bind to paste weakly. All the samples were made using the same procedure.

6.4 Casting and Curing

The concrete samples were cast in different sizes as required by the tests. The mixtures were cast into the pre-oiled moulds in three layers and vibrated by means of a vibrating table to remove any entrapped air. It was observed that a geopolymer concrete stick hard to the mould and oiling of the moulds is very important to allow release of the samples.

Taftan specimens were de-moulded 24 hours after casting and cured in two curing regimes and at three different temperatures:

1) Sealed curing: Three series of specimens were sealed wrapped in a special plastic covering which was tested to be impermeable and stored in a controlled room kept at three different temperature equal to 20± 2, 40± 2 and 60± 2° C.

2) Fog curing: Three series of the specimens were cured in the fog chamber set at three different temperatures equal to 20±2, 40±2 and 60±2°C and compressive and splitting tensile strength were measured. One series was fog cured at 40±2°C for other measurements.

Shahindej specimens were all cured in sealed curing conditions. This is because the zeolites minerals in this pozzolan have inherently high water absorption and are sensitive to shrinkage. Thus, in the sealed curing condition the water in the system participates in the chemical reactions and there would not be more water available to cause expansion and shrinkage of these minerals, while curing in fog condition causes absorption of excess water after the chemical reaction is finished and loss of this free absorbed water, causes micro cracks and high reduction of the strength. Thus Shahindej pozzolan in a natural state would be suitable for concrete works in which curing at more than 60°C without pressure is practical. Otherwise warm condition with pressure improves the performance. In pre-cast concrete works curing at 80°C and 18MPa uniaxial pressure between two Mylar sheets would produce a good material. It was found in section 4.4.1 that untreated Shahindej pozzolan needed at least 60°C curing to provide moderate to high strength and the optimum temperature for curing calcined Shahindej was found to be 20°C. Therefore ARSH concrete mixes were cured at 60°C and ACSH mixes were cured at 20°C.

After the high temperature curing regime, the specimens were kept in air until testing. Fog cured samples were put in the air 24 hours before testing and sealed cured samples an hour, to gain the ambient temperature and humidity.

6.5 Workability

Workability generally defines the ease of handling, placing and compaction of a concrete. A workable concrete is one that requires minimum amount of energy to produce a consolidated composite with low air content, thus achieving its characteristic hardened properties.

6.5.1 Workability tests

Workability of concrete is a complex property and numerous attempts have been made to quantitatively measure this important property. Some of the tests for measuring the parameters of workability are:

- Slump test
- Compacting factor test
- Vebe time test
- Flow table test
- Two point test G.H. Tattersall of Sheffield University (Tattersall, 1991, 1976 in Day, 1999)
- Viscometer and rheometer which are modern determinations of workability

These are chosen based on the type of concrete, its application, and the location of the casting. In this research Slump and Vebe time were measured for all of the concrete mixes.

6.5.2 Slump Test

The Slump test is the most commonly used method for measuring consistency of concrete. It does not measure all factors contributing to workability. However, it is used conventionally as a control test and gives an indication of the uniformity of concrete from batch to batch. Repeated batches of the same mix, brought to the same slump, will have the same water content and water binder ratio, provided the weights of aggregate and binder are uniform and aggregate grading is within acceptable limits.

The apparatus for conducting the slump test essentially consists of a metallic mould in the form of a frustum of a cone having bottom diameter, top diameter and height equal to 20, 10, and 30 cm respectively. The mould is placed on a smooth, horizontal

and rigid surface. The mould is then filled in four layers and each layer is tamped 25 times by the tamping rod. The mould is removed from the concrete by raising it slowly and carefully in vertical direction. This allows the concrete to subside and the subsidence shows the slump of concrete. Hence, slump was measured for all mixes in accordance with BS EN 12350-2:2000 and the results of the slump tests are presented in Table 6.3 and Figure 6.3.

6.5.3 Vebe time Test

Vebe test is a good indirect laboratory measurement of the workability of concrete. This test consists of a vibrating table, a metal pot, a sheet metal cone, and a standard iron rod. Slump test as described earlier is performed, placing the slump cone inside the sheet metal cylindrical pot of the consistometer. The glass disc attached to the swivel arm is turned and placed on the top of the concrete in the pot. The electrical vibrator is then switched on and simultaneously a stop watch started. The vibration is continued until such time as the conical shape of the concrete disappears and the concrete assumes a cylindrical shape. This can be judged by observing the glass disc from the top. Immediately when the concrete fully assumes a cylindrical shape, the stop watch is switched off. The time in seconds required for the shape of concrete to change is known as the vebe time. This was measured for all mixes in accordance with BS 1881: 1670 and the results of these tests are presented in Table 6.3 and Figure 6.4.

6.5.4 Results and Discussions

The results of the slump tests and vebe time tests are presented in Table 6.3, and Figures 6.3 and 6.4. The results show low workability concrete for OPC control mixes while the CM1 having the lower slump than CM2 which has a higher w/c ratio. The fresh geopolymer is usually classified as "sticky" when compared to normal OPC mixes (Roy and Silsbee 1992; Hardjito et al. 2002), specially if the reaction happens in the presence of soluble silicates (Fernandez-Jimenez et al. 2006). The slump results also show low workability for this type of concrete and the vebe time for the geopolymer concrete based on activation of natural pozzolans is much more than for OPC concretes because they are inherently highly plastic and sticky

concretes. In this type of concrete increasing the w/b ratio and calcination the pozzolan both increase the slump and cause more workable geopolymer concrete.

6.6 Setting Time

In actual construction dealing with cement paste, mortar or concrete, certain amount of time is required for mixing, transporting and placing. During this time cement paste, mortar or concrete should be in a plastic condition. The setting times refer to the time interval for which these products remain in plastic condition or change from a fluid to a rigid state. An arbitrary division has been made for setting time as initial and final setting time. The initial setting is regarded as the time in which paste or concrete remains plastic or workable. While, the final setting time corresponds to the time required for the matrix to reach the stage where it has completely lost its plasticity and has started to attain its mechanical strength. During the time between the initial and final set, the matrix is stiff and cannot be reshaped.

6.6.1 Test Procedure

The mixing procedure followed the steps described in section 6.3. The mortar was placed in a special shaped mould immediately after mixing. The setting time was determined using the Vicat apparatus in accordance to BS EN 196-3:1995. The apparatus consists of a steel needle which acts under a prescribed weight of 300 ± 1 g to penetrate the mortar. The penetration was repeated every 10 min and during the interval the sample was kept in a chamber under a controlled temperature (the same as the curing temperatures used i.e. 20, 40, 60°C for Taftan; 60°C and 20°C for untreated and calcined Shahindej, respectively) and 90% relative humidity.

The initial setting time was recorded when the sample was sufficiently stiff that the needle penetrated no deeper than 4 ± 1 mm from the bottom. The final set occurred when the special needle penetrated the mortar to a depth of only 0.5 mm.

6.6.2 Results and Discussion

The results of the initial and final setting times for the various mixes are listed in Table 6.4 and plotted in Figures 6.5 and 6.6.

As expected, the initial setting time was shorter for higher temperature curing. The setting characteristic of mixes shows that setting is generally fast, and on average it took about 8 to 15 minutes from start to end of setting of the mortar with optimum concentration of activator except for untreated Shahindej pozzolan (Table 6.3 and Figure 6.6). The different pozzolans investigated behaved differently in affecting the initial and final setting time of geopolymer concretes which depend on the properties of the main mineral phases. Shahindej pozzolan has inherently higher silicate content compared to Taftan pozzolan and its higher SiO_2 concentration may be responsible for the delay in its setting as is observed in the results. It took about 120 minutes from start to end of setting for untreated Shahindej pozzolan. The amount of SiO_2 detected for calcined Shahindej was similar to what was determined for untreated Shahindej pozzolan, but the source of silicate related to opal which reacts rapidly with an aqueous alkaline solution, thus it took 13 minutes from start to end of setting for calcined Shahindej pozzolan (Table 6.3 and Figure 6.6).

Blended systems of OPC and natural pozzolan generally present a prolonged setting time when compared to a control Portland cement. Turanli et al. (2004) studied the replacement of 35, 45, and 55% of OPC for Turkish volcanic tuff and reported that the blended cements showed quiet different setting times according to pozzolan content. Considering W/C for normal consistency, the blended cement containing 55% natural pozzolan exhibited shorter initial and final setting times equal to 105 and 157(min) when compared with reference Portland cement. While for the blended cement containing 35% pozzolan, the reverse is true and these are equal to 190 and 315(min), respectively.

The BS EN 197-1:2000 prescribes a minimal initial setting time of Portland cement: if the designed 28 days compressive strength is 32.5 MPa, the initial setting time cannot be less than 75 min; if it is 42.5 MPa not less than 60 min; and if it is 52.5 MPa not less than 45 min. In comparison with OPC concrete, most of the geopolymer concrete mixes seems not to show an acceptable initial setting time according to the BS EN 197-1:2000.

As the concentration of alkaline hydroxide increases, the setting time of the mortars always decreased. When the dosage of activator increased from 2.5 to 5 Molar, it slightly decreased the initial and final setting time, but the further increase of

activator dosage from 5 to 7.5 Molar markedly decreased the initial and final setting times (Table 6.4 and Figure 6.5).

6.7 Air Content

The exact air content in concrete is extremely important as it affects the various properties of concrete including workability, strength and the resistance of concrete in severe environmental conditions. If the air content is found to be very low, it causes insufficient workability while the presence of high air content or voids, greatly reduces the strength of concrete.

There are mainly three methods for measuring air content of fresh concrete:

- Gravimetric Method
- Volumetric Method
- Pressure Method

In this investigation the pressure method was used because it is the best method for finding the air content of fresh concrete due to its superiority and ease of operation over other methods.

6.7.1 Test Procedure

The air content was determined in accordance with BS EN 12350-7:2000. According to the pressure method the vessel was filled with concrete, compacted in three layers in a standard manner and stuck off level. A cover was then clamped in position and water added until it spilled from the tube of the cover and then pressure was applied by means of a pump. The pressure is then transmitted to the air entrained in the concrete, which contracts accordingly. Then the water level falls. The pressure is then increased to a predetermined value as indicated by a small pressure gauge mounted on the cover. For this type of concrete, the glass gauge tube is so calibrated that the percentage of air by volume is indicated directly. The results reported the volume of air as a percentage of volume of concrete.

6.7.2 Results and Discussion

The air content of the various mixes is listed in Table 6.3 and plotted in Figure 6.7. The air content of different activated pozzolans is compared to control mixes. It is evident from the results that increasing the water/binder ratio is associated with the reduction of the air content. This could be due to a reduction in the viscosity of the concrete. Although the vebe result of ATAF2 did not suffer from air entrapment as much as expected. Also for different pozzolans the more viscous they are, the higher was the air content.

6.8 Summary

The main conclusions drawn from this chapter are summarized as follows:

1) In pozzolans containing zeolites and clayey minerals, such as Shahindej, the optimum amount of water to binder ratio for achieving the highest compressive strength, is the summation of its plastic limit and aggregate water absorption (Figure 6.2).

2) In alkali activated pozzolan concrete, the procedure for adding the reaction mixtures to the pozzolan materials and aggregates is important for achieving high compressive strength. Highest strength occurs if alkaline hydroxide solution is added and mixed with natural pozzolan first, then followed by adding the sodium silicate solution.

3) Geopolymer concrete based on activation of natural pozzolan has low workability and the vebe time for this type of concrete is much longer than for OPC concretes due to the sticky nature of geopolymer concrete.

4) Geoploymer paste sets rapidly; usually there is about 15 minutes between the beginning and end of setting. The initial and final setting time of alkali activated pozzolan concrete depends on the properties of the main mineral phases. In natural pozzolans, the higher the amount of silicate concentration the longer the setting time, unless the silicate source consists of minerals such as opal which reacts rapidly with an aqueous alkaline solution.

5) The setting time of alkali activated natural pozzolan decreases when the dosage of alkaline hydroxide increases.

6) The relationship between paste setting time and mix temperature shows that as the mix temperature increases the setting time of the paste decreases.

7) Increasing the water to binder ratio is associated with a reduction in air content.

Table 6.1 Grading for the fine and coarse aggregates

Fine aggregate

Sieve size	% Passed
4.75 mm	99
2.36 mm	90
1.18 mm	85
600 microns	77.5
300 microns	37.5
150 microns	–

Coarse aggregate

Sieve size	%Passed
20 mm	100
14 mm	95
10 mm	67.5
5 mm	5
2.36 mm	–

Table 6.2 Concrete Mix Proportion

Mix No.	Natural Pozzolan (kg/m^3)	OPC (kg/m^3)	Alkaline Hydroxide (kg/m^3)	Water Glass (cc/m^3)	Water (kg/m^3)	Total Water (kg/m^3)	Total Binder (kg/m^3)	Fine Agg. (kg/m^3)	Coarse Agg. (kg/m^3)	W/B%
CM1	_	403	_	_	180	181.3	403	577.82	1227.88	0.45
CM2	_	357	_	_	195	196.35	357	702	1119.65	0.55
ATAF1	391	_	66.27	34.18	157.78	180	403	578.17	1228.8	0.45
ATAF2	344	_	71.82	36.9	171	195	357	702	1121	0.55
ARSH	417.43	_	66.91	31.83	159.31	180	428.57	498.8	1282.63	0.42
ACSH	417.43	_	66.91	31.83	159.31	180	428.57	498.8	1282.63	0.42

Table 6.3 Fresh concrete properties of the mixes investigated

Concrete Mix No.	Slump (mm)	Vebe Consistometer (seconds)	Air Content (%)	Setting time (min)	
				Initial	Final
CM1	60.0	3.0	2.3	180	270
CM2	65.0	2.0	1.65	-	-
ATAF1	10.0	25.0	2.2	60	75
ATAF2	71.0	12.0	1.5	-	-
ARSH	25.0	27.0	2.8	60	180
ACSH	35.0	22.0	2.5	37	50

Table 6.4 Initial and Final setting time of different mixes (with different activator concentrations and mix temperatures)

Mix Temperature	Mix No.	Activator Concentration (Molar)	Setting time (min)	
			Initial	Final
20	CM1	-	180	270
20	ATAF	2.5	375	405
		5.0	310	330
		7.5	60	75
40	ATAF	2.5	244	264
		5.0	233	248
		7.5	48	60
60	ATAF	2.5	92	100
		5.0	90	99
		7.5	15	23
60	ARSH	2.5	112	375
		5.0	95	270
		7.5	60	180
20	ACSH	2.5	295	330
		5.0	155	180
		7.5	37	50

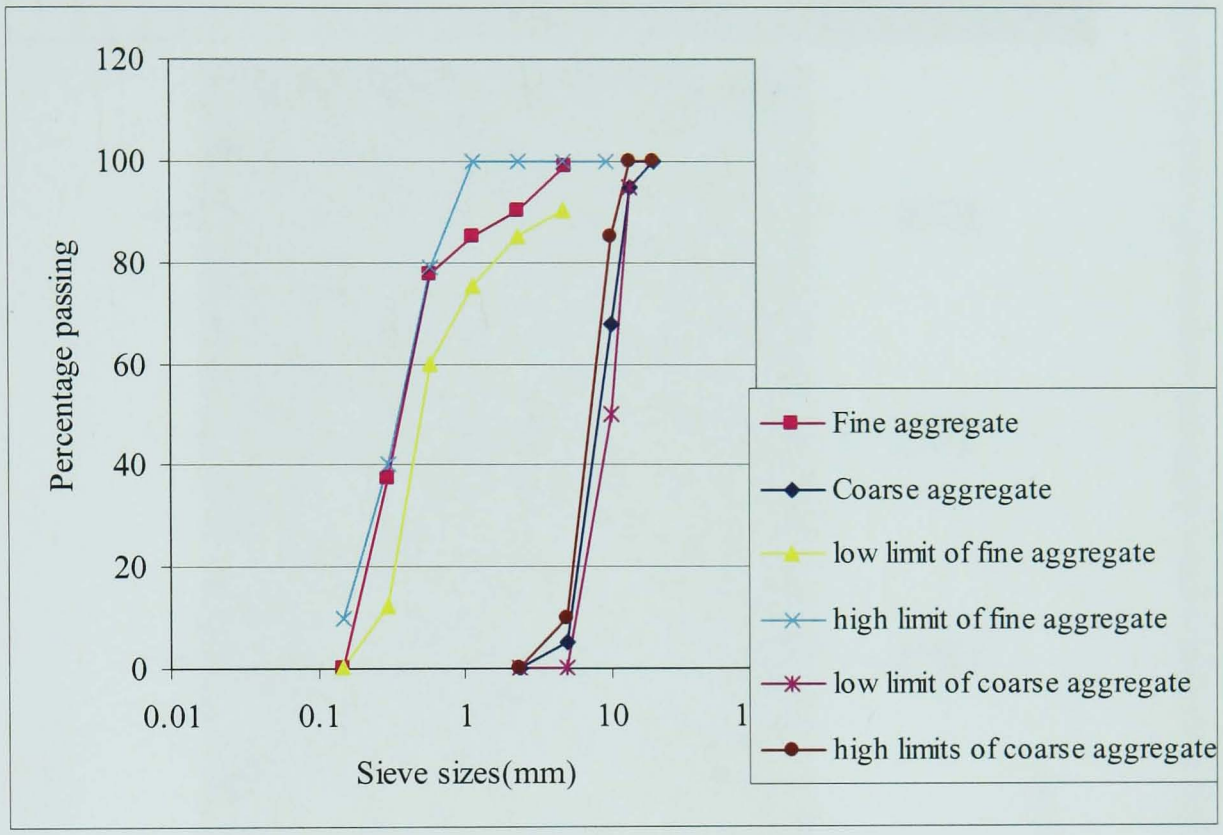

Figure 6.1 Grading limits and size distribution curves for the fine and coarse aggregates

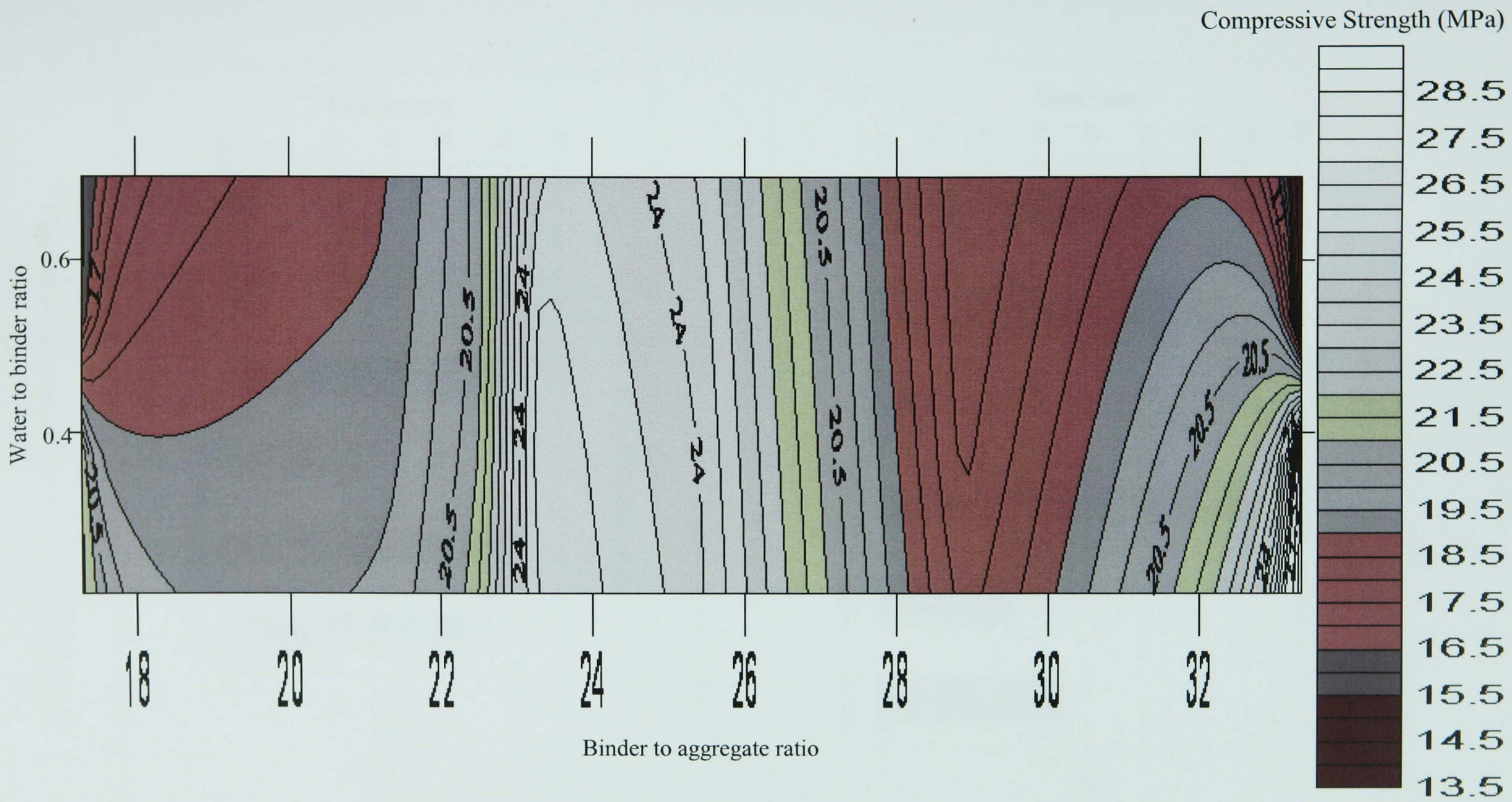

Figure 6.2 Compressive strength contour of activated untreated Shahindej pozzolan versus different amount of water to binder and binder to aggregate ratio (16 samples were tested)

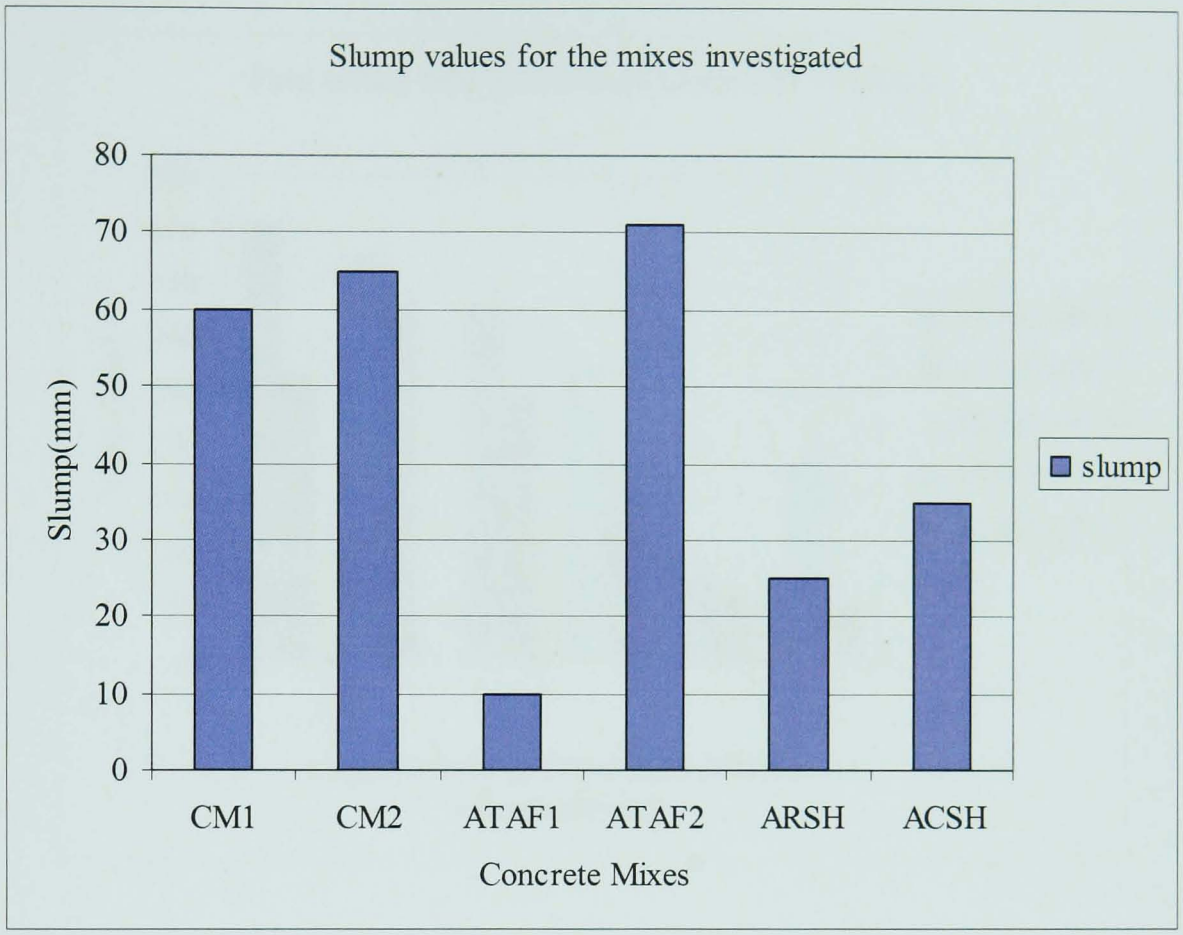

Figure 6.3 Slump values for mixes investigated

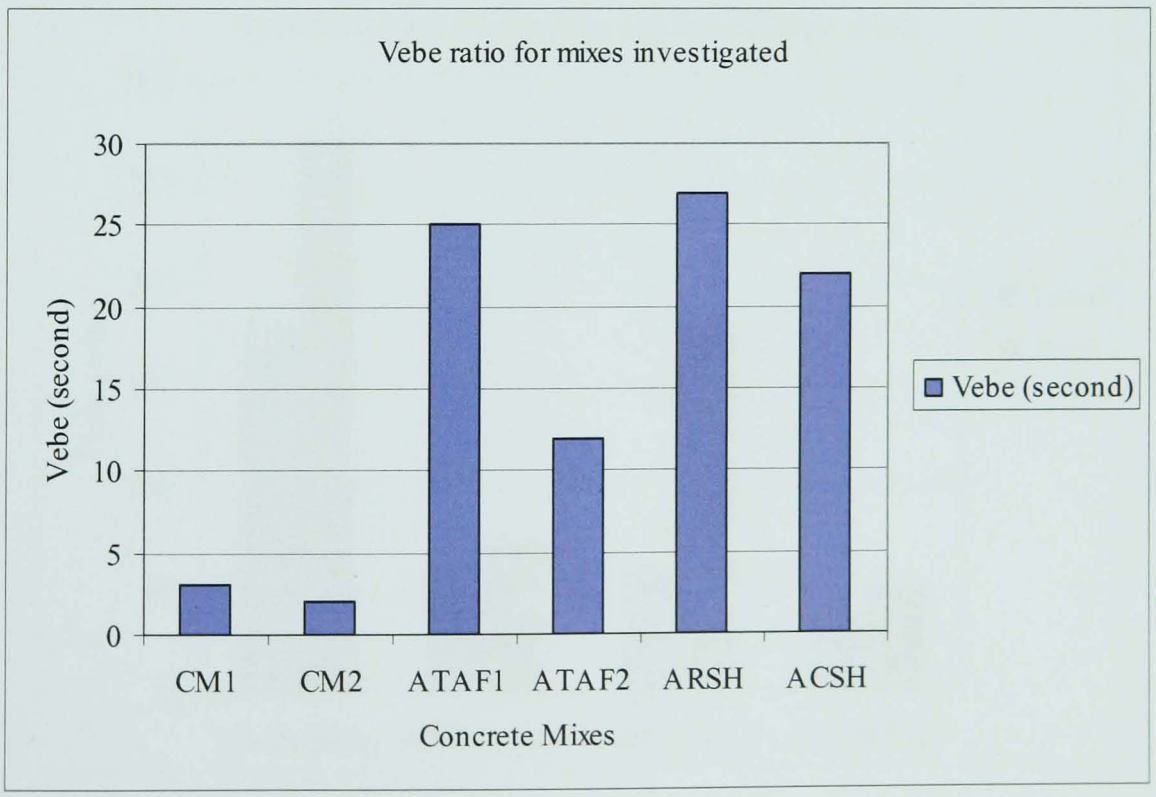

Figure 6.4 Vebe results for the mixes investigated

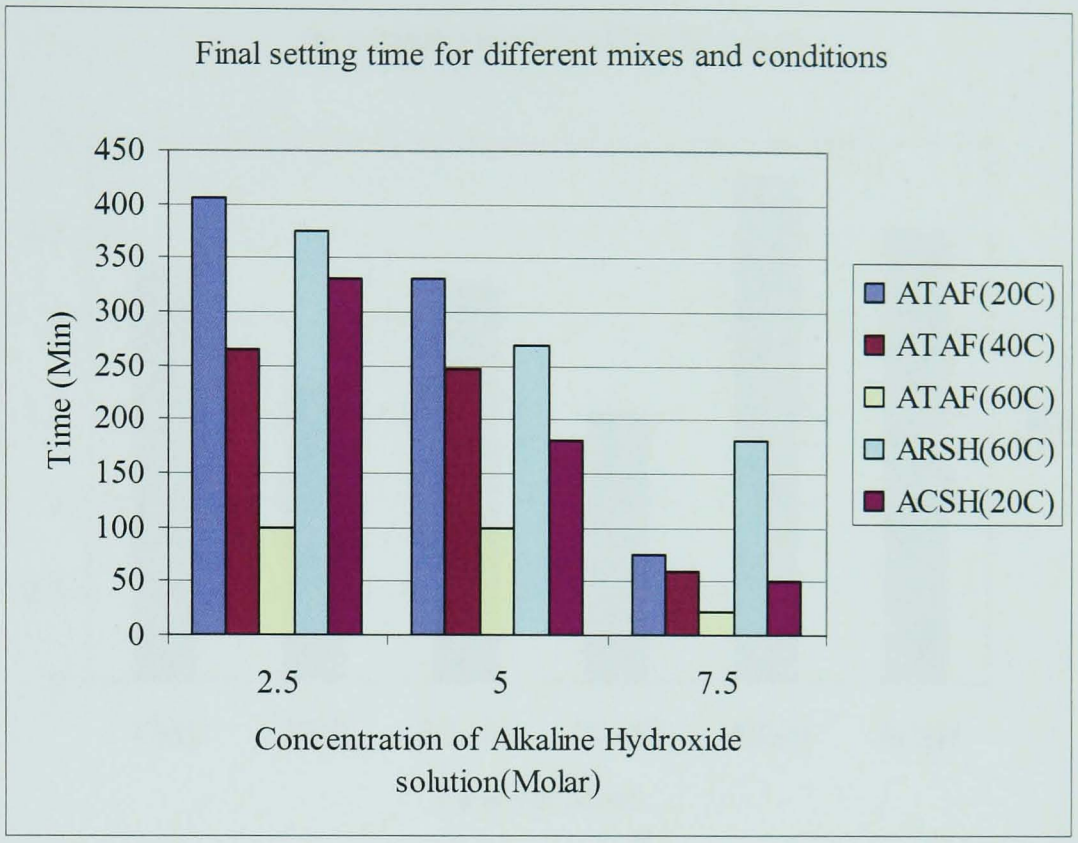

Figure 6.5 Influence of activator concentration and mix temperature on final setting time

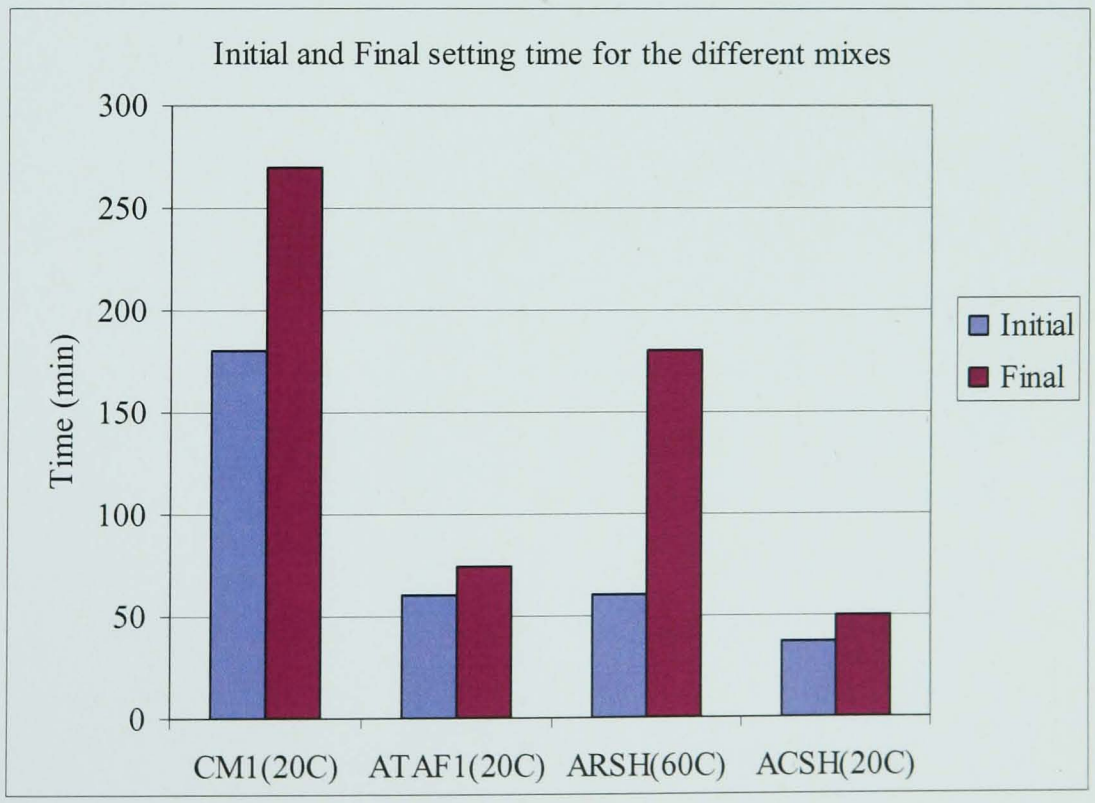

Figure 6.6 Initial and final setting time for different mixes

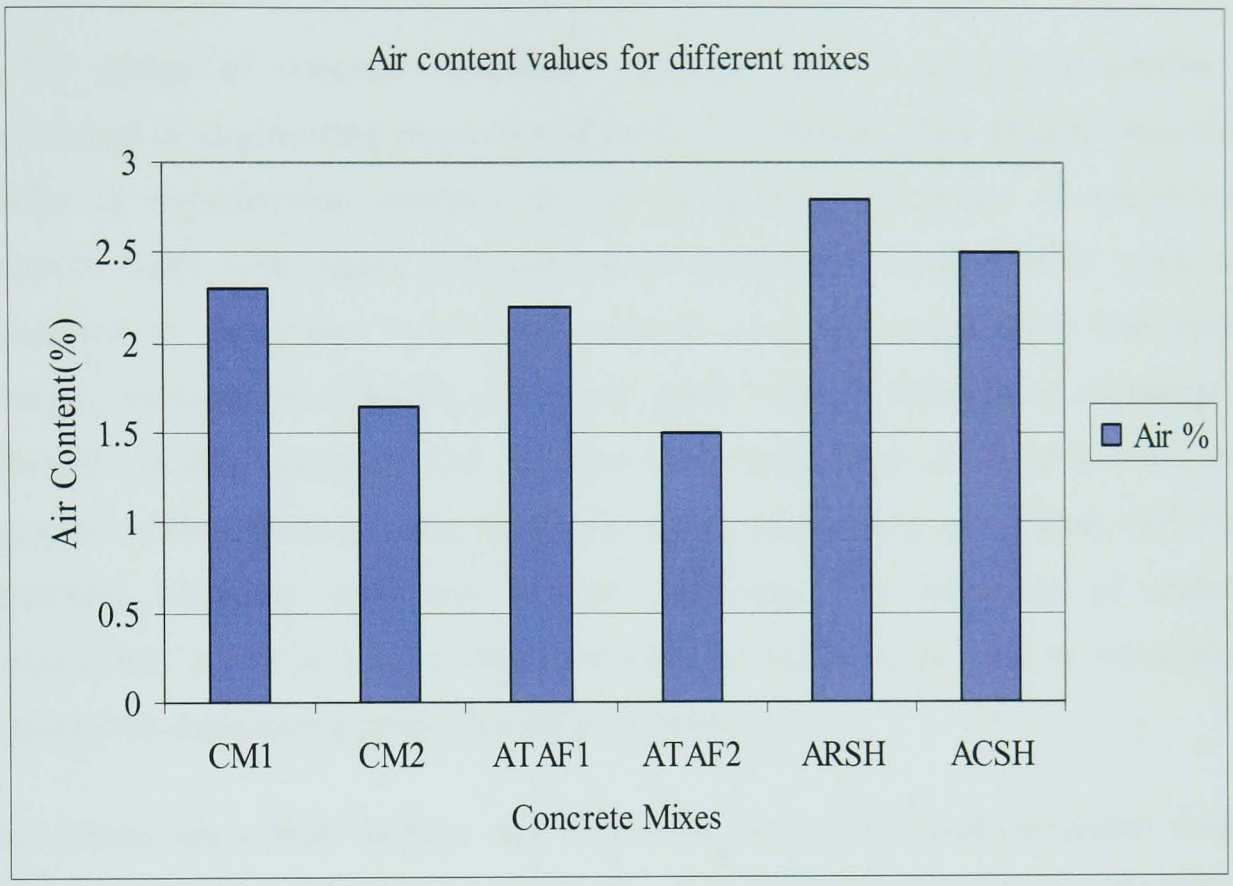

Figure 6.7 Air content values for different mixes investigated

7. ENGINEERING PROPERITIES OF GEOPOLYMER CONCRETE

7.1 Introduction

In the design of concrete structures, engineers use, or assume a number of mechanical or engineering properties of hardened concrete. This chapter reports the results of experimental research on the engineering properties of geopolymer concrete made with alkali activated natural pozzolans. Experimental work was conducted to determine mechanical strength such as compressive and tensile strength; modulus of elasticity; ultrasonic pulse velocity and drying shrinkage of different concrete mixtures. The mixtures were made from alkali activated Taftan Pozzolan with different water to binder ratios and curing conditions and from Shahindej Pozzolan with and without calcining. The influence of material composition, water to binder ratio and curing conditions as well as correlations between the engineering properties are presented.

The results show that mortars and concretes made with alkali activated natural pozzolan develop moderate to high mechanical strength and modulus of elasticity and shrink much less than ordinary Portland cement (OPC) concrete with same workability.

7.2 Compressive Strength

The compressive strength of concrete is one of the major criteria adopted to evaluate the quality of concrete for different applications, and structural design of concrete is usually based on its value. Strength of concrete, as already discussed in chapter 6, is its resistance to stress and it may be measured in a number of ways, amongst which, uniaxial compressive strength is probably the most important. The mechanics of failure is a complex phenomenon. It can be assumed that the concrete in resisting failure generates both cohesion and internal friction. The cohesion and internal friction developed by concrete in resisting failure are related mostly to the water to binder ratio and curing temperature. In other words, based on the original water to binder ratio rule, for a given binder and acceptable aggregates, the strength that may be developed by workable mixture of binder, aggregate and water (under the same mixing, curing and testing conditions) is influenced by:

- Ratio of binder to aggregate

- Grading, surface texture, shape, strength and stiffness of aggregate particles
- Maximum size of aggregate
- Curing temperature

In the above list, the water to binder ratio primarily affects the strength, whereas the other factors indirectly affect the strength of concrete by affecting the water to binder ratio (Shetty, 1982).

This section gives the details of the investigation carried out to evaluate the compressive strength of activated Taftan, calcined and uncalcined Shahindej pozzzolan and the influence of water to binder ratio and curing condition on compressive strength development.

7.2.1 Test Procedure

In order to determine the compressive strength of geopolymer concrete, each mixture was prepared as 100x100x100 mm cubes and the compressive strength for these samples was tested according to BS EN 12390-3:2000. Details of casting and curing are described in section 6.4. Three samples for each formulation were tested at 1, 7, 14, 28, 90, 180 and 365 days, and the average compressive strength values reported as the results.

The compressive strength was calculated from the formula below:

$$f_c = P/A \qquad (7\text{-}1)$$

Where:

f_c is compressive strength in N/mm^2 (MPa)

P is maximum load applied to the cube in N

A is the area of concrete surface in mm^2

The crushing machine used for measuring the compressive strength was fixed at a constant rate of load increase of 2.5 kN/s.

7.2.2 Results and Discussion

The results of the compressive strength tests on concrete using activated natural pozzolan and control Portland cement mixes are presented in Figures 7.1 to 7.10. In Figures 7.3 to 7.10 errors of a similar magnitude to those in Figure 7.2 are expected.

The results of the compressive strength versus age, for the different mixes are presented in Figure 7.1; the upper graph shows results up to 28 days to highlight the increase in strength at early ages and the lower graph shows the long term strength development up to 365 days. In all cases, the strengths of the concretes increased with age. The rate of strength gain is high at early ages and gradually decreases at longer ages. Geopolymer concrete mixes mostly showed lower strengths than OPC control mixes at early ages, but they reached the same and even higher strengths than OPC mixes after long-term aging with the compressive strength of ATAF1 geopolymer concrete mix is 39.7MPa after 28 days and being higher than the comparable OPC control mix (29.2MPa). The results of long-term compressive strength tests show that all the geopolymer concrete mixes have higher compressive strengths than the OPC control mixes after 365 days with the exception of the ARSH mix. ATAF1 and ACSH have the highest compressive strength equal to 43.5MPa, while ATAF2 reaches 39.1MPa more than that for the CM2 control mix. In the ARSH mix the compressive strength after 365 days was 30.2MPa.

Figures 7.2 and 7.3 show the early age and long term compressive strength for the control concrete mixes CM1 and CM2 which indicate higher compressive strength due to fog curing conditions at early age but the results show higher strength for sealed curing condition in long-term. This seems to show that sealing is done well and no loss of water occurred during the maturity of concrete.

It is well known that the lack of curing greatly reduces the strength development of concrete. Figure 7.4 to 7.7 clearly show the effect of different curing temperatures in sealed and fog curing conditions. Generally, the sealed condition gave the best results in the long term, the similar to these for OPC control concrete, although the difference between the two conditions is not significant.

The results suggest that the optimum temperature for curing alkali-activated Taftan pozzolan is 60°C at early ages but curing at 40°C under sealed conditions gave the highest strength results in the long-term (Figures 7.4 to 7.7). It was found in section 4.4.1 that untreated Shahindej pozzolan needed at least 60°C curing to satisfy moderate to high strength and the optimum temperature for curing calcined Shahindej was found to be 20°C. Therefore ARSH concrete mixes were cured at 60°C and ACSH mixes were cured at 20°C.

The water to binder ratio has been found to affect the strength of geopolymer concrete mixes as much as OPC concrete mixes while the minimum amount of water needed in the system to complete the chemical reactions is more important than in OPC concrete mixes (Figures 7.8 to 7.10). The effect of water content is illustrated in Figure 7.11 by plotting the 28 day compressive strength versus the water-to-geopolymer solids ratio by mass. The test data shown in Figure 7.11 demonstrate that the compressive strength of geopolymer concrete decreased as the ratio of water-to geopolymer solids by mass increased giving rise to more free water in the geopolymer concrete leading to a more porous microstructure. The trends of these test results are similar to those observed by Hardjito et al (2004*c*) and Barbosa et al (2000) for their tests on geopolymer concretes. The results shown in Figure 7.11 also confirm that an increase in the curing temperature increased the concrete compressive strength.

7.3 Splitting Tensile Strength

Concrete is generally known to be weak in tension. There are three types of tests for tensile strength: direct tension test, flexure test, and splitting tension test. In this section the tensile strength is determined by the splitting cylinder test which is most commonly used as indirect measure of tensile strength. The result will be discussed in this section. Results show that the tensile strength is related to the mix material composition and proportion of ingredients and it is greatly affected by curing conditions as well.

7.3.1 Test Procedure

The splitting tensile strength of all mixes was measured using 100mm Φ x 200mm length cylinders. The samples were prepared and splitting tensile tests performed as

described in BS EN 12390-6:2000. The specimens were tested in duplicate sets at 7, 14, 28, 90, 180 days and the average results are reported.

The splitting tensile strength was calculated from the following formula:

$$f_t = 2P/\pi LD \qquad (7\text{-}2)$$

Where:

f_t is splitting tensile strength in N/mm^2 (MPa)

P is failure load applied to the cylinder in N

L is the length of concrete specimen in mm

D is the diameter of concrete specimen in mm

7.3.2 Results and Discussion

The results of the indirect tensile strength tests up to 180 days are shown in Figures 7.12 to 7.14.

The trend in tensile strength is similar to that obtained for compressive strength, increasing with time. Figure 7.12 illustrates there was a difference in the development in tensile strength of different mixes. As far as the geopolymer concrete mixes based on activated natural pozzolan are concerned, higher strengths were observed at longer ages in comparison with control OPC mixes. At early age, the geopolymer concrete mixes showed lower tensile strength results than the OPC control mix, while the ATAF1 mix gave 3.57MPa after 28 days, higher than the corresponding OPC control mix at 2.67MPa. The results show that the long term tensile strengths of activated Taftan geopolymer concrete mixes are higher than those of OPC control mixes, 3.69 and 3.0MPa after 365 days compared to CM1 and CM2 at 2.81 and 1.99, respectively. For ACSH and ARSH mixes, the tensile strength after 365 days is 1.96 and 1.3MPa, respectively.

The tensile strength of this type of concrete is more sensitive to improper curing than its compressive strength, the same as in OPC concrete. This may be due to an inferior gel formation as a result of improper curing. Figure 7.13 illustrates the effect of curing conditions and temperatures on tensile strength of concrete made from activated natural pozzlans. The optimum temperature of curing was 40°C, the same as that found for compressive strength.

Figure 7.14 also shows that a higher water to binder ratio resulted in lower tensile strength, the same as for OPC mixes.

7.4 Static Modulus of Elasticity

Knowledge of the elastic modulus of concrete is essential in the determination of the deflection of concrete structures. As a general rule the higher the modulus of elasticity, the better the quality of the concrete. The modulus of elasticity is usually divided in two: static and dynamic. The static modulus of elasticity gives the strain response to an applied stress of known intensity. The dynamic modulus is determined by means of vibration methods with only a negligible stress being applied. The value of dynamic modulus of elasticity computed from an ultrasonic pulse velocity method is somewhat higher than those determined by the static method. This is because the modulus of elasticity as determined by dynamic modulus is unaffected by creep (Shetty, 1982).

The static modulus of elasticity is a property of concrete that expresses the ratio, within the elastic limit, between a certain range of unit stress and the corresponding strain or unit elongation. In this section only the static modulus of elasticity will be studied and an attempt is made to provide information on the elastic properties of alkali activated natural pozzolans from tests carried out under uniaxial compression conditions.

7.4.1 Test Procedure

The static modulus of elasticity was determined according to BS1881-121:1983 standard by subjecting 100mm Φ x 200mm cylinder specimens to uni-axial compression and measuring the deformation by means of dial gauges fixed between certain gauge lengths. Dial gauge reading divided by gauge length gives the strain while load applied divided by area of cross section gives the stress. A series of readings were taken and the stress-strain relationship was established. The modulus of elasticity found from actual loading is called static modulus of elasticity.

As specified by the standard, the maximum stress applied was 1/3 of the ultimate compressive strength. The minimum stress used to avoid any movement from the

cylinder was 0.5MPa. All the samples were subjected to three loading cycles. The static modulus of elasticity in compression (E_c) is given by the formula:

$$E_c = \frac{\Delta_\sigma}{\Delta_\varepsilon} = \frac{\sigma_a - \sigma_b}{\varepsilon_a - \varepsilon_b} \qquad (7\text{-}3)$$

Where:

σ_a is the upper loading stress (1/3 of the ultimate strength)

σ_b is the basic stress (0.5MPa)

ε_a is the mean strain under upper loading stress

ε_b is the mean strain under basic stress

7.4.2 Results and Discussion

Results of the static modulus of elasticity tests are shown in Figures 7.15 and 7.16. In a similar way to the compressive strength results, the static modulus of elasticity increased with age. This improvement was rapid such that in the first 28 days as the most of the modulus value was generally achieved. During the first 14 days the mixes made with activated natural pozzolans have mostly shown lower values of static modulus of elasticity than OPC concrete mixes, except for the ATAF1 mix. The static modulus of elasticity for ATAF1, ATAF2, ACSH, and ARSH mixes after 14 days was 33.96, 14.03, 15.81, and 8.57GPa, respectively with that for the CM1 mix was 26.55GPa. Long term results show that the static elastic modulus of some of alkali activated natural pozzolans such as ATAF1 and ACSH are around 5% to 20% more than OPC mixes. However, the ARSH mix shows much lower value of static modulus of elasticity than OPC concrete mixes. The long term static modulus of elasticity of ATAF1, ATAF2, ACSH, and ARSH mixes were 32.7, 26.8, 33.6, 10.7GPa in comparison with OPC concrete mixes for which the value was 29GPa.

The elastic modulus was affected by the curing temperatures and conditions. At early ages the static modulus of elasticity increased with increasing the curing temperature up to a limit which seems to be related to the water to binder ratio (Figure 7.16). For ATAF1 with a water to binder ratio of 0.45, the elastic modulus increased with increasing curing temperature up to 40°C but decreased when the curing temperature rose to 60°C. For ATAF2 mixes where the water to binder ratio was 0.55, the temperature where the highest static modulus of elasticity was obtained rose to 60°C.

However, over the long term the results drop to the same value as the mix cured at 40°C. Fernandez-Jimenez, Palomo et al. (2006) show the static modulus of elasticity of alkali activated fly ash concrete samples frequently reduces slightly with curing temperature increases from 25°C to 40 °C.

7.5 Ultrasonic Pulse Velocity

The velocity of ultrasonic pulses travelling in a material depends on the density and elastic properties of that material. Ultrasonic pulse velocity method consists of measuring the time of travel for an ultrasonic pulse, passing through the concrete. The pulse generator consists of an electronic circuit for generating pulses and a transducer for transforming these electronic pulses into mechanical energy. This method can be used to determine the setting characteristics, strength, and modulus of elasticity of concrete, as well as durability of concrete including detection and measurement of cracks and deterioration. The measurement of pulse velocity is affected by a number of factors regardless of the properties of the concrete including smoothness of contact surface under test to maintain good acoustical contact between the surface of concrete and the face of each transducer, temperature of concrete for preventing the reduction of pulse velocity at temperature more than 30°C, and moisture condition of concrete.

7.5.1 Test Procedure

A PUNDIT instrument was used to measure the ultrasonic pulse velocity in accordance with BS 1881: part 203: 1986. The measurement was conducted on 100mm square by 500mm long prism. Duplicate sets of samples were tested at 28, 90, and 180 days.

For measuring the ultrasonic pulse velocity, a pulse of longitudinal vibration is produced by a 50mm diameter 54 kHz electro acoustical transducer and picked up by another transducer after travelling a known path length (500mm). The pulse velocity is given by:

$$V=L/T \qquad (8\text{-}4)$$

Where V=ultrasonic pulse velocity (km/sec)

L=path length or distance travelled by pulse (mm)

T=transit time (μsec)

7.5.2 Results and Discussion

Figure 7.17 shows the results for the ultrasonic pulse velocity test for all mixes. ACSH and ATAF1 achieved the highest values followed by ATAF2 which has a higher w/b and the lowest ARSH despite its low density. All of the geopolymer concrete mixes showed lower ultrasonic pulse velocities than the OPC concrete mixes, even with the same or higher compressive strength. The results are tabulated in Table 7.1. Comparing the results with Table 7.2, which gives the pulse velocity rating as suggested by Central Water and Power Research Station, Khadakwasla (India), indicates that a lower velocity corresponds to the same compressive strength. It seems that in geopolymer concrete, despite its lower density the velocity of ultrasonic pulses is lower than in OPC concrete.

7.6 Drying Shrinkage properties

Volume change is one of the most detrimental properties of concrete, which affects the long-term strength and durability as it causes unsightly and damaging cracks in concrete. It is the loss of water held in gel capillary pores that causes the change in the volume. Many internal and external factors can affect the drying shrinkage of hardened cement pastes. The internal factors include the nature of the pozzolan, nature of the activator, dosage of activator, water to binder ratio and degree of polymerization. The external factors include curing temperature, additives, relative humidity, and the rate and time of drying. The relative humidity of the atmosphere, water/binder ratio, and aggregate properties including its grading and modulus of elasticity and curing condition prior to drying are important factors which influence the magnitude of drying shrinkage. This section presents the test carried out and the results obtained for geopolymer concrete mixes. The results are discussed and conclusions derived from the results.

7.6.1 Test Procedure

In the present work, the changes in length of 75 x 75 x 280 mm concrete prisms were measured by conventional mechanical equipment. Predrilled metal studs were fixed

to either end of the concrete specimen with adhesive at a preset spacing with the aid of a standard calibration bar. The distance between each of two pins located into the stud holes was measured to an accuracy of about 0.0025 mm at fixed times. One end of the reference rod was designed as the top and it was kept uppermost during all measurements. The prisms were placed in the apparatus with the marked end uppermost and were rotated slowly around the contact surfaces to measure the changes in length. For each mix two specimens were cast and cured for 3 and 7 days. The prisms were then left in a room controlled at 20°C and 70% humidity and chemical shrinkage was measured using the length comparator in accordance with BS 812: Part 120: 1989. The comparator and a concrete prism are shown in Figure 7.18.

7.6.2 Results and Discussion

The shrinkage/time curves are shown in Figures 7.19 to 7.21. From this investigation the following observations can be made:

1) The graphs show that while the amount of shrinkage increased with time, the rate of shrinkage decreased rapidly with time. The rate of shrinkage in Taftan pozzolan mixture was similar to but not as rapid as the rate of development of compressive strength and the amount of shrinkage seems to be constant after 60 days. However, in Shahindej pozzolan, the rate of shrinkage was more rapid than the development of strength and it became constant value after 14 days.

2) In OPC concrete, one of the important factors which influenced the magnitude of shrinkage was the water to cement ratio of concrete which usually increased with an increases of this ratio. The total water to binder ratio also has a significant effect on the shrinkage properties of geopolymer concretes but seems to be contrary to the behaviour of OPC concrete, where lower drying shrinkage resulted from higher water to binder ratios. It may be that the lower water/binder ratios reduces the efficiency of the cross linking (Figure 2.1b) as it must occur within in a restricted space, so it may be incomplete. Hence shrinkage is more than occurs for a higher water to binder ratio as further efficient cross linking is made before water removal. The

maximum amount of final drying shrinkage for the ATAF2 mix ($514x10^{-6}$) was 43% of that for ATAF1 ($1185x10^{-6}$) at 180 days.

3) The results show that for a given water to binder ratio, the drying shrinkage at all ages varies with different curing regimes and temperatures. In concrete made from alkali activated natural pozzolan, the higher the curing temperature, the lower the amount of drying shrinkage measured. This is possibly because further cross links are made as a result of water removal by the higher temperature and follows the pattern reported by Wallah and Rangan (2006). The lowest amount of drying shrinkage for different curing temperatures correspond to ATAF1 and ATAF2 mixes for which values of $239x10^{-6}$ and $161x10^{-6}$ respectively were achieved for mixes cured at 60°C. Fog curing showed higher amounts of drying shrinkage. This phenomenon may be related to more water being retained in the pores causing a looser microstructure giving rise to higher shrinkage. Similar finding are reported by Zuhua et al. (2009) for calcined kaolin-based geopolymer.

4) The curing period affects the amount of drying shrinkage as well. In the specimens cured for a period of three days, it seems the chemical reactions are incomplete, thus there is little water in the gel pores available for shrinkage while for samples cured at 7 days or more, more water is available to cause more shrinkage.

7.7 Relationship between Engineering Properties

Statistical correlations that were obtained between the different results of properties measured in the laboratory are presented in this section. The relationships are empirical in nature and have certain limitations because a number of factors including the mineral and chemical properties of natural pozzolan, water to binder ratio, age and curing, affect these relationships. However, the relationships contribute to an understanding of the development of the properties.

7.7.1 Relationship between Compressive and Tensile Strength

Compressive and tensile strength of concrete are closely related, but the tensile strength increases with age at a lower rate than the compressive strength. Thus they

are not related proportionally. Most of the empirical formulae combining both tensile and compressive strength are in the following form:

$$f_t = k\,(f_c)^n \qquad (7\text{-}5)$$

Where k and n are coefficients in which n varies between 0.5 and 0.75 (Neville, 1995)

In general, the relationship between the compressive strength and the tensile strength seems to be determined by the effect of various factors on properties of concrete. It is known that not only the curing age and conditions but also the characteristics of the concrete mixture, such as the composition of the pozzolan, the properties of activators, water to binder ratio, and the type of aggregate affect the tensile compressive relationship to varying degrees.

A relationship between compressive strength and splitting tensile strength would be expected. These results show that as compressive strength increases, the tensile strength also increases, see Figures A7.1 to A7.5. Using power regression analysis carried out between the compressive strength and the splitting tensile strength of each of the 6 mixes for different curing regimes and temperatures. The regression equation and the correlation coefficient are given in Table A7.1.

It can be seen that in nearly all mixes the splitting tensile strength is highly correlated with the compressive strength. However due to the variation in the source mineral, water to binder ratio and curing conditions, activated calcined Shahindej and activated Taftan pozzolan with higher water binder ratio which cured at 60˚C have higher correlation coefficient, respectively. Referring to equation 7-5 and the data in Table A7.1, the values of n range from 0.1 to 0.7 and those of k from 0.2 to 1.4 for OPC mixes. In comparison in alkali activated natural pozzolans, the values of n range from 0.2 to 1.5 and those of k from 0.03 to 1.5. The results of splitting tensile strength versus compressive strength for different mixes made from activated natural pozzolans are shown in Figure 7.22. It can be seen that two different trend lines can be identified. Comparing the data points to what was presented in Figures A7.2 and A7.4 shows that the Group I data points correspond to activated Taftan pozzolan cured at 20°C and 40°C in sealed and fog and at 60°C in fog curing conditions while Group II data points correspond to activated Taftan mixes cured at 60°C in sealed curing condition and activated Shahindej pozzolan mixes in both untreated and

calcined states. Whereas the tensile strength is highly dependant on the bond between aggregates and the paste, the heat curing may not necessarily enhance the interface of aggregate/gel to the same order as enhancing the strength of the gel itself. The weakness of Group II mixes in splitting tensile strength seems to be related to the high temperature of curing in the absence of water since water in the sealed curing condition cannot be replenished to enhance the paste bonding properties especially at the interface of the paste and the aggregates. The low tensile strength is also observed when the pozzolan contains sodic zeolites with high loss on ignition and soluble silicon, such as Shahindej is used, which suggests resulting in poor bonding with aggregates. This follows the pattern reported by Fernandez-Jimenez et al (2006) about the presence of silicate ions in the alkaline solution substantially which has negative effect on the very strong matrix/aggregate bond. Power regression analysis showed that the formulae appropriate for two groups of geopolymer concretes based on activated natural pozzolans are as follows:

AANP Concrete Group I: $f_t = 0.05(f_c)^{1.19}$ $R^2=0.776$ (7-6)

AANP Concrete Group II: $f_t = 0.02(f_c)^{1.19}$ $R^2=0.639$ (7-7)

Comparing the correlation between the splitting tensile strength and the compressive strength for geopolymer concrete based on activated natural pozzolans to that of normal OPC shows that more tensile strength with natural pozzolan (Group I) for the same compressive strength when it is more than 22.5MPa (Figure 7.22).

7.7.2 Relationship between Compressive Strength and Modules of Elasticity

At the same stress/strength ratio, stronger OPC concrete has higher strain. On the other hand stronger concrete has higher modulus of elasticity. This implies that stronger the concrete the stronger is the gel and hence there is less strain for a given load which gives higher modulus of elasticity. The modulus of elasticity of OPC concrete increases approximately with the square root of the strength. The basic form of equation is generally suggested by BS8110: part 2: 1985 and ACI 318-83 to adequately describe the relationship between static modulus of elasticity and compressive strength as follows:

$$Es=k\,(fc)^{n} \qquad (7\text{-}8)$$

Where k and n are coefficients is suggested in the above standards due to concrete density and the shape for the sample used to determine the compressive strength (cube or cylinder).

In this investigation the static modulus of elasticity values for concrete mixes have been plotted against their respective cube and cylinder compressive strength values to explore the opportunity for an analogous geopolymer concrete formula to the relationships suggested by BS8110: part 2: 1985 and ACI 318-83 for calculating the static modulus of elasticity versus compressive strength.

The static modulus of elasticity values of concrete mixes in this research have been plotted against their respective cubic and cylinder compressive strength values, as shown in Figures A7.6 to A7.14. Figures A7.15 to A7.19 present the relationship between the static modulus of elasticity and the splitting tensile strength of all concrete mixes. Power regression analysis was then carried out between the static modulus of elasticity values and the compressive strength and afterward the splitting tensile strength of each of the 6 mixes for different curing regimes and temperatures. For the concrete mixes used in this investigation separate equations relating to the static elastic modulus and strength were found. The regression equations and the correlation coefficients relating the static modulus of elasticity and the cubic and cylinder compressive strength and the splitting tensile strength are given in Tables A7.2, A7.3 and A7.4, respectively.

It can be seen that for geopolymer concrete based on activated natural pozzolans, in 80% of mixes, the static modulus of elasticity is highly correlated with the cubic compressive strength and in nearly all mixes the static modulus of elasticity is highly correlated with the cylinder compressive strength. It can be observed that in the former correlation activated calcined Shahindej, activated Taftan pozzolan with lower water binder ratio cured at 40°C fog condition and activated untreated Shahindej pozzolan have higher correlation coefficient, respectively. In the latter case activated calcined Shahindej, and activated Taftan pozzolan mix cured at 60°C sealed condition, have higher correlation coefficient.

Referring to equation 7-8 and with respect to Table A7.2 for cubic compressive strength the major values of n range from 0.3 to 0.4 and those of k from 7.5 to 10 for

OPC mixes compared to the values of n ranging from 0.5 to 2.0 and those of k from 0.1 to 2.4 for alkali activated natural pozzolans. The results of static modulus of elasticity versus cube compressive strength for different mixes made from activated natural pozzolans are shown in Figure 7.24 and power regression analysis showed that the formulae reached for geopolymer concrete based on activated natural pozzolans are probably as follows:

$$Es= (fcu)^{0.9} \qquad R^2=0.682 \qquad (7\text{-}9)$$

This implies that at the same cube compressive strength, OPC concrete has higher static modulus of elasticity especially for lower amount of compressive strength which occurs at early age.

Considering Table A7.3 for cylinder compressive strength the values of n range from 0.5 to 1.7 and those of k from 0.07 to 3.6 for alkali activated natural pozzolans, and drawing the results of static modulus of elasticity versus cylinder compressive strength for different mixes made from activated natural pozzolans in Figure 7.25 with power regression analysis, the formulae reached for geopolymer concrete based on activated natural pozzolans would be as follows:

$$Es= 1.6(fcyl)^{0.82} \qquad R^2=0.696 \qquad (7\text{-}10)$$

It can be observed that the correlation between cube and cylinder compressive strengths shown in Figure 7.23 is high and cylinders show lower compressive strength as is expected. Comparing equation (Eq. 7-10) with the formulae suggested by ACI 318-83 standard for conventional concrete implies that when the compressive strength is more than 28MPa, the mixes made with activated natural pozzolans have shown higher values of static modulus of elasticity than OPC concrete mixes (Figure 7.25).

In this investigation for predicting the static modulus of elasticity from splitting tensile strength of concretes based on alkali activated natural pozzolans from the equation 7-11, the values of n range from 0.3 to 2.5 and those of k from 1.8 to 20.6:

$$Es=k\,(f_t)^n \qquad (7\text{-}11)$$

With respect to Table A7.4 and Figure A7.20, the formulae relating modulus of elasticity, Es (GPa) versus splitting tensile strength, f_t (MPa) reached for geopolymer concrete based on activated natural pozzolans is proposed:

$$Es = 12.5 (f_t)^{0.7} \qquad R^2=0.584 \qquad (7\text{-}12)$$

Hence, the above formulae and comparing the correlation between the static modulus of elasticity and the splitting tensile strength for geopolymer concrete based on activated natural pozzolans to that of normal OPC concrete in Figure A7.20 shows that higher splitting tensile strength is expected for alkali activated natural pozzolan concrete than OPC concrete, having the same static modulus of elasticity.

7.7.3 Relationship between Compressive Strength and Ultrasonic Pulse Velocity

A high pulse velocity in concrete is generally indicative of concrete with high compressive strength and good quality. Table 7.2 gives the pulse velocity rating as suggested by Central Water and Power Research Station, Khadakwasla (India) corresponding to different ranges of compressive strength (Shetty, 1982). In this investigation, an attempt has been made to formulate an equation that describes the relationship between UPV and strength of this type of concrete. Therefore, the values of ultrasonic pulse velocity against compressive strength were plotted in Figure 7.26. The relationship between pulse velocity, V (km/sec), and compressive strength, f_c (MPa) fitted equations as follows:

OPC concrete: $V=0.29 f_c^{0.776}$ $R^2=0.996$ (7-13)

AANP concrete: $V=0.44 f_c^{0.616}$ $R^2=0.786$ (7-14)

The equations obtained have good correlation for both concretes and ultrasonic pulse velocity in the geopolymer concrete despite its inherent property of lower density relative to OPC concrete having the same compressive strength. Therefore pulse velocity techniques can be successfully used for the estimation of strength of the geopolymer concrete mixes made with alkali activated natural pozzolans.

7.8 Summary

The main results drawn from the investigation of the engineering properties of geopolymer concrete made from activating natural pozzolans (i.e. alkali activated natural pozzolan or AANP) are summarized as follows:

1) Geopolymer concrete from activated natural pozzolans generally have lower strengths than OPC mixes at early ages, but they reach the same or even higher strengths than OPC mixes after long-term curing.

2) The optimum temperature for curing alkali-activated natural pozzolans in concrete is different for the different pozzolans and seems mostly related to the main mineral phases in the natural pozzolan. Each pozzolan shows a different response to a temperature rise and raising the temperature is more helpful to the reaction processes in pozzolans such as Taftan and uncalcined Shahindej, which contain feldspars and zeolites as the main mineral phases, which seem to need higher activation energy to react. For Shahindej, which contains zeolite minerals such as clinoptilolite, it was shown that when it was calcined the resulting pozzolan could be activated at room temperature.

3) The strength of geopolymer concrete decreases with the ratio of water to geopolymer solids by mass increases. This allows more entrapment of water within the geopolymer paste and makes a looser microstructure in this type of concrete.

4) During the first 14 days, activated natural pozzolan concrete mixes generally have lower values of static modulus of elasticity than OPC concrete mixes. However, the long term results show that the static elastic modulus of alkali activated natural pozzolans concrete is generally around 5 to 20% higher than for OPC mixes.

5) The elastic modulus of AANP concrete is affected by the curing temperatures. At early ages the static modulus of elasticity increased with increasing curing temperature to a limit which seems to be related to the water to binder ratio. If water is lost due to evaporation when curing at higher

temperature before the full strength is gained, the static modulus of elasticity decreases.

6) It seems that the ultrasonic pulse velocity in the geopolymer concrete is lower than in OPC concrete of the same compressive strength.

7) The AANP concrete mixes exhibit lower drying shrinkage in comparison with the OPC mixes of the same water to binder and cement to aggregate ratios.

8) In sealed curing conditions, the higher the water to binder ratio for geopolymer concrete, the lower is the amount of drying shrinkage. This is possibly because for the lower water/binder ratios, the cross linking is not as efficient as it must occur in a restricted space and may well not be completed.

9) In concrete made with alkali activated natural pozzolan, the higher the curing temperature, the lower the amount of drying shrinkage resulted, which is possibly because further cross linking is made as a result of water removal by the higher temperature and follows the pattern reported by Wallah and Rangan (2006).

10) Fog curing shows higher amount of drying shrinkage. This phenomenon may be related to the retention of water by the geopolymer matrix giving rise to a looser microstructure in this type of concrete. This may cause more shrinkage and follows that found by Zuhua et al. (2009).

Table 7.1 The pulse velocity and the corresponding compressive strength of different mixes

Mixes	Age(days)	Velocity(km/sec)	Compressive strength(MPa)
CM1 cured at 20°C Sealed	28	3.95	29.8
	90	5.0	39.23
	180	4.95	39
CM2 cured at 20°C Sealed	28	3.5	24.78
	90	4.7	36.78
	180	4.6	36
ATAF1cured at 40°C Sealed	28	3.39	39.7
	90	4.0	35.6
	180	4.5	40.97
ATAF2 cured at 40°C Sealed	28	3.03	21.36
	90	4.2	38.72
	180	4.2	38.06
ARSH cured at 60°C Sealed	28	3.0	24
	90	3.8	33.15
	180	3.5	30.2
ACSH cured at 20°C Sealed	28	3.0	24.54
	90	4.5	40.26
	180	4.5	40.56

Table 7.2 Quality criteria suggested by Central Water and Power Research Station Khadakwasla (India)

Velocity (km/sec)	Classification (Quality)	Compressive strength(Kg/cm^2)
4.0 and above	Very good	300 to 350
3.5 to 4.0	Good	250 to 300
3.0 to 3.5	Medium	200 to 250
3.0 and below	Poor	150 to 200

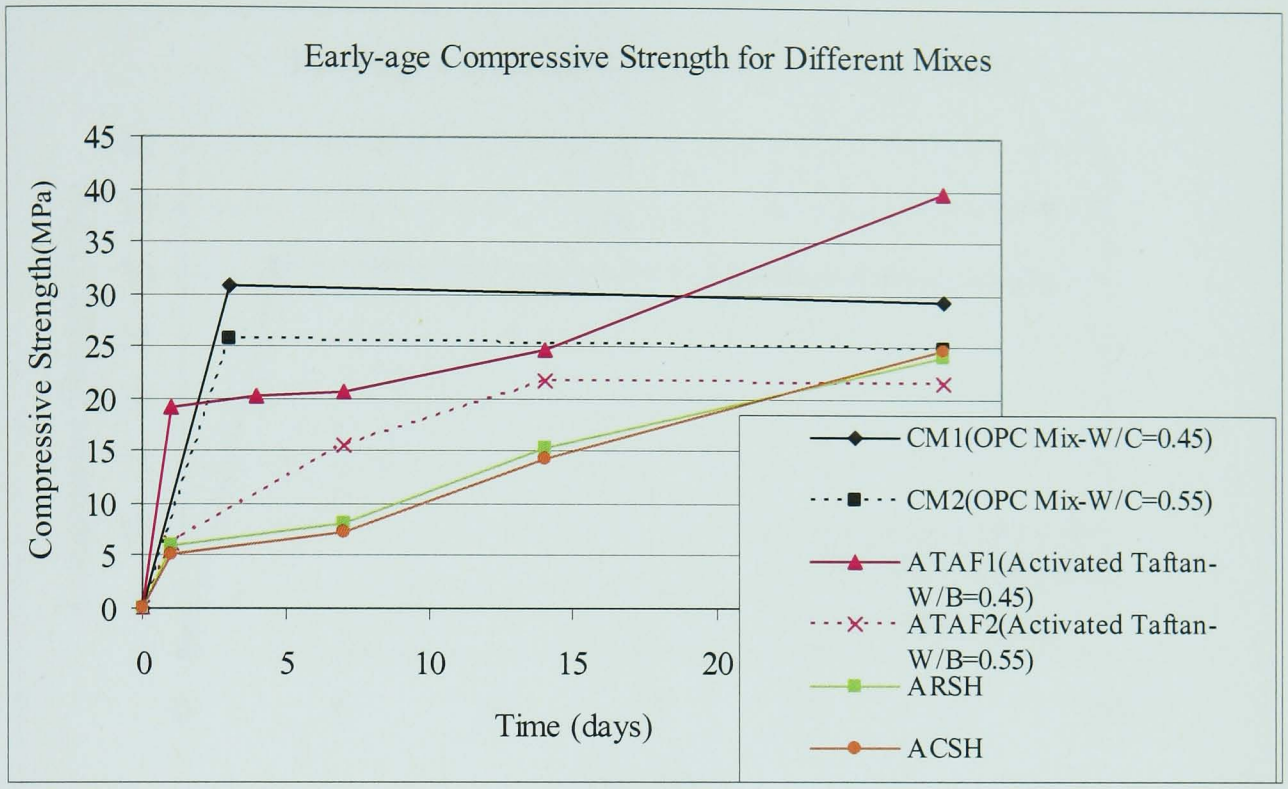

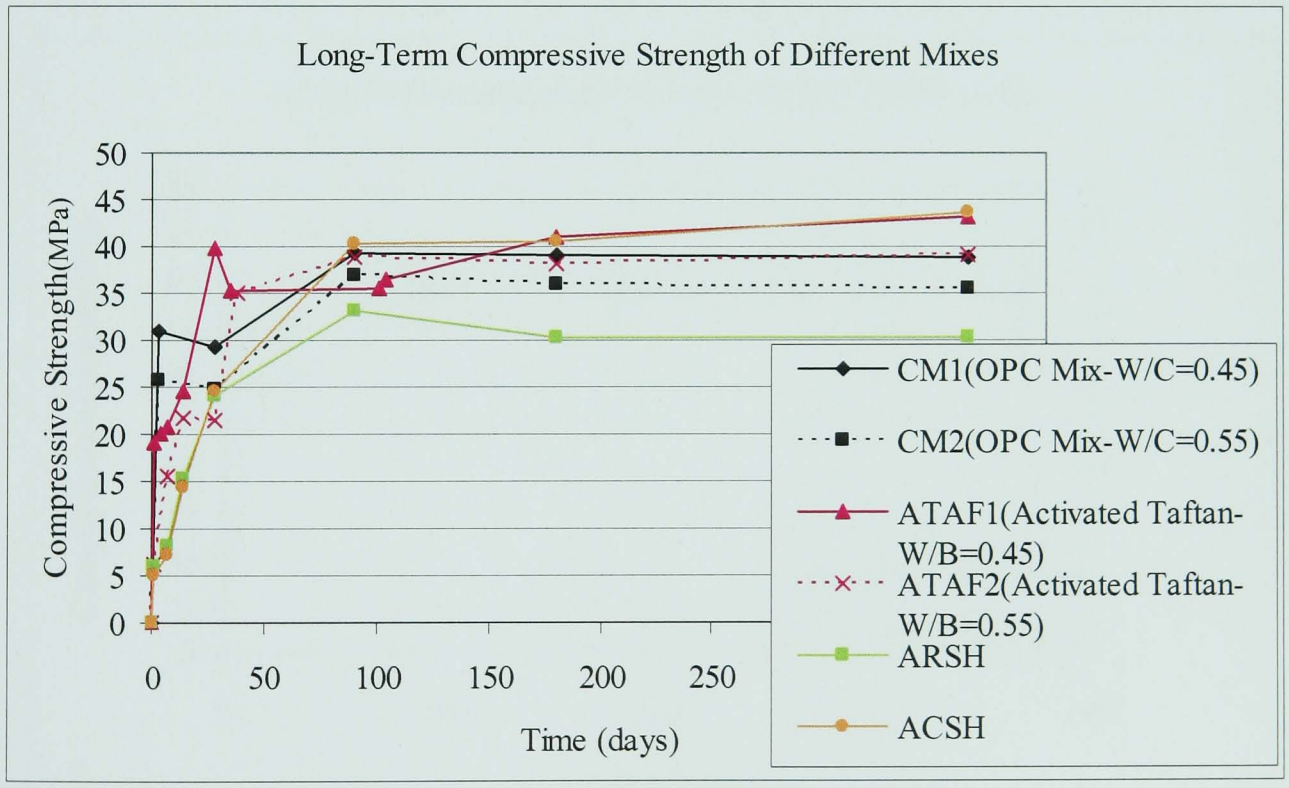

Figure 7.1 Early-age and long-term compressive strength development for different mixes under sealed curing condition (CM1, CM2, and ACSH were cured at 20°C, ATAF1 and ATAF2 were cured at 40°C and ARSH was cured at 60°C which were the best curing temperature in each case)

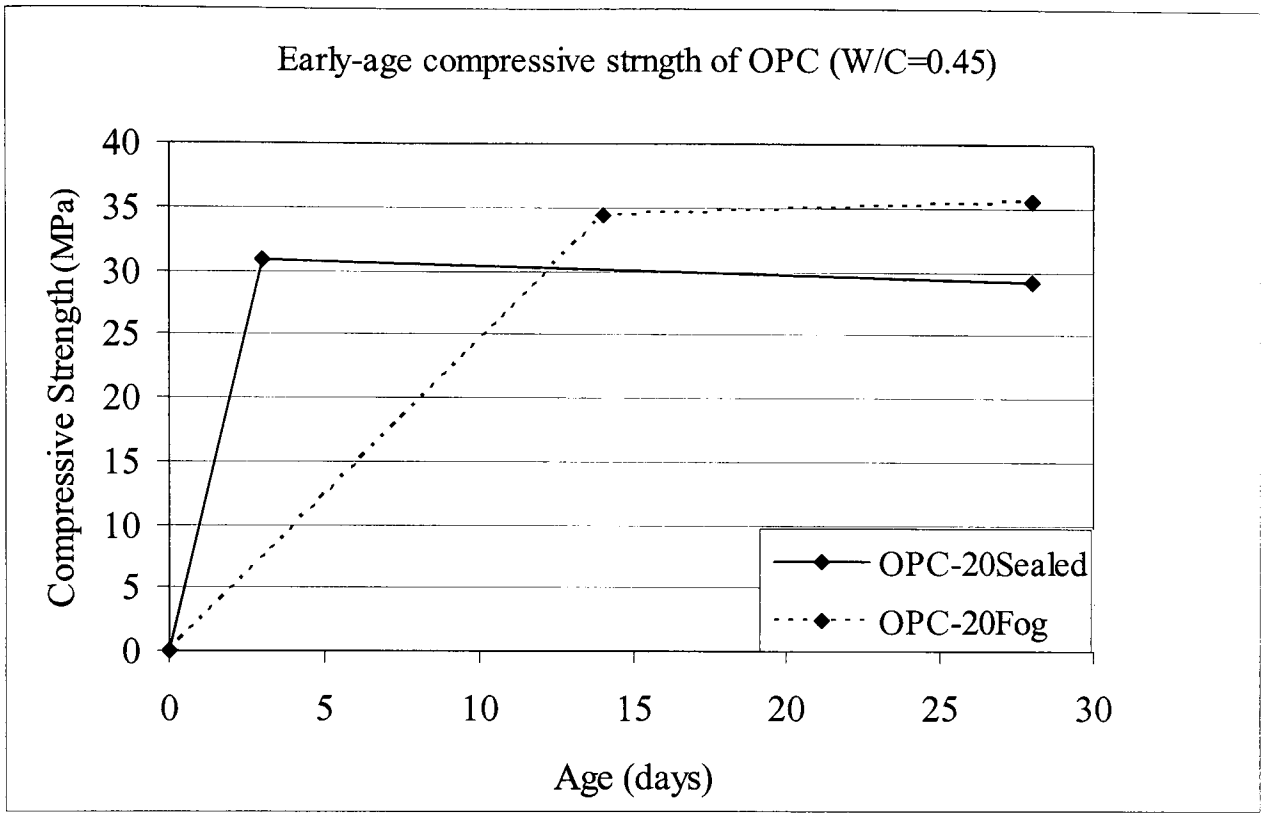

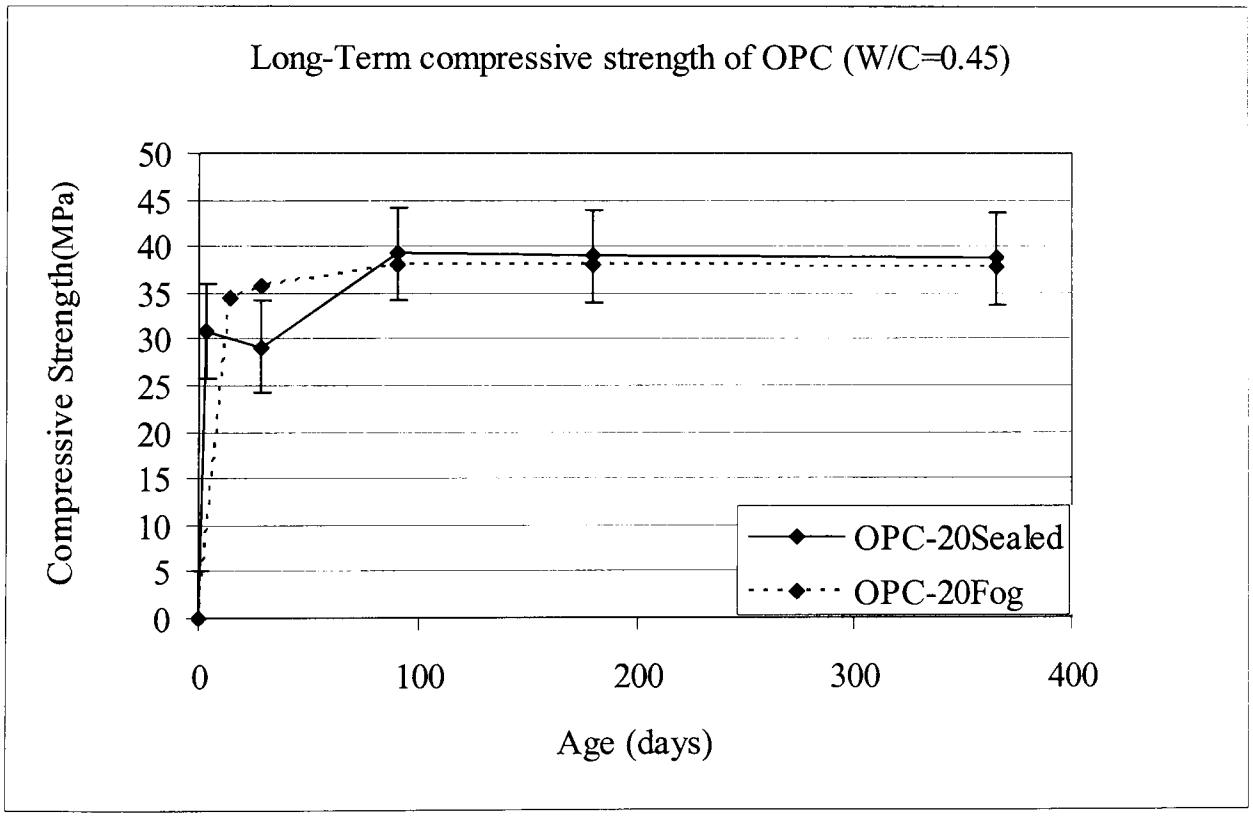

Figure 7.2 Effect of curing conditions on compressive strength development of CM1 mix

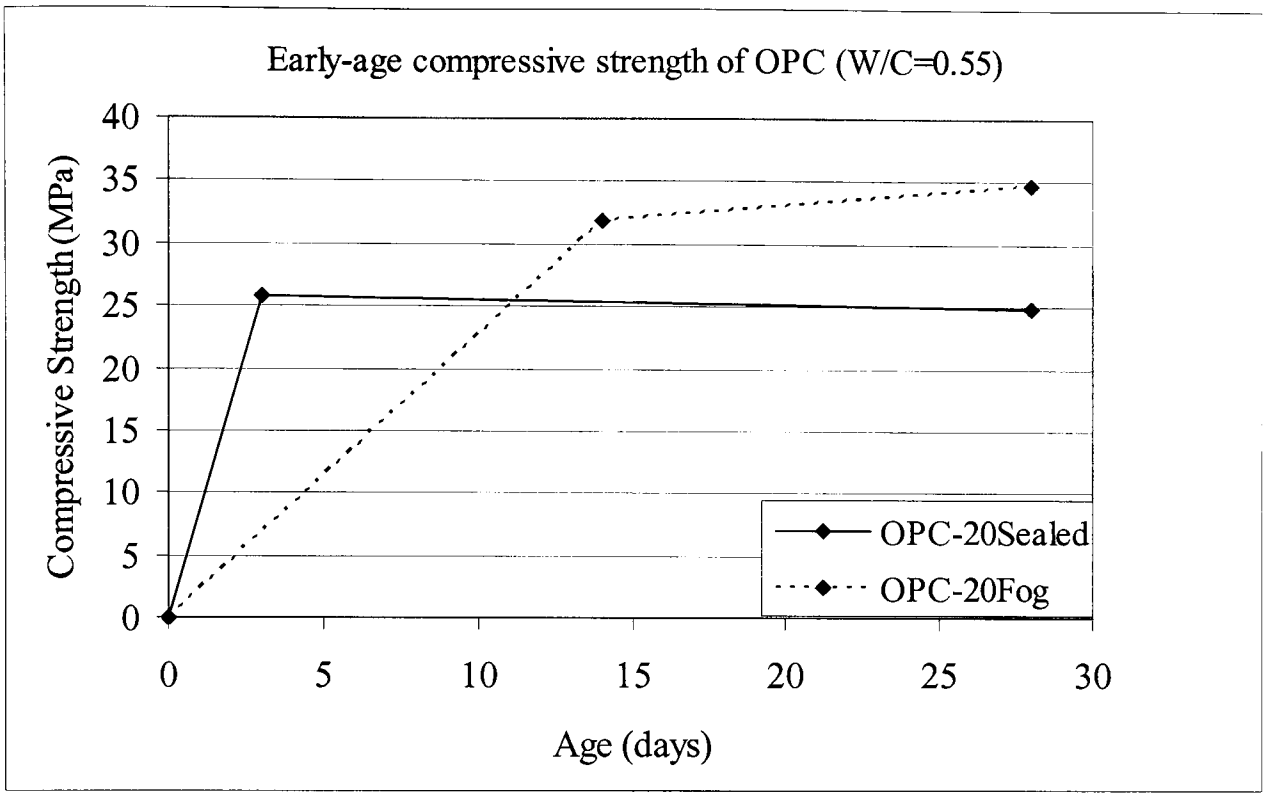

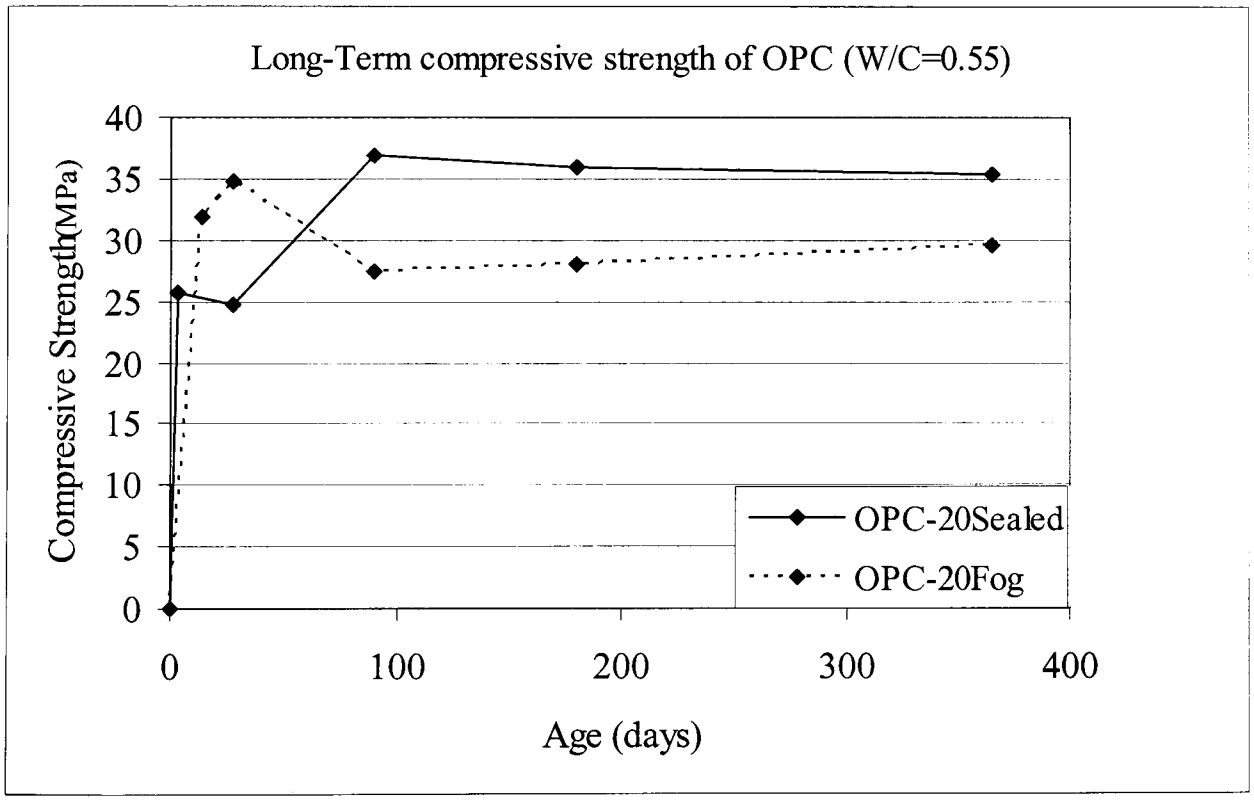

Figure 7.3 Effect of curing conditions on compressive strength development of CM2 mix

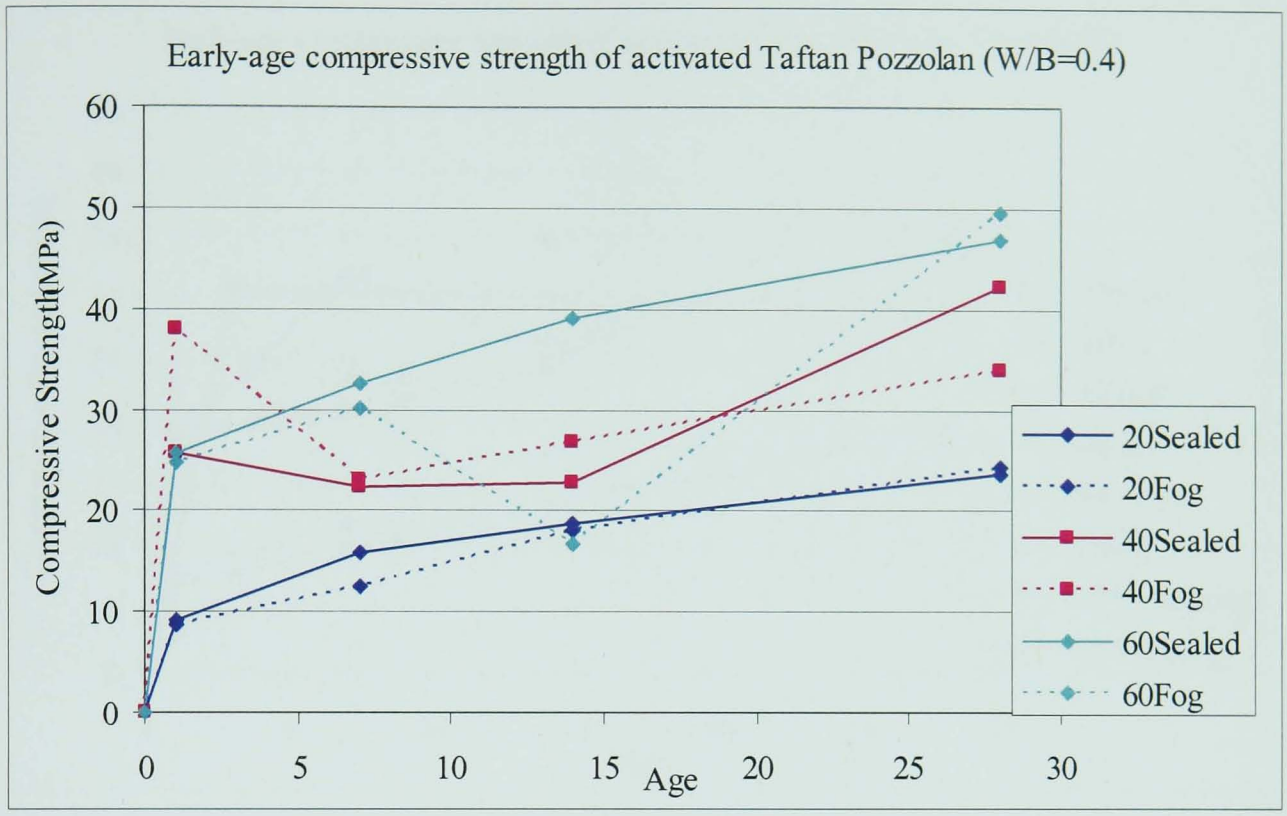

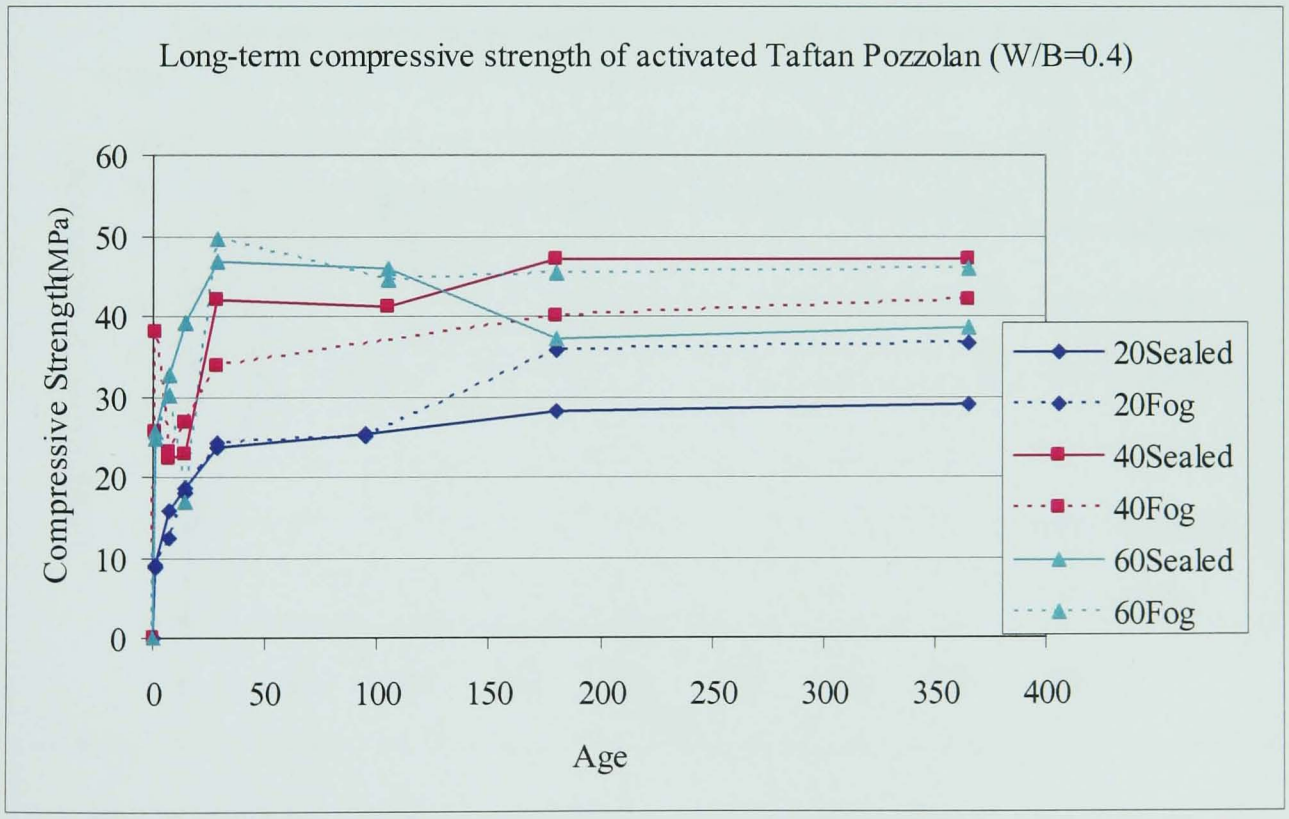

Figure 7.4 Effect of different curing condition and curing temperature on compressive strength development for activated Taftan pozzolan with water to binder ratio equal to 0.4

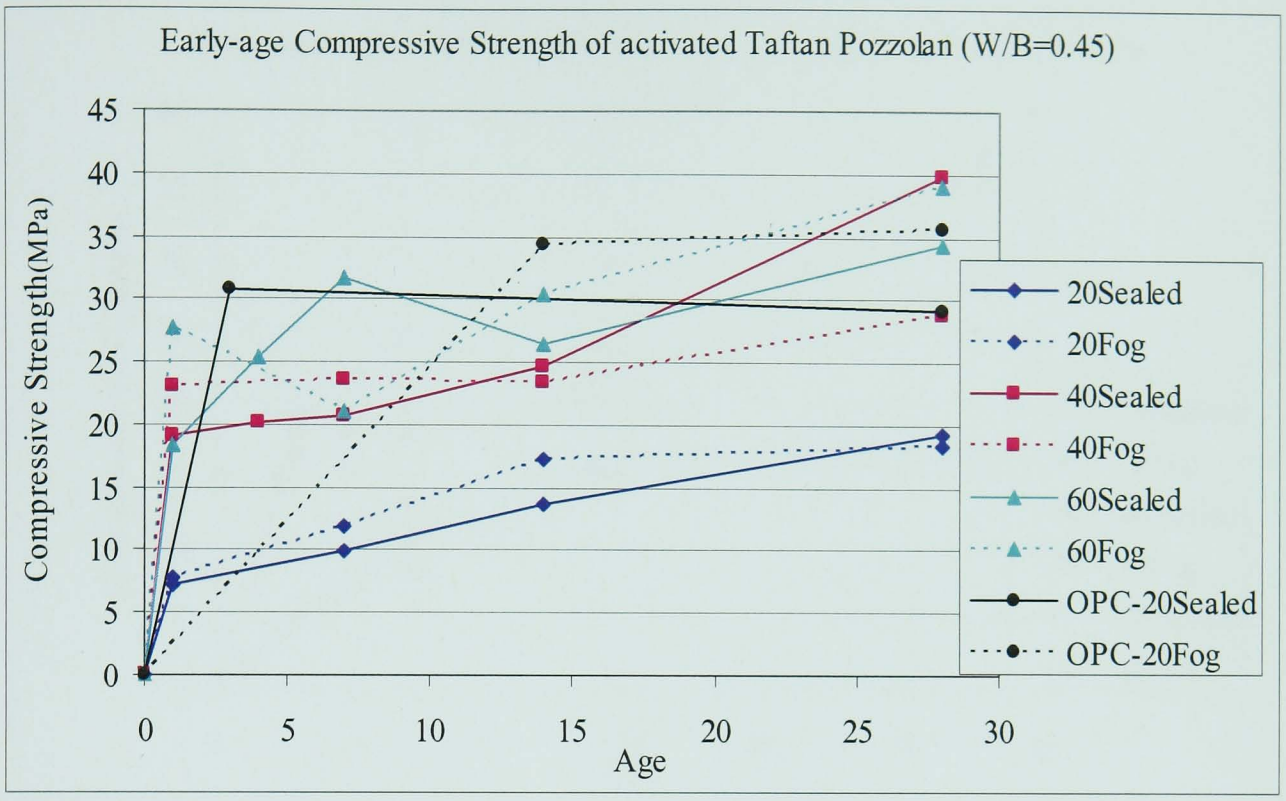

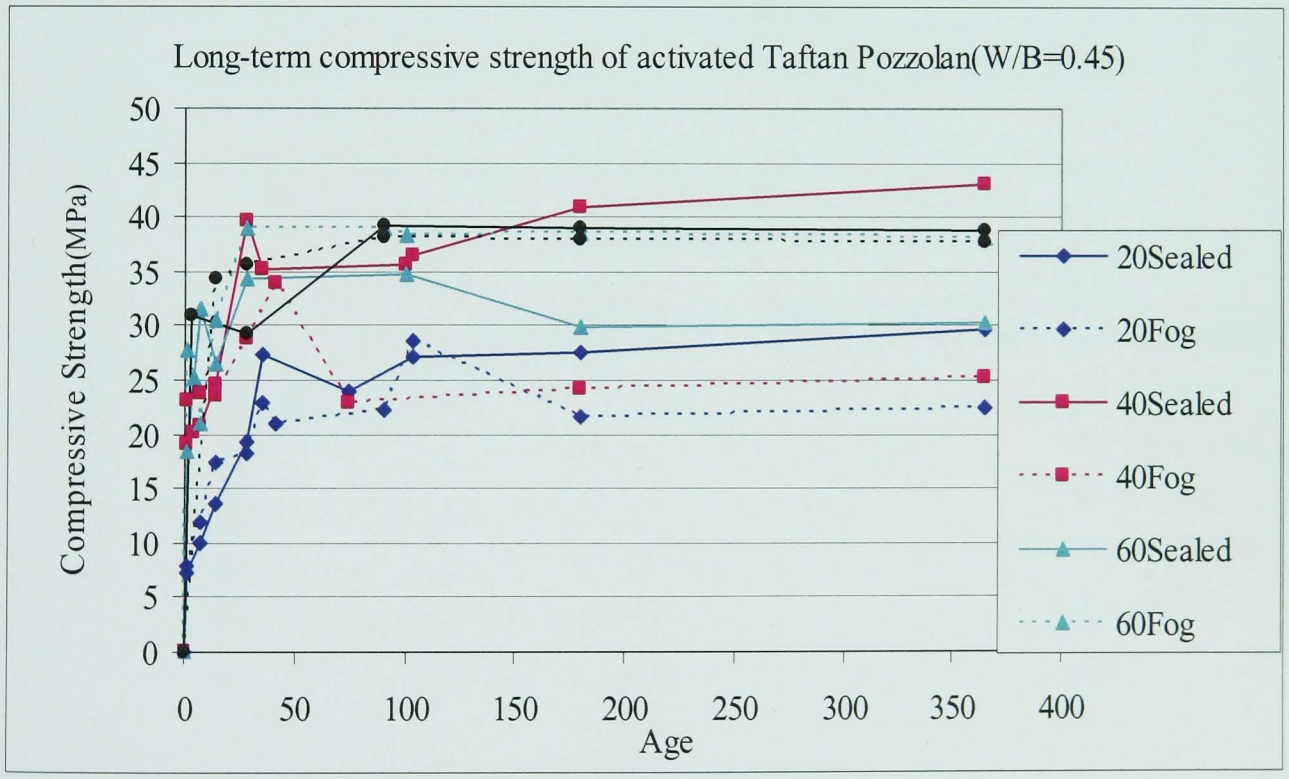

Figure 7.5 Effect of different curing condition and curing temperature on compressive strength development for ATAF1 mix and comparing with CM1 mix

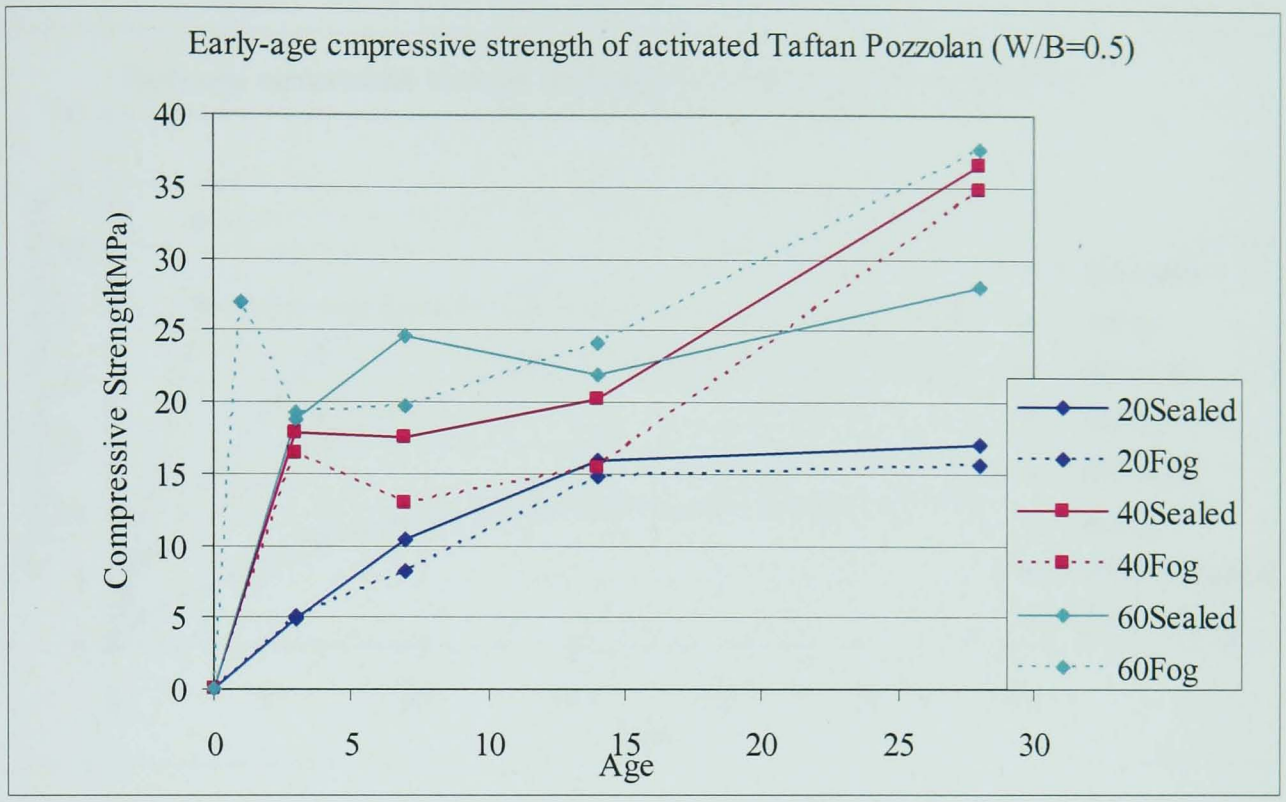

Figure 7.6 Effect of different curing condition and curing temperature on compressive strength development for activated Taftan pozzolan with water to binder ratio equal to 0.5

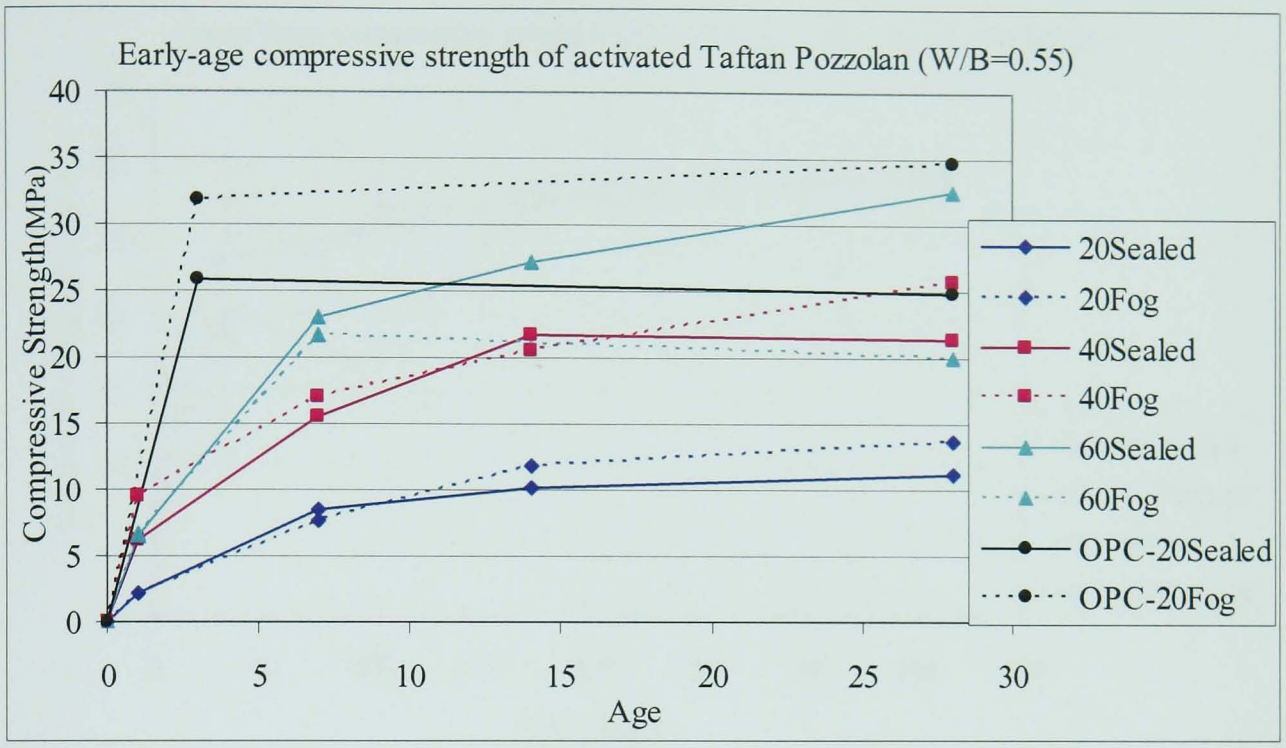

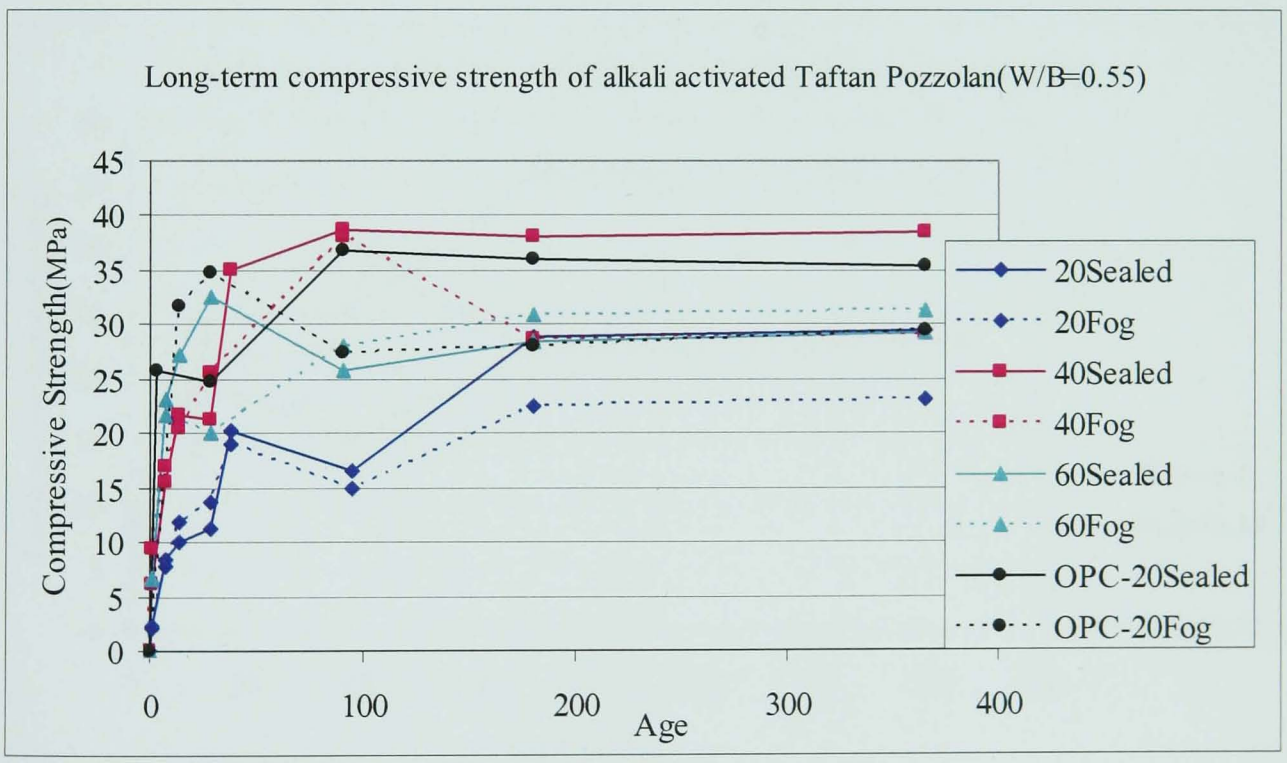

Figure 7.7 Effect of different curing condition and curing temperature on compressive strength development for ATAF2 mix and comparing with CM2 mix

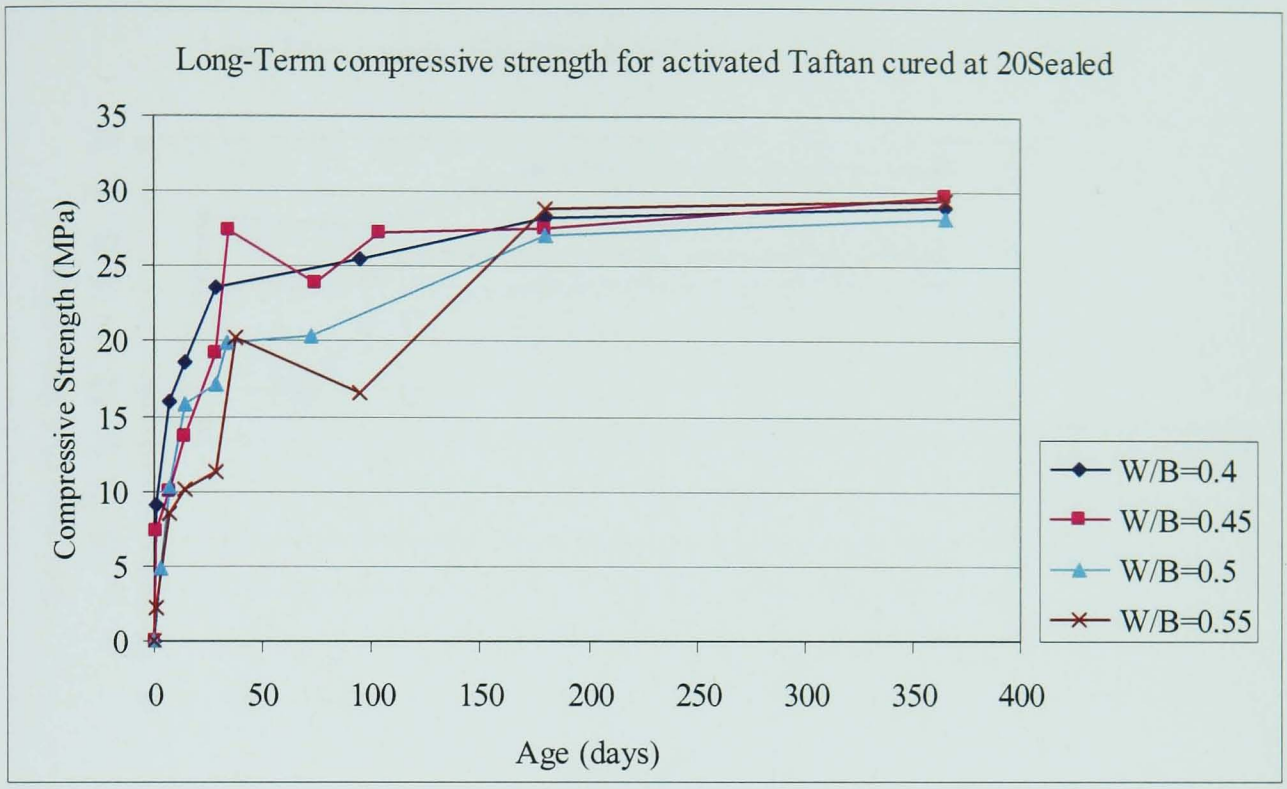

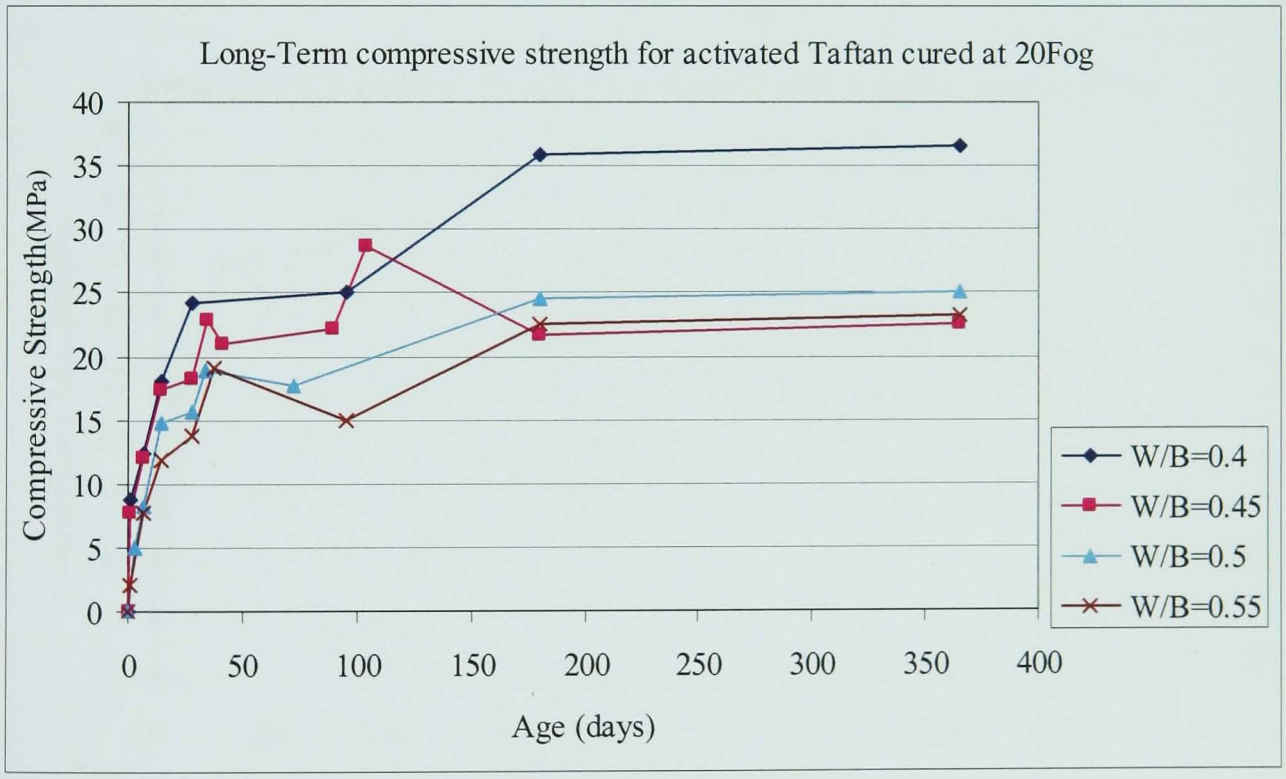

Figure 7.8 Effect of water to binder ratio on compressive strength development for activated Taftan pozzolan cured at 20°C

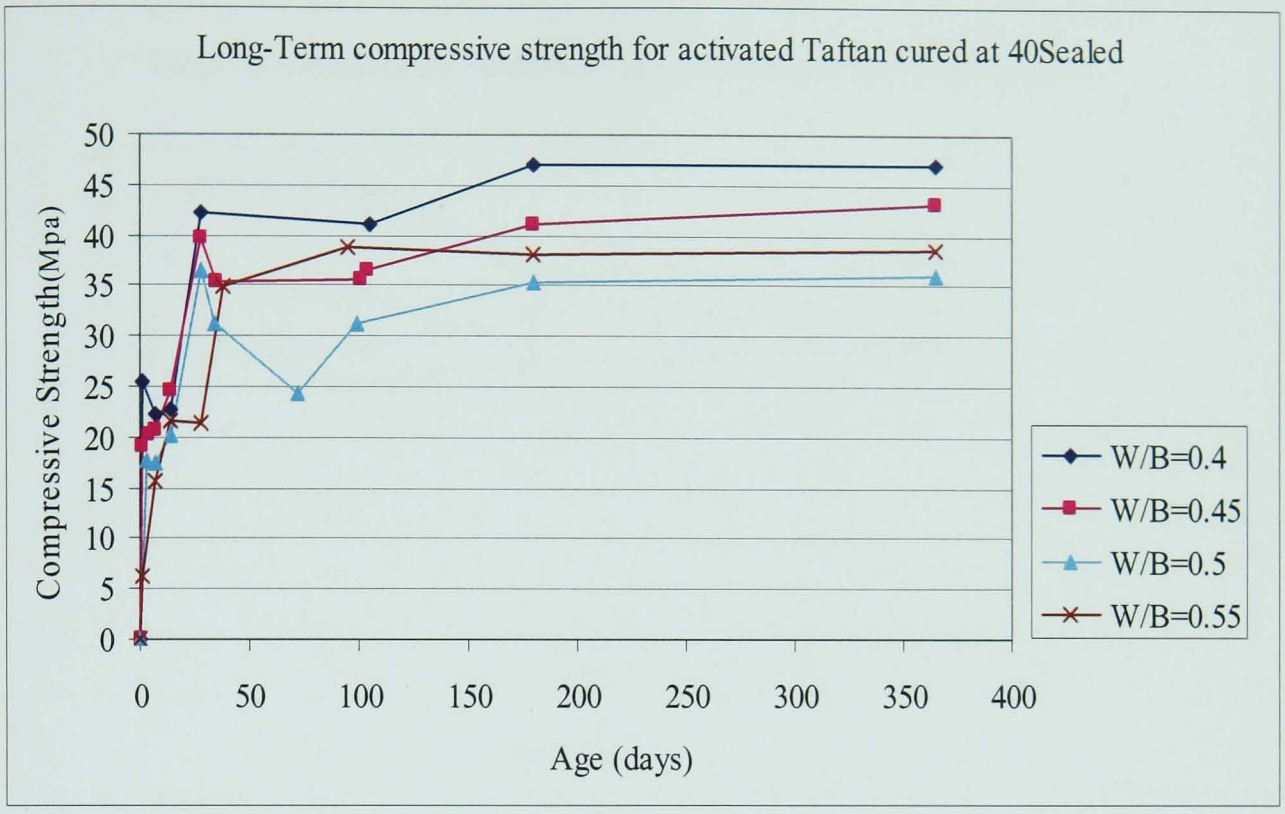

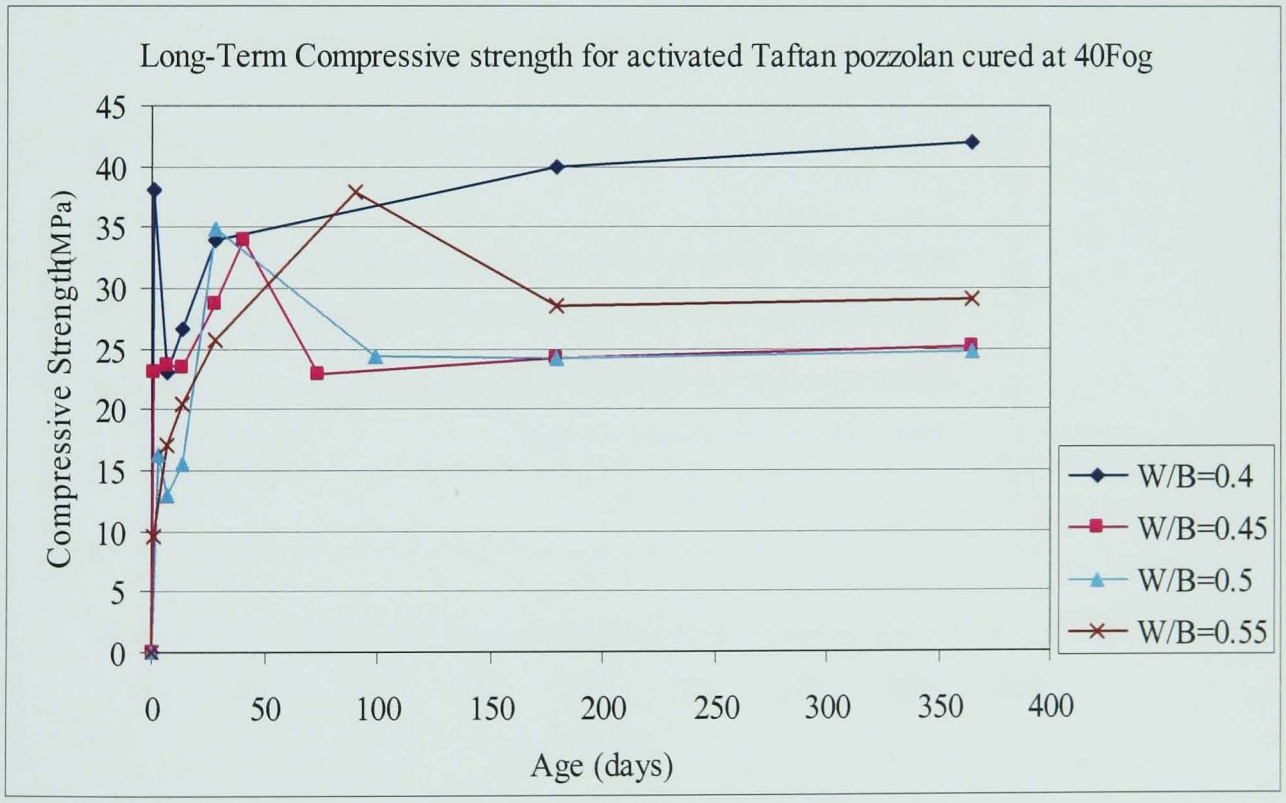

Figure 7.9 Effect of water to binder ratio on compressive strength development for activated Taftan pozzolan cured at 40°C

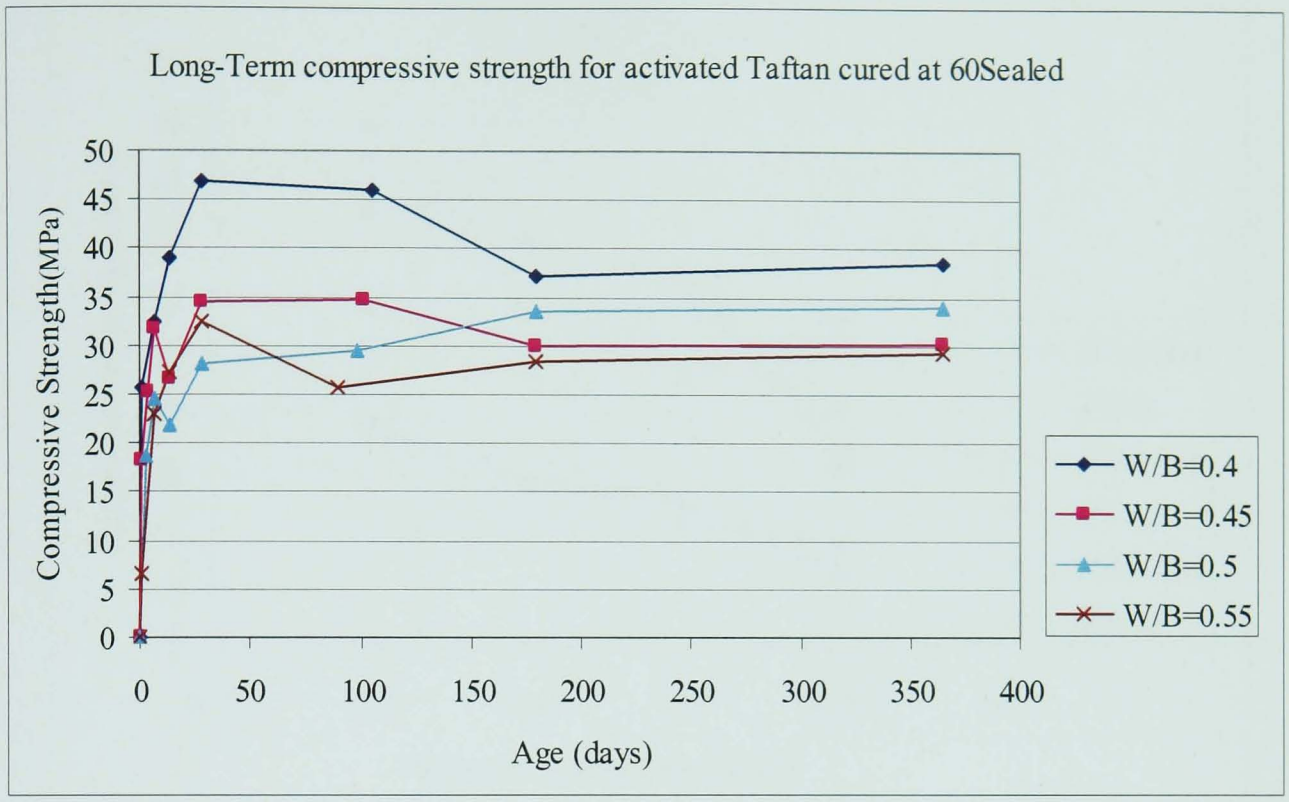

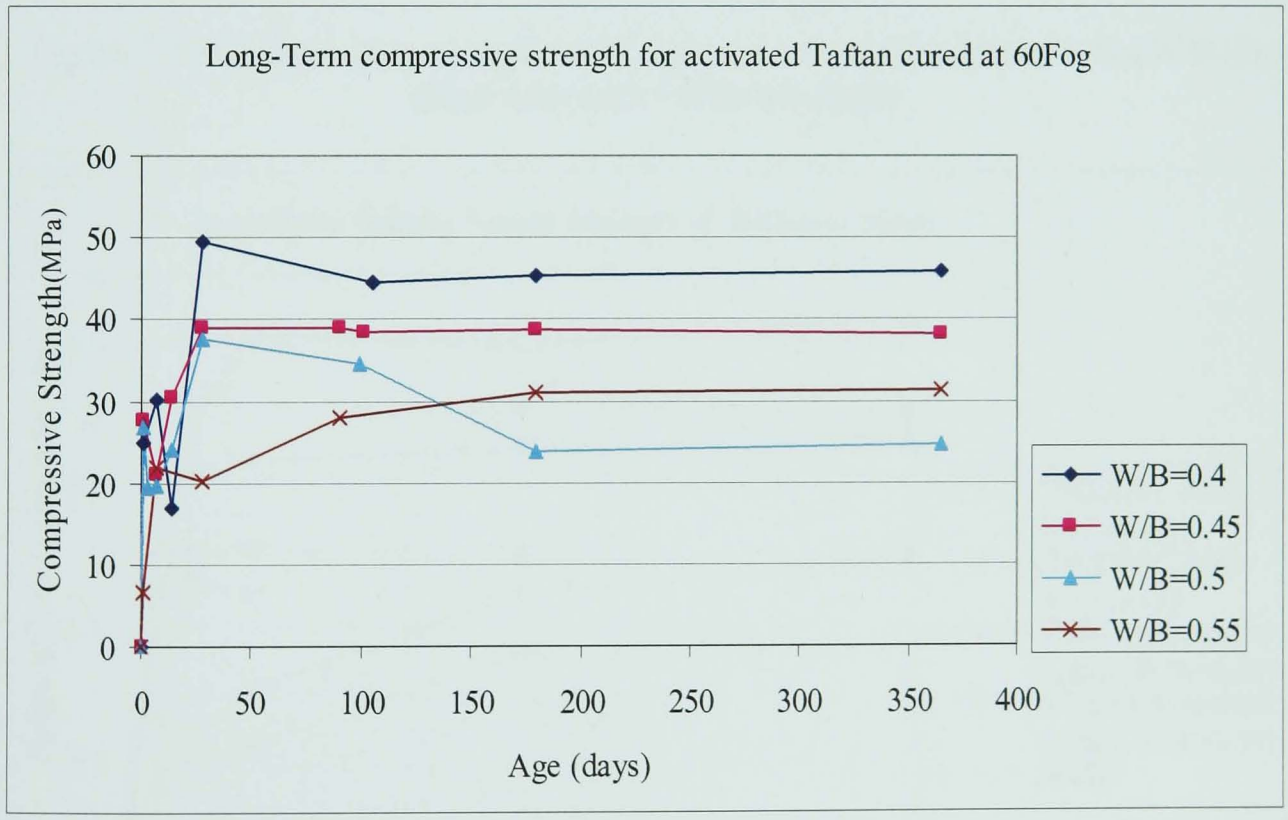

Figure 7.10 Effect of water to binder ratio on compressive strength development for activated Taftan pozzolan cured at 60°C

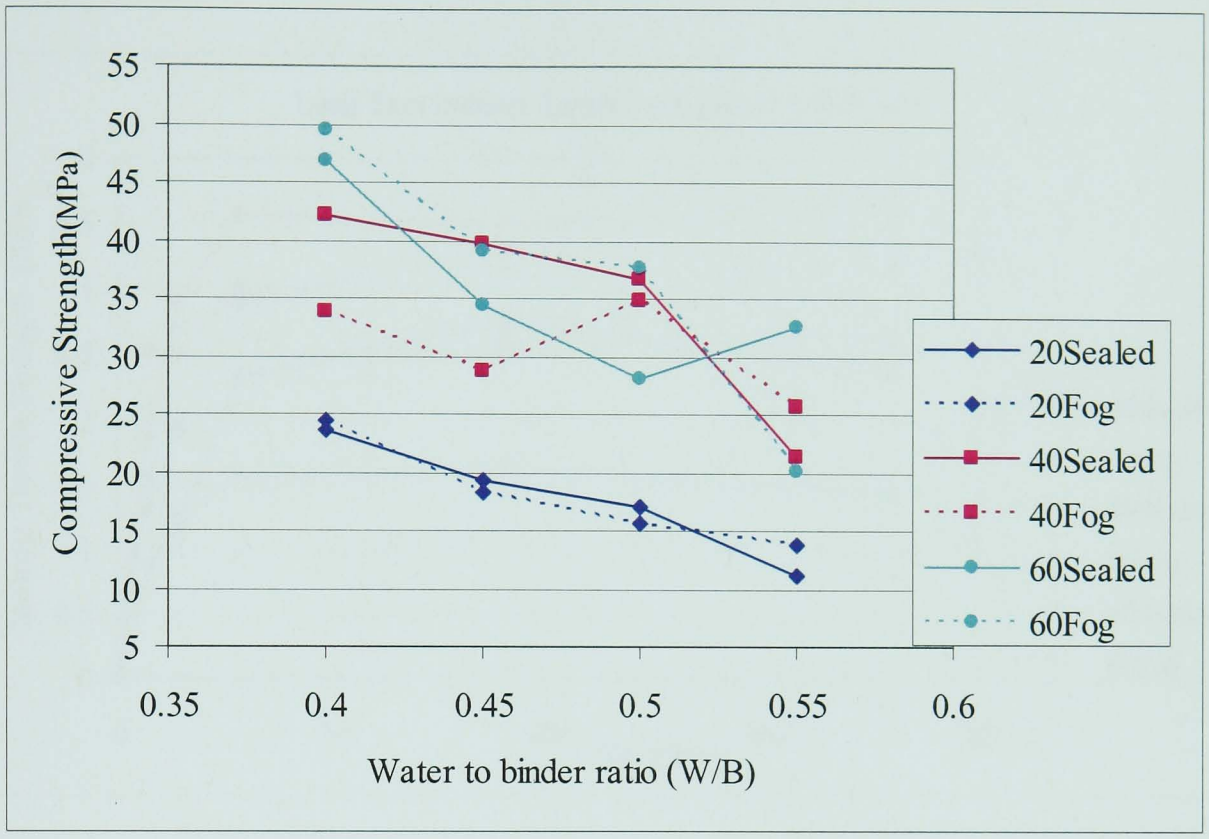

Figure 7.11 Compressive strength at 28 days versus water to binder ratio(W/B)for alkali activated Taftan pozzolan

Figure 7.12 Long-term indirect tensile strength development for different mixes under sealed curing condition (CM1, CM2, and ACSH were cured at 20°C, ATAF1 and ATAF2 were cured at 40°C and ARSH was cured at 60°C which were the best curing temperature in each case)

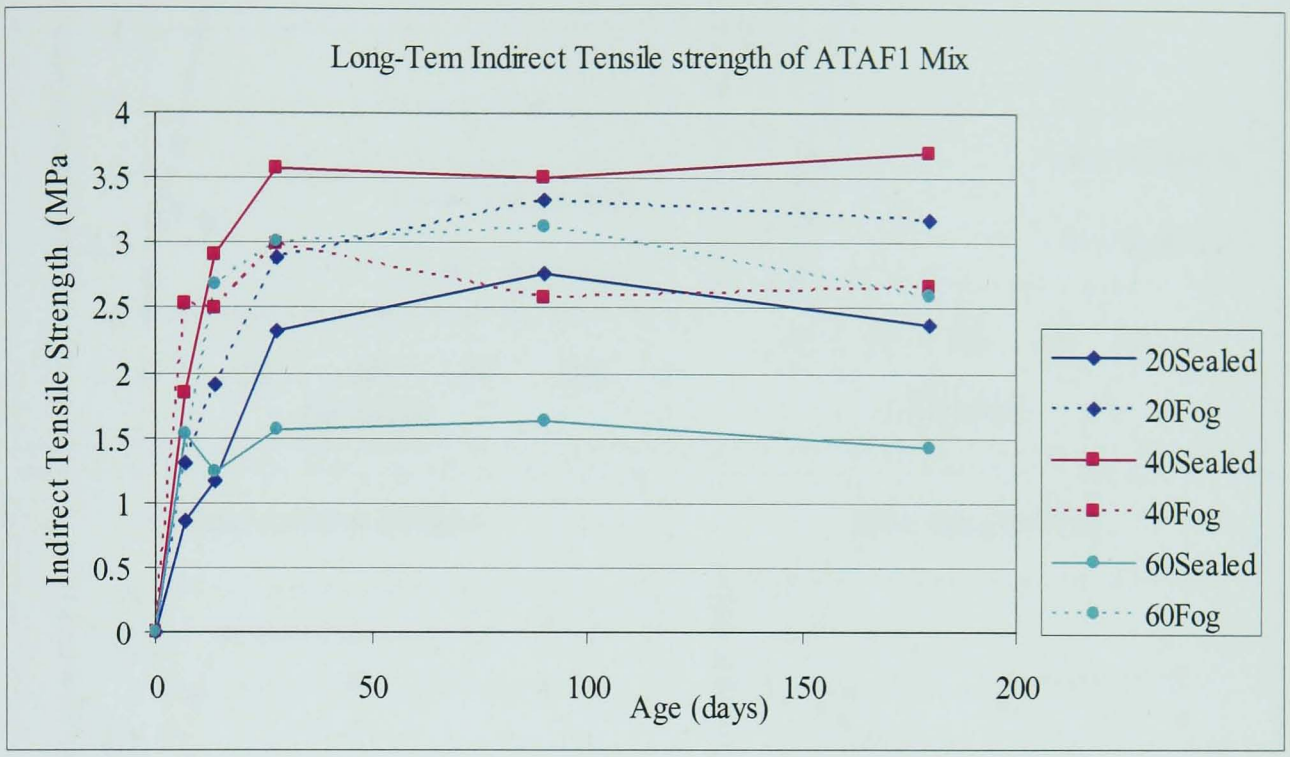

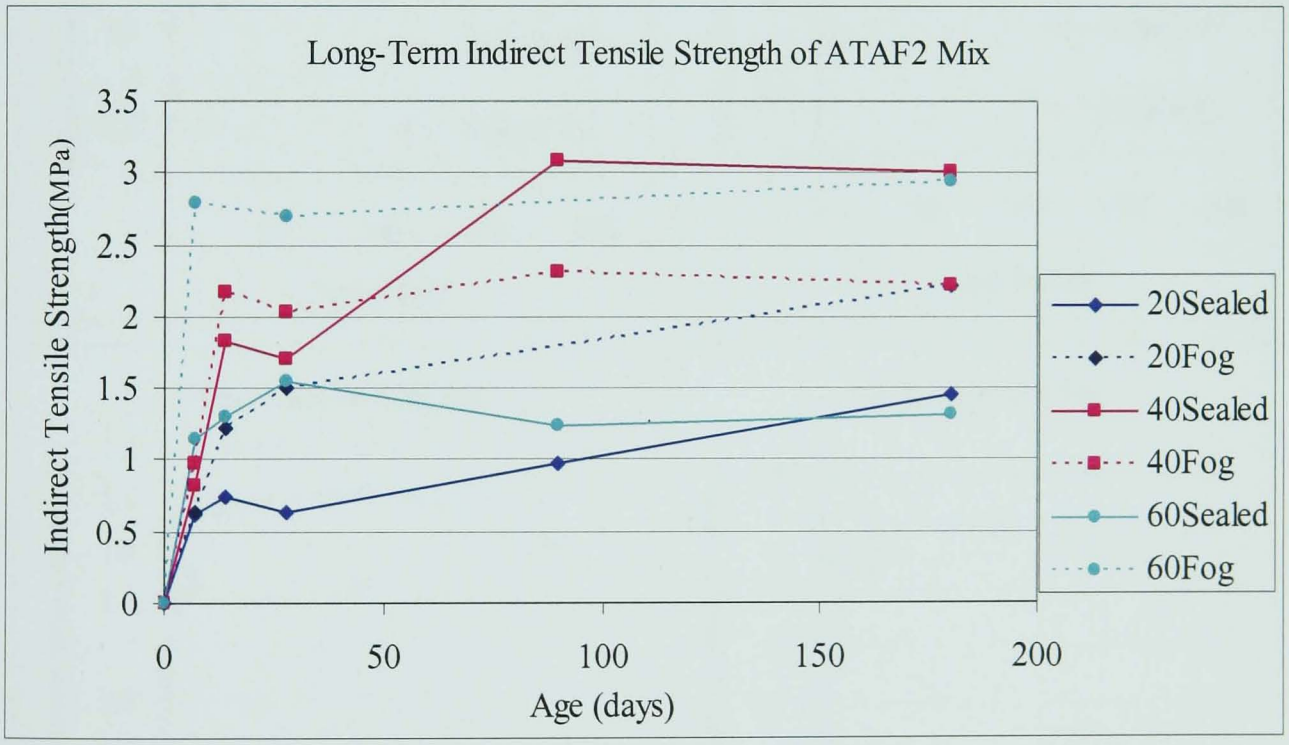

Figure 7.13 Effect of different curing condition and curing temperature on indirect tensile strength development for ATAF1 and ATAF2 mixes

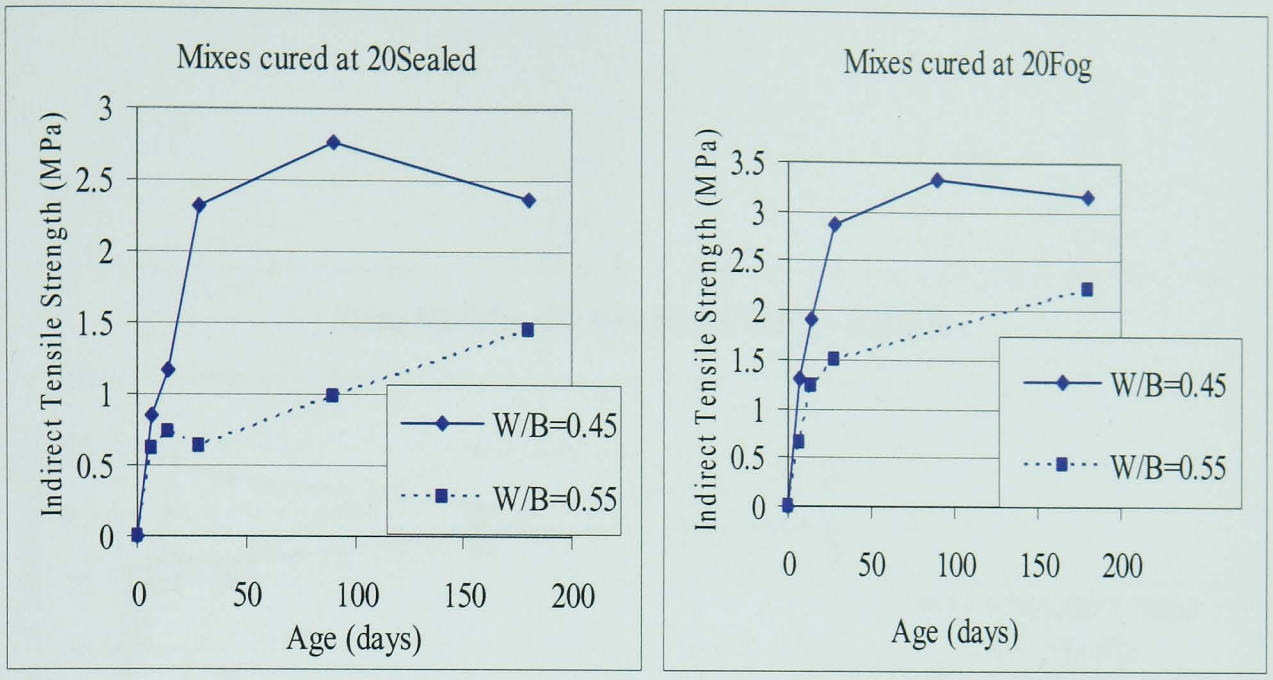

Figure 7.14 Effect of water to binder ratio on indirect tensile strength development for activated Taftan pozzolan cured at different curing condition (sealed and fog) and temperatures

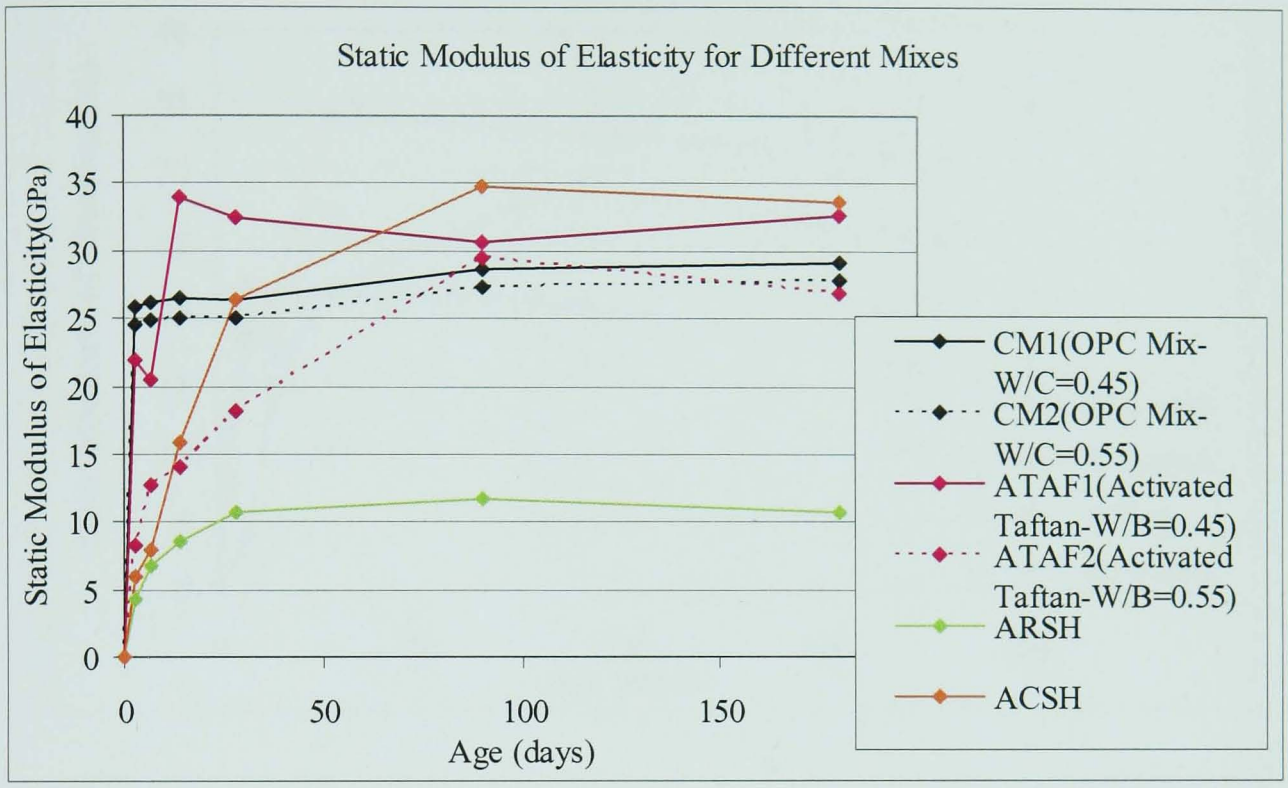

Figure 7.15 Long-term static modulus of elasticity development for different mixes under sealed curing condition (CM1, CM2, and ACSH were cured at 20°C, ATAF1 and ATAF2 were cured at 40°C and ARSH was cured at 60°C which were the best curing temperature in each case)

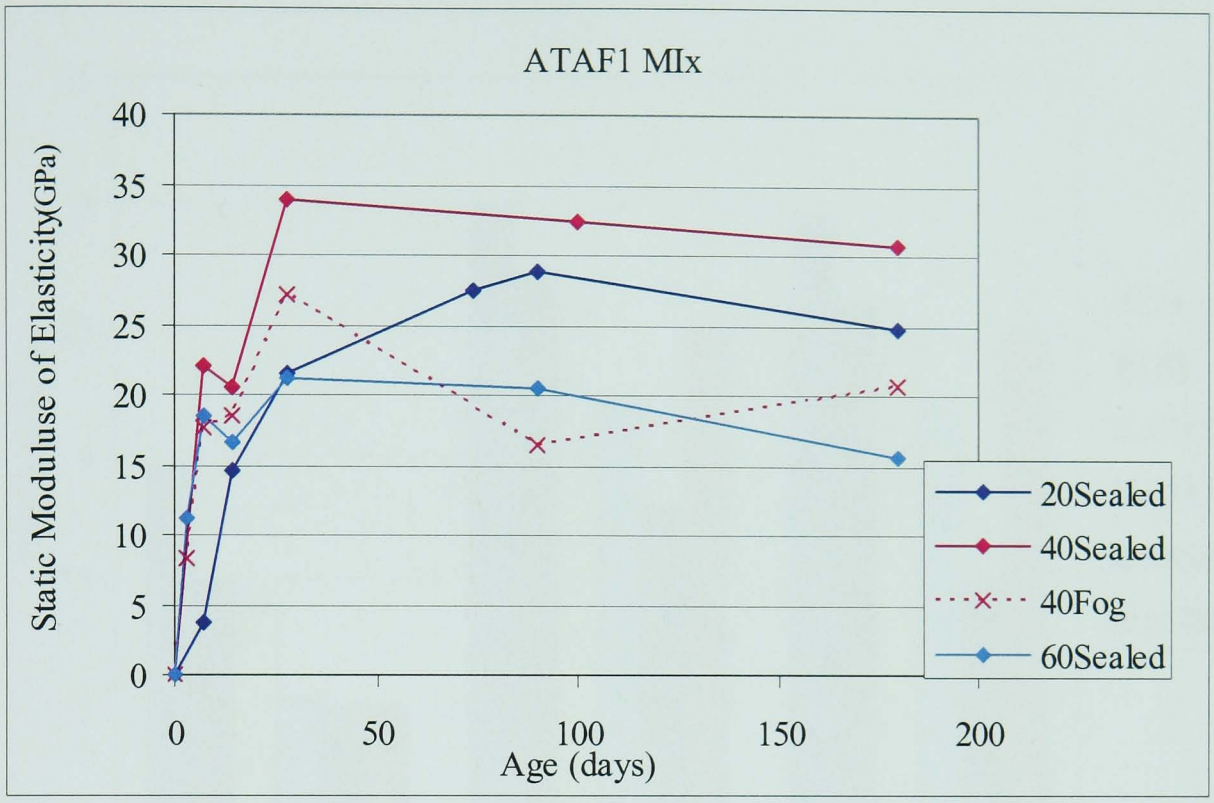

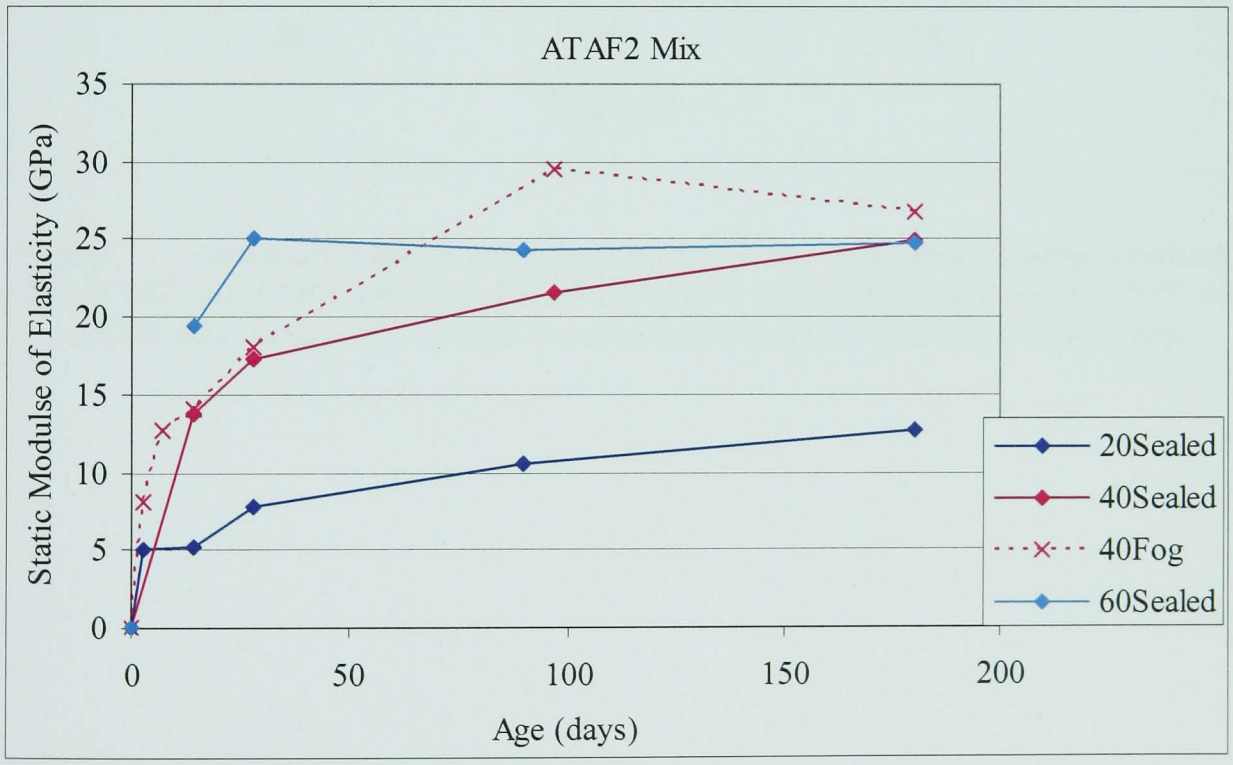

Figure 7.16 Effect of different curing condition and curing temperature on static modulus of elasticity development for ATAF1 and ATAF2 mixes

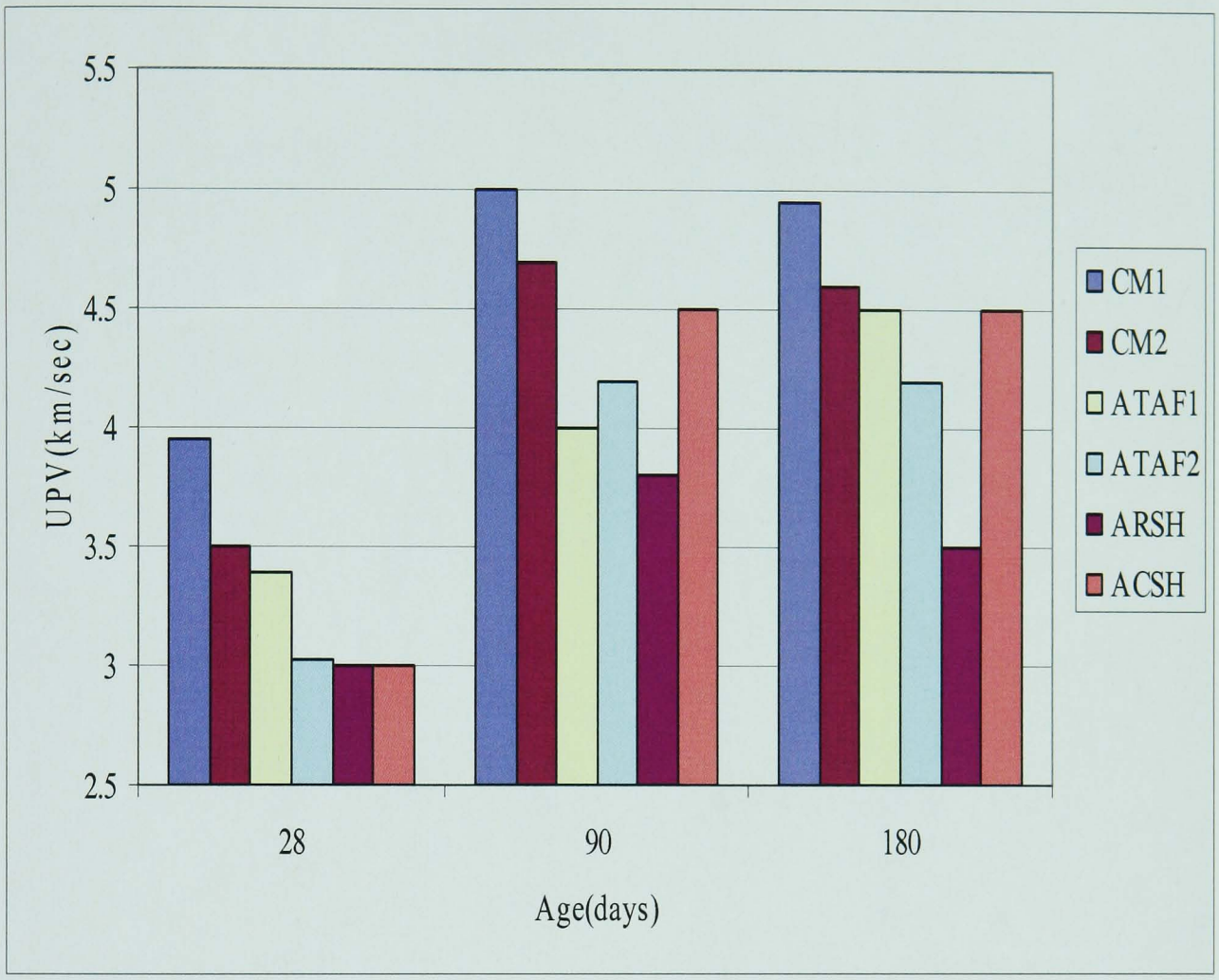

Figure 7.17 Ultrasonic pulse velocity for different mixes under sealed curing condition (CM1, CM2, and ACSH were cured at 20°C, ATAF1 and ATAF2 were cured at 40°C and ARSH was cured at 60°C which were the best curing temperature for each one)

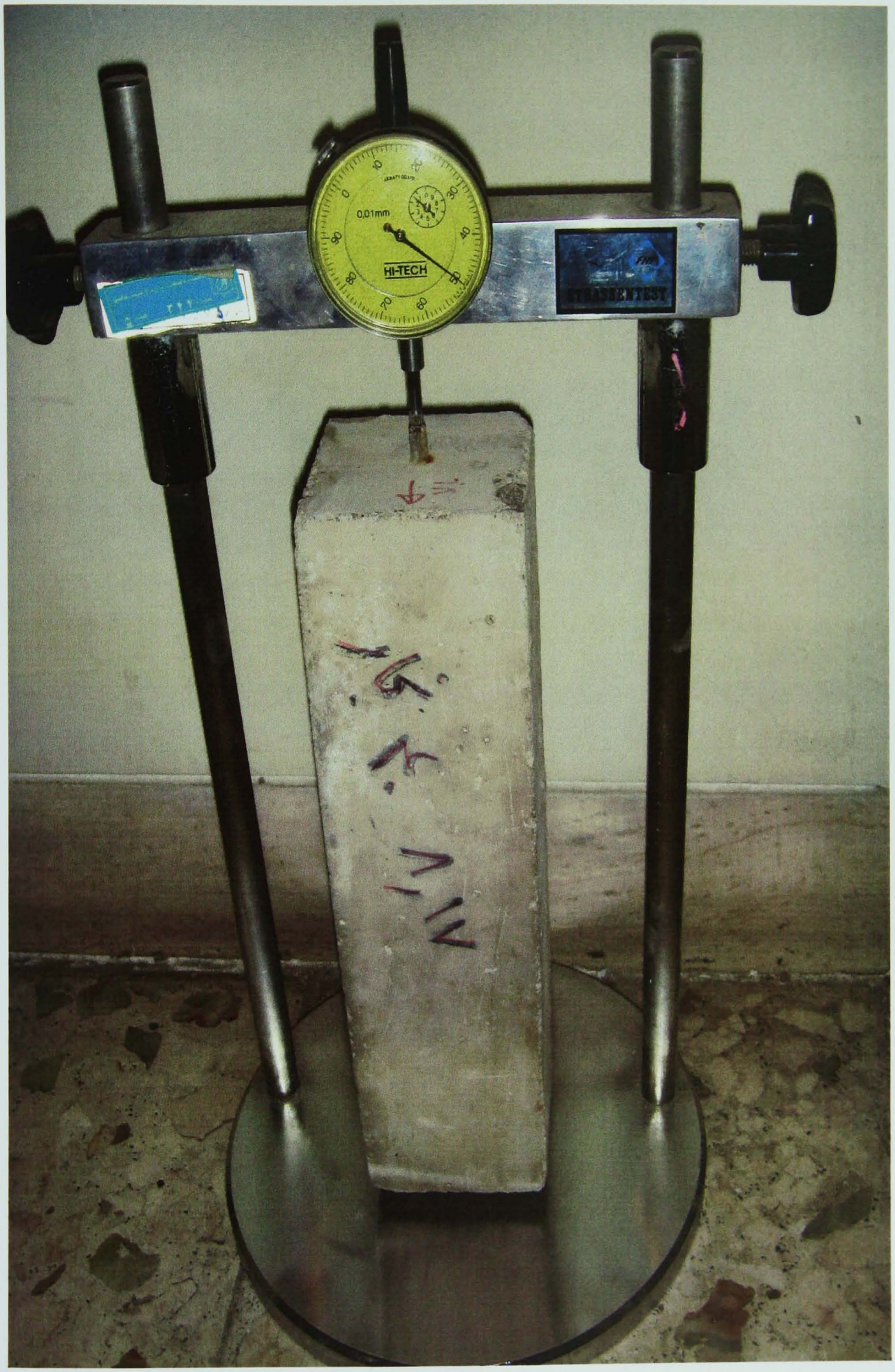

Figure 7.18 The comparator and concrete prism

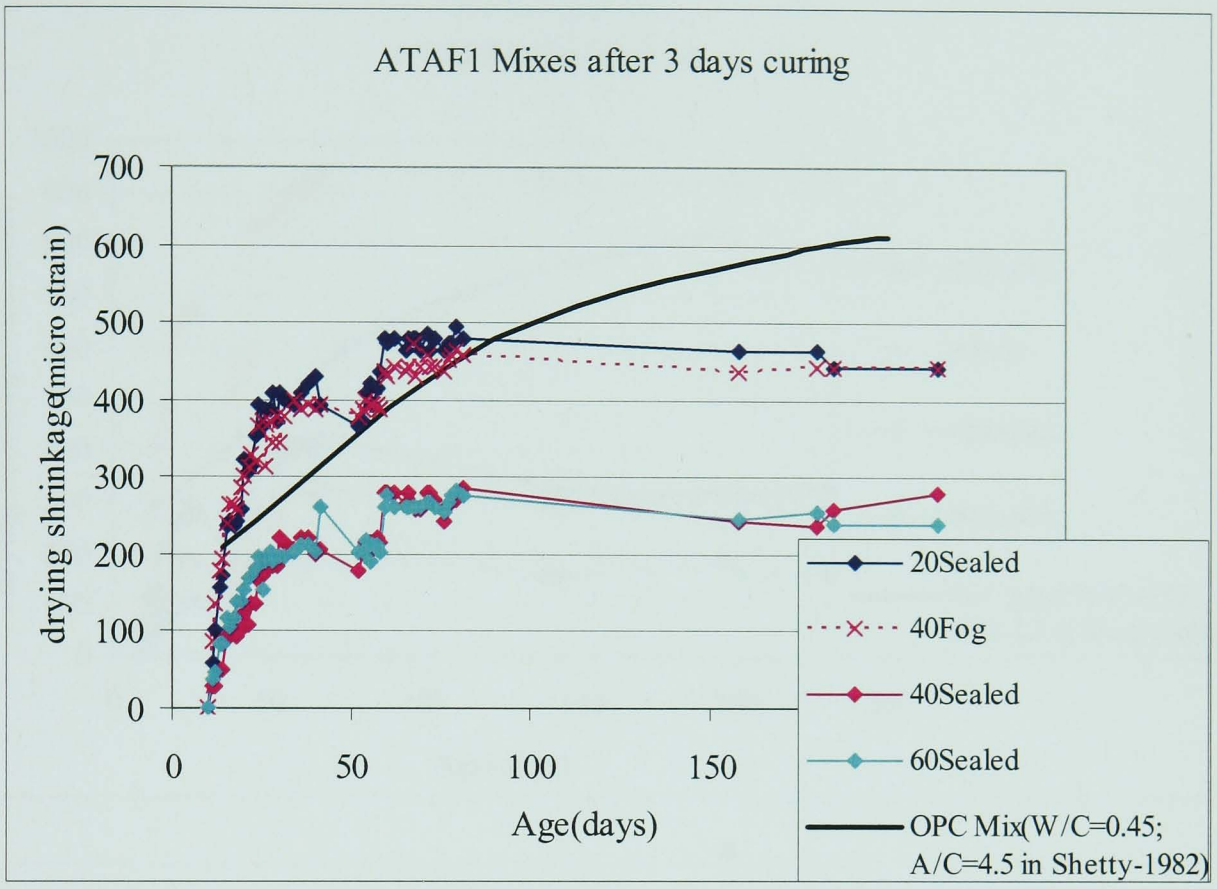

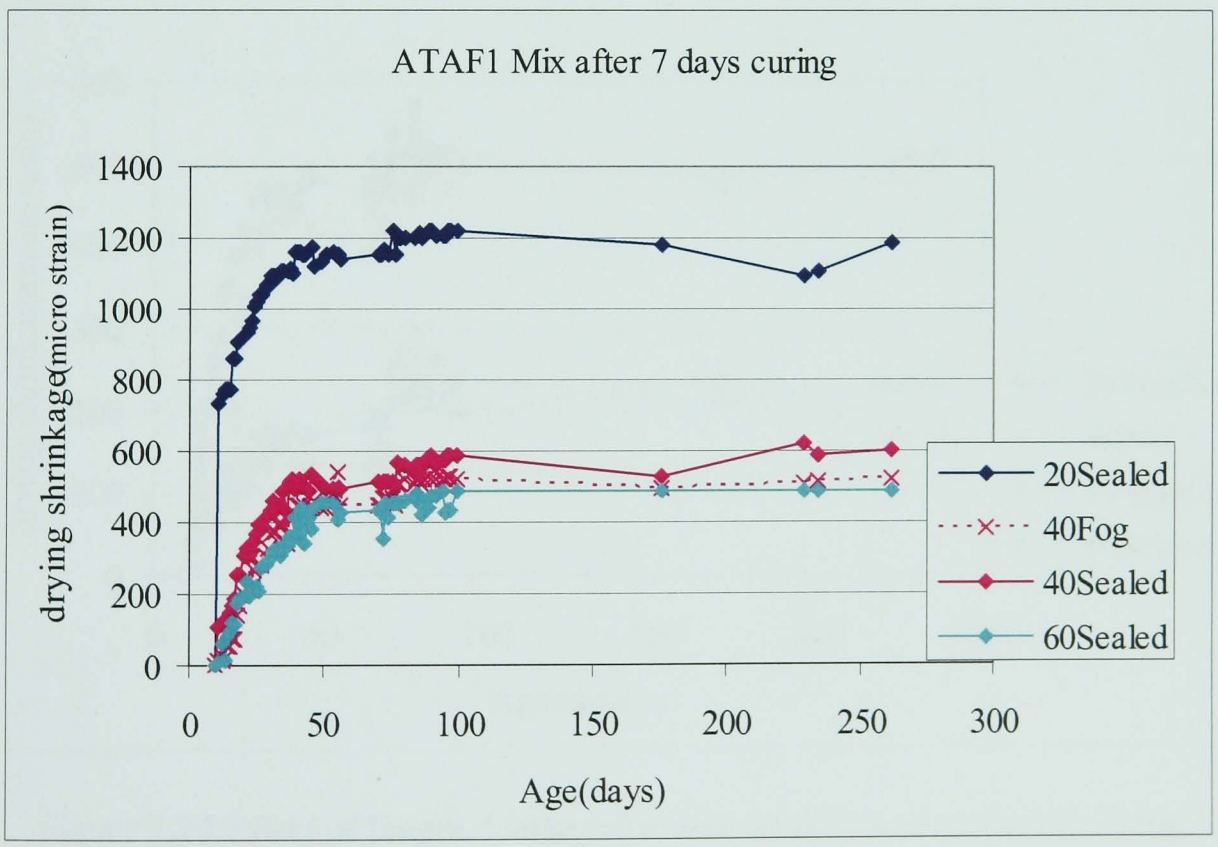

Figure 7.19 Effect of length, temperature and condition of curing on drying shrinkage development with age for ATAF1 mix with comparison with OPC

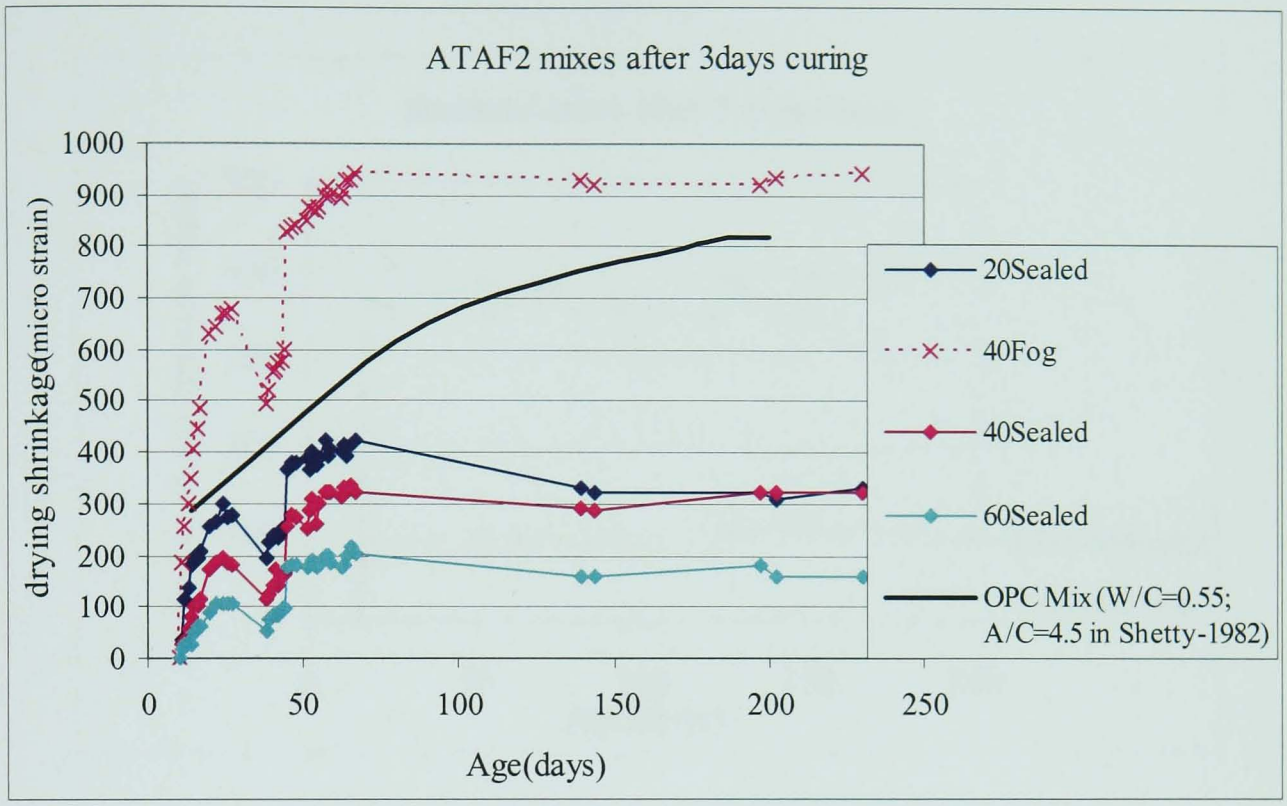

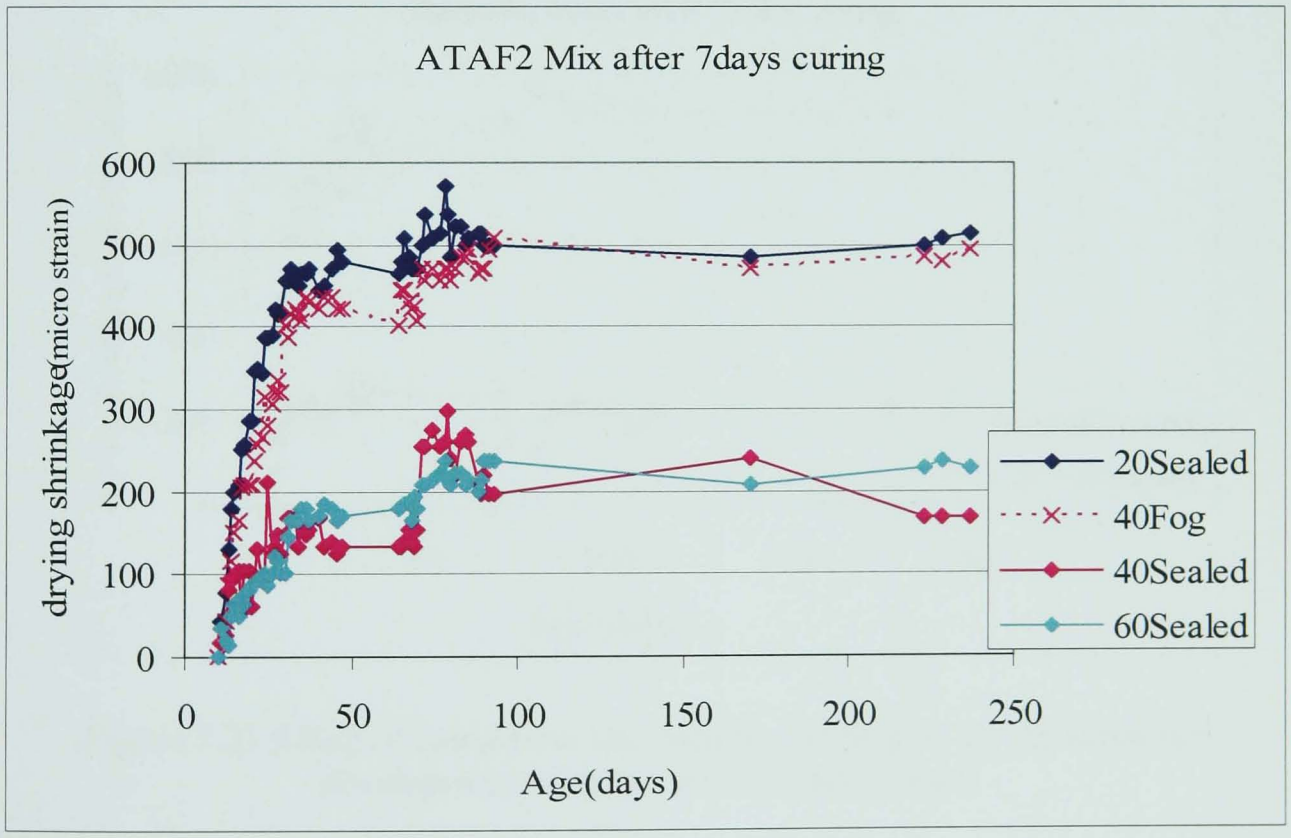

Figure 7.20 Effect of length, temperature and condition of curing on drying shrinkage development with age for ATAF2 mix with comparison with OPC

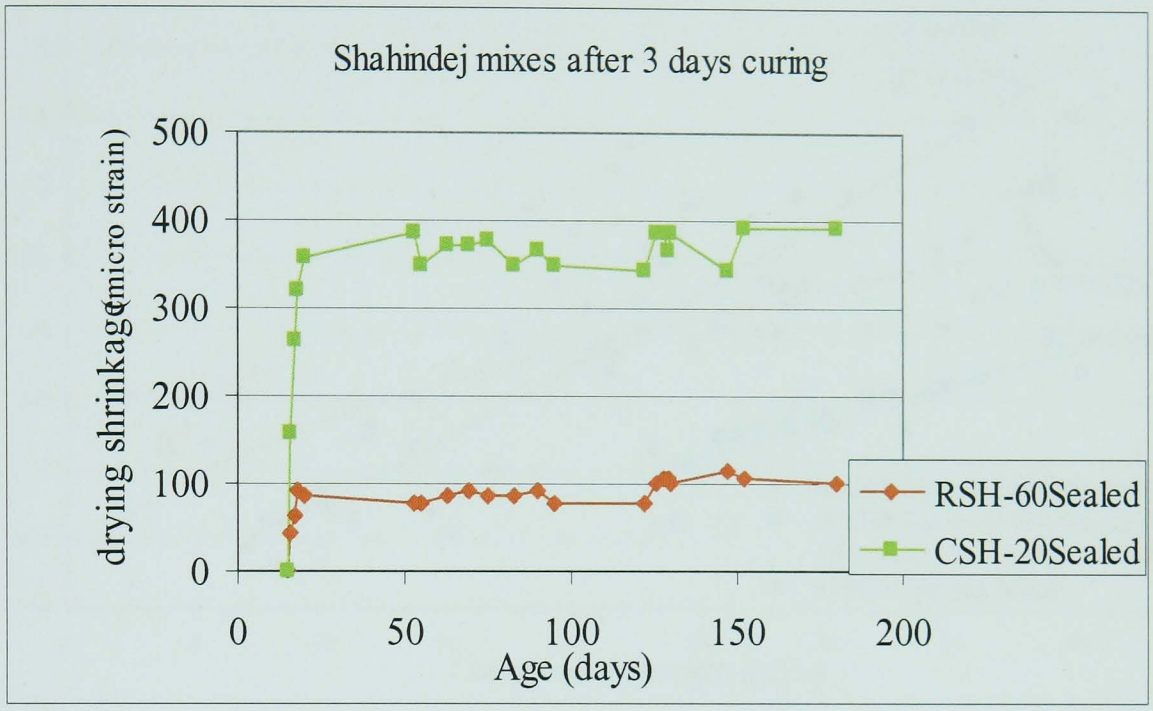

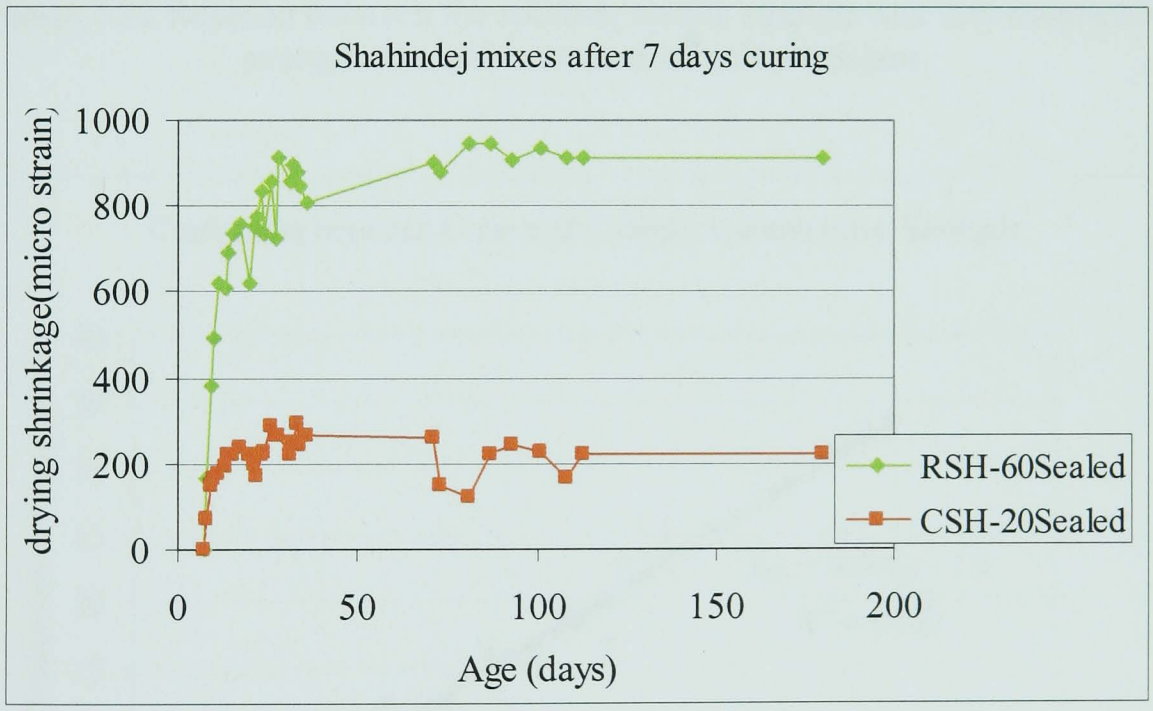

Figure 7.21 Effect of calcination and length of curing on drying shrinkage development with age for Shahindej mixes

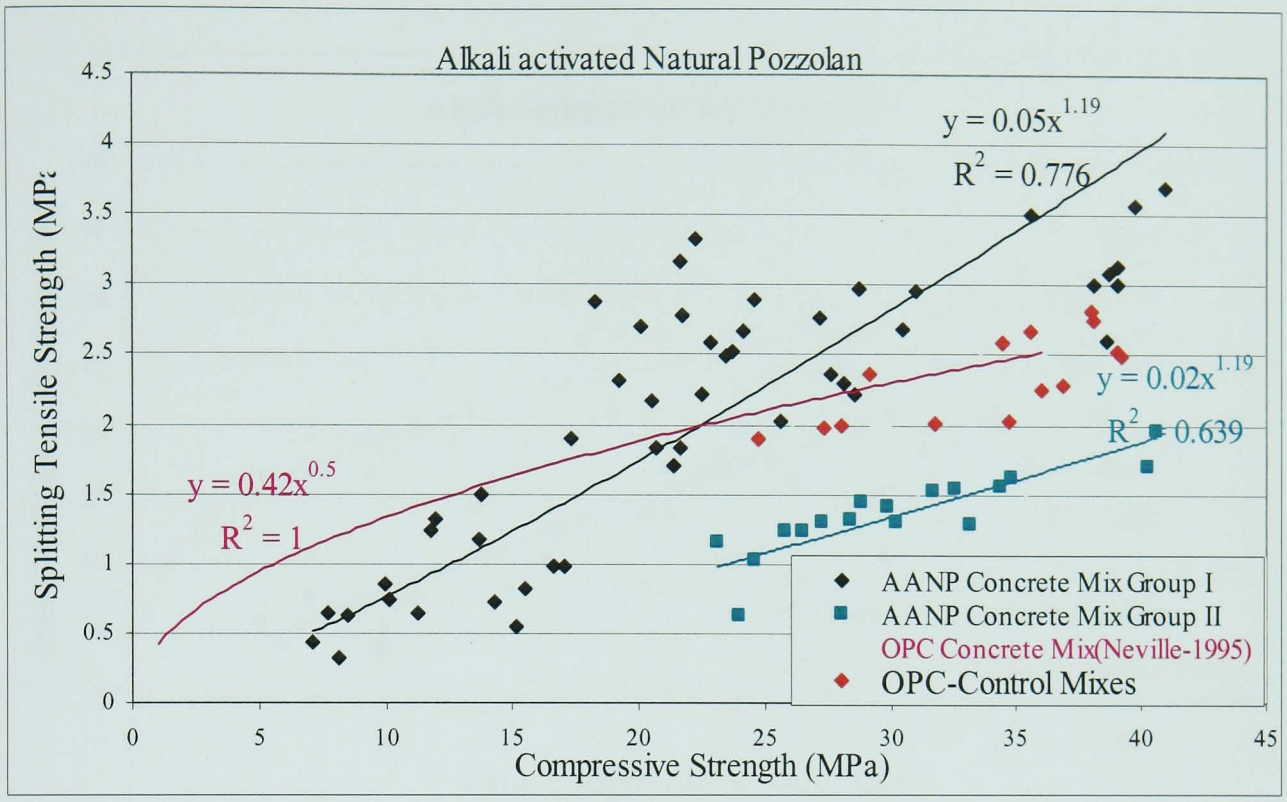

Figure 7.22 Relation between the splitting tensile strength and the compressive strength of alkali activated natural pozzolans

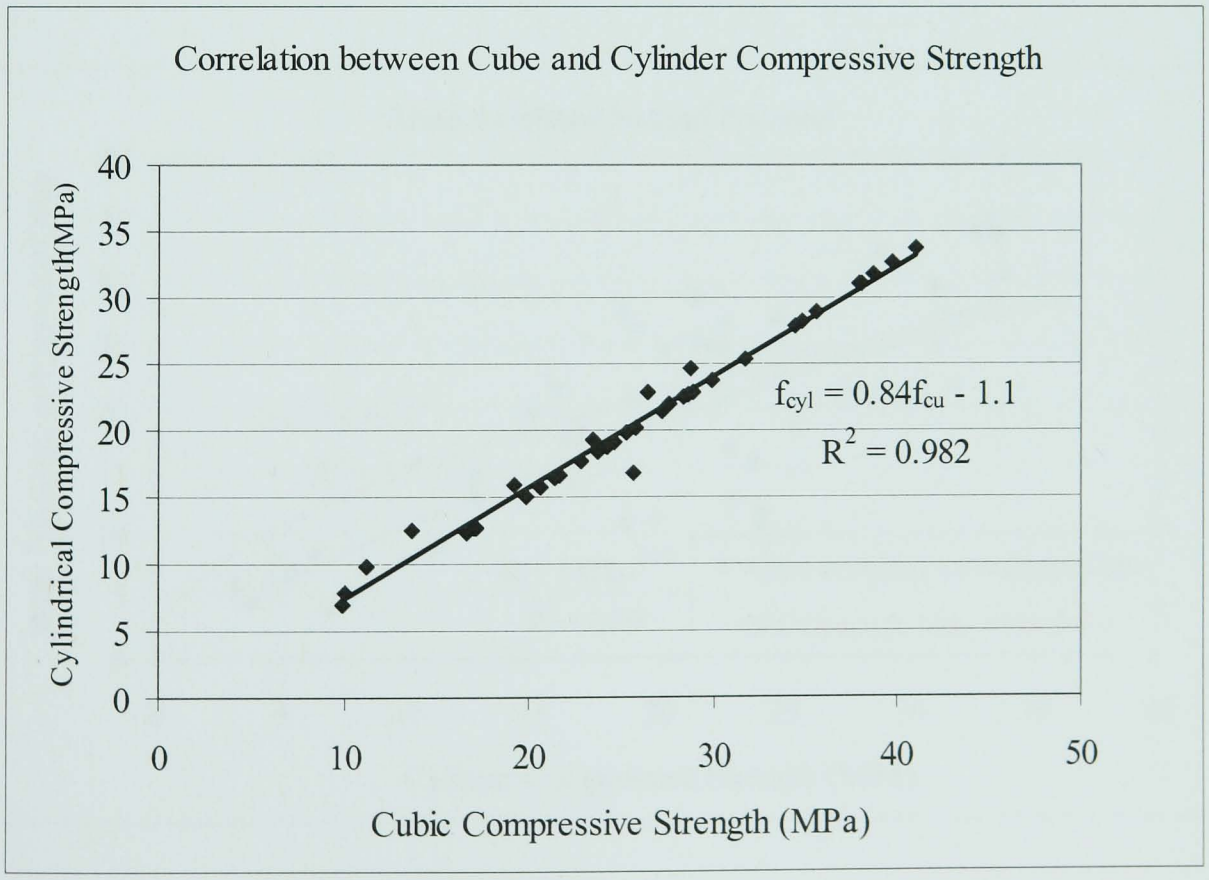

Figure 7.23 Correlation between cube and cylinder compressive strength

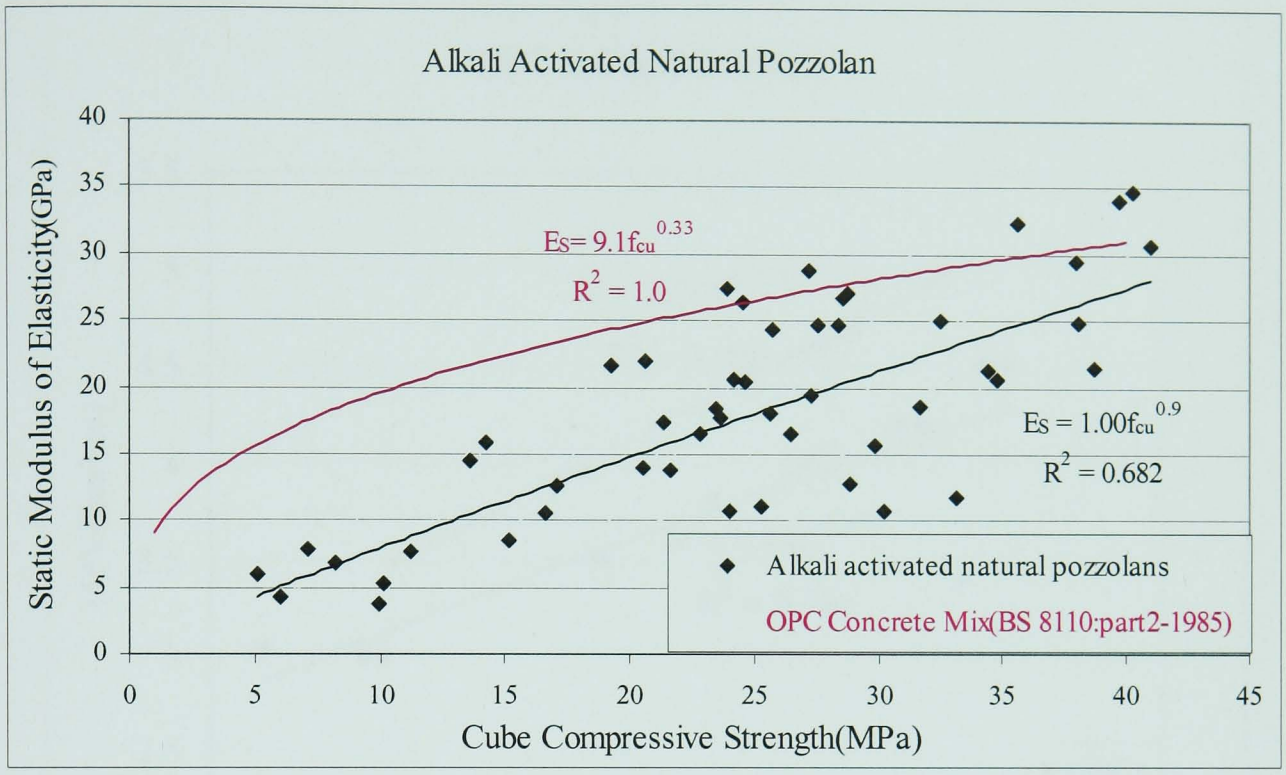

Figure 7.24 Relation between the static modulus of elasticity and the cube compressive strength of Alkali activated natural pozzolans

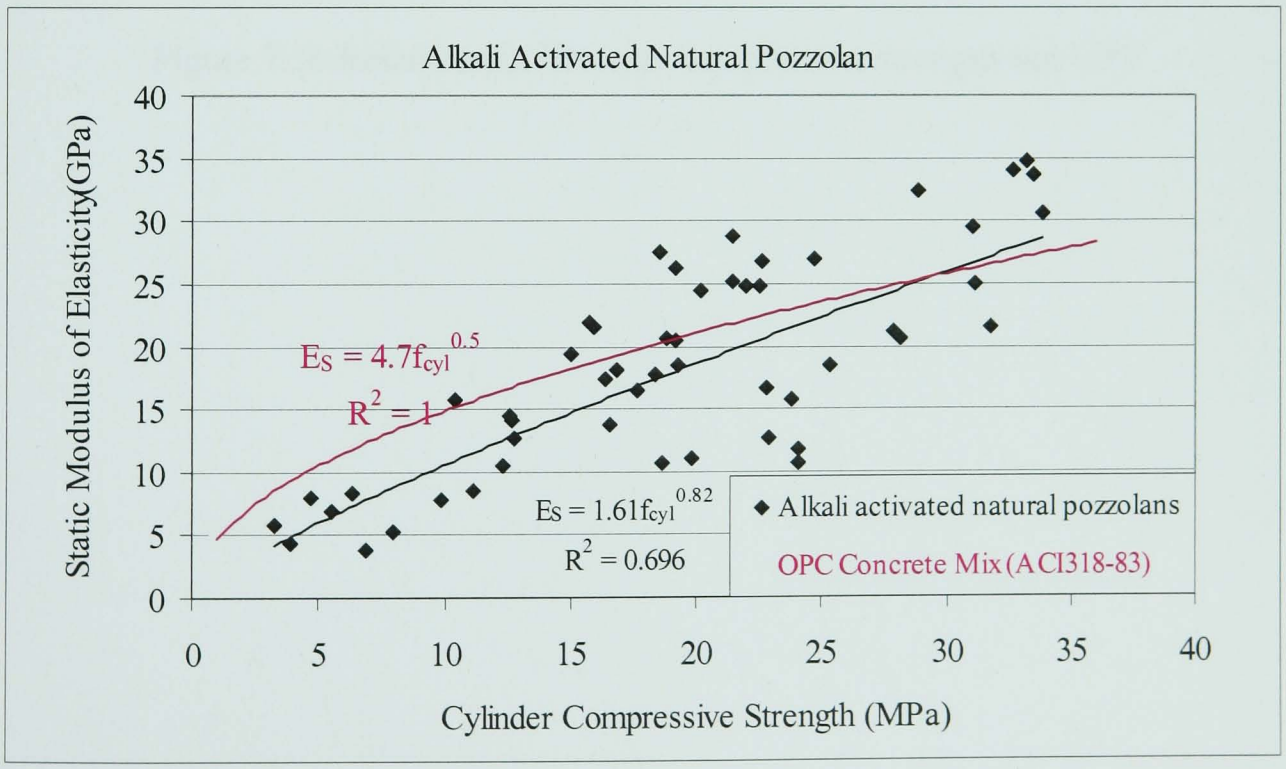

Figure 7.25 Relation between the static modulus of elasticity and the cylinder compressive strength of Alkali activated natural pozzolans

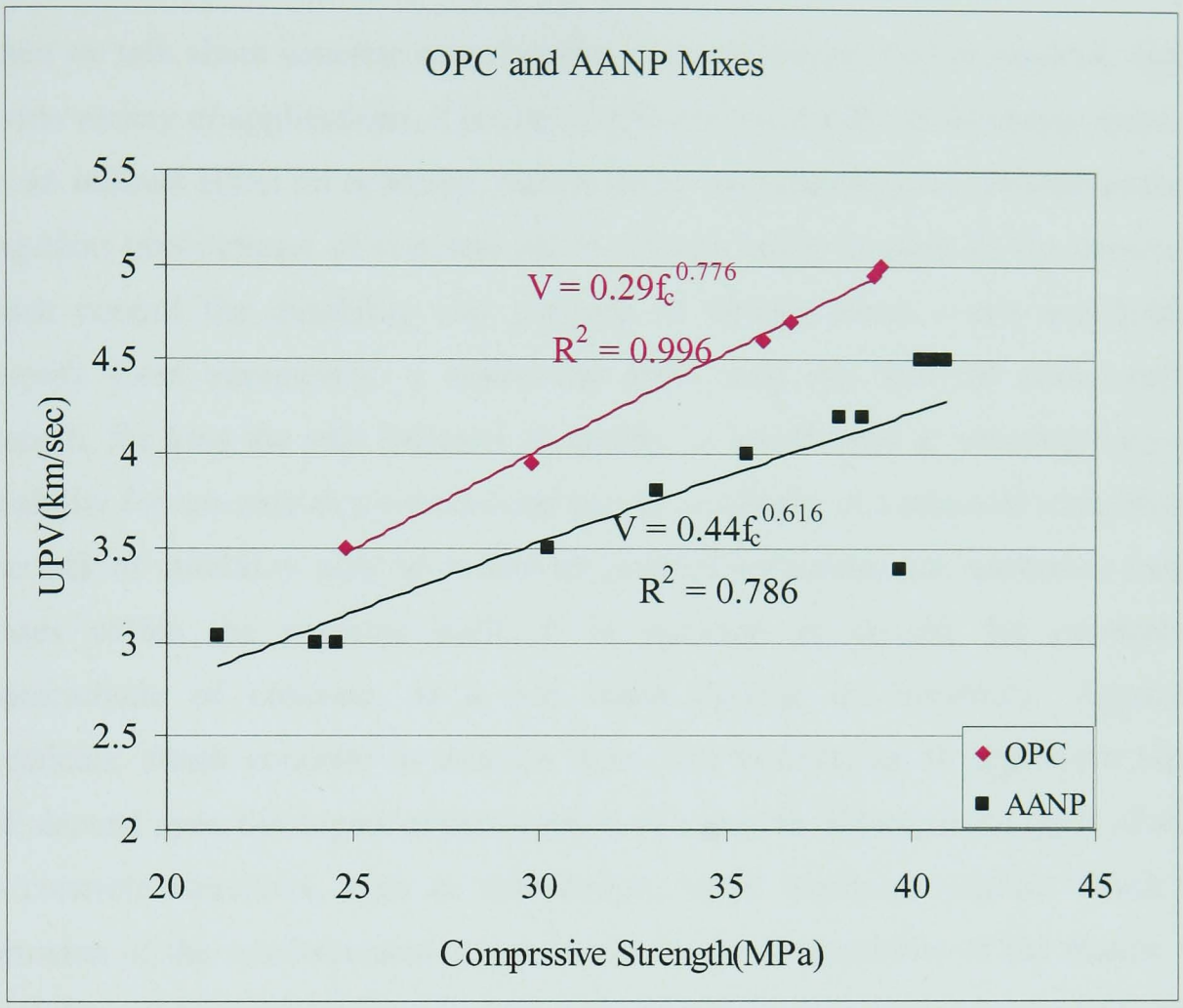

Figure 7.26 Relationship between compressive strength and UPV

8. DURABILITY PROPERTIES OF GEOPOLYMER CONCRETE

8.1 Introduction

When we talk about concrete as an important versatile construction material, used in a wide variety of applications, it is very important to consider its durability since this has an indirect effect on economy, serviceability and maintenance. Determination of long-term performance of concrete led to interest being focused on the parameters which control the durability and methods of testing which could meaningfully quantify these parameters. A realization grew long ago that the cube crushing strength, for long the sole indicator of quality, is insufficient in ensuring long-term durability for concrete as a material and the serviceability of a structure made from it. The lack of durability may be caused by external environmental reasons or internal causes within the concrete itself. It is pertinent to discuss the permeability characteristic of concrete, as it has much bearing on durability. Aggressive chemicals, attack concrete in solution form. The penetration of aggressive liquids will depend upon the degree of permeability of concrete. Hence, some types of attack on concrete structures, such as carbonation, water leaching; sulphate attack and corrosion of the reinforcement are governed by the permeability of the matrix. The durability of structures made of reinforced concrete is dependent on the mechanisms of movement of aggressive fluids within the micro-structure of concrete. Pore structure has long been recognized as strongly related to many, if not all, aspects of durability. The concrete acts as a protection barrier for the reinforcing bars against potentially damaging matter such as acids, chlorides, and CO_2. Thus it is felt that some form of permeability test might be devised which would have the necessary features and can provide information about the resistance to the ingress of aggressive chemicals through the porous system. The concrete might suffer from chemical internal sources and their interactions as in the presence of contaminants or harmful materials in the concrete ingredients. Deterioration may also occurs due to the presence of an aggressive chemical environment that contains materials such as chlorides and sulphates that attack the concrete, causes volume changes in it. This chapter presents the results of oxygen permeability, chloride permeability, and sulphate resistance tests carried out to study the possibility of external element penetration and volume changes in the AANP concrete leading to studying the durability of this type of geopolymeric concrete.

8.2 Oxygen permeability

Oxygen permeability method to measure permeability of pastes, mortars or concrete employs the use of oxygen (Cabrera and Lynsdale 1988; Cabrera and Claisse 1999; Basheer 2001; Khan and Lynsdale 2002). This method is intended to be suitable for concretes with a specific permeability coefficient k to oxygen within the range of 10^{-14} to 10^{-19} m^2 and has the advantage of being capable of examining the permeability of samples collected "in situ". The samples are usually smaller than water permeability measurement samples and therefore, the flow equilibrium condition is quicker and rapidly achieved, reducing the time for testing which makes oxygen permeability method easier to perform than water permeability measurement (Cabrera and Lynsdale 1988). The influence of sample size on permeating fluid can be seen in the equation derived from D'Arcy's law of flow, which is used to calculate the intrinsic permeability of the sample.

8.2.1 Samples Preparation

To study the permeability of concrete by gas permeability measurement, a procedure for removing the pore moisture before the actual measurement of this property, normally called preconditioning, is an unavoidable necessity. The moisture content of the sample, affects oxygen permeability considerably since due to surface tension can not be pushed out by oxygen. In OPC concrete mixes, incomplete drying results in residual water being present in the pore system, which will block the passage of gas through the specimen and thus lower permeability values, are obtained. On the other hand, drying at high temperatures may result in shrinkage cracking and modification of pore structure, leading to incorrect permeability values obtained. Therefore, the results are specific to the drying regime used prior to testing. It seems that in geopolymer concrete especially those subjected to high temperature curing the phenomena of shrinkage cracking due to drying at high temperatures is not as important as for OPC concrete. This is because the water removed from geopolymer concrete is not combined or bound water, since it does not participate in the reaction. The water is just a medium which promotes the geopolymerisation and it must be eliminated once the reaction is over and it has been found that the higher the curing temperature the lower the amount of drying shrinkage. Another parameter that affects the oxygen flow is the inlet pressure employed (P_2) and high inlet pressure

may cause less flow due to more scattering and conflict of air bubbles with each other and tube wall (Klingenberg effect) so the intrinsic permeability varies with different pressures.

Cylinders of 150 mm of diameter by 50 mm height were cast for oxygen permeability and cured in the manner mentioned in section 6.4. Gas permeability on samples pre-dried at different temperatures (20, 40, 50, 80, and 105°C) is reported in the literature for OPC concretes (Lynsdale, 1989; Carcasses et al., 2002). In this investigation, to reduce the shrinkage effect, the samples were dried at 50°C±5°C until constant weight was reached and kept in vacuum desiccators at 20°C±2°C until testing. Oxygen permeability was performed on three samples of each concrete mix at 7, 28, 90 days with different curing conditions.

8.2.2 Test Procedure

The apparatus used for the test is schematically shown in Figure 8.1. The sample is placed in a rubber sleeve, while kept inside a stainless steel capped cell. Two discs with a smooth face must face the sample. These have the function of distributing (lower disc) and collecting (upper disc) the oxygen from the outer part to the centre of the sample. The rubber tube is inserted in the cell such that it is deflated by the valve that exists through the hole in the side of the cell. The cover is placed on the cell and fixed using six hand screws. The oxygen supply is connected to the pressure control valve. By connecting the output of the cell situated on the upper face to the distribution block, leaving the three valves closed and inflating the rubber tube, oxygen is forced to flow vertically through the sample. A bubble flow meter records the flow rate (V) after the steady state is achieved (approximately 20 minutes after the beginning of the test).

The following equation, derived from D'Arcy's law of flow, is used to calculate the intrinsic permeability of the sample:

$$k = \frac{2P_2Vl \times 2.02 \times 10^{-16}}{A(P_1^2 - P_2^2)} \qquad (8\text{-}1)$$

Where:

k is the intrinsic permeability (m^2)

l is the length of the specimen (m)

A is the cross-sectional area of specimen (m^2)

V is the flow rate (cm^3/s).

P_1 is the absolute applied pressure (bar)

P_2 is the pressure at which the flow rate is measured, usually 1 bar.

For oxygen at a temperature of 20°C the dynamic viscosity may be taken at $2.02x10^{-5}$ $N.s.m^{-2}$ and the coefficient 2.02×10^{-16} does the transformation of the units and provides the final results in m^2.

The result of oxygen permeability values is calculated at five absolute inlet pressure stages reading for each mix and at each age by plotting a regression line for flow rate versus (P_1^2-P_2^2) to determine the average permeability. This helps to demonstrate the extent of deviation of the results from linearity and detect any outlying result due to abnormal behaviour of the apparatus. A systematic deviation from linearity with the points lying on a smooth convex curve is normal. The deviation from linearity of the curve is mainly due to the inaccuracy in the assumption that the flow of oxygen through concrete is laminar.

8.2.3 Results and Discussion

The results of oxygen permeability for the different mixes are presented in Figure 8.2. It can be clearly seen that permeability decreases with age, especially at early ages. The permeability of ARSH and ACSH Mixes decreases at a faster rate between 7 and 28 days but is slower after 28 days. ATAF2 shows higher permeability at 28 and 90 days in comparison with the ATAF1 mixes which may be related to lower water to binder ratio in the latter which produce less capillary pores. It is also observed from the results that calcining Shahindej pozzolan will reduce the permeability of the mix at 90 days. The oxygen permeability of the ATAF2 and ARSH mixes are equal to $5x10^{-17}m^2$ at 90 days while ACSH and ATAF1 mixes show permeability equal to $1.5x10^{-17}$ and $2x10^{-17}m^2$, respectively. In general, the alkali activated natural pozzolan specimens show lower permeability in comparison with the normal OPC concrete at 90 days although at 7 days the permeability is higher. This behaviour follows what was seen for the compressive strength of activated pozzolan cement concretes.

Figure 8.2 shows that oxygen permeability reduces as the water to binder ratio is reduced. This effect is greater at early ages for alkali activated Taftan pozzolan. It is also clear from the results that the difference in oxygen permeability of alkali activated Taftan mixes with water to binder ratios between 0.55 and 0.45 is higher than the comparable OPC mixes. This fact means that by increasing the water to binder ratio, there is more free water in the geopolymer concrete which makes looser microstructure with higher permeability in this type of concrete rather than OPC concrete.

The effect of curing on oxygen permeability for the alkali activated Taftan pozzolan mixes is shown in Figure 8.3. It is very clear that permeability of these mixes decreases sweeping toward 40°C sealed curing condition and curing at higher temperature decreases the permeability of alkali activated natural pozzolan geopolymer concrete. This is possibly because the water in the geopolymer structure is just a medium which promotes the geopolymerisation with further cross linking made as a result of water removal by the higher temperature. This results in pore space blockage.

8.3 Chloride permeability

Concrete is very widely used in the construction of harbours, docks, breakwaters, and other structures that are exposed to the action of seawater. The discussion on durability of concrete in seawater is a matter of much importance. Concrete in seawater may suffer due to attack of dissolved chemicals on the products of hydration, crystallization of salts within the concrete under condition of alternate wetting and drying, frost action, mechanical attrition, impact of by waves and corrosion of reinforcements embedded in it. It is well known that a high concentration of chloride salts in solution deteriorates reinforced concretes. One of the most common causes of concrete deterioration is corrosion of the embedded reinforcing steel which occurs when chloride ions penetrate concrete. This type of deterioration is prevalent not only in structures near to saline sources such as marine structures but also in road bridges exposed to cyclic de-icing salt applications. A common method of preventing such deterioration is to prevent chlorides from penetrating the structure to the level of the reinforcing steel bar by using impenetrable concrete. There is much literature suggesting the use of pozzolanic

material improves the durability of reinforced concrete against sea water by preventing the leaching of calcium hydroxide and calcium sulphate, both of which are soluble in sea water. Massazza (1985) concluded that pozzolanic or slag cements (>60% slag) are more durable due to reduced permeability than pure Portland cements, and noted that lime-pozzolana mortar used by the Romans in sea works are still in good condition.

This section discusses the usefulness of the rapid ASTM C1202-97 RCPT (Rapid Chloride Permeability Test) and long term Bulk Diffusion Test (NordTest NTBuild 443) methods for assessing the chloride permeability characteristics of geopolymer concrete based on alkali activated natural pozzolans. The disadvantages of the RCPT method are discussed generally and for this type of concrete, and the results are compared with the long term Bulk Diffusion Test method. The influence of type, age, water to binder ratio, curing conditions and temperatures were studied.

8.3.1 Samples Preparation

Specimens were cast for all the concrete mixes with different water to binder ratios in the form of 15cm cubes using metal moulds. The cast specimens after de-moulding, were cured according to section 6.4 for different curing conditions and temperatures for 7, 28 and 90 days. These cubes were then cut into 10cm diameter by 15cm thick cores. From these cores, 2.5cm thickness was removed from each side and then the remaining section was cut into two equal parts which provide two 5cm thick by 10cm diameter specimens for each mix proportion and curing condition.

In order to assure full saturation of the samples before testing their ability to resist chloride ion penetration in accordance to the ASTM C1202-97 (RCPT) test, the samples were dried to a constant weight in an oven kept at 50°C±5°C before being vacuum saturated with de-ionised water and in the apparatus shown in Figure 8.4.

8.3.2 Test Procedure

Capillary absorption, hydrostatic pressure, and diffusion are the means by which chloride ions can penetrate concrete. The most familiar method is diffusion, the movement of chloride ions under a concentration gradient. For this to occur, the concrete must have a continuous liquid phase within the pores and there must be a

chloride ion concentration gradient. There are various methods for assessing chloride penetration of concrete depending on mechanisms of chloride ion transportation. In the ASTM C1202 (AASHTO T277) in the test referred to as RCPT, a water-saturated, 5cm thick, 10cm diameter concrete specimen is subjected to 60V applied DC voltage for 6 hours using the apparatus shown in Figure 8.4. In one reservoir is a 3.0% NaCl solution and in the other reservoir is a 0.3M NaOH solution. The total charge passed is determined and this is used to rate the concrete according to the following criteria:

Chloride Ion Penetrability	Charge Passed (coulombs)	Total integral chloride to 41mm depth after 90-days ponding test
High	>4000	>1.3
Moderate	2000-4000	0.8-1.3
Low	1000-2000	0.55-0.8
Very Low	100-1000	0.35-0.55
Negligible	<100	<0.35

The specimens were subjected to 20V applied DC voltage for 6 hours in this investigation because of the alkaline activators which give rise to existing conductive pore solutions in this type of concrete. Here, the pore solution chemistry of geopolymer concrete in turn can have a very significant effect on the conductivity of pore solution or the RCPT results for concrete and will bias the results upwards, causing when the specimens are subjected to a higher applied DC voltage. It should be mentioned that for voltage more than this amount, the current exceeded 500mA and the test was terminated quickly in order not to damage the system due to heating which would lead to a further increase in the charge passed. Thus the test is non-standard in terms of ASTM C1202.

In the bulk diffusion test (NordTest NTBuild 443) which has been developed to overcome some of the deficiencies of the salt ponding test (AASHTO T259) to measure diffusion, the test specimen is saturated to prevent any initial sorption effects when the chloride solution is introduced and the sides and bottom face of the prepared samples are sealed. The only face left uncovered is the one exposed to a 2.8M NaCl solution. The samples are left this way for 90 days before evaluation. At the end of this time the samples are removed and to evaluate the sample, the profile of the concrete is determined by mounting the sample in a lathe with a diamond tipped bit. The sample is level so that the axis of advance of the bit is perpendicular

to the surface of the sample. A pass is made at each depth to grind the concrete sample to dust, which is then collected. This is repeated at greater and greater depths, at depth increments on the order of 5mm. The chloride content of the powder is then determined according to AASHTO T260. The error function solution of Fick's Second Law is then fitted to the curve and a diffusion value and surface chloride concentration is determined. Therefore the experimental data are fitted to the equation (8-2) which is the linearized form of the solution to Fick's second law:

$$Lnc= \ln(m/\sqrt{\pi}Dt)-x^2/(4Dt) \qquad (8\text{-}2)$$

Where c=concentration of chloride per mass of sample at distance x and time t (%), m= total amount of diffusing chloride, D= diffusion coefficient (m^2/s)

Linear regression of lnc versus x^2 yields slope $-1/(4Dt)$ and intercept $\ln(m/\sqrt{\pi}Dt)$ from which the diffusion coefficient(D) and the total amount of diffusing chloride(m) can be obtained.

8.3.3 Results and Discussions

There are a number of criticisms of the RCPT technique, although this test has been adopted as a standard. The main criticisms are:

- The high voltage applied leads to an increase in temperature, especially for low quality concretes, which further increases the charge passed.
- The measurements are made before steady-state migration is achieved.
- The current passed is related to all ions in the pore solution not just chloride ions.

With respect to above points for low quality concretes, which further increases the charge passed (Malek and Roy, 1996), and as the temperature rise is related to the product of the current and the voltage, they heat more. The lower the quality of concrete, the greater the current at a given voltage and thus the greater heat energy produced. This heating leads to a further increase in the charge passed, more than what would be experienced if the temperature remained constant. Thus, poor quality concrete looks even worse than it would be otherwise.

Another difficulty with the RCPT test is that it depends on the conductivity of the concrete being in some way related to the chloride ion penetrability. Actually, the rapid chloride ion permeability test is essentially a measurement of electrical

conductivity, which depends on both the pore structure and chemistry of pore solution (Shi, 2004). For a given specimen size and applied voltage, the recorded initial current can be regarded as a representative of electrical conductivity of the specimen. For different concrete mixtures, electrical conductivity can be significantly affected by the change in pore solution composition (Shi et al., 2006). Thus, any conducting material such as a conductive pore solution present in the concrete sample will bias the results, causing them to be too high. These conductors all influence the results so that a higher coulomb value than would otherwise be recorded is determined. The method still could serve as a quality control test and can qualify a mix, but not necessarily disqualify it (Ozyildirim, 1994). If an acceptably low rating is achieved, it is known that the concrete is not worse than that, at least within the precision of the least method.

With due attention to above mentioned issues, voltages low enough to avoid heating the samples while high enough to ensure sufficiently short test duration equal to 6 hours was considered. Thus different voltages were checked and finally the voltage applied was 20V DC, which allowed control of the current and temperature rise to a value acceptable and similar to the values reached by OPC concrete specimens when subjected to 60V DC for 6 hours.

The results of the rapid chloride permeability test (RCPT) for different mixes at various ages are illustrated in Figure 8.5. These results show that in the activated natural pozzolan geopolymer mixes a higher charge is passed than OPC mixes at all ages. It should be mentioned that OPC concrete specimens were subjected to 60V DC as in the standard ASTM C1202. The measurements for all samples were made when the steady-state migration was achieved after 6 hours, thus the comparison of the results could be independent of the voltage applied. This clearly demonstrates that the incorporation of alkali solution for activation natural pozzolans leads to an increase in RCPT values. The ATAF1, ATAF2 mixes show the lowest RCPT value equal to 2704 and 2750 coulombs for 6 hours at 90 days while ARSH and ACSH mixes show the highest values equal to 3027 and 3007 coulombs, respectively.

Chloride permeability reduces with age with a higher rate of reduction at early age. At later ages the effect of chemical progress on the permeability seems to cause a

change in the porosity of the geopolymer concrete microstructure and this leads to the reduction of chloride permeability results.

For all the ages investigated, ATAF2 mixes show higher chloride permeability than ATAF1 mixes. Thus, the same as in OPC concrete mixes, chloride permeability increases as the water to binder ratio increases.

The effect of curing on the alkali activated Taftan pozzolan mixes with different water to binder ratio (ATAF1 and ATAF2) is demonstrated in Figure 8.6. For both mixes, the specimens cured at 40°C sealed conditions show the lowest chloride permeability. This may be due to the temperature being optimum for activation of natural pozzolan.

The results of long-term chloride absorption including the experimental Cl^- concentration profiles determined at 90 days are shown in Figure 8.7 and have been adjusted to a particular solution of Fick's second law of diffusion chloride to obtain the corresponding diffusion coefficients and the total amount of diffusing chloride. The diffusion coefficient and total integral chloride contents after 90 days ponding are presented in Table 8.3. Comparing the total integral chloride penetration to 41mm depth after 90-days ponding test to AASHTO standard shows moderate chloride ion penetrability. While relatively high chloride diffusion coefficient for geopolymeric concrete mixes compared to OPC concrete was achieved. The amount of Cl^- present in each concrete specimen depends on the nature of concrete: the less porous concrete (ATAF1 cured at 40°C sealed) absorbs less Cl^- with equality of other test conditions (Table 8.3). The percentage of chloride penetration was lower in concrete mixes with lower water to binder ratio showing that this ratio affects the chloride penetration. This reduction is due to the formation of tighter pore structure which is one of the main parameters that affect chloride penetration.

8.4 Sulphate Resistance

Sulphate attack is known to produce significant degradation in concrete structures and refers to the deterioration of concrete resulting from chemical reactions occurring when concrete is exposed to a solution containing a sufficiently high concentration of dissolved sulphates. This is particularly prevalent in arid regions where naturally occurring sulphate minerals are present in water and ground water. It

was established that deterioration of concrete due to sulphate attack is generally attributed to reaction of Portland cement hydration products with sulphate ions to form expansive reaction products after hardening, which produces internal stress and a subsequent disruption of the concrete. The reaction between these substances, particularly aluminates, in the presence of sulphate and water produce ettringite and gypsum and causes expansion of OPC concrete. The expansion leading to deterioration usually starts at edges and corners and is followed by progressive cracking with an irregular pattern. The lower the permeability of concrete, the higher the resistance of concrete to sulphate attack. Thus, the factors reducing the permeability of concrete have a beneficial effect on reducing the vulnerability of concrete to sulphate attack.

Hakkinen (1986, 1987) evaluated the sulphate resistance of both alkali activated slag cement and Portland cement. The Portland cement samples were destroyed in 10% Na_2SO_4 solution after two years and in 10% $MgSO_4$ solution after one year, while the alkali activated slag cement samples survived well.

It seems that the majority of pozzolans improve the sulphate resistance of geopolymer mixes based on alkali activated natural pozzolans in comparison with ordinary Portland cement concrete. The simplest explanation for this is the lack of the C_3A content, as would be the case were OPC present in the mix. In this type of concrete the aluminates, that are also prone to attack in OPC concrete by monosulfate, are held in stable alumina silicate hydrates which are more resistant to sulphate solutions. Secondly, in comparison with OPC there is much less calcium present in natural pozzolan and Slag to provide gypsum precipitation. In addition to the properties of natural pozzolans, the properties of activators and the curing regime can affect the sulphate attack resistance of the alkali activated concrete mixture. The use of non-silicate alkaline activators increased the sulphate corrosion resistance of the alkali-activated slag cement in the $MgSO_4$ solution (Shi et al., 2006). While steam curing of the specimens made with water-glass with a modulus from 1 to 3 decreased the sulphate corrosion resistance compared to the specimens cured under normal conditions (Shi et al., 2006).

The resistance to sulphate attack of geopolymer concrete formed by alkali activation of natural pozzolan is assessed and discussed in the next section.

8.4.1 Sample Preparation and Test Method for Sulphate Resistance

During this study, experiments were carried out on mixes made from 3 different pozzolans including Taftan, as well as both untreated and calcined Shahindej pozzolans. A comparison is made between specimens which were immersed in a sulphate solution and those were cured in their previous curing conditions in sealed or fog form. The specimens were cast in the form of 100mm cubes as described in section 6.2.6 for measuring the change of compressive strength and in the form of 25x25x285mm mortar prisms in order to measure the expansion. After de-moulding the samples were cured according to section 6.4 using different curing conditions and temperatures. Then the specimens were immersed in a solution consisting of 2.5% Na_2SO_4 and 2.5% $MgSO_4$ by weight of water for 7 days. The containers were left in a room controlled at 20°C for 6 months. The solutions in containers were replaced every two weeks for the first 3 months and then at 4 months interior.

8.4.2 Test Procedure

The methods for testing sulphate attack, are classified into three groups: the changes in the strength of the specimens, the changes in the length of the specimens, and chemical analysis. The second measurement was done according to ASTM C1012-95a standard and the chemical elements were detected from X-Ray Diffraction (XRD) recorded.

8.4.2.1 Compressive Strength

In order to assess the variation in compressive strength between specimens subjected to sulphate attack and those cured normally in sealed or fog conditions, 100mm concrete cubes with curing conditions according to sections 6.4 were cast. The compressive strength of both samples in and out of the sulphate solution were measured periodically over 6 months to find the difference in the strength of cubes put in the sulphate solution and those left to cure in previous curing conditions according to sections 6.4. For any one mix and age, two cubes were tested.

8.4.2.2 Expansion Test

In this test the rates of expansion of 25x25x285mm mortar prisms were measured. The test procedure is similar to that described in section 7.6.1. For each mix two specimens were immersed in the solution.

8.4.2.3 X-ray Diffraction Test

X-ray diffraction was used to identify the crystalline products present in mortars after immersing samples in sulphate solution up to 90 days. A thin layer was carefully removed away from the sample surface by grinding and its x-ray diffraction result compared to the result achieved for the powder prepared from the middle of the sample. This resulted in finding the difference in phases between the centre and edge of the sample after immersion in sulphate.

8.4.3 Results and Discussions

Results of the tests carried out to show the effects of added chemicals on the compressive strength of this type of concrete when it is present inside the sulphate solution which are presented in Figure 8.8. It seems that migration of alkalis from geopolymer mixes into sulphate solution and the interaction between sulphate solution and this type of concrete makes the completion of chemical reaction slower in the specimens cured at higher temperature and sealed conditions. In addition to migration of alkalis from geopolymers into the solution, the XRD results show there was also diffusion of magnesium in the surface layer of geopolymers, which improved their strength according to Bakharev (2005). The strength of all sulphate cured concrete are less than the samples cured outside of the solution initially with except in Taftan samples cure at 20°C sealed condition. The trend of compressive strength development is to increase, except in ATAF2 cured at 40°C fog condition and ARSH concrete mixes. The results can be confirmed by the previous investigations carried out on alkali activated cements (Shi et al., 2006).

The results of expansion tests are shown in Figure 8.9, as expansion versus time. The highest absolute expansion is recorded for ARSH mortar prism which was the most affected by sulphate solution and the lowest amount is recorded for ATAF cured at 40°C and sealed condition. The latter was only slightly expanded when exposed to

sulphate solution for up to 6 months. The percentages of expansion of samples that have been immersed in sulphate solution versus their strength reductions are presented in Figure 8.10. The results show that these two parameters are highly correlated exponentially. It can be observed that the maximum percentage of expansion which occurred for ARSH mixes was 0.086 percent which is less than 0.1% which British Standard suggests for OPC concretes.

For comparison of crystalline compounds, samples from surfaces and middles of cubes were analysed. The chemical composition of the reaction products are shown in Figures A8.1 (a) to A8.1 (i) and are summarized in Table 8.4. It can be seen that the peaks for the crystals of reaction products in the surface of alkali activated natural pozzolan mortar specimens, reduce to a lower level for the same compounds detected for samples prepared from the middle of cubes, after 3 month in sulphate solution. It is seen that the main crystalline compounds present in the surface and middle part of specimens consist of albite ($NaAlSi_3O_8$) and quartz (SiO_2) with the crystalline phases of hornblende for activated Taftan samples and clinoptilolite for activated Shahindej samples. While the crystalline products conformed due to the ponding of the samples in sulphates solutions in the surface of specimens with higher intensities than what is found in the middle of specimens, consisted mostly of sodium aluminium sulphate [$Na_3Al(SO_4)_3$] and/or langbeinite [$K_2Mg_2(So_4)_3$] which may cause expansion in this type of concrete. Comparison of the X-ray traces of samples taken from the surface and middle of specimen shows that for activated calcined Shahindej samples the penetration of sulphate is inconsiderable and for activated raw Shahindej the peaks are only related to sodium aluminium sulphate. For ATAF1 mix cured at 40°C some hydrated sulphate salts such as leonite [$K_2Mg(SO_4)_2$, $4H_2O$] were detected on the surface of samples. Although the intensity of sulphate crystalline compound peaks in the middle of the specimens is lower than what was found for the surface of the specimens, the results show that in this type of concrete sulphate could penetrate in the concrete. This can be confirmed since that the trace of sulphate combination in the core of all samples except ACSH was observed. Therefore further study is needed to find out the resistance of this type of concrete to sulphate attack.

8.5 Relationship between Oxygen Permeability and Compressive Strength

It is always desirable to be able to predict the long term permeability of concrete from cube compressive strength, which is the first tool used by civil engineers to judge concrete quality. However, the developments in concrete technology indicate that the durability of concrete should be assessed separately; Lynsdale (1989) has found that permeability is not only a function of strength but also porosity and pore size distribution.

Figures A8.2 to A8.5 present the relationship between the oxygen permeability and the compressive strength for all concrete mixes. Power regression analysis was then carried out between the compressive strength and oxygen permeability for each mix with different water to binder ratio and curing conditions and temperatures. The consequent regression curves for alkali activated Taftan pozzolan and AANP mixes are shown in Figures A8.4 and 8.11. The regression equation and the correlation coefficients are given in Table A8.1. It can be seen that in all mixes the oxygen permeability is highly correlated with the compressive strength.

A general relationship between oxygen permeability and compressive strength of concretes has been found by Costa et al. (1992), which is independent of the type of cement, water to cement ratio and curing time. The relationships follow the equation:

$$Y=AX^{-B} \qquad (8\text{-}3)$$

Where:

Y is coefficient of permeability (m^2)

X is compressive strength (MPa)

A and B are constants

Using the above formula (equation 8-3) and with respect to Table A8.1, the values of A ranges from $4.4\text{x}10^{-15}$ to $5.5\text{x}10^{-13}$ and that of B from 1.0 to 2.35 for OPC mixes comparative to the values of A ranges from $5.46\text{x}10^{-15}$ to $2.61\text{x}10^{-12}$ and that of B from 1.3 to 3.35 for alkali activated natural pozzolans eliminating two scattered points. The results of oxygen permeability versus cube compressive strength for different mixes made from activated natural pozzolans were shown in Figure 8.11 and power regression analysis showed that the formulae for geopolymer concrete is as follows: $Y=3.37\text{x}10^{-14}X^{-1.98}$ $R^2=0.887$ (8-4)

It can be observed that the above coefficients are compatible to the amounts suggested by Costa et al. (1992) in the Proc. 9th Internat. Congress Chem. Cement (i.e. $A=2.576x10^{-13}$ and $B=2.62$).

The relationship between the oxygen permeability and compressive strength of alkali activated natural pozzolan concrete is compared to OPC concrete in Figure 8.11. It can be seen that for the same compressible strength, lower permeability is found in for AANP concrete.

Capillary pores are formed as consequence of excess mixing water. The water to cement ratio, therefore, affects this kind of porosity as well as the activating process. As a consequence, low permeability concrete may be indirectly achieved by placing maximum limits on the water content ratio. In this way the starting point for the durability requirements for concrete in the European pre-standard ENV 206 is to limit the maximum water to cement ratio. Therefore a general relationship can be found between oxygen permeability dependent of compressive strength and water to binder ratio to consider the effect of porosity. The correlation between air permeability and each of the above two parameter for alkali activated Taftan Pozzolan is presented as follows:

$$K=9.81x10^{-14}(f_c)^{-2.39} \quad (R^2=0.878, \text{Sig.}=0.005) \quad (8\text{-}5)$$

$$K=[5.46(W/B)-2.24]\,x10^{-16} \quad (R^2=0.819, \text{Sig.}=0.013) \quad (8\text{-}6)$$

Where K= coefficient of permeability (m^2), f_c=compressive strength (MPa) and W/B=water to binder ratio

The number of measurements is N=8 and N=6 respectively. Therefore the degree of freedom would be (N-2=6 and 4) and R should more than 0.707 and 0.811 which has occurred for the above equations. On the other hand, R^2 shows that values up to 82.0% are justified. The statistical significance level indicates that the regression assumption is correct.

After finding two simplified power and linear models, which were proposed for prediction air permeability incorporating compressive strength and water to binder ratio respectively, a non-linear model was tried with the combination of the two models input parameters using the least squares technique. It was found that Eq. (8-

7) fits well for the above model. The coefficients for Eq. (8-7) are given in Table 8.2. Therefore considering non-linear regression, the following model was found and confirmed by back substituting:

$$K= b_0+b_1 (W/B) + b_2 (f_c)^{-2.39} \qquad (8\text{-}7)$$

Where K= coefficient of permeability (m^2), f_c=compressive strength (MPa) and W/B=water to binder ratio

Fig. 8.12 shows the relationship with good agreement between the predicted and observed permeability. The correlation of the best fit, R^2, is higher than 0.95, again demonstrating the good accuracy of the statistical model.

8.6 Relationship between Chloride Permeability and Compressive Strength

The results of chloride permeability against compressive strength for the mixes investigated are plotted in Figure A8.6 to A8.9. An attempt has been made to arrive at a possible correlation between chloride permeability and compressive strength. Generally the trend is that an increase in the compressive strength is accompanied by a decrease in the chloride permeability values. The regression equation and the correlation coefficients are given in Table A8.2. It can be seen that in all mixes the chloride permeability is highly correlated with the compressive strength.

Considering exponential correlation with below formula:

$$Y=Ae^{-Bx} \qquad (8\text{-}8)$$

Where Y= charge passed (coulombs)

X=cubic compressive strength (MPa)

A and B are constants

With respect to Table A8.2, for OPC mixes the values of A range from $6.4x10^3$ to $7.1x10^3$ and that of B from 0.02 to 0.03. On the other hand for alkali activated natural pozzolans the values of A range from $9.8x10^3$ to $2.0x10^5$ and of B from 0.03 to 0.12. The results of chloride permeability versus cube compressive strength for different mixes made from activated natural pozzolans are shown in Figure 8.13. Exponential regression analysis showed that the formulae found for activated natural pozzolan geopolymer concrete seems to be as follows:

$$Y=10731e^{-0.04x} \quad R^2=0.795 \qquad (8\text{-}9)$$

Comparing charge passes through geopolymer concrete and normal concrete in Figure 8.13 shows that up to compressive strength equal to 33MPa, the charge passed through AANP concrete is more than OPC concrete but reverse happens for compressive strength more than it. The reason for this might be that increasing the compressive strength shows that most of the alkaline ion struggled in the reaction so the conductivity of the paste was reduced.

8.7 Relationship between Chloride Permeability and Oxygen Permeability

Generally the trend is that an increase in the oxygen permeability is accompanied by an increase in the chloride permeability values. The regression equation and the correlation coefficients are given in Figure 8.14. It can be seen that the chloride permeability is highly correlated with the oxygen permeability. The relationship for geopolymer concrete based on activated natural pozzolans seems to follow the equation:

$$Y=AX^B \qquad (8\text{-}10)$$

Where:

Y is charge passed (coulombs)

X is coefficient of permeability (m^2)

A and B are constants and equal to 2108.8 and 0.36 respectively.

8.8 Concluding summary

The main results drawn from the present investigation on the durability properties of the alkali activated natural pozzolan concrete are summarised as follows:

1) In general, the alkali activated natural pozzolan concrete has lower permeability in comparison with the normal OPC concrete at 90 days, although permeability is higher at 7 days. The same pattern of behaviour occurs for compressive strength.

2) Oxygen permeability reduces in alkali activated natural pozzolan concretes as the water to binder ratio reduces. This effect is greater in the geopolymer concrete than in OPC mixes, since there is more free water which makes looser microstructure with higher permeability in this type of concrete, compared with OPC concrete.

3) Curing at higher temperature decreases the permeability of alkali activated natural pozzolan geopolymer concrete. This is possibly because the water in the geopolymer structure is just a medium which promotes the geopolymerisation with further cross linking made as a result of water removal at higher temperature. This results in pore space blockage, stronger structure with more binding and lower shrinkage (as found earlier in Chapter 7 for mixes at elevated temperature).

4) The rapid chloride permeability test gives misleadingly high results for alkali activated geopolymer concrete. This is probably due to the very high alkali ion concentration in the pore solution promoting higher electrical conductivity though the geopolymer concrete. This effect seems to reduce with age due to a change in the porosity of the geopolymer concrete microstructure.

5) The voltage which allowed control of the current and temperature rise to a value acceptable and similar to the values reached by OPC concrete specimens when subjected to 60V DC, was 20V DC in geopolymer concrete.

6) As for OPC concrete mixes, chloride permeability of geopolymer concrete investigated increases as the water to binder ratio increases.

7) The long-term chloride ponding results indicate that chloride ion penetrability of geopolymer concrete is moderate to high. Chloride penetration was lower in concrete mixes with lower water to binder ratio. This reduction may be due to the formation of tighter pore structure which is one of the main parameters that affect chloride penetration.

8) Based on 6 months results, this investigation suggests that alkali activated geopolymer concrete is much more resistant to sulfate attack than OPC concrete. However, longer periods of exposure to aggressive solutions is needed to confirm the superior sulfate resistance of AANP concrete.

Table 8.1 The measured parameters used as input for finding nonlinear model to predict permeability of alkali activated Taftan pozzolan

Curing temperature	W/B	f_c(MPa)	K(m^2)
20S	0.45	19.22	1.1E-16
20S	0.55	11.21	2.58E-16
40S	0.45	39.7	1E-17
40S	0.55	21.36	9.18E-17
40E	0.45	28.72	1.45E-17
40E	0.55	25.64	7.5E-17
60S	0.45	34.38	4E-17
60S	0.55	27.25	6.14E-17

Table 8.2 Nonlinear regression coefficients and correlation coefficient (R^2) for predicting permeability of alkali activated Taftan pozzolan

Coefficients	Nonlinear model
b_0	$-8.58x10^{-17}$
b_1	$2.24x10^{-16}$
b_2	$7.34x10^{-14}$
Correlation coefficient (R^2)	0.952

Table 8.3 Chloride diffusion coefficient and total integral chloride% to 45mm depth after 90 days ponding

Mix	Curing Conditions	Ponding diffusion coefficient D(m^2/s;$x10^{-11}$)	Total integral chloride %	Chloride Ion Penetrability
ATAF1	20Sealed	10.5	1.0	Moderate
ATAF1	40Fog	10.8	1.1	Moderate
ATAF1	40Sealed	13.4	0.8	Moderate
ATAF1	60Sealed	16.7	1.1	Moderate
ATAF2	20Sealed	17.3	1.13	Moderate
ATAF2	40Fog	10.8	1.11	Moderate
ATAF2	40Sealed	8.6	1.03	Moderate
ATAF2	60Sealed	5.9	0.63	Low
ARSH	60Sealed	5.0	0.7	Low
ACSH	20Sealed	7.5	1.0	Moderate

Table 8.4 Summary of X-ray diffraction results show the existence of sulphate phases and achieved from the powder prepared from the surface and the middle of the samples immersed in sulphate solution

Mix	Water to Binder Ratio (W/B)	Curing Condition and Temperature	Position of Sampling	Sulphate Phases	Mineral Name of Sulphate Phases
ATAF1	0.45	Sealed curing at 20°C	Surface	$Na_3Al(SO_4)_3$ $K_2Mg_2(SO_4)_3$	Sodium Aluminium Sulphate Langbeinite
ATAF1	0.45	Sealed curing at 20°C	Middle	$Na_3Al(SO_4)_3$ $K_2Mg_2(SO_4)_3$	Sodium Aluminium Sulphate Langbeinite
ATAF1	0.45	Fog curing at 40°C	Surface	$Na_3Al(SO_4)_3$ $K_2Mg_2(SO_4)_3$ $(MgAl)_5(SiAl)_8O_{20}(OH)_2,8H_2O$ $K_2Mg(SO_4)_2,4H_2O$	Sodium Aluminium Sulphate Langbeinite Palyigorskite Leonite
ATAF1	0.45	Fog curing at 40°C	Middle	$Na_3Al(SO_4)_3$ $K_2Mg_2(SO_4)_3$	Sodium Aluminium Sulphate Langbeinite
ATAF2	0.55	Fog curing at 40°C	Surface	$Na_3Al(SO_4)_3$ $K_2Mg_2(SO_4)_3$ $K_2Mg(SO_4)_2,6H_2O$	Sodium Aluminium Sulphate Langbeinite Picromerite
ATAF2	0.55	Fog curing at 40°C	Middle	$Na_3Al(SO_4)$ $K_2Mg_2(SO_4)_3$ $K_2Mg(SO_4)_2,6H_2O$	Sodium Aluminium Sulphate Langbeinite Picromerite

Table 8.4 Summary of X-ray diffraction results show the existence of sulphate phases and achieved from the powder prepared from the surface and the middle of the samples immersed in sulphate solution (continue)

Mix	Water to Binder Ratio (W/B)	Curing Condition and Temperature	Position of Sampling	Sulphate Phases	Mineral Name of Sulphate Phases
ATAF1	0.45	Sealed curing at 40°C	Surface	$Na_3Al(SO_4)_3$ $K_2Mg_2(SO_4)_3$ $(MgAl)_5(SiAl)_8O_{20}(OH)_2,8H_2O$ $K_2Mg(SO_4)_2,4H_2O$	Sodium Aluminium Sulphate Langbeinite Palyigorskite Leonite
ATAF1	0.45	Sealed curing at 40°C	Middle	$Na_3Al(SO_4)_3$ $K_2Mg_2(SO_4)_3$	Sodium Aluminium Sulphate Langbeinite
ATAF2	0.55	Sealed curing at 40°C	Surface	$Na_3Al(SO_4)_3$ $K_2Mg_2(SO_4)_3$	Sodium Aluminium Sulphate Langbeinite
ATAF2	0.55	Sealed curing at 40°C	Middle	$Na_3Al(SO_4)_3$ $K_2Mg_2(SO_4)_3$	Sodium Aluminium Sulphate Langbeinite
ATAF1	0.45	Sealed curing at 60°C	Surface	$Na_3Al(SO_4)_3$ $K_2Mg_2(SO_4)_3$	Sodium Aluminium Sulphate Langbeinite
ATAF1	0.45	Sealed curing at 60°C	Middle	$Na_3Al(SO_4)_3$ $K_2Mg_2(SO_4)_3$	Sodium Aluminium Sulphate Langbeinite
ATAF2	0.55	Sealed curing at 60°C	Surface	$Na_3Al(SO_4)_3$ $K_2Mg_2(SO_4)_3$	Sodium Aluminium Sulphate Langbeinite
ATAF2	0.55	Sealed curing at 60°C	Middle	$Na_3Al(SO_4)_3$ $K_2Mg_2(SO_4)_3$	Sodium Aluminium Sulphate Langbeinite
ACSH	0.42	Sealed curing at 20°C	Surface	$Na_3Al(SO_4)_3$ $K_2Mg_2(SO_4)_3$	Sodium Aluminium Sulphate Langbeinite
ACSH	0.42	Sealed curing at 20°C	Middle	$Na_3Al(SO_4)_3$	Sodium Aluminium Sulphate
ARSH	0.42	Sealed curing at 60°C	Surface	$Na_3Al(SO_4)_3$ $K_2Mg_2(SO_4)_3$	Sodium Aluminium Sulphate Langbeinite
ARSH	0.42	Sealed curing at 60°C	Middle	$Na_3Al(SO_4)_3$	Sodium Aluminium Sulphate

Figure 8.1 Oxygen permeability apparatus

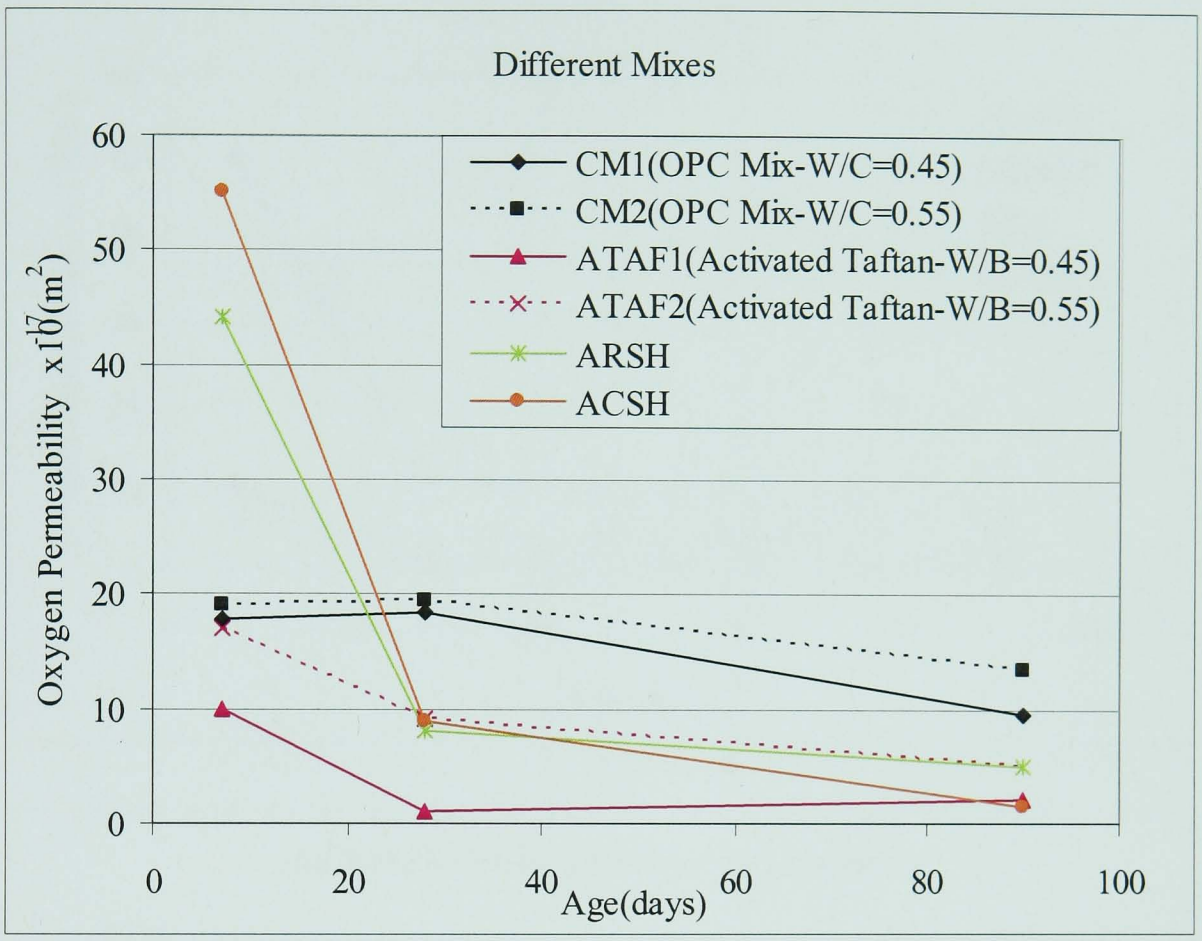

Figure 8.2 Oxygen permeability development for different mixes under sealed curing conditions (CM1, CM2, and ACSH were cured at 20°C, ATAF1 and ATAF2 were cured at 40°C and ARSH was cured at 60°C which were the best curing temperature in each case)

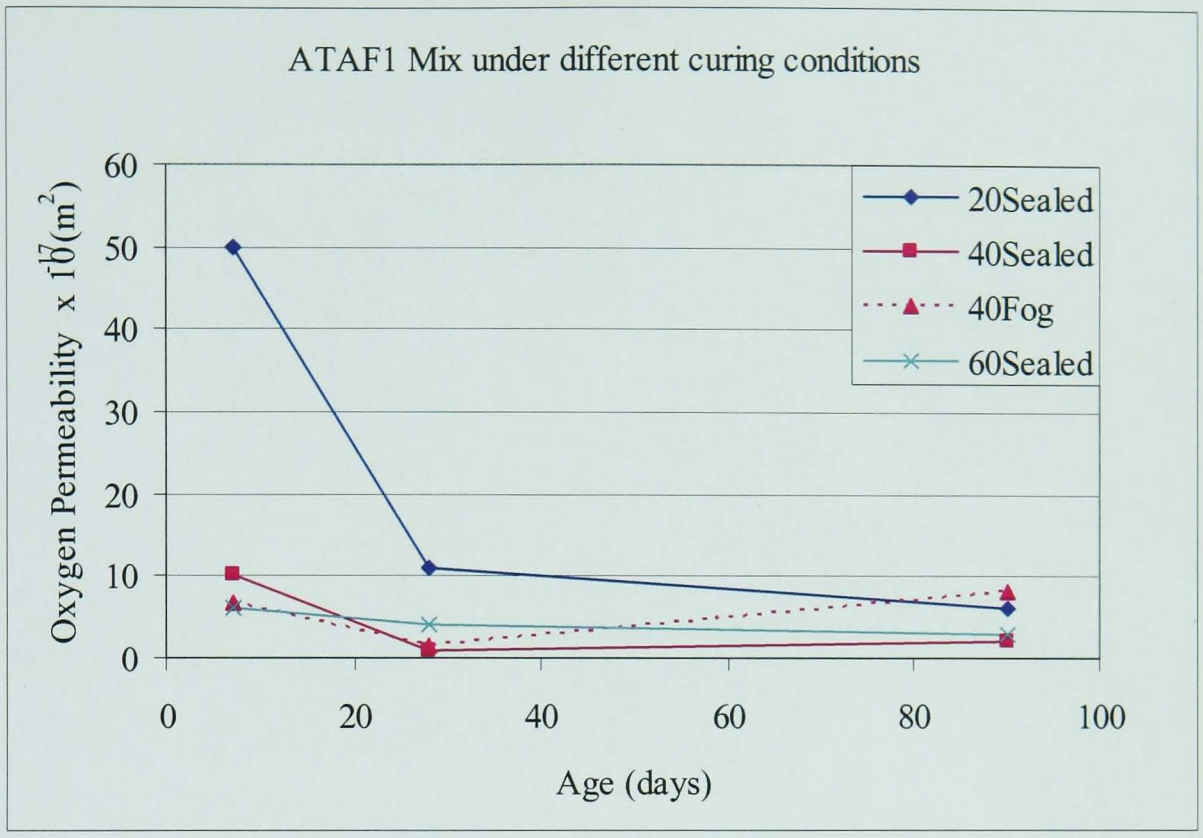

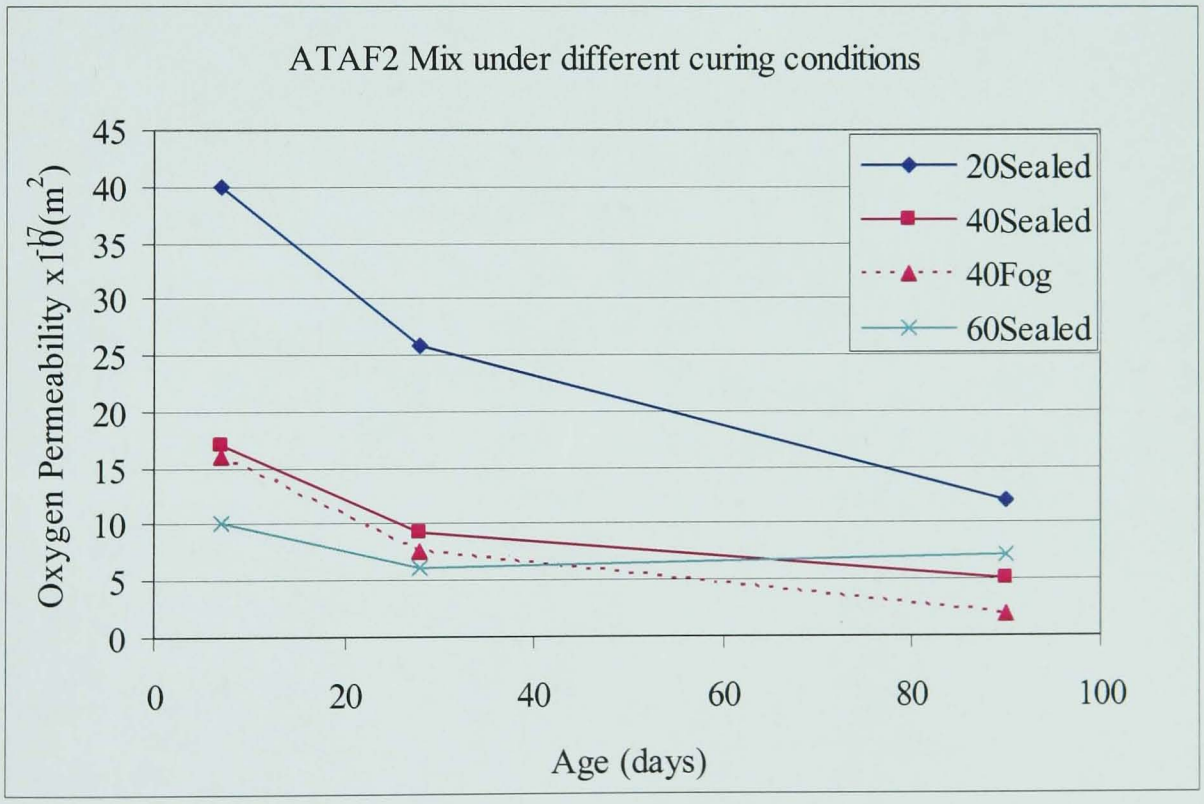

Figure 8.3 Effect of curing conditions on oxygen permeability of alkali activated Taftan pozzolan

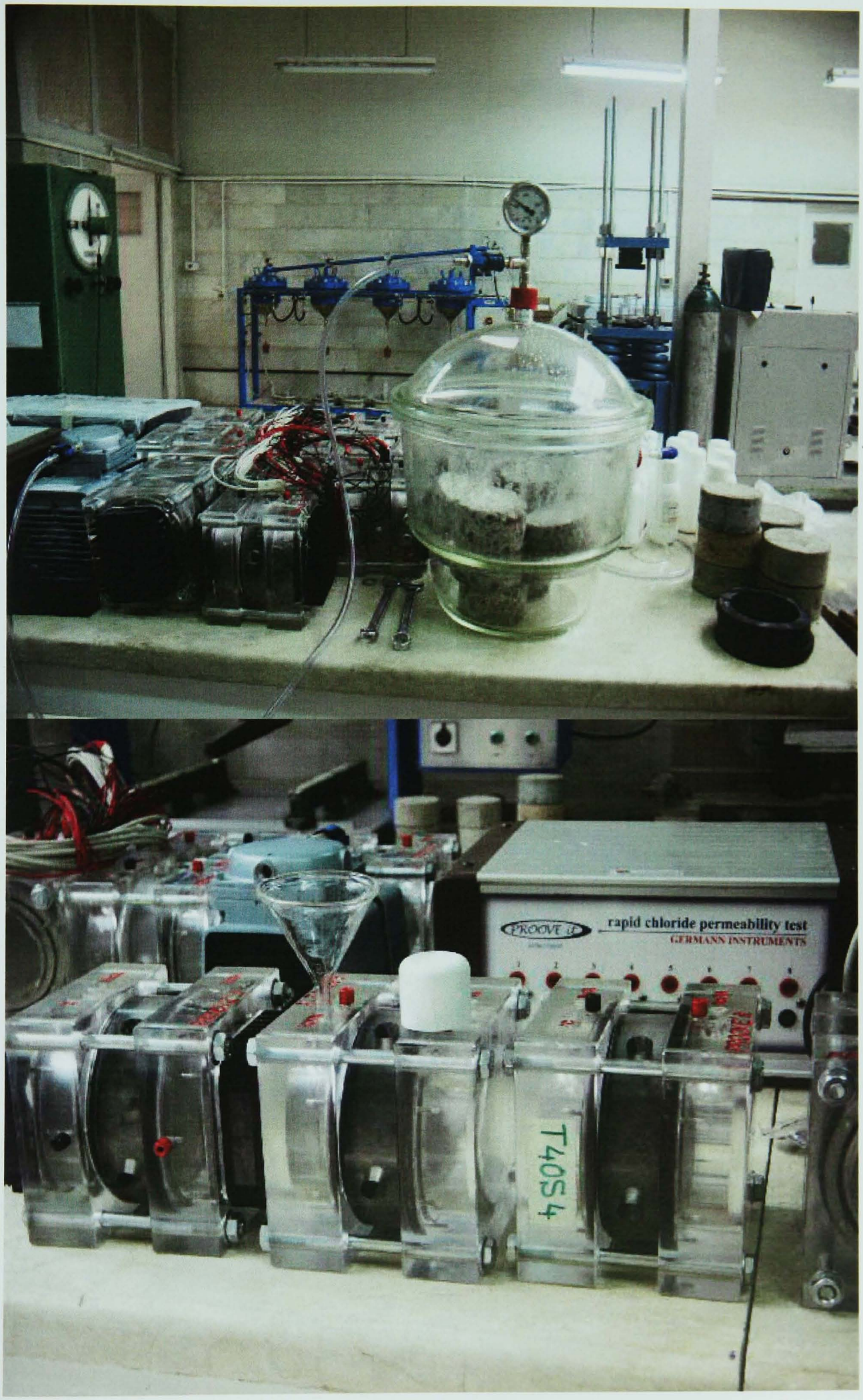

Figure 8.4 Top: Vacuum saturation and Bottom: Rapid chloride permeability test apparatus

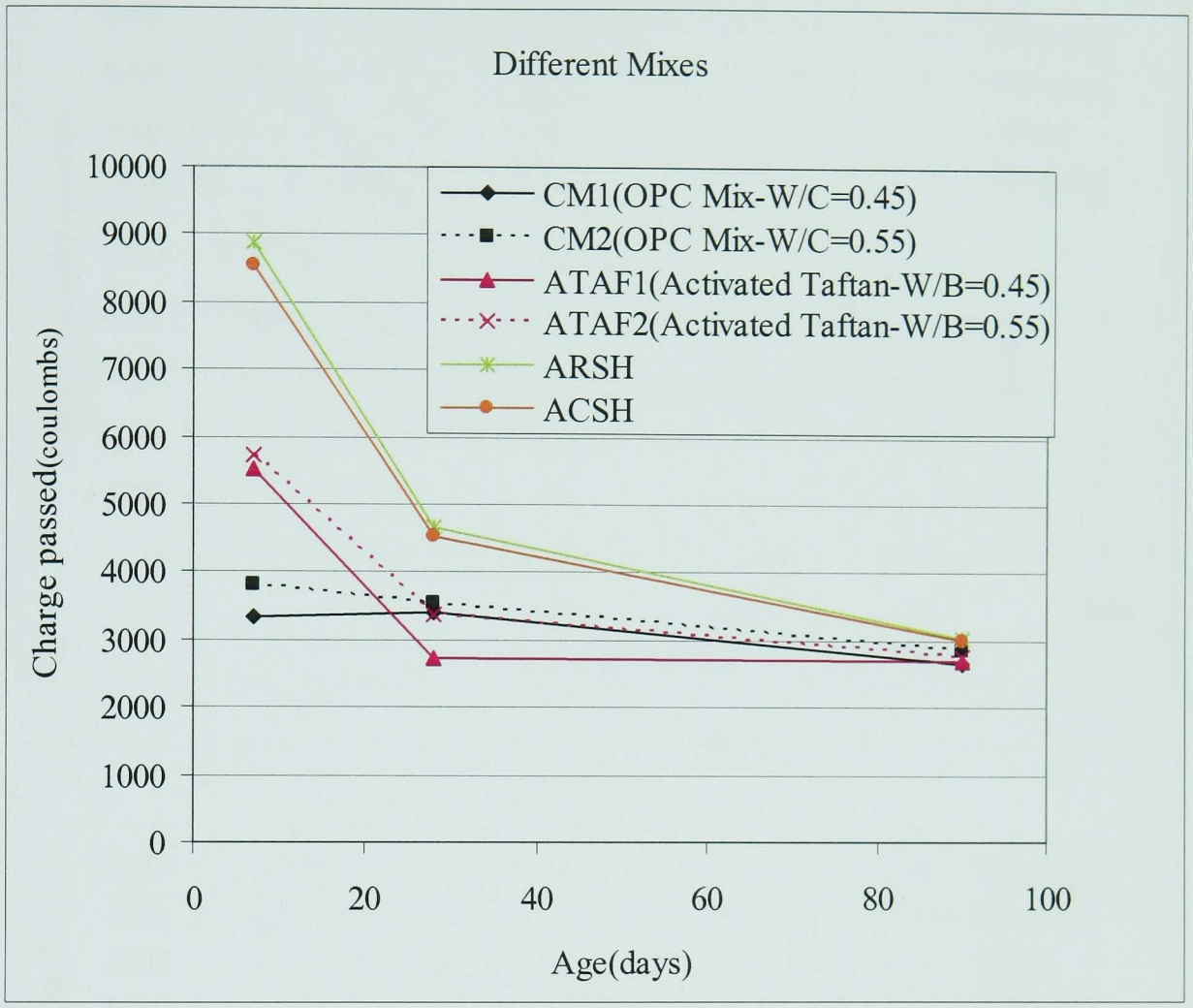

Figure 8.5 Chloride permeability of various mixes at different ages under sealed curing conditions (CM1, CM2, and ACSH were cured at 20°C, ATAF1 and ATAF2 were cured at 40°C and ARSH was cured at 60°C which were the best curing temperature in each case)

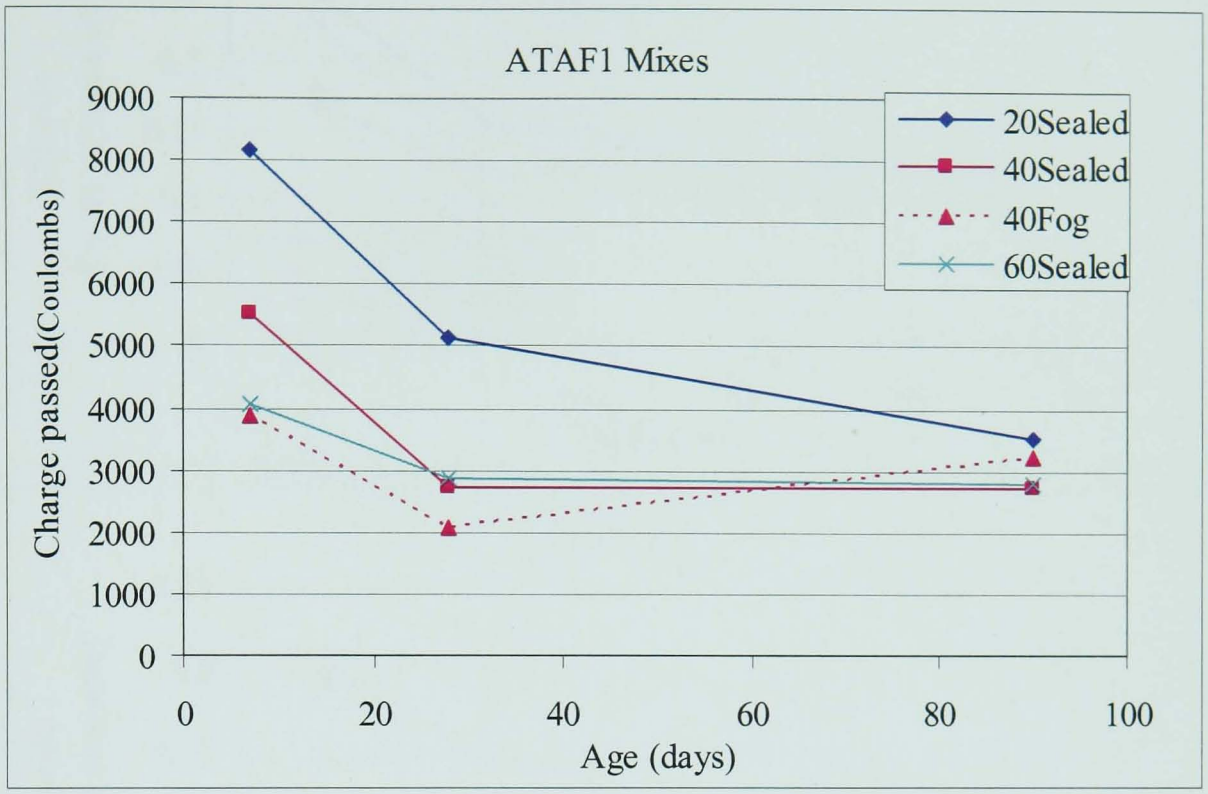

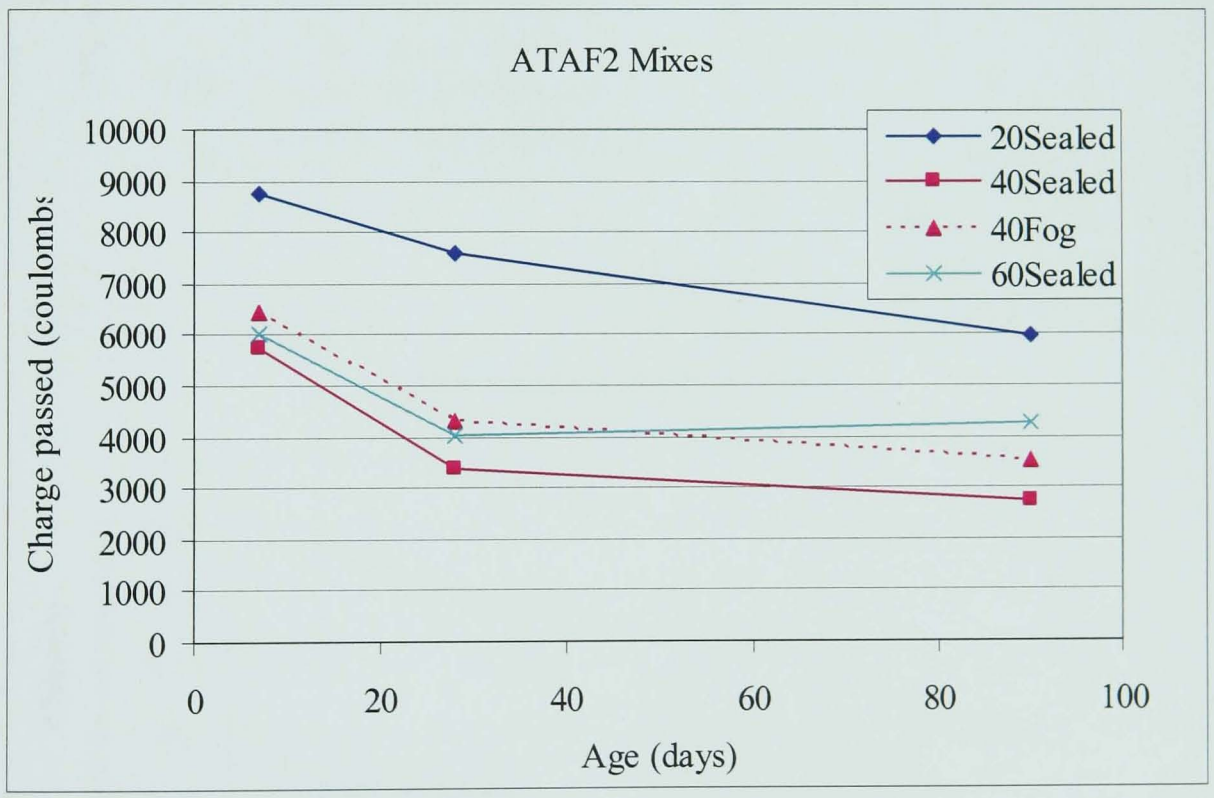

Figure 8.6 Effect of curing conditions on chloride permeability for ATAF1 and ATAF2 Mixes

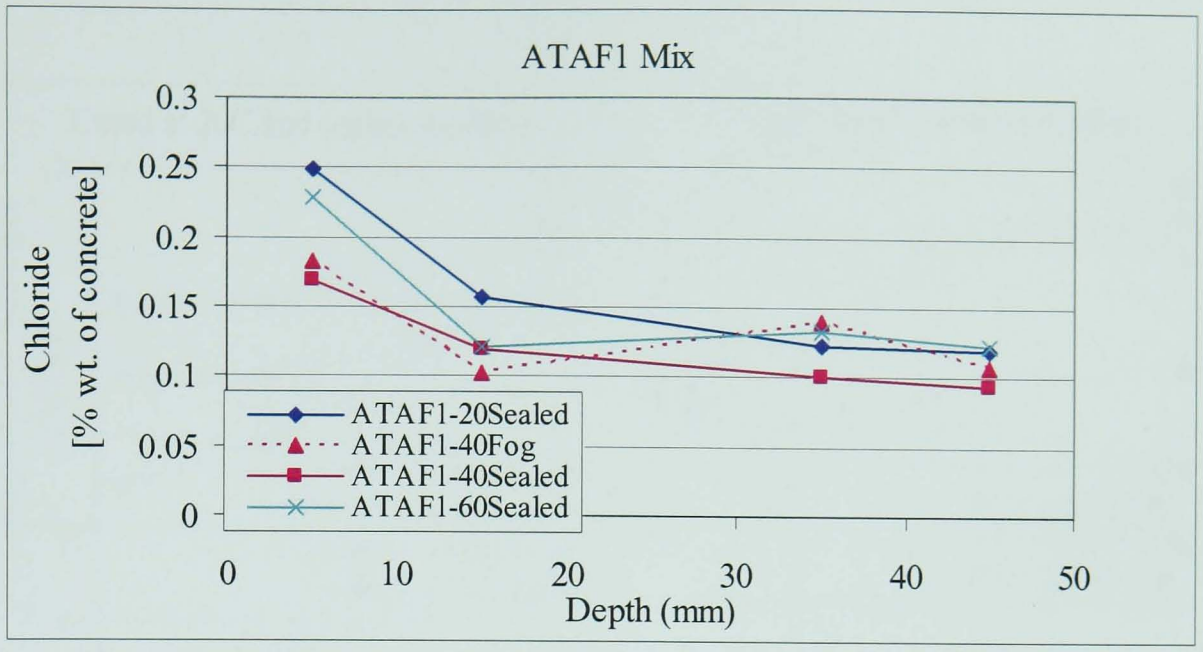

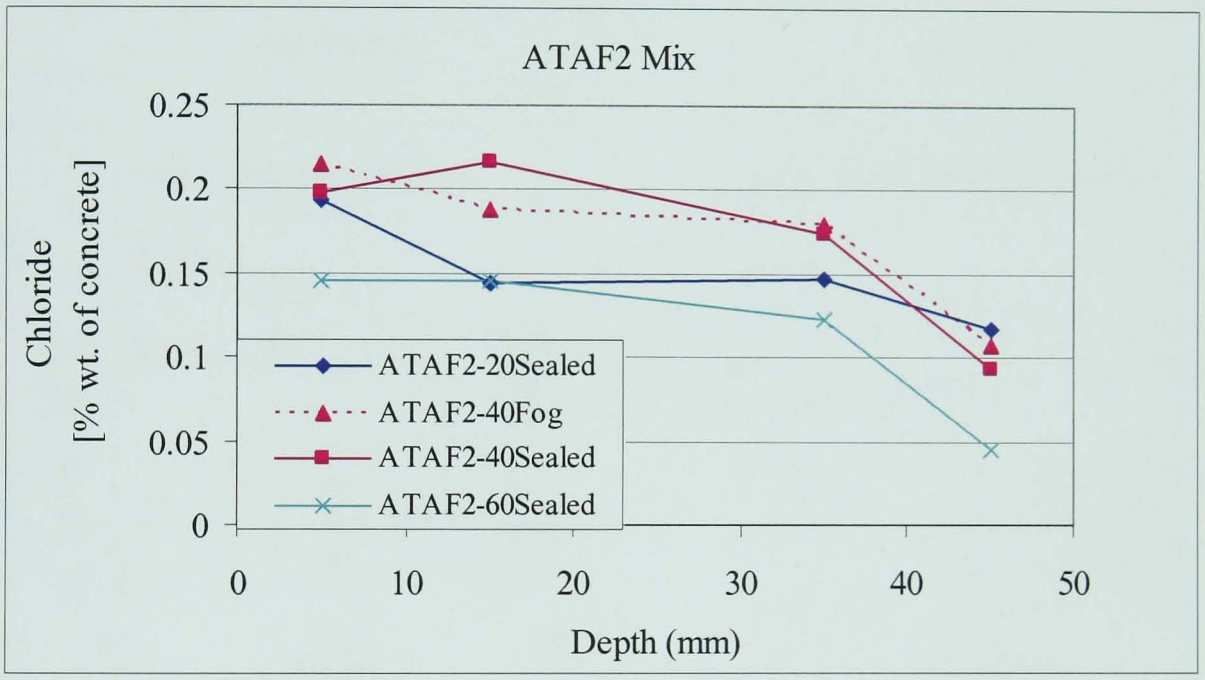

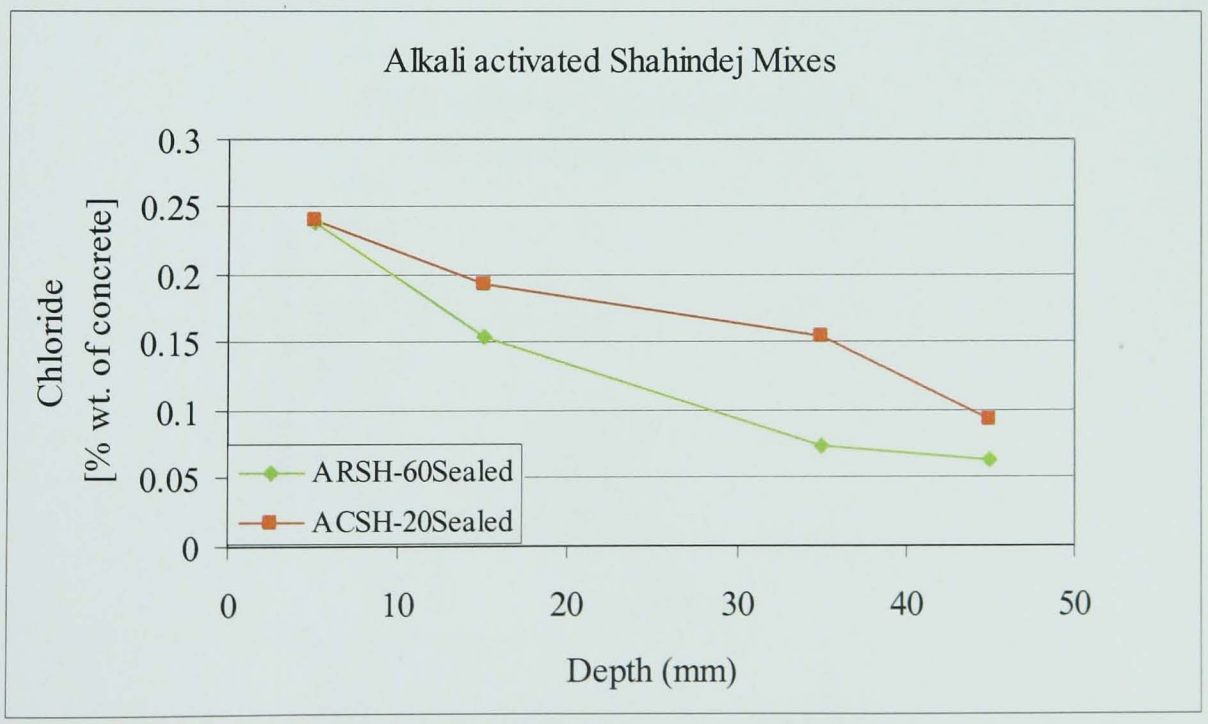

Figure 8.7 Chloride [% wt. of concrete] versus depth of samples for different material and curing conditions

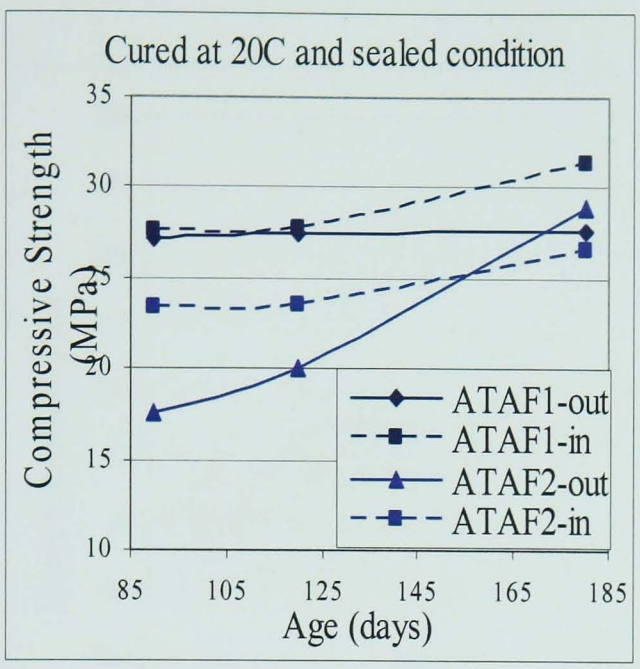

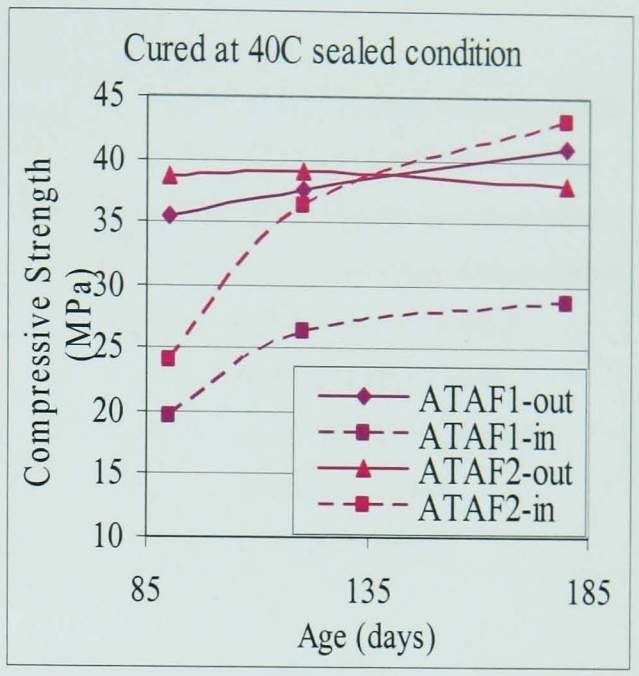

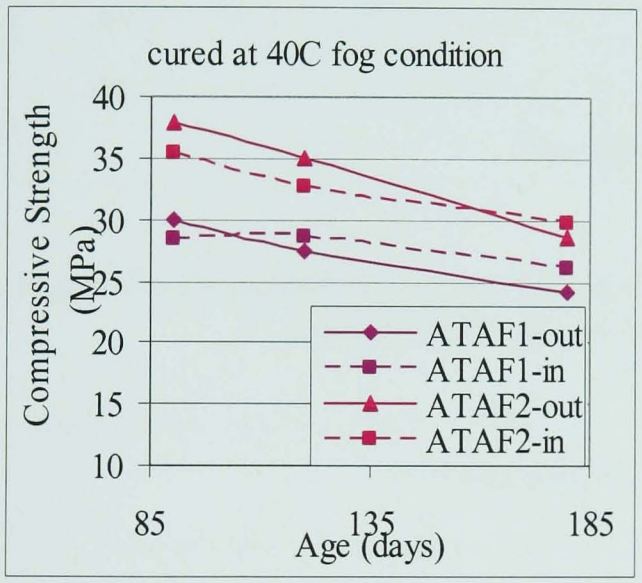

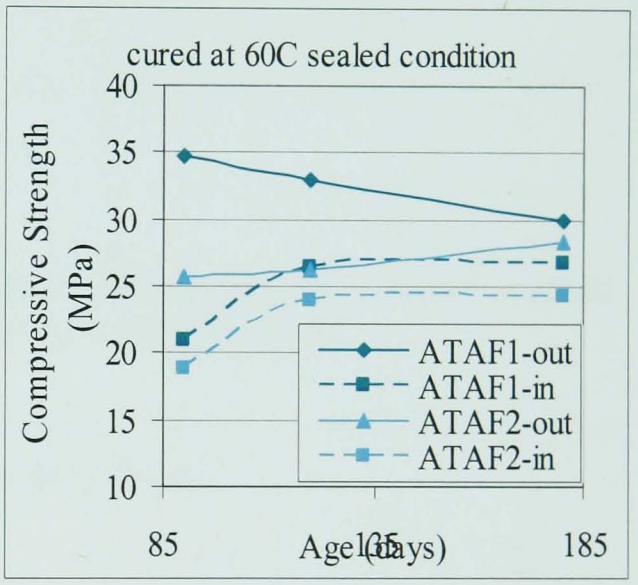

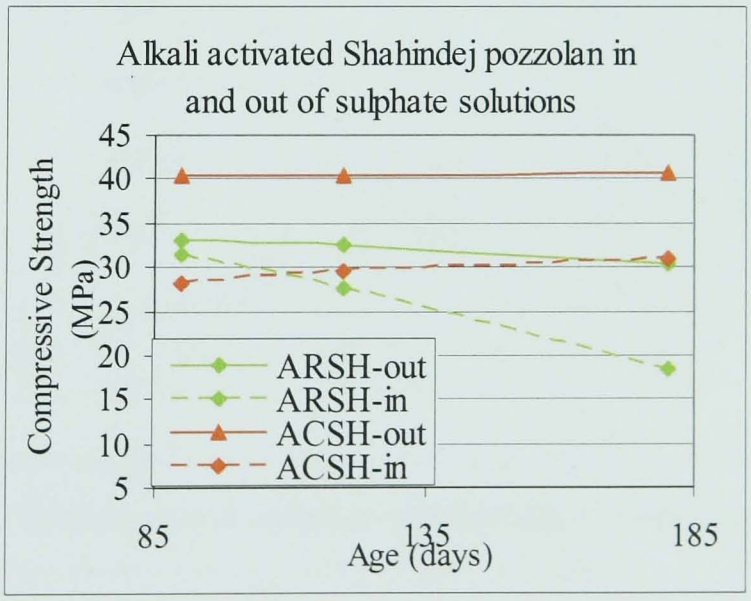

Figure 8.8 Compressive strength for ATAF1 and ATAF2 Mixes cured under different condition and temperatures, ARSH, and ACSH in and out of the sulphate solution

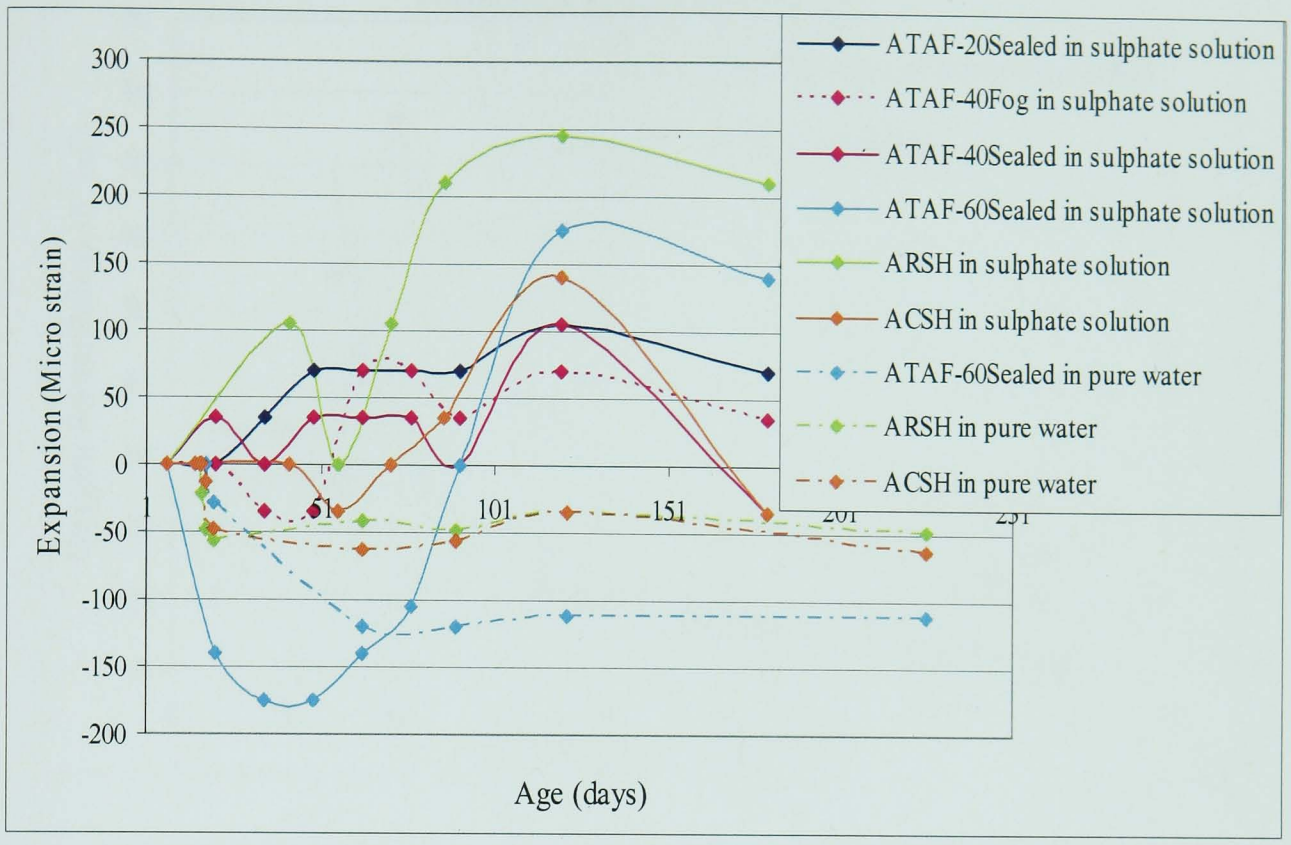

Figure 8.9 Expansion at various ages for geopolymer mortar mixes based on alkali activated natural pozzolan in sulphate solution

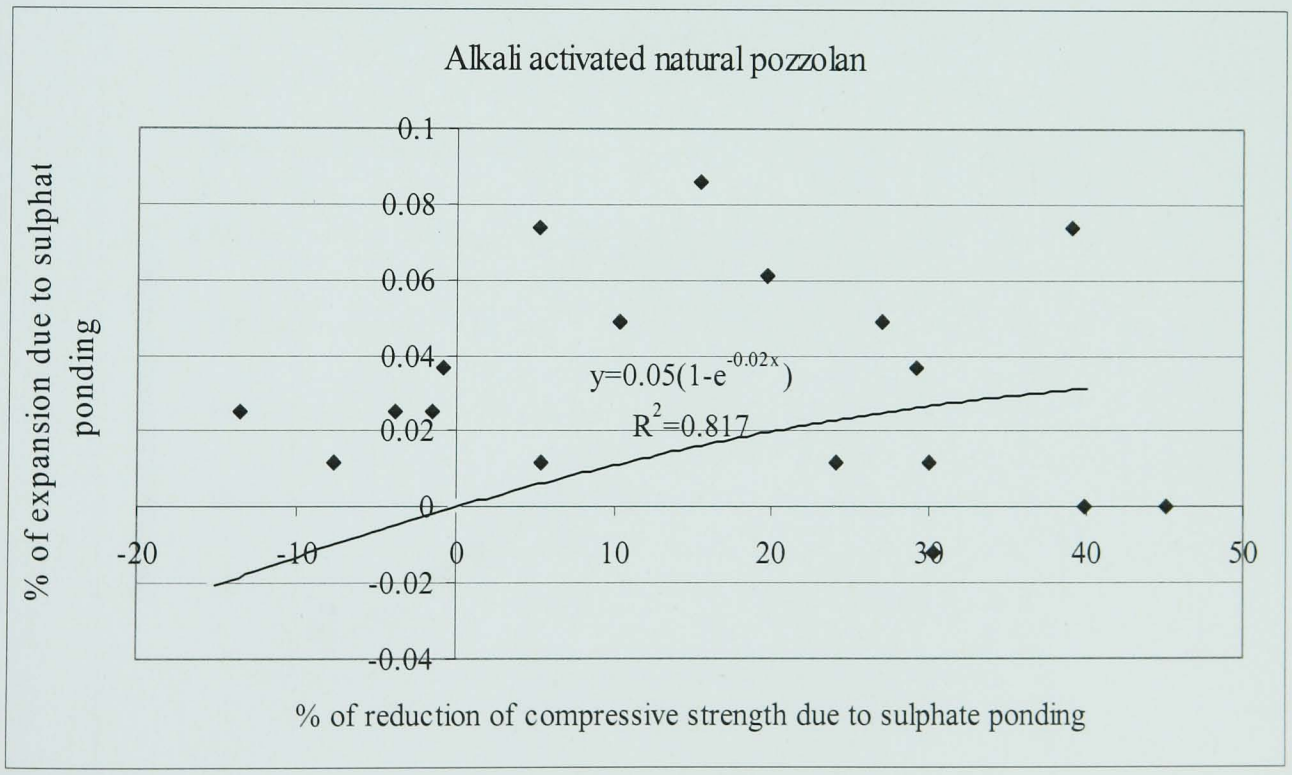

Figure 8.10 Correlation between the percentage of expansion and reduction of strength at various ages for geopolymer mortar mixes based on alkali activated natural pozzolan in sulphate solution (W/B for mixes is same)

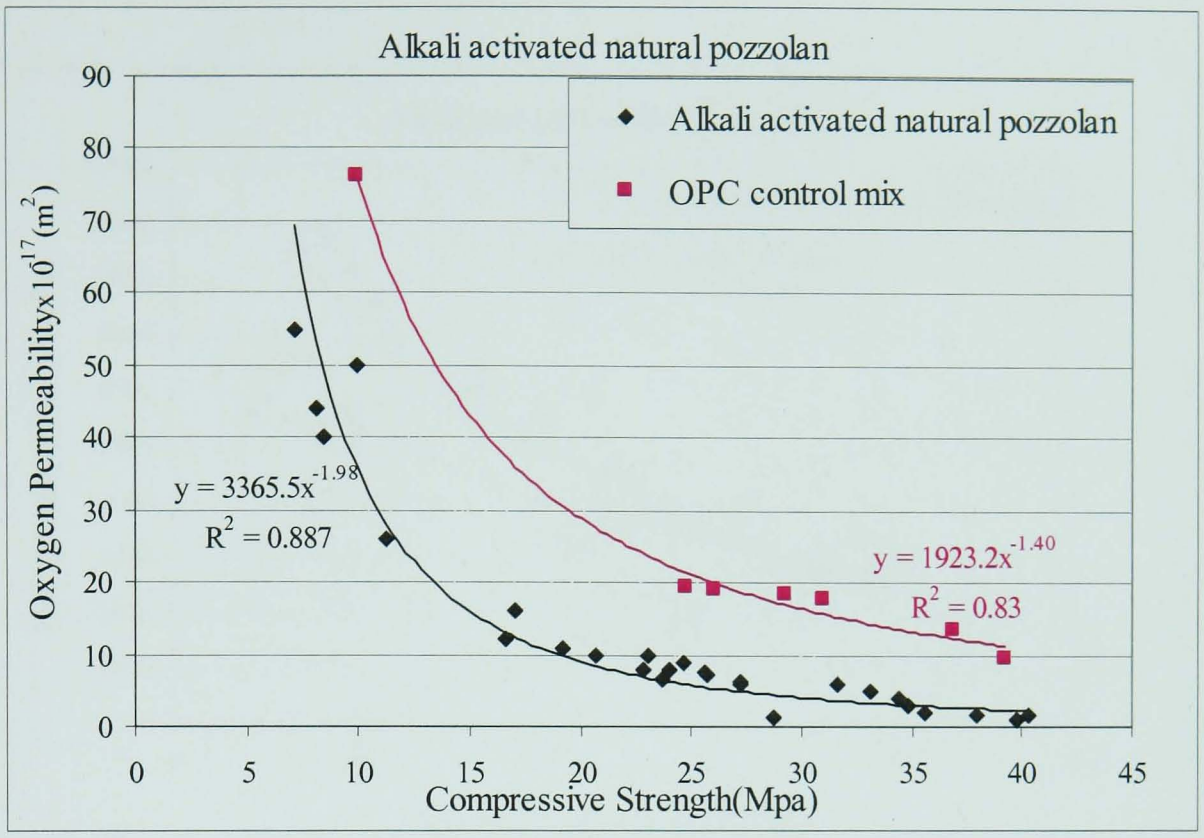

Figure 8.11 Relation between the oxygen permeability and the compressive strength of alkali activated natural pozzolans geopolymer concrete

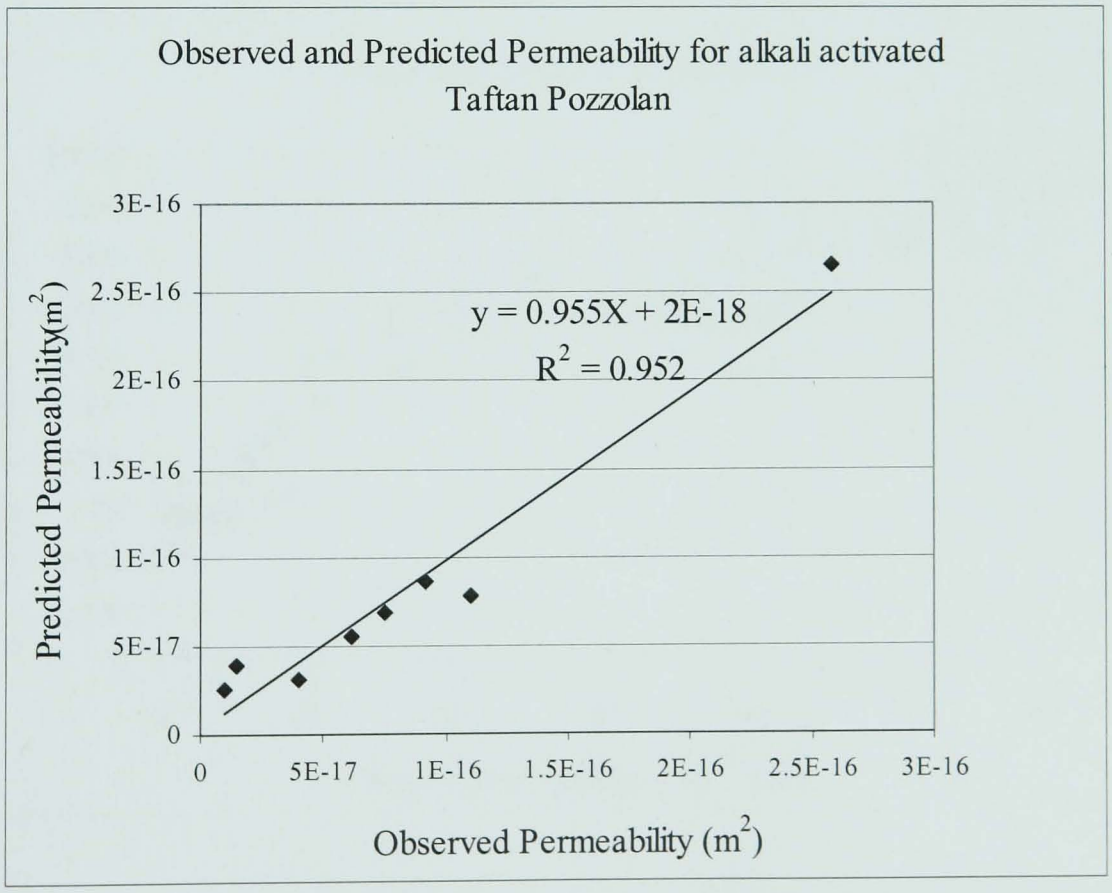

Figure 8.12 The relationship between the predicted and observed permeability in Taftan pozzolan

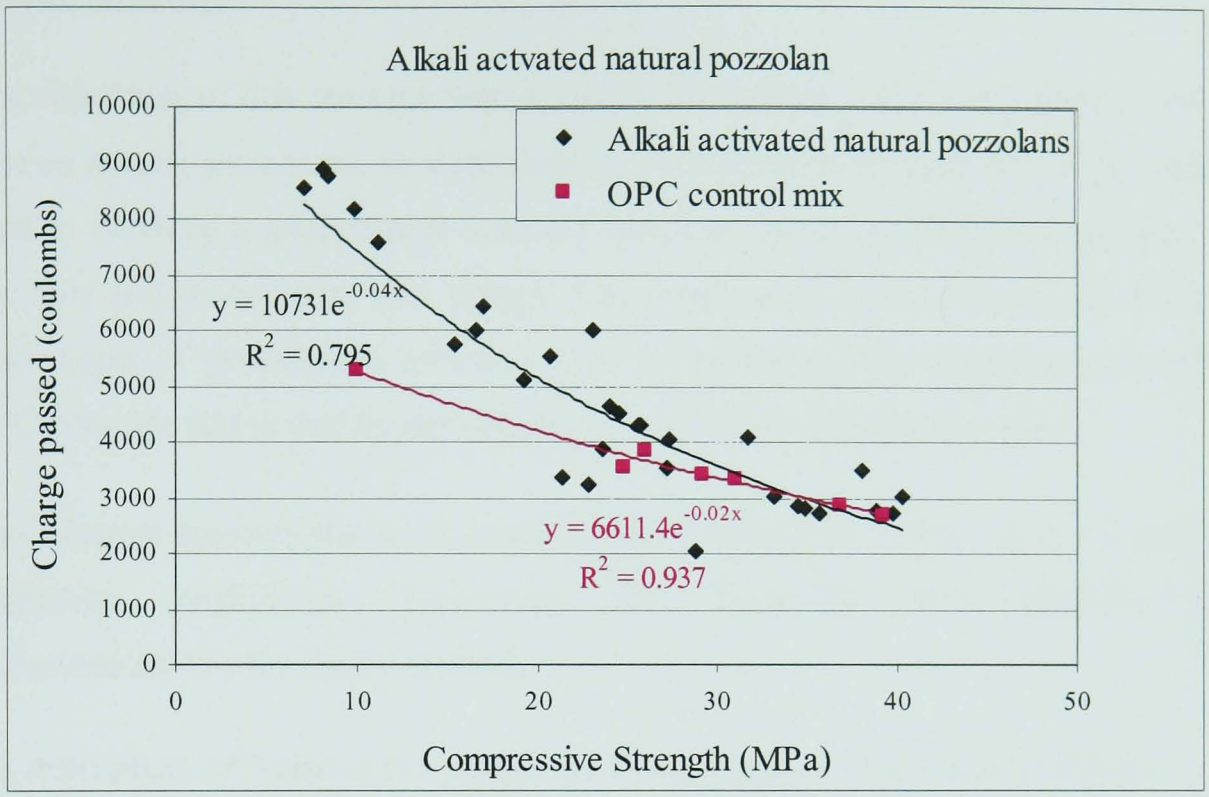

Figure 8.13 Relation between the chloride permeability and the compressive strength of geopolymer concrete based on alkali activated natural pozzolans

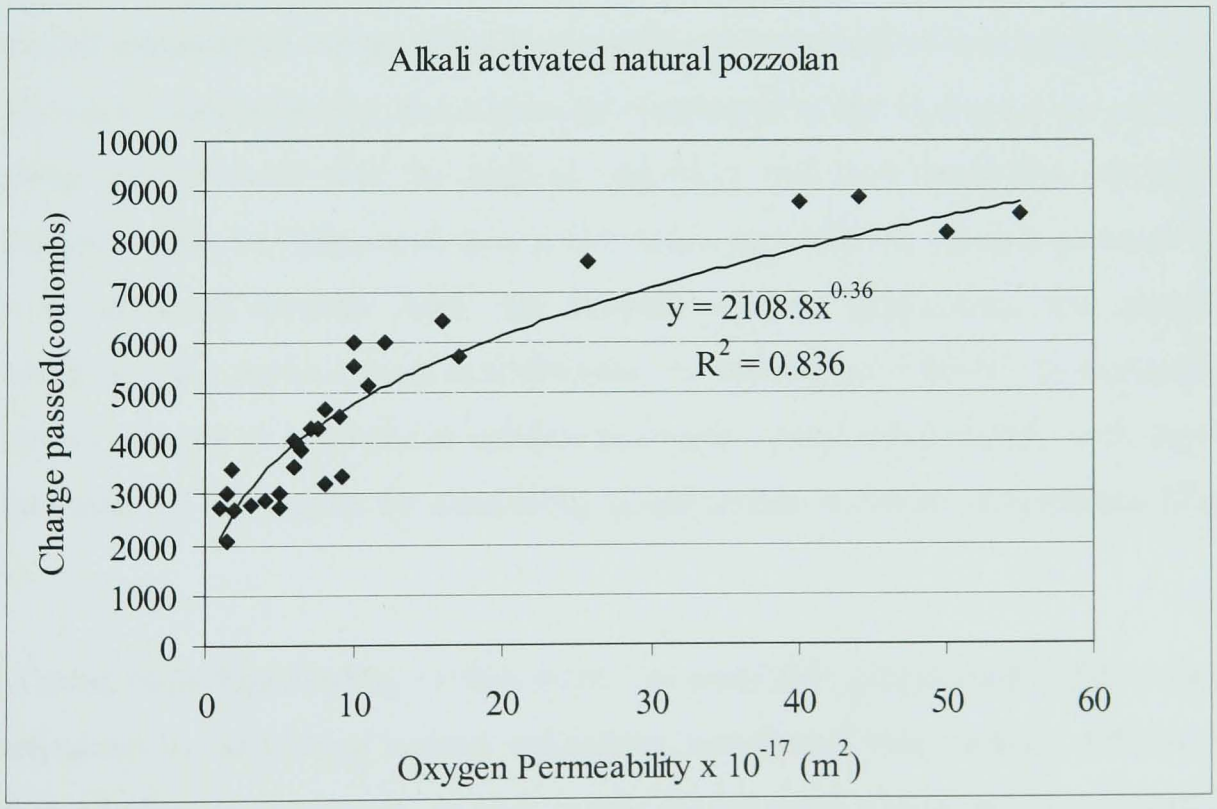

Figure 8.14 Relation between the chloride permeability and the oxygen permeability of geopolymer concrete based on alkali activated natural pozzolans

9. CONCLUSIONS AND RECOMMENDATIONS FOR FUTURE RESEARCH

9.1 Introduction

The objectives of this research were to study the intrinsic nature of different types of Iranian natural pozzolans, to determine the activators and methods which could be used to produce a geopolymer concrete based on alkali activated natural pozzolan (AANP) and to optimise mix design. The mechanical behaviour and durability of these types of geopolymer concrete were investigated and compared with normal OPC concrete mixes cast by the author and also reported in the literature.

This chapter presents the main conclusions regarding pozzolanic activity, activator properties, engineering properties, and durability and suggests some recommendations for future research.

9.2 Activation of Natural Pozzolans for Production of Geopolymer Binder

The primary aim of this study has been to investigate the characteristics of five pozzolans from Iran (Table 9.1), both in their natural state and after calcination at different temperatures, as sources for the preparation of geopolymer binders. Elevated temperature curing of pastes containing the pozzolans was considered. This study used alkali solubility and compressive strength as the indicators for pozzolanic activity, and showed that the highest reactivity and best behaviour resulted for pozzolanas such as Taftan with low L.O.I. and a high soluble calcium content which can be activated directly from raw material without calcination. For pozzolans containing sodic zeolites, such as Shahindej, on calcination at 800°C, its clinoptilolite minerals convert to amorphous opaline materials which react readily with aqueous alkali making it suitable for producing geopolymers at room temperature (Figure 9.1).

The most important finding of this work has been that geopolymer binders can be synthesized by activating natural pozzolans, condensed with sodium silicate in a highly alkaline environment. A new model is presented which allows prediction of the alkali activated pozzolan strength versus their alkali solubility, chemical composition and crystallinity.

In section 4.5, a model has been proposed for assessing the pozzolanic reactivity of pozzolans in both natural and calcined forms in terms of compressive strength of the pozzolanic based geopolymer binder to save both resources and time. The correlation between compressive strength and relevant parameters includes the alkali solubility, alkali content, activity index, loss on ignition, the ratio of (SiO_2+Al_2O_3+CaO) in solution to (SiO_2+Al_2O_3+CaO) mineral (obtained from ICP measurements) and quartz percentage was investigated one by one. A linear model was tried combining the first three parameters as inputs in order to find compressive strength using the least squares technique with the effect of curing temperatures in section 4.6. This model was improved with a nonlinear model which considered three further parameters including L.O.I., the ratio of [(SiO_2+Al_2O_3+CaO) solution/ (SiO_2+Al_2O_3+CaO) mineral] from ICP tests and the quartz percentage thus obtaining better correlation ($R>0.93$) between the predicted and observed values of compressive strength of pozzolanic based geopolymer binder.

This investigation has shown that the most efficient activator for activating natural pozzolans is a combination of potassium hydroxide and sodium silicate solution. The optimum dosage of activators is determined by a new method which draws the strength contours versus different molarities of alkaline hydroxide and various ratios of alkaline hydroxide to alkaline silicate allowing the islands of ideal compositions to be defined. The results show that for pozzolans containing high soluble silicate with low alkalinity, a sodium silicate with lower SiO_2 to Na_2O ratios gives higher strengths but when a calcined or a natural form with higher alkalinity is used the reverse is true. Using mineral additives including kaolinite, other calcined pozzolans such as Shahindej pozzolan, and lime when added to Taftan pozzolan as solid precursor is found to give approximately the same strength, although it seems that the gel obtained is more impermeable than when the pozzolan is activated without mineral additives.

9.3 Mix Design, Procedure and Curing Temperature

This research has successfully used geopolymer binders made from alkali-activated natural pozzolan to produce concrete instead of using an OPC cement paste. To produce the best paste and ongoing mix designs, the effect of water content was

studied and it was found that the minimum water to binder ratio for concrete mixtures made with activated natural pozzolans should be at least equal to the sum of plastic limits which is determined by falling cone test and aggregate water absorption. This amount would prepare a low workability concrete that achieves the maximum strength when hardened. The proportioning of the concrete mixture was based on the BRE method of mix design considering the approaches for determining the minimum water to binder. Then, the amount of cement was substituted with the same quantity of natural pozzolan plus the solids in water-glass with the water in the activator also taken as part of the total mix water.

To achieve the best results in geopolymer concrete, mixing should be done in three stages by adding the hydroxide alkaline solution to the natural pozzolan first, followed by an alkaline silicate solution, and then adding the mixed paste to aggregates.

This type of binder usually needs higher than room temperature for curing to be activated since pozzolans such as Taftan, which contain feldspars as main mineral phases, seems to need a higher activation energy to be activated with alkali. For Shahindej it was shown that when pozzolans which contain zeolite minerals such as clinoptilolite are calcined they can be activated at room temperature.

9.4 Fresh Properties of AANP Concrete

In this type of concrete, which can be classified as 'sticky' concrete, calcination of Shahindej pozzolan increases the slump and results in a more workable geopolymer concrete. Pozzolans with higher silicate content and aluminate may delay the setting time of alkali activated natural pozzolan which decreases when the curing temperature and dosage of alkaline hydroxide increases.

9.5 Engineering Properties of AANP Concrete

Geopolymeric concrete mixes based on activated natural pozzolans mostly have shown lower strength and modulus of elasticity than OPC mixes at early ages, but they reach the same and even higher strength and modulus of elasticity than OPC mixes after long-term curing (Figure 9.2). It is concluded that concrete made with an alkali activated natural pozzolan develops moderate to high mechanical strength and

modulus of elasticity and shrinks much less than ordinary OPC. All of the geopolymer concrete mixes show lower ultrasonic pulse velocity than OPC concrete mixes even though they have higher compressive strengths despite lower densities. In this investigation, an attempt has been made to formulate the equations to describe the relationship between splitting tensile strength, static modulus of elasticity and UPV of AANP concrete and its compressive strength in section 7.7. It is shown that the relationships provide some idea of prediction of the properties while justifies the variation of these parameters more than 78, 68, and 78 percent respectively.

9.6 Durability Properties of AANP Concrete

This type of concrete has shown that oxygen permeability lies in the same ranges as OPC concrete. The Rapid Chloride Permeability Test (ASTM C1202) was not found to be applicable for geopolymer concrete because of the conductive pore solution that exists due to the presence of alkaline activators in the pore solution. A reduced voltage was used and the results of long term chloride absorption shows that the resistance of alkali activated natural pozzolan concrete when subjected to chloride attack was moderate.

On exposure to sulphate solution, while the compressive strength development does not show significant reduction in most samples, XRD traces show sulphate compounds were observed in the core of AANP concrete and thus further study is needed to confirm the resistance of AANP concrete to sulphate attack for longer periods of time. In section 8.5 a general relationship was found to predict the oxygen permeability of AANP concrete from its compressive strength (Figure 9.3). For alkali activated Taftan mixes this relationship is improved by considering the effect of water to binder ratio. The correlation of the model is higher than 0.95 which shows a good agreement between the experimental and calculated air permeability coefficients.

9.7 Evaluation of Carbon footprint and Cost for AANP Concrete

Two potential advantages of concrete made with alkali activated natural pozzolans compared with other binders are its carbon footprint and cost. Increased pressure to improve sustainability within the concrete industry makes these factors very important. The relation between CO_2 footprint and cost of AANP concrete and its

compositions in comparison with Portland-based cements is roughly quantified in this section.

9.7. 1 Environmental Benefits

De-carbonation of lime and calcination of cement clinker release CO_2 as a reaction product in OPC concrete while the use of an alkaline hydroxide or silicate activating solution rather than water for cement hydration does reintroduce some CO_2. Production of these activators needs temperature similar to de-carbonation of lime in OPC manufacture. The CO_2 emission of AANP concrete can be quantified in terms of its compositions. Referring to Table 6.2, 110kg of activator is needed to be mixed with 400kg pozzolan to produce $1m^3$ of AANP concrete which has the CO_2 emission equal to 27.5% of the same amount of OPC, when pozzolan used in natural state (It is estimated that the production of 1 tone of OPC results in the release of 1 tone of CO_2). If the calcined form is used, the CO_2 emission of AANP concrete would be the summation of CO_2 emission due to producing the required activators and the amount related to calcination procedure. Since the temperature required for calcination these materials, is half of that needed to de-carbonate lime, the CO_2 emission for calcinations of these materials can be considered 50% of equal OPC production. Therefore, in this case the CO_2 emission of AANP concrete increases to 77.5% of the amount emitted by the same weight of OPC. Hence the AANP concrete manufacture is liable to reduce CO_2 emission from 22.5% to 72.5% compared to OPC production.

9.7.2 Supply and Cost of activators

Referring to Table 6.2, 66kg of potassium hydroxide and 46kg (considering density equal to 1.35 kg/m^3) of water-glass as activator is needed to be mixed with 400kg pozzolan to produce $1m^3$ of AANP concrete. Although, these activators have different prices in different markets, the cost of industrial potassium hydroxide (25kg KOH Flake UNSD made in KOREA costs £52) and water-glass [25 lbs (11.35 kg) water-glass solution is sold by Sheffield Pottery in U.K. for 12$] is considered equal to £2.1 and £0.73 per kg, respectively. Hence calculating as a rule of thumb the activators required for activating 400kg pozzolans cost £173 and considering 25kg of pozzolan to be comparable to the price of OPC in 25kg bags, the price of required activators would be £11 per 25kg.

9.8 Application Aspects of AANP Concrete

Geopolymer concrete made from alkali activated natural pozzolan is a new type of concrete which needs a very good control on site to be used as a comparable alternative to OPC concrete. However its drawbacks, such as loss of workability, quick setting time and the health and safety implications of working with strong alkali solutions can easily be adapted in applications such as pre-cast concrete and mass concretes as in dam construction where roller compacted AANP concrete may be a viable construction method. This type of concrete, especially in countries with greater resources of natural pozzolan, can help decrease energy consumption and environmental impacts.

9.8 Future Research on AANP Concrete

In view of the experience gained from this study the following suggestions for future study in the activation of natural pozzolan to produce geopolymer concrete as construction material are:

1. Standardise the mix design methods for alkali activated natural pozzolans as a binder according to the classification of the materials presented in section 2.3 and specify the optimum proportions of activator, precursor and additive and properties.

2. Study blending of natural pozzolans as raw materials, which vary in their chemical compositions, with other raw minerals to compensate for the deficiency of oxides such as SiO_2, Al_2O_3 and CaO to overcome some of the problems related to workability and setting time.

3. Study the compatibility between geopolymer mortars / concretes with admixtures and the effect of superplasticizers which can perform a very effective role in producing concrete by using activated natural pozzolan with high silica content.

4. Investigate further mixes with different water to binder ratios to find out the effect of this parameter on drying shrinkage of geopolymer concrete.

5. Conduct extensive investigation on the chemical reaction between binder, water and aggregate to understand the heat produced due to the chemical reaction, microstructure of hardened paste and interaction of the binder with aggregates considering different procedures of mixing and various curing conditions.

6. Although the curing of AANP concrete seems to be an exothermic reaction and has better properties at higher curing temperature, it seems not to create high heat due to its chemical reaction, so it would be useful to do further investigation on this phenomenon by measuring the heat of reaction of this type concrete.

7. Study the potential use of alkali activated natural pozzolan mortars and concretes in the pre-cast concrete industry with respect to possibility of using high temperatures or autoclaving curing conditions and considering the restriction factors.

8. Although different tests were done in this research to find out whether sulphate attacks this type of concrete or not, further study is needed to confirm the resistance of AANP concrete to sulphate attack for longer periods of time.

9. Extensively study the durability properties of geopolymer mortars and concretes based on alkali activation of natural pozzolan to find its vulnerability to chemical attack including presence of reactive aggregates and carbonation, together with the investigation the use of additives.

Table 9.1 Mineralogy of investigated pozzolans

Material	Shahindej Pozzolan	Sahand Pozzolan	Sirjan Pozzolan	Rafsanjan Pozzolan	Taftan Pozzolan
Minerals	Clinoptiolite	Albite	Albite	Montmorillonite	Albite
	Albite	Hornblende	Montmorillonite	Albite	Hornblende
	Quartz	Quartz	Quartz	Hornblende	Quartz
	Calcite	Muscovite	Biotite	Biotite	-
	-	-	-	Calcite	-
	-	-	-	Quartz	-
	-	-	Amorphous	Amorphous	Amorphous

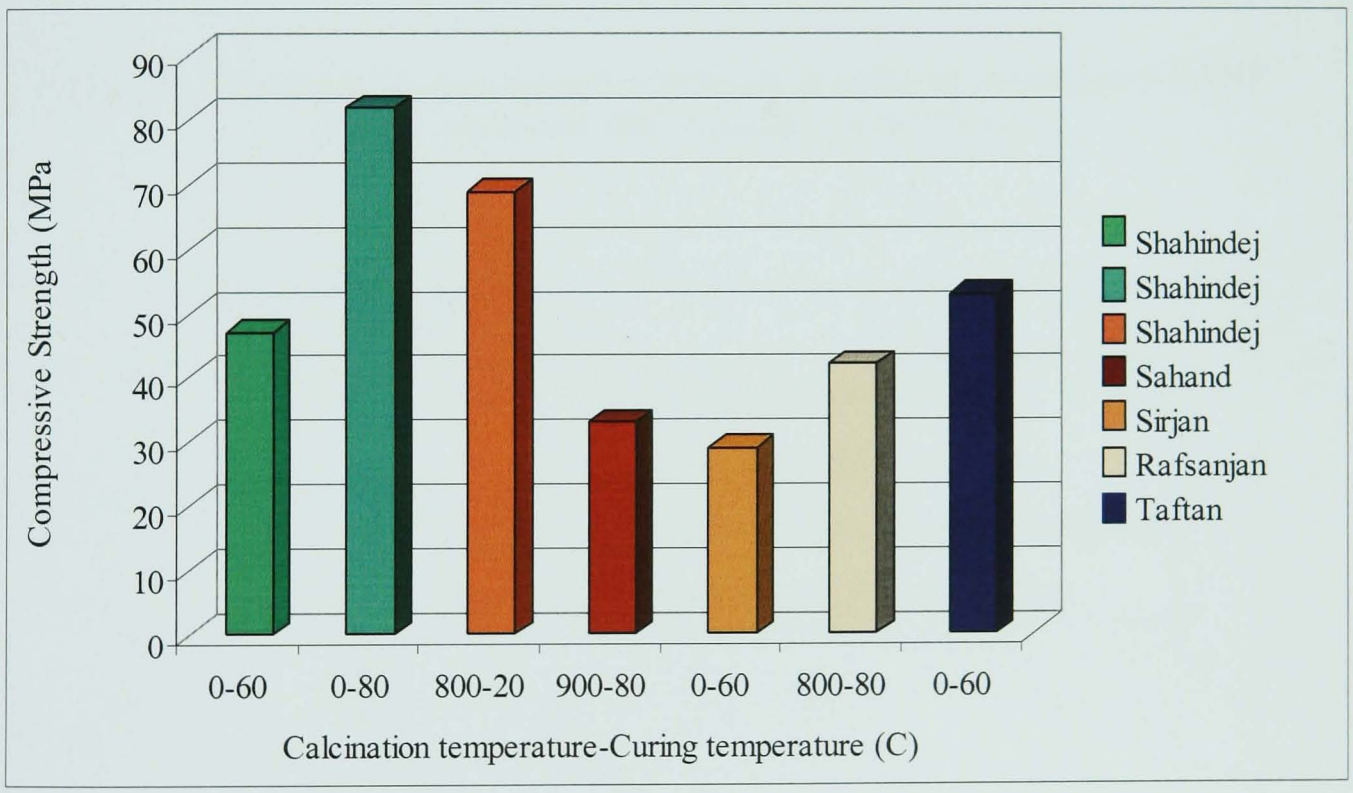

Figure 9.1 Different calcination and curing temperatures with related compressive strengths of investigated pozzolans

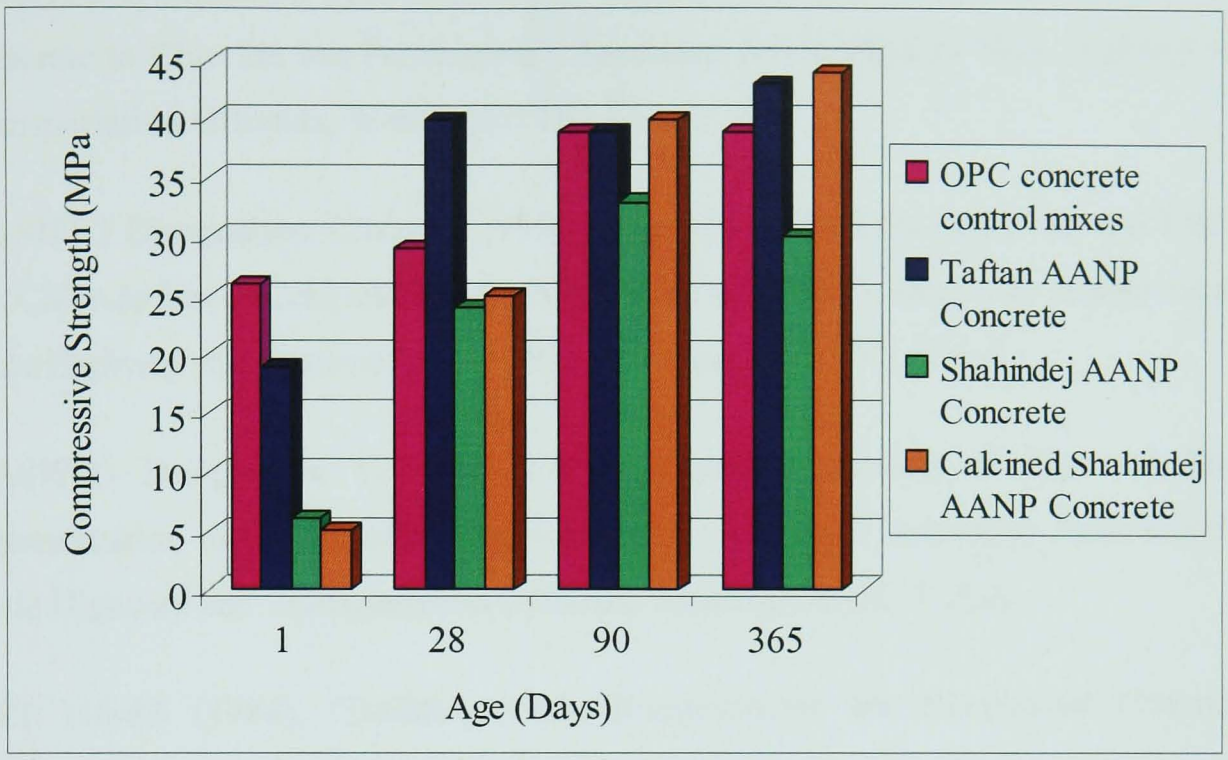

Figure 9.2 Comparison of compressive strength of different investigated AANP concrete mixes and OPC concrete control mixes

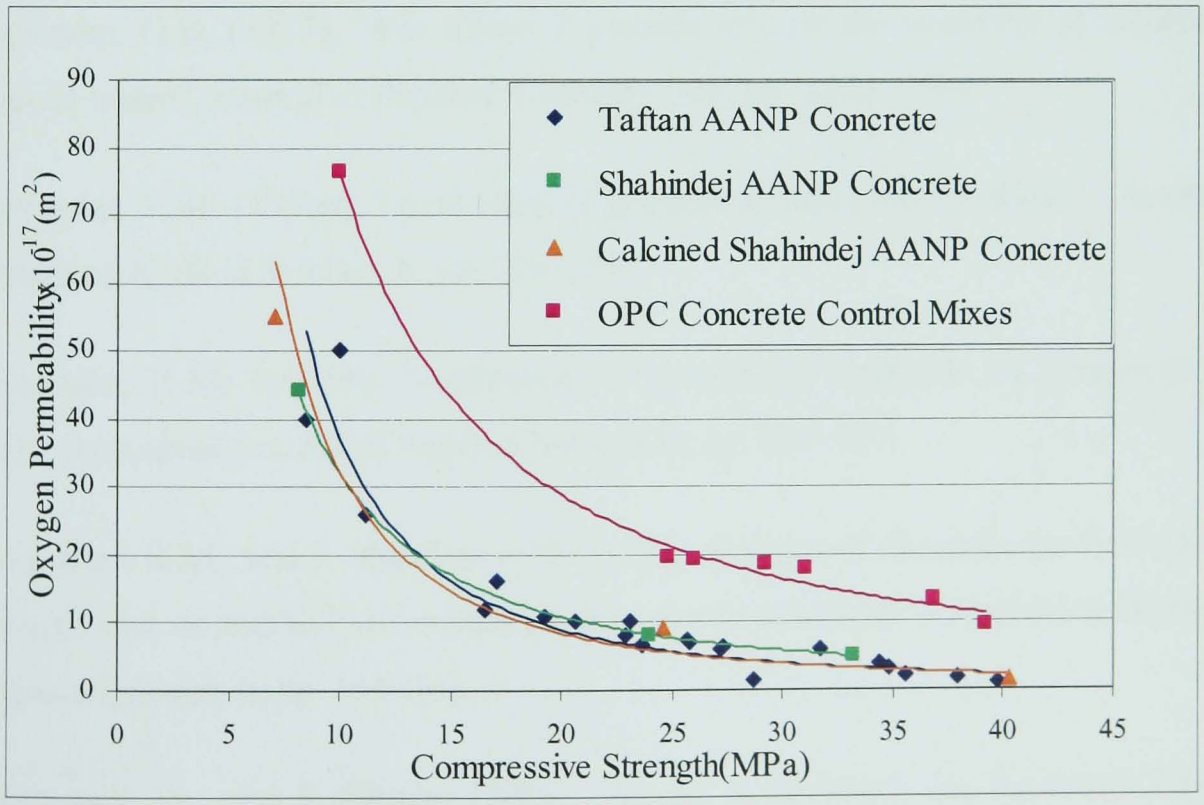

Figure 9.3 Comparison of the oxygen permeability of different AANP concrete mixes and OPC concrete control mixes

REFERENCES

AASHTO Designation T259-80 (1980), "Standard Method of Test for Resistance of Concrete to Chloride Ion Penetration", American Association of State Highway and Transportation Officials, Washington DC, U.S.A

AASHTO Designation T260-94 (1994), "Standard Method for Sampling and Testing for Chloride Ion in Concrete and Concrete Raw Materials", American Association of State Highway and Transportation Officials, Washington DC, U.S.A

AASHTO Designation T277-83 (1993), "Standard Method of Test for Rapid Determination of the Chloride Permeability of Concrete", American Association of State Highway and Transportation Officials, Washington DC, U.S.A

ACI 318-83 (1984), "Building Code Requirements for Reinforced Concrete", American Concrete Institute, Committee 318

Alexander, K.M. (1960), "Reactivity of ultra fine powders produced from siliceous rocks", Journal of American Concrete Institute, 57, pp. 557–569

Alexander, G.B. (1957), "The effect of particle size on the solubility of amorphous silica in water", Journal of Physical Chemistry, 61, pp. 1563–1564

Alexander, K.M. (1955*a*), "Activation of pozzolanic materials by alkali", .Australian Journal of Applied Science, 6, pp. 224–229

Alexander, K.M. (1955*b*), "Activation of pozzolanic materials by treatment with acid", Australian Journal of Applied Science, 6, pp. 327–333

Alexander, K.M., and J. Wardlaw (1955*c*), "Limitations of the pozzolan-lime mortars strength test as method of comparing pozzolanic reactivity", Australian Journal of Applied Science, 6, pp. 334–342

Allahverdi, A., and F. Skvara (2001), "Nitric Acid Attack on Hardened Paste of Geopolimeric Cements-Part I", Ceramics-Silikaty, 45(3), pp. 81-88

Allahverdi, A., and F. Skvara, (2001), "Nitric Acid Attack on Hardened Paste of Geopolimeric Cements-Part II", Ceramics-Silikaty, 45(4), pp. 143-149

Al-Otaibi, S., C.J. Lynsdale, and J.H. Sharp (2001), "Performance of Alkali-Activated Slag Concrete", In Proc. Sustainable Development of Cement and Concrete, San Francisco

Antonic´, T., A. Cˇiz¨mek, B. Subotic´ (1994), "Dissolution of amorphous aluminosilicate zeolite precursors in alkaline solutions: Part 2. Mechanism of the dissolution", Journal of Chemical Society, Faraday Trans. 90 _13, pp. 1973–1977

Antonic´, T., A. Cˇiz¨mek, C. Kosanovic´, B. Subotic´ (1993), "Dissolution of amorphous aluminosilicate zeolite precursors in alkaline solutions: Part 1. Kinetics of the dissolution", Journal of Chemical Society, Faraday Trans. 89_11, pp. 1817–1822

Asavapisit, S., D. Chotklang (2004), "Solidification of electroplating sludge using alkali-activated pulverized fuel ash as cementitious binder", Cement and Concrete Research, 34, pp. 349–353

ASTM C39/C39M-05e2 (2005), "Standard Test Method for Compressive Strength of Cylindrical Concrete Specimens", American Society for Testing and Materials, USA

ASTM C-311-07 (2007), "Standard Test Methods for Sampling and Testing Fly ash or Natural Pozzolans for use in Portland-Cement Concrete", American Society for Testing and Materials, USA

ASTM C-618-08a (2008), "Standard Specification for Coal Fly Ash and Raw or Calcined Natural Pozzolan for Use in Concrete", American Society for Testing and Materials, USA

ASTM C 1012-95a (1995), "Standard Test Method for Length Change of Hydraulic-Cement Mortars Exposed to a Sulfate Solution", American Society for Testing and Materials, USA

ASTM C 1202-97 (1997), "Standard Test Method for Electrical Indication of Concrete's Ability to Resist Chloride Ion Penetration", American Society for Testing and Materials, USA

ASTM D854-06 (2006), "Standard Test Methods for Specific Gravity of Soil Solids by Water Pycnometer", American Society for Testing and Materials, USA

ASTM D5550-06 (2006) "Standard Test Method for Specific Gravity of Soil Solids by Gas Pycnometer", American Society for Testing and Materials, USA

Babushkin, V.I., G.M. Matveyev, O.P. Mchedlov-Petrossyan (1985), "Thermodynamics of Silicates", Springer-Verlag, Berlin, pp. 276–281

Bakharev T. (2005), "Durability of geopolymer materials in sodium and magnesium sulphate solutions", Cement and Concrete Research, 35, pp. 1233 –1246

Bakhareva T., J.G. Sanjayana, Y. B. Cheng (2002), "Sulfate attack on alkali-activated slag concrete", Cement and Concrete Research, 32, pp. 211 –216

Bakhareva T., J.G. Sanjayana, Y. B. Cheng (2000), "Effect of admixtures on properties of alkali-activated slag concrete", Cement and Concrete Research, 30, pp.1367–1374

Bakhareva T., J.G. Sanjayana, Y. B. Cheng (1999*a*), "Alkali activation of Australian slag cements", Cement and Concrete Research, 29, pp.113–120

Bakhareva T., J.G. Sanjayana, Y. B. Cheng (1999*b*), "Effect of elevated temperature curing on properties of alkali –activated concrete", Cement and Concrete Research, 29(10), 1619-1626

Bao-min, W., W. Li-jiu (2004), "Development of studies and applications of activation techniques of fly ash", International Workshop on Sustainable Development and Concrete Technology, pp. 159-169

Barbosa, V.F.F., K.J.D. MacKenzie, and C. Thaumaturgo, (2000), "Synthesis and characterisation of materials based on inorganic polymers of alumina and silica: sodium polysialate polymers", International Journal of Inorganic Materials, Vol. 2, pp. 309-317

Basheer, P. A. M. (2001),"Permeation analysis", Handbook of analytical techniques in concrete science and technology, V. S. Ramachandran, J. J. Beaudoin, and William Andrew Publishing, pp. 985

Bear, J., Y. Bachmat (1990), "Introduction to modeling and transport phenomena in porous Media", Kluwer, Dodrecht, the Netherlands

Bell, J., W.M. Kriven (2004), "Nanoporosity in Geopolymeric Cements", Microscopy and Microanalysis 04, Proceeding 62nd Annual Meeting of Microscopy Society of America, Vol. 10, pp. 590

Bell, F.G. (2000), "Engineering Properties of Soils and Rocks", 4th ed., Blackwell, Oxford

Berry, E.E., R.T. Hemmings, and B.J. Cornelius (1988), "Speciation in size and density fractionated fly-ash, III. The influence of HCl leaching on the glassy constituents of a high-Ca fly ash", Proceedings of Materials Research Society, v. 113, pp.55–63

Bhardwaj, M.C., V. S. Batra, and U.V. Sastry (1980), "Effect of admixtures on pozzolana concrete", Indian Concrete Journal, 54, pp.134–138

Bilodeau and Mohan Malhotra (2003), "High-Volume Fly Ash System: Concrete Solution for Sustainable Development", ACI Material Journal, Vol.1, No.1

Breck, D.W. (1974), "Zeolite Molecular Sieves", Interscience, New York

BS 1881: 1670 Determination of Vebe time, London, British Standard Institution

BS 1881-121:1983 Testing concrete —Part 121: Method for determination of static modulus of elasticity in compression, London, British Standard Institution

BS 8110-2:1985 Structural use of concrete -Part 2: Code of practice for special circumstances, London, British Standard Institution

BS 1881-203:1986 Testing concrete —Part 203: Method for determination of ultrasonic pulse velocity, London, British Standard Institution

BS 812-120:1989 Testing concrete —Part 120: Method for determination of Shrinkage, London, British Standard Institution

BS 882:1992, Specification for aggregates from natural sources for concrete, London, British Standard Institution

BS EN 196-3:1995 Methods of testing cement- Part 3: Determination of setting time and soundness. London, British Standard Institution.

BS EN 197-1:2000 Cement- Part1: Composition, specifications and conformity criteria for common cements, London, British Standard Institution,

BS EN 12350-2:2000 Testing fresh concrete: Slump test, London, British Standard Institution

BS EN 12350-7:2000 Testing fresh concrete: Air content, Pressure methods, London, British Standard Institution

BS EN 12390-3:2000 Testing hardened concrete: Compressive strength of test specimens, London, British Standard Institution

BS EN 12390-6:2000 Testing hardened concrete: Tensile splitting strength of test specimens, London, British Standard Institution

BS EN 12620:2002 Aggregates for concrete, London, British Standard Institution

Brough, A.R., A. Atkinson (2002), "Sodium silicate-based, alkali-activated slag mortars Part I. Strength, hydration and microstructure", Cement and Concrete Research, 32, pp. 865–879

Brougha, A.R., M. Hollowayb, J. Sykesb, A. Atkinsona (2000), "Sodium silicate-based alkali-activated slag mortars Part II: The retarding effect of additions of sodium chloride or malic acid", Cement and Concrete Research, 30, pp. 1375–1379

Buchwald, A., Ch. Kaps, M. Hohmann (2003), "Alkali-activated binders and pozzolan cement binders-compete binder reaction or two sides of the same story". Academic press, University of Weimar, Germany

Butt, Y. M., and L.N. Rashkovich (1961), "The hardening of binders at elevated temperature", Academic Press, Moscow (in Russian)

Cabrera, J. G., and P. A. Claisse (1999), "Oxygen and water vapour transport in cement-silica fume pastes", Construction and building materials 13, pp. 405-414

Cabrera, J. G., A.R. Cusens, and C. J. Lynsdale (1989), "Porosity and Permeability as Indicators of Concrete Performance", IABSE Report, Vol. 57/1, pp. 249-254

Cabrera, J. G., and C. J. Lynsdale (1988), "A new gas permeameter for measuring the permeability of mortar and concrete", Magazine of Concrete Research 40(144), pp. 177-182

Carcasses, M., A. Abbas, J.P. Ollivier, and J. Verdier (2002), "An optimised preconditioning procedure for gas permeability measurement", Materials and Structures, 35(1), pp. 22-27

Chatterjee, M.K., and D. Lahiri (1967), "Pozzolanic activity in relation to specific surface of some artificial pozzolans", Transaction of Indian Ceramic Society, 26, pp. 65-74

Cheng, T.W. and J.P. Chiu (2003), "Fire-resistant geopolymer produced by granulated blast furnace slag", Minerals Engineering, Vol. 16, pp. 205-210

Coad, J.R., (1974), "Natural pozzolans, In Lime and alternative cements", edited by R. Spence, Intermediate Technology Development Group, London, pp. 46–48

Collinsa, F., J.G. Sanjayan (2000), "Effect of pore size distribution on drying shrinkage of alkali-activated", Cement and Concrete Research, 30, pp. 1401– 1406

Collins, F.G., J.G. Sanjayan, (1999), "Workability and mechanical properties of alkali activated slag concrete", Cement and Concrete Research, 29, pp. 455–458

Comrie, D.C., J. Davidovits (1988), "Long term durability of hazardous toxic and nuclear waste disposals Geopolymer", 1st European Conference on Soft Mineralurgy, Compiegne, France, 1, pp. 125–134

Costa, J., C.J. Lynsdale, and N.B. Milestone (2007) "Alkali activation of flyash for production of geopolymer concrete", A dissertation submitted to University of Sheffield in fulfilment of the requirement for the degree of master of philosophy, U.K

Costa, U., M. Fucoetti, F. Massazza (1992), "Permeability and diffusion of gasses in concrete", Proceeding 9th International Congress of Chemistry of Cement, NCB, New Delhi, India, Vol. 5, pp. 107-114

Costa, U., F. Massazza (1981), "Natural pozzolanas and fly ashes: analogies and differences", Materials Research Society, Annual meeting, Boston Mass., pp. 134-144

Costa, U., and F. Massazza (1977), "Influence of thermal treatment on the activity of some natural pozzolans with lime", Il Cemento, 77, pp.105–122

Costa, U., and F. Massazza (1974), "Factors affecting the reaction with lime of Italian pozzolans", Il Cemento, 74, pp.131–139

Darvishzadeh, A., (1983), "Esfordi Phosphate deposit", Tehran University Journal of Science, 13 (in Farsi)

Dave, N.G., (1981), "Pozzolanic wastes and their activation to produce improved lime pozzolana mixtures", In Proceedings of 2nd Australian conference on engineering materials, Edited by D.J. Cook, Sydney, pp. 623–638

Davidovits, J., (2003), "Building Materials", McMullen

Davidovits, J., (1999), "Chemistry of Geopolymeric Systems, Terminology", Presented at the Geopolymer 99 International Conference, France

Davidovits, J., (1994*a*), "Geopolymers, man-made rock geosynthesis and the resulting development of very early high strength cement", Journal of Materials Education, 16 (2-3), pp. 91-139

Davidovits, J., (1994*b*), "High-alkali cements for 21st century concretes in concrete technology, past, present and future", Proceedings of V. Mohan Malhotra Symposium, Editor: P. Kumar Metha, ACI SP- 144, pp. 383-397

Davidovits, J., (1994*c*), "Properties of Geopolymer Cements", in First International Conference on Alkaline Cements and Concretes, SRIBM, Kiev State Technical University, Kiev, Ukraine, pp. 131-149

Davidovits, J., M. Davidovits, N. Davidovits, (1994*d*), "Process for obtaining a geopolymeric alumino-silicate and products thus obtained", U.S. Patent no. 5,342,595

Davidovits, J., (1991), "Geopolymers: inorganic polymeric new materials", Journal of Thermal Analysis, 37, pp. 1633–1656

Davidovits, J., D.C. Comrie, J.H. Paterson, D.J. Ritcey (1990), "Geopolymeric concretes for environmental protection", Concrete International Conference, France, pp. 30–40

Davidovits, J., (1988*a*), "Geopolymer chemistry and properties", First European Conference on Soft Mineralurgy, Compiegne, France, 1, pp. 25–48

Davidovits, J., (1988*b*), "Geopolymers of the first generation: SILIFACE-Process", First European Conference on Soft Mineralurgy, Compiegne, France, 1, pp. 49–67

Davidovits, J., M. Davidovics (1988), "Geopolymer room temperature ceramic matrix for composites", Ceramic Engineering Science Proc. 9, pp. 835–842

Davidovits, J., J.L. Sawyer (1985), "Early High-Strength Mineral Polymer", US Pattent No.4, pp. 509-985

Davidovits, J., (1982), "Mineral Polymers and Methods of Making Them", U.S. Pat. No. 4,349,486

Day, Ken W., (1999), "Concrete mix design, quality control and specification", Published by Taylor & Francis, ISBN 0419243305, 9780419243304, 2nd Edition, pp. 313-318

Day, R.L., and C. Shi (1994), "Relationship between strength development of lime–natural pozzolan pastes and the blaine fineness of the natural pozzolans", Cement and Concrete Research, 24, pp.1485–1491

Day, R.L., (1988), "Natural pozzolans for building in Latin America", In Proceedings of project identification meeting on local building materials, Nairobi, Kenya. British Science Council, U.K,

Deer, W.A., R.A. Howie, J. Zussman, (1992), "An Introduction to the Rock-forming Minerals", 2nd edition Longman, England,

Dent Glasser, L.S., G. Harvey (1984*a*), "The unexpected behaviour of potassium aluminosilicate solutions", Journal of Chemistry Society, Chemistry Communication 13, pp. 664–665

Dent Glasser, L.S., G. Harvey (1984*b*), "The gelation behaviour of aluminosilicate solutions containing Na+, K+, Cs+, and Me4N+", Journal of Chemistry Society, Chemistry Communication 13, pp. 1250–1252

Dent Glasser, L.S., (1982), "Sodium silicates", Chemistry Br. 18, pp. 33–39

Devidal, J. L., J. L Dandurand, R. R. Gout (1994), "Solubility of kaolinite in alkaline solutions at hydrothermal conditions", Goldschmidt Conference, Edinburgh, Mineral Magazine 58A, pp. 223–224

Douglas, E., A. Bilodeau, J. Brandstetr, V. M. Malhotra (1991), "Alkali Activated Ground Granulated Blast-Furnace Slag Concrete: Preliminary Investigation", Cement and Concrete Research, Vol. 21, pp. 101-108, Printed in the USA

Ezatian, F., (2002), " Atlas of Igneous Rocks: Classification and Nomenclatures", Ministry of Industries and Mines, Geological Survey of Iran (GSI) (in Farsi)

Ezatian, F., (1998), "Optical Mineralogy of Silicates with Coloured Atlas", Ministry of Mines and Metals, Geological Survey of Iran (GSI) (in Farsi)

Fan, Y., S. Yin, Z. Wen, J. Zhong (1999), "Activation of fly ash and its effects on cement properties", Cement and Concrete Research, 29, pp. 467–472

Fernandez-Jimenez, A. M., A. Palomo, et al., (2006), "Engineering properties of alkali activated fly ash concrete." ACI - Materials Journals 103(2), pp. 106-112.

Fernandez-Jimenez, A. M., and A. Palomo (2005), "Composition and microstructure of alkali activated fly ash binder: Effect of the activator", Cement and Concrete Research, 35(10), pp. 1984-1992

Ferna´ndez-Jime´nez, A., (2000), "Cementos de escorias activadas alcalinamente: influencia de las variables y modelizacio´n del proceso", Doctoral Thesis,UAM

Fernilndez-Jimhez, A., F. Puertas (1997), "Alkali-activated slag cements: kinetic studies", Cement and Concrete Research, Vol. 27, No. 3, pp. 359-368

Freidin, C., (2003), "Alkali-activated cement based on natural SiO2-containing material Part I. Strength, hydration, microstructure and durability", Cement and Concrete Research 33, pp.1417–1422

Gasteiger, H.A., W.J. Frederick, R.C. Streisel (1992), "Solubility of aluminosilicates in alkaline solutions and a thermodynamic equilibrium model", Industrial Engineering Chemistry Research 31, pp.1183–1190

Glukhovsky, V.D., (1981), "Slag-Alkali Concretes Produced from Fine-Grained Aggregate", Vishcha Shkola, Kiev, Russia (in Russian)

Glukhovsky, V.D., G.S. Rostovskaja, G.V. Rumina (1980), "High strength slag-alkaline cements", Proceedings of 7th International Congress on Chemistry of Cement, Paris, 3, V164–V168

Glukhovsky, V.D., V.A. Pakhomov (1978), "Slag-Alkali Cements and Concretes", Budivelnik Publishers, Kiev, Russia (in Russian)

Gregg, S.J., (1961), "The surface chemistry of solids", Chapman and Hall Ltd., London

Hakkinen, T., (1993), "The influence of slag content on the microstructure, permeability and mechanical properties of concrete Part 2: Technical properties and theoretical examinations", Cement and Concrete Research, Vol. 23, pp. 518-530

Hakkinen, T., (1987), "Durability of alkali activated slag concrete", Nordic Concrete Research, No. 6, pp. 81-94

Hakkinen, T., (1986), "Properties of alkali activated slag concrete", VTT Research Notes, Technical Research Centre of Finland (VTT), Finland, No. 540

Hansen, K. D., and W. G. Reinhardt (1991), "Roller-Compacted Concrete Dams", McGraw-Hill, ISBN 9780070260726

Hanzlicek, T., M. Steinerova (2002), "Investigation of dissolution of aluminosilicate in aqueous alkaline solution under laboratory conditions", Ceramic-silikaty, 46(3), pp.97-103

Hardjito, D., S.E. Wallah, D.M. J. Sumajouw, & B.V. Rangan (2004*a*), "On The Development of Fly Ash-Based Geopolymer Concrete", ACI Materials Journal, Accepted for publication

Hardjito, D., S.E. Wallah, D.M. J. Sumajouw & B.V. Rangan (2004*b*), "The Stress-Strain Behaviour of Fly Ash-Based Geopolymer Concrete", in ACMSM 18,A.A. Balkema Publishers - The Netherlands, Perth, Australia

Hardjito, D., S.E. Wallah, D.M. J. Sumajouw & B.V. Rangan (2004*c*), "Factors influencing the compressive strength fly-ash based geopolymer concrete", Jurusan Teknik Sipil, Fakultas Teknik Sipil dan Perencanaan – Universitas Kristen Petra, Vol. 6, No. 2, pp.88-96

Hardjito, D., S.E. Wallah, D.M. J. Sumajouw & B.V. Rangan (2003*a*), "Geopolymer Concrete: Turn Waste into Environmentally Friendly Concrete", Presented at the International Conference on Recent Trends in Concrete Technology and Structures (INCONTEST), Coimbatore, India, Kumaraguru College of Technology

Hardjito, D., S.E. Wallah, D.M. J. Sumajouw & B.V. Rangan (2003*b*), "Properties of fly ash-based Geopolymer Concrete: Influence of mixture composition and curing temperature", Presented at the Ninth East Asia-Pacific Conference on Structural Engineering and Construction (EASEC), Bali, Indonesia

Hardjito, D., S.E. Wallah, and B.V. Rangan (2002), "Study on Engineering Properties of Fly ash-based Geopolymer Concrete", Journal of the Australasian Ceramic Society, Vol. 38, pp. 44-47

Heath, C. O. Jr., and N.R. Brandenburg (1953), "Pozzolanic properties of several Oregon pumicites", Oregon State College Engineering Experiment Station Bulletin, 34, pp. 5–26

Hemmings, R.T., E.E. Berry, W.S. Langley, G.G. Carette (1989), "Beneficiated flyash: hydration, microstructure and strength development in Portland cement", In: Proceedings of the First International Conference on Fly ash, Silica Fume, Slag and Natural Pozzolans in Concrete, SP-114, Detroit, USA, pp. 241-273

Hendricks, W.M., A.T. Bell, C.J. Radke (1991), "Effect of organic and alkali metal cations on the distribution of silicate anions in aqueous solutions", Journal of Physical Chemistry 95, pp. 9513–9518

Hos, J.P., P.G. McCormick, and L.T. Byrne (2002), "Investigation of a Synthetic Aluminosilicate Inorganic Polymer", Journal of Material Science, 37, pp. 2311-2316

Iller, R.K., (1979), "The chemistry of silica — solubility, polymerization, colloid and surface properties, and biochemistry", John Wiley and Sons, New York

Jawed, I., and J. Skalny (1983), "The influence of alkali sulphates on the properties of cement and concrete", World Cement, No. 11, pp. 325–330

Jawed, I., and J. Skalny (1978), "Alkalis in cement: a review, II. Effects of alkalis on hydration and performance of Portland cement", Cement and Concrete Research, 8, pp. 37–52

Johansen, V., (1976), "Influence of alkalis on the strength development", In The effect of alkalis on the properties of concrete, London, pp. 81–97

Kaewmanee, K., and H. Okamura (2001), "A New Testing Method For Creep Behaviour of Self-Compacting Concrete Early Age", A dissertation submitted to Kochi University of Technology in partial fulfilment of the requirement for the degree of master of engineering

Khan, M. I., and C.J. Lynsdale (2002), "Strength, permeability, and carbonation of high-performance concrete", Cement and Concrete Research. 32, pp. 123-131

Korneev, V.L., V.V. Danilov, A.S. Brykov, E.Yu. Aleshunina (2000), "Acid-proof Formulation Based on Hydrated Sodium Silicate Powder", Russian Journal of Applied Chemistry, Vol. 73, No. 10, pp.1691

Kriven, W. M., J.L. Bell, M. Gordon, S. Mallicoat (2003), "Microstructure and microchemistry of fully reacted geopolymers and geopolymer matrix composites", Ceramic Transactions, 153, pp. 227-252

Laney, B.E., (1993), "Geopolymer-modified gypsum-based construction materials", U.S. Patent no. 5,194,091

Larew, H.G., (1976), "The use of volcanic ash compounds for construction projects in Iceland", Report No.CE-3447-101-76, Department of Civil Engineering, University of Virginia

Lea, F.M., (1988), "The chemistry of cement and concrete", 3rd and 4th Edition, Edward Arnold, New York, 1974

Lea, F.M., (1983), "The chemistry of pozzolans", In Proceedings of 3rd Symposium on the Chemistry of Cements, Stockholm, pp. 460–490

Lee, W. K. W., and J.S.J. Van Deventer (2004), "The interface between natural siliceous aggregates and geopolymers", Cement and Concrete Research, 34, pp. 195-206

Lee, W. K. W., & J.S.J. Van Deventer (2003*a*), "The interface between natural siliceous aggregates and geo-polymers", Cement and Concrete Research 34, Issue 2, pp. 195-206

Lee, W.K.W., J.S.J. Van Deventer (2003*b*), "Use of infrared spectroscopy to study geopolymerization of heterogeneous amorphous aluminosilicates", Langmuir, 19, pp. 8726-8734

Lee, W.K.W., J.S.J. Van Deventer (2002*a*), "The effects of inorganic salt contamination on the strength and durability of geopolymers", Colloid and Surfaces: A 211, pp. 115–126

Lee, W.K.W., J.S.J. Van Deventer (2002*b*), "The effect of ionic contaminants on the early-age properties of alkali-activated fly ash-based cements", Cement and Concrete Research, 32, pp. 577–584

Liji, Y., (1991), "Alkali-activated slag cement based radioactive waste forms". Cement and Concrete Research, Vol. 21, pp. 16-20

Maghsoudi, A.A., (2001), "Kerman Pozzolans", University of Bahonar, Kerman, Iran (in Farsi)

Malek, R.I.A., D.M. Roy, (1996), "The Permeability of Chloride Ions in Fly Ash-Cement Pastes, Mortars and Concrete", MRS Symposium, Material Research Society, Pittsburgh, Vol. 113, pp.291-300

Malhotra, V. M., (2002*a*), "High-Performance High-Volume Fly Ash Concrete", ACI Concrete International, vol. 24, no. 7, pp. 1-5

Malhotra, V. M., (2002*b*), "Introduction: Sustainable Development and Concrete Technology", ACI Concrete International, vol. 24, no. 7, pp. 22

Malhotra, V. M., (1999), "Making Concrete "Greener" With Fly Ash", ACI Concrete International, vol. 21, no. 5, pp. 61-66

Malone, P.G., T. Kirkpatrick, C.A. Randall (1986), "Potential applications of alkali-activated alumino-silicate binders in military operations", Report WESrMPrGL-85-15, U.S. Army Corps of Engineers, Vicksburg, MI

Malquori, G., (1960), "Portland–pozzolan cement", In Proceedings of 4th International Symposium on the Chemistry of Cement, Washington, Vol. II, pp. 983–1000

Massazza, F., (2003), "Structures and Performance of Cements", University of Sheffield, England

McCormick, A.V., A.T. Bell, C.J. Radke (1989*a*), "Evidence from alkali-metal NMR spectroscopy for ion pairing in alkaline silicate solutions", Journal of Physical Chemistry, 93 _5, pp. 1733–1737

McCormick, A.V., A.T. Bell, C.J. Radke (1989*b*), "Influence of alkali-metal cations on silicon exchange and silicon-29 spin relaxation in alkaline silicate solutions", Journal of Physical Chemistry, 93 _5, pp. 1737–1741

McCormick, A.V., A.T. Bell, C.J. Radke (1989*c*), "Multinuclear NMR investigation of the formation of aluminosilicate anions", Journal of Physical Chemistry, 93 _5, pp. 1741–1744

McDonald, M., J.L. Thompson (2004), "Sodium Silicate a Binder for the 21st Century", National Silicates and PQ Corporation of Industrial Chemicals Division

Mielenz, R.C., L.P. Witte, and O.J. Glantz (1950), "Effect of calcinations on natural pozzolans", In Proceedings of symposium on use of pozzolanic materials in mortars and concretes, ASTM STP-99, San Francisco, pp. 43–91

Millers, J.G., and T.D. Oulton (1970), "Proto-tropy in kaolinite during percussive grinding", Clay and Clay Minerals, 18, pp. 313–323

Milestone, Neil. B., (1978), "A rapid method for estimating the reactivity of pozzolanic materials", Report No. C.D.2273, Department of Scientific and industrial research, New Zealand

Moran, W.T., and J.L. Gilliland (1950), "Summary of methods for determining pozzolanic activity", In Proceedings of symposium on use of pozzolanic materials in mortars and concretes, ASTM STP-99, San Francisco, pp. 109–131

Mortureux, B., H. Hornain, E. Qautier, and M. Regourd (1980), "Comparison of the reactivity of different pozzolans", In Proceedings of the 7th international congress on the chemistry of cement and concrete, Paris, pp. IV/110–115

Murat, M., M. Driouche (1988), "Chemical reactivity of thermally activated clay minerals: Estimation by dissolution in hydrofluoric acid", Cement and Concrete Research, 18, pp. 221- 228

Neville, A. M., (1995), "Properties of Concrete", Essex, England, Pearson Educational Limited

Nickel, E.H., M.C. Nichols (1991), "Mineral Reference Manual", Van Nostrand-Reinhold, New York

Nord Test Method: Bulk Diffusion Test (NordTest NTBuild 443) (1995), Nordtest, Espoo, Finland, Proj. 443-94

Ortega, E. A., C. Cheeseman, J. Knight, M. Loizidou (2000), "Properties of alkali-activated clinoptilolite", Cement and Concrete Research, 30, pp. 1641-1646

Ozyildirim, C., (1994), "Rapid Chloride Permeability Testing of Silica-Fume Concrete", Cement Concrete and Aggregates, CCAGPD, Vol. 16, No. 1, pp. 53-56

Palomo, A., J.I. Lo´pez de la Fuente (2003), "Alkali-activated cementitous materials: Alternative matrices for the immobilisation of hazardous wastes Part I. Stabilisation of boron", Cement and Concrete Research, 33, pp. 281–288

Palomo, A., S. Alonso (2000), "Recycling fly ashes for making precast components", 2nd International Symposium on Prefabrication, Concrete Association of Finland, Helsinki, Finland, pp. 50– 61

Palomo, A., M.T. Blanco-Varela, M.L. Granizo, F. Puertas, T. Vazquez, and M.W. Grutzeck (1999*a*), "Chemical stability of cementitious materials based on metakaolin", Cement and Concrete Research, Vol. 29, pp. 997-1004

Palomo, A., M.W. Grutzeck, and M.T. Blanco (1999*b*), "Alkali-activated fly ashes, a cement for the future", Cement and Concrete Research, Vol. 29, pp. 1323-1329

Palomo, A., F. Puertas, M.T. Blanco, ML. Granizo (1997), "Alkaline activation of metakaolin: influence of synthesis parameters, In Proceeding of the Tenth International Congress on Chemistry of Cement, Goteborg, Vol. 3, pp. 3-113

Palomo, A., A. Macias, M.T. Blanco, F. Puertas (1992), "Physical, chemical and mechanical characterisation of geopolymers", Proceedings of the 9th International Congress on the Chemistry of Cement, pp. 505–511

Phair, J.W., J.S.J. Van Deventer (2001), "Effect of silicate activator pH on the leaching and material characteristics of waste-based inorganic polymers", Mineral Engineering 14, pp. 289– 304

Popovics, S., (1992), "Concrete materials: Properties, Specifications and Testing", 2nd edition Noyes Data Corp., Park Ridge, NJ, USA

Pu, X. (1999), "Investigation on pozzolanic effect of mineral additives in cement and concrete by specific strength index", Cement and Concrete Research 29, pp. 951-955

Puertas, F., T. Amat, A. Ferna´ndez-Jime´nez, T. Va´zquez (2003), "Mechanical and durable behaviour of alkaline cement mortars reinforced with polypropylene fibres", Cement and Concrete Research, 33, pp. 2031–2036

Puertas, F., S. MartõÂnez-RamõÂrez, S. Alonso, T. VaÂzquez (2000), "Alkali-activated fly ash/slag cement Strength behaviour and hydration products", Cement and Concrete Research, 30, pp. 1625-1632

Qing-Hua, C., and S.L. Sarkar (1994), "A study of rheological and mechanical properties of mixed alkali activated slag pastes", Advanced Cement Based Materials 1, pp. 178-184

Rahier, H., M. Biesemans, B. Van Mele, J. Wastiels, X. Wu (1996), "Low-temperature synthesized aluminosilicate glasses: Part I. Low-temperature reaction stoichiometry and structure of a model compound", Journal of Material Science, 31, pp. 71–79

Ramezanianpour, A.A., A. Ghazimoradi (1992), "Evaluation of pozzolans of Iran", Building and Housing Research Center (in Farsi)

Ramezanianpour, A.A., J.G. Cabrera (1987), "Engineering properties and durability of mortars and concretes", Ph.D Thesis, Leeds University, 1987

Rossi, G., and L. Forchielli (1976), "Porous structure and reactivity with lime of some natural Italian pozzolans", Il Cemento, 76, pp. 215–221

Rowles, M. and B. O'Connor (2003), "Chemical optimisation of the compressive strength of aluminosilicate geopolymers synthesised by sodium silicate activation of metakaolinite", Journal of Materials Chemistry, Vol. 13, 2003, pp. 1161-1165

Roy, D. M., (1999), "Alkali-Activated Cements, Opportunities and Challenges". Cement and Concrete Research, Vol. 29, No. 2, pp. 249-254

Roy, D. M., and M.R. Silsbee (1992), "Alkali activated cementitious materials: An overview", Materials Research Society Proceedings

Scian, A.N., J.M.P. Lopez, and E. Pereira (1991), "Mechanochemical activation of high alumina cements — hydration characteristics", Cement and Concrete Research, 21, pp. 51–60

Shetty, M.S., (1982),"Concrete Technology", Published by S. Chand & Company Ltd, Ram Nagar, New Delhi

Shi, C., P.V. Krivenko, D. Roy (2006), "Alkali-Activated Cement and Concretes", Taylor & Francis, London and New York

Shi, C., (2004), "Effect of mixing proportions of concrete on its electrical conductivity and the rapid chloride permeability test (ASTM C1202 or AASHTO T277) results", Cement and Concrete Research, 34, pp. 537-545

Shi, C., (2001), "An Overview on the activation of reactivity of natural pozzolans", Canadian Journal of Civil Engineering, Vol. 28, pp. 778-786

Shi, C., and R.L. Day (2001), "Comparison of different activation methods for enhancing reactiovity of pozzolans", Cement and Concrete Research, 31, pp. 813–818

Shi, C., and R.L. Day (2000*a*), "Pozzolanic reactions in the presence of chemical activators — part I: reaction kinetics", Cement and Concrete Research, 30, pp. 51–58

Shi, C., and R.L. Day (2000*b*), "Pozzolanic reactions in the presence of chemical activators — part II: reaction mechanisms", Cement and Concrete Research. 30, pp. 607–613

Shi, C., J. Qian (2000*c*), "High performance cementing materials from industrial slags — a review", Resources, Conservation and Recycling, 29, pp. 195–207

Shi, C., and R.L. Day (1996*a*), "Some factors affecting early hydration of alkali-activated slag cement", Cement and Concrete Research, Vol. 26, No. 3, pp. 439-441

Shi, C., and R.L. Day (1996*b*), "Strength, Pore structure and Permeability of Alkali-activated Slag Mortars", Cement and Concrete Research, Vol. 26, No. 12, pp. 1789-1799

Shi, C., and R.L. Day (1993*a*), "Acceleration of strength gain of lime–natural pozzolan cements by thermal activation", Cement and Concrete Research, 23, pp. 824–832

Shi, C., and R.L. Day (1993*b*), "Chemical activation of blended cement made with lime and natural pozzolans", Cement and Concrete Research, 23, pp. 1389–1396

Shi, C., X. Wu, and M. Tang, (1993*c*), "Research on alkaliactivated cementitious systems in China", Advances in Cement and Concrete Research, 5(17), pp. 1–7

Shi, C., (1992*a*), "Activation of natural pozzolans, fly ashes and blast furnace slag", Ph.D. Thesis, The University of Calgary, Calgary, Alta

Shi, C., R.L. Day, X. Wu, and M. Tang (1992*b*), "Comparison of the microstructure and performance of alkali-slag and Portland Cement pastes", In Proceedings of 9th international congress on the chemistry of cement, New Delhi, Vol. III, pp. 298–304

Shi, C., (1987), "An investigation of the activation of Granulated Phosphorus slag", M. Sc. Thesis, Nanjing Institute of Tekology (innChinese), 75p

Sun, W., Y. Zhang, W. Lin, Z. Liu (2004), "In situ monitoring of the hydration process of K-PS geopolymer cement with ESEM", Cement and Concrete Research, 34, pp. 935–940

Swaddle, T.W., J. Salerno, P.A. Tregloan (1994), "Aqueous aluminates, silicates, and aluminosilicates", Chemistry Society Review, pp. 319–325

Swanepoel, J. C. & C.A. Strydom (2002), "Utilisation of fly ash in a geopolymeric material", Applied Geochemistry, Vol. 17, No. 8, pp. 1143-1148

Takemoto, K., and H. Uchikawa (1980), "Hydration of pozzolanic cement", In Proceedings of 7th international congress on the chemistry of cement, Paris, Vol. 1 (Principal Reports), pp. 2/1–2/29

Tang, X. and C. Shi (1988), "Silicate Construction Products (in Chinese)", No. 1, pp. 28-32

Taylor H., (1997), "Cement Chemistry", Second edition, Thomas Telford, London

Teixeira-Pinto, A., P. Fernandes, and S. Jalali (2002), "Geopolymer manufacture and application - main problems when using concrete technology", presented at the Geopolymers 2002 International Conference, Melbourne, Australia, Siloxo Pty. Ltd

Turanli, L., B. Uzal, F. Bektas (2004), "Effect of material characteristics on the properties of blended cements containing high volumes of natural pozzolans", Cement and Concrete Research, 34, pp. 2277-2282

Turriziani, R., (1964), "Aspects of chemistry of pozzolans in the chemistry of cements", Edited by H.F.W. Taylor, Academic Press, London and New York, Vol. 2, pp. 69–86

Van Brakel, J., (1981), "A special issue devoted to mercury Porosimetry", Powder Technology 29 (1), pp. 1-209

Van Jaarsveld, J.G.S., J.S.J. Van Deventer, and G.C. Lukey (2002), "The effect of composition and temperature on the Properties of fly Ash and kaolinite-based geopolymers", Chemical Engineering Journal, Vol. 89, pp. 63-73

Van Jaarsveld, J.G.S., J.S.J. Van Deventer (1999*a*), "Effect of alkali metal activator on the properties of fly ash based geopolymers", Industrial Engineering Chemistry Research, 38, pp. 3932–3941

Van Jaarsveld, J.G.S., J.S.J. Van Deventer, A. Schwartzman (1999*b*), "The potential use of geo-polymeric materials to immobilise toxic metals: Part II: Material and leaching characteristics", Minerals Engineering, 12, pp. 75– 91

Van Jaarsveld, J.G.S., J.S.J. Van Deventer, A. Schwartzman (1999*c*), "The potential use of geopolymeric materials to immobilise toxic metals: Part II. Material and leaching characteristics", Minerals Engineering, 12 _1, pp. 75–91

Van Jaarsveld, J.G.S., J.S.J. Van Deventer, L. Lorenzen (1998), "Factors affecting the immobilisation of metals in geopolymerised fly ash", Metallurgical and Materials Transactions B 29B, pp. 283–291

Van Jaarsveld, J.G.S., J.S.J. Van Deventer, L. Lorenzen (1997), "The potential use of geopolymeric materials to immobilise toxic metals: Part I. Theory and applications", Mineral Engineering, 10 _7, pp. 659–669

Wallah, S.E., B.V. Rangan (2006), "Low-Calcium Fly Ash-Based Geopolymer Concrete: Long-Term Properties", Research Report GC2, Faculty of Engineering, Curtin Technology, Perth

Wallah, S. E., D. Hardjito, D.M.J. Sumajouw, & B.V. Rangan (2004*a*), "Creep Behaviour of Fly Ash-Based Geopolymer Concrete", in Seventh CANMET/ACI International Conference on Recent Advances in Concrete Technology, Supplementary Papers, Las Vegas, USA, pp. 49-60

Wallah, S. E., D. Hardjito, D.M.J. Sumajouw, & B.V. Rangan (2004*b*), "Geopolymer Concrete: A Key for Better Long-Term Performance and Durability", in International Conference on Fibre Composites, High Performance Concretes and Smart Materials, Vol. I, ed. V. S. Parameswaran, Chennai, India, pp. 527-539

Wallah, S. E., D. Hardjito, D.M.J. Sumajouw, & B.V. Rangan (2003), "Sulfate resistance of fly ash-based geopolymer concrete", presented at the Concrete in The Third Millenium, in 21st Biennial Conference of The Concrete Institute of Australia, Brisbane, Queensland, Australia

Wang, S., K.L. Scrivener, P.L. Pratt (1994), "Factors affecting the strength of alkali-activated slag", Cement and Concrete Research, Vol.24, No. 6, pp. 1033-1043

Xiaodong, S., Y. Sheng, W. Xuequan, T. Mingshu, Y. Liji (1994), "Immobilization of simulated high level wastes into AASC waste form" Cement and Concrete Research, Vol. 24, pp. 133-138

Xiea, Z., Y. Xib (2001), "Hardening mechanisms of an alkaline-activated class F fly ash", Cement and Concrete Research, 31, pp. 1245–1249

Xu, H., J.S.J. Van Deventer (2003), "The effect of alkali metals on the formation of geopolymeric gels from alkali-feldspar", Colloids and Surfaces A: Physicochemistry Engineering Aspects, Vol. 216, pp. 27-44

Xu, H., J.S.J. Van Deventer (2002*a*), "Micro-structural characterisation of geopolymers synthesised from kaolinite/stilbite mixtures using XRD, MAS-NMR, SEM/EDX, TEM/EDX, and HREM", Cement and Concrete Research 32, pp. 1705-1716

Xu, H., J.S.J. Van Deventer (2002*b*), "Geopolymerisation of multiple minerals", Minerals Engineering, Vol. 15, pp. 1131-1139

Xu, H., J.S.J. Van Deventer (2002*c*), "Micro-structural characterisation of geopolymers synthesised from kaolinite/stilbite mixtures using XRD, MAS-NMR, SEM/EDX, TEM/EDX, and HREM", Cement and Concrete Research, 32, pp. 1705-1716

Xu, H., J.S.J. Van Deventer (2000), "The geopolymerisation of aluminosilicate minerals", International Journal of Mineral Processing, Vol. 59, pp. 247-266

Yip, C.K., G.C. Lukey, J.S.J. Van Deventer (2005), "The coexistence of geo-polymeric gel and calcium silicate hydrate at the early stage of alkaline activation", Cement and Concrete Research, 35, pp. 1688-1697

Zuhua, Z., Y. Xiao, Z. Huajun, C. Yue (2009), "Role of water in the synthesis of calcined kaolin-based geopolymer", Applied Clay Science, 43, pp. 218–223

APPENDIX

Table A7.1 Relation between splitting tensile strength and compressive strength

Mix-Curing	Correlation Coefficient	Equation of power regression
CM1-20Sealed	0.927	$Y=0.23X^{0.69}$
CM1-20Fog	0.937	$Y=1.23X^{0.2}$
CM2-20Sealed	0.999	$Y=0.44X^{0.45}$
CM2-20Fog	0.987	$Y=1.43X^{0.1}$
ATAF1-20Sealed	0.924	$Y=0.07\ X^{1.12}$
ATAF1-20Fog	0.913	$Y=0.03X^{1.54}$
ATAF1-40Sealed	0.848	$Y=0.15X^{0.88}$
ATAF1-40Fog	0.868	$Y=0.26X^{0.73}$
ATAF1-60Sealed	0.964	$Y=0.06X^{0.94}$
ATAF1-60Fog	0.942	$Y=0.57X^{0.45}$
ATAF2-20Sealed	0.947	$Y=0.13X^{0.71}$
ATAF2-20Fog	0.963	$Y=0.07X^{1.16}$
ATAF2-40Sealed	0.922	$Y=0.03X^{1.29}$
ATAF2-40Fog	0.841	$Y=0.05X^{1.12}$
ATAF2-60Sealed	0.981	$Y=0.15X^{0.66}$
ATAF2-60Fog	0.976	$Y=1.52X^{0.19}$
ATAF	0.511	$Y=0.13X^{0.85}$
ARSH-60Sealed	0.900	$Y=0.04X^{0.96}$
ACSH-20Sealed	0.983	$Y=0.08X^{0.83}$
ASH	0.874	$Y=0.06X^{0.9}$
Alkali activated natural pozzolans	0.502	$Y=0.1X^{0.9}$

X is cube compressive strength (MPa) and Y is splitting tensile strength (MPa)

Table A7.2 Relation between static modulus of elasticity and cube compressive strength

Mix-Curing	Correlation Coefficient	Equation of power regression
CM1-20Sealed	0.909	$Y=7.41X^{0.37}$
CM1-20Fog	0.998	$Y=0.78X$
CM2-20Sealed	0.931	$Y=9.91X^{0.28}$
CM2-20Fog	0.980	$Y=8.16X^{0.34}$
ATAF1-20Sealed	0.847	$Y=0.10X^{1.73}$
ATAF1-40Sealed	0.846	$Y=2.42X^{0.70}$
ATAF1-40Fog	0.942	$Y=0.27X^{2.06}$
ATAF1-60Sealed	0.786	$Y=0.08X^{1.59}$
ATAF2-20Sealed	0.835	$Y=1.14X^{0.74}$
ATAF2-40Sealed	0.797	$Y=1.89X^{0.69}$
ATAF2-40Fog	0.912	$Y=0.43X^{1.18}$
ATAF2-60Sealed	0.134	$Y=5.13X^{0.45}$
ATAF	0.686	$Y=0.54X^{1.09}$
ARSH-60Sealed	0.918	$Y=1.99X^{0.52}$
ACSH-20Sealed	0.991	$Y=1.50X^{0.86}$
ASH	0.673	$Y=1.53X^{0.73}$
Alkali activated natural pozzolans	0.682	$Y=X^{0.9}$

X is cube compressive strength (MPa) and Y is static modulus of elasticity (GPa)

Table A7.3 Relation between static modulus of elasticity and cylinder compressive strength

Mix-Curing	Correlation Coefficient	Equation of power regression
ATAF1-20Sealed	0.944	$Y=0.16X^{1.72}$
ATAF1-40Sealed	0.846	$Y=3.58X^{0.63}$
ATAF1-40Fog	0.905	$Y=0.32X^{1.39}$
ATAF1-60Sealed	0.938	$Y=0.07X^{1.73}$
ATAF2-20Sealed	0.836	$Y=1.24X^{0.77}$
ATAF2-40Sealed	0.792	$Y=2.75X^{0.62}$
ATAF2-40Fog	0.949	$Y=1.21X^{0.95}$
ATAF2-60Sealed	0.958	$Y=3.29X^{0.66}$
ATAF	0.691	$Y=1.03X^{0.97}$
ARSH-60Sealed	0.921	$Y=2.62X^{0.47}$
ACSH-20Sealed	0.992	$Y=2.48X^{0.76}$
ASH	0.686	$Y=2.28X^{0.66}$
Alkali activated natural pozzolans	0.696	$Y=1.61X^{0.82}$

X is cylinder compressive strength (MPa) and Y is static modulus of elasticity (GPa)

Table A7.4 Relation between static modulus of elasticity and splitting tensile strength

Mix-Curing	Correlation Coefficient	Equation of power regression
CM1-20Sealed	0.750	$Y=15.54X^{0.66}$
CM1-20Fog	0.933	$Y=1.64X^{2.86}$
CM2-20Sealed	0.916	$Y=19.2X^{0.44}$
CM2-20Fog	0.998	$Y=3.65X$
ATAF1-20Sealed	0.849	$Y=6.88X^{1.47}$
ATAF1-40Sealed	0.562	$Y=14.1X^{0.6}$
ATAF1-40Fog	0.855	$Y=1.76X^{2.49}$
ATAF1-60Sealed	0.599	$Y=12.73X^{0.96}$
ATAF2-20Sealed	0.732	$Y=9.17X$
ATAF2-40Sealed	0.733	$Y=10.53X^{0.7}$
ATAF2-40Fog	0.445	$Y=12.42X^{0.7}$
ATAF2-60Sealed	0.105	$Y=20.62X^{0.41}$
ATAF	0.630	$Y=10.89X^{0.84}$
ARSH-60Sealed	0.808	$Y=10.66X^{0.33}$
ACSH-20Sealed	0.941	$Y=20.39X^{0.97}$
ASH	0.665	$Y=16.03X^{0.81}$

X is splitting tensile strength (MPa) and Y is static modulus of elasticity (GPa)

Table A8.1 Relation between oxygen permeability and compressive strength

Mix-Curing	Correlation Coefficient	Equation of power regression
CM1-20Sealed	0.980	$Y=54032X^{-2.35}$
CM2-20Sealed	0.996	$Y=444.82X^{-0.97}$
OPC	0.83	$Y=1923.2X^{-1.4}$
ATAF1-20Sealed	0.996	$Y=6493.2X^{-2.13}$
ATAF1-40Sealed	0.981	$Y=261162X^{-3.35}$
ATAF1-40Fog	0.999	$Y=2x10^{11}X^{-7.56}$
ATAF1-60Sealed	0.904	$Y=3x10^{10}X^{-6.45}$
ATAF2-20Sealed	0.996	$Y=1876X^{-1.79}$
ATAF2-40Sealed	0.97	$Y=545.66X^{-1.29}$
ATAF2-40Fog	0.966	$Y=41127X^{-2.73}$
ATAF2-60Sealed	0.999	$Y=103488X^{-2.95}$
ATAF	0.872	$Y=4307.3X^{-2.06}$
ARSH-60Sealed	1.0	$Y=1160.7X^{-1.56}$
ACSH-20Sealed	0.943	$Y=2971X^{-1.96}$
ASH	0.94	$Y=2097.9X^{-1.8}$
Alkali activated natural pozzolans	0.887	$Y=3365.5X^{-1.98}$

X= Cubic compressive strength of concrete (MPa); Y = Oxygen permeability x $10^{-17}(m^2)$

Table A8.2 Relation between chloride permeability and compressive strength

Mix-Curing	Correlation Coefficient	Equation of power regression
CM1-20Sealed	0.990	$Y=7183.6e^{-0.03X}$
CM2-20Sealed	0.892	$Y=6382.3e^{-0.02X}$
OPC	0.937	$Y=6611.4e^{-0.02X}$
ATAF1-20Sealed	0.999	$Y=13161e^{-0.05X}$
ATAF1-40Sealed	0.952	$Y=12350e^{-0.04X}$
ATAF1-40Fog	0.837	$Y=30526e^{-0.09X}$
ATAF1-60Sealed	0.995	$Y=201389e^{-0.12X}$
ATAF2-20Sealed	0.998	$Y=12898e^{-0.05X}$
ATAF2-40Sealed	0.744	$Y=74207e^{-0.03X}$
ATAF2-40Fog	0.919	$Y=9817.2e^{-0.03X}$
ATAF2-60Sealed	0.953	$Y=57767e^{-0.1X}$
ATAF	0.741	$Y=10597e^{-0.04X}$
ARSH-60Sealed	0.999	$Y=12707e^{-0.04X}$
ACSH-20Sealed	0.991	$Y=10424e^{-0.03X}$
ASH	0.969	$Y=11141e^{-0.04X}$
Alkali activated natural pozzolans	0.795	$Y=10731e^{-0.04X}$

X= Cubic compressive strength of concrete (MPa); Y = Chloride permeability (coulombs)

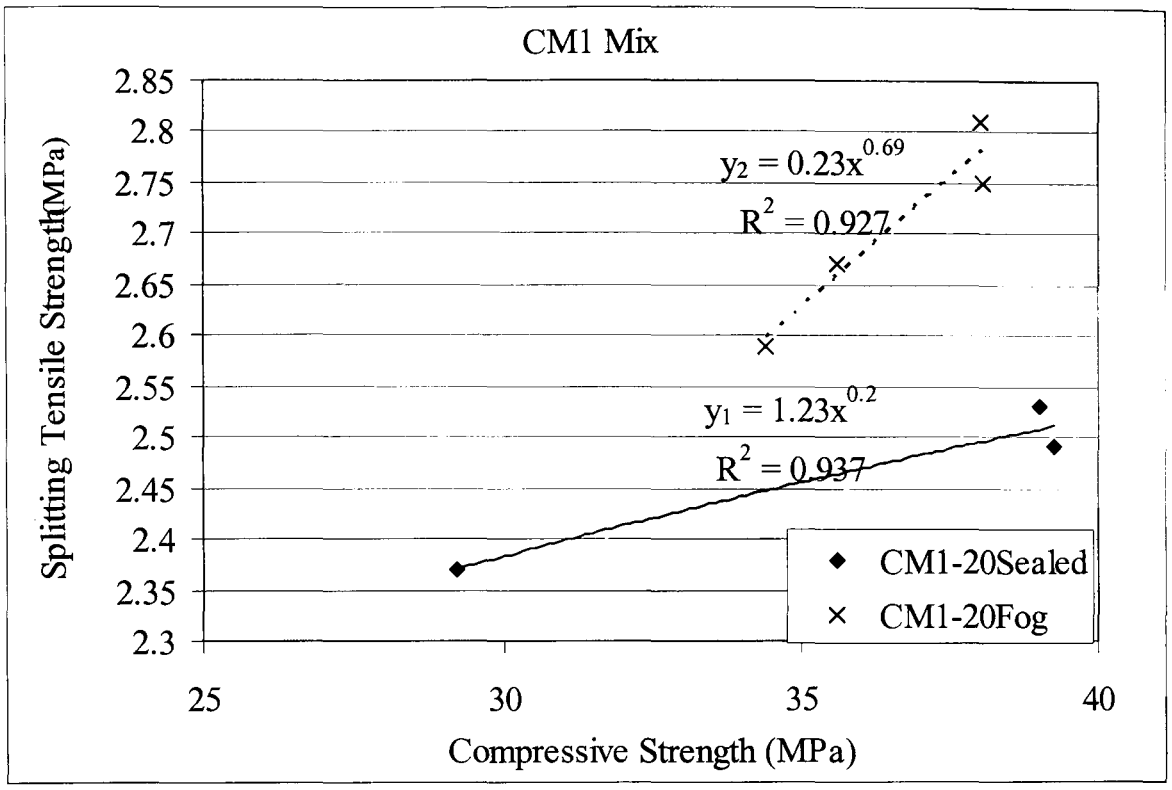

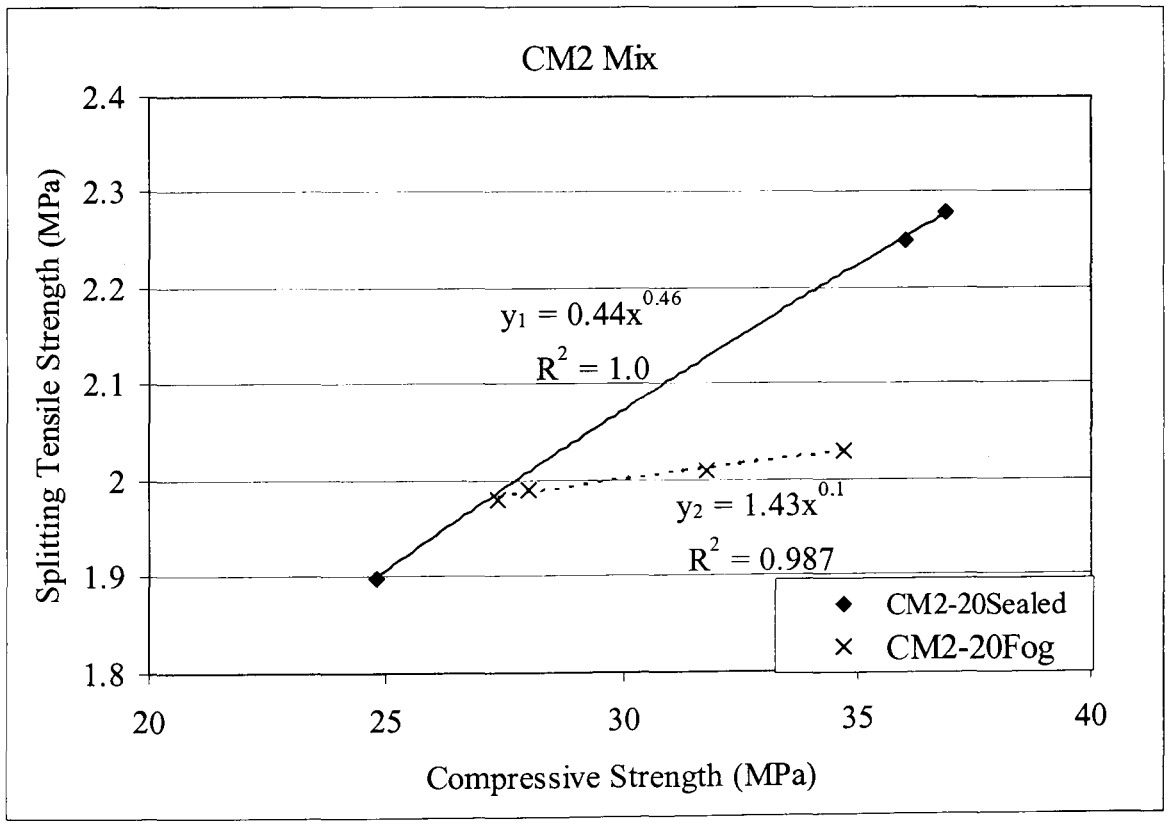

Figure A7.1 Relation between the splitting strength and the compressive strength of CM1 and CM2 under different curing conditions

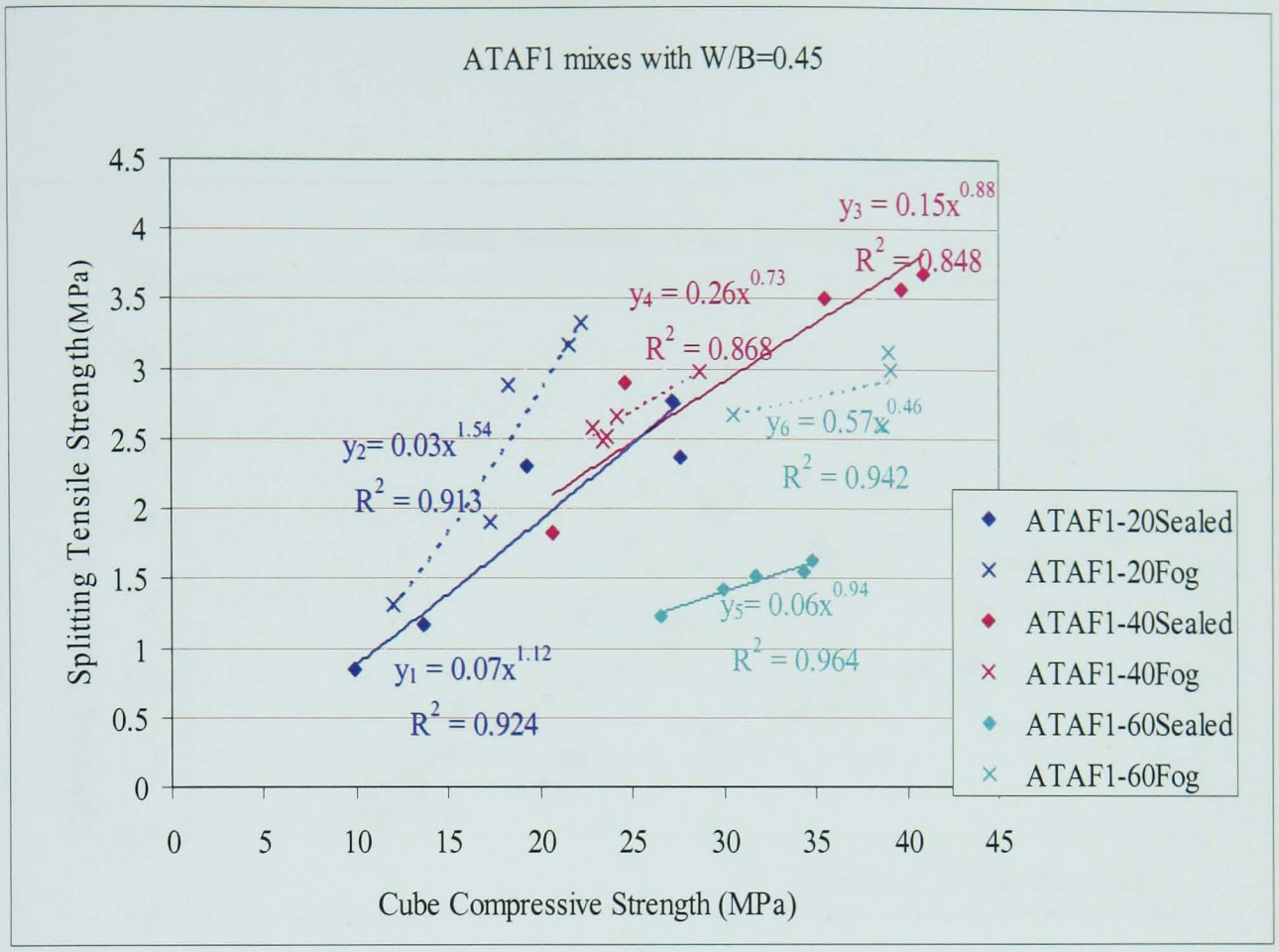

Figure A7.2 Relation between the splitting strength and the compressive strength of ATAF1 and ATAF2 under different curing conditions

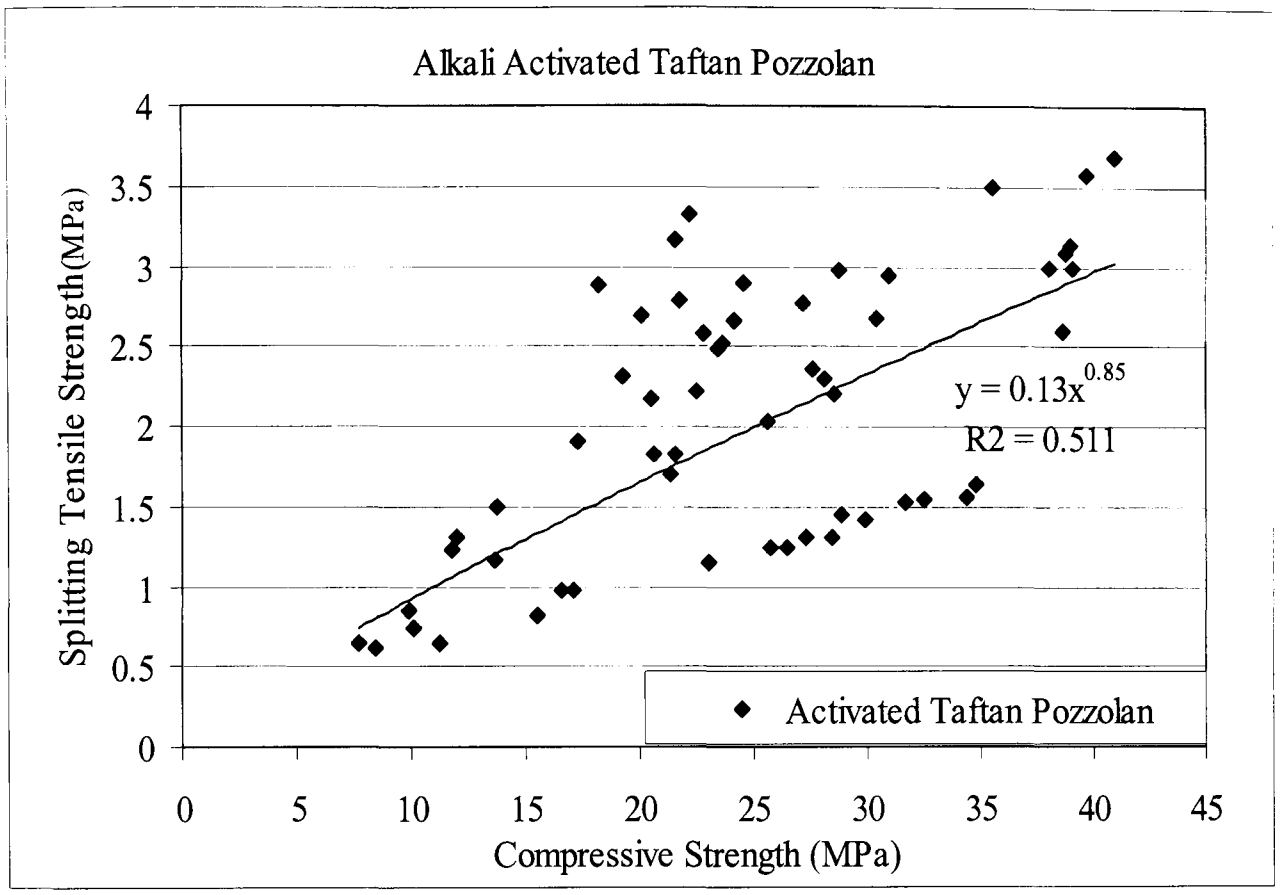

Figure A7.3 Relation between the splitting tensile strength and the compressive strength of activated Taftan Pozzolan

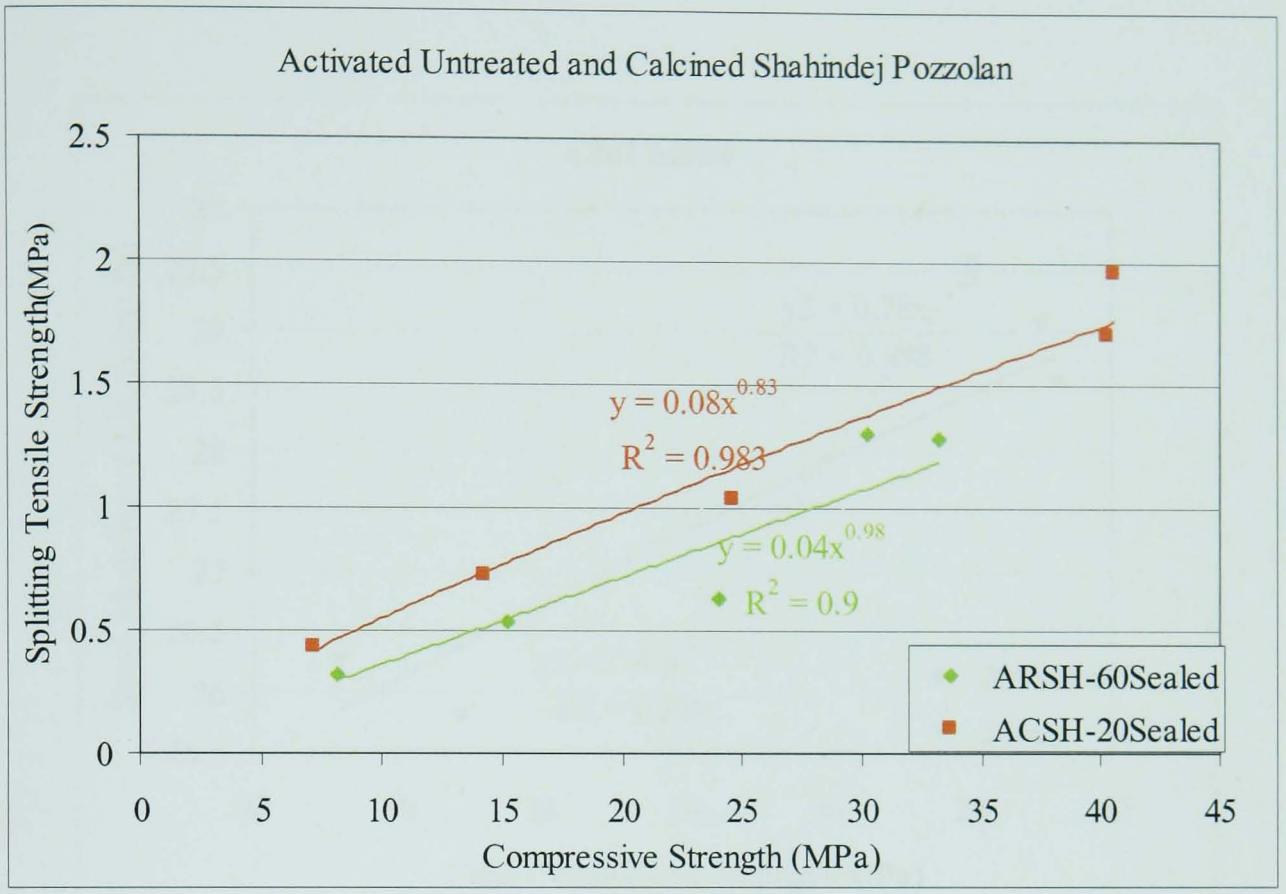

Figure A7.4 Relation between the splitting tensile strength and the compressive strength of ARSH and ACSH mixes

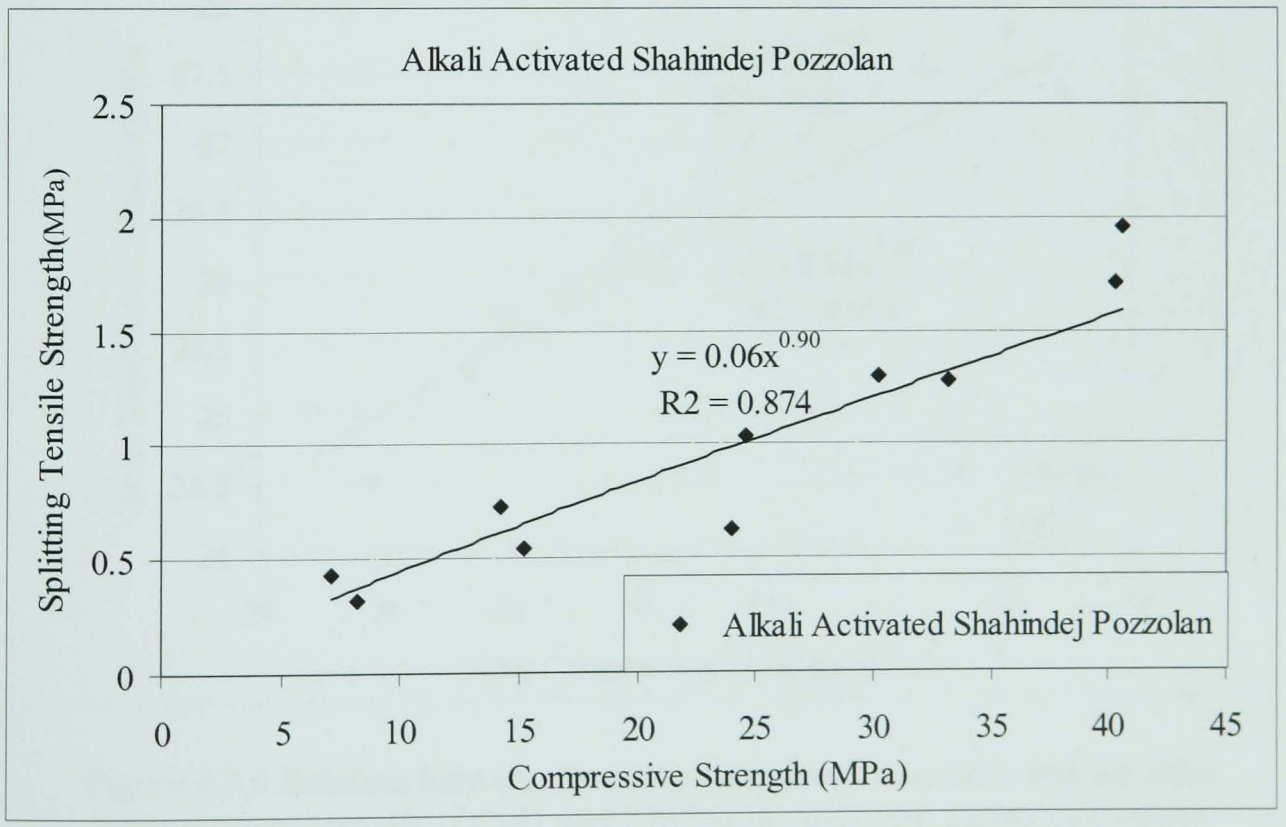

Figure A7.5 Relation between the splitting tensile strength and the compressive strength of alkali activated Shahindej mixes

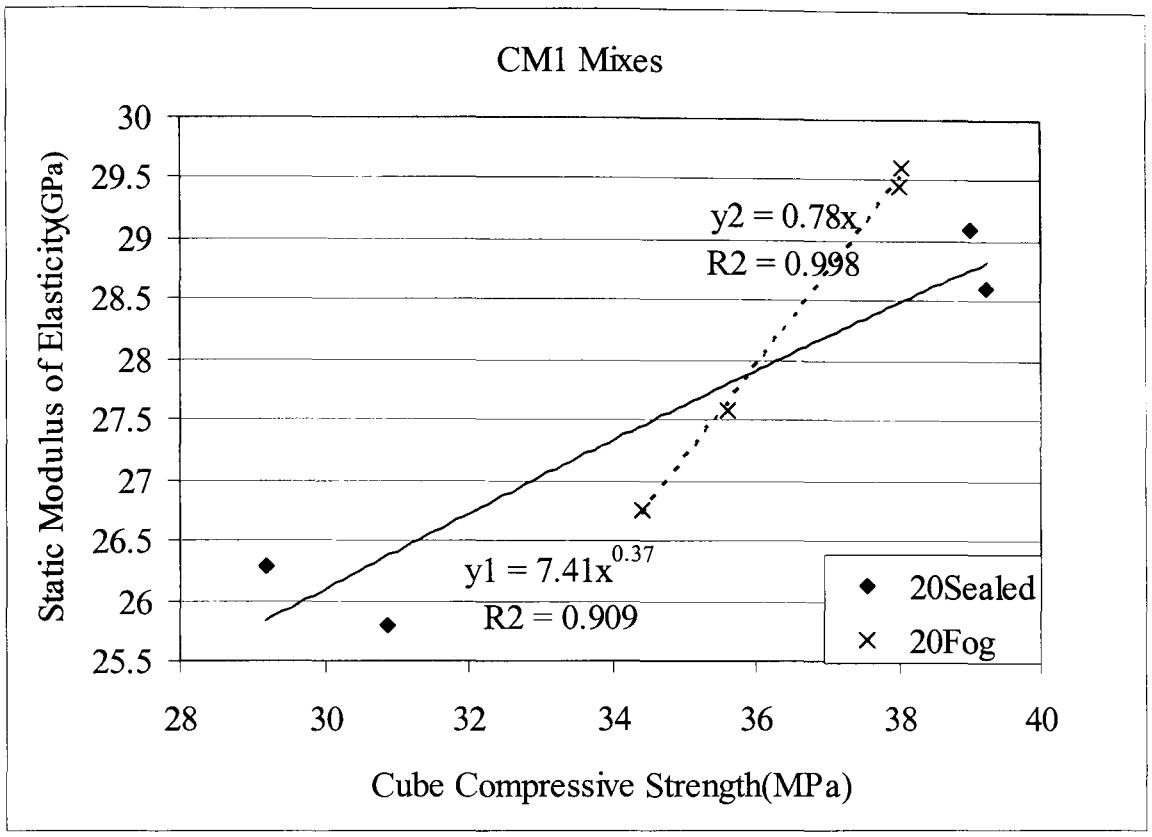

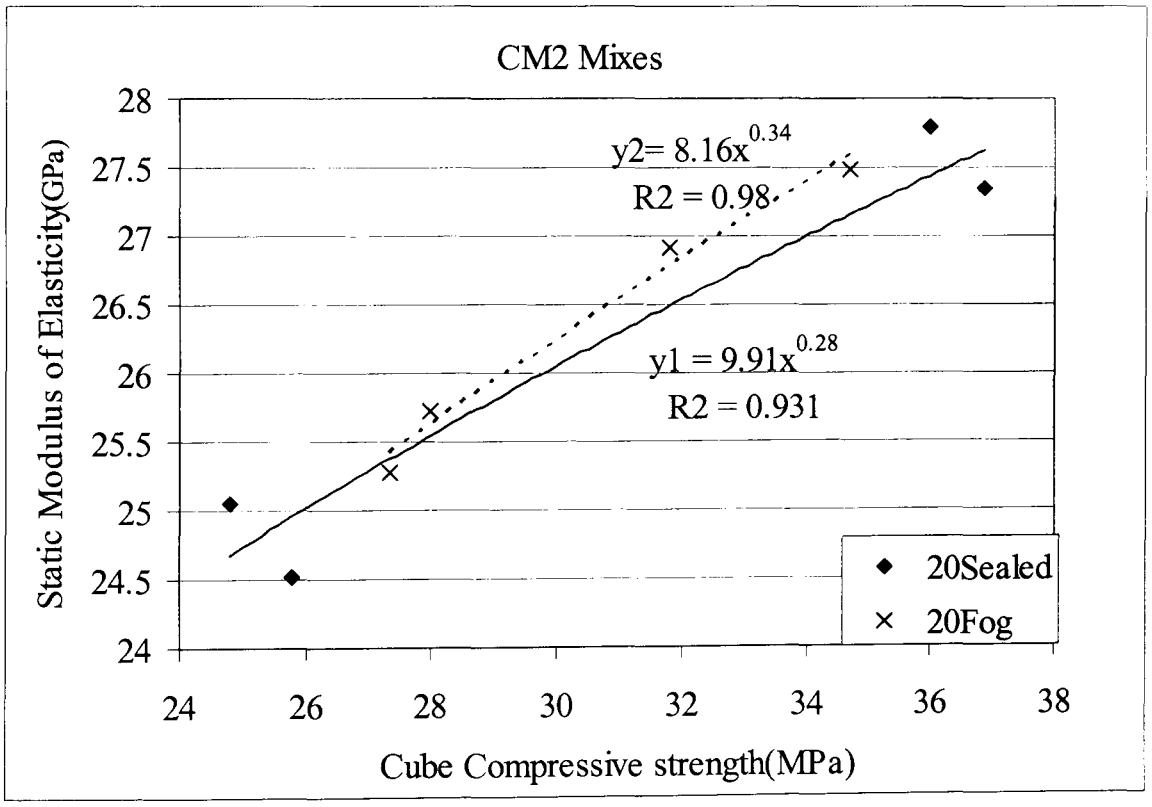

Figure A7.6 Relation between the static modulus of elasticity and the cube compressive strength of CM1 and CM2 under different curing conditions

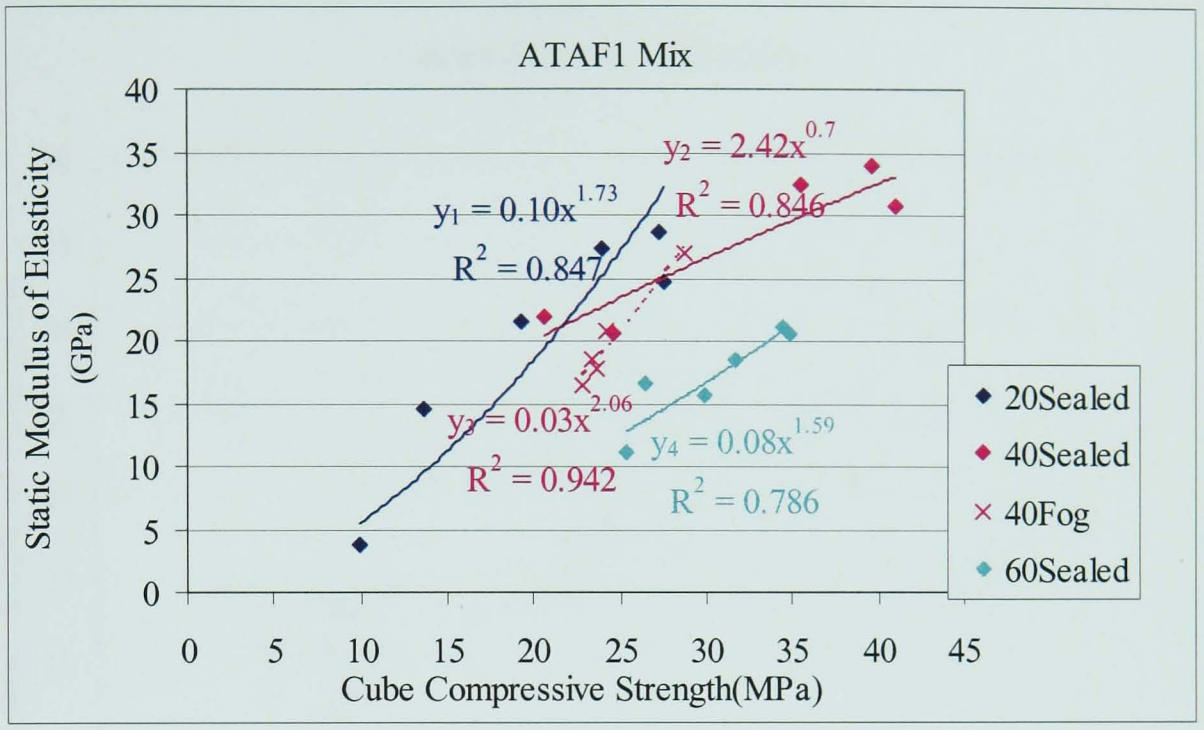

Figure A7.7 Relation between the static modulus of elasticity and the cube compressive strength of ATAF1 and ATAF2 under different curing conditions

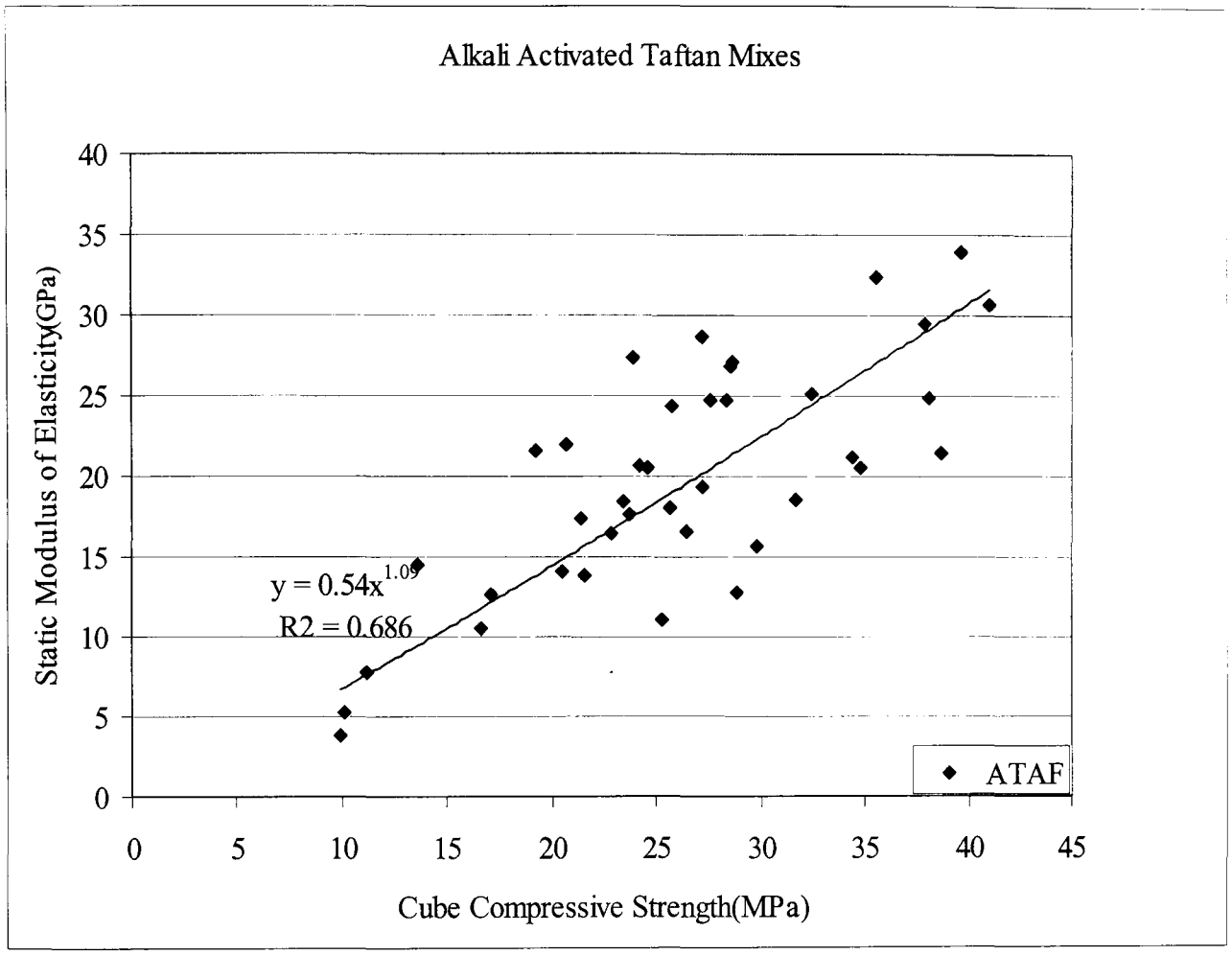

Figure A7.8 Relation between the static modulus of elasticity and the cube compressive strength of alkali activated Taftan pozzolan

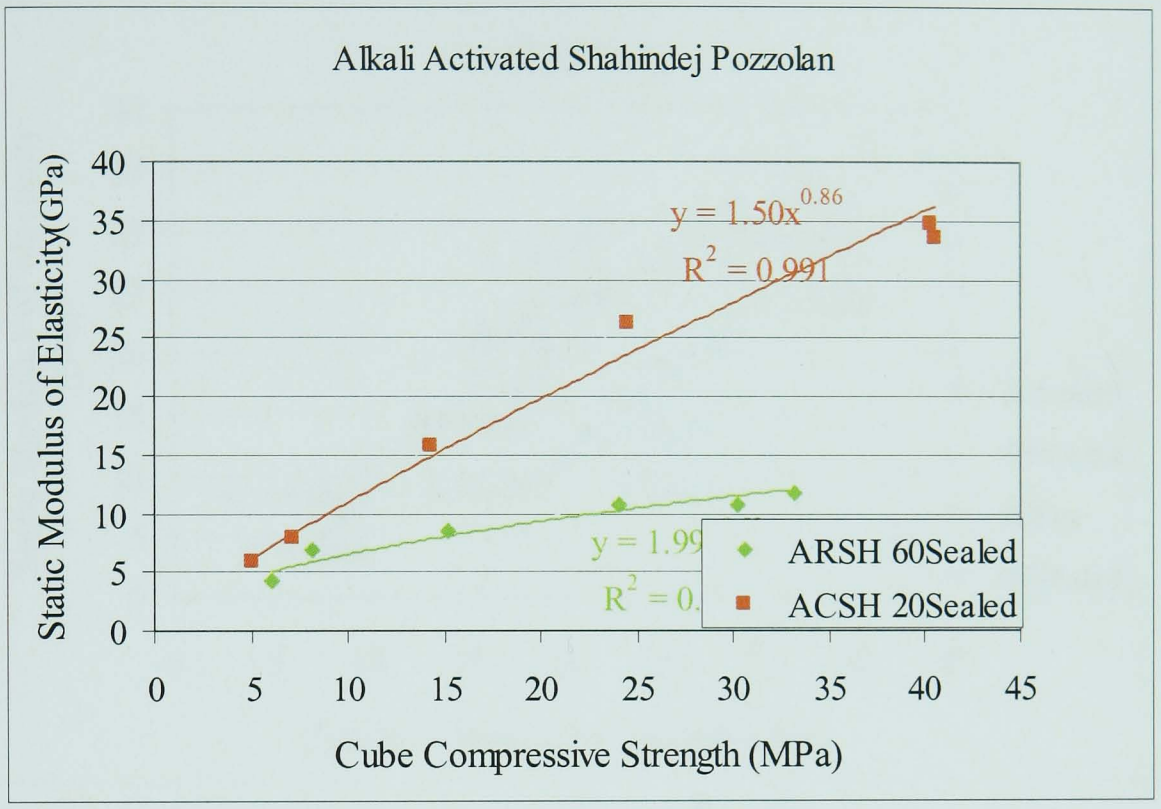

Figure A7.9 Relation between the static modulus of elasticity and the cube compressive strength of ARSH and ACSH Mixes

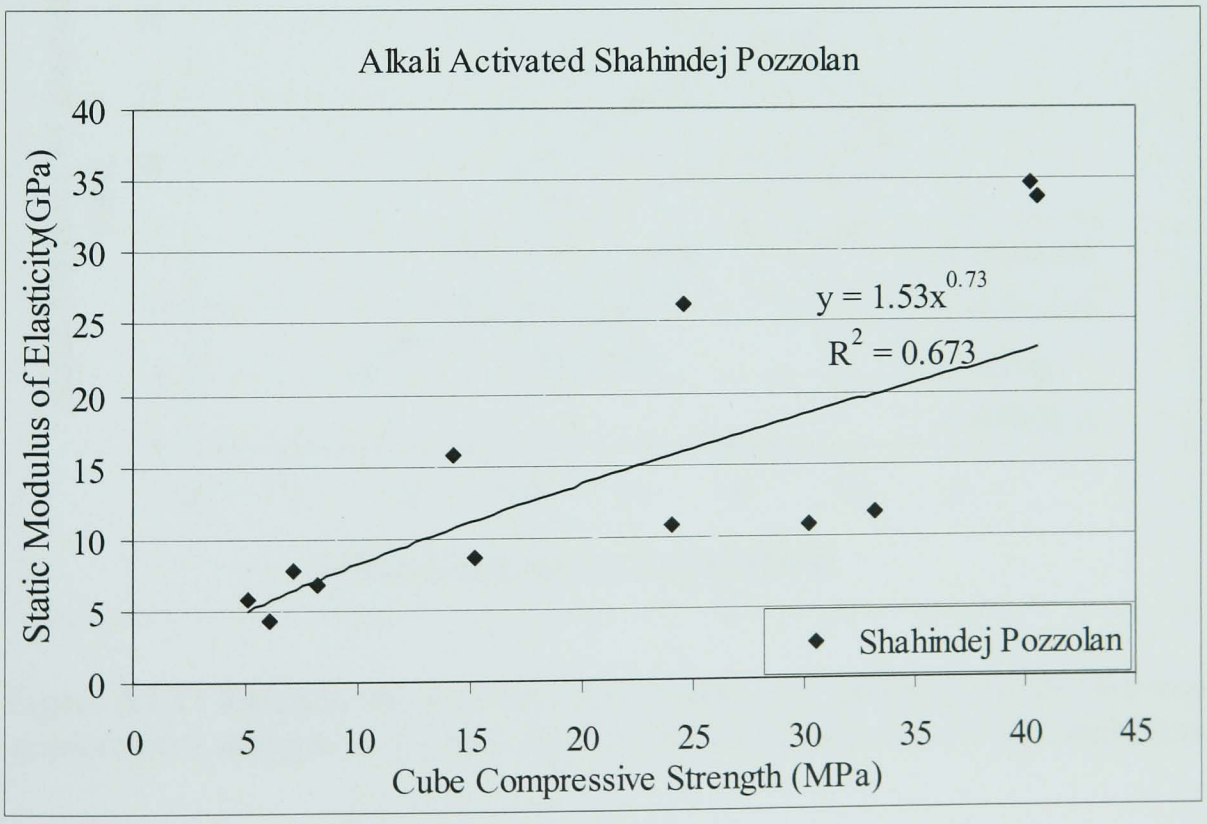

Figure A7.10 Relation between the static modulus of elasticity and the cube compressive strength of alkali activated Shahindej mixes

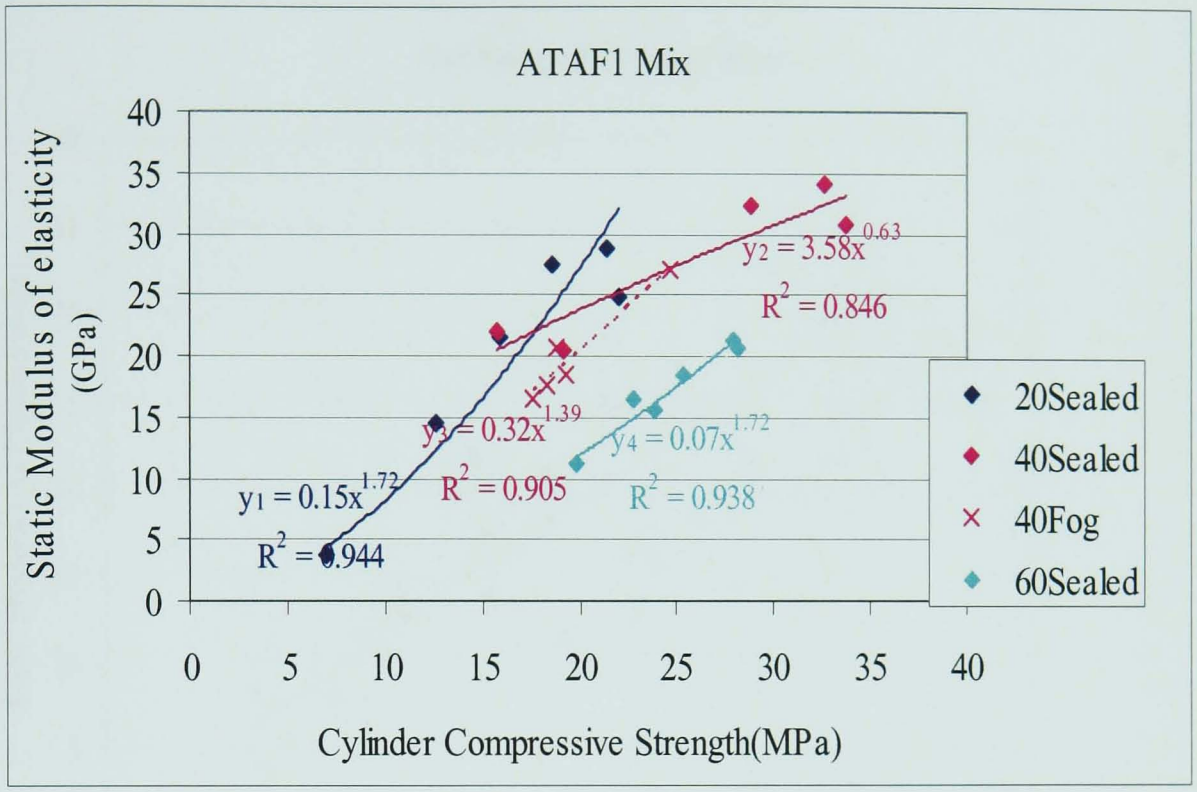

Figure A7.11 Relation between the static modulus of elasticity and the cylinder compressive strength of ATAF1 and ATAF2 under different curing conditions

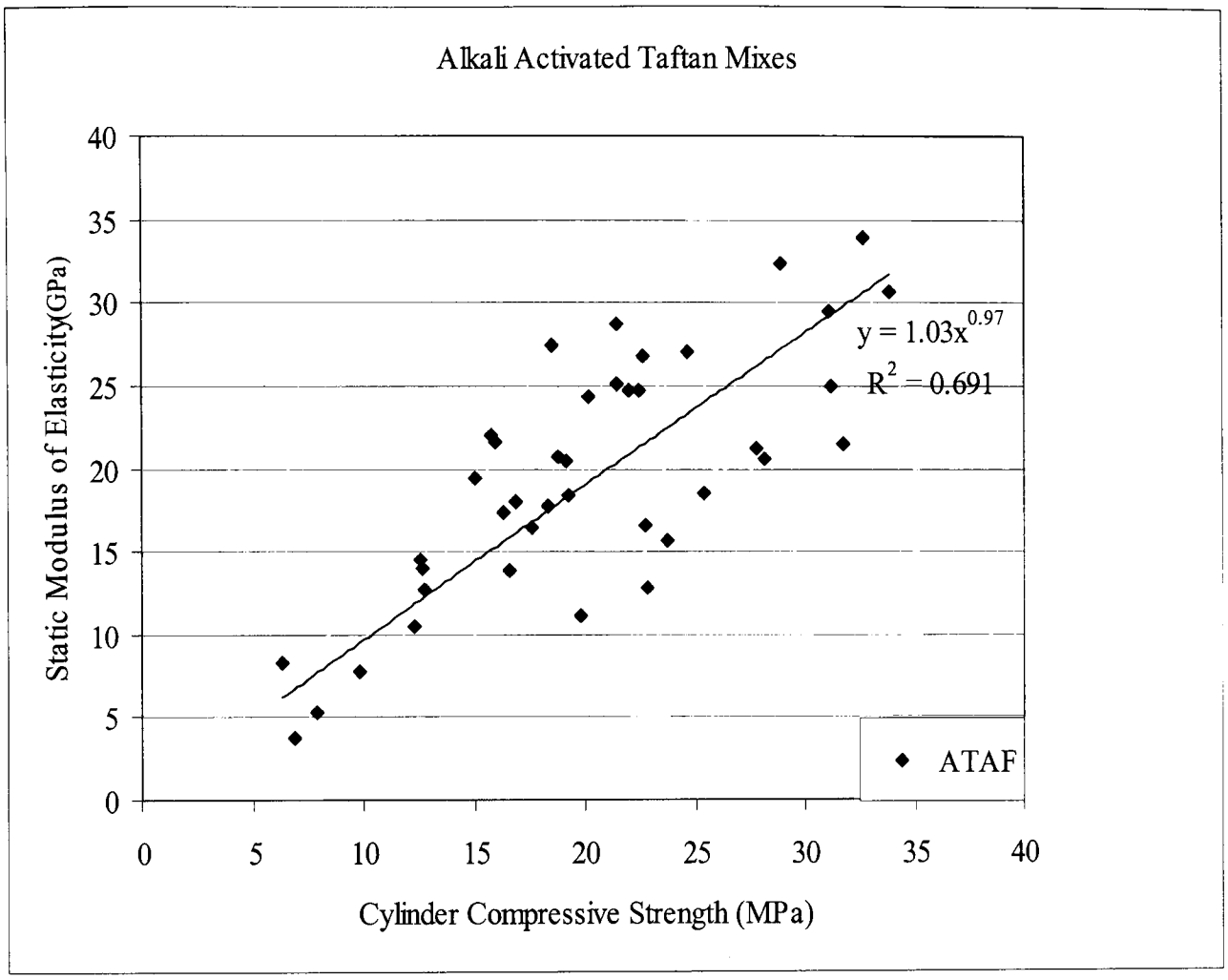

Figure A7.12 Relation between the static modulus of elasticity and the cylinder compressive strength of alkali activated Taftan Mixes

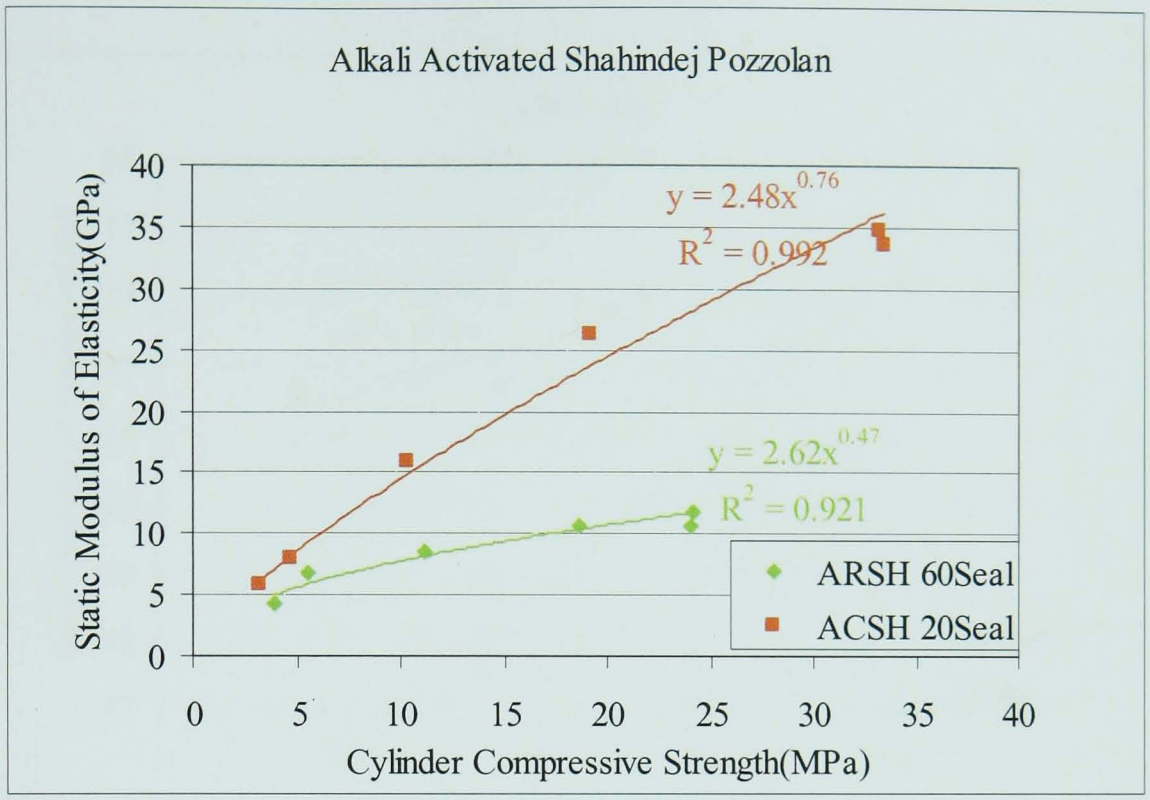

Figure A7.13 Relation between the static modulus of elasticity and the cylinder compressive strength of ARSH and ACSH Mixes

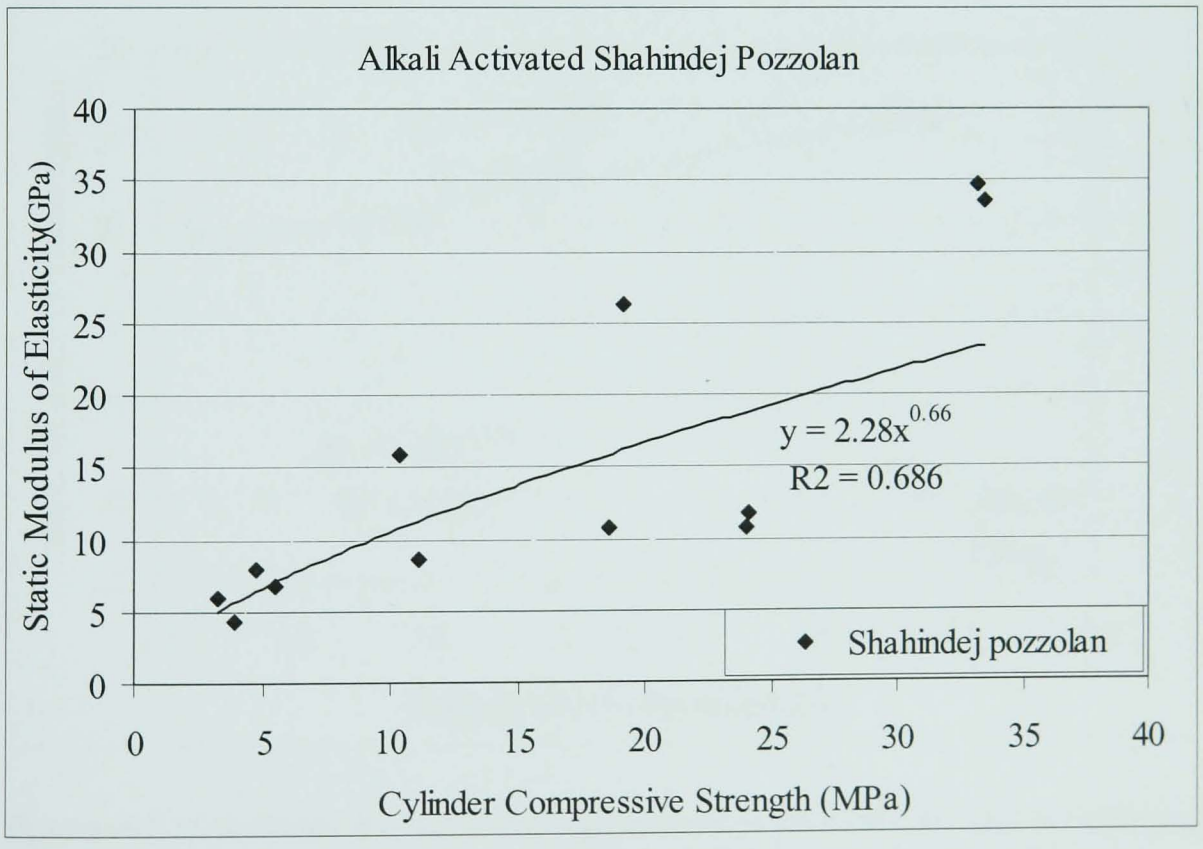

Figure A7.14 Relation between the static modulus of elasticity and the cylinder compressive strength of alkali activated Shahindej Mixes

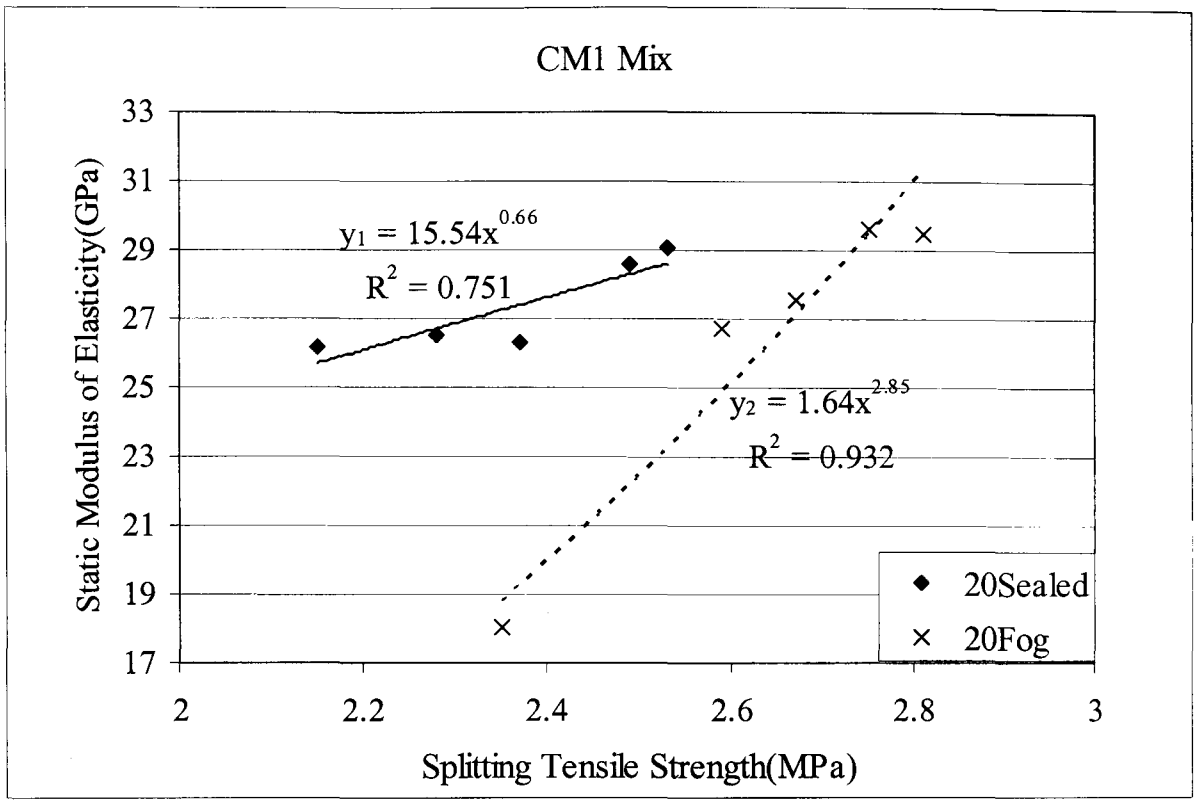

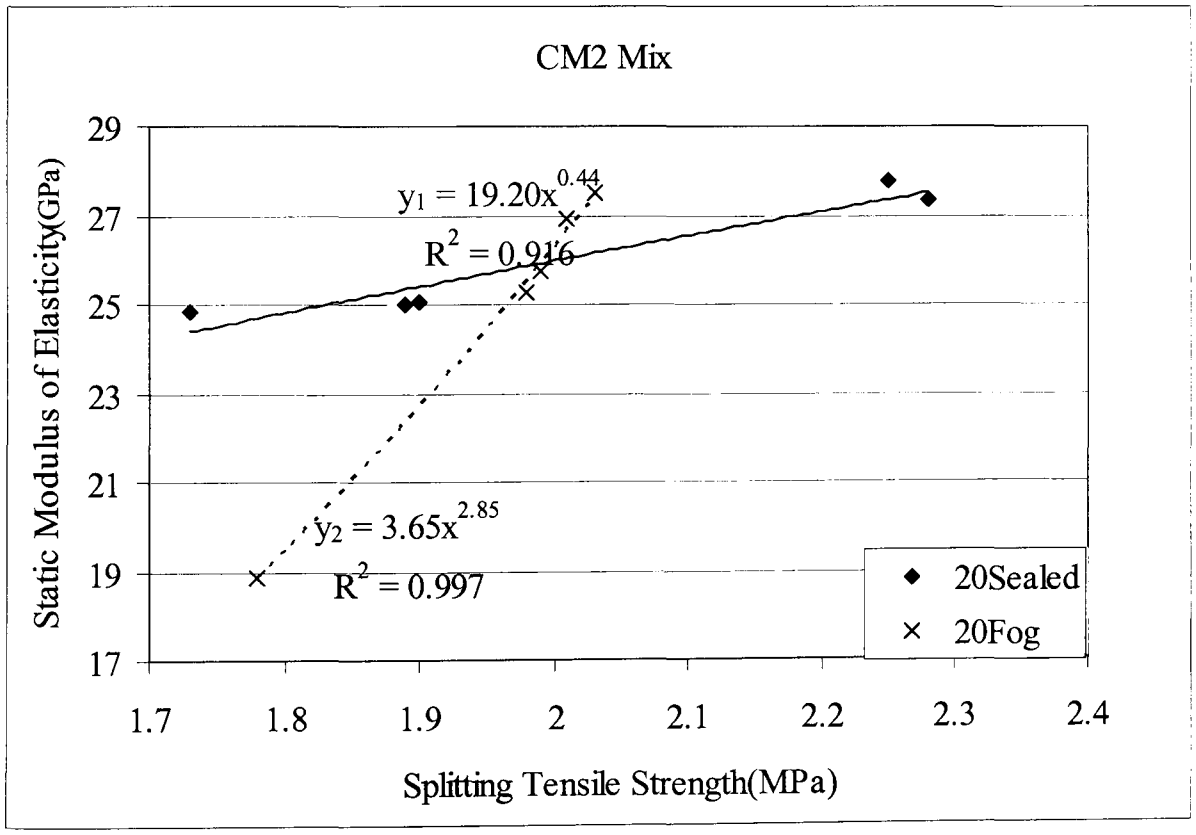

Figure A7.15 Relation between the static modulus of elasticity and the splitting tensile strength of CM1 and CM2 under different curing conditions

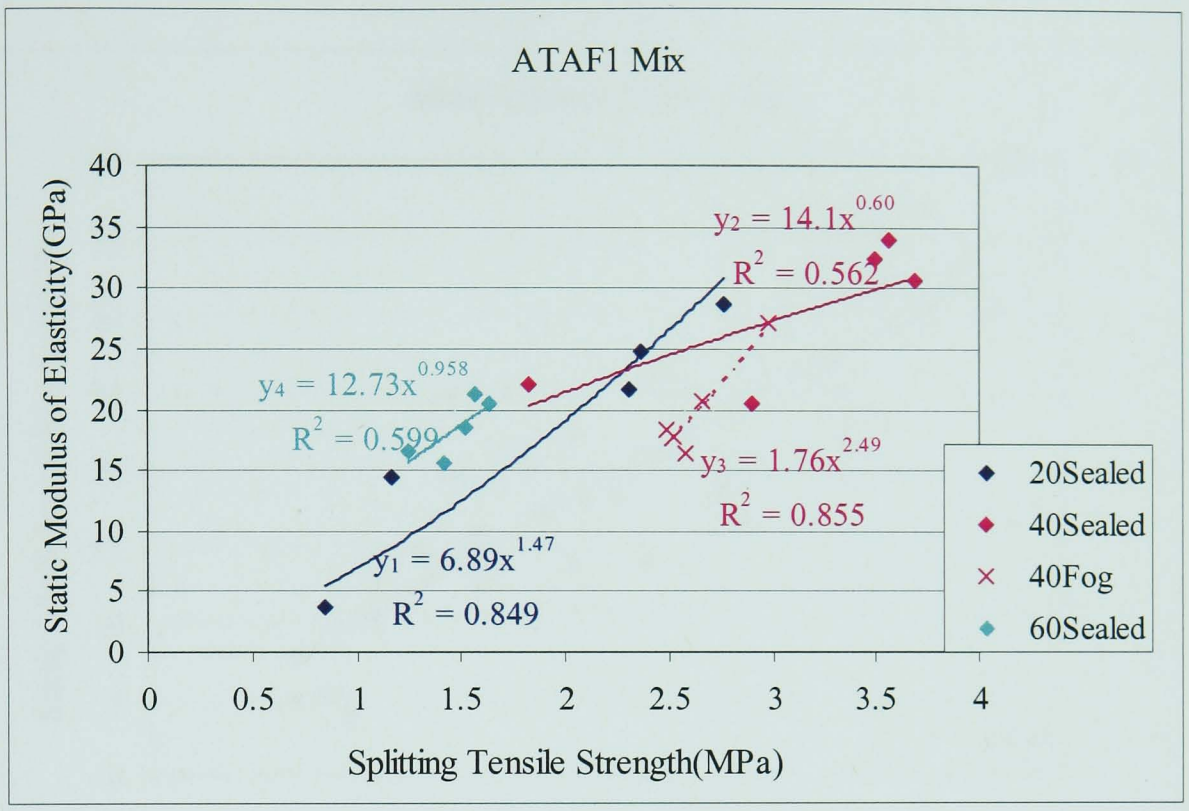

Figure A7.16 Relation between the static modulus of elasticity and the splitting tensile strength of ATAF1 and ATAF2 under different curing conditions

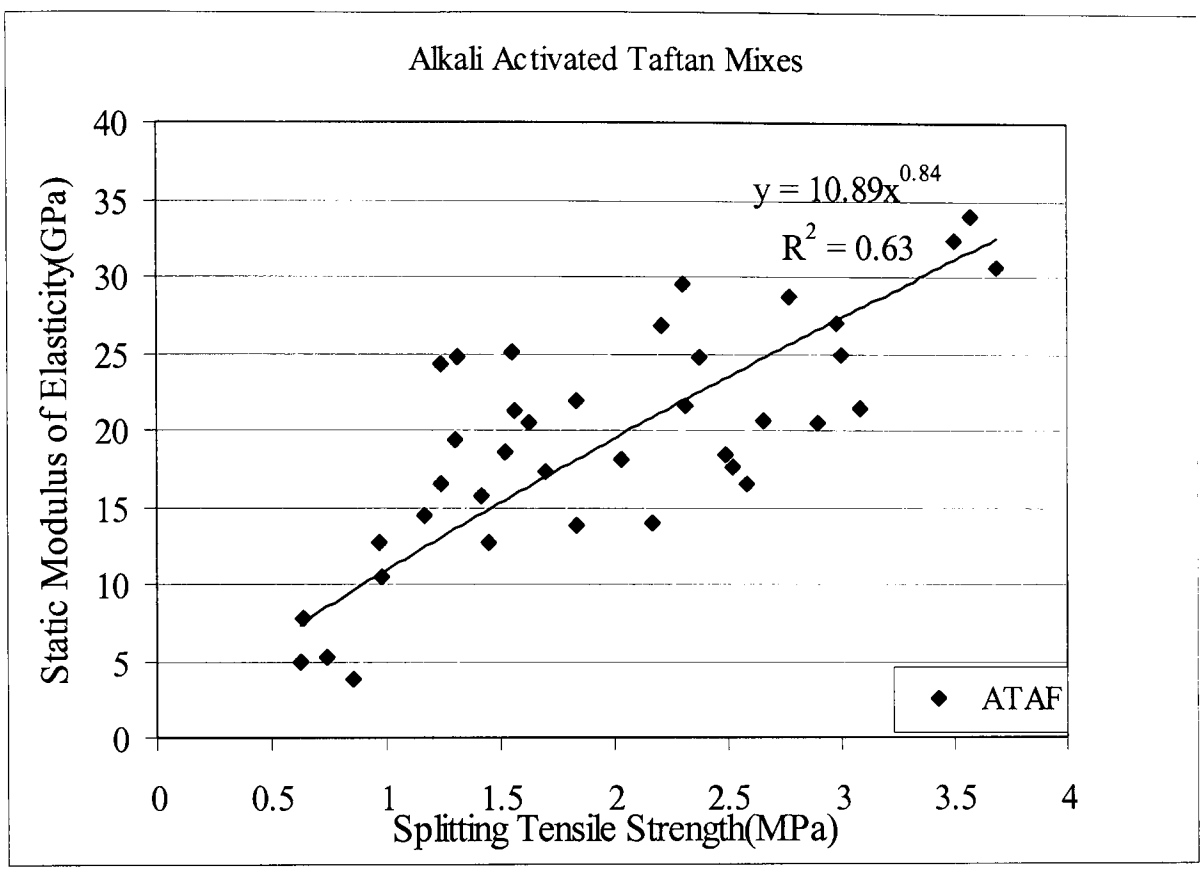

Figure A7.17 Relation between the static modulus of elasticity and the splitting tensile strength of alkali activated Taftan Mixes

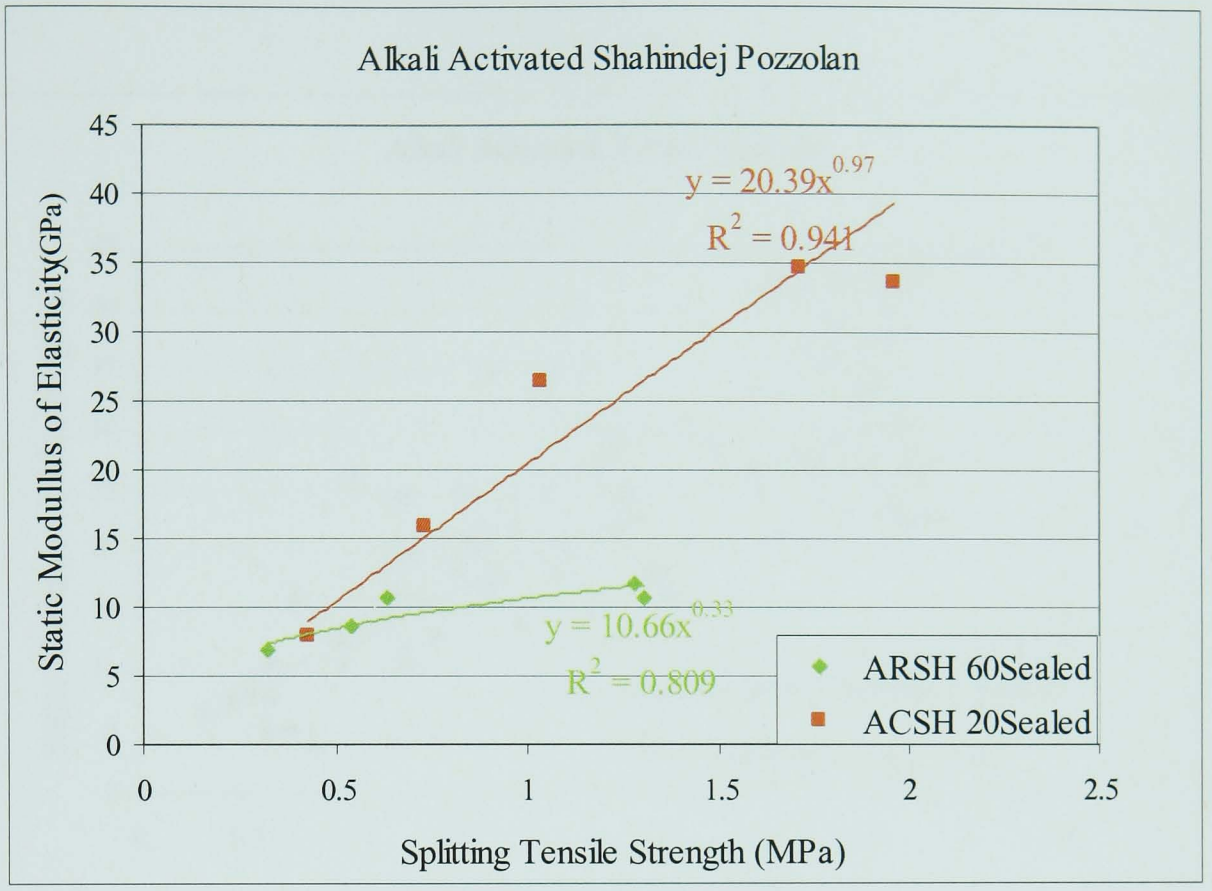

Figure A7.18 Relation between the static modulus of elasticity and the splitting tensile strength of ARSH and ACSH mixes

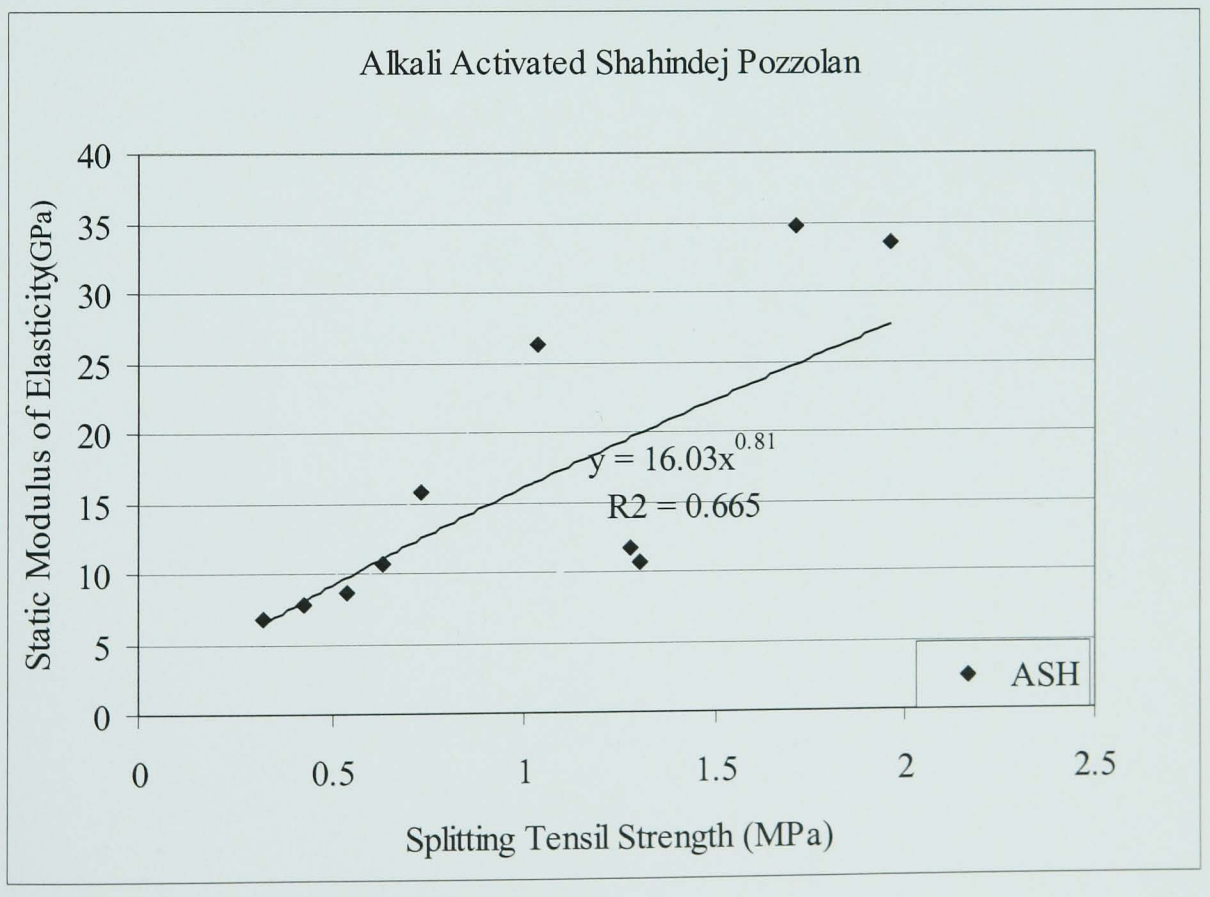

Figure A7.19 Relation between the static modulus of elasticity and the splitting tensile strength of alkali activated Shahindej Mixes

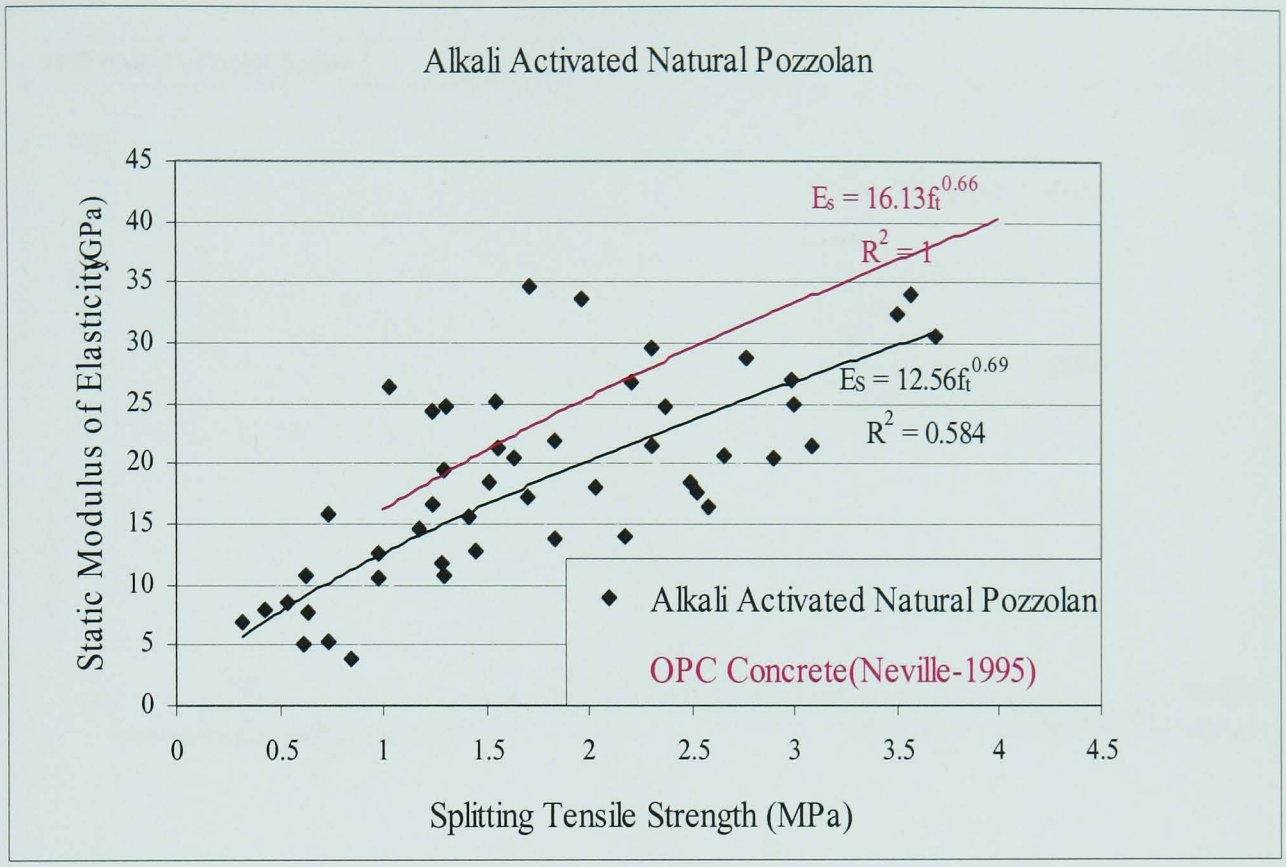

Figure A7.20 Relation between the static modulus of elasticity and the splitting tensile strength of alkali activated natural pozzolans

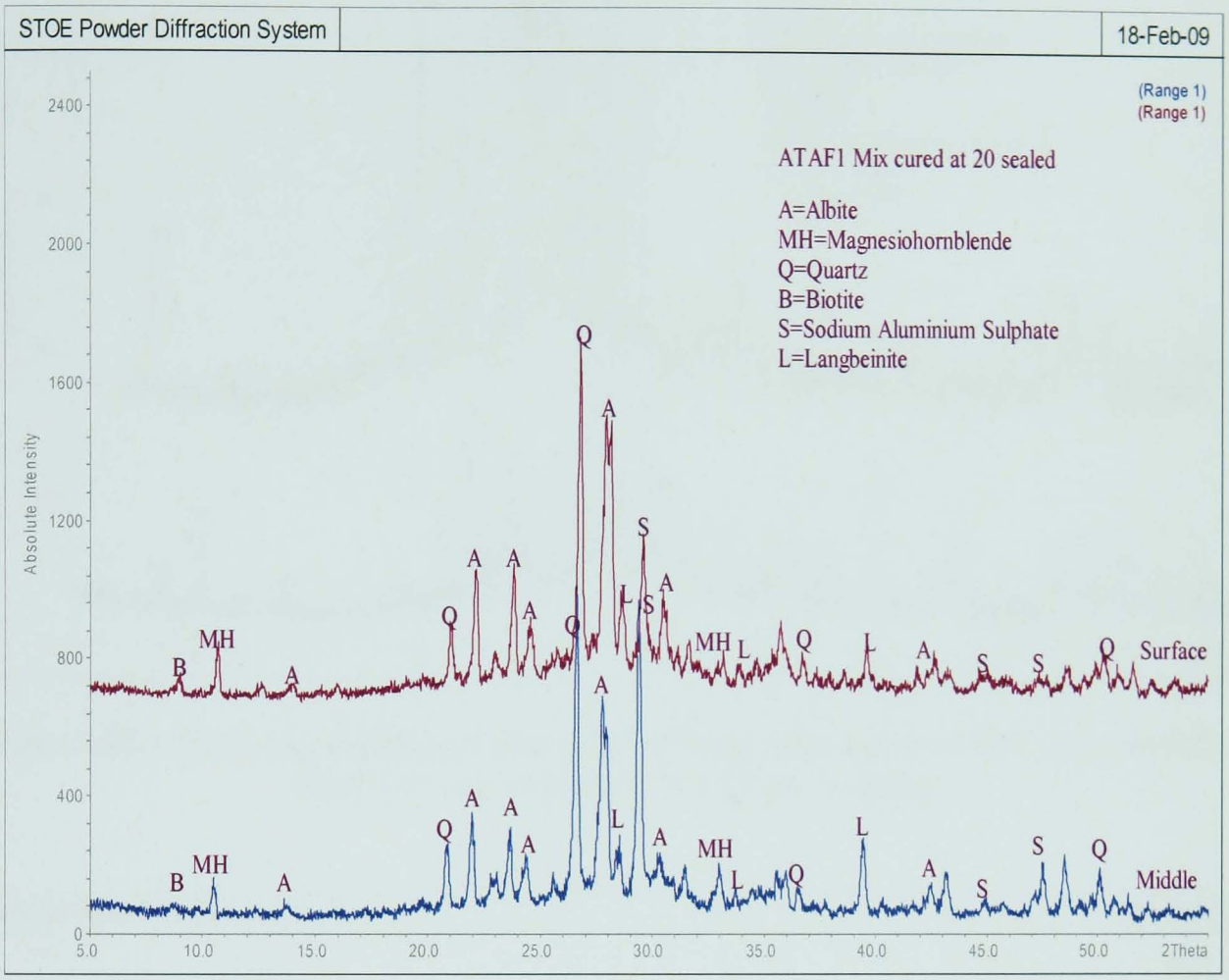

Figure A8.1 (a) X-ray diffraction traces for ATAF1 Mix cured at 20°C sealed condition after 3 month exposure in sulphate solution

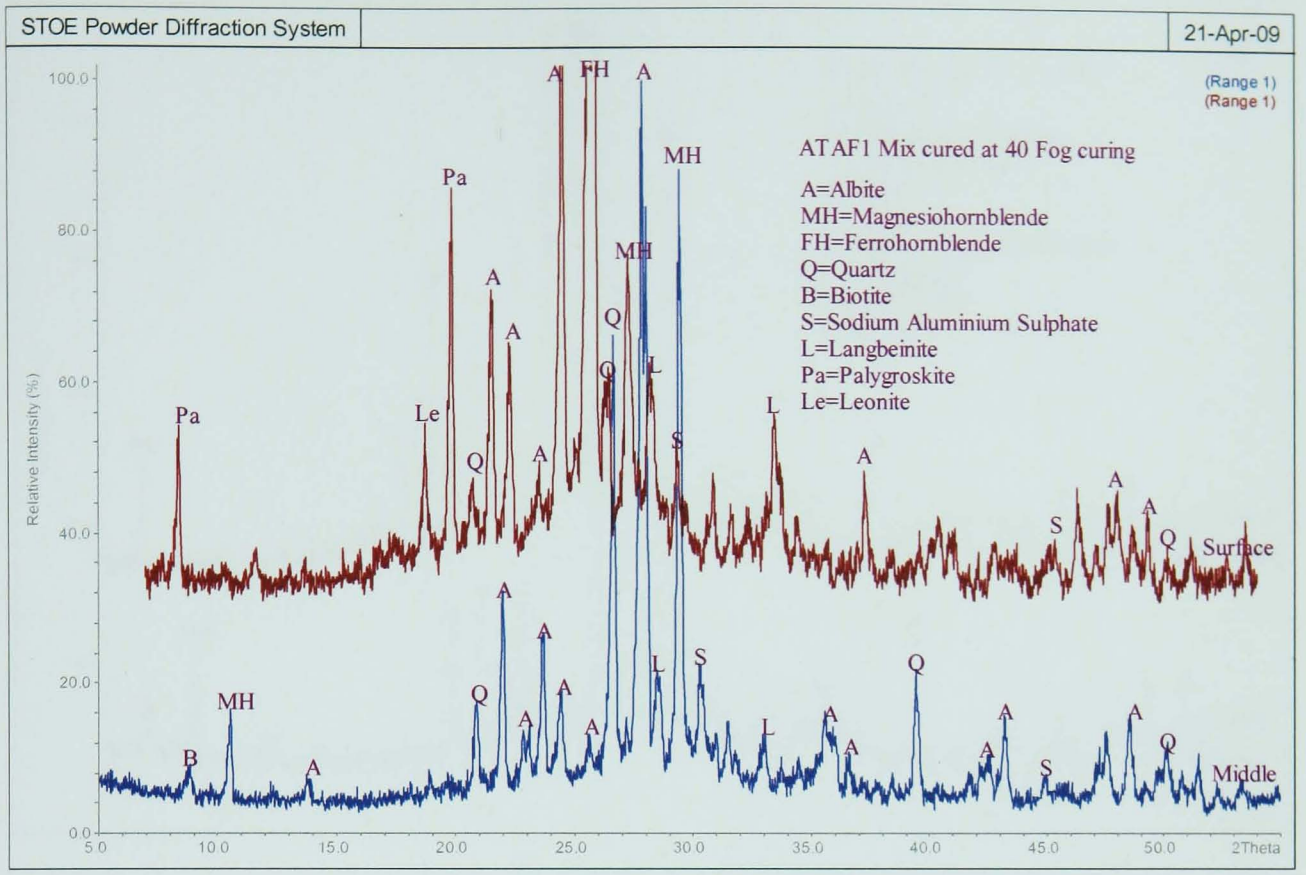

Figure A8.1 (b) X-ray diffraction traces for ATAF1 Mix cured at 40°C fog condition after 3 month exposure in sulphate solution

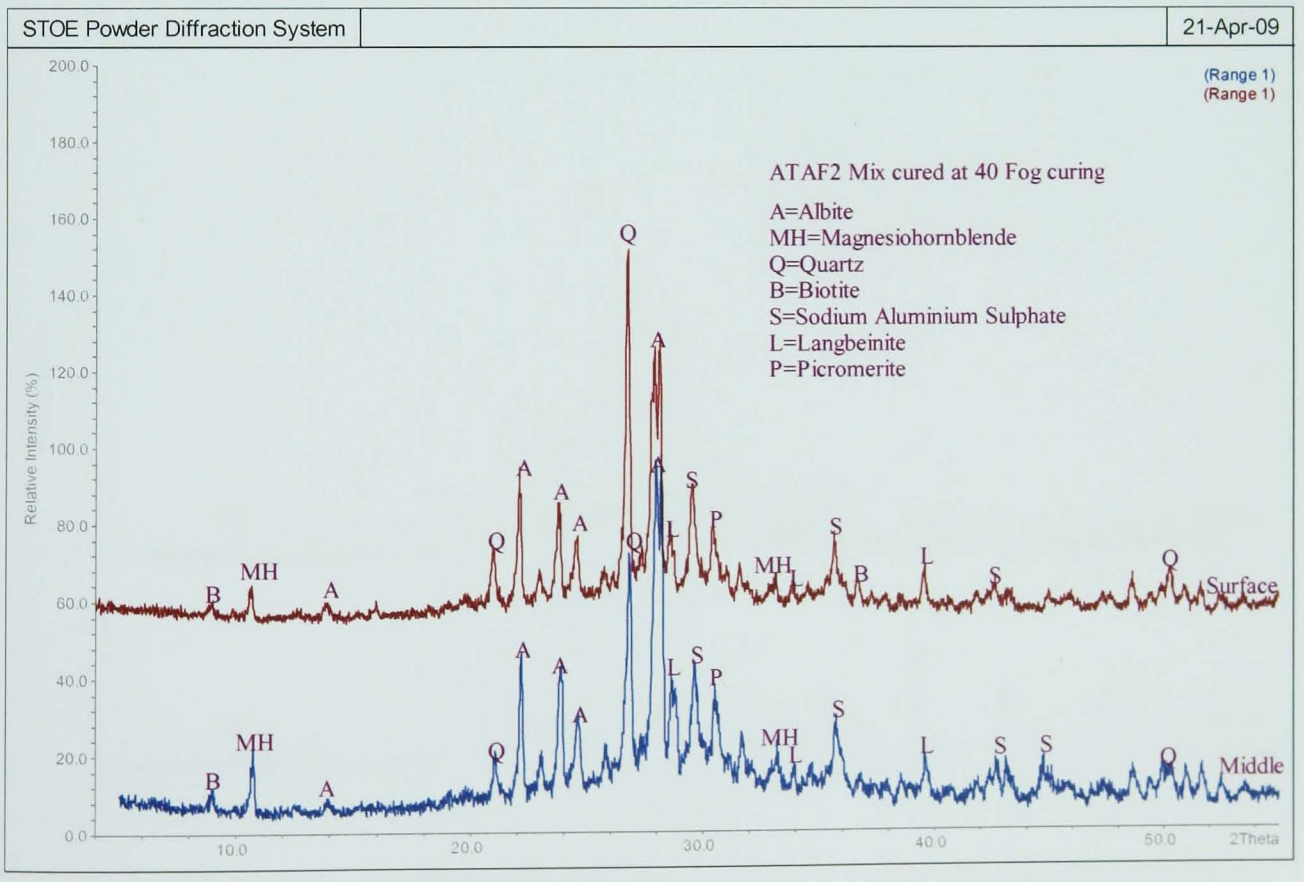

Figure A8.1 (c) X-ray diffraction traces for ATAF2 Mix cured at 40°C fog condition after 3 month exposure in sulphate solution

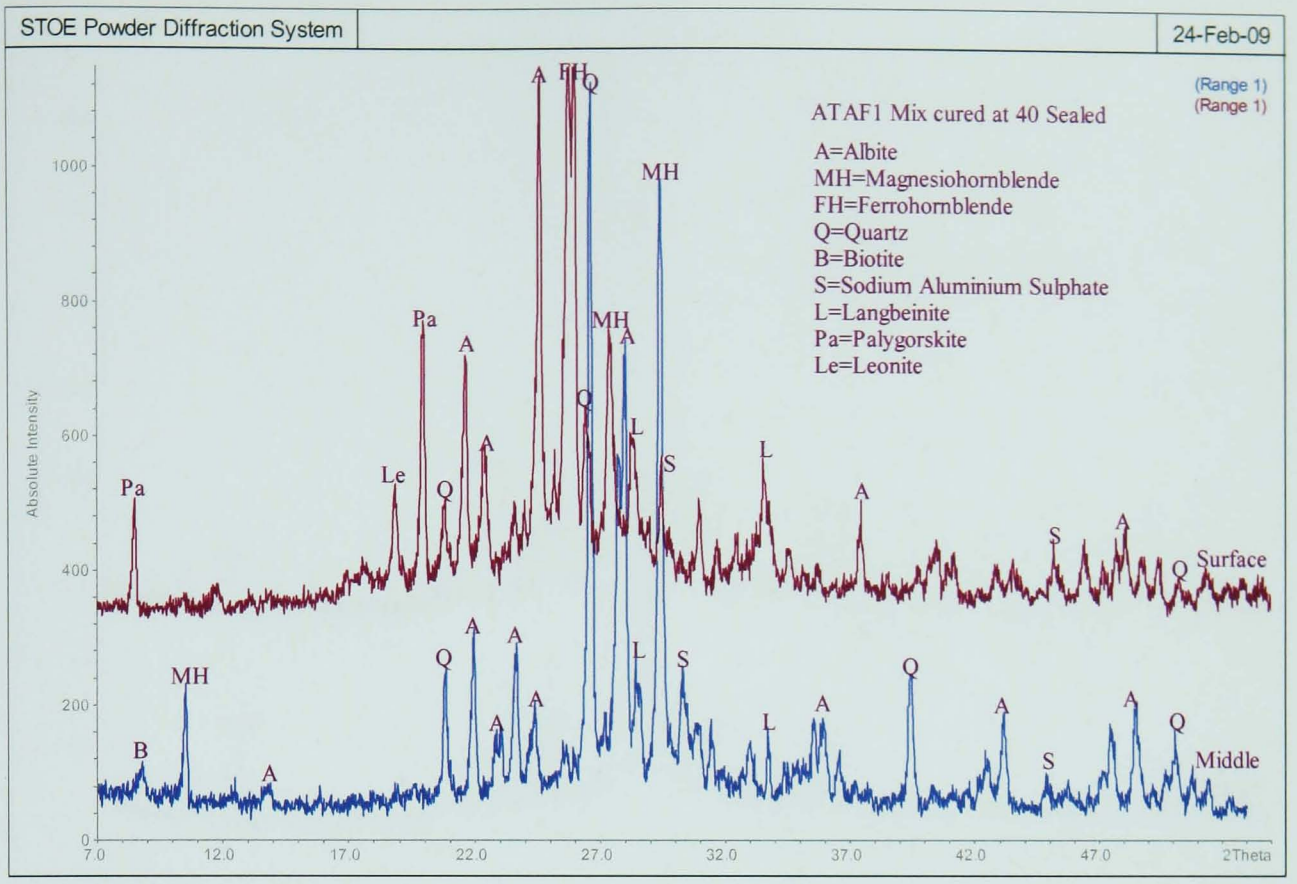

Figure A8.1 (d) X-ray diffraction traces for ATAF1 Mix cured at 40ºC sealed condition after 3 month exposure in sulphate solution

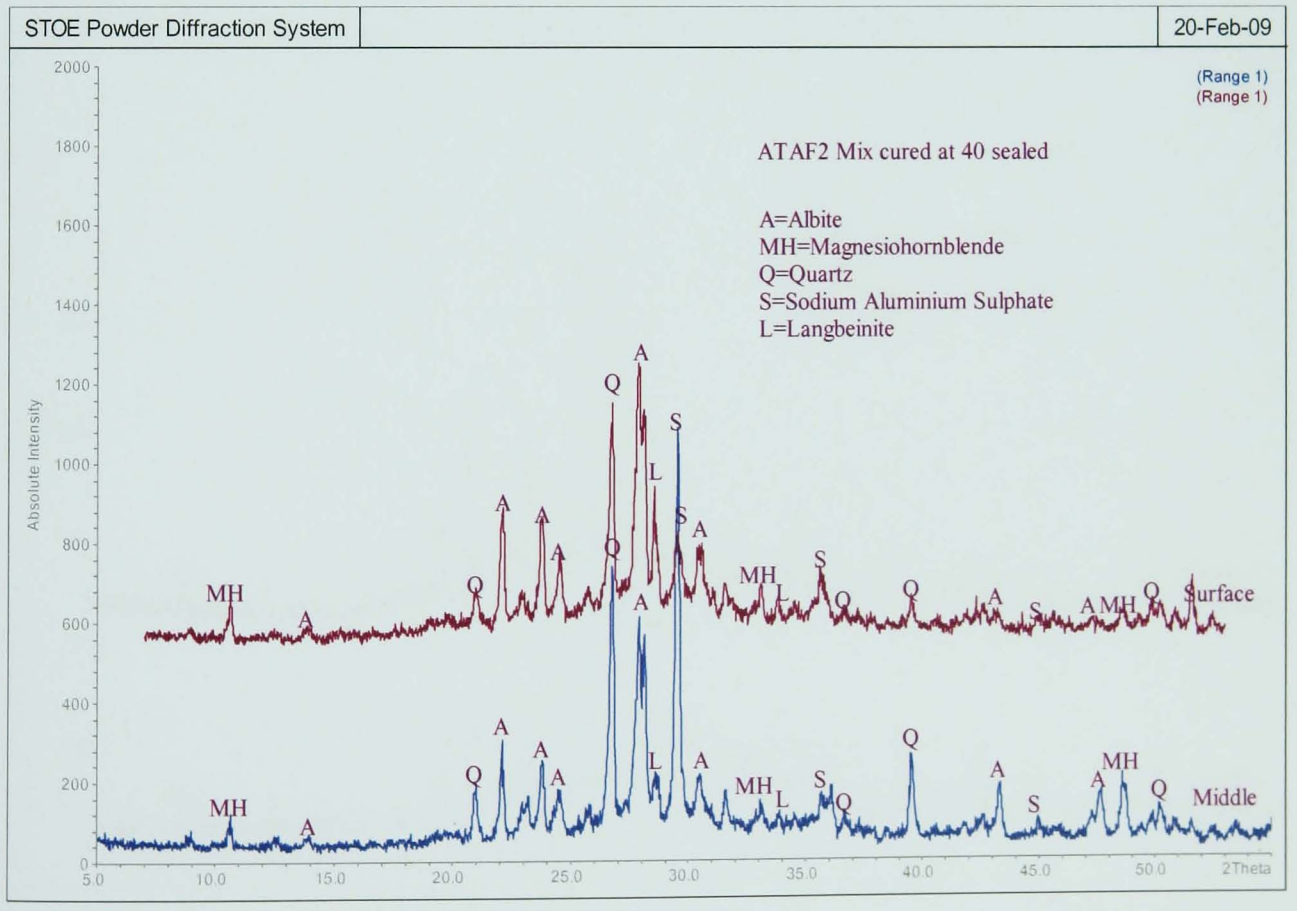

Figure A8.1 (e) X-ray diffraction traces for ATAF2 Mix cured at 40ºC sealed condition after 3 month exposure in sulphate solution

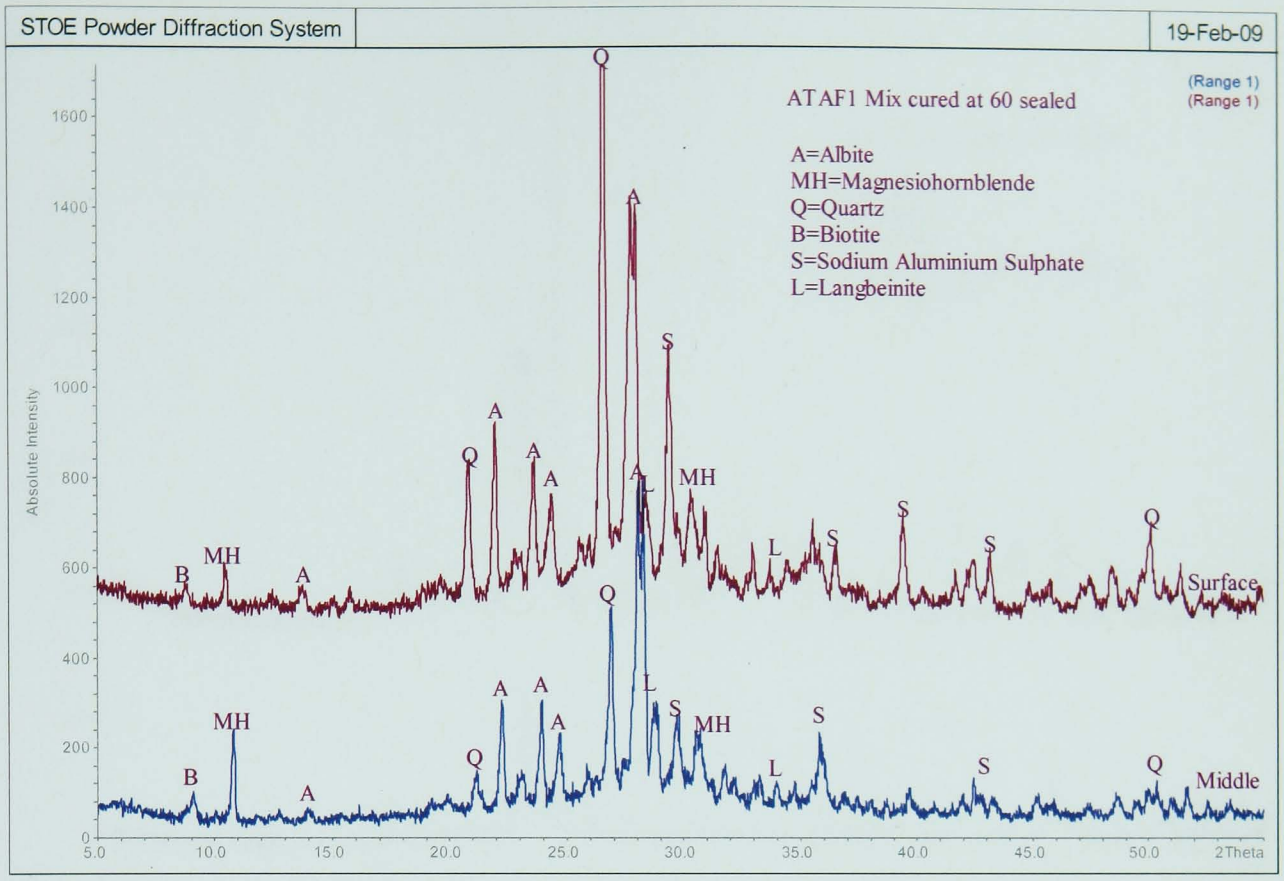

Figure A8.1 (f) X-ray diffraction traces for ATAF1 Mix cured at 60ºC sealed condition after 3 month exposure in sulphate solution

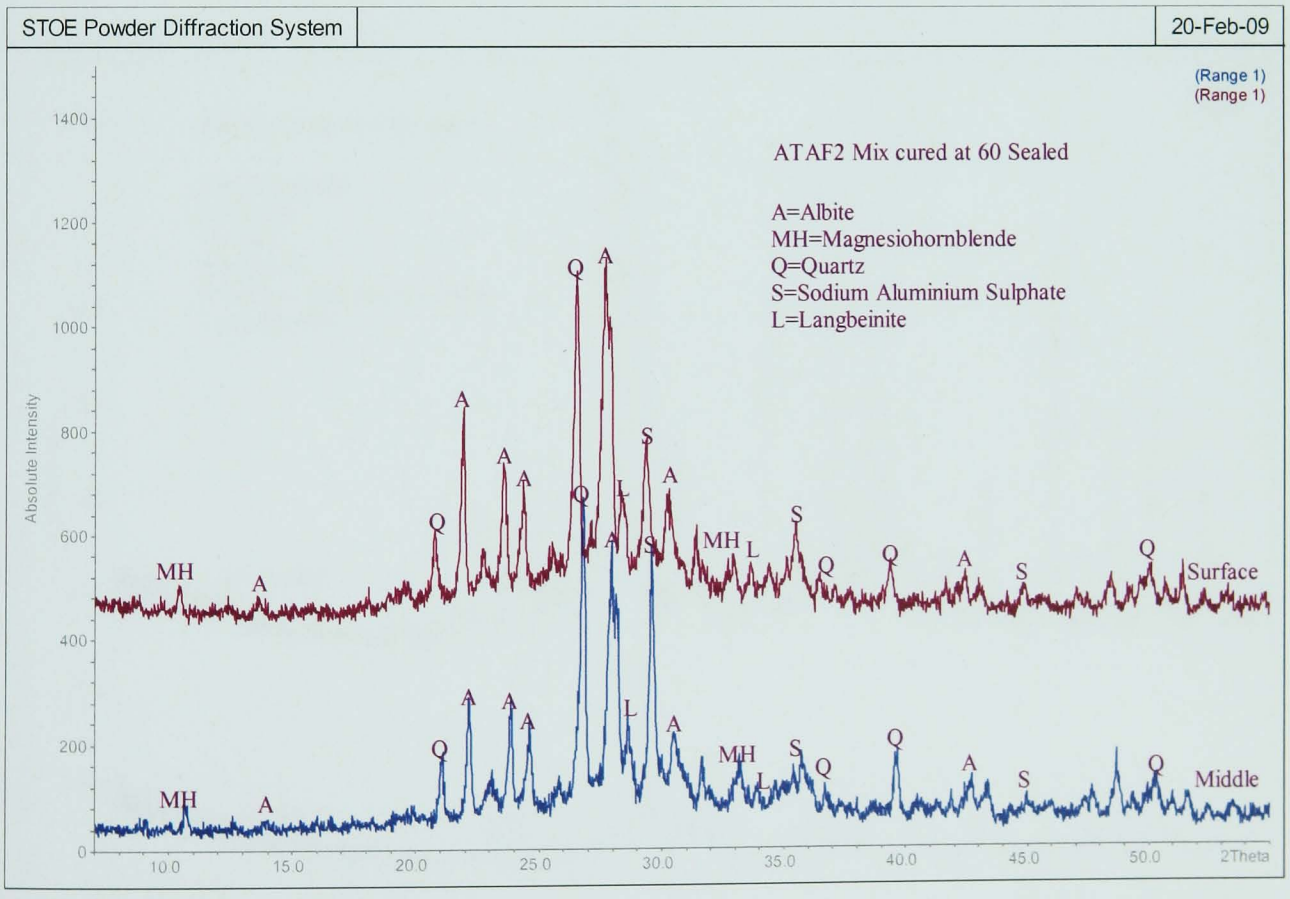

Figure A8.1 (g) X-ray diffraction traces for ATAF2 Mix cured at 60ºC sealed condition after 3 month exposure in sulphate solution

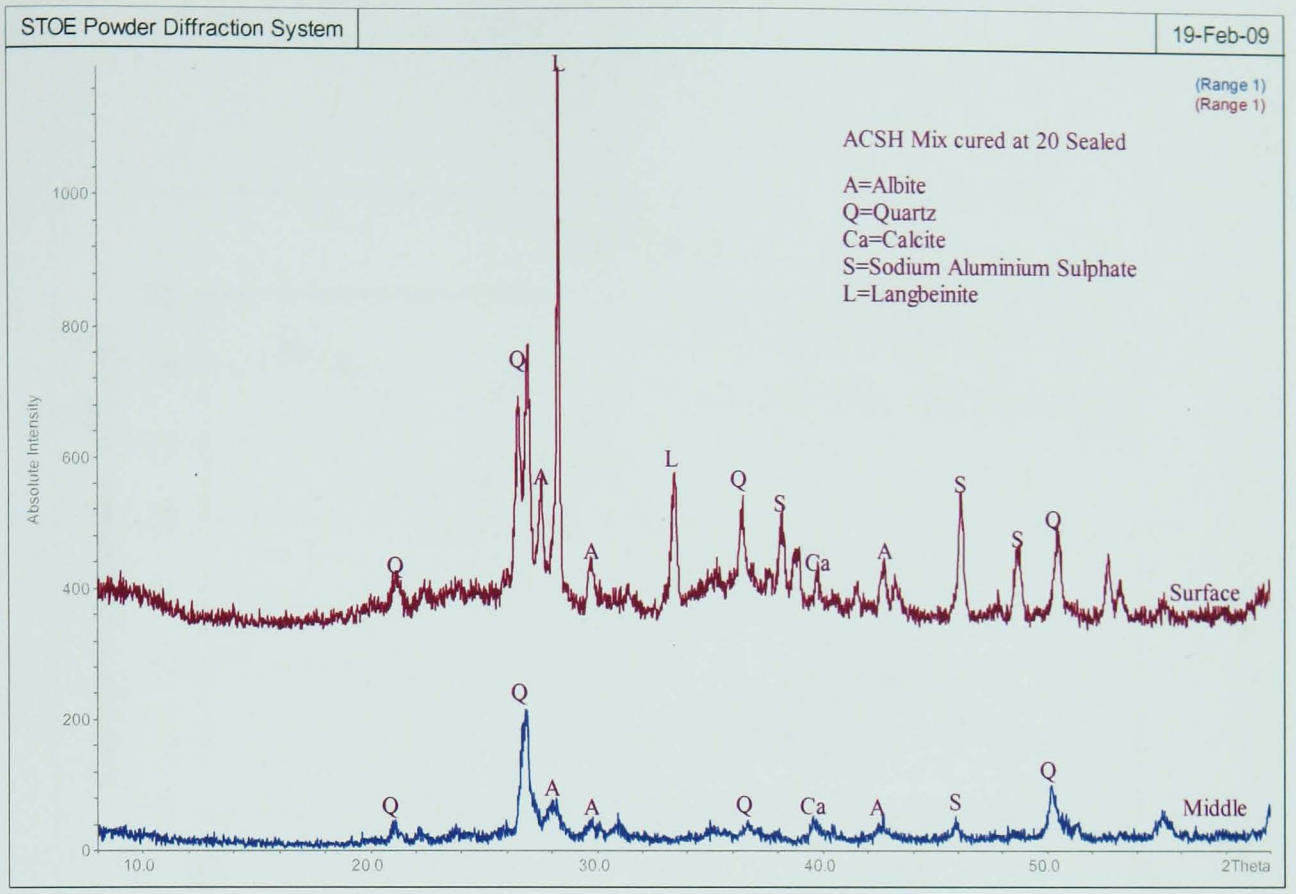

Figure A8.1 (h) X-ray diffraction traces for ACSH Mix cured at 20°C sealed condition after 3 month exposure in sulphate solution

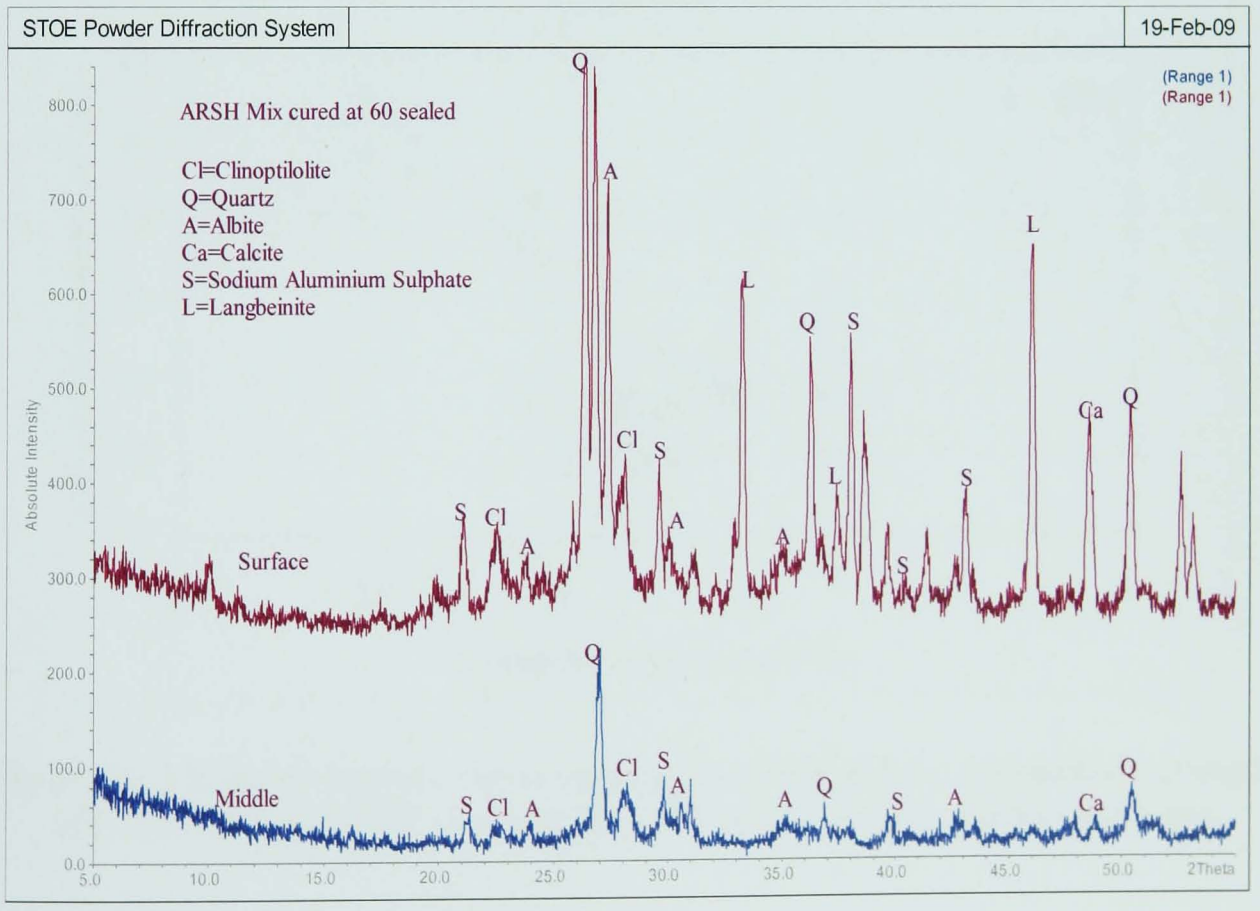

Figure A8.1 (i) X-ray diffraction traces for ARSH Mix cured at 60°C sealed condition after 3 month exposure in sulphate solution

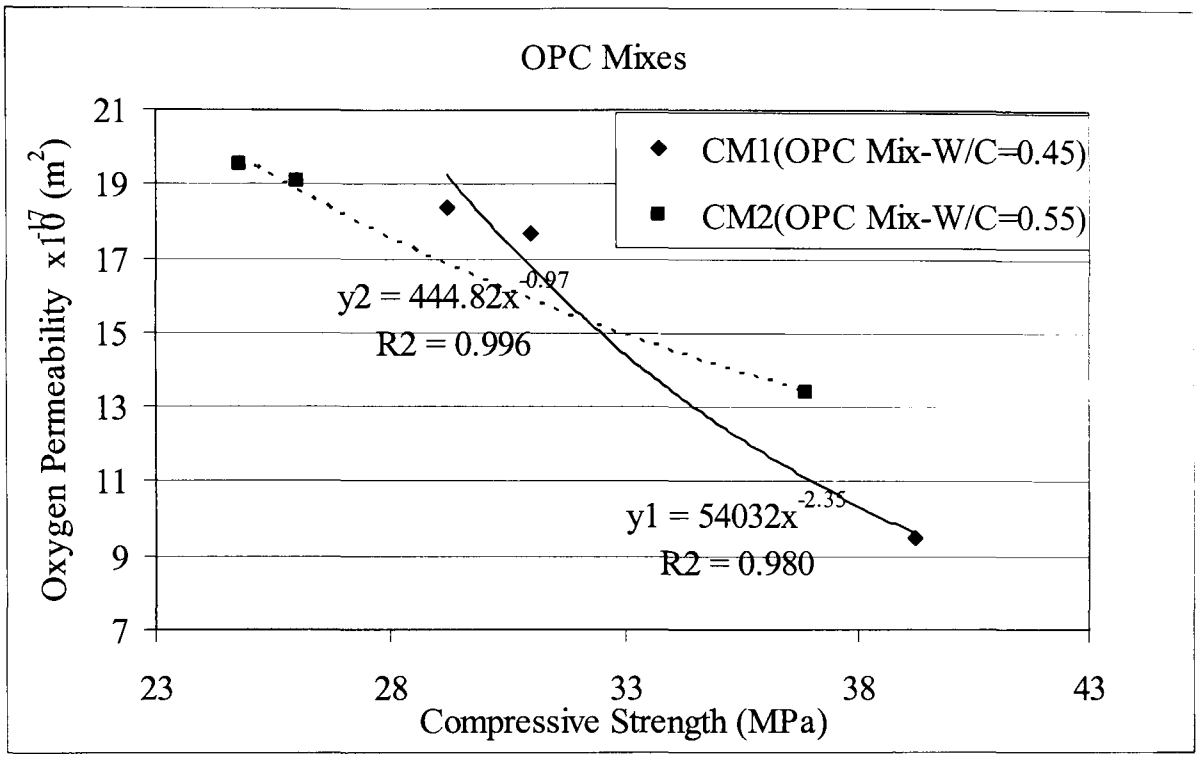

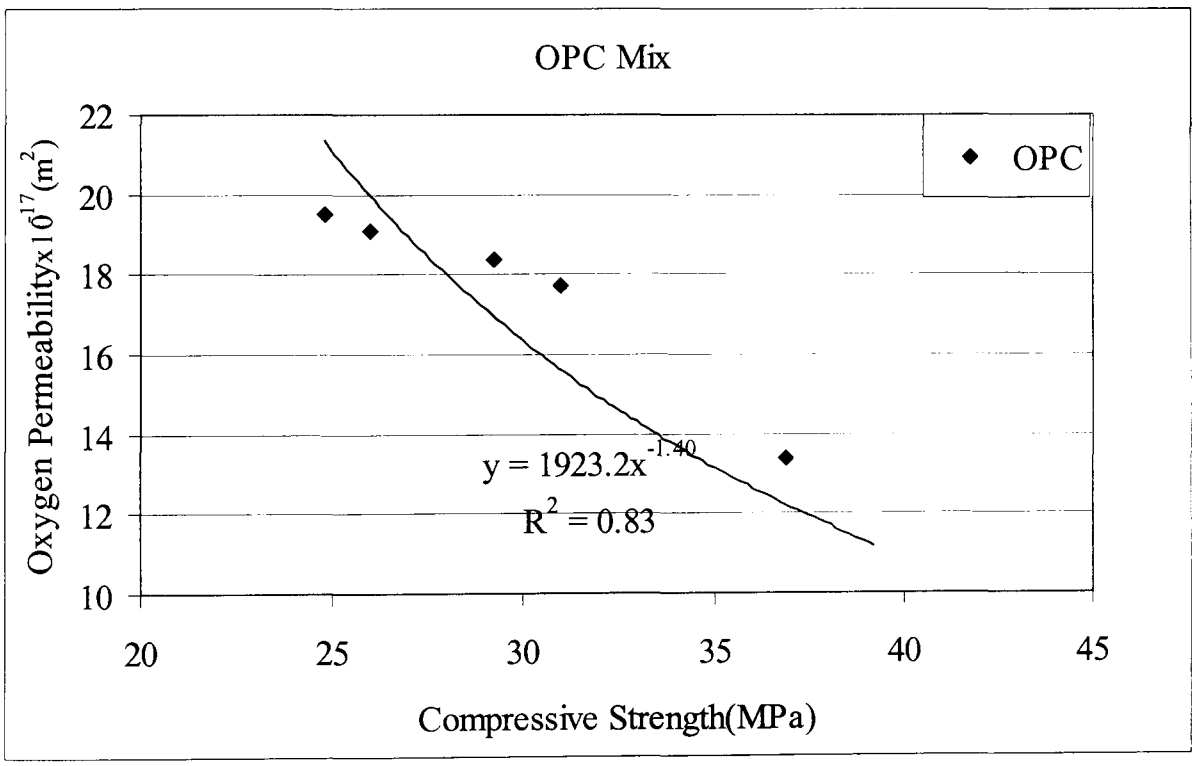

Figure A8.2 Relation between the oxygen permeability and the compressive strength of CM1, CM2 and OPC concrete generally under different curing conditions

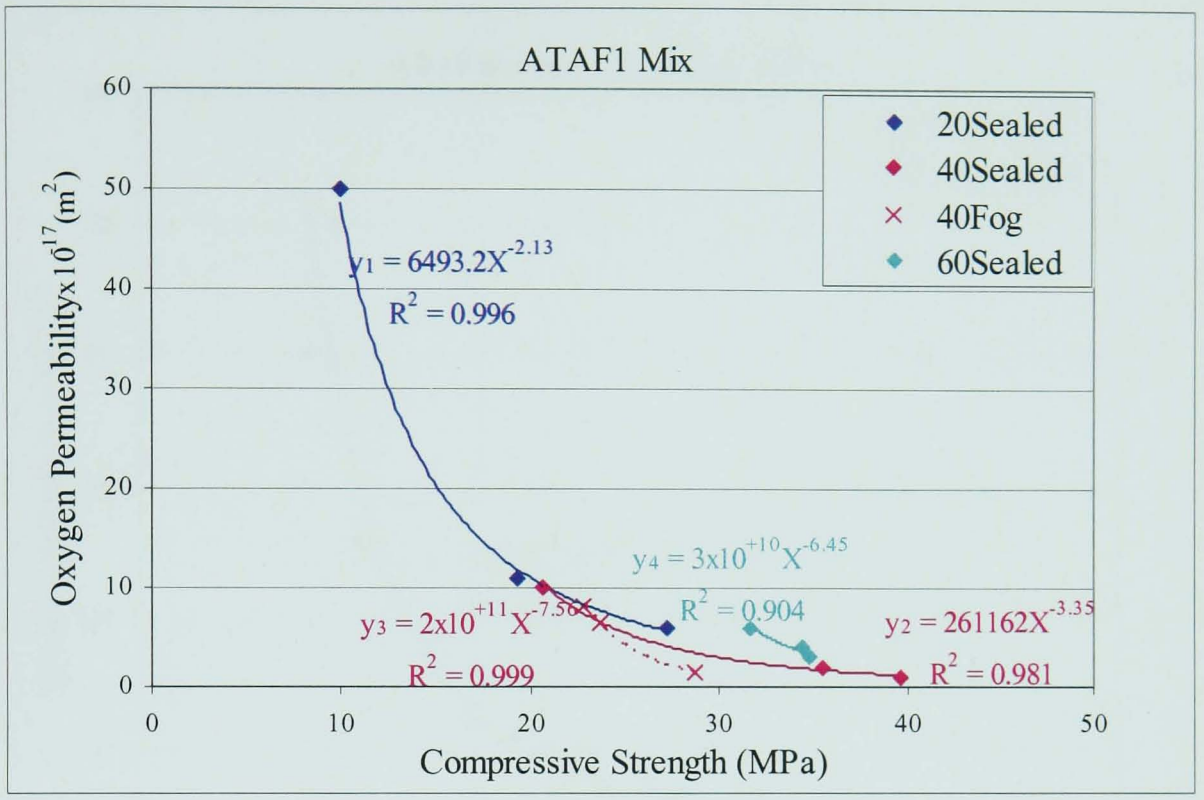

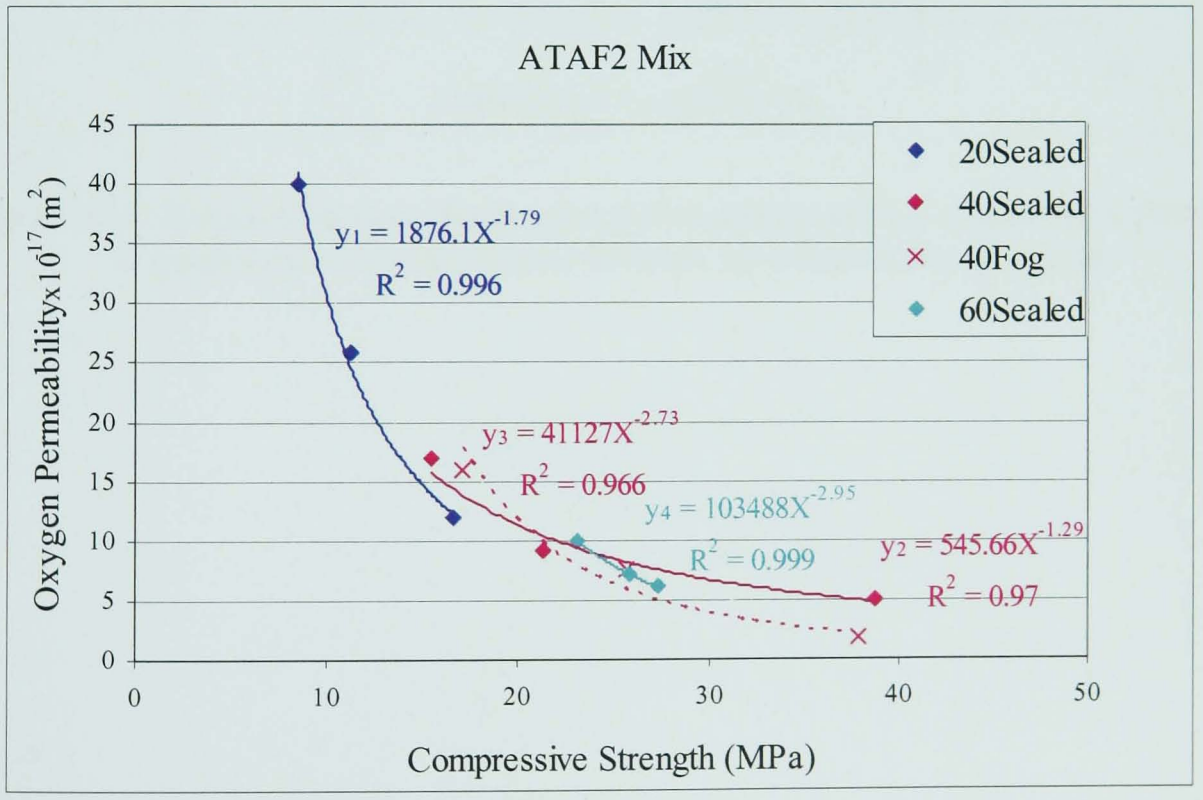

Figure A8.3 Relation between the oxygen permeability and the compressive strength of ATAF1, and ATAF2 mixes under different curing conditions

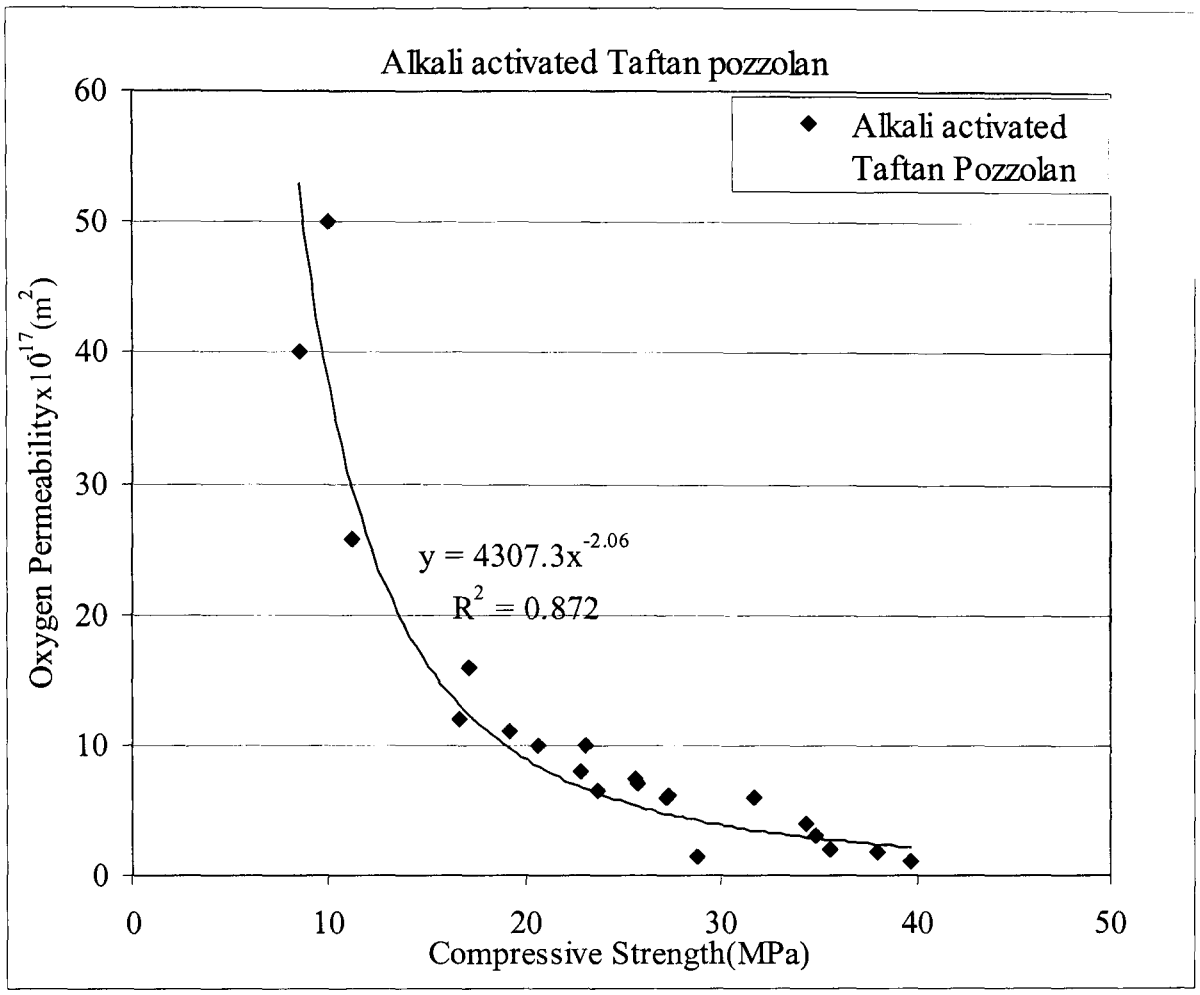

Figure A8.4 Relation between the oxygen permeability and the compressive strength of geopolymer concrete based on alkali activated Taftan pozzolan

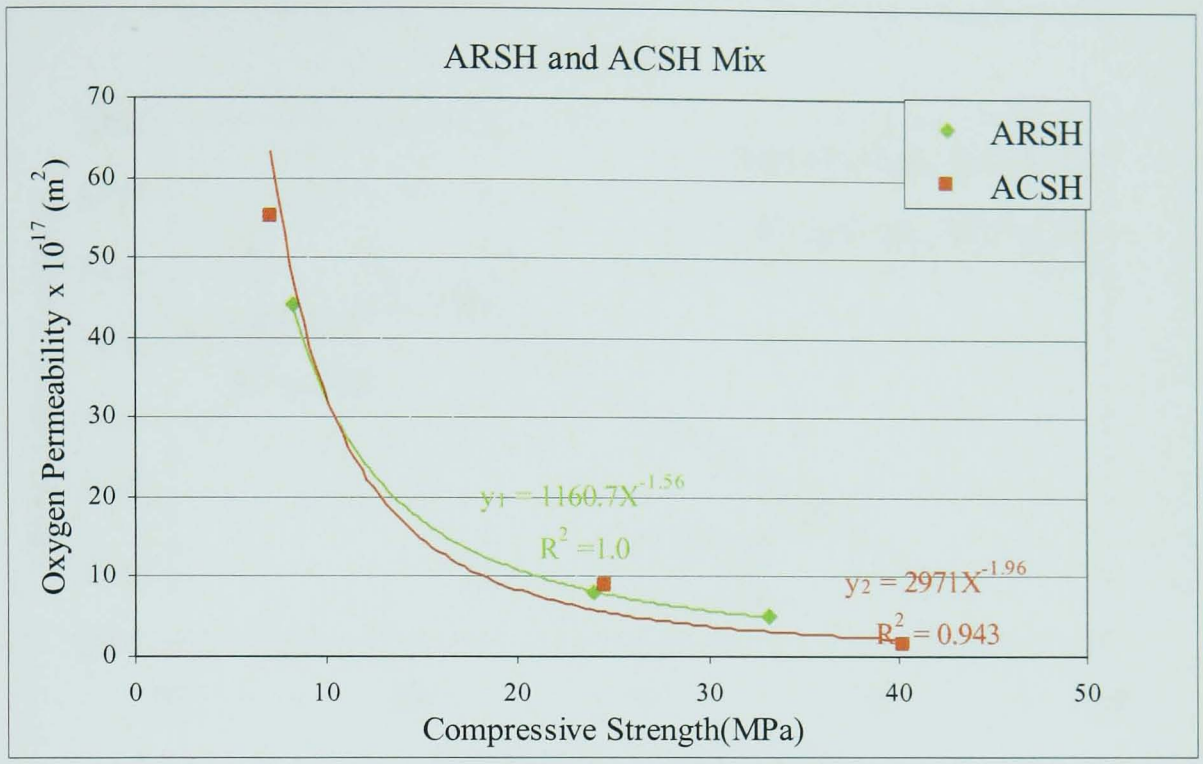

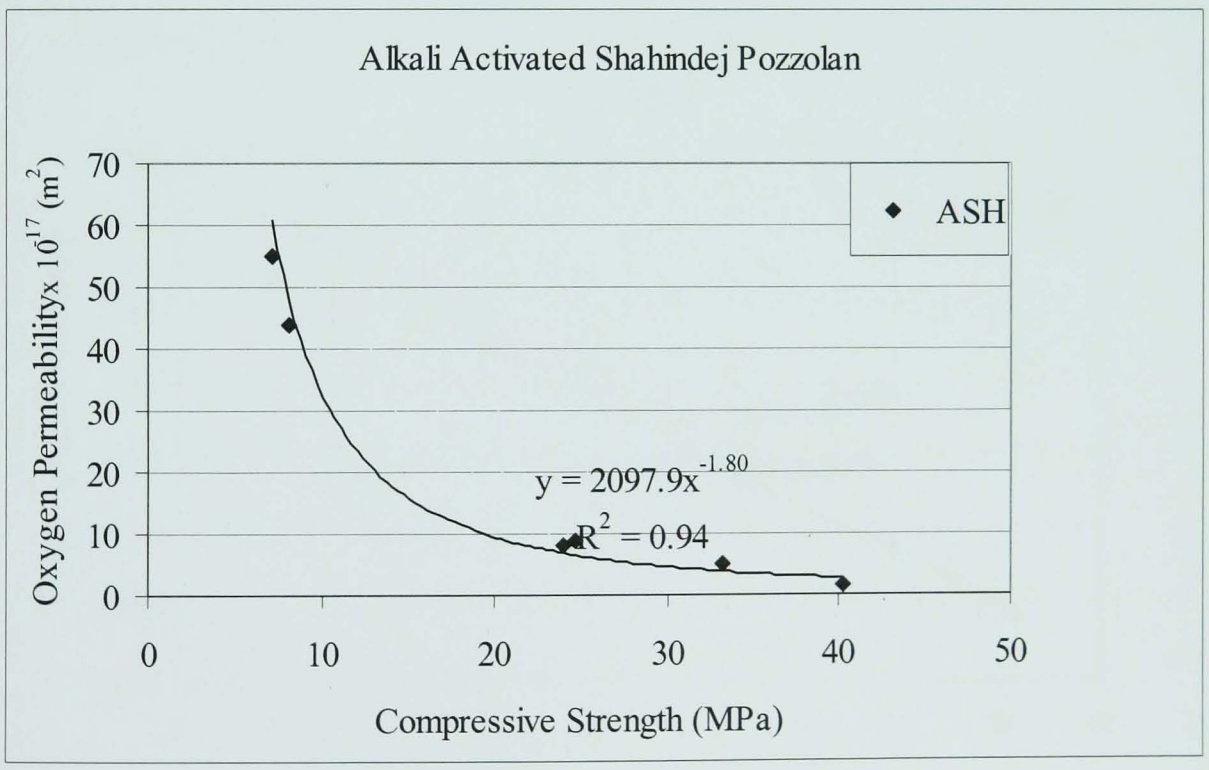

Figure A8.5 Relation between the oxygen permeability and the compressive strength of ARSH and ACSH mixes separately and totally

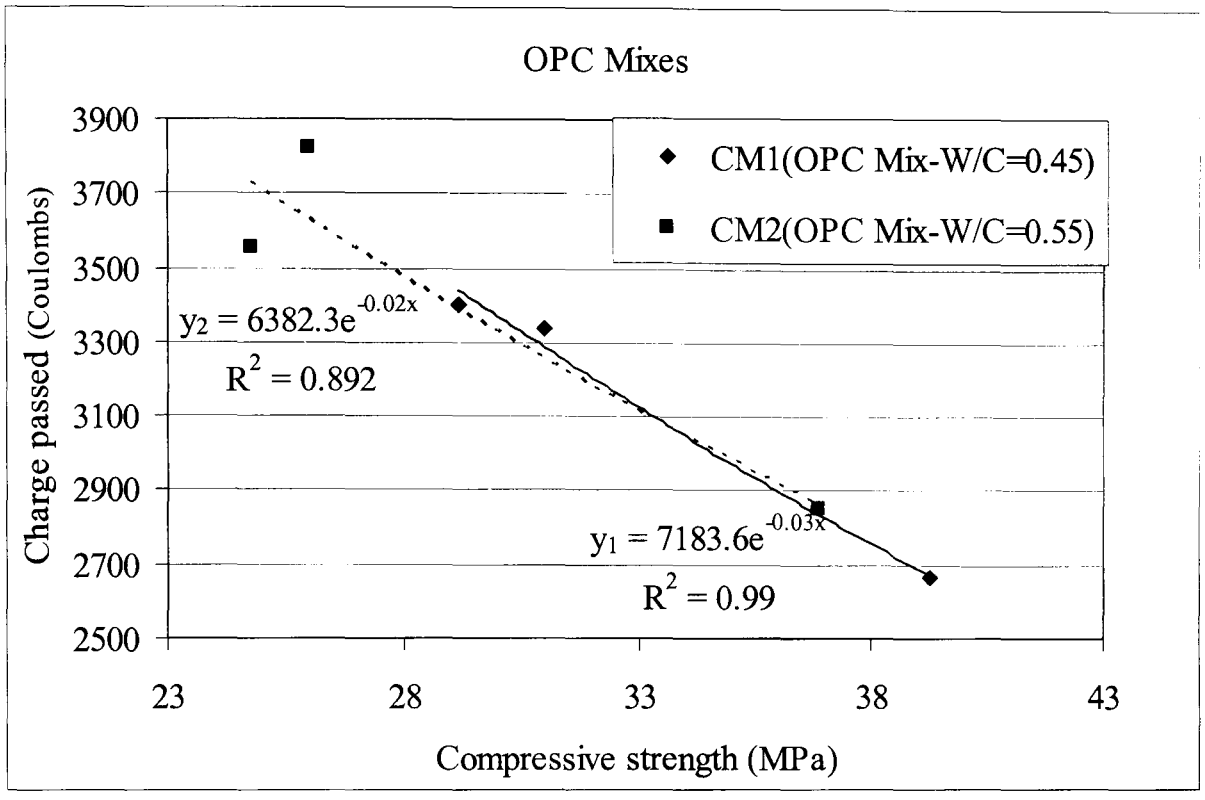

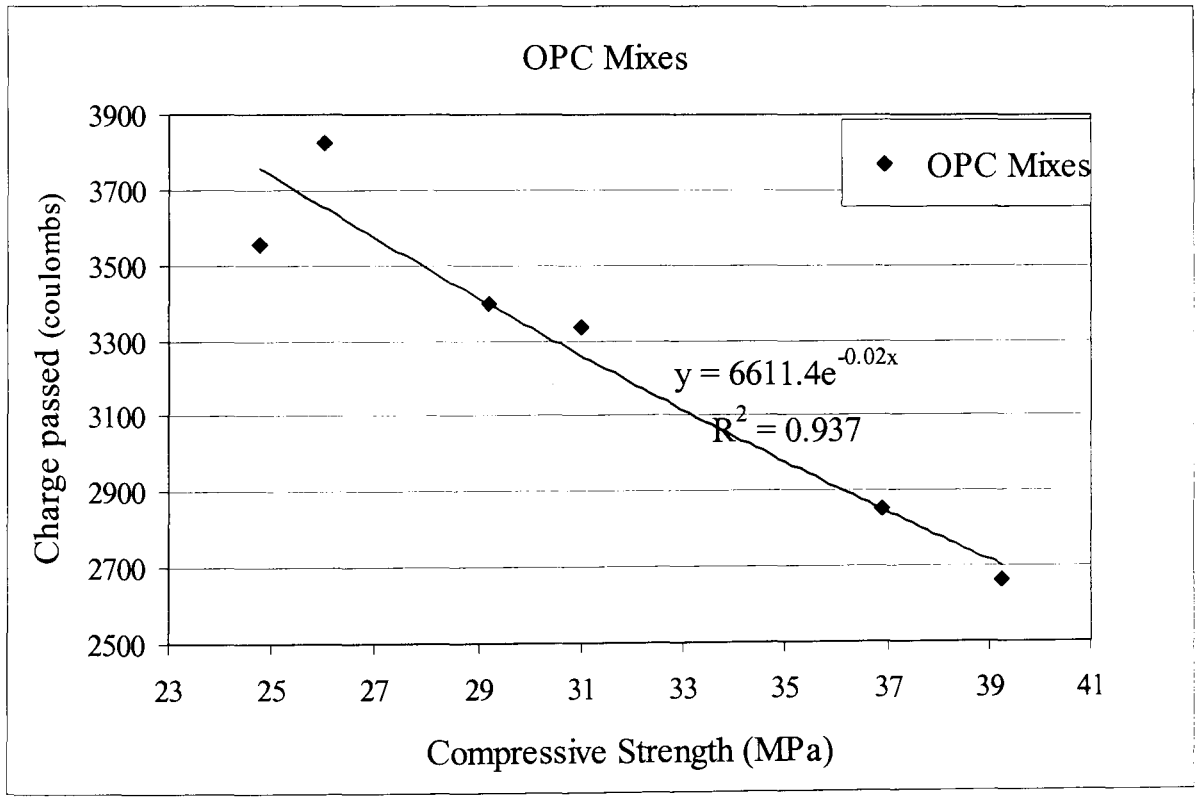

Figure A8.6 Relation between the chloride permeability and the compressive strength of CM1, CM2 and OPC concrete generally under different curing conditions

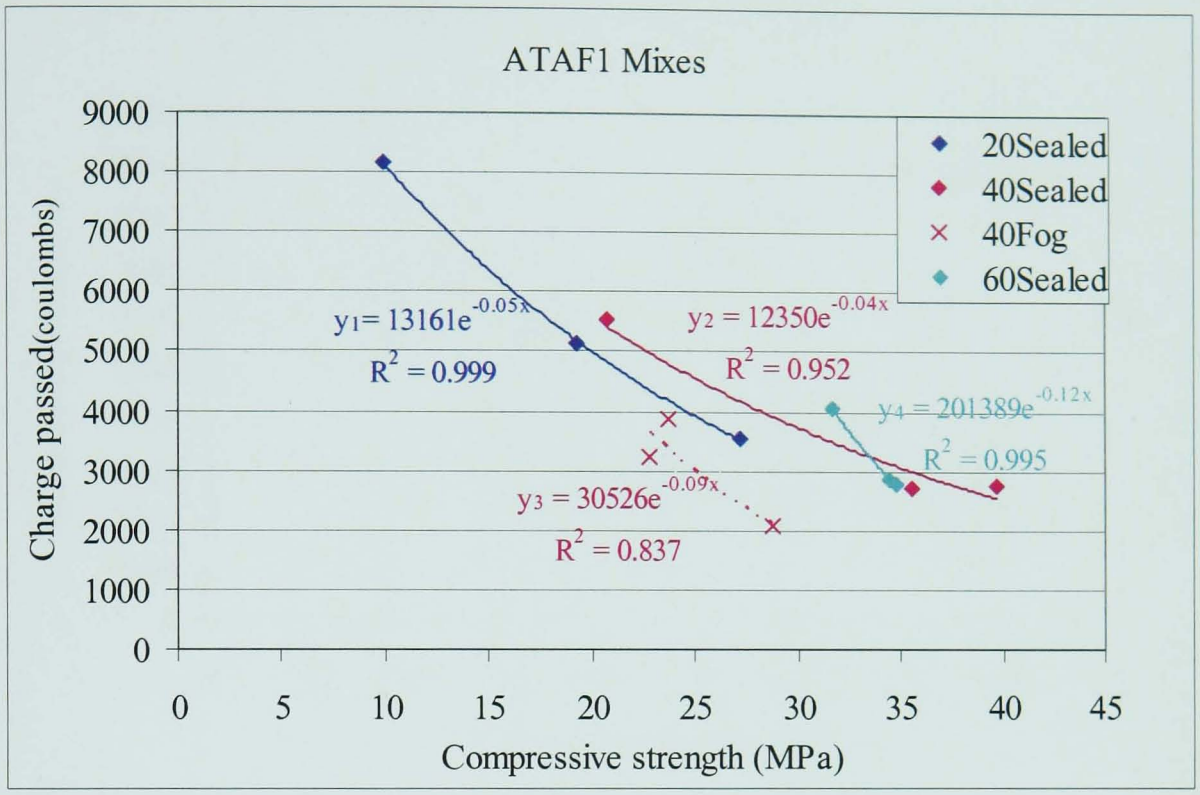

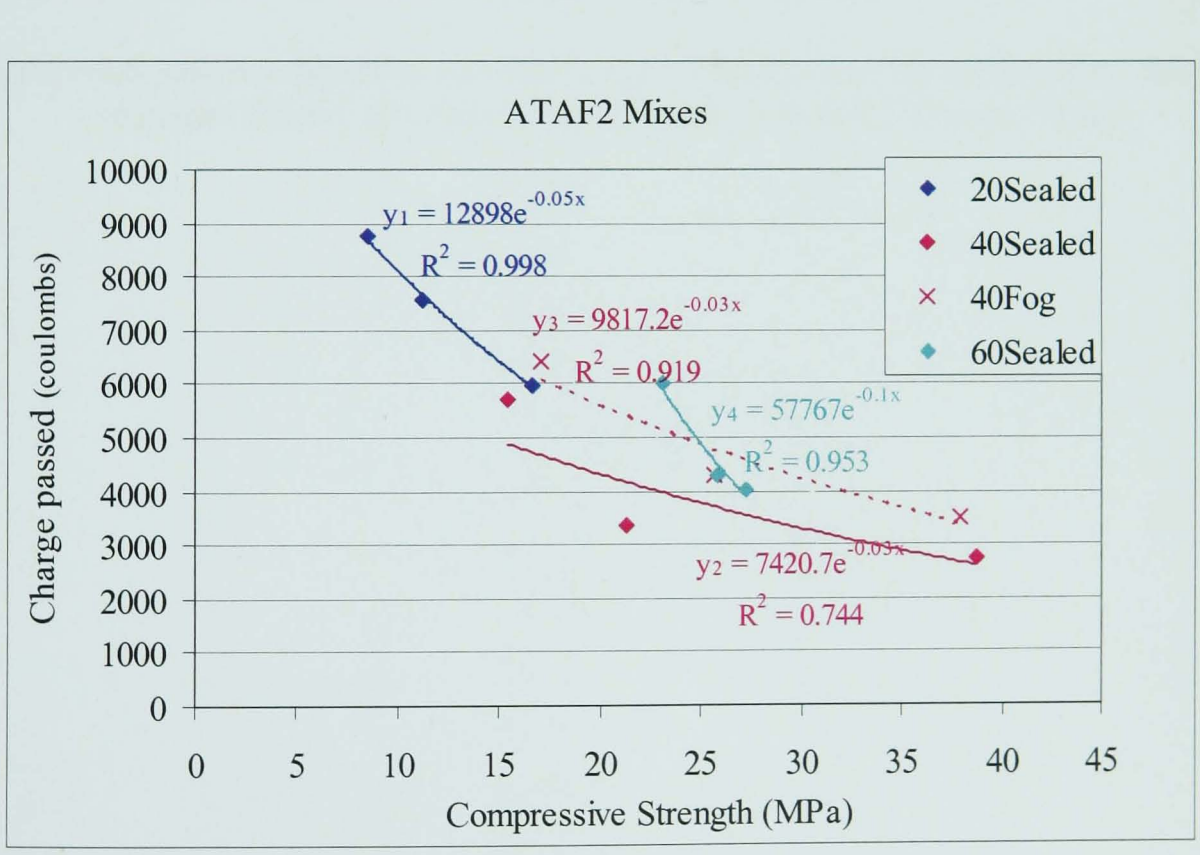

Figure A8.7 Relation between the chloride permeability and the compressive strength of ATAF1, and ATAF2 mixes under different curing conditions

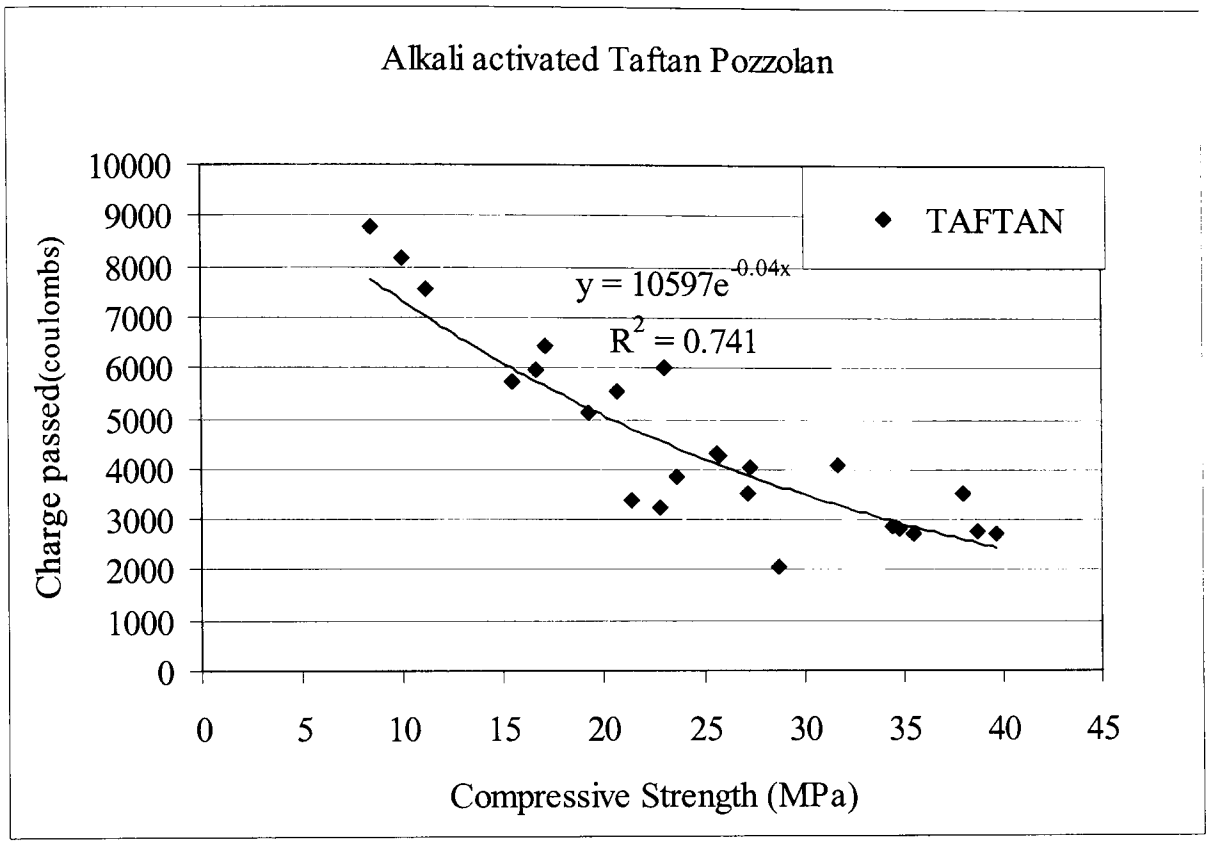

Figure A8.8 Relation between the chloride permeability and the compressive strength of geopolymeric concrete based on alkali activated Taftan pozzolan

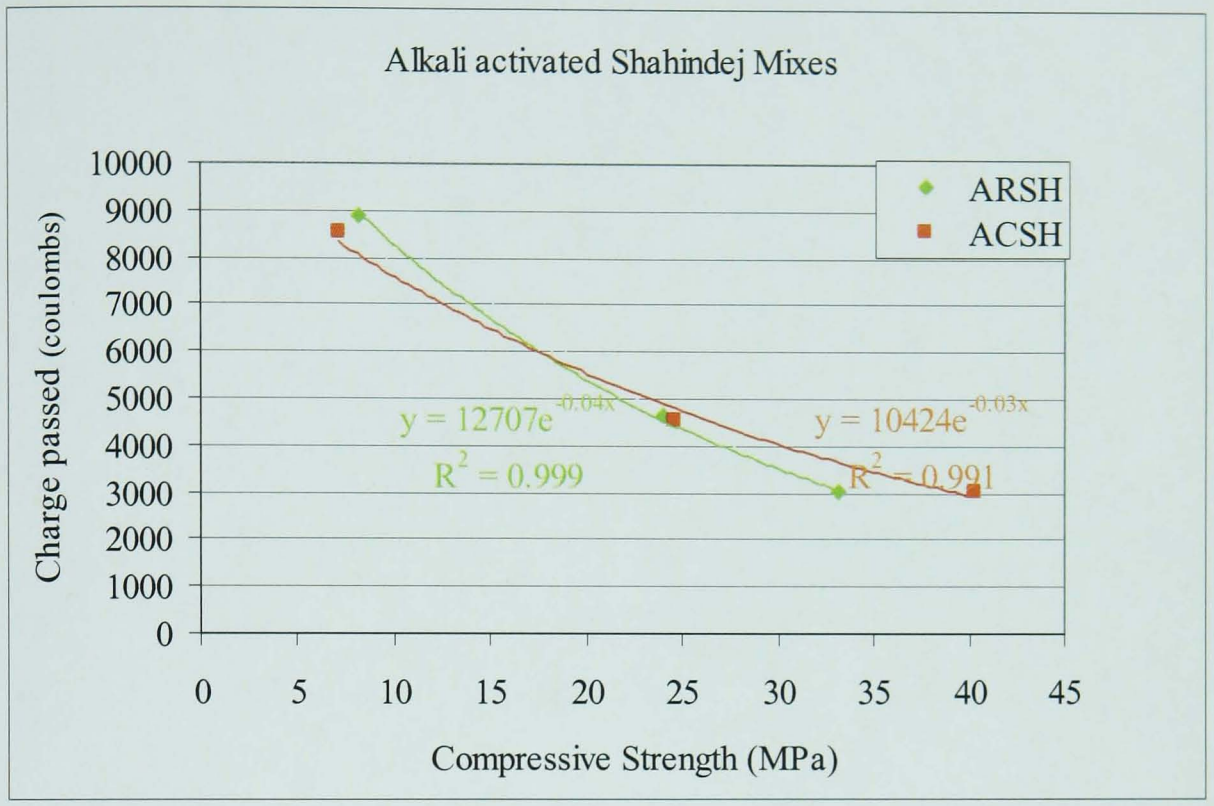

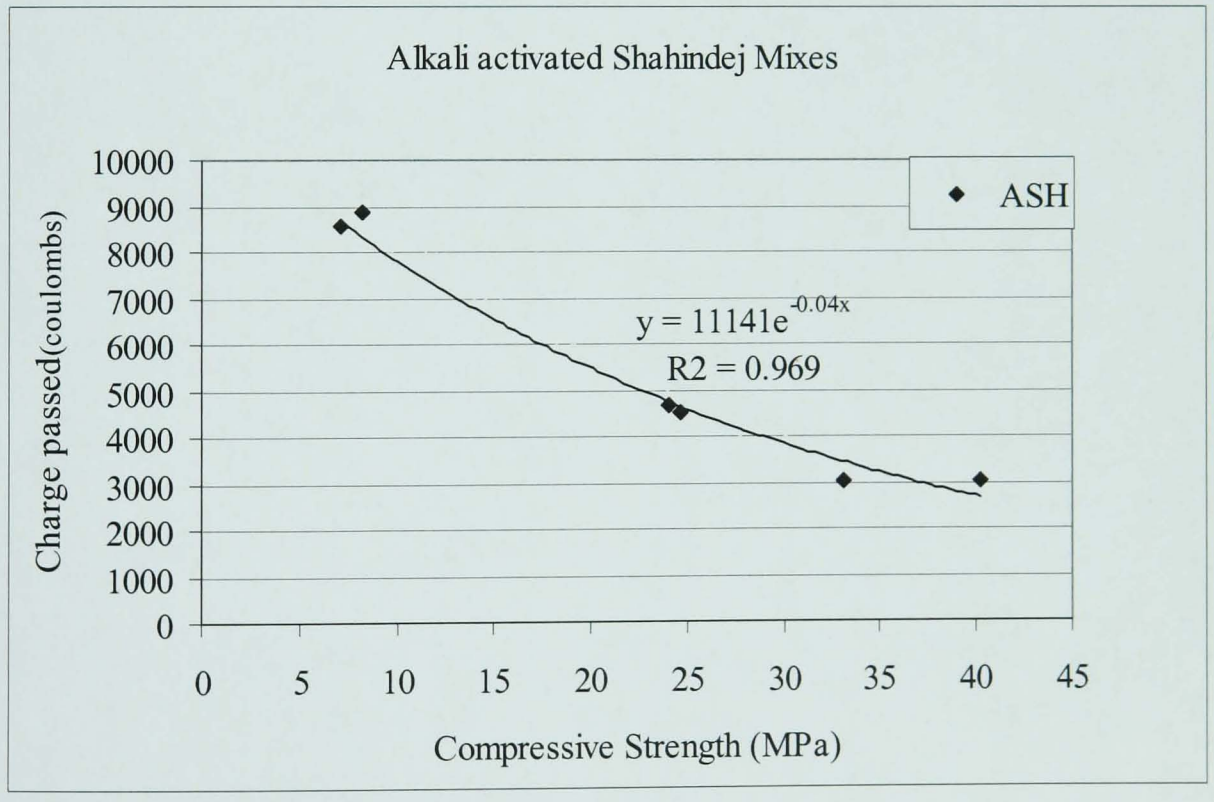

Figure A8.9 Relation between the chloride permeability and the compressive strength of ARSH and ACSH mixes separately and totally